PNNL-15377

Pacific Northwest
National Laboratory
Operated by Battelle for the
U.S. Department of Energy

2005 Closure Assessments for WMA-C Tank Farms: Numerical Simulations

V. L. Freedman
Z. F. Zhang
S. R. Waichler
S. K. Wurstner

September 2005

Prepared for the U.S. Department of Energy
under Contract DE-AC05-76RL01830

DISCLAIMER

PACIFIC NORTHWEST NATIONAL LABORATORY
operated by

BATTELLE
for the
UNITED STATES DEPARTMENT OF ENERGY
under Contract DE-AC05-76RL01830

Printed in the United States of America
Available to DOE and DOE contractors from the
Office of Scientific and Technical Information,
P.O. Box 62, Oak Ridge, TN 37831-0062;
ph: (865) 576-8401
fax: (865) 576-5728
email: reports@adonis.osti.gov

Available to the public from the National Technical Information Service,
U.S. Department of Commerce, 5285 Port Royal Rd., Springfield, VA 22161
ph: (800) 553-6847
fax: (703) 605-6900
email: orders@ntis.fedworld.gov
online ordering: http://www.ntis.gov/ordering.htm


This document was printed on recycled paper.
(9/2003)

PNNL-15377

2005 Closure Assessments for WMA-C Tank Farms: Numerical Simulations

V. L. Freedman
Z. F. Zhang
S. R. Waichler
S. K. Wurstner

September 2005

Prepared for
the U.S. Department of Energy
under Contract DE-AC05-6RL01830

Pacific Northwest National Laboratory
Richland, WA 99352

Summary

In support of CH2M HILL Hanford Group, Inc.'s (CHG) closure of the Hanford Site Single-Shell Tank (SST) Waste Management Area (WMA) tank farms, numerical simulations of flow and solute transport were executed to investigate different potential contaminant source scenarios that may pose long-term risks to groundwater from the closure of the C Tank Farm (WMA C). The simulations were based on the initial assessment effort but implemented a revised approach that examined a range of key parameters and multiple base cases. Four potential source types were identified to represent the four base cases and included past leaks, diffusion releases from residual wastes, leaks during retrieval, and ancillary equipment sources. Using a two-dimensional cross section through the C Tank Farm (Tanks C-103 through C-112) and a unit release from Tank C-112, two solutes [uranium-238 (^{238}U) and technetium-99 (^{99}Tc)] were transported through the problem domain. To evaluate the effect of sorption on contaminant transport, seven sorption coefficients were simulated for ^{238}U. Apart from differences in source releases, all four base cases used the same median parameter values to describe flow and contaminant transport at the WMA C. Forty-six additional cases were also run that examined individual transport responses to the upper and lower limits of the median parameter values implemented in the base-case systems. These cases included varying the preclosure recharge rate, the barrier recharge rate, the degraded barrier recharge rate, and aquifer and vadose zone saturated hydraulic conductivities. Initial depth of past leaks and the magnitude of the diffusion coefficient in the diffusion release scenario were also investigated.

Increasing the preclosure recharge rate increased peak concentrations and accelerated their arrival times at the fenceline compliance point, while the reverse trend occurred when decreasing the preclosure recharge rate. However, the extent of the impact was most significant for the past leak, because the initial release of the contaminant was already close to the water table. Because this rate only represented a short period of time (~80 years) relative to the entire simulation, the impact on leaks initially positioned closer to the tanks was smaller because their peaks occurred much later in the simulations.

Of the three recharge period estimates, the barrier operational recharge estimate (2032–2532) had little impact on peak concentrations and arrival times at the fenceline in all four of the base-case scenarios. The degraded barrier recharge rate had its largest impact on the diffusion case. Peak concentrations and arrival times in the diffusion case were significantly affected because the contaminants were still being released during the degraded barrier recharge period (2532–12032). By contrast, the other base cases simulated more rapid release scenarios, and all of the contaminants had been released into the profile by the time the degraded barrier recharge rate became effective.

Peak concentrations decreased and arrival times were accelerated at the fenceline by a small measure for increases in the estimates of aquifer hydraulic conductivity, while the reverse was true for the lower estimates. This response was the same among all of the release scenarios. By contrast, changes in the saturated hydraulic conductivities of the vadose zone produced more dissimilar results due to the highly nonlinear behavior of transport in the vadose zone. The only generalizations that could be made were that the peak concentrations for the more conservative solutes increased when the saturated hydraulic conductivities increased. When lower estimates of the saturated hydraulic conductivities were simulated, peak concentrations for the more conservative solutes decreased. By contrast, the more strongly retarded species tended to demonstrate opposite trends. Increasing the saturated hydraulic conductivities caused peak concentrations to decrease, while decreases in peak concentrations at the fenceline occurred when upper estimates of the saturated hydraulic conductivities were simulated.

Contents

Figures

Tables

1.0 Introduction

The U.S. Department of Energy (DOE) is charged with evaluating the impacts associated with closure of the single shell tanks (SSTs) and double shell tanks (DSTs) at the Hanford tank farms. In keeping with this charge, DOE began a series of field investigations for the Waste Management Areas (WMAs) at the tank farms. Under the Tri-Party Agreement (TPA) (TPA M-45-98-03) (Ecology et al. 1989), the SSTs and DSTs are Resource Conservation and Recovery Act (RCRA) hazardous waste management units that will eventually be closed under Washington State Dangerous Waste regulations (WAC 173-303). Assessments like the one presented in this report for WMA C are being conducted or are planned for each WMA to evaluate impacts to groundwater resources (i.e., the concentration of contaminants in the groundwater). Hence, this report is one of the first in a series to evaluate the effects of tank closure and establishes a template for reporting results. Results from these analyses may affect current operations or future decisions on retrieval of tank waste and closure of the tank farms.

The specific objectives of the numerical assessment presented in this report were to quantify the risks posed by tank closure at WMA C. These simulations were based on an initial assessment of closure performed in fiscal year 2003 (Zhang et al. 2003) but implemented a revised approach that examined a range of key parameters with four base cases distinguished by the contaminant release type. These potential sources included past leaks, diffusion releases from residual wastes, leaks during retrieval, and ancillary equipment sources. All four base cases used the same median parameter values to describe flow and contaminant transport at the WMA C. Forty-six additional cases were run to examine changes in peak concentrations and arrival times at downstream compliance points when the upper and lower bounds of select median parameter values were implemented. In each of these additional simulations, only one parameter was varied so that any deviations from the base case could be attributed to the "sensitivity" of the system to the altered parameter.

Rather than focus on a comparison among the base cases, this report emphasizes the comparison of peak concentrations and arrival times of the sensitivity cases to their corresponding base case. This approach permits an analysis of the impacts in the uncertainty of the parameter estimates to each of the potential contaminant release scenarios.

This report is divided into sections that generally follow the procedures used to execute the simulations. First, objectives are summarized, followed by a description of each of the numerical simulations. Next, the process of converting the data provided in the Modeling Data Package (MDP) (Khaleel et al. 2003) into input files for the STOMP simulator is described. Much of this discussion relies on the reader having access to the STOMP guide documents and focuses on the correlation between the MDP and STOMP input cards. Implementation of the diffusion release model described in Khaleel et al. (2003) in the STOMP simulator (White and Oostrom 2000a, 2000b) is also described. This is followed by the source releases, movement of contaminants through the vadose zone to the groundwater, and movement of contaminants through the groundwater to points of compliance.

The principal objective of these investigations was to execute the simulations specified in the MDP using widely accepted, scientifically based computational software and reporting the generated results. To promote an open exchange of scientific knowledge and ideas, the software used in this study will be made available, upon request, to the U.S. government and its contractors. To ensure that these simulations can be repeated in the future, the source coding, input files, and output files have been stored in

electronic form and are also available to the U.S. government and its contractors. Although Battelle – Pacific Northwest Division maintains a copyright on the STOMP simulator, the U.S. government retains a paid-up, nonexclusive, irrevocable worldwide license to reproduce, prepare derivative works, and perform and display publicly by or for the U.S. government, including the right to distribute to other government contractors. Numerical simulation of contaminant migration through the vadose zone and unconfined aquifer beneath the C Tank Farm required converting information in the MDP into electronic input that could be interpreted by the STOMP simulator, executing the software, and translating the simulation output into graphical form for reporting. This procedure is described in the final section of the report.

1.1 Modeling Approach

The scope and data required to perform the numerical simulations are documented in the MDP (Khaleel et al. 2003) provided by CH2M HILL Hanford Group, Inc. and updated in an unpublished letter of instruction.(a) The numerical simulations were executed with the STOMP simulator (White and Oostrom 2000a, 2000b), which modeled the vadose zone as an aqueous-gas porous media system where transport through the gas phase was neglected. All simulations used the infinite dilution assumption for coupling fluid flow and contaminant transport.

Fluid flow within the vadose zone was described using Richard's equation, whereas contaminant transport was described using the conventional advective-dispersive transport equation with an equilibrium linear sorption coefficient (K_d) formulation. Stratigraphic information for the cross sections was based on the studies of Lindsey and Reynolds (2001) and the MDP (Khaleel et al. 2003). These cross sections include dipping strata and, when combined with the Polmann (1990) model for anisotropy in unsaturated soils, allow the simulator to model the enhanced spreading at the fine- to coarse-grained interfaces and the increased downslope movement of water along these interfaces.

Modeling parameters used to describe soil-moisture retention, phase relative permeability, saturated hydraulic conductivity (intrinsic permeability), and bulk density (porosity) for individual strata were based on data collected from 200 Area soils (Khaleel et al. 2003). For each stratum (soil type) defined on the cross-section stratigraphy, the small-scale laboratory measurements were scaled spatially upward using the Polmann (1990) model to obtain equivalent horizontal and vertical unsaturated hydraulic conductivities as a function of mean tension. This scaling technique yielded a mathematical expression describing macroscopic anisotropy in the unsaturated hydraulic conductivity as a function of mean tension for each stratum. When multiple soil samples were available for a given stratum, arithmetic averaging of van Genuchten parameters (van Genuchten 1980) was used to define the soil-moisture retention function for each stratum. When multiple soil samples were unavailable for a given stratum, data from other sites in the 200 Areas were used. Hydraulic properties were determined from laboratory measurements of soil moisture retention and unsaturated hydraulic conductivity when available. This approach avoided extrapolating unsaturated hydraulic conductivities (van Genuchten 1980, Mualem 1976) to dry conditions based on a saturated conductivity estimate (Khaleel et al. 1995). To reflect field conditions, laboratory data were corrected for the presence of any gravel fraction in the sediment samples (Khaleel and Relyea 1997).

(a) Connelly MP. 2004. CH2M HILL Hanford Group, Richland, Washington.

1.2 Model Application

A steady flow simulation was run to establish flow conditions for the C Tank Farm before the tank farm was in place. Steady flow conditions for the preconstruction period were established using a constant surface recharge of meteoric water and fixing the aquifer flux across the cross section. No solute transport was considered during the steady flow simulations. Transient simulations involved both fluid flow and solute transport and were simulated in a single stage. The transient simulations started with the flow conditions from the preconstruction simulation and responded to the source release and changes in meteoric recharge caused by barrier emplacement and degradation. Throughout the entire transient simulation, nodes representing the tanks were inactive and considered impermeable. Before tank closure, the impermeable nodes represented tanks filled with waste. The after closure scenario assumed that tanks were filled with grout and that tank degradation was negligible.

Initial conditions for solute concentrations were based on the source type and assumed lateral extent for ^{238}U and ^{99}Tc (Khaleel et al. 2003). As specified by the data package, two contaminant species (^{99}Tc and ^{238}U) were used to represent a range of constituent mobility in these analyses. A two-dimensional northwest-to-southeast cross section through the C Tank Farm, traversing four SSTs, was used to model fluid flow and solute transport. Hence, concentrations do not account for spreading or dilution of solutes in the third dimension. Grid resolutions for all simulations were 1 m in the horizontal and 1 m in the vertical. The simulation domain extended horizontally 180 m to the fenceline boundary. From the ground surface, the simulation domain extended vertically to 15 m below the water table and as much as 97 m below ground surface (bgs).

Several potential contaminant sources were considered, including retrieval leaks (spills), past leaks, and residual tank waste from tanks and tank ancillary equipment. Each source was simulated as a unit inventory release. Unit inventory releases of the contaminants were used for solute transport so that inventories could be scaled eventually to the estimated leak inventory for the C Tank Farm independently of the applied water. All unit releases in the simulations originated from C-112, the tank farthest from the exit boundary. Releases from this tank were considered so that contaminant transport behavior beneath each of the tanks could be analyzed.

For all of the simulation cases, results from vadose zone-aquifer simulations were then transported using streamtube modeling to its downstream compliance points. The streamtube model is an analytical model with the assumption that the aquifer is homogeneous and the flow is one-dimensional while the transport is three dimensional. The results from the streamtube model were examined by comparing them with the results of simulations by the Hanford Site-Wide Groundwater Model (SGM). The SGM is a three-dimensional finite element model based on the Coupled Fluid, Energy, and Solute Transport (CFEST-96) code (Gupta et al. 1987; Gupta 1996).

In keeping with the approach taken for modeling fluid flow, solute transport properties for bulk density, diffusivity, and dispersivity were specified for each stratum. Contaminant mobility was defined through an equilibrium linear sorption coefficient (K_d). Uncertainty remains about the linear sorption coefficient and the applicability of a linear-sorption model for ^{238}U. For example, Kaplan et al. (1996) found that, when uranium was in the form of uranyl, the K_d values were functions of pH and soil moisture content and remained nearly constant in solution concentrations of 3.3 and 100 μg/L. Consequently, Kaplan et al. (1996) concluded that a more complicated sorption model did not necessarily result in better

performance. As a result, a range of linear sorption coefficients was used in the modeling to assess the migration behavior of ^{238}U (e.g., K_d = 0.02, 0.1, 0.2, 0.6, 1.0, 2.0, and 5.0 mL/g). There is little doubt, however, that the linear sorption coefficient (K_d) for ^{99}Tc is close to 0 mL/g in Hanford sediments. This low K_d, coupled with its long half-life (2.03×10^5 yr), allows ^{99}Tc to migrate long distances in both the vadose zone and groundwater, posing a threat to groundwater quality for a long period of time.

2.0 Case Descriptions

The flow and solute transport simulations executed in this report were initially specified in the MDP (Khaleel et al. 2003) and updated in an unpublished letter of instruction.(a) This suite of simulations investigated the impacts on groundwater resources from potential contaminant sources, which included retrieval leaks (spills), past leaks, and diffusion release from residual tank waste and ancillary equipment sources. Also investigated in this study was the system response to changes in individual parameter estimates. In general, the base cases implemented median estimates for key parameters. The system response to changes in the parameter values was investigated using the upper and lower parameter bounds. In this document, simulations that examined changes in peak concentrations and arrival times at downstream compliance points relative to the base cases are termed sensitivity runs. Although the term "sensitivity" is not used here in a classical statistical context, it is used in this document to describe the transport response, or sensitivity, to the individual changes in parameter values.

A two-dimensional cross section representing a northwest-southeast transect through the C Tank Farm was used for the computational domain. No scaling of concentrations and water sources was performed to convert the reported concentrations to an effective concentration in three dimensions. The following simulations represent the four bases cases, identified by source type, that were conducted for the cross section for Tanks C-112, C-109, C-106, and C-103:

- **Past Leak (Base Case 1)**: Past inventory leak with a unit release between Tanks C-112 and C-109
- **Diffusion Release (Base Case 2)**: Diffusion release from residual waste leachates following tank closure using a unit release at Tank C-112
- **Potential Retrieval Leak (Base Case 3)**: Inventory leaks during retrieval using a unit release at Tank C-112
- **Ancillary Equipment Source (Base Case 4)**: Residual waste leachates from tank ancillary equipment following closure using a unit release at Tank C-112.

Sensitivity runs that examined the effect of using upper and lower boundary estimates for key parameter values were carried out in 46 additional simulations. Below is a list of the key parameters that were changed to determine changes in peak concentration and arrival time responses. After a brief description, the median value used in the base-case scenario is listed, followed by the lower and upper parameter bounds used in the sensitivity cases. The parameter values used in these simulations are summarized in Table 2.1. Because the importance of the parameter value depended on the source type, Table 2.2 summarizes the sensitivity runs that were carried out for each of the four base cases. The label used for shorthand notation in tables in this document is shown in parentheses and listed as subcase name in Table 2.1.

- **Preclosure Recharge (recharge)**: These sensitivity cases refer to the recharge period with the highest rate, 1945–2032. In 1945, Hanford operations began at the WMA C which created conditions for enhanced water infiltration. In 2032, a protective barrier was emplaced for tank closure, which significantly reduced the recharge rate relative to the Hanford operational period [median: 100 mm/yr, lower bound: 40 mm/yr, upper bound: 140 mm/yr].

(a) Connelly MP. 2004. CH2M HILL Hanford Group, Richland, Washington.

Table 2.1. Key Parameters Used in Base (median) and Sensitivity Cases (lower and upper bounds). Parameters not listed were the same in all simulations.

	Parameters Varied in Sensitivity Cases						
	Preclosure Recharge Rate (mm/yr)	**Barrier Recharge Rate (mm/yr)**	**Degraded Barrier Recharge Rate (mm/yr)**	**Aquifer Hydraulic Conductivity (m/d)**	**Vadose Zone Hydraulic Conductivity (scale factor)**	**Plume Depth (ft bgs)**	**Diffusion Release Rate (cm^2/s)**
Subcase name	recharge	barrier	barrier_deg	ksat_aq	ksat_vz	plume	diffusion
Lower bound	40	0.1	0.5	2000	0.1	170	1×10^{-14}
Median	100	0.5	1.0	3000	1.0	150	1×10^{-9}
Upper bound	140	1.0	3.5	4000	10.0	130	1×10^{-8}

Table 2.2. Source Types[(a)] Run with Upper and Lower Parameter Bounds Listed in Table 2.1 (no checkmark indicates that simulations using upper and lower parameter bounds were not conducted for the corresponding source type)

	Parameters Varied in Sensitivity Cases						
	Preclosure Recharge Rate	**Barrier Recharge Rate**	**Degraded Barrier Recharge Rate**	**Aquifer Hydraulic Conductivity**	**Vadose Zone Hydraulic Conductivity**	**Plume Depth**	**Diffusion Release Rate**
Past Leak	✓	✓	✓	✓	✓	✓	
Diffusion release	✓	✓	✓	✓	✓		✓
Retrieval leak	✓	✓	✓	✓	✓		
Ancillary equipment release	✓	✓	✓	✓	✓		
(a) Base cases are identified by source type.							

- **Barrier Recharge (barrier)**: These sensitivity cases refer to the recharge period 2032 – 2532, when the protective barrier was emplaced, following tank closure. The effective recharge rate was significantly reduced when the barrier was fully operational [median: 0.5 mm/yr, lower bound: 0.1 mm/yr, upper bound: 1.0 mm/yr].
- **Degraded Barrier Recharge (barrier_deg)**: These sensitivity cases refer to the recharge period 2532 – 12032, when the protective barrier was assumed to undergo degradation. The effective recharge rate was increased during this period to account for enhanced infiltration relative to the period when the barrier was fully operational [median: 1.0 mm/yr, lower bound: 0.5 mm/yr, upper bound: 3.5 mm/yr].
- **Aquifer Hydraulic Conductivity (ksat_aq)**: Due to uncertainty in the aquifer hydraulic conductivity, these sensitivity cases examined a wide range in the aquifer hydraulic conductivity parameter. The aquifer hydraulic conductivity was changed for both the steady-state, pre-Hanford operations simulation, as well as for the duration of the transient simulation, 1945–12032 [median: 3000 m/d, lower bound: 2000 m/d, upper bound: 4000 m/d].

- **Vadose Zone Saturated Hydraulic Conductivity (ksat_vz)**: Due to uncertainty in the estimates of the unsaturated parameters, these sensitivity cases examined the impact that one of the most sensitive vadose zone parameters, the saturated hydraulic conductivity, has on transport. For both the steady-state, pre-Hanford operations simulation, as well as for the duration of the transient simulation, 1945 – 12032, the saturated hydraulic conductivity parameter was scaled for each of the material types in the vadose zone [median: scale_factor = 1, lower bound: scale_factor = 0.1, upper bound: scale_factor = 10.0].
- **Plume Depth (plume)**: Due to uncertainty in the depth to which existing plumes from past leaks have migrated, the subsurface placement of the unit release in the past leak scenario was varied for the sensitivity cases corresponding to Base Case 1. For these cases, an instantaneous unit release was assumed to have occurred on January 1, 2000 [median: 150 ft bgs, lower bound: 170 ft bgs, upper bound: 130 ft bgs].
- **Rate of Diffusion (diffusion)**: In these sensitivity cases, the uncertainty in the diffusion release rate from tank residual wastes was investigated. The upper and lower bounds of the parameter estimate were changed only for the diffusion-dominated release model used in Base Case 2 [median: 1×10^{-9} cm^2/s, lower bound: 1×10^{-14} cm^2/s, upper bound: 1×10^{-8} cm^2/s].

Simulations were executed for a period of compliance of 10,000 years. Tank degradation was assumed to be negligible in the years following closure (2032–12032). Once tank closure occurred, it was assumed that grout replaced the tank wastes in the impermeable tank structures. Initial flow conditions for the first stages of the simulation were established with a steady-state flow simulation that assumed a natural infiltration rate of 3.5 mm/yr. The base cases are described in the sections that follow.

2.1 Past Leak (150-ft depth)

This scenario (Base Case 1) investigated a past leak at a depth of 150 ft bgs (45.7 m) with an inventory distribution between Tanks C-112 and C-109 and a width of 25 ft (7.6 m). The release began on the first day of the year 2000. A unit release of each of the contaminant species (^{99}Tc and ^{238}U) was simulated. The ^{238}U contaminant was simulated with seven different linear sorption coefficients (K_d = 0.02, 0.1, 0.2, 0.6, 1.0, 2.0, and 5.0 mL/g).

2.2 Residual Tank Waste (diffusion dominated)

This scenario (Base Case 2) investigated a residual tank waste source using a diffusion-dominated release model and a diffusion coefficient of 1×10^{-8} cm^2/s. The release occurred over the bottom width of Tank C-112 with a source thickness of 0.825 m. The leak began on the first day of the year 2032, when tank closure has been completed and the barrier emplaced. A unit release of each of the contaminant species (^{99}Tc and ^{238}U) was simulated. The ^{238}U contaminant was simulated with seven different linear sorption coefficients (K_d = 0.02, 0.1, 0.2, 0.6, 1.0, 2.0, and 5.0 mL/g).

2.3 Potential Retrieval Leak (8,000 gal)

This scenario (Base Case 3) investigated a potential retrieval leak of 8,000 gallons that was in the lower-right corner of Tank C-112 and began on the first day of the year 2000. The leak lasted 14 days and contained a unit release of each of the contaminant species (^{99}Tc and ^{238}U). The ^{238}U was simulated with seven different linear sorption coefficients (K_d = 0.02, 0.1, 0.2, 0.6, 1.0, 2.0, and 5.0 mL/g).

2.4 Ancillary Equipment Leak (30 ft depth)

This scenario (Base Case 4) investigated a past leak at a depth of 30 ft bgs (9.1 m) and an inventory distribution between Tanks C-112 and C-109 and a width of 25 ft (7.6 m). The release began on the first day of the year 2000. A unit release of each of the contaminant species (^{99}Tc and ^{238}U) was simulated. The ^{238}U contaminant was simulated with six different linear sorption coefficients (K_d = 0.01, 0.03, 0.1, 0.3, 0.6, and 1.0 mL/g).

3.0 Technical Approach

A multistep approach was used to execute the simulations described in the modeling data package (Khaleel et al. 2003). In brief, the approach involved converting information in the data package to a suite of input files, executing the STOMP simulator, translating the simulation results into graphical form, and determining solute concentrations at the compliance points. This section provides an overview, followed by a more extensive review of these steps. In this discussion, MDP refers to the modeling data package (Khaleel et al. 2003), which was updated by an unpublished letter of instruction.(a)

3.1 Overview

Two types of input are defined in a STOMP simulation: 1) a simulation control and material definition file, and 2) a soil zonation file. Modeling input data stored in these files were developed from the modeling data package in conjunction with the discretization of the physical domain. The physical domain was a northwest-southeast two-dimensional cross section in the C Tank Farm. The physical domain was discretized using a Cartesian grid with uniform horizontal and vertical spacing of 1 m.

Graphical representations of geologic interpretations and engineered structures in the C Tank Farm subsurface (Khaleel et al. 2003, Appendix B) were converted to zonation maps based on the Cartesian discretization of the physical domain. Hydrologic properties, as defined in the MDP, for each of six identified soil types were converted to input in the form of STOMP input cards. Transport property data for the two contaminants and six soil-type combinations were converted to input in the form of STOMP input cards. The conceptual model was then completed by converting boundary conditions and sources, as specified in the MDP, into input in the form of STOMP input cards, specifying execution controls and requesting output data.

Time-varying surface recharge and tank leaks required a transient flow solution to be executed with the solute transport calculations. The transient flow and transport simulations were initiated using a steady flow solution to the boundary value problem using the initial boundary values. This approach neglects time variations in surface recharge prior to the start of simulation. The steady flow initial condition was generated with a simulation to steady flow conditions. The same steady-state flow solution was used for each of the simulations executed in this work. This represented the preconstruction time period for the C Tank Farm. This simulation did not involve solute transport and was executed as a transient simulation from a unit-gradient initial condition to a steady flow condition that honored the surface recharge and unconfined aquifer flux. The steady flow and transient simulations were executed on a Linux workstation. For compatibility between platforms, the input, zonation, and inventory files were maintained in an ASCII format.

The steady flow solution was then used as an initial condition for the transient flow and solute transport cases executed in this work. Because tank degradation was assumed to be negligible in the years following closure (2032–12032), the tank structures were assumed to be impermeable and were represented by inactive nodes in the simulation domain.

(a) Connelly MP. 2004. CH2M HILL Hanford Group, Richland, Washington.

Simulation results were written to three types of output files: 1) a reflected input and reference node file, 2) a series of plot files, and 3) a series of surface-flux files. The reflected input and reference node file contains a translation of the input files as interpreted by the simulator (e.g., with unit conversions) and a time sequence of the simulation history and chosen variables (e.g., aqueous pressure, moisture content, solute concentrations, Darcy fluxes) at selected grid locations. Plot files contain variable data for all grid points at selected simulation times. These files are used to generate color-scaled plots and animations through Tecplot.(a) A utility program, PlotTec, is used to translate STOMP plot files into Tecplot-formatted input files. Surface-flux files contain rate and integral information about fluxes crossing user-defined internal or external boundaries. Solute fluxes and aqueous fluxes at the downgradient domain boundary within the groundwater are used to calculate average solute concentrations and source rates. Surface-flux files are also used to generate rate and integral plots of solutes exiting the computational domain and entering the groundwater. A utility program, Surfcalc, was used to translate STOMP surface-flux files into formatted input files suitable for plotting.

Solute breakthrough curves for the aquifer, or solute concentrations as a function of time at the compliance points outside the C Tank Farm, were computed by extrapolating solute concentrations exiting the STOMP computational domain. An analytical solution to the advection-dispersion equation for solute transport through a saturated porous media in three dimensions was used, following the approach described by Baetslé (1969) and documented in Domenico and Schwartz (1990). This approach assumed that the solute originated at a point source as a series of slugs released over time. The method of superposition was used to integrate the slug releases. The solute mass from each slug migrated from the point source by advective-dispersive transport in a steady, uniform flow field. As the solute mass was transported advectively with the flow, it spread longitudinally and transversely via hydrodynamic dispersion and molecular diffusion. The mass flux of solute used as input was computed from the STOMP surface file output for mass flux exiting the 15-m-thick aquifer at the east side of the domain. Aquifer recharge along the groundwater flow path was neglected in translating solute concentrations to the compliance points.

3.2 Modeling Data Package

Meteoric recharge and parameters for vadose zone flow and transport were provided in the MDP. Selected data are repeated in this section for the base cases only. Simulations that examine the sensitivity of the contaminant transport response to changes in select parameters are detailed in Section 3.3.

3.2.1 Recharge Estimates

Portions of the C Tank Farm surfaces were covered with gravel to prevent vegetative growth and provide radiation shielding for workers. Bare gravel surfaces, however, enhance the net infiltration of meteoric water compared with undisturbed, naturally vegetated surfaces. Between tanks, infiltration is further enhanced by the effect of percolating water being diverted by the impermeable sloping surface of the tank domes.

(a) Amtec Engineering, Inc. 2002. Tecplot, Version 9.0. Amtec, Bellevue, Washington.

Recharge rates for all cases were varied to represent various stages of tank and barrier construction. For example, the beginning of the simulation represents the tank preconstruction period, and recharge is estimated at 3.5 mm/yr. Once the tanks are in place in the year 1945, recharge rates increase to their current estimate of 100 mm/yr. In the year 2032, a protective barrier is installed at the surface, and the recharge rate estimate decreases to 0.5 mm/yr. The recharge rate is increased to 1 mm/yr when degradation of the barrier occurs in the year 2532. These values are summarized in Table 3.1.

Table 3.1. Recharge Estimates (Khaleel et al. 2003)

Years	Pre-1945	1945–2032	2032–2532	2532–12032
Recharge Rate (mm/yr)	3.5	100.0	0.5	1.0

3.2.2 Vadose Zone Flow and Transport Properties

Upscaled values of parameters for fluid flow and solute transport for the vadose zone were used in these investigations. Details for computing upscaled parameters are provided in Khaleel et al. (2003). Fluid flow parameters for the vadose zone include soil moisture retention characteristics and saturated hydraulic conductivity. Solute transport parameters include bulk density, diffusivity, sorption coefficients, and macrodispersivity. Table 3.2 lists the bulk density and the composite, fitted van Genuchten-Mualem parameters (van Genuchten 1980) for various strata at the C Tank Farm. The material type numbers are identical to those indicated in the MDP (Section 4.2).

Table 3.2. Composite van Genuchten-Mualem Parameters for Various Strata at the C Tank Farm (Khaleel et al. 2003, Appendix C)

Strata/Material Type	Number of Samples	ρ_b	θ_s	θ_r	α 1/cm	n	l	K_s cm/s
Backfill (1)	10	2.13	0.1380	0.0100	0.0210	1.3740	0.5	5.60e-04
Sand H2 (2)	12	1.76	0.3819	0.0443	0.117	1.6162	0.5	9.88e-05
Gravelly sand H3 (3)	8	2.07	0.2688	0.0151	0.0197	1.4194	0.5	5.15e-04
Gravelly sand H1 (4)	11	1.94	0.2126	0.0032	0.0141	1.3730	0.5	2.62e-04
Hanford-Ringold/ Plio-Pleistocene (5)	10	2.13	0.1380	0.0100	0.0210	1.3740	0.5	5.60e-04
Aquifer (Ringold gravels)	10	2.13	0.25[(a)]	0.0100	0.0210	1.3740	0.5	3.47e+00
(a) Represents the effective porosity of the aquifer.								

3.2.3 Stochastic Model for Macroscopic Anisotropy

Variable tension-dependent anisotropy provides a framework for upscaling small-scale laboratory measurements to the effective (i.e., upscaled) properties for the large-scale tank farm vadose zone. A stochastic model (Polmann 1990) was used to evaluate tension-dependent anisotropy for sediments at the

C Tank Farm; details are in Khaleel et al. (2003, Appendix C). The following is a brief description of the variable anisotropy model used in this investigation.

Yeh et al. (1985) analyzed steady unsaturated flow through heterogeneous porous media using a stochastic model; parameters such as hydraulic conductivity were treated as random variables rather than deterministic quantities. The Gardner (1958) relationship was used by Yeh et al. (1985) to describe unsaturated hydraulic conductivity as a function of saturated hydraulic conductivity and tension according to Equation (3.1):

$$K(\psi) = K_S \exp(-\beta\psi) \tag{3.1}$$

where K is the unsaturated hydraulic conductivity, K_S is the saturated hydraulic conductivity, ψ is the tension, and β is a fitting parameter. Eq. (3.1) can be written as shown in Eq. (3.2). This form is referred to as the log-linear model:

$$\ln K(\psi) = \ln K_s - \beta\psi \tag{3.2}$$

because the log of the hydraulic conductivity is linearly related to the tension through a constant slope. A constant slope, however, is often inadequate for describing $\ln K(\psi)$ over the range of tension of interest for field applications. As an alterative, β can be approximated locally by straight lines over a range of tensions. The $\ln K_S$ term can then be derived by extrapolating the local slopes to zero tension.

Using a linear correlation model between the zero-tension intercept and β, Polmann (1990) presented a generalized model that accounts for the cross-correlation of the local soil property (i.e., $\ln K_S$ and β) residual fluctuations. Compared with the uncorrelated $\ln K_S$ and β model, partial correlation of the properties was shown to have a significant impact on the magnitude of the effective parameters derived from the stochastic theory. The Polmann (1990) equations for deriving the effective parameters are shown in Eq. (3.3) through (3.6):

$$\langle LnK(\psi)\rangle = \langle LnK_s\rangle - A\langle\psi\rangle - \frac{\sigma^2_{LnKs}\lambda\left[p - p^2\langle\psi\rangle - \zeta^2\langle\psi\rangle\right]}{(1+A\lambda)} \tag{3.3}$$

$$\sigma^2_{LnK(\psi)} = \frac{\sigma^2_{LnKs}\left[(1-p\langle\psi\rangle)^2 + \zeta^2\langle\psi\rangle^2\right]}{(1+A\lambda)} \tag{3.4}$$

$$K_h^{eq} = \exp\left[\langle LnK(\psi)\rangle + \frac{\sigma^2_{LnK(\psi)}}{2}\right] \tag{3.5}$$

$$K_v^{eq} = \exp\left[\langle LnK(\psi)\rangle - \frac{\sigma^2_{LnK(\psi)}}{2}\right] \tag{3.6}$$

where

σ^2_{LnK} = the variance of log unsaturated conductivity

$\langle \psi \rangle$ = the mean tension

σ^2_{LnKs} = the variance of $\ln K_s$

$\langle Ln K_s \rangle$ = the mean of $\ln K_s$

p = the slope of the β versus $\ln K_s$ regression line

$$\zeta = \frac{\sigma_\delta}{\sigma_{LnKs}}$$

σ_δ = the standard deviation of the residuals in the β versus $\ln K_s$ regression

A = the mean slope, β, for $\ln K_s$ versus ψ

λ = the vertical correlation length for $\ln K_s$

K_h^{eq} = the equivalent unsaturated horizontal hydraulic conductivity

K_v^{eq} = the equivalent unsaturated vertical hydraulic conductivity.

Macroscopic anisotropy parameter estimates for the strata at the C Tank Farm are listed in Table 3.3. Details on these parameters and their derivation are included in Khaleel et al. (2003, Appendix C) and White et al. (2001).

Table 3.3. Macroscopic Anisotropy Parameters Based on Polmann Equations for Strata at the C Tank Farm (Khaleel et al. 2003, Section 4.2)

Strata/Material Type	No. of Samples	$\langle Ln K_s \rangle$	σ^2_{LnKs}	p	ζ	λ (cm)	A
Backfill (1)	10	-15.76	3.56	-1.1e-4	1.84e-4	30	0.00371
Sand H2 (2)	12	-14.59	1.50	-7.2e-4	6.55e-4	50	0.00620
Gravelly sand H3 (3)	11	-14.85	1.94	-2.6e-4	2.50e-4	30	0.00368
Gravelly sand H1 (4)	8	-15.30	1.83	-5.6e-4	5.16e-4	50	0.00415
Hanford-Ringold/ Plio-Pleistocene (5)	10	-15.76	3.56	-1.1E-4	1.84E-4	30	0.00371

3.2.4 Dispersivity

Field-scale dispersivities were selected based on an extensive literature review presented in the MDP (Khaleel et al. 2003) and a small-scale field experiment. The field measurements performed at the Hanford site used KCL as a tracer (Ward et al. 1998) and were consistent with the concept of scale-dependent dispersivities that is prevalent in the literature. This scale dependence occurs for dispersivities that increase with time or distance until an asymptotic value is reached. These field-scale dispersivities

are referred to here as macrodispersivities. Based on a stochastic solution, Gelhar and Axness (1983) estimated the asymptotic value of macrodispersivity as

$$\alpha_L = \sigma^2_{\ln K_{sat}} \lambda \tag{3.7}$$

where αL is the longitudinal dispersivity, $\sigma^2_{\ln K_{sat}}$ is the variance of the log saturated hydraulic conductivity, and λis the vertical correlation scale for log saturated hydraulic conductivity.

In addition to the size of the flow domain and vadose zone soil heterogeneities, dispersivities are also a function of soil moisture content. Russo (1993) suggested that vadose zone macrodispersivities can be defined similar to saturated media estimates because the product of the variance and the correlation scale for the log conductivity of both saturated and unsaturated media are similar in magnitude. Hence, in this work, the Gelhar and Axness (1983) equation is modified to account for unsaturated conditions with the following

$$\alpha_L\left(\langle\varphi\rangle\right) = \sigma^2_{\ln K} \lambda \tag{3.8}$$

where the longitudinal macrodispersivity depends on the mean tension <φ>. To obtain macrodispersivity estimates using Eq. (3.8), an estimate of the vertical correlation scale for unsaturated conductivity is needed. A value of 30 cm was assumed for the correlation length at WMA C for all five strata. The resulting macrodispersivity estimates for the nonreactive species are listed in Table 3.4. Transverse dispersivities are estimated as one-tenth of the longitudinal macrodispersivities (Gelhar et al. 1992).

Table 3.4. Nonreactive Macrodispersivity Estimates for Strata at the C Tank Farm

Strata/Material	$\sigma^2_{\ln K}$	Correlation Length λ, cm	α_L, cm	α_T, cm
Backfill (1)	4.54	30	~150	~15
Sand H2 (2)	4.60	30	~150	~15
Gravelly sand H3 (3)	3.19	30	~100	~10
Gravelly sand H1 (4)	4.95	30	~100	~10
Hanford-Ringold/ Plio-Pleistocene (5)	4.54	30	~150	~15
Aquifer (Ringold gravels)	4.54	30	~150	~15

3.2.4.1 Enhanced Macrodispersivity for Reactive Species

Enhanced spreading may occur due to reactive species that are sorbed in the subsurface. When sorption occurs during contaminant transport, the migration through geologic media is retarded, thereby enhancing dispersion. Enhanced macrodispersion is then a function of the solute and the soil properties that affect sorption (Gelhar 1993; Talbott and Gelhar 1994). This enhancement can be described mathematically as

$$\alpha_{L_E} = \alpha_L \left\{ \left[1 + \gamma \frac{\sigma_R}{\overline{R}\sigma_{\ln K}} \sqrt{\zeta} \right]^2 + (1-\zeta) \frac{\sigma_R^2 \lambda_h}{\overline{R}\sigma^2_{\ln K} \lambda} \gamma^2 \right\} \tag{3.9}$$

where α_{L_E} is the enhanced longitudinal macrodispersivity, γ is the ratio of harmonic to geometric mean for unsaturated hydraulic conductivity, and λ_h is the horizontal correlation scale (Talbott and Gelhar 1994). The ratio of λ_h/λ is assumed to be approximately equal to one. The retardation factor is related to the distribution coefficient by the following

$$\overline{R} = 1 + \frac{\overline{\rho}_b \overline{K}_d}{\overline{\theta}} \tag{3.10}$$

where R can be described statistically by an effective retardation, $\overline{R}$ and its standard deviation σ_R. The symbols $\overline{\rho}_b$, $\overline{K}_d$ and $\overline{\theta}$ represent the averages of the bulk density (g/cm^3), distribution coefficient (mL/g) and water content (cm^3/cm^3), respectively.

Stochastic analysis results for macrodispersivity enhancement for the five strata are presented in Table 3.5 for the reactive species (^{238}U). The macrodispersivity enhancement ranged from 1.06 for sandy sediments to about 1.12 for gravelly sand. In this analysis, the unsaturated hydraulic conductivities were evaluated at a tension of 100 cm via the fitted van Genuchten-Mualem relation with a distribution coefficient (K_d) of 0.6. It is assumed that the ratio $\sigma_R/\overline{R}$ is constant for the range of distribution coefficients used in this analysis.

Table 3.5. Reactive Enhanced Macrodispersivity (α_{L_E}/α_L) Estimates for Strata at the C Tank Farm

Strata/Material	$\sigma_R/\overline{R}$	γ	ζ	α_{L_E}/α_L
Backfill (1)	0.43	0.26	0.38	1.067
Sand H2 (2)	0.67	0.13	0.58	1.063
Gravelly sand H3 (3)	0.38	0.32	0.72	1.120
Gravelly sand H1 (4)	0.50	0.20	0.42	1.062
Hanford-Ringold/ Plio-Pleistocene (5)	0.43	0.26	0.38	1.067

3.2.5 Diffusivity

It was assumed that the effective, large-scale diffusion coefficients for all strata at the C Tank Farm were a function of volumetric moisture content and could be expressed using the Millington and Quirk (1961) empirical relation, as shown in Eq. 3.11:

$$D_e(\theta) = D_o \frac{\theta^{10/3}}{\theta_s^2} \tag{3.11}$$

where D_e is the effective diffusion coefficient of an ionic species, D_o is the molecular diffusion coefficient for the species in water, θ is the water content, and θ_s is the saturated water content. The molecular diffusion coefficient for all species in pore water was assumed to be 2.5 x 10^{-5} cm^2/s (Kincaid et al. 1995).

3.2.6 Diffusion-Dominated Release Model

A diffusion release model was implemented in the STOMP simulator for describing radionuclide releases from the tank wastes (Zhang et al. 2003). It is used to simulate the release of contaminants from stabilized (e.g., grouted) tank wastes. With little or no advection through the waste container, the release can be modeled as a diffusion-limited process given as (Khaleel and Connelly 2003)

$$Q(t) = \frac{I}{d}\sqrt{\frac{D_e}{\pi t}} \tag{3.12}$$

where D_e is the effective diffusion coefficient. I is the total inventory defined as

$$I = C_0 \sum_i V_i = C_0 V_T \tag{3.13}$$

where C_o is the initial contaminant concentration and V_T is the total volume of all cells. Two values, the diffusion coefficient within the waste source (D_e) and the source thickness (d), were required as inputs to the STOMP simulator. The source thickness was assumed to be 0.825 m. Values for the diffusion coefficient are given in Table 2.1.

In the diffusion model, the average release rate for the current time step was determined by integrating the rate equations at the beginning and end of each time step. The release rate was then determined by differencing the integrated rates over the time step. A closed-form integral solution was used to determine the average release rate for the diffusion-dominated model. The total amount of mass released is given as

$$M(t) = \frac{2I}{d}\sqrt{\frac{D_e t}{\pi}} \tag{3.14}$$

where M is the current quantity of the contaminant (in Ci) at time t.

3.3 Source Terms

The source terms in these analyses consisted of four different source types, including 1) leaks during retrieval, 2) past leaks and spills, 3) residual waste leachate from tanks following closure, and 4) residual

waste leachate from tank ancillary equipment following closure. For the cases simulating past leaks, these scenarios represent tank waste that leaked into the vadose zone prior to retrieval and closure activities. For the retrieval leakage scenarios, this source type represents leaks that might occur during waste retrieval operations using water-based sluicing. Releases from the tank residual wastes may occur over an extended period following the closure of the tank farm. Contaminant migration would occur when infiltrating water comes into contact with the tanks or tank ancillary equipment. Dissolved contaminants then have the potential to mobilize in the vadose zone and enter the groundwater table.

For all cases presented in this report, sources are located near or at C-112, the tank farthest from the exit boundary. All sources are simulated as a unit curie so that results can be scaled when actual source inventories are known. Two additional cases were run with a unit source at each of the four tanks in the cross section. These cases are presented to compare the transport behavior of the contaminants in the various tanks.

3.4 Input File Generation

Two types of input files were used to drive the STOMP simulator: 1) a simulation control file and material definition (input) and 2) a soil zonation file (zonation). All input files were written and stored in ASCII text format. The simulation control and material definition input files were assembled using a conventional text editor, whereas the zonation file was generated with a utility program.

3.4.1 Input File

As described in the STOMP User's Guide (White and Oostrom 2000a), the input file is divided into cards that group common data (e.g., solution control, hydraulic properties, output control, boundary conditions). The input files for the simulated cases will be provided in electronic form (see Section 5).

3.4.2 Zonation File

The zonation file is an ordered listing (i.e., I, J, K indexing) of integers that identify the rock/soil type for every grid cell in the computational domain. Inactive nodes are assigned an integer value of zero, and rock/soil types are assigned numbers in accordance with the ordered listing of rock/soil types in the rock/soil zonation card. For example, an integer value of one in the zonation file refers to backfill, and a value of 3 refers to gravelly sand H3. Zonation files for the executed simulations were generated for the C cross section shown in Figure 3.1 (also shown in MDP, Appendix B). Color delineated images of the zonation files for the C Tank Farm cross sections are shown in Figures 3.2 and 3.3. In Figure 3.2, the preconstruction period for the tank farm is shown. Figure 3.3 shows the post-construction tank farm cross section, where the H1 gravelly sand unit has been replaced with backfill material around the tanks. These files were generated from digitized versions of the geologic cross sections for the C Tank Farm (Figure 3.1).

The cross section containing Tanks C-112, -109, -106 and -103 (Figure 3.2b), was modeled using a computation domain with a horizontal extent of 180 m, a vertical extent of 97 m, and unit width. Spacing of 1 m was used for the computational grid in both the horizontal and vertical directions. The geology for both of these cross sections is a primarily layered system created by alluvial deposition, with a more permeable gravely sand stratum that forms the foundation for the tank bottoms.

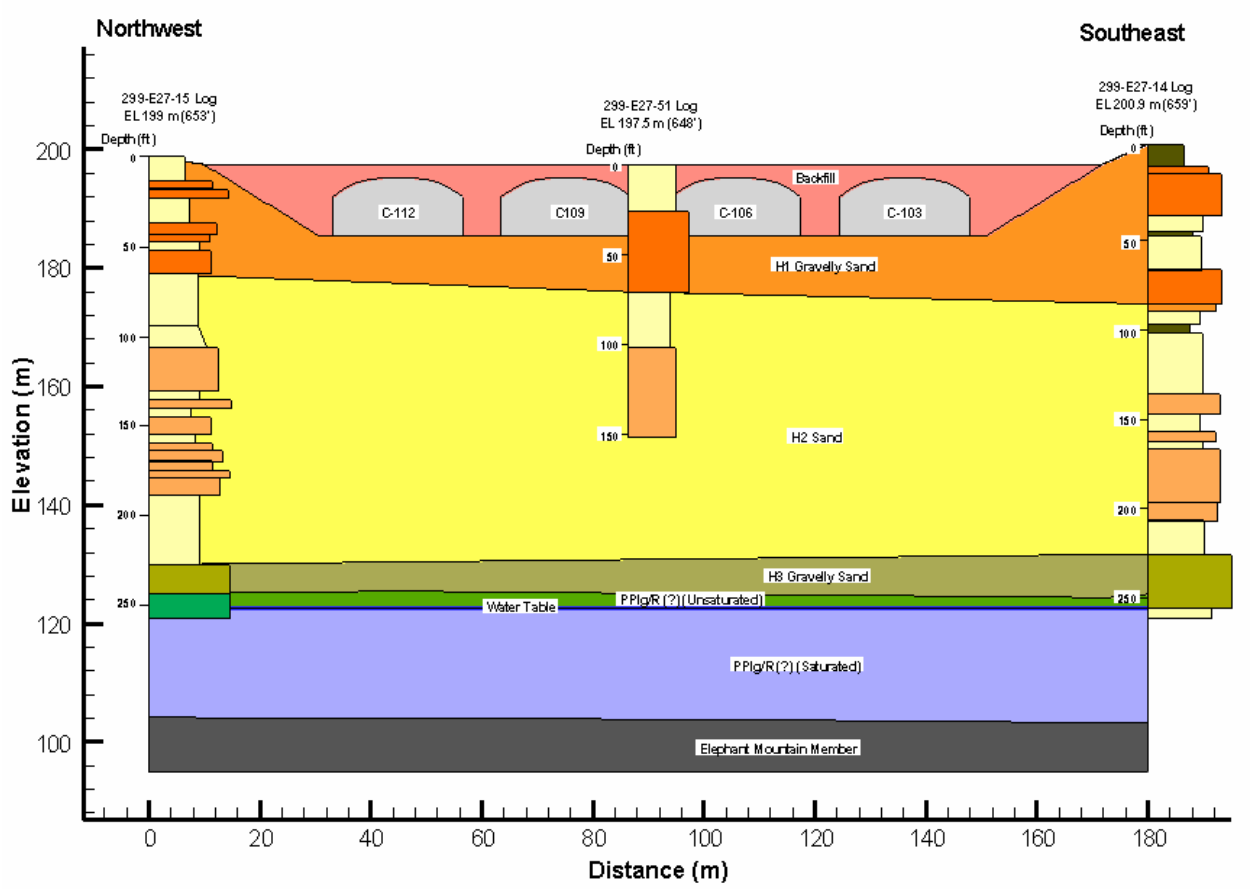

Figure 3.1. Northwest-Southeast Cross Section for the C Tank Farm Through Tanks C-112, C-109, C-106 and C-103 (after Khaleel et al. 2003)

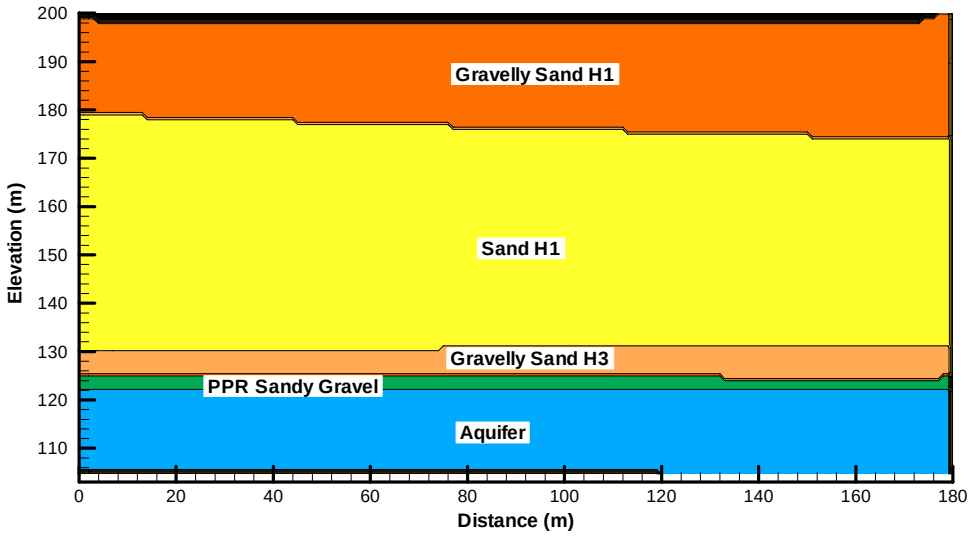

Figure 3.2. Rock/Soil Zonation for the Preconstruction Period of C Tank Farm

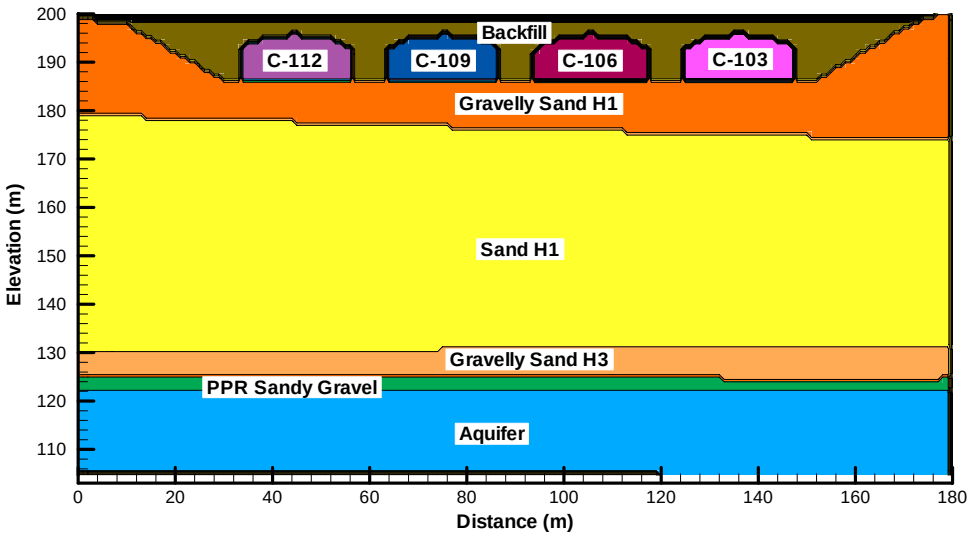

Figure 3.3. Rock/Soil Zonation for the Post-Construction Periods of the C Tank Farm

3.5 STOMP Execution

The reported simulations were executed on Linux workstations. All executables were generated from a single source code that is readable and available in electronic form (Section 6). Executing the simulator required two steps: 1) compiling the source code with a parameters definition file and 2) executing the compiled code on a workstation or personal computer. The executable forms of the STOMP simulator were generated for these investigations using the default level of optimization for each compiler. STOMP was coded following ASCII FORTRAN 77 protocols and yielded no warning or error messages during compilation. The size of the computational domains (~18,000 nodes) necessitates the use of a conjugate gradient linear system solver with a compact storage scheme for the Jacobian matrix. The STOMP simulator uses the SPLIB solver (Bramley and Wang 1995) for sparse linear systems for solutions implementing conjugate gradient solvers. The SPLIB solver is a collection of libraries that must be assembled on the executing computer and linked to the STOMP simulator during compilation. The SPLIB files and instructions necessary to complete the compilation and execution of the STOMP simulator will be available in electronic form (Section 6).

3.6 Result Translation

For these investigations, the STOMP simulator read a series of input files and generated an output file, surface flux files, and a series of plot files. As described previously, the STOMP output file contains reflected data from the input files, simulation progression information, and reference-node output. The output files were used only for verification and simulation tracking. Input, output, plot, and surface-flux files are located in the simulation case directories and will be available in electronic format (Section 5).

Because a two-dimensional cross section through the C Tank Farm was used, reported concentrations are for a unit width inventory. No scaling of concentrations and water sources was performed to convert the reported concentrations to a three-dimensional plume.

Concentration calculations for the breakthrough curves presented in the appendixes were made using STOMP output values for solute mass and water mass fluxes at the fenceline. These data were recorded in STOMP surface files and used to calculate average groundwater concentrations and average fenceline concentrations. Both concentration calculations were scaled using the water flux at the fenceline rather than aquifer thickness. For example, average concentrations at the fenceline (C_{fl}) were computed as

$$C_{fl} = \frac{Solute\ Mass\ Flux\ at\ Fence\ Line\,(Ci/day)}{Water\ Mass\ Flux\ Fenceline\,(L/day)} \tag{3.15}$$

Similarly, average concentrations at the water table (C_{wt}) were calculated as

$$C_{wt} = \frac{Solute\ Mass\ Flux\ at\ Water\ Table\,(Ci/day)}{Water\ Mass\ Flux\ Fenceline\,(L/day)} \tag{3.16}$$

Fenceline concentrations were then used as sources in the analytic aquifer streamtube model described in the next section to predict concentrations at the distal compliance points.

3.7 Analytical Groundwater Transport Modeling

The instantaneous point source model (Baetslé 1969) for a three dimensional space, as reported by Domenico and Schwartz (1990), is shown in Eq. (3.17):

$$C(x,y,z,t) = \left[\frac{C_0 V_0}{\left(8(\pi t)^{3/2}\left(D_x D_y D_z\right)^{1/2}\right)}\right] \exp\left[-\frac{(x-vt)^2}{4D_x t} - \frac{y^2}{4D_y t} - \frac{z^2}{4D_z t} - \lambda_t t\right] \tag{3.17}$$

where C is the solute concentration as a function of position and time (pCi/L or μg/L), C_0V_0 is the instantaneous source of solute mass (pCi or μg), D_x, D_y, D_z are spatial components of the hydrodynamic dispersion coefficient (m^2/yr), x,y,z are spatial distances from the solute source (m), t is the time (yr), λ_t is the solute species radioactive decay half-life (yr), and v is the pore-water velocity (m/yr). The spatial components of hydrodynamic dispersion coefficients include dispersive and diffusive elements, according to Eq. (3.19):

$$D_i = \alpha_i v + D_m \quad for\ i = x,y,z \tag{3.18}$$

where α_i is the dispersivity (m), and D_m is the molecular diffusion coefficient (m^2/yr).

If the soil sorption of solute is assumed to be linear, the transport of a reactive solute can also be described by Eq. (3.16). The dispersivities, D*, and the pore-water velocity, v*, of a reactive solute relate to those, D and v, of a conservative solute as

$$D^* = D/R \text{ and } v^* = v/R \quad (3.19)$$

where R is the retardation factor and is defined as

$$R = 1 + \rho_b K_d/\theta \quad (3.19)$$

and θ is volumetric soil water content.

The streamtube model considered longitudinal and transverse dispersion as well as molecular diffusion. To simulate the transport of solutes from temporally dispersed source, the analytical groundwater model assumed transport from a series of solute slugs. The method of superposition was used to integrate the individual slug sources.

The concentration at compliance points was calculated by a FORTRAN code (point_3d.f) that implemented the instantaneous pulse equation. Contaminants at the WMA C fenceline were then transported using the streamtube model to the downstream compliance points, the 200 Area exclusion boundary and the Columbia River. The distance to each compliance point along the groundwater flow path was based on streamlines derived from the CFEST Site-wide groundwater model described in Section 5. Average groundwater velocities were also based on the CFEST Site-wide groundwater model. The y and z directions were assigned values of zero, signifying that the point of observation was along the longitudinal center line.

Input into the streamtube model included STOMP mass fluxes at the fenceline, as well as velocity, distance and dispersivities from the Site-wide model. These mass fluxes from the fenceline were routed independently to each of the downstream compliance points. For example, the sources at the fenceline, not the exclusion boundary, were used as input for routing contaminants to the Columbia River. The 10,032-year period for the WMA C analysis, between years 2000 and 12032, was modeled using 10,032 uniformly spaced solute release events. Because the half-lives of Tc-99 and U-238 are large relative to the time scale of the simulation (10^7 and 10^9 years, respectively), radiological decay of the species was not considered.

4.0 Simulation Results

This section reports key fluid flow and solute transport behavior, breakthrough curves, and mass balances for the C Tank Farm simulations at the groundwater table, fenceline, and two downgradient compliance points. Two-dimensional simulations in STOMP were used to determine fluid flow and solute transport behavior at the groundwater table and fenceline for the C-112 to C-103 cross section. Resulting concentrations were not scaled to account for spreading and dilution associated with a three-dimensional plume.

As discussed in Section 2, because tank closure occurred in January 2032 and tank degradation was assumed to be negligible, tank structures were assumed to be impermeable even after closure. Once emplaced, the tanks were represented by inactive nodes in the simulation domain. Initial flow conditions were established with a steady-state flow simulation prior to tank emplacement.

Four base cases are presented and are distinguished by source type: past leaks, diffusion releases from residual wastes, leaks during retrieval, and ancillary equipment leaks. Apart from differences in source releases, all four base cases involved a unit contaminant release and used the same median parameter values to describe flow and contaminant transport at the WMA C. Forty-six additional cases were also run that examined individual transport responses to the upper and lower limits of the median parameter values implemented in the base-case systems. These cases are summarized in Tables 2.1 and 2.2. These additional simulations are termed sensitivity cases because they are used to evaluate differences in peak concentrations and arrival times relative to their respective base cases. Although the term is not used in a classical statistical sense, the sensitivity cases in this work document the transport response to changes in individual parameter values.

An analytical, one-dimensional streamtube model that accounts for three-dimensional diffusion and dispersion was used to predict solute transport behavior at the downstream compliance points. The first streamline segment extended from the C-Tank Farm fenceline to the 200 Area exclusion boundary and the second from the C Tank Farm fenceline to the Columbia River. Radioactive decay was not considered because ^{99}Tc and ^{238}U have long half-lives.

4.1 Section Organization

Inventory profiles, mass fluxes, cumulative activities, and breakthrough curves (BTC) are organized by source type. All of the plots associated with the results for past leaks are found in Appendix B. Likewise, plots associated with diffusion release simulations are found in Appendix C, retrieval leak plots are in Appendix D, and ancillary equipment plots are located in Appendix E. Appendix A contains saturation distributions for all of the cases at select output times.

Seven different sorption coefficients (K_d = 0.02, 0.1, 0.2, 0.6, 1.0, 2.0, and 5.0 mL/g) were used to simulate a wide range of retardation for the ^{238}U species. However, for $K_d \geq 0.60$ mL/g, the solute travel times were so long that the amount of mass migrating into the groundwater was insignificant. In the majority of cases, for $K_d \geq 1.0$, the peak concentrations were zero. As a result, these cases are not described in the text, but the results are recorded in Tables F.1–F.64.

Although peak concentrations and arrival times are recorded for all species, only plots for a ^{238}U with a K_d of 0.2 mL/g and 0.6 mL/g are shown in the appendixes. ^{99}Tc plots are also presented so that conservative (^{99}Tc, K_d = 0.0 mL/g), slightly retarded (K_d = 0.2 mL/g) and strongly retarded (K_d = 0.6 mL/g) solute transport are represented graphically in this report. To maintain reasonably sized appendixes, BTCs tracing concentrations at the downstream compliance points are only shown for the easterly flow path. The notation "U_K_d" is used to represent each of the uranium contaminant species from Tank C-112. For example, U_0.01 represents the uranium contaminant with K_d = 0.01 mL/g.

Saturation and concentration distribution profiles show interfaces between the material types. Tank outlines are shown in these figures, even though tank closure occurred in the year 2032. Hence, figures predicting water and solute transport movement after these dates show tanks as permeable structures. However, tanks were assumed to be filled with grout, and tank degradation was assumed to be negligible. Tank outlines exist in these figures only as points of reference but were modeled as impermeable structures.

Because solute concentrations at the groundwater table were scaled by the water flux at the fenceline (see Eq. 3.17, Section 3.7), BTCs at the groundwater and fenceline compliance points demonstrated similar behavior. Though contaminant concentrations are reported in curies for the sake of simplicity, the term "mass" is substituted for "activity."

Concentrations and arrival times relative to the base cases are presented in tables for each uncertainty scenario for the fenceline compliance point. In Appendix F, a complete set of tables is presented for the peak mass fluxes and arrival times at the groundwater table and the fenceline (Tables F.1 through F.32), and the peak concentrations and arrival times at the groundwater table, fenceline, exclusion boundary, and Columbia River (Tables F.33 through F.64). The mass balance for each contaminant in each case is summarized in Tables F.65 through F.96.

Plot-file output for all of the simulations was generated at the beginning (year 2000) and after leak events. This included output for the years 2001, 2005, 2010, 2010+14 days, 2011, 2020, 2032, 2050, 2100, 2200, 2300, 2400, 2500, 3000, 4000, 5000, 6000, 8000, 10000, and 12032.

In the sections that follow, results are reported for each base case, followed by the results of the associated sensitivity cases. Peak concentrations and arrival times for the median parameter value (base case) and the upper and lower parameter bounds (sensitivity cases) are directly compared for simulations with the same source type. A summary description and brief interpretation of results follows the individual case descriptions.

4.2 Initial Conditions and Saturation Distributions

4.2.1 Initial Saturation Distribution (1945)

The initial moisture condition in 1945 for all cases was achieved by running a simulation for the cross section using a recharge rate of 3.5 mm/yr for 1000 years (see Figure A.1a). Because this period represents the preconstruction period of the C Tank Farm, the simulation was run without the four tanks in place. These conditions yielded a mean water content in the vadose zone of 0.147 m^3/m^3 for all cases

except the sensitivity cases investigating the impact of the saturated hydraulic conductivity in the vadose zone (Figure 4.1a–c). When the saturated hydraulic conductivity for each of the material types was scaled by the upper parameter bound (10.0), the average water content in the vadose zone was 0.127 m^3/m^3 (Figures 4.1d and A.1b). When the saturated hydraulic conductivity for each of the material types was scaled by the lower parameter bound (0.10), the average water content in the vadose zone was 0.177 m^3/m^3 (Figures 4.1d and A.1c).

4.2.2 Preclosure Saturation Distribution (1945–2032)

From 1945 to 2032, the recharge was assumed to increase from the preconstruction estimate of 3.5 mm/yr to the current base case (median) value of 100 mm/yr. This change was due to the replacement of the gravel-sand layer at the top of the domain (unit H1, see Figure 3.2) with a porous backfill material, which increased the mean water content by 33% (0.195 m^3/m^3) in the vadose zone by the year 2000 (Figures 4.1 and A.2a). For the sensitivity cases investigating the uncertainty in the preclosure recharge estimate, the mean water contents increased by 38% (0.202 m^3/m^3) for the upper recharge estimate of 140 mm/yr, and only by 16% (0.168 m^3/m^3) for the lower recharge estimate of 40 mm/yr (Figure 4.1a). These saturation distributions are shown in Figures A.2b and A.2c.

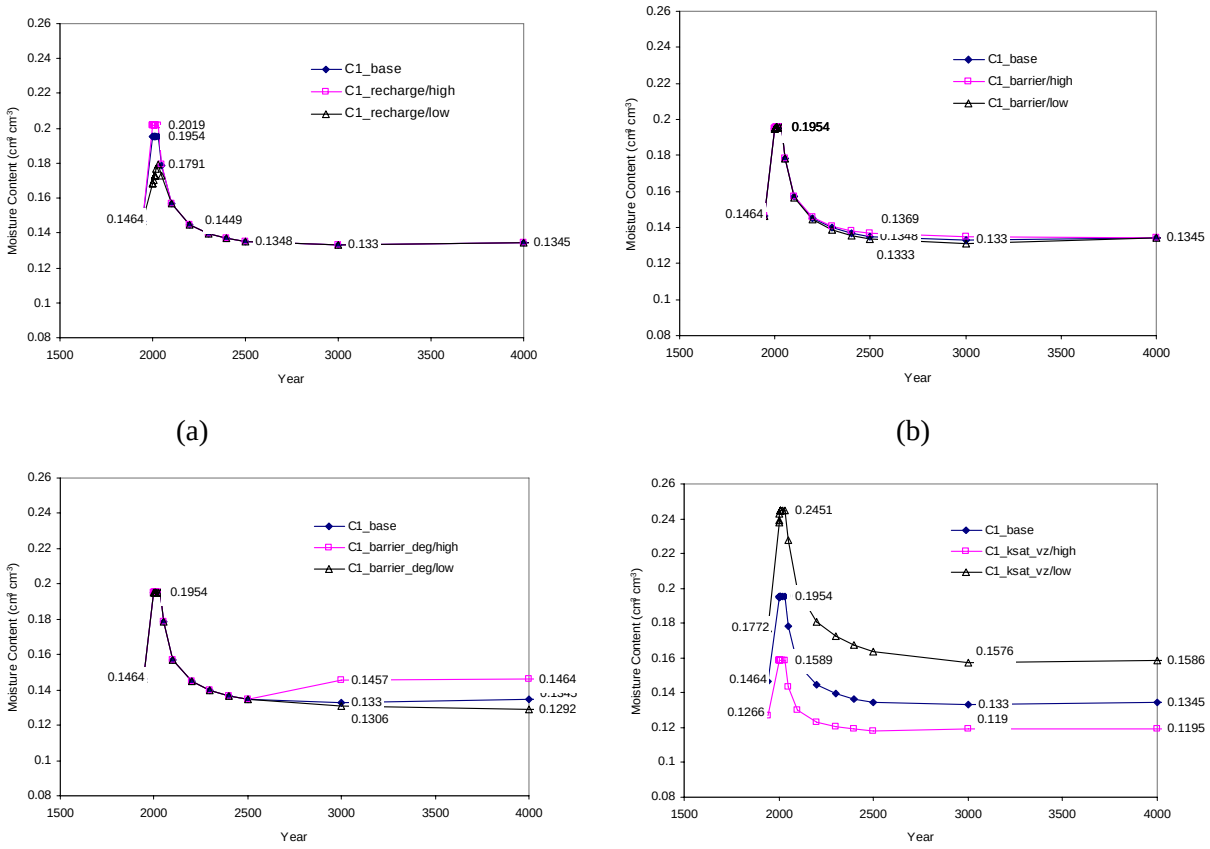

Figure 4.1. Time Course of the Vadose Zone Average Water Contents of Different Cases. The curves for the diffusion and aquifer conductivity variation were identical to that of the base case.

Figures A.3a and A.3b also show saturation distributions for the year 2000 but for the sensitivity cases that account for uncertainty in the saturated hydraulic conductivity of the vadose zone. As shown in Figure 4.1d, for the upper bound scale factor the mean water content increased by 25% (0.159 m^3/m^3). For the lower bound, the mean water content increased by 34% (0.238 m^3/m^3).

4.2.3 Barrier Saturation Distribution (2032–2532)

From 2032 to 2532, the annual recharge rate was decreased to the median barrier design value of 0.5 mm/yr, causing a subsequent decrease in the soil water content. With the exception of sensitivity cases investigating uncertainty in barrier design recharge rate and the saturated hydraulic conductivity for the vadose zone in the year 2500, the mean water content in the vadose zone for all other cases was 0.135 m^3/m^3. This was a decrease of 31% from the year 2050 (see Figures 4.1a and A.3a). For the cases that altered the preclosure recharge rates, this meant a decrease of 33 and 17% for the upper and lower estimates, and the effect of increased recharge on moisture content at early times was insignificant by the year 2500.

Figures A.3b and A.3c show the saturation distributions for the year 2500 for the sensitivity cases investigating uncertainty in the barrier design recharge rate. The upper recharge rate estimate for the barrier was 1 mm/yr, which yielded an average water content of 0.137 m^3/m^3, as shown in Figure 4.1b. The lower recharge rate estimate for the barrier was 0.1 mm/yr, yielding an average water content of 0.133 m^3/m^3, also shown in Figure 4.1b. These values differ by only 1% from the average moisture content for the cases shown in Figure A.3a, suggesting that the uncertainty in the barrier recharge rate may have only a small effect on transport predictions.

Shown in Figures A.3d and A.3e are the saturation distributions in the year 2500 for the upper and lower saturated hydraulic conductivity estimates in the vadose zone. For the upper-bound scale factor, the mean water content decreased by 25% (0.118 m^3/m^3), and for the lower-bound scale factor, the mean decreased by 31% (0.164 m^3/m^3) (see Figure 4.1d).

4.2.4 Degraded Barrier Saturation Distribution (2532–12032)

Beginning in the year 2532 the barrier degraded, increasing the recharge rate to its base case (median) value of 1.0 mm/yr. With the exception of sensitivity cases investigating uncertainty in the degraded barrier recharge rate and the saturated hydraulic conductivity for the vadose zone, by the end of the simulations at year 12032 the mean water content was 0.135 m^3/m^3 (see Figures 4.1a and A.4a). This moisture content represented less than 1% decrease in average moisture content from the previous recharge period.

The upper estimate of the degraded barrier recharge rate was 3.5 mm/yr. This recharge rate yielded an average water content of 0.146 m^3/m^3 (see Figures 4.1c and A.4b), the same average computed for the preconstruction period with the same recharge rate. This moisture content was only 8% higher than the average resulting from the median value. The lower estimate of the degraded barrier recharge rate was 0.5 mm/yr. The average water content was 0.129 m^3/m^3 (see Figures 4.1c and A.4c), only 4% lower than the average resulting from the median value estimate.

Shown in Figures A.4d and A.4e are the saturation distributions in the year 12032 for the upper and lower saturated hydraulic conductivity estimates in the vadose zone. For the upper-bound scale factor, the mean water content was 0.120 m^3/m^3, and for the lower-bound scale factor, the mean decreased to 0.159 m^3/m^3 (Figure 4.1d).

4.3 Past Leaks (Case 1)

Base Case 1 predicted transport behavior for contaminants originating from past leaks. In addition to sensitivity cases that examined uncertainty in recharge rates and saturated hydraulic conductivities, uncertainty in the source depth was also examined in two additional sensitivity cases. For all of these cases, the inventory was located between Tanks C-112 and C-109 with a source width of 22.9 ft (7 m). The base-case depth emplacement was at 150 ft below the ground surface (bgs). A unit release of each of the contaminant species (^{99}Tc and ^{238}U) was simulated.

4.3.1 Base Case (depth = 150 ft)

The saturation distributions for the Past Leak Case 1 scenario are shown for the years 2000, 2500, and 12032 in Figures A.2a, A.3a, and A4a, which represent the three different stages of the protective surface barrier. The concentration distributions of contaminants ^{99}Tc, U_0.20, and U_0.60 in 2048, the year when the peak ^{99}Tc concentration occurs at the fenceline, are shown in Figure B.1. These figures show that the contaminants with higher values of K_d were not as dispersed as the conservative solute, ^{99}Tc. Only contaminants with a $K_d \leq 2.00$ mL/g reached the fenceline by the end of the simulation in 12032 (see Tables F.1–F.64).

The peak concentration of ^{99}Tc at the fenceline was 8.07×10^{-8} Ci/L. The percent of the ^{99}Tc peak for ^{238}U compounds with different K_d values at the fenceline were 56.1% for U_0.02, 4.21% for U_0.10, 0.56% for U_0.20, and 0.02% for U_0.60. The peak concentrations for U_1.00 and U_2.00 were so small that the percent of peak for both solutes was nearly zero. The arrival times for the peak fenceline concentrations were years 2051 for ^{99}Tc, 2057 for U_0.02, 2095 for U_0.10, and 9621 for U_0.20. For U_0.60, the peak occurs at the end of the simulation, indicating that the true peak has not yet occurred. These results are summarized in Tables 4.1 and F.33–F.64 along with peak concentrations and arrival times at the downstream compliance points.

The mass flux, cumulative mass, and BTCs of ^{99}Tc, U_0.20, and U_60 are shown in Figures B.3–B.5. While the curves of mass flux and BTCs for ^{99}Tc had a single distinct peak, the same curves for U_0.20 exhibited double peaks. By the year 12032, the percentage of contaminants that had exited the fenceline was 100% for ^{99}Tc and U_0.02, 93.4% for U_0.10, 56.2% for U_0.20, 5.10×10^{-3}% for U_0.60, and 0% for U_1.00, U_2.00, and U_5.00 (see Tables 4.1 and F.1–F.32).

Table 4.1. Peak Concentrations and Arrival Times at the WMA Fenceline for Case 1

Base Case	
^{99}Tc	
Peak Concentration	8.07E-08 Ci/L
Arrival Time	2051 yr
Cumulative Mass	1.003 Ci
U_0.02	
Peak Concentration	4.53E-08 Ci/L
Arrival Time	2057 yr
Cumulative Mass	1.002 Ci
U_0.10	
Peak Concentration	3.40E-09 Ci/L
Arrival Time	2095 yr
Cumulative Mass	0.934 Ci
U_0.20	
Peak Concentration	4.54E-10 Ci/L
Arrival Time	9621 yr
Cumulative Mass	0.562 Ci
U_0.60	
Peak Concentration	1.57E-11 Ci/L
Arrival Time	12032 yr
Cumulative Mass	0.005 Ci

4.3.2 Preclosure Recharge Sensitivity Cases

The preclosure recharge sensitivity cases investigated the uncertainty in the recharge estimate and its impact on peak concentrations and arrival times at the groundwater table, fenceline and downstream compliance points. To evaluate effects associated with the lower bound of the preclosure recharge rate, the median recharge rate of 100 mm/yr for the period 1945–2032 was changed to 40 mm/yr. Likewise, to examine the impact of the upper bound, preclosure recharge rate, the median recharge was set to 140 mm/yr for the same period.

For the 140-mm/yr preclosure recharge rate, the saturation distributions at years 2000, 2500, and 12032 are shown in Figures A.2b, A.4a, and A.6a. Saturation distributions for 2500 and 12032 are the same as the base case. The concentration distributions of the contaminants in 2042,t the year the ^{99}Tc peak concentration occurs, are shown in Figure B.6 and the final concentration distribution (in 12032) in Figure B.7. The mass flux, cumulative mass, and BTCs of ^{99}Tc, U_0.20, and U_0.60 are shown in Figures B.8 through B.10. Only contaminants with a $K_d \leq 2.00$ mL/g reached the fenceline by the end of the simulation in 12032 (see Tables F.1–F.64).

For the 4- mm/yr preclosure recharge rate, saturation distributions at years 2000, 2500, and 12032 are shown in Figures A.2c, A.4a, and A.6a. Saturation distributions for 2500 and 12032 are the same as the base case. The concentration distributions of the contaminants in 2119, the year the ^{99}Tc peak concentration occurs, are shown in Figure B.11 and the final concentration distribution (in 12032) in Figure B.12.

The mass flux, cumulative mass, and BTCs of ^{99}Tc, U_0.20, and U_0.60 are shown in Figures B.12–B.15. Only contaminants with a $K_d \leq 1.00$ mL/g reached the fenceline by the end of the simulation in 12032 (see Tables F.1–F.64)

The peak concentrations, arrival times and cumulative mass for ^{99}Tc and ^{238}U with $K_d \leq 0.60$ mL/g are shown in Table 4.2, which also reports concentrations, arrival times, and the cumulative mass relative to the base-case predictions. A graphical representation of relative concentrations and arrival times is shown in Figure 4.2, along with the results from the other sensitivity cases.

The results in Table 4.2 demonstrate that the system was sensitive to the magnitude of the preclosure recharge rate. This was evidenced by the differences in peak concentrations, their arrival times and the cumulative mass reaching the fenceline compliance point. Not only were the peak concentrations higher for the high recharge case, but the arrival times were earlier, especially for U_0.20, whose peak arrival time was more than 7,000 years earlier than the base preclosure recharge rate scenario.

Table 4.2. Peak Concentrations and Arrival Times at WMA Fenceline for Case 1 for Different Preclosure Recharge Rates

Parameter	Upper Bound (140 mm/yr)	Lower Bound (40 mm/yr)
^{99}Tc		
Peak Concentration[(a)]	1.39E-07 Ci/L (1.72)	1.19E-08 Ci/L (0.15)
Arrival Time[(b)]	2042 yr (-9)	2119 yr (68)
Cumulative Mass[(c)]	1.004 Ci (1.001)	1.000 Ci (0.997)
U_0.02		
Peak Concentration	9.47E-08 Ci/L (2.09)	4.79E-09 Ci/L (0.11)
Arrival Time	2046 yr (-11)	2156 yr (99)
Cumulative Mass	1.004 Ci (1.002)	0.998 Ci (0.996)
U_0.10		
Peak Concentration	1.20E-08 Ci/L (3.53)	7.24E-10 Ci/L (0.21)
Arrival Time	2064 yr (-31)	7173 yr (5078)
Cumulative Mass	0.961 Ci (1.029)	0.840 Ci (0.900)
U_0.20		
Peak Concentration	7.51E-10 Ci/L (1.65)	4.63E-10 Ci/L (1.02)
Arrival Time	2101 yr (-7520)	>= >= 12032 yr (2411)
Cumulative Mass	0.662 Ci (1.178)	0.353 Ci (0.629)
U_0.60		
Peak Concentration	2.82E-11 Ci/L (1.80)	3.67E-12 Ci/L (0.23)
Arrival Time	>= >= 12032 yr (0)	>= >= 12032 yr (0)
Cumulative Mass	0.011 Ci (2.216)	0.001 Ci (0.157)
(a) Numbers in parentheses indicate concentration ratio relative to base case.		
(b) Numbers in parentheses indicate deviations in arrival time relative to base case.		
(c) Numbers in parentheses indicate cumulative mass ratio relative to base case.		

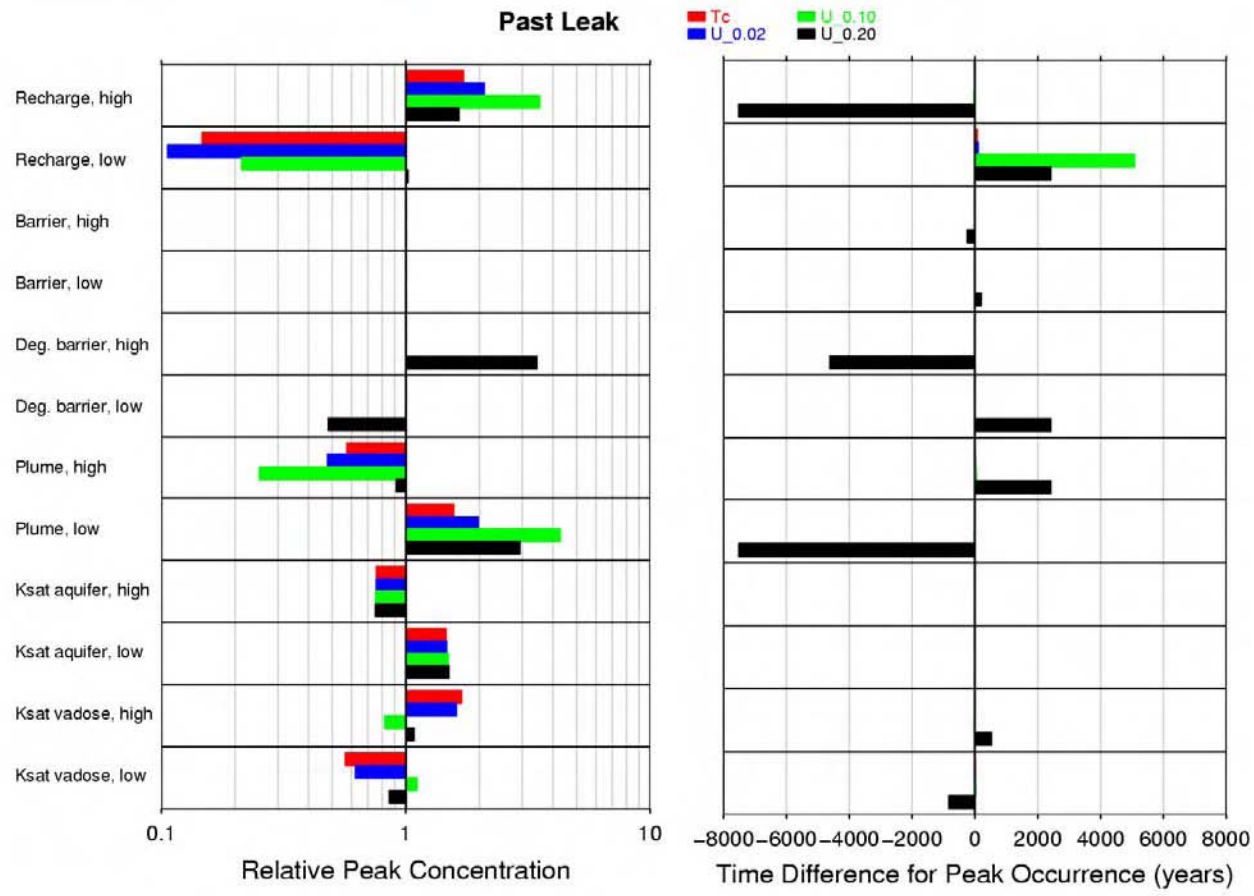

Figure 4.2. Relative Peak Concentrations and Arrival Times for All Past Leak Sensitivity Cases

Consistent with theoretical expectation, the peak concentrations and arrival times for the low recharge case demonstrated opposite trends. With the exception of U_0.20, peak concentrations on average, were 0.16 times lower than the corresponding base case. Breakthroughs for the peak concentrations exhibited a more significant delay for the retarded species than the acceleration exhibited by the high recharge case. For example, for ^{99}Tc, the delay relative to the base case was 68 years, versus nine-year acceleration for the high recharge case. For U_0.02 and U_0.10, the delays were even more significant, at 99 years (versus 11) and 5078 years (versus 31).

The U_0.20 peak concentration for the low recharge case occurred at the end of the simulation, and demonstrated a higher peak relative to the base case. This result was contrary to the trends exhibited by the other ^{238}U species. Although only 63% of the mass transported to the fenceline in the base case migrated to the same location in the low recharge case, the peak concentration was higher because of the longer residence time in the vadose zone due to the lower recharge rate. This phenomenon is noted in the breakthrough curve for U_0.20 (Figure B.14c). In this figure, the first peak is dampened considerably relative to the peak exhibited by the base case for U_0.20 (Figure B.4c).

4.3.3 Barrier Recharge Sensitivity Cases

The barrier recharge sensitivity cases investigated the uncertainty in the estimate of recharge before barrier degradation occurred and its impact on peak concentrations and arrival times at the groundwater table, fenceline, and downstream compliance points. To evaluate effects associated with the lower bound of the barrier recharge rate, the median recharge rate of 0.5 mm/yr for the period 2032–2532 was changed to 0.1 mm/yr. Likewise, to examine the impact of the upper bound, barrier recharge rate, the median recharge was set to 1 mm/yr for the same period.

For the 1-mm/yr post-closure recharge rate, the saturation distributions at years 2000, 2500, and 12032 are shown in Figures A.2a, A.4b, and A.6a. The saturation distributions for the years 2000 and 12032 are the same as the base case. The concentration distributions of the contaminants in 2051, the year the ^{99}Tc peak concentration occurs, are shown in Figure B.16 and the final concentration distributions (in 12032) in Figure B.17. The mass flux, cumulative mass, and BTCs of ^{99}Tc, U_0.20, and U_0.60 are shown in Figures B.18–B.20. Only contaminants with a $K_d \leq 2.00$ mL/g reached the fenceline by the end of the simulation in 12032 (see Tables F.1–F.64).

For the 0.1-mm/yr post-closure recharge rate, the saturation distributions at years 2000, 2500, and 12032 are shown in Figures A.2a, A.4c, and A.6a. The saturation distributions for the years 2000 and 12032 are the same as the base case. The concentration distributions of the contaminants in 2051, the year the ^{99}Tc peak concentration occurs, are shown in Figure B.21 and the final concentration distributions (in 12032) in Figure B.22. The mass flux, cumulative mass, and BTCs of ^{99}Tc, U_0.20, and U_0.60 are shown in Figures B.23–B.25. Only contaminants with a $K_d \leq 2.00$ mL/g reached the fenceline by the end of the simulation in 12032 (see Tables F.1–F.64).

The peak concentrations, arrival times, and cumulative mass for ^{99}Tc and ^{238}U with $K_d \leq 0.60$ mL/g are shown in Table 4.3, which also reports concentrations, arrival times, and the cumulative mass relative to the base-case predictions. A graphical representation of relative concentrations and arrival times is shown in Figure 4.2, along with the results from the other sensitivity cases.

The results in Table 4.3 show that, in general, the uncertainty in the barrier recharge estimate had only a small effect on contaminant transport predictions. Peak concentrations for both the high and low barrier recharge estimates were the same as those predicted for the base case. The total mass of the solutes reaching the fenceline compliance point did not differ by a large measure for either the upper or lower bound estimates. The primary effect of the different barrier recharge estimates lay in the arrival time for U_0.20. Under high barrier recharge conditions, the arrival time was accelerated by more than 200 years due to the larger recharge rate. With a low barrier recharge estimate, the arrival time was delayed by nearly the same period of time due to the reduction in recharge.

Table 4.3. Peak Concentrations and Arrival Times at the WMA Fenceline for Case 1 for Different Barrier Recharge Rates

Parameter	Upper Bound (1.0 mm/yr)	Lower Bound (0.1 mm/yr)
^{99}Tc		
Peak Concentration[(a)]	8.07E-08 Ci/L (1.00)	8.07E-08 Ci/L (1.00)
Arrival Time[(b)]	2051 yr (0)	2051 yr (0)
Cumulative Mass[(c)]	1.003 Ci (1.000)	1.003 Ci (1.000)
U_0.02		
Peak Concentration	4.53E-08 Ci/L (1.00)	4.53E-08 Ci/L (1.00)
Arrival Time	2057 yr (0)	2057 yr (0)
Cumulative Mass	1.002 Ci (1.000)	1.002 Ci (1.000)
U_0.10		
Peak Concentration	3.41E-09 Ci/L (1.00)	3.40E-09 Ci/L (1.00)
Arrival Time	2095 yr (0)	2095 yr (0)
Cumulative Mass	0.940 Ci (1.006)	0.929 Ci (0.995)
U_0.20		
Peak Concentration	4.55E-10 Ci/L (1.00)	4.54E-10 Ci/L (1.00)
Arrival Time	9376 yr (-245)	9819 yr (198)
Cumulative Mass	0.579 Ci (1.031)	0.547 Ci (0.975)
U_0.60		
Peak Concentration	1.72E-11 Ci/L (1.10)	1.44E-11 Ci/L (0.92)
Arrival Time	>= >= 12032 yr (0)	>= >= 12032 yr (0)
Cumulative Mass	0.006 Ci (1.137)	0.005 Ci (0.902)

(a) Numbers in parentheses indicate concentration ratio relative to base case.
(b) Numbers in parentheses indicate deviations in arrival time relative to base case.
(c) Numbers in parentheses indicate cumulative mass ratio relative to base case.

4.3.4 Degraded Barrier Recharge Sensitivity Cases

The degraded barrier recharge sensitivity cases investigated the uncertainty in the degraded barrier recharge estimate and its effect on peak concentrations and arrival times at the groundwater table, fenceline and downstream compliance points. To evaluate effects associated with the lower-bound degraded barrier recharge rate, the median recharge rate of 1 mm/yr for the period 2532–12032 was changed to 0.5 mm/yr, which assumed that no degradation occurred. Likewise, to examine the effect of the upper-bound degraded barrier recharge rate, the median recharge was set to 3.5 mm/yr for the same period, which is the pre-Hanford operations recharge rate.

For the 3.5-mm/yr barrier degradation recharge rate, saturation distributions at years 2000, 2500, and 12032 are shown in Figures A.2a, A.4a, and A.6b. Saturation distributions for 2000 and 2500 are the same as the base case. The concentration distributions of the contaminants in 2051, the year the ^{99}Tc peak concentration occurs, are shown in Figure B.26 and the final concentration distributions (in 12032) in Figure B.27. The mass flux, cumulative mass, and BTCs of ^{99}Tc, U_0.20, and U_0.60 are shown in Figures B.28–B.30. All contaminants reached the fenceline by the end of the simulation, but the more retarded species were at very small concentrations (e.g., 10^{-19} Ci/L for U_5.00) (see Tables F.1–F.64).

For the 0.5-mm/yr barrier degradation recharge rate, the saturation distributions at years 2000, 2500, and 12032 are shown in Figures A.2a, A.4a, and A.6c. The saturation distributions for the years 2000 and 2500 are the same as the base case. The concentration distributions of the contaminants in 2051, the year the ^{99}Tc peak concentration occurs, are shown in Figure B.31 and the final concentration distributions (in 12032) in Figure B.32. The mass flux, cumulative mass, and BTCs of ^{99}Tc, U_0.20, and U_0.60 are shown in Figures B.33–B.35. Only contaminants with a $K_d \leq 1.00$ mL/g reached the fenceline by the end of the simulation in 12032 (see Tables F.1–F.64).

The peak concentrations, arrival times and cumulative mass for ^{99}Tc and ^{238}U with $K_d \leq 0.60$ mL/g are shown in Table 4.4 along with concentrations, arrival times, and the cumulative mass relative to the base-case predictions. A graphical representation of relative concentrations and arrival times is shown in Figure 4.2 along with the results from the other sensitivity cases.

Table 4.4 shows that the uncertainty in the degraded barrier recharge estimate had little effect on peak concentrations but a significant effect on the total mass reaching the fenceline compliance point. Nearly two times more U_0.20 mass and 94 times more U_0.60 mass reached the fenceline in the high degraded

Table 4.4. Peak Concentrations and Arrival Times at the WMA Fenceline for Case 1 for Different Degraded Barrier Recharge Rates

Parameter	Upper Bound (3.5 mm/yr)	Lower Bound (0.5 mm/yr)
^{99}Tc		
Peak Concentration[(a)]	8.07E-08 Ci/L (1.00)	8.07E-08 Ci/L (1.00)
Arrival Time[(b)]	2051 yr (0)	2051 yr (0)
Cumulative Mass[(c)]	1.003 Ci (1.000)	1.003 Ci (0.999)
U_0.02		
Peak Concentration	4.53E-08 Ci/L (1.00)	4.53E-08 Ci/L (1.00)
Arrival Time	2057 yr (0)	2057 yr (0)
Cumulative Mass	1.002 Ci (1.000)	0.994 Ci (0.992)
U_0.10		
Peak Concentration	3.40E-09 Ci/L (1.00)	3.40E-09 Ci/L (1.00)
Arrival Time	2095 yr (0)	2095 yr (0)
Cumulative Mass	1.000 Ci (1.071)	0.740 Ci (0.792)
U_0.20		
Peak Concentration	1.56E-09 Ci/L (3.44)	2.19E-10 Ci/L (0.48)
Arrival Time	5007 yr (-4614)	>= >= 12032 yr (2411)
Cumulative Mass	0.998 Ci (1.776)	0.258 Ci (0.459)
U_0.60		
Peak Concentration	6.52E-10 Ci/L (41.53)	1.14E-12 Ci/L (0.07)
Arrival Time	11126 yr (-906)	>= >= 12032 yr (0)
Cumulative Mass	0.477 Ci (93.431)	0.000 Ci (0.078)
(a) Numbers in parentheses indicate concentration ratio relative to base case.		
(b) Numbers in parentheses indicate deviations in arrival time relative to base case.		
(c) Numbers in parentheses indicate cumulative mass ratio relative to base case.		

barrier recharge scenario. The opposite trend occurred for the low degraded barrier recharge scenario. Less than half of the U_0.20 mass predicted in the base-case scenario reached the fenceline in the low degraded barrier recharge case. Similarly, only 7% of the U_0.60 mass reached the fenceline relative to the base case.

Another major impact in the uncertainty of the degraded barrier recharge rate is in the peak arrival times for the more retarded species, U_0.20 and U_0.60. For the high case, the arrival time for U_0.20 occurred more than four thousand years earlier than in the base case, and in the low case more than 2000 years later. The peak concentration arrival time for U_0.60 for the upper estimate was nearly 1000 years earlier than the base case. Like the base case, the peak arrival time for the lower estimate occurred at the end of the simulation.

4.3.5 Depth of Plume

The depth of plume placement investigated the uncertainty in the estimate of the plume depth in the vadose zone and its impact on peak concentrations and arrival times at the groundwater table, fenceline, and downstream compliance points. To evaluate effects associated with the lower bound of the plume depth, the median value for the plume depth was decreased from 150 ft to 170 ft bgs. Likewise, to examine the impact of the upper bound of the plume depth, the median value was changed to 130 ft bgs.

For the 130-ft depth for plume placement, the saturation distributions at year 2000, 2500, and 12032 are shown in Figures A.2a, A.4a, and A.6a, which were the same as the base case. The concentration distributions of the contaminants in 2058, the year the ^{99}Tc peak concentration occurs, are shown in Figure B.36 and the final concentration distributions (in 12032) in Figure B.37. The mass flux, cumulative mass, and BTCs of ^{99}Tc, U_0.20, and U_0.60 are shown in Figures B.38–B.40. Only contaminants with a $K_d \leq 1.00$ mL/g reached the fenceline by the end of the simulation in 12032 (see Tables F.1–F.64).

For the 170-ft depth for plume placement, the saturation distributions at year 2000, 2500, and 12032 are shown in Figures A.2a, A.4a, and A.6a, which were the same as the base case. The concentration distributions of the contaminants in 2044, the year the ^{99}Tc peak concentration occurs, are shown in Figure B.41 and the final concentration distributions (in 12032) in Figure B.42. The mass flux, cumulative mass, and BTCs of ^{99}Tc, U_0.20, and U_0.60 are shown in Figures B.43–B.45. Only contaminants with $K_d \leq 2.00$ mL/g reached the fenceline by the end of the simulation in 12032 (see Tables F.1–F.64).

The peak concentrations, arrival times, and cumulative mass for ^{99}Tc and ^{238}U with $K_d \leq 0.60$ mL/g are shown in Table 4.5, which also reports concentrations, arrival times, and the cumulative mass relative to the base-case predictions. A graphical representation of relative concentrations and arrival times is shown in Figure 4.2, along with the results from the other sensitivity cases.

Results in Table 4.5 show that the peak concentrations and their corresponding arrival times were sensitive to the depth of the past leak. A ±20-ft placement of the plume led to a 50% change in the ^{99}Tc peak concentrations relative to the base case. Arrival times for the more conservative species, ^{99}Tc, U_0.02, and U_0.10, differed by tens of years relative to the base case for both upper and lower depths.

Table 4.5. Peak Concentrations, Arrival Times at the WMA Fenceline for Case 1 for Different Plume Depths

Parameter	Upper Bound (130 ft bgs)	Lower Bound (170 ft bgs)
^{99}Tc		
Peak Concentration[(a)]	4.63E-08 Ci/L (0.57)	1.27E-07 Ci/L (1.57)
Arrival Time[(b)]	2058 yr (7)	2044 yr (-7)
Cumulative Mass[(c)]	1.002 Ci (0.999)	1.003 Ci (1.000)
U_0.02		
Peak Concentration	2.17E-08 Ci/L (0.48)	8.99E-08 Ci/L (1.98)
Arrival Time	2067 yr (10)	2048 yr (-9)
Cumulative Mass	1.000 Ci (0.998)	1.003 Ci (1.001)
U_0.10		
Peak Concentration	8.57E-10 Ci/L (0.25)	1.46E-08 Ci/L (4.29)
Arrival Time	2136 yr (41)	2069 yr (-26)
Cumulative Mass	0.855 Ci (0.916)	0.980 Ci (1.050)
U_0.20		
Peak Concentration	4.16E-10 Ci/L (0.92)	1.33E-09 Ci/L (2.93)
Arrival Time	>= >= 12032 yr (2411)	2109 yr (-7512)
Cumulative Mass	0.355 Ci (0.633)	0.785 Ci (1.398)
U_0.60		
Peak Concentration	2.07E-12 Ci/L (0.13)	8.97E-11 Ci/L (5.71)
Arrival Time	>= >= 12032 yr (0)	>= >= 12032 yr (0)
Cumulative Mass	0.001 Ci (0.098)	0.045 Ci (8.843)
(a) Numbers in parentheses indicate concentration ratio relative to base case.		
(b) Numbers in parentheses indicate deviations in arrival time relative to base case.		
(c) Numbers in parentheses indicate cumulative mass ratio relative to base case.		

For the more retarded species, U_0.20, differences in arrival times were much larger; ~7500 years earlier for the lower depth and ~2500 years later for the upper depth. When the plume was placed closer to the water table, the peak concentration for U_0.20 was nearly three times higher than the base case. For the upper depth, the same peak was only 10% lower than predicted in the base case. Although plume placement affected peak concentrations and arrival times for all species, the most significant effect resulted with U_0.20 and the placement of the plume closer to the water table.

Differences in cumulative mass reaching the fenceline compliance point demonstrated consistent trends. For both depths, the cumulative mass for the more conservative species (^{99}Tc, U_0.02, and U_0.10) were close to the predictions in the base case. For the more retarded species, however, larger differences in the cumulative mass resulted. At the upper depth, the cumulative mass at the fenceline for U_0.20 was ~60% less than the base case, and for U_0.60 ~10% less. At the lower depth, the cumulative mass was 1.4 and 8.8 times higher than predictions made in the base case.

4.3.6 Aquifer Hydraulic Conductivity

The aquifer hydraulic conductivity sensitivity cases investigated the uncertainty in the estimate of the aquifer hydraulic conductivity and its impact on peak concentrations and arrival times at the groundwater table, fenceline, and downstream compliance points. To evaluate impacts associated with the lower bound of the aquifer hydraulic conductivity, the median value of 3000 m/d was changed to 2000 m/d. Likewise, to examine the effect of the upper bound of the aquifer hydraulic conductivity, the median value was changed to 4000 m/d for both the steady-state and transient simulations.

For the upper bound of the aquifer saturated hydraulic conductivity (4000 m/d), the saturation distributions at years 2000, 2500, and 12032 are shown in Figures A.2a, A.4a, and A.6a, which are the same as the base case. The concentration distributions of the contaminants in 2050, the year the ^{99}Tc peak concentration occurs, are shown in Figure B.46 and the final concentration distributions (in 12032) in Figure B.47. The mass flux, cumulative mass, and BTCs of ^{99}Tc, U_0.20, and U_0.60 are shown in Figures B.48–B.50. Only contaminants with a $K_d \leq 2.00$ mL/g reached the fenceline by the end of the simulation in 12032 (see Tables F.1–F.64).

For the lower bound of the aquifer saturated hydraulic conductivity (2000 m/d), the saturation distributions at years 2000, 2500, and 12032 are shown in Figures A.2a, A.4a, and A.6a, which are the same as the base case. The concentration distributions of the contaminants in 2052, the year the ^{99}Tc peak concentration occurs, are shown in Figure B.51 and the final concentration distributions (in 12032) in Figure B.52. The mass flux, cumulative mass, and BTCs of ^{99}Tc, U_0.20, and U_0.60 are shown in Figures B.53–B.55. Only contaminants with a $K_d \leq 2.00$ mL/g reached the fenceline by the end of the simulation in 12032 (see Tables F.1–F.64).

The peak concentrations, arrival times, and cumulative mass for ^{99}Tc and ^{238}U with $K_d \leq 0.60$ mL/g are shown in Table 4.6, which also reports concentrations, arrival times, and the cumulative mass relative to the base-case predictions. A graphical representation of relative concentrations and arrival times is shown in Figure 4.2, along with the results from the other sensitivity cases.

Results in Table 4.6 show that the uncertainty in the estimate of aquifer hydraulic conductivity has its largest impact on the peak concentrations at the fenceline. For the upper estimate of hydraulic conductivity, peak concentrations for all the solutes were approximately 0.75 times lower than the base case because higher velocities increased dispersion. For the lower estimate, peak concentrations for all solutes were approximately 1.5 times higher due to less dispersion during transport.

Arrival times for both cases were close to the predictions in the base case, differing by only a few years. For the upper estimate travel times were accelerated, and peak arrivals were earlier than in the base case. The opposite trend occurred for the lower estimate of hydraulic conductivity. Given that ^{99}Tc required three years to reach the fenceline once it entered the water table in the base case, only small differences in arrival times were expected for the upper and lower estimates of aquifer hydraulic conductivity.

Consistent with theoretical expectation, the mass reaching the fenceline for both sensitivity cases was nearly the same as in the base case. Given the short residence time in the aquifer, the magnitude of the saturated hydraulic conductivity had little effect on the mass arriving at the fenceline.

Table 4.6. Peak Concentrations and Arrival Times at the WMA Fenceline for Case 1 for Different Aquifer Hydraulic Conductivity Estimates

Parameter	Upper Bound (4000 m/d)	Lower Bound (2000 m/d)
^{99}Tc		
Peak Concentration[(a)]	6.12E-08 Ci/L (0.76)	1.18E-07 Ci/L (1.46)
Arrival Time[(b)]	2050 yr (-1)	2052 yr (1)
Cumulative Mass[(c)]	1.003 Ci (1.000)	1.004 Ci (1.000)
U_0.02		
Peak Concentration	3.43E-08 Ci/L (0.76)	6.66E-08 Ci/L (1.47)
Arrival Time	2056 yr (-1)	2058 yr (1)
Cumulative Mass	1.002 Ci (1.000)	1.002 Ci (1.000)
U_0.10		
Peak Concentration	2.56E-09 Ci/L (0.75)	5.05E-09 Ci/L (1.49)
Arrival Time	2093 yr (-2)	2099 yr (4)
Cumulative Mass	0.934 Ci (1.000)	0.934 Ci (1.000)
U_0.20		
Peak Concentration	3.41E-10 Ci/L (0.75)	6.81E-10 Ci/L (1.50)
Arrival Time	9616 yr (-5)	9624 yr (3)
Cumulative Mass	0.562 Ci (1.000)	0.561 Ci (0.999)
U_0.60		
Peak Concentration	1.18E-11 Ci/L (0.75)	2.34E-11 Ci/L (1.49)
Arrival Time	>= >= 12032 yr (0)	>= >= 12032 yr (0)
Cumulative Mass	0.005 Ci (1.000)	0.005 Ci (1.000)
(a) Numbers in parentheses indicate concentration ratio relative to base case.		
(b) Numbers in parentheses indicate deviations in arrival time relative to base case.		
(c) Numbers in parentheses indicate cumulative mass ratio relative to base case.		

4.3.7 Vadose Zone Saturated Hydraulic Conductivity

The vadose zone saturated hydraulic conductivity sensitivity cases investigated the uncertainty in the estimate of the saturated hydraulic conductivity for each strata in the vadose zone and its effect on peak concentrations and arrival times at the groundwater table, fenceline, and downstream compliance points. To evaluate effects associated with the lower bound of the saturated hydraulic conductivities, the median values for the saturated hydraulic conductivity was decreased by an order of magnitude for each material type. Likewise, to examine the effect of the upper bound of the saturated hydraulic conductivities, the median values were increased by an order of magnitude for each material type.

For the upper bound on the estimated saturated hydraulic conductivity for all materials in the vadose zone (scale factor = 10.0), the saturation distributions at years 2000, 2500, and 12032 are shown in Figures A.3b, A.5a, and A.7a, respectively. The concentration distributions of the contaminants in 2042, the year the ^{99}Tc peak concentration occurs, are shown in Figure B.56 and the final concentration distributions (in 12032) in Figure B.57. The mass flux, cumulative mass, and BTCs of ^{99}Tc, U_0.20, and U_0.60 are shown in Figures B.58–B.60. Only contaminants with a $K_d \leq 1.00$ mL/g reach the fenceline by the end of the simulation in 12032 (see Tables F.1–F.64).

For the lower bound on the estimated saturated hydraulic conductivity for all materials in the vadose zone (scale factor = 0.10), the saturation distributions at years 2000, 2500, and 12032 are shown in Figures A.3c, A.5b, and A.7b, respectively. The concentration distributions of the contaminants in the year the ^{99}Tc peak concentration occurred (2062) are shown in Figure B.61, and the final concentration distributions in the year 12032 are shown in Figure B.62. The mass flux, cumulative mass, and BTCs of ^{99}Tc, U_0.20, and U_0.60 are shown in Figures B.63–B.65. Only contaminants with a $K_d \leq 2.00$ mL/g reach the fenceline by the end of the simulation in 12032 (see Tables F.1–F.64).

The peak concentrations, arrival times and cumulative mass for ^{99}Tc and ^{238}U with $K_d \leq 0.60$ mL/g are shown in Table 4.7, which also reports concentrations, arrival times, and the cumulative mass relative to the base-case predictions. A graphical representation of relative concentrations and arrival times is shown in Figure 4.2, along with the results from the other sensitivity cases.

Table 4.7. Peak Concentrations and Arrival Times at the WMA Fenceline for Case 1 for Different Vadose Zone Saturated Hydraulic Conductivity Estimates

Parameter	Upper Bound (10.0 scale factor)	Lower Bound (0.1 scale factor)
^{99}Tc		
Peak Concentration[(a)]	1.36E-07 Ci/L (1.69)	4.57E-08 Ci/L (0.57)
Arrival Time[(b)]	2042 yr (-9)	2062 yr (11)
Cumulative Mass[(c)]	1.003 Ci (1.000)	1.002 Ci (0.998)
U_0.02		
Peak Concentration	7.29E-08 Ci/L (1.61)	2.82E-08 Ci/L (0.62)
Arrival Time	2046 yr (-11)	2070 yr (13)
Cumulative Mass	1.002 Ci (1.000)	0.998 Ci (0.996)
U_0.10		
Peak Concentration	2.79E-09 Ci/L (0.82)	3.78E-09 Ci/L (1.11)
Arrival Time	2069 yr (-26)	2122 yr (27)
Cumulative Mass	0.944 Ci (1.010)	0.901 Ci (0.965)
U_0.20		
Peak Concentration	4.92E-10 Ci/L (1.08)	3.89E-10 Ci/L (0.86)
Arrival Time	10145 yr (524)	8795 yr (-826)
Cumulative Mass	0.537 Ci (0.957)	0.565 Ci (1.007)
U_0.60		
Peak Concentration	9.57E-12 Ci/L (0.61)	2.87E-11 Ci/L (1.83)
Arrival Time	>= >= 12032 yr (0)	>= >= 12032 yr (0)
Cumulative Mass	0.003 Ci (0.529)	0.012 Ci (2.333)
(a) Numbers in parentheses indicate concentration ratio relative to base case.		
(b) Numbers in parentheses indicate deviations in arrival time relative to base case.		
(c) Numbers in parentheses indicate cumulative mass ratio relative to base case.		

The results in Table 4.7 show that distinct impacts resulted from scaling the saturated hydraulic conductivity in the vadose zone. For the conservative species, ^{99}Tc, U_0.02, and U_0.10, arrival times were tens of years earlier for the upper estimate of saturated hydraulic conductivity and tens of years later for the lower estimate. In the former case, higher conductivities resulted in faster travel times but lower soil

moisture content. For the lower estimate of saturated hydraulic conductivity, the converse was true: slower travel times for the conservative species, but overall, higher soil moisture content.

These trends, however, were reversed for the more retarded species, U_0.20. For the higher saturated hydraulic conductivity case, the peak concentration arrival time was more than 500 years later than the base case, and for the lower estimate more than 800 years earlier. Due to retardation, more U_0.20 mass was left in the domain relative to the conservative species when the high recharge period ended. The low recharge boundary condition due to the protective barrier essentially resulted in a system that was dominated by gravity drainage. For the lower estimate of saturated hydraulic conductivity, the higher soil moisture content accelerated solute transport, whereas for the upper estimate, the lower soil moisture content resulted in a slower travel time.

An additional factor contributing to the different trends amongst the solutes was the dependence of the retardation factor on soil moisture content. Lower soil moisture contents resulted in higher retardation factor, which also contributed to delaying the arrival time of U_0.20 for the higher saturated hydraulic conductivity estimate. The opposite trend occurred for the lower estimate, where the higher soil moisture contents resulted in a lower retardation factor.

Peak concentrations for ^{99}Tc and U_0.02 were more than 1.5 times higher than the base case for the upper estimates of saturated hydraulic conductivity. This is expected, given the lower moisture and faster travel times for this case. However, the peak concentration for U_0.10 was only ~80% of the base-case prediction, whereas the peak for U_0.20 was almost 10% greater than its base-case value. The lower moisture content resulted in a higher solute concentration for U_0.20. For U_0.10, the amount of mass remaining when gravity drainage occurred was less than the mass of U_0.20, resulting in dilution of the U_0.10 peak relative to the base case. This phenomenon was apparent at the fenceline where the cumulative mass was slightly higher (1%) than the base case. For U_0.60, the higher retardation factor from the decreased soil moisture content likely lowered the peak to ~60% of the base-case prediction. This was also noted in the cumulative mass at the fenceline, which was only half the base-case prediction.

The opposite trends in peak concentrations were observed for the lower estimates of saturated hydraulic conductivity. Due to the higher moisture content, the peak concentration for U_0.20 was more dilute (~80%). For U_0.10, the peak concentration was higher (~10%) because more mass remained in the system once gravity drainage occurred. With the lower retardation factor due to the higher moisture, an increase in the peak occurred relative to the base case. For U_0.60, the lower retardation factor likely caused the peak estimate to be ~1.8 times greater than the base-case prediction. This was also noted in the cumulative mass at the fenceline, which was more than double that of the base-case prediction.

4.3.8 Past Leak Summary

The effects of the preclosure recharge rate, barrier recharge rate, degraded barrier recharge rate, plume depth, aquifer hydraulic conductivity, and saturated hydraulic conductivity of the vadose zone are shown in Figure 4.2 and summarized below.

The system was sensitive to the magnitude of the preclosure recharge rate. Not only were the peak concentrations higher for the high recharge (140 mm/yr) case, but the arrival times were earlier. The peak concentrations and arrival times for the low recharge (40 mm/yr) case demonstrated opposite trends.

Breakthroughs for the peak concentrations exhibited a more significant delay for the retarded species than the acceleration exhibited by the high recharge case.

In general, the uncertainty in the barrier recharge estimate had only a small impact on contaminant transport predictions. Peak concentrations for both the high and low barrier recharge estimates were the same as those predicted for the base case. The uncertainty in the degraded barrier recharge estimate had little effect on peak concentrations but a significant effect on the total mass reaching the fenceline compliance point. The uncertainty of the degraded barrier recharge rate had stronger effect on the peak arrival times for the more retarded species.

The peak concentrations and their corresponding arrival times were sensitive to the depth of the past leak. A ±20-ft placement of the plume led to a ~60% change in the ^{99}Tc peak concentrations relative to the base case. For both depths, the cumulative mass for the more conservative species (^{99}Tc, U_0.02, and U_0.10) were close to the predictions in the base case. For the more retarded species, however, larger differences in the cumulative mass resulted.

The uncertainty in the estimate of aquifer hydraulic conductivity had a significant effect on the peak concentrations at the fenceline. For the upper estimate of hydraulic conductivity, peak concentrations for all the solutes were approximately 25% of that in the base case because higher velocities increased dispersion. For the lower estimate, peak concentrations for all solutes were approximately 50% higher than base-case predictions. For the upper estimate, travel times were accelerated and peak arrivals were earlier than those in the base case. The opposite trend occurred for the lower estimate of hydraulic conductivity. The amount of mass reaching the fenceline for both sensitivity cases was nearly the same as the base case.

Distinct effects resulted from scaling the saturated hydraulic conductivity in the vadose zone. For ^{99}Tc and U_0.02, arrival times were earlier for the upper estimate of saturated hydraulic conductivity and later for the lower estimate. Peak concentration for both ^{99}Tc and U_0.02 were higher than the base case for the upper estimates of saturated hydraulic conductivity. The opposite trends in peak concentrations were observed for the lower estimates of saturated hydraulic conductivity; however, the peak concentration for U_0.10 was higher rather than lower than the base-case prediction.

4.4 Diffusion Release (Case 2)

Base Case 2 predicted transport behavior for a diffusion release scenario. This type of release occurs when water infiltrates stabilized residual tank wastes and mobilizes contaminants at a rate determined by the rate of infiltrating water and the amount of dispersion occurring within the source. In addition to sensitivity cases that examined uncertainty in recharge rates and saturated hydraulic conductivities, uncertainty in the rate of diffusion was also examined in two additional sensitivity cases. For all of these cases, the inventory was located beneath Tank C-112 with a source width of 72.2 ft (22.0 m) that spanned the width of the tank. The base-case diffusion coefficient for the source release was 1×10^{-9} cm^2/s. The diffusion release of the contaminants began on the first day of the year 2032. A unit release of each of the contaminant species (^{99}Tc and ^{238}U) was simulated.

4.4.1 Base Case (diffusion coefficient = 1 x 10^{-9} cm^2/s)

The saturation distributions for the diffusion release Case 2 scenario are shown for the years 2000, 2500, and 12032 in Figures A.2a, A.3a, and A4a, which represent the three stages of the protective surface barrier. The concentration distributions of contaminants ^{99}Tc, U_0.20, and U_0.60 are shown in Figure C.1 for 10483, the year when the peak concentration occurred at the fenceline for ^{99}Tc. These figures show that the contaminants with higher values of K_d were not as dispersed as the conservative solute, ^{99}Tc. Only contaminants with a $K_d \leq 0.20$ mL/g reached the fenceline by the end of the simulation in 12032 (see Table 4.8).

The peak concentration of ^{99}Tc at the fenceline was 1.64×10^{-10} Ci/L. The percent of the ^{99}Tc peak for ^{238}U compounds with different K_d values at the fenceline were 79.9% for U_0.02 and 0.67% for U_0.10. The peak concentration of U_0.20 was so small that the percent of peak was zero. The arrival time for the ^{99}Tc peak fenceline concentrations was the year 10483; all other arrival times were at the end of the simulation, indicating that the true peak had not yet occurred. These results are summarized in Tables 4.8 and F.33–F.64 along with peak concentrations and arrival times at the downstream compliance points.

The mass flux, cumulative mass, and BTCs for ^{99}Tc and U_0.20 are shown in Figures C.3–C.4. No plots are shown for U_0.60 because it did not reach the water table by the end of the simulation. The plots for U_0.20 (Figure C.4) show only a small amount of mass (10^{-8} Ci) reaching the water table by 12032. By the year 12032, the percentage of contaminants that had exited the fenceline was 11.2% for ^{99}Tc, 5.02% for U_0.02, and 0.01% for U_0.10 (Tables 4.8 and F.1–F.32).

Table 4.8. Peak Concentrations and Arrival Times at the WMA Fenceline for Case 2

Base Case	
^{99}Tc	
Peak Concentration	1.64E-10 Ci/L
Arrival Time	10483 yr
Cumulative Mass	0.112 Ci
U_0.02	
Peak Concentration	1.31E-10 Ci/L
Arrival Time	12032 yr
Cumulative Mass	0.051 Ci
U_0.10	
Peak Concentration	1.10E-12 Ci/L
Arrival Time	12032 yr
Cumulative Mass	0.000 Ci
U_0.20	
Peak Concentration	2.27E-16 Ci/L
Arrival Time	12032 yr
Cumulative Mass	0.000 Ci
U_0.60	
Peak Concentration	0.00E+00 Ci/L
Arrival Time	12032 yr
Cumulative Mass	0.000 Ci

4.4.2 Preclosure Recharge Sensitivity Cases

The preclosure recharge sensitivity cases investigated the uncertainty in the recharge estimate and its effect on peak concentrations and arrival times at the groundwater table, fenceline, and downstream compliance points. To evaluate impacts associated with the lower bound of the preclosure recharge rate, the median recharge rate of 100 mm/yr for the period 1945–2032 was changed to 40 mm/yr. Likewise, to examine the effects of the upper-bound preclosure recharge rate, the median recharge was set to 140 mm/yr for the same period.

For the 140-mm/yr preclosure recharge rate, the saturation distributions at years 2000, 2500, and 12032 are shown in Figures A.2b, A.4a, and A.6a; those for 2500 and 12032 are the same as the base case. The concentration distributions of the contaminants in 10483, the year ^{99}Tc peak concentration occurs, are shown in Figure C.5 and the final concentration distribution (in 12032) in Figure C.6. The mass flux, cumulative mass, and BTCs for ^{99}Tc and U_0.20 are shown in Figures C.7 and C.8. No plots are shown for U_0.60 because it did not reach the fenceline by the end of the simulation. The plots for U_0.20 (Figure C.8) show only a small mass (10^{-8} Ci) reaching the water table by 12032. Only contaminants with $K_d \leq 0.20$ mL/g reached the fenceline by the end of the simulation in 12032 (Table 4.9).

Table 4.9. Peak Concentrations and Arrival Times at the WMA Fenceline for Case 2 for Different Preclosure Recharge Estimates

Parameter	Upper Bound (140 mm/yr)	Lower Bound (40 mm/yr)
^{99}Tc		
Peak Concentration[(a)]	1.64E-10 Ci/L (1.00)	1.64E-10 Ci/L (1.00)
Arrival Time[(b)]	10483 yr (0)	10484 yr (1)
Cumulative Mass[(c)]	0.113 Ci (1.001)	0.112 Ci (1.000)
U_0.02		
Peak Concentration	1.31E-10 Ci/L (1.00)	1.31E-10 Ci/L (1.00)
Arrival Time	>= 12032 yr (0)	>= 12032 yr (0)
Cumulative Mass	0.051 Ci (1.000)	0.051 Ci (0.998)
U_0.10		
Peak Concentration	1.10E-12 Ci/L (1.00)	1.10E-12 Ci/L (1.00)
Arrival Time	>= 12032 yr (0)	>= 12032 yr (0)
Cumulative Mass	0.000 Ci (1.000)	0.000 Ci (1.000)
U_0.20		
Peak Concentration	2.28E-16 Ci/L (1.00)	2.23E-16 Ci/L (0.98)
Arrival Time	>= 12032 yr (0)	>= 12032 yr (0)
Cumulative Mass	0.000 Ci (-)	0.000 Ci (-)
U_0.60		
Peak Concentration	0.00E+00 Ci/L (0.00)	0.00E+00 Ci/L (0.00)
Arrival Time	>= 12032 yr (0)	>= 12032 yr (0)
Cumulative Mass	0.000 Ci (-)	0.000 Ci (-)

(a) Numbers in parentheses indicate concentration ratio relative to base case.
(b) Numbers in parentheses indicate deviations in arrival time relative to base case.
(c) Numbers in parentheses indicate cumulative mass ratio relative to base case.

For the 40-mm/yr preclosure recharge rate, saturation distributions at years 2000, 2500, and 12032 are shown in Figures A.2c, A.4a, and A.6a. Saturation distributions for 2500 and 12032 are the same as the base case. The concentration distributions of the contaminants in 10484, the year the ^{99}Tc peak concentration occurs, are shown in Figure C.9 and the final concentration distribution (12032) in Figure C.10. The mass flux, cumulative mass, and BTCs for ^{99}Tc and U_0.20 are shown in Figures C.11–C.12. No plots are shown for U_0.60 because it did not reach the fenceline by the end of the simulation. The plots for U_0.20 (Figure C.12) show only a small mass (10^{-8} Ci) reaching the water table by 12032. Only contaminants with $K_d \leq 0.20$ mL/g reached the fenceline by the end of the simulation in 12032 (Table 4.9).

The peak concentrations, arrival times, and cumulative mass for ^{99}Tc and ^{238}U with $K_d \leq 0.60$ mL/g are shown in Table 4.9, which also reports concentrations, arrival times, and the cumulative mass relative to the base-case predictions. A graphical representation of relative concentrations and arrival times is shown in Figure 4.3 along with the results from the other sensitivity cases.

Because the diffusive release of the contaminants began in the year 2032, the year the protective barrier was emplaced, the preclosure recharge rate had no real effect on peak concentrations and arrival times for any of the species (Table 4.9). In 2032, the recharge rate was reduced to its base-case value of 0.5 mm/yr. Hence, variations in the preclosure recharge rate affected the moisture content distribution when the contaminant release began; however, the release rate was slow relative to the drying of the soil profile. Only a minor difference in the U_0.20 peak concentration resulted (0.98 times the base-case prediction) because its slower transport meant it was more affected by the lower moisture in the soil.

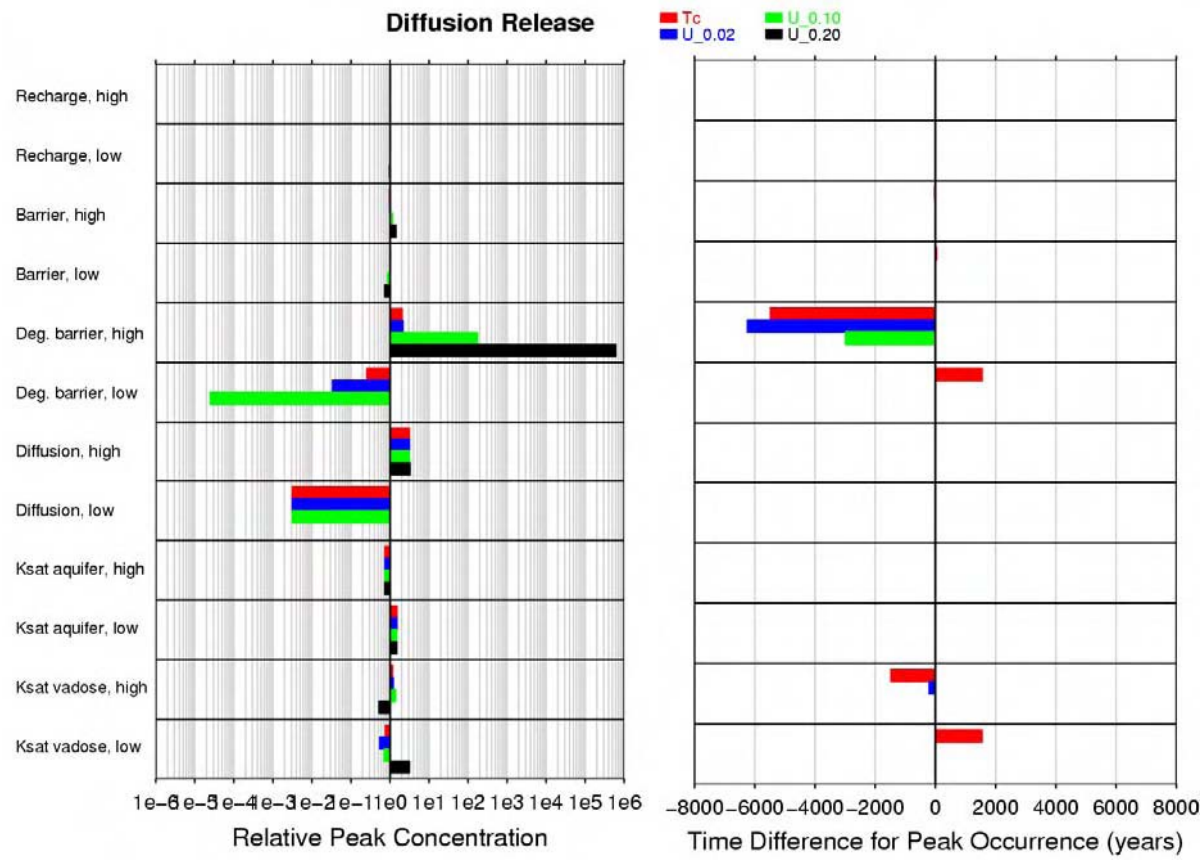

Figure 4.3. Relative Peak Concentrations and Arrival Times for All Diffusion Sensitivity Cases

4.4.3 Barrier Recharge Sensitivity Cases

The barrier recharge sensitivity cases investigated 1) the uncertainty in the estimate of recharge before barrier degradation occurred and 2) its impact on peak concentrations and arrival times at the groundwater table, fenceline and downstream compliance points. To evaluate impacts associated with the lower bound of the barrier recharge rate, the median recharge rate of 0.5 mm/yr for the period 2032–2532 was changed to 0.1 mm/yr. Likewise, to examine the impact of the upper bound, barrier recharge rate, the median recharge was set to 1 mm/yr for the same period.

For the 1-mm/yr post-closure recharge rate, the saturation distributions at years 2000, 2500, and 12032 are shown in Figures A.2a, A.4b, and A.6a. Those for 2000 and 12032 are the same as the base case. The concentration distributions for 10458, the year when the ^{99}Tc peak concentration occurs, are shown in Figure C.13 and the final concentration distributions (in 12032) in Figure C.14. The mass flux, cumulative mass, and BTCs for ^{99}Tc and U_0.20 are shown in Figures C.15 and C.16. There are no plots for U_0.60 because it did not reach the fenceline by the end of the simulation. The plots for U_0.20 (Figure C.16) show only a small mass (10^{-8} Ci) reaching the water table by 12032. Only contaminants with $K_d \leq 0.20$ mL/g reached the fenceline by the end of the simulation in 12032 (Table 4.10).

Table 4.10. Peak Concentrations and Arrival Times at the WMA Fenceline for Case 2 for Different Barrier Recharge Estimates

Parameter	Upper Bound (1.0 mm/yr)	Lower Bound (0.1 mm/yr)
^{99}Tc		
Peak Concentration[(a)]	1.61E-10 Ci/L (0.98)	1.67E-10 Ci/L (1.02)
Arrival Time[(b)]	10458 yr (-25)	10517 yr (34)
Cumulative Mass[(c)]	0.113 Ci (1.007)	0.112 Ci (0.994)
U_0.02		
Peak Concentration	1.30E-10 Ci/L (0.99)	1.31E-10 Ci/L (1.00)
Arrival Time	>= 12032 yr (0)	>= 12032 yr (0)
Cumulative Mass	0.052 Ci (1.030)	0.049 Ci (0.972)
U_0.10		
Peak Concentration	1.28E-12 Ci/L (1.16)	9.73E-13 Ci/L (0.88)
Arrival Time	>= 12032 yr (0)	>= 12032 yr (0)
Cumulative Mass	0.000 Ci (2.000)	0.000 Ci (1.000)
U_0.20		
Peak Concentration	3.22E-16 Ci/L (1.42)	1.66E-16 Ci/L (0.73)
Arrival Time	>= 12032 yr (0)	>= 12032 yr (0)
Cumulative Mass	0.000 Ci (-)	0.000 Ci (-)
U_0.60		
Peak Concentration	0.00E+00 Ci/L (0.00)	0.00E+00 Ci/L (0.00)
Arrival Time	>= 12032 yr (0)	>= 12032 yr (0)
Cumulative Mass	0.000 Ci (-)	0.000 Ci (-)

(a) Numbers in parentheses indicate concentration ratio relative to base case.
(b) Numbers in parentheses indicate deviations in arrival time relative to base case.
(c) Numbers in parentheses indicate cumulative mass ratio relative to base case.

For the 0.1-mm/yr post-closure recharge rate, the saturation distributions at years 2000, 2500, and 12032 are shown in Figures A.2a, A.4c, and A.6a. Saturation distributions for 2000 and 12032 are the same as the base case. The concentration distributions of the contaminants in 10517, the year the ^{99}Tc peak concentration occurs, are shown in Figure C.17 and the final concentration distributions (year 12032) in Figure C.18. The mass flux, cumulative mass, and BTCs for ^{99}Tc and U_0.20 are shown in Figures C.19 and C.20. There are no plots for U_0.60 because it did not reach the fenceline by the end of the simulation. The same plots for U_0.20 (Figure C.20) show only a small amount of mass (10^{-8} Ci) reaching the water table by 12032. Only contaminants with a $K_d \leq 0.20$ mL/g reached the fenceline by the end of the simulation in 12032 (Table 4.10).

The peak concentrations, arrival times, and cumulative mass for ^{99}Tc and ^{238}U with $K_d \leq 0.60$ mL/g are shown in Table 4.10, which also reports concentrations, arrival times, and cumulative mass relative to the base-case predictions. A graphical representation of relative concentrations and arrival times is shown in Figure 4.3 along with the results from the other sensitivity cases.

Table 4.10 shows that the uncertainty in the barrier recharge estimate had only a small effect on peak concentrations and arrival times. The high barrier recharge rate diluted conservative species (e.g., ^{99}Tc and U_0.02) but increased peak concentrations for more retarded species. For the low barrier recharge rate case, the highest peak occurred for ^{99}Tc, and the peak concentration for U_0.10 was lower than predicted in the base case. Differences in the amount of mass transported to the fenceline were ±1 to 3%; the higher estimate resulted in more mass and the lower estimate in less mass relative to the base case.

The 500-year duration of the barrier recharge rate played an important role in reversing trends for both cases. For the high barrier recharge rate, the increased rate accelerated transport to the water table and diluted ^{99}Tc, as noted in the arrival time that was 25 years earlier than the base case. Once the recharge rate was increased to the degraded barrier rate of 1 mm/yr, more U_0.10 was present in the vadose zone than ^{99}Tc. The effect of the subsequent drying of the soil profile caused the concentration of U_0.10 to increase by the end of the simulation. The drying did not affect the ^{99}Tc peak because of its proximity to the water table.

By contrast, the low recharge estimate diluted the peak concentration for U_0.10 and increased the peak for ^{99}Tc. The low recharge rate reduced moisture content and delayed the ^{99}Tc peak arrival time by 34 years. The reduced moisture content also contributed to the slight increase in the ^{99}Tc peak, 1.02 times more than the base-case prediction. For U_0.10, the peak was diluted by ~10%, but this peak occurred at the end of the simulation, indicating that its concentration was still increasing at the end of the simulation. Hence, the apparent dilution may only be an artifact of the length of the simulation.

4.4.4 Degraded Barrier Recharge Sensitivity Cases

The degraded barrier recharge sensitivity cases investigated the uncertainty in the degraded barrier recharge estimate and its effect on peak concentrations and arrival times at the groundwater table, fenceline, and downstream compliance points. To evaluate impacts associated with the lower bound of the degraded barrier recharge rate, the median recharge rate of 1-mm/yr for the period 2532–12032 was changed to 0.5 mm/yr, which assumed that no degradation occurred. Likewise, to examine the effect of the upper-bound degraded barrier recharge rate, the median recharge was set to 3.5 mm/yr for the same period, which is the pre-Hanford operations recharge rate.

For the 3.5-mm/yr barrier degradation recharge rate, the saturation distributions at years 2000, 2500, and 12032 are shown in Figures A.2a, A.4a, and A.6b. Saturation distributions for 2000 and 2500 are the same as the base case. The concentration distributions of the contaminants in 5004, the year the ^{99}Tc peak concentration occurs, are shown in Figure C.21 and the final concentration distributions (in 12032) in Figure C.22. The mass flux, cumulative mass, and BTCs for ^{99}Tc, U_0.20, and U_0.60 are shown in Figures C.23–C.25. Only contaminants with $K_d \leq 0.60$ mL/g reached the fenceline by the end of the simulation in 12032 (see Table 4.11).

For the 0.5 mm/yr barrier degradation recharge rate, the saturation distributions at years 2000, 2500, and 12032 are shown in Figures A.2a, A.4a, and A.6c. Saturation distributions for 2000 and 2500 are the same as the base case. The concentration distributions of the contaminants in 12032, the year the ^{99}Tc peak concentration occurred, are shown in Figure C.26. This indicates that, because this was the final year of simulation, the concentration of ^{99}Tc was still increasing and the true peak never occurred. The mass flux, cumulative mass, and BTCs for ^{99}Tc are shown in Figure C.27. There are no plots for U_0.20 and U_0.60 because they did not reach the fenceline by the end of the simulation end. Only contaminants with $K_d \leq 0.10$ mL/g reached the fenceline by the end of the simulation in 12032 (Table 4.11).

Table 4.11. Peak Concentrations and Arrival Times at the WMA Fenceline for Case 2 for Different Degraded Barrier Recharge Estimates

Parameter	Upper Bound (3.5 mm/yr)	Lower Bound (0.5 mm/yr)
^{99}Tc		
Peak Concentration[(a)]	3.38E-10 Ci/L (2.06)	4.19E-11 Ci/L (0.26)
Arrival Time[(b)]	5004 yr (-5479)	>= 12032 yr (1549)
Cumulative Mass[(c)]	0.210 Ci (1.871)	0.010 Ci (0.088)
U_0.02		
Peak Concentration	2.82E-10 Ci/L (2.15)	4.44E-12 Ci/L (0.03)
Arrival Time	5791 yr (-6241)	>= 12032 yr (0)
Cumulative Mass	0.200 Ci (3.945)	0.001 Ci (0.014)
U_0.10		
Peak Concentration	1.92E-10 Ci/L (174.55)	2.74E-17 Ci/L (0.00)
Arrival Time	9043 yr (-2989)	>= 12032 yr (0)
Cumulative Mass	0.146 Ci (1458.000)	0.000 Ci (0.000)
U_0.20		
Peak Concentration	1.38E-10 Ci/L (607929.52)	0.00E+00 Ci/L (0.00)
Arrival Time	>= 12032 yr (0)	>= 12032 yr (0)
Cumulative Mass	0.050 Ci (-)	0.000 Ci (-)
U_0.60		
Peak Concentration	1.91E-14 Ci/L (0.00)	0.00E+00 Ci/L (0.00)
Arrival Time	>= 12032 yr (0)	>= 12032 yr (0)
Cumulative Mass	0.000 Ci (-)	0.000 Ci (-)

(a) Numbers in parentheses indicate concentration ratio relative to base case.
(b) Numbers in parentheses indicate deviations in arrival time relative to base case.
(c) Numbers in parentheses indicate cumulative mass ratio relative to base case.

The peak concentrations, arrival times, and cumulative mass for ^{99}Tc and ^{238}U with $K_d \leq 0.60$ mL/g are shown in Table 4.11, which also reports concentrations, arrival times, and the cumulative mass relative to the base-case predictions. A graphical representation of relative concentrations and arrival times is shown in Figure 4.3 along with the results from the other sensitivity cases.

The results in Table 4.11 show that the uncertainty in the degraded barrier recharge estimate had a significant effect on peak concentrations and arrival times. For the upper recharge estimate, the peak ^{99}Tc arrival time was accelerated by more than 5,000 years. The arrival time delay due to reduced recharge could not be precisely quantified because all peaks, including ^{99}Tc, occurred at the end of the simulation.

Because of the slow release for the entire duration of the simulation, the extended period (9,500 yr) defining the degraded barrier recharge has a significant effect on the amount of mass transported to the water table. This effect increased with the value of the distribution coefficient. For example, in the high recharge case, the peak concentration for ^{99}Tc and U_0.02 was ~2 times the base-case value. For U_0.10, the peak concentration was ~175 times higher than the base case and more than 60,000 times more for U_0.20. Similar reductions in peak concentrations for the low recharge case were noted (e.g., 0.255 and 0.03 times the base-case value for ^{99}Tc and U_0.02, respectively). These values, however, would likely be much higher if the peak had occurred before then end of the simulation.

A significant impact also occurred on the total mass reaching the fenceline compliance point. Nearly twice the ^{99}Tc and nearly four times the U_0.02 reached the fenceline in the high degraded barrier recharge scenario. The opposite occurred for the low degraded barrier recharge scenario; less than 10% of the ^{99}Tc mass predicted in the base-case scenario reached the fenceline in the low degraded barrier recharge case. Similarly, only 1% of the U_0.02 mass reached the fenceline relative to the base case.

4.4.5 Diffusion Coefficient

The diffusion sensitivity cases investigated the uncertainty in the estimate of the diffusion coefficient and its impact on peak concentrations and arrival times at the groundwater table, fenceline, and down-stream compliance points. To evaluate impacts associated with the lower bound of the diffusion coefficient, the median value was decreased from 1×10^{-9} cm^2/s to 1×10^{-14} cm^2/s. Likewise, to examine the impact of the upper bound of the diffusion coefficient, the median value was changed to 1×10^{-8} cm^2/s.

For the upper estimate of the diffusion coefficient (1×10^{-8} cm^2/s), the saturation distributions at years 2000, 2500, and 12032 are shown in Figures A.2a, A.4a, and A.6a, which are the same as the base case. The concentration distributions of contaminants in 10483, when the ^{99}Tc peak concentration occurs, are shown in Figure C.28 and the final concentration distribution (in 12032) in Figure C.29. The mass flux, cumulative mass, and BTCs for ^{99}Tc and U_0.20 are shown in Figures C.30 and C.31. There are no plots for U_0.60 because it did not reach the fenceline by the end of the simulation. The plots for U_0.20 (Figure C.31) show only a small mass (10^{-8} Ci) reaching the water table by 12032. Only contaminants with $K_d \leq 0.20$ mL/g reached the fenceline by the end of the simulation in 12032 (Table 4.12).

For the low estimate of the diffusion coefficient (1×10^{-14} cm^2/s), the saturation distributions at years 2000, 2500, and 12032 are shown in Figures A.2a, A.4a, and A.6a, which are the same as the base case. The concentration distributions of the contaminants in 10482, the year the ^{99}Tc peak concentration occurred, are shown in Figure C.32 and the final concentration distributions (in 12032) in Figure C.33.

Table 4.12. Peak Concentrations and Arrival Times at the WMA Fenceline for Case 2 for Different Diffusion Estimates

Parameters	Upper Bound (1×10^{-8} cm^2/s)	Lower Bound (1×10^{-14} cm^2/s)
^{99}Tc		
Peak Concentration[(a)]	5.19E-10 Ci/L (3.16)	5.19E-13 Ci/L (0.003)
Arrival Time[(b)]	10483 yr (0)	10482 yr (-1)
Cumulative Mass[(c)]	0.356 Ci (3.164)	0.000 Ci (0.004)
U_0.02		
Peak Concentration	4.13E-10 Ci/L (3.15)	4.13E-13 Ci/L (0.003)
Arrival Time	>= 12032 yr (0)	>= 12032 yr (0)
Cumulative Mass	0.160 Ci (3.160)	0.000 Ci (0.004)
U_0.10		
Peak Concentration	3.48E-12 Ci/L (3.16)	3.47E-15 Ci/L (0.003)
Arrival Time	>= 12032 yr (0)	>= 12032 yr (0)
Cumulative Mass	0.000 Ci (4.000)	0.000 Ci (0.000)
U_0.20		
Peak Concentration	7.38E-16 Ci/L (3.25)	0.00E+00 Ci/L (0.000)
Arrival Time	>= 12032 yr (0)	>= 12032 yr (0)
Cumulative Mass	0.000 Ci (-)	0.000 Ci (-)
U_0.60		
Peak Concentration	0.00E+00 Ci/L (0.00)	0.00E+00 Ci/L (0.000)
Arrival Time	>= 12032 yr (0)	>= 12032 yr (0)
Cumulative Mass	0.000 Ci (-)	0.000 Ci (-)

(a) Numbers in parentheses indicate concentration ratio relative to base case.
(b) Numbers in parentheses indicate deviations in arrival time relative to base case.
(c) Numbers in parentheses indicate cumulative mass ratio relative to base case.

The mass flux, cumulative mass, and BTCs for ^{99}Tc are shown in Figure C.34. Plots are not shown for U_0.20 and U_0.60 because they did not reach the fenceline by simulation end. Only contaminants with a $K_d \leq 0.10$ mL/g reached the fenceline by the end of the simulation in 12032 (see Table 4.12).

The peak concentrations, arrival times, and cumulative mass for ^{99}Tc and ^{238}U with $K_d \leq 0.60$ mL/g are shown in Table 4.12, which also reports concentrations, arrival times, and cumulative mass relative to base-case predictions. A graphical representation of relative concentrations and arrival times is shown in Figure 4.3 along with the results from the other sensitivity cases.

The uncertainty in the estimate of the diffusion rate had a significant effect on the total amount of mass reaching the water table (Table 4.12). There were large differences between the upper and lower diffusion rate bounds—over three times more mass for the higher rate and 300 times less mass for the lower rate. These large differences could be attributed to the absolute difference in the magnitude of the diffusion rate coefficient. Relative to the median value, the upper estimate was only one order of magnitude larger. By contrast, the lower estimate of the diffusion coefficient was six orders of magnitude smaller than the median base-case value. The large difference between upper and lower parameter

bounds also had a significant effect on peak concentrations. Similar to cumulative mass, the high diffusion coefficient resulted in peak concentrations that were three times higher than the base case for all solutes, and the lower estimate predicted peaks that were more than 300 times less. Despite these differences, peak concentration arrival times were unaffected by the magnitude of the diffusion coefficient. Other factors like recharge rates have a more significant effect on contaminant travel times.

4.4.6 Aquifer Hydraulic Conductivity

The aquifer hydraulic conductivity sensitivity cases investigated the uncertainty in the estimate of the aquifer hydraulic conductivity and its impact on peak concentrations and arrival times at the groundwater table, fenceline, and downstream compliance points. To evaluate impacts associated with the lower bound of the aquifer hydraulic conductivity, the median value of 3000 m/d was changed to 2000 m/d. Likewise, to examine the effect of the upper bound of the aquifer hydraulic conductivity, the median values was changed to 4000 m/d for both the steady-state and transient simulations.

For the upper bound of the aquifer saturated hydraulic conductivity (4000 m/d), the saturation distributions at years 2000, 2500, and 12032 are shown in Figures A.2a, A.4a, and A.6a, which are the same as the base case. The concentration distributions of the contaminants in year 10483, when the ^{99}Tc peak concentration occurs, are shown in Figure C.35 and the final concentration distributions (year 12032) in Figure C.36. The mass flux, cumulative mass, and BTCs for ^{99}Tc and U_0.20 are shown in Figures C.37 and C.38. There are no plots for U_0.60 because it did not reach the fenceline by the end of the simulation. The plots for U_0.20 (Figure C.38) show only a small amount of mass (10^{-8} Ci) reaching the water table by 12032. Only contaminants with a $K_d \leq 0.20$ mL/g reached the fenceline by the end of the simulation in 12032 (see Table 4.13).

For the lower bound of the aquifer saturated hydraulic conductivity (2000 m/d), the saturation distributions at years 2000, 2500, and 12032 are shown in Figures A.2a, A.4a, and A.6a, which are the same as the base case. The concentration distributions of the contaminants in year 10485, when the ^{99}Tc peak concentration occurs, are shown in Figure C.39 and final concentration distribution (year 12032) in Figure C.40. The mass flux, cumulative mass, and BTCs for ^{99}Tc and U_0.20 are shown in Figures C.41 and C.42. There are no plots for U_0.60 because it did not reach the fenceline by the end of the simulation. The plots for U_0.20 (Figure C.42) show only a small amount of mass (10^{-8} Ci) reaching the water table by 12032. Only contaminants with a $K_d \leq 0.20$ mL/g reached the fenceline by the end of the simulation in 12032 (see Table 4.13)

The peak concentrations, arrival time, and cumulative mass for ^{99}Tc and ^{238}U with $K_d \leq 0.60$ mL/g are shown in Table 4.13, as are concentrations, arrival times, and cumulative mass relative to the base-case predictions. A graphical representation of relative concentrations and arrival times is shown in Figure 4.3, along with the results from the other sensitivity cases.

Table 4.13 shows that the uncertainty in the estimate of aquifer hydraulic conductivity has its largest impact on peak concentrations at the fenceline. For the upper estimate of hydraulic conductivity, peak concentrations for all solutes were approximately 0.75 times lower than the base case because higher velocities increased dispersion. For the lower estimate, peak concentrations for all solutes were approximately 1.5 times higher due to less dispersion during transport.

Table 4.13. Peak Concentrations and Arrival Times at the WMA Fenceline for Case 2 for Different Aquifer Hydraulic Conductivity Estimates

Parameter	Upper Bound (4000 m/d)	Lower Bound (2000 m/d)
^{99}Tc		
Peak Concentration[(a)]	1.23E-10 Ci/L (0.75)	2.46E-10 Ci/L (1.50)
Arrival Time[(b)]	10483 yr (0)	10485 yr (2)
Cumulative Mass[(c)]	0.113 Ci (1.001)	0.112 Ci (1.000)
U_0.02		
Peak Concentration	9.81E-11 Ci/L (0.75)	1.96E-10 Ci/L (1.50)
Arrival Time	>= 12032 yr (0)	>= 12032 yr (0)
Cumulative Mass	0.051 Ci (1.000)	0.051 Ci (0.998)
U_0.10		
Peak Concentration	8.28E-13 Ci/L (0.75)	1.64E-12 Ci/L (1.49)
Arrival Time	>= 12032 yr (0)	>= 12032 yr (0)
Cumulative Mass	0.000 Ci (1.000)	0.000 Ci (1.000)
U_0.20		
Peak Concentration	1.69E-16 Ci/L (0.74)	3.38E-16 Ci/L (1.49)
Arrival Time	>= 12032 yr (0)	>= 12032 yr (0)
Cumulative Mass	0.000 Ci (-)	0.000 Ci (-)
U_0.60		
Peak Concentration	0.00E+00 Ci/L (0.00)	0.00E+00 Ci/L (0.00)
Arrival Time	>= 12032 yr (0)	>= 12032 yr (0)
Cumulative Mass	0.000 Ci (-)	0.000 Ci (-)

(a) Numbers in parentheses indicate concentration ratio relative to base case.
(b) Numbers in parentheses indicate deviations in arrival time relative to base case.
(c) Numbers in parentheses indicate cumulative mass ratio relative to base case.

The arrival time for ^{99}Tc was the same as the base case for the high estimate and two years later for the low estimate. Given that ^{99}Tc required three years to reach the fenceline once it entered the water table in the base case, only small differences in arrival times were expected for the upper and lower estimates of aquifer hydraulic conductivity.

Consistent with theoretical expectation, the amount of mass reaching the fenceline for both sensitivity cases were nearly the same as in the base case. Given the short residence time in the aquifer, the magnitude of the saturated hydraulic conductivity had little effect on the mass arriving at the fenceline.

4.4.7 Vadose Zone Saturated Hydraulic Conductivity

The vadose zone saturated hydraulic conductivity sensitivity cases investigated the uncertainty in the estimate of the saturated hydraulic conductivity for each strata in the vadose zone and its effect on peak

concentrations and arrival times at the groundwater table, fenceline, and downstream compliance points. To evaluate effects associated with the lower bound of the saturated hydraulic conductivities, the median values for the saturated hydraulic conductivity was decreased by an order of magnitude for each material type. Likewise, to examine the impact of the upper bound of the saturated hydraulic conductivities, the median values were increased by an order of magnitude for each material type.

For the upper bound on the estimated saturated hydraulic conductivity for all materials in the vadose zone (scale factor = 10.0), the saturation distributions at years 2000, 2500, and 12032 are shown in Figures A.3b, A.5a, and A.7a, respectively. The concentration distributions of the contaminants in 9005, the year the ^{99}Tc peak concentration occurs, are shown in Figure C.43 and the final concentration distributions (year 12032) in Figure C.44. The mass flux, cumulative mass, and BTCs for ^{99}Tc and U_0.20 are shown in Figures C.45 and C.46. No plots are shown for U_0.60 because it did not reach the fenceline by the end of the simulation. The plots for U_0.20 (Figure C.46) show only a small amount of mass (10^{-9} Ci) reaching the water table by 12032. Only contaminants with $K_d \leq 0.20$ mL/g reached the fenceline by the end of the simulation in 12032 (Table 4.14).

For the lower bound on the estimated saturated hydraulic conductivity for all materials in the vadose zone (scale factor = 0.10), the saturation distributions at years 2000, 2500, and 12032 are shown in Figures A.3c, A.5b, and A.7b, respectively. The concentration distributions of the contaminants in 12032, the year the peak concentration of ^{99}Tc occurred and the final year in the simulation, are shown in Figure C.47. The mass flux, cumulative mass, and BTCs for ^{99}Tc are shown in Figures C.48 and C.49. There are no plots for U_0.60 because it did not reach the fenceline by the end of the simulation. The plots for U_0.20 (Figure C.49) show only a small amount of mass (10^{-10} Ci) reaching the water table by 12032. Only contaminants with $K_d \leq 0.20$ mL/g reached the fenceline by the end of the simulation in 12032 (see Table 4.14).

The peak concentrations, arrival times, and cumulative mass for ^{99}Tc and ^{238}U with $K_d \leq 0.60$ mL/g are shown in Table 4.14, which also reports concentrations, arrival times, and the cumulative mass relative to the base-case predictions. A graphical representation of relative concentrations and arrival times is shown in Figure 4.3, along with the results from the other sensitivity cases.

Increasing the saturated hydraulic conductivities in the vadose zone allowed the contaminants to spread more laterally (Figures C.43–C.44) relative to the base case (Figures C.1–C.2). As shown in Table 4.14, the conservative species, ^{99}Tc and U_0.02, arrival times were much earlier for the upper estimate of hydraulic conductivity, 1,477 and 212 years, respectively. In both cases, higher conductivities resulted in faster travel times but lower soil moisture content. For the lower estimate of saturated hydraulic conductivity the converse was true. Slower travel times for the conservative species but higher soil moisture content resulted overall.

These trends, however, were reversed for the more retarded species, U_0.20. The relative concentration fractions (0.529 for the high case and 3.15 for the low case) show that U_0.20 has a lower peak concentration with the higher estimate of saturated hydraulic conductivity and a larger peak with the lower estimate. For both cases, two factors affect this result. The first was the amount of mass left in the domain relative to the base case when the high recharge period ended and gravity drainage occurred. The low case had more mass in the domain at the end of this period. The second factor was the dependence of the retardation factor on soil moisture content. Lower soil moisture contents resulted in higher retardation

Table 4.14. Peak Concentrations and Arrival Times at the WMA Fenceline for Case 2 for Different Aquifer Hydraulic Conductivity Estimates

Parameters	Upper Bound (10.0 scale factor)	Lower Bound (0.1 scale factor)
^{99}Tc		
Peak Concentration[(a)]	1.89E-10 Ci/L (1.15)	1.26E-10 Ci/L (0.77)
Arrival Time[(b)]	9005 yr (-1478)	>= 12032 yr (1549)
Cumulative Mass[(c)]	0.146 Ci (1.297)	0.058 Ci (0.514)
U_0.02		
Peak Concentration	1.57E-10 Ci/L (1.20)	7.19E-11 Ci/L (0.55)
Arrival Time	11824 yr (-208)	>= 12032 yr (0)
Cumulative Mass	0.080 Ci (1.577)	0.022 Ci (0.431)
U_0.10		
Peak Concentration	1.51E-12 Ci/L (1.37)	7.79E-13 Ci/L (0.71)
Arrival Time	>= 12032 yr (0)	>= 12032 yr (0)
Cumulative Mass	0.000 Ci (2.000)	0.000 Ci (1.000)
U_0.20		
Peak Concentration	1.20E-16 Ci/L (0.53)	7.14E-16 Ci/L (3.15)
Arrival Time	>= 12032 yr (0)	>= 12032 yr (0)
Cumulative Mass	0.000 Ci (-)	0.000 Ci (-)
U_0.60		
Peak Concentration	0.00E+00 Ci/L (0.00)	0.00E+00 Ci/L (0.00)
Arrival Time	>= 12032 yr (0)	>= 12032 yr (0)
Cumulative Mass	0.000 Ci (-)	0.000 Ci (-)

(a) Numbers in parentheses indicate concentration ratio relative to base case.
(b) Numbers in parentheses indicate deviations in arrival time relative to base case.
(c) Numbers in parentheses indicate cumulative mass ratio relative to base case.

factor, which delayed and therefore diluted the peak concentration arrival time of U_0.20 for the higher saturated hydraulic conductivity estimate. The opposite trend occurred for the lower estimate. Higher soil moisture contents resulted in a lower retardation factor, transporting more mass to the water table and increasing the peak concentration of U_0.20 relative to the base case.

4.4.8 Diffusion Release Summary

The effects of the preclosure recharge rate, barrier recharge rate, degraded barrier recharge rate, diffusion coefficient, aquifer hydraulic conductivity, and saturated hydraulic conductivity of the vadose zone are shown in Figure 4.3 and summarized in this section.

Because the diffusive release of the contaminants began in the year 2032, the year the protective barrier was emplaced, the preclosure recharge rate had no real effect on peak concentrations and arrival times for any of the species. The peak concentrations and arrival times for all the solutes for the two preclosure recharge sensitivity cases were almost identical to the base-case predictions.

The uncertainty in the barrier recharge estimate had a small impact on peak concentrations and arrival times. The increase of barrier recharge from 0.5 to 1.0 mm/yr produced a slightly lower peak concentration and shorter travel time. By contrast, the decrease of barrier recharge from 0.5 to 0.1 mm/yr produced a slightly higher peak concentration and a longer travel time.

The uncertainty in the degraded barrier recharge estimate had a significant impact on peak concentrations and arrival times. For the upper recharge estimate, the peak arrival time for ^{99}Tc was accelerated by more than 5,000 years. For the low barrier recharge (0.5 mm/yr) case, no peak concentrations occurred for any of the solutes at the fenceline by the end of the simulation. More mass reached the fenceline in the high degraded barrier recharge scenario and less mass reached the fenceline in the low degraded barrier recharge scenario.

The uncertainty in the estimate of the diffusion rate had a significant impact on the total amount of mass that migrated outside the fenceline. Large differences resulted between the upper and lower diffusion rate bounds, more than three times more mass for the higher rate and more than 300 times less mass for the lower rate. Similar results were obtained for the peak concentrations. Despite these differences, peak concentration arrival times were unaffected by the magnitude of the diffusion coefficient.

The uncertainty in the estimate of aquifer hydraulic conductivity had its most significant impact on peak concentrations at the fenceline. For the upper estimate of hydraulic conductivity (4000 m/d), peak concentrations for all the solutes were approximately 0.75 times the base-case predictions. For the lower estimate (2000 m/d), peak concentrations for all solutes were approximately 1.5 times those of the base case. Arrival times, when different than the base case, differed only by a couple of years.

In the upper bound case, higher vadose zone conductivities resulted in a faster travel velocity but lower soil moisture content. For the lower estimate of saturated hydraulic conductivity, the converse was true: slower travel velocity but higher soil moisture content. For ^{99}Tc, arrival times were ~1500 years earlier for the upper estimate of saturated hydraulic conductivity, and ~1500 years later for the lower estimate. The impact on peak concentration was relatively small. Increasing the saturated hydraulic conductivities in the vadose zone allowed more lateral spreading of the contaminants relative to the base case because the soil was drier and hence more anisotropic.

4.5 Retrieval Leak (Case 3)

Base case 3 predicted transport behavior for contaminants originating from leaks that might occur during waste retrieval operations using water-based sluicing. In this scenario, a retrieval leak was assumed to have occurred over a two-week period with a unit release of each contaminant in 8,000 gallons of water. For the base and sensitivity cases, the inventory was located at the lower right-hand corner of Tank C-112. The leak occurred on the first day in the year 2000.

4.5.1 Base Case

The saturation distributions for the Retrieval Leak Case 3 scenario are shown for the years 2010+14 days (2010.04), 2500, and 12032 in Figures A.8a, A.4a, and A6a, which represent saturation after the retrieval leak occurs, saturation after barrier emplacement, and saturation distribution after barrier

degradation. The concentration distributions of contaminants ^{99}Tc, U_0.20, and U_0.60 in 2121, when the peak ^{99}Tc concentration occurred at the fenceline, are shown in Figure D.1, which depicts that the contaminants with higher values of K_d were not as dispersed as the conservative solute, ^{99}Tc. Only contaminants with $K_d \leq 0.20$ mL/g reached the fenceline by the end of the simulation in 12032 (see Table 4.15 and Figure D.2).

The peak concentration of ^{99}Tc at the fenceline was 1.34×10^{-9} Ci/L. The percent of the ^{99}Tc peak for ^{238}U compounds with different K_d values at the fenceline were 60.2% for U_0.02, 21.6% for U_0.10, and 0.49% for U_0.20. The peak concentrations for U_0.60, U_1.00, and U_2.00 were zero. The arrival times for the peak fenceline concentrations were year 2121 for ^{99}Tc and 7687 for U_0.02. All other peak arrival times occurred at the end of the simulation in the year 12032, when concentrations were still increasing. These results are summarized in Tables 4.15 and F.33–F.64, along with peak concentrations and arrival times at the downstream compliance points.

The mass flux, cumulative mass, and BTCs of each contaminant are shown in Figures D.3 and D.4. No plots are shown for U_0.60 because it did not reach the water table by the end of the simulation. While the mass flux and BTCs for ^{99}Tc exhibit a double peak, the same curves for U_0.20 increase monotonically. By the year 12032, the percentage of contaminants that have exited the fenceline is 99% of ^{99}Tc, 90.1% of U_0.02, 12% of U_0.10, 0.15% of U_0.20, and 0% of U_1.00, U_2.00, and U_5.00 (Tables 4.15 and F.1–F.32).

Table 4.15. Peak Concentrations and Arrival Times at the WMA Fenceline for Case 3

Base Case	
^{99}Tc	
Peak Concentration	1.34E-09 Ci/L
Arrival Time	2121 yr
Cumulative Mass	0.990 Ci
U_0.02	
Peak Concentration	8.07E-10 Ci/L
Arrival Time	7687 yr
Cumulative Mass	0.901 Ci
U_0.10	
Peak Concentration	2.89E-10 Ci/L
Arrival Time	12032 yr
Cumulative Mass	0.120 Ci
U_0.20	
Peak Concentration	6.50E-12 Ci/L
Arrival Time	12032 yr
Cumulative Mass	0.002 Ci
U_0.60	
Peak Concentration	0.00E+00 Ci/L
Arrival Time	12032 yr
Cumulative Mass	0.000 Ci

4.5.2 Preclosure Recharge Sensitivity Cases

The preclosure recharge sensitivity cases investigated the uncertainty in the recharge estimate and its impact on peak concentrations and arrival times at the groundwater table, fenceline, and downstream compliance points. To evaluate impacts associated with the lower bound of the preclosure recharge rate, the median recharge rate of 100 mm/yr for the period 1945–2032 was changed to 40 mm/yr. Likewise, to examine the effect of the upper-bound preclosure recharge rate, the median recharge was set to 140 mm/yr for the same period.

For the 140-mm/yr preclosure recharge rate, the saturation distributions at years 2010 + 14 days (2010.04), 2500, and 12032 are shown in Figures A.8a, A.4a, and A.6a. Saturation distributions for 2500 and 12032 are the same as the base case. The concentration distributions of the contaminants in 2087, the year the ^{99}Tc peak concentration occurs, are shown in Figure D.5 and the final concentration distribution (in 12032) in Figure D.6. The mass flux, cumulative mass, and BTCs for ^{99}Tc and U_0.20 are shown in Figures D.7 and D.8. No plots are shown for U_0.60 because it did not reach the fenceline by the end of the simulation. Only contaminants with $K_d \leq 0.20$ mL/g reached the fenceline by the end of the simulation in 12032 (see Table 4.16).

For the 40 mm/yr preclosure recharge rate, the saturation distributions at years 2010 + 14 days (2010.04), 2500, and 12032 are shown in Figures A.8a, A.4a, and A.6a. Saturation distributions for 2500 and 12032 are the same as the base case. The concentration distributions of the contaminants in 6964, the year the ^{99}Tc peak concentration occurs, are shown in Figure D.9 and the final concentration distribution (year 12032) in Figure D.10. The mass flux, cumulative mass, and BTCs for ^{99}Tc and U_0.20 are shown in Figures D.11 and D.12. Plots are not shown for U_0.60 because it did not reach the fenceline by the end of the simulation. Only contaminants with $K_d \leq 0.20$ mL/g reached the fenceline by the end of the simulation in 12032 (see Table 4.16).

The peak concentrations, arrival times, and cumulative mass for ^{99}Tc and ^{238}U with $K_d \leq 0.60$ mL/g are shown in Table 4.16, which also reports concentrations, arrival times, and cumulative mass relative to base-case predictions. A graphical representation of relative concentrations and arrival times is shown in Figure 4.4, along with the results from the other sensitivity cases.

The results reported in Table 4.16 show that the estimate of the preclosure recharge rate impacted peak concentrations, arrival times and the cumulative mass reaching the fenceline compliance point. For the high recharge case, more mass reached the fenceline compliance point relative to the base case with larger values of the distribution coefficient (e.g., 1.0004, 1.034, 1.469 and 2.200 times more for ^{99}Tc, U_0.02, U_0.10 and U_0.20, respectively). For the low recharge case, less mass reached the fenceline relative to the base case with smaller values of the distribution coefficient (e.g., 0.986, 0.909, 0.443 and 0.200 times less ^{99}Tc, U_0.02, U_0.10 and U_0.20, respectively). Not only were the peak concentrations higher for the “high” recharge case, but the arrival times were earlier. Although ^{99}Tc was only ~30 years earlier than the base case, the U_0.02 peak concentration arrived more than 5,000 years earlier than the base preclosure recharge rate scenario.

Table 4.16. Peak Concentrations and Arrival Times at the WMA Fenceline for Case 3 for Different Preclosure Recharge Estimates

Parameter	Upper Bound (140 mm/yr)	Lower Bound (40 mm/yr)
^{99}Tc		
Peak Concentration[(a)]	3.68E-09 Ci/L (2.75)	1.10E-09 Ci/L (0.82)
Arrival Time[(b)]	2087 yr (-34)	6964 yr (4843)
Cumulative Mass[(c)]	0.994 Ci (1.004)	0.977 Ci (0.986)
U_0.02		
Peak Concentration	9.13E-10 Ci/L (1.13)	8.74E-10 Ci/L (1.08)
Arrival Time	2105 yr (-5582)	9012 yr (1325)
Cumulative Mass	0.931 Ci (1.034)	0.819 Ci (0.909)
U_0.10		
Peak Concentration	3.50E-10 Ci/L (1.21)	1.75E-10 Ci/L (0.61)
Arrival Time	>= 12032 yr (0)	>= 12032 yr (0)
Cumulative Mass	0.176 Ci (1.469)	0.053 Ci (0.443)
U_0.20		
Peak Concentration	1.29E-11 Ci/L (1.98)	1.69E-12 Ci/L (0.26)
Arrival Time	>= 12032 yr (0)	>= 12032 yr (0)
Cumulative Mass	0.003 Ci (2.200)	0.000 Ci (0.200)
U_0.60		
Peak Concentration	0.00E+00 Ci/L (0.00)	0.00E+00 Ci/L (0.00)
Arrival Time	>= 12032 yr (0)	>= 12032 yr (0)
Cumulative Mass	0.000 Ci (-)	0.000 Ci (-)

(a) Numbers in parentheses indicate concentration ratio relative to base case.
(b) Numbers in parentheses indicate deviations in arrival time relative to base case.
(c) Numbers in parentheses indicate cumulative mass ratio relative to base case.

Consistent with theoretical expectation, the peak concentrations and arrival times for the low recharge case, in general, demonstrated opposite trends. Peak concentrations were 0.821, 0.606, and 0.206 times lower than the corresponding base case for ^{99}Tc, U_0.10, and U_0.20. For U_0.02, however, the relative concentration was 8% higher than the base case. Because the first peak from the high recharge rate was dampened relative to the base case, more mass was available for transport in the vadose zone to the fenceline compliance point. This translated to a higher peak concentration and delay in arrival time relative to the base case. This effect was not observed for U_0.10 because the true peak had not yet occurred. Concentrations for the more retarded species were still increasing by the end of the simulation.

The arrival time for ^{99}Tc exhibited a more significant delay in the low recharge case than the acceleration exhibited by the high recharge case. The arrival time was nearly 5,000 years later than the base case and 40 years earlier than the high recharge case. For U_0.02, this trend was reversed. The arrival time for U_0.02 in the low recharge case was delayed by ~1,300 years, whereas the arrival time in the high recharge case was more than 5,500 years earlier. This earlier breakthrough for U_0.02 accounts for the increase in relative peak concentrations for ^{238}U species with increasing distribution coefficient.

4.5.3 Barrier Recharge Sensitivity Cases

The barrier recharge sensitivity cases investigated the uncertainty in the estimate of recharge before barrier degradation occurred, and its impact on peak concentrations and arrival times at the groundwater table, fenceline and downstream compliance points. To evaluate impacts associated with the lower bound of the barrier recharge rate, the median recharge rate of 0.5 mm/yr for the period 2032–2532 was changed to 0.1 mm/yr. Likewise, to examine the impact of the upper bound, barrier recharge rate, the median recharge was set to 1.0 mm/yr for the same period.

For the 1 mm/yr post-closure recharge rate, the saturation distributions at years 2010 + 14 days (2010.04), 2500, and 12032 are shown in Figures A.8a, A.4b, and A.6a. Saturation distributions for 2010.04 and 12032 are the same as the base case. Concentration distributions of the contaminants in 2122, the year the ^{99}Tc peak concentration occurred, are shown in Figure D.13 and the final concentration distributions (in 12032) in Figure D.14. The mass flux, cumulative mass, and BTCs for ^{99}Tc and U_0.20 are shown in Figures D.15 and D.16. No plots are shown for U_0.60 because it did not reach the fenceline by the end of the simulation. Only contaminants with $K_d \leq 0.20$ mL/g reached the fenceline by the end of the simulation in 12032 (Table 4.17).

For the 0.1-mm/yr post-closure recharge rate, the saturation distributions at years 2010 + 14 days (2010.04), 2500, and 12032 are shown in Figures A.8a, A.4c, and A.6a. Saturation distributions for 2010.04 and 12032 are the same as the base case. The concentration distributions of the contaminants in 2121, the year the ^{99}Tc peak concentration occurred, are shown in Figure D.17 and the final concentration distributions (in 12032) in Figure D.18. The mass flux, cumulative mass, and BTCs for ^{99}Tc and U_0.20 are shown in Figures D.19 and D.20. No plots are shown for U_0.60 because it did not reach the fenceline by the end of the simulation. Only contaminants with a $K_d \leq 0.20$ mL/g reached the fenceline by the end of the simulation in 12032 (Table 4.17).

The peak concentrations, arrival times and cumulative mass for ^{99}Tc and $_{238}$U with $K_d \leq 0.60$ mL/g are shown in Table 4.17, which also reports concentrations, arrival times, and the cumulative mass relative to the base-case predictions. A graphical representation of relative concentrations and arrival times is shown in Figure 4.4, along with the results from the other sensitivity cases.

Table 4.17 shows that in general, the uncertainty in the barrier recharge estimate had only a small impact on contaminant transport predictions for the more retarded species (e.g., $K_d \geq 0.10$). Peak concentrations for both the high and low barrier recharge estimates were the same as those predicted for the base case for ^{99}Tc and U_0.02. For U_0.10 and U_0.20, the concentrations were ~10% higher in high recharge case and ~10% lower for the lower estimate of barrier recharge.

The total mass of the solutes reaching the fenceline compliance point did not differ by a large measure for either the upper- or lower-bound estimates. The primary impact of the different barrier recharge estimates was in the arrival time for U_0.02. Under high barrier recharge conditions, the arrival time was accelerated by more than 200 years due to the larger recharge rate. With a low barrier recharge estimate, the arrival time was delayed by nearly the same period of time, due to the reduction in recharge.

Table 4.17. Peak Concentrations and Arrival Times at the WMA Fenceline for Case 3 for Different Barrier Recharge Estimates

Parameter	Upper Bound (1.0 mm/yr)	Lower Bound (0.1 mm/yr)
^{99}Tc		
Peak Concentration[(a)]	1.34E-09 Ci/L (1.00)	1.34E-09 Ci/L (1.00)
Arrival Time[(b)]	2122 yr (1)	2121 yr (0)
Cumulative Mass[(c)]	0.992 Ci (1.002)	0.989 Ci (0.998)
U_0.02		
Peak Concentration	8.07E-10 Ci/L (1.00)	8.07E-10 Ci/L (1.00)
Arrival Time	7444 yr (-243)	7883 yr (196)
Cumulative Mass	0.913 Ci (1.013)	0.891 Ci (0.988)
U_0.10		
Peak Concentration	3.07E-10 Ci/L (1.06)	2.74E-10 Ci/L (0.95)
Arrival Time	>= 12032 yr (0)	>= 12032 yr (0)
Cumulative Mass	0.132 Ci (1.106)	0.110 Ci (0.919)
U_0.20		
Peak Concentration	7.64E-12 Ci/L (1.18)	5.69E-12 Ci/L (0.88)
Arrival Time	>= 12032 yr (0)	>= 12032 yr (0)
Cumulative Mass	0.002 Ci (1.133)	0.001 Ci (0.800)
U_0.60		
Peak Concentration	0.00E+00 Ci/L (0.00)	0.00E+00 Ci/L (0.00)
Arrival Time	>= 12032 yr (0)	>= 12032 yr (0)
Cumulative Mass	0.000 Ci (-)	0.000 Ci (-)

(a) Numbers in parentheses indicate concentration ratio relative to base case.
(b) Numbers in parentheses indicate deviations in arrival time relative to base case.
(c) Numbers in parentheses indicate cumulative mass ratio relative to base case.

4.5.4 Degraded Barrier Recharge Sensitivity Cases

The degraded barrier recharge sensitivity cases investigated the uncertainty in the degraded barrier recharge estimate and its effect on peak concentrations and arrival times at the groundwater table, fenceline, and downstream compliance points. To evaluate impacts associated with the lower bound of the degraded barrier recharge rate, the median recharge rate of 1 mm/yr for the period 2532–12032 was changed to 0.5 mm/yr, which assumed that no degradation occurred. Likewise, to examine the impact of the upper bound, degraded barrier recharge rate, the median recharge was set to 3.5 mm/yr for the same period, which is the pre-Hanford operations recharge rate.

For the 3.5-mm/yr barrier degradation recharge rate, the saturation distributions at years 2010 + 14 days (2010.04), 2500, and 12032 are shown in Figures A.8a, A.4a, and A.6b. Saturation distributions for 2010.04 and 2500 are the same as the base case. The concentration distributions of contaminants in 3738, the year the ^{99}Tc peak concentration occurs, are shown in Figure D.21 and final concentration distributions (year 12032) in Figure D.22. The mass flux, cumulative mass, and BTCs for ^{99}Tc, U_0.20, and

U_0.60 are shown in Figures D.23–D.25. Only contaminants with $K_d \leq 1.00$ mL/g reached the fenceline by the end of the simulation in 12032 (see Tables F.1–F.64).

For the 0.5 mm/yr barrier degradation recharge rate, the saturation distributions at years 2010 + 14 days (2010.04), 2500, and 12032 are shown in Figures A.8a, A.4a, and A.6c. Saturation distributions for 2010.04 and 2500 are the same as the base case. The concentration distributions of the contaminants in 2121, the year the ^{99}Tc peak concentration occurred, are shown in Figure D.26 and the final concentration distributions (year 12032) in Figure D.27. The mass flux, cumulative mass, and BTCs for ^{99}Tc and U_0.20 are shown in Figures D.28 and D.29. No plots are shown for U_0.60 because it did not reach the fenceline by the end of the simulation. Only contaminants with $K_d \leq 0.20$ mL/g reached the fenceline by the end of the simulation in 12032 (Table 4.18).

The peak concentrations, arrival times, and cumulative mass for ^{99}Tc, and ^{238}U with $K_d \leq 0.60$ mL/g are shown in Table 4.18, which also reports concentrations, arrival times, and the cumulative mass relative to base-case predictions. A graphical representation of relative concentrations and arrival times is shown in Figure 4.4, along with the results from the other sensitivity cases.

Table 4.18. Peak Concentrations and Arrival Times at WMA Fenceline for Case 3 for Different Degraded Barrier Recharge Estimates

Parameters	Upper Bound (3.5 mm/yr)	Lower Bound (0.5 mm/yr)
^{99}Tc		
Peak Concentration[(a)]	3.30E-09 Ci/L (2.46)	1.34E-09 Ci/L (1.00)
Arrival Time[(b)]	3738 yr (1617)	2121 yr (0)
Cumulative Mass[(c)]	1.000 Ci (1.010)	0.805 Ci (0.813)
U_0.02		
Peak Concentration	2.72E-09 Ci/L (3.37)	4.06E-10 Ci/L (0.50)
Arrival Time	4342 yr (-3345)	11623 yr (3936)
Cumulative Mass	1.000 Ci (1.110)	0.482 Ci (0.535)
U_0.10		
Peak Concentration	1.60E-09 Ci/L (5.54)	2.50E-11 Ci/L (0.09)
Arrival Time	6890 yr (-5142)	>= 12032 yr (0)
Cumulative Mass	0.995 Ci (8.324)	0.011 Ci (0.093)
U_0.20		
Peak Concentration	1.04E-09 Ci/L (160.00)	1.16E-13 Ci/L (0.02)
Arrival Time	10157 yr (-1875)	>= 12032 yr (0)
Cumulative Mass	0.721 Ci (480)	0.000 Ci (0.000)
U_0.60		
Peak Concentration	3.95E-12 Ci/L (0.25)	0.00E+00 Ci/L (0.00)
Arrival Time	>= 12032 yr (0)	>= 12032 yr (0)
Cumulative Mass	0.001 Ci (0.098)	0.000 Ci (-)

(a) Numbers in parentheses indicate concentration ratio relative to base case.
(b) Numbers in parentheses indicate deviations in arrival time relative to base case.
(a) Numbers in parentheses indicate cumulative mass ratio relative to base case.

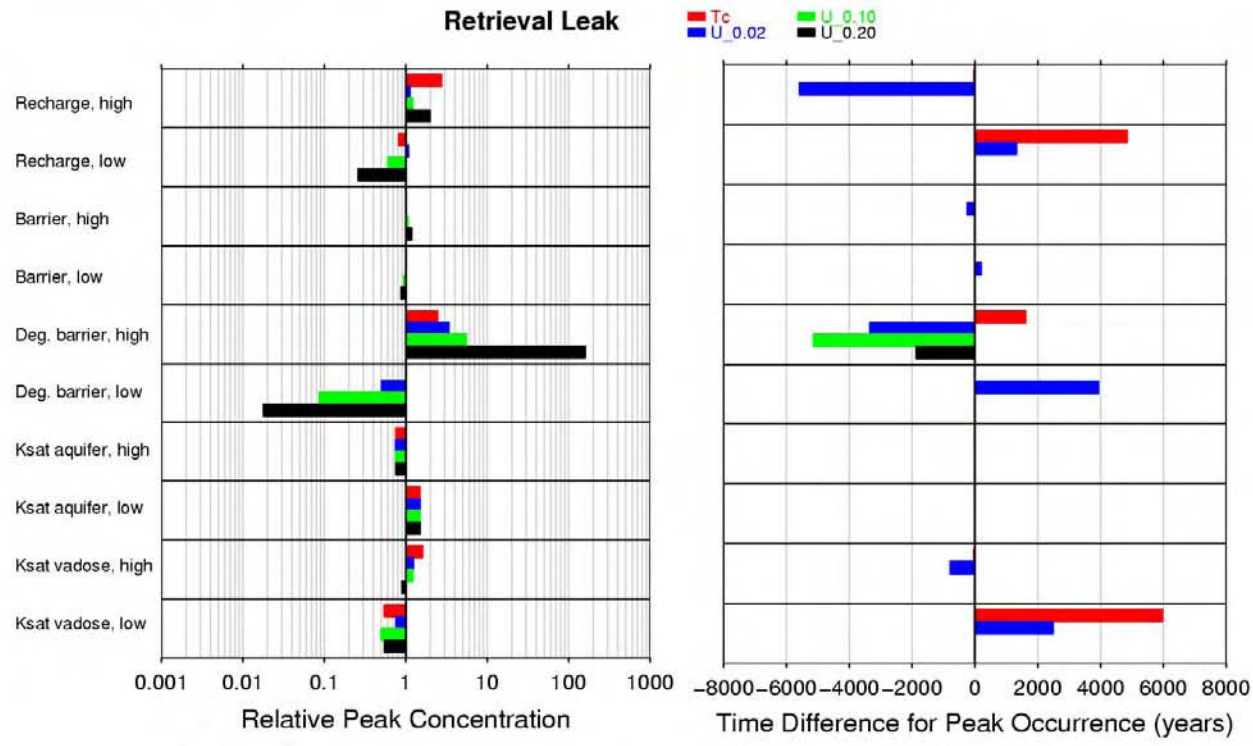

Figure 4.4. Relative Peak Concentrations and Arrival Times for Retrieval Leak Sensitivity Cases

Table 4.18 shows that uncertainty in the degraded barrier recharge estimate had a significant effect on peak concentrations, arrival times, and the total mass reaching the fenceline compliance point. The effect was greatest with the most retarded species. For example, peak concentrations for U_0.20 were 160 times higher in the high degraded barrier recharge estimate and more than 50 times smaller in the low degraded barrier recharge estimate. The U_0.20 mass reaching the fenceline was so small that it is reported as zero in Table 4.18 in the low degraded barrier recharge case. Similarly, the U_0.20 mass reaching the fenceline in the high recharge case was 480 times larger than that transported to the fenceline in the base case.

Arrival times were accelerated for the retarded species in the high recharge case and delayed in the lower estimate of the degraded barrier recharge rate. For ^{99}Tc, the peak concentration occurred more than 1,500 years later than the base case because the higher recharge rate increased ^{99}Tc concentrations at later times. This effect is noted in Figure D.23, which shows that the second peak in the BTC is higher than the first. In the base-case retrieval leak scenario, the first peak is higher than the second (see Figure D.3).

4.5.5 Aquifer Hydraulic Conductivity

The aquifer hydraulic conductivity sensitivity cases investigated the uncertainty in the estimate of the aquifer hydraulic conductivity and its effect on peak concentrations and arrival times at the groundwater table, fenceline, and downstream compliance points. To evaluate impacts associated with the lower bound of the aquifer hydraulic conductivity, the median value of 3000 m/d was changed to 2000 m/d. Likewise, to examine the effect of the upper bound of the aquifer hydraulic conductivity, the median values was changed to 4000 m/d for both the steady-state and transient simulations.

For the upper bound of the aquifer saturated hydraulic conductivity (4000 m/d), the saturation distributions at year 2010 + 14 days (2010.04), 2500, and 12032 are shown in Figures A.8a, A.4a, and A.6a. Saturations are the same as the base case. The concentration distributions of contaminants in 2120, the year the ^{99}Tc peak concentration occurs, are shown in Figure D.30 and final concentration distributions (in 12032) in Figure D.31. The mass flux, cumulative mass, and BTCs for ^{99}Tc and U_0.20 are shown in Figures D.32 and D.33. No plots are shown for U_0.60 because it did not reach the fenceline by the end of the simulation. Only contaminants with $K_d \leq 0.20$ mL/g reached the fenceline by the end of the simulation in 12032 (Table 4.19).

For the lower bound of the aquifer saturated hydraulic conductivity (2000 m/d), saturation distributions at year 2010 + 14 days (2010.04), 2500, and 12032 are shown in Figures A.8a, A.4a, and A.6a. Saturations in 2500 and 12032 are the same as the base case. The concentration distributions of contaminants in 2123, the year the ^{99}Tc peak concentration occurred, are shown in Figure D.34 and final concentration distributions (in 12032) in Figure D.35. The mass flux, cumulative mass, and BTCs for ^{99}Tc and U_0.20 are shown in Figures D.36–D.37. No plots are shown for U_0.60 because it did not reach the fenceline by the end of the simulation. Only contaminants with $K_d \leq 0.20$ mL/g reached the fenceline by the end of the simulation in 12032 (Table 4.19).

Table 4.19. Peak Concentrations, Arrival Times at the WMA Fenceline for Case 3 for Different Aquifer Hydraulic Conductivity Estimates

Parameter	Upper Bound (4000 m/d)	Lower Bound (2000 m/d)
^{99}Tc		
Peak Concentration[(a)]	1.01E-09 Ci/L (0.75)	2.00E-09 Ci/L (1.49)
Arrival Time[(b)]	2120 yr (-1)	2123 yr (2)
Cumulative Mass[(c)]	0.990 Ci (1.000)	0.990 Ci (1.000)
U_0.02		
Peak Concentration	6.06E-10 Ci/L (0.75)	1.21E-09 Ci/L (1.50)
Arrival Time	7686 yr (-1)	7688 yr (1)
Cumulative Mass	0.901 Ci (1.000)	0.901 Ci (1.000)
U_0.10		
Peak Concentration	2.17E-10 Ci/L (0.75)	4.33E-10 Ci/L (1.50)
Arrival Time	>= 12032 yr (0)	>= 12032 yr (0)
Cumulative Mass	0.120 Ci (1.001)	0.119 Ci (0.998)
U_0.20		
Peak Concentration	4.89E-12 Ci/L (0.75)	9.72E-12 Ci/L (1.50)
Arrival Time	>= 12032 yr (0)	>= 12032 yr (0)
Cumulative Mass	0.002 Ci (1.000)	0.001 Ci (0.933)
U_0.60		
Peak Concentration	0.00E+00 Ci/L (0.00)	0.00E+00 Ci/L (0.00)
Arrival Time	>= 12032 yr (0)	>= 12032 yr (0)
Cumulative Mass	0.000 Ci (-)	0.000 Ci (-)

(a) Numbers in parentheses indicate concentration ratio relative to base case.
(b) Numbers in parentheses indicate deviations in arrival time relative to base cases
(c) Numbers in parentheses indicate cumulative mass ratio relative to base case.

The peak concentrations, arrival times, and cumulative mass for ^{99}Tc and ^{238}U with $K_d \leq 0.60$ mL/g are shown in Table 4.19, which also reports concentrations, arrival times, and cumulative mass relative to base-case predictions. A graphical representation of relative concentrations and arrival times is shown in Figure 4.4 along with the results from the other sensitivity cases.

Results in Table 4.19 demonstrate that uncertainty in the estimate of aquifer hydraulic conductivity had its largest impact on the peak concentrations at the fenceline. For the upper estimate of hydraulic conductivity, peak concentrations for all solutes were approximately 0.75 times lower than the base case because higher velocities increased dispersion. For the lower estimate, peak concentrations for all solutes were approximately 1.5 times higher due to less dispersion during transport.

Arrival times for both cases were close to the predictions in the base case and differed by only one or two years. For the upper estimate, travel times were accelerated and peak arrivals earlier than the base case. The opposite trend occurred for the lower estimate of hydraulic conductivity. Given that ^{99}Tc required three years to reach the fenceline once it entered the water table in the base case, only small differences in arrival times were expected for the upper and lower estimates of aquifer hydraulic conductivity. Consistent with theoretical expectation, the amount of mass reaching the fenceline for both sensitivity cases was nearly the same in the base case. Given the short residence time in the aquifer, the magnitude of the saturated hydraulic conductivity had little effect on the mass arriving at the fenceline.

4.5.6 Vadose Zone Saturated Hydraulic Conductivity

The vadose zone saturated hydraulic conductivity sensitivity cases investigated the uncertainty in the estimate of the saturated hydraulic conductivity for each strata in the vadose zone and its impact on peak concentrations and arrival times at the groundwater table, fenceline, and downstream compliance points. To evaluate impacts associated with the lower bound of the saturated hydraulic conductivities, the median values for the saturated hydraulic conductivity was decreased by an order of magnitude for each material type. Likewise, to examine the effect of the upper bound of the saturated hydraulic conductivities, the median values were increased by an order of magnitude for each material type.

For the upper bound on the estimated saturated hydraulic conductivity for all materials in the vadose zone (scale factor = 10.0), saturation distributions at year 2010 + 14 days (2010.04), 2500, and 12032 are shown in Figures A.8b, A.5a, and A.7a, respectively. The concentration distributions of contaminants in 2079, the year the peak ^{99}Tc concentration occurs, are shown in Figure D.38 and final concentration distributions (year 12032) in Figure D.39. The mass flux, cumulative mass, and BTCs for ^{99}Tc and U_0.20 are shown in Figures D.40 and D.41. No plots are shown for U_0.60 because it did not reach the fenceline by the end of the simulation. Only contaminants with $K_d \leq 0.20$ mL/g reached the fenceline by the end of the simulation in 12032 (Table 4.20).

For the lower bound on the estimated saturated hydraulic conductivity for all materials in the vadose zone (scale factor = 0.10), saturation distributions at year 2010 + 14 days (2010.04), 2500, and 12032 are shown in Figures A.8c, A.5c, and A.7c, respectively. The concentration distributions of the contaminants in 8097, the year the ^{99}Tc peak concentration occurs, are shown in Figure D.42 and the final concentration distributions (year 12032) in Figure D.43. The mass flux, cumulative mass, and BTCs for ^{99}Tc and

Table 4.20. Peak Concentrations and Arrival Times at WMA Fenceline for Case 3 for Different Vadose Zone Saturated Hydraulic Conductivity Estimates

Parameters	Upper Bound (10.0 scale factor)	Lower Bound (0.1 scale factor)
^{99}Tc		
Peak Concentration[(a)]	2.16E-09 Ci/L (1.61)	7.27E-10 Ci/L (0.54)
Arrival Time[(b)]	2079 yr (-42)	8097 yr (5976)
Cumulative Mass[(c)]	0.999 Ci (1.009)	0.846 Ci (0.855)
U_0.02		
Peak Concentration	9.99E-10 Ci/L (1.24)	6.12E-10 Ci/L (0.76)
Arrival Time	6900 yr (-787)	10179 yr (2492)
Cumulative Mass	0.968 Ci (1.074)	0.619 Ci (0.687)
U_0.10		
Peak Concentration	3.52E-10 Ci/L (1.22)	1.43E-10 Ci/L (0.49)
Arrival Time	>= 12032 yr (0)	>= 12032 yr (0)
Cumulative Mass	0.137 Ci (1.146)	0.053 Ci (0.439)
U_0.20		
Peak Concentration	5.84E-12 Ci/L (0.90)	3.56E-12 Ci/L (0.55)
Arrival Time	>= 12032 yr (0)	>= 12032 yr (0)
Cumulative Mass	0.001 Ci (0.800)	0.001 Ci (0.533)
U_0.60		
Peak Concentration	0.00E+00 Ci/L (0.00)	0.00E+00 Ci/L (0.00)
Arrival Time	>= 12032 yr (0)	>= 12032 yr (0)
Cumulative Mass	0.000 Ci (-)	0.000 Ci (-)

(a) Numbers in parentheses indicate concentration ratio relative to base case.
(b) Numbers in parentheses indicate deviations in arrival time relative to base case.
(c) Numbers in parentheses indicate cumulative mass ratio relative to base case.

U_0.20 are shown in Figures D.44 and D.45. No plots are shown for U_0.60 because it did not reach the fenceline by the end of the simulation. Only contaminants with $K_d \leq 0.20$ mL/g reached the fenceline by the end of the simulation in 12032 (Table 4.20).

The peak concentrations, arrival times, and cumulative mass for ^{99}Tc and ^{238}U with $K_d \leq 0.60$ mL/g are shown in Table 4.20, which also reports concentrations, arrival times, and cumulative mass relative to base-case predictions. A graphical representation of relative concentrations and arrival times is shown in Figure 4.4, along with the results from the other sensitivity cases.

The results in Table 4.20 show that for the upper estimate of saturated hydraulic conductivity, arrival times were ~ 40 and ~800 years earlier for the conservative species, ^{99}Tc and U_0.02, respectively. For the lower estimate of saturated hydraulic conductivity, arrival times were delayed by thousands of years. The higher conductivities resulted in faster travel times but lower soil moisture content. For the lower estimate of saturated hydraulic conductivity, higher moisture content and significantly delayed travel times resulted for the conservative species. No assessments of arrival times could be made with respect to ^{238}U species with higher distribution coefficients in both sensitivity cases because their peaks occurred in the final year of simulation, when concentrations were still increasing.

Peak concentrations for the more conservative species were, on average, ~ 1.4 times higher than base-case predictions for the upper estimate of saturated hydraulic conductivity. The exception to this trend was the peak concentration estimate for U_0.20, which was only 90% of its base-case prediction. Because the peak concentration was reported in the final year of simulation, the true peak did not occur, but it is likely the true peak for U_0.20 would show a similar trend as a more conservative species.

For the lower bound of saturated hydraulic conductivity, peak concentrations were on average, 0.60 times lower than the base-case predictions. Unlike the upper bound estimate, the percent of peak concentrations were not monotonic. For example, the largest percent of peak concentration, 0.76, was for U_0.02, whereas the other percent of peaks were ~0.5. However, the peaks reported for the more retarded species (U_0.10 and U_0.20) occurred during the final year of simulation, which obfuscates the comparisons to the base-case predictions.

In general, less mass was transported to the fenceline for the lower estimate of saturated hydraulic conductivity and more mass for the upper estimate. This is consistent with theoretical expectation as higher hydraulic conductivities should result in more mass being transported from the vadose zone to the groundwater table.

4.5.7 Retrieval Leak Summary

The effects of the preclosure recharge rate, barrier recharge rate, degraded barrier recharge rate, aquifer hydraulic conductivity, and saturated hydraulic conductivity of the vadose zone are shown in Figure 4.4 and summarized in this section.

For the high recharge case (140 mm/yr), the peak concentrations were higher and arrival times earlier. The peak concentrations and arrival times for the low recharge case (40 mm/yr), in general, demonstrated opposite trends. The arrival time for ^{99}Tc exhibited a more significant delay in the low recharge case than the acceleration exhibited by the high recharge case.

The uncertainty in the barrier recharge estimate had only a small impact on contaminant transport predictions for the more retarded species (e.g., ~5% in peak concentrations for ^{238}U with $K_d \geq 0.10$. The peak concentrations, arrival times, and total mass of ^{99}Tc and U_0.02 reaching the fenceline compliance point were nearly the same as that of the base case for either the upper or lower bound estimates.

The uncertainty in the degraded barrier recharge estimate had a significant effect on peak concentrations, arrival times, and total mass reaching the fenceline compliance point. The effect was greatest with the most retarded species. Peak concentrations were higher in the high degraded barrier recharge estimate and smaller in the low degraded barrier recharge estimate. For the highly retarded species, which still resided in the vadose zone when the barrier degraded, arrival times were accelerated in the high recharge case and delayed in the lower estimate of the degraded barrier recharge rate.

The uncertainty in the estimate of aquifer hydraulic conductivity had an effect on peak concentrations at the fenceline but little effect on arrival time and cumulative mass. For the upper estimate of hydraulic conductivity, peak concentrations for all solutes were ~0.75 times the base-case prediction. For the lower estimate, peak concentrations for all solutes were ~1.5 times the base case.

For the upper estimate of saturated hydraulic conductivity, arrival times earlier than the base-case predictions. The higher conductivities resulted in shorter travel times but lower soil moisture content. For the lower estimate of saturated hydraulic conductivity, the higher moisture content resulted with travel times that were significantly delayed. In general, less mass was transported to the fenceline for the lower estimate of saturated hydraulic conductivity, and more mass for the upper estimate.

4.6 Ancillary Equipment (Case 4)

Base Case 4 investigated contaminant transport behavior from residual ancillary equipment wastes. These releases can occur when ancillary equipment left behind after closure activities comes into contact with water. For the base and sensitivity cases, the inventory was located 30 ft bgs between Tanks C-112 and C-109 and was 20 ft wide. The ancillary equipment leak occurred on the first day in the year 2000.

4.6.1 Base Case

The saturation distributions for the Ancillary Equipment Case 4 scenario are shown for years 2000, 2500, and 12032 in Figures A.2a, A.4a, and A6a, which represent the three stages of the protective surface barrier. The concentration distributions of ^{99}Tc, U_0.20, and U_0.60 in 5717, the year when the peak ^{99}Tc concentration occurred at the fenceline, are shown in Figure E.1. This figure shows that the contaminants with higher values of K_d were not as dispersed as the conservative solute ^{99}Tc. Only contaminants with $K_d \leq 0.20$ mL/g reached the fenceline by the end of the simulation in 12032 (Table 4.21).

Table 4.21. Peak Concentrations and Arrival Times at the WMA Fenceline for Case 4

Base Case	
^{99}Tc	
Peak Concentration	1.03E-09 Ci/L
Arrival Time	5717 yr
Cumulative Mass	0.990 Ci
U_0.02	
Peak Concentration	8.40E-10 Ci/L
Arrival Time	7842 yr
Cumulative Mass	0.892 Ci
U_0.10	
Peak Concentration	2.53E-10 Ci/L
Arrival Time	12032 yr
Cumulative Mass	0.090 Ci
U_0.20	
Peak Concentration	3.11E-12 Ci/L
Arrival Time	12032 yr
Cumulative Mass	0.001 Ci
U_0.60	
Peak Concentration	0.00E+00 Ci/L
Arrival Time	12032 yr
Cumulative Mass	0.000 Ci

The peak concentration of ^{99}Tc at the fenceline was 1.03×10^{-9} Ci/L. The percent of the ^{99}Tc peak for ^{238}U compounds with different K_d values at the fenceline were 81.6% for U_0.02, 24.6% for U_0.10, and 0.30% for U_0.20. The peak concentrations for U_0.60, U_1.00, and U_2.00 were zero. The arrival times for the peak fenceline concentrations were year 5717 for ^{99}Tc and 7842 for U_0.02. All other peak arrival times occurred at the end of the simulation, year 12032, when concentrations were still increasing. These results are summarized in Tables 4.21 and F.33–F.64, along with peak concentrations and arrival times at the downstream compliance points.

The mass flux, cumulative mass, and BTCs of each contaminant are shown in Figures E.3–E.4. No plots are shown for U_0.60 because it did not reach the water table by the end of the simulation. While the curves of mass flux and BTCs for ^{99}Tc exhibit a double peak, the same curves for U_0.20 increase monotonically. By the year 12032, the percentage of contaminants that had exited the fenceline was 99% for ^{99}Tc, 89.2% for U_0.02, 0.09% for U_0.10, and 0% for U_0.20 (see Tables 4.21 and F.1–F.32).

4.6.2 Preclosure Recharge Sensitivity Cases

The preclosure recharge sensitivity cases investigated the uncertainty in the recharge estimate and its impact on peak concentrations and arrival times at the groundwater table, fenceline and downstream compliance points. To evaluate impacts associated with the lower bound of the preclosure recharge rate, the median recharge rate of 100 mm/yr for the period 1945–2032 was changed to 40 mm/yr. Likewise, to examine the impact of the upper bound, preclosure recharge rate, the median recharge was set to 140 mm/yr for the same period.

For the 140 mm/yr preclosure recharge rate, the saturation distributions at years 2000, 2500, and 12032 are shown in Figures A.2a, A.4a, and A.6a, which are the same as the base-case saturations. The concentration distributions of the contaminants at the year the ^{99}Tc peak concentration occurs (2095) are shown in Figure E.5, and the final concentration distribution in the year 12032 is shown in Figure E.6. The mass flux, cumulative mass, and BTCs for ^{99}Tc and U_0.20 are shown in Figures E.7–E.8. No plots are shown for U_0.60 because it did not reach the fenceline by the end of the simulation. Only contaminants with $K_d \leq 0.20$ mL/g reached the fenceline by the end of the simulation in 12032 (Table 4.22).

For the 40-mm/yr preclosure recharge rate, the saturation distributions at years 2000, 2500, and 12032 are shown in Figures A.2a, A.4a, and A.6a, which are the same as base-case saturations. Concentration distributions of the contaminants in 7540, the year the ^{99}Tc peak concentration occurred, are shown in Figure E.9 and the final concentration distribution (in 12032) in Figure E.10. The mass flux, cumulative mass, and BTCs for ^{99}Tc and U_0.20 are shown in Figures E.11 and E.12. No plots are shown for U_0.60 because it did not reach the fenceline by the end of the simulation. Only the contaminants with a $K_d \leq 0.20$ mL/g reached the fenceline by the end of the simulation in 12032 (Table 4.22).

The peak concentrations, arrival times, and cumulative mass for ^{99}Tc and ^{238}U with $K_d \leq 0.60$ mL/g are shown in Table 4.22, which also reports concentrations, arrival times, and cumulative mass relative to base-case predictions. A graphical representation of relative concentrations and arrival times is shown in Figure 4.5, along with the results from the other sensitivity cases.

Table 4.22. Peak Concentrations and Arrival Times at the WMA Fenceline for Case 4 for Different Preclosure Recharge Estimates

Parameters	Upper Bound (140 mm/yr)	Lower Bound (40 mm/yr)
^{99}Tc		
Peak Concentration[(a)]	3.83E-09 Ci/L (3.72)	1.22E-09 Ci/L (1.18)
Arrival Time[(b)]	2095 yr (-3622)	7540 yr (1823)
Cumulative Mass[(c)]	0.995 Ci (1.006)	0.964 Ci (0.974)
U_0.02		
Peak Concentration	7.92E-10 Ci/L (0.94)	9.38E-10 Ci/L (1.12)
Arrival Time	2133 yr (-5709)	9745 yr (1903)
Cumulative Mass	0.937 Ci (1.051)	0.745 Ci (0.835)
U_0.10		
Peak Concentration	3.50E-10 Ci/L (1.38)	8.42E-11 Ci/L (0.33)
Arrival Time	>= 12032 yr (0)	>= 12032 yr (0)
Cumulative Mass	0.170 Ci (1.889)	0.017 Ci (0.192)
U_0.20		
Peak Concentration	1.06E-11 Ci/L (3.41)	1.46E-13 Ci/L (0.05)
Arrival Time	>= 12032 yr (0)	>= 12032 yr (0)
Cumulative Mass	0.003 Ci (4.167)	0.000 Ci (0.000)
U_0.60		
Peak Concentration	0.00E+00 Ci/L (0.00)	0.00E+00 Ci/L (0.00)
Arrival Time	>= 12032 yr (0)	>= 12032 yr (0)
Cumulative Mass	0.000 Ci (-)	0.000 Ci (-)

(a) Numbers in parentheses indicate concentration ratio relative to base case.
(b) Numbers in parentheses indicate deviations in arrival time relative to base case.
(c) Numbers in parentheses indicate cumulative mass ratio relative to base case.

The results reported in Table 4.22 show that the estimate of the preclosure recharge rate impacted peak concentrations, arrival times and the cumulative mass reaching the fenceline compliance point. For the high recharge case, more mass reached the fenceline compliance point relative to the base case with larger values of the distribution coefficient (e.g., 1.006, 1.051, 1.889, and 4.167 times more for ^{99}Tc, U_0.02, U_0.10, and U_0.20, respectively). For the low recharge case, less mass reached the fenceline relative to the base case with smaller values of the distribution coefficient (e.g., 0.974, 0.835, 0.192, and 0.000 times less ^{99}Tc, U_0.02, U_0.10, and U_0.20, respectively).

Despite the consistent trends in cumulative mass arriving at the fenceline compliance point, in the high recharge scenario, peak concentrations seemingly demonstrated an inconsistency. Peak concentrations relative to the base case were expected to increase with increasing recharge. Although peak concentrations for ^{99}Tc, U_0.10, and U_0.20 were higher than base-case predictions (3.72, 1.38, and 3.41, respectively), for U_0.02, the peak concentration decreased (0.94 times lower than the base case). This result, however, occurred due to the timing of the mass arriving at the groundwater table. In all cases, changes in the recharge rate cause the BTCs to exhibit dual peaks for the more conservative species. In the base case, the second peak was higher than the first, with an arrival time in the year 7842. In the high

recharge case, the additional water flux caused the peak recharge for U_0.02 to occur nearly 6000 years earlier, but the peak was diluted with respect to the second peak in the base case. This effect did not occur for the more conservative ^{99}Tc because the first peaks in the BTC were higher than the second in both the base and high recharge rate scenarios.

Because arrival times for ^{238}U species with $K_d > 0.10$ occurred in the final year of simulation, a comparison of arrival times for only ^{99}Tc and U_0.02 could be made. Consistent with theoretical expectation, a higher recharge rate translated into earlier peak arrival times by thousands of years. For the lower estimate of recharge, the reverse effect was observed. Arrival times for peak concentrations were delayed by nearly 2000 years for both ^{99}Tc and U_0.02.

4.6.3 Barrier Recharge Sensitivity Cases

The barrier recharge sensitivity cases investigated the uncertainty in the estimate of recharge before barrier degradation occurred, and its impact on peak concentrations and arrival times at the groundwater table, fenceline and downstream compliance points. To evaluate impacts associated with the lower bound of the barrier recharge rate, the median recharge rate of 0.5 mm/yr for the period 2032–2532 was changed to 0.1 mm/yr. Likewise, to examine the impact of the upper bound, barrier recharge rate, the median recharge was set to 1 mm/yr for the same period.

For the 1-mm/yr post-closure recharge rate, the saturation distributions at years 2000, 2500, and 12032 are shown in Figures A.2a, A.4b, and A.6a. The saturation distributions for 2000 and 12032 are the same as the base case. The concentration distributions of the contaminants in 5474, the year the ^{99}Tc peak concentration occurred, are shown in Figure E.13 and the final concentration distributions (in 12032) in Figure E.14. The mass flux, cumulative mass, and BTCs for ^{99}Tc and U_0.20 are shown in Figures E.15–E.16. No plots are shown for U_0.60 because it did not reach the fenceline by the end of the simulation. Only contaminants with $K_d \leq 0.20$ mL/g reached the fenceline by the end of the simulation in 12032 (Table 4.23).

For the 0.1-mm/yr post-closure recharge rate, the saturation distributions at years 2000, 2500, and 12032 are shown in Figures A.2a, A.4c, and A.6a. The saturation distributions for 2000 and 12032 are the same as the base case. The concentration distributions of the contaminants in 5912, the year the ^{99}Tc peak concentration occurred, are shown in Figure E.17 and the final concentration distributions (in 12032) in Figure E.18. The mass flux, cumulative mass, and BTCs for ^{99}Tc and U_0.20 are shown in Figures E.19 and E.20. No plots are shown for U_0.60 because it did not reach the fenceline by the end of the simulation. Only contaminants with $K_d \leq 0.20$ mL/g reached the fenceline by the end of the simulation in 12032 (Table 4.23).

The peak concentrations, arrival times, and cumulative mass for ^{99}Tc and ^{238}U with $K_d \leq 0.60$ mL/g are shown in Table 4.23, which also reports concentrations, arrival times, and cumulative mass relative to base-case predictions. A graphical representation of relative concentrations and arrival times is shown in Figure 4.5, along with the results from the other sensitivity cases.

Table 4.23. Peak Concentrations and Arrival Times at the WMA Fenceline for Case 4 for Different Barrier Recharge Estimates

Parameter	Upper Bound (1.0 mm/yr)	Lower Bound (0.1 mm/yr)
^{99}Tc		
Peak Concentration[(a)]	1.03E-09 Ci/L (1.00)	1.03E-09 Ci/L (1.00)
Arrival Time[(b)]	5474 yr (-243)	5912 yr (195)
Cumulative Mass[(c)]	0.992 Ci (1.002)	0.988 Ci (0.998)
U_0.02		
Peak Concentration	8.40E-10 Ci/L (1.00)	8.40E-10 Ci/L (1.00)
Arrival Time	7599 yr (-243)	8039 yr (197)
Cumulative Mass	0.904 Ci (1.014)	0.880 Ci (0.987)
U_0.10		
Peak Concentration	2.71E-10 Ci/L (1.07)	2.37E-10 Ci/L (0.94)
Arrival Time	>= 12032 yr (0)	>= 12032 yr (0)
Cumulative Mass	0.101 Ci (1.123)	0.082 Ci (0.907)
U_0.20		
Peak Concentration	3.79E-12 Ci/L (1.22)	2.64E-12 Ci/L (0.85)
Arrival Time	>= 12032 yr (0)	>= 12032 yr (0)
Cumulative Mass	0.001 Ci (1.167)	0.001 Ci (0.833)
U_0.60		
Peak Concentration	0.00E+00 Ci/L (0.00)	0.00E+00 Ci/L (0.00)
Arrival Time	>= 12032 yr (0)	>= 12032 yr (0)
Cumulative Mass	0.000 Ci (-)	0.000 Ci (-)

(a) Numbers in parentheses indicate concentration ratio relative to base case.
(b) Numbers in parentheses indicate deviations in arrival time relative to base case.
(c) Numbers in parentheses indicate cumulative mass ratio relative to base case.

Table 4.23 shows that in general, the uncertainty in the barrier recharge estimate had its largest impact on peak concentration arrival times. Because the peak concentrations for ^{238}U species with $K_d \geq 0.10$ occurred in the final year of simulation, only the arrival times for ^{99}Tc and U_0.02 could be evaluated. In the high barrier recharge case, arrival times were accelerated by ~250 years for both ^{99}Tc and U_0.02. For the low case, arrival times were similarly delayed by ~200 years.

Peak concentrations, however, were not impacted by a large measure. Variations in the recharge rate only affected peak concentrations for the more retarded species (e.g., $K_d \geq 0.10$) because the more conservative species were transported more quickly through the domain by the higher preclosure recharge rate. Peak concentrations for both the high and low barrier recharge estimates were the same as those predicted for the base case for ^{99}Tc and U_0.02. For U_0.10, the concentrations were ~10% higher in high recharge case and ~10% lower for the lower estimate of barrier recharge. For U_0.20, the concentrations were ~20% higher in the high recharge case and ~15% lower in the low recharge case.

The total mass of the solutes reaching the fenceline compliance point did not differ by a large measure for either the upper- or lower-bound estimates. For the high barrier recharge estimate, the

amount of mass reaching the fenceline relative to the base case increased with increasing value of the distribution coefficient (e.g., 1.002, 1.014, 1.123, and 1.167 for ^{99}Tc, U_0.02, U_0.10, and U_0.20, respectively). The opposite trend occurred for the low barrier recharge case (e.g., 0.998, 0.987, 0.907, and 0.833 for ^{99}Tc, U_0.02, U_0.10, and U_0.20, respectively).

4.6.4 Degraded Barrier Recharge Sensitivity Cases

The degraded barrier recharge sensitivity cases investigated the uncertainty in the degraded barrier recharge estimate and its impact on peak concentrations and arrival times at the groundwater table, fenceline, and downstream compliance points. To evaluate impacts associated with the lower bound of the degraded barrier recharge rate, the median recharge rate of 1 mm/yr for the period 2532–12032 was changed to 0.5 mm/yr, which assumed that no degradation occurred. Likewise, to examine the impact of the upper-bound degraded barrier recharge rate, the median recharge was set to 3.5 mm/yr for the same period, which is the pre-Hanford operations recharge rate.

For the 3.5-mm/yr barrier degradation recharge rate, the saturation distributions at years 2000, 2500, and 12032 are shown in Figures A.2a, A.4a, and A.6b. Saturation distributions for 2000 and 2500 are the same as the base case. The concentration distributions of the contaminants in 3760, the year the ^{99}Tc peak concentration occurred, are shown in Figure E.21 and the final concentration distributions (in 12032) in Figure E.22. The mass flux, cumulative mass, and BTCs for ^{99}Tc, U_0.20, and U_0.60 are shown in Figures E.23–E.25. Only contaminants with $K_d \leq 1.00$ mL/g reached the fenceline by the end of the simulation in 12032 (see Tables F.1–F.64).

For the 0.5 mm/yr barrier degradation recharge rate, the saturation distributions at years 2000, 2500, and 12032 are shown in Figures A.2a, A.4a, and A.6c. Saturation distributions for 2000 and 2500 are the same as the base case. The concentration distributions of contaminants in 2197, when the ^{99}Tc peak concentration occurred, are shown in Figure E.26 and the final concentration distributions (in 12032) in E.27. The mass flux, cumulative mass, and BTCs for ^{99}Tc and U_0.20 are shown in Figures E.28 and E.29. No plots are shown for U_0.60 because it did not reach the fenceline by the end of the simulation. Only contaminants with $K_d \leq 0.20$ mL/g reached the fenceline by the end of the simulation in 12032 (Table 4.24).

The peak concentrations, arrival times, and cumulative mass for ^{99}Tc and ^{238}U with $K_d \leq 0.60$ mL/g are shown in Table 4.24, which also reports concentrations, arrival times, and cumulative mass relative to the base-case predictions. A graphical representation of relative concentrations and arrival times is shown in Figure 4.5, along with the results from the other sensitivity cases.

Table 4.24 shows that the uncertainty in the degraded barrier recharge estimate had a significant effect on peak concentrations, arrival times, and total mass reaching the fenceline compliance point. Peak concentrations were 3.35, 3.35, 6.36, and 334 times higher than the base-case prediction in the high degraded barrier case for ^{99}Tc, U_0.02, U_0.10, and U_0.20. For U_0.60, the peak was 0.14 times the base-case prediction, but its concentration was still increasing at the end of the simulation. For the low degraded barrier recharge case, peak concentrations relative to the base case decreased with increasing values of distribution coefficient (e.g., 0.75, 0.50, 0.06, and 0.01 for ^{99}Tc, U_0.02, U_0.10, and U_0.20).

Changes in the degraded barrier recharge rate had the greatest impact on the most retarded species. For example, the peak concentration for U_0.20 was more than 300 times higher in the high degraded

Table 4.24. Peak Concentrations, Arrival Times at the WMA Fenceline for Case 4 for Different Degraded Barrier Recharge Estimates

Parameter	Upper Bound (3.5 mm/yr)	Lower Bound (0.5 mm/yr)
^{99}Tc		
Peak Concentration[(a)]	3.45E-09 Ci/L (3.35)	7.71E-10 Ci/L (0.75)
Arrival Time[(b)]	3760 yr (-1957)	2197 yr (-3520)
Cumulative Mass[(c)]	1.000 Ci (1.010)	0.795 Ci (0.803)
U_0.02		
Peak Concentration	2.81E-09 Ci/L (3.35)	4.23E-10 Ci/L (0.50)
Arrival Time	4400 yr (-3442)	11925 yr (4083)
Cumulative Mass	1.000 Ci (1.122)	0.445 Ci (0.499)
U_0.10		
Peak Concentration	1.61E-09 Ci/L (6.36)	1.45E-11 Ci/L (0.06)
Arrival Time	7050 yr (-4982)	>= 12032 yr (0)
Cumulative Mass	0.994 Ci (11.039)	0.005 Ci (0.056)
U_0.20		
Peak Concentration	1.04E-09 Ci/L (334.41)	1.96E-14 Ci/L (0.01)
Arrival Time	10405 yr (-1627)	>= 12032 yr (0)
Cumulative Mass	0.684 Ci (1140.500)	0.000 Ci (0.000)
U_0.60		
Peak Concentration	2.22E-12 Ci/L (0.14)	0.00E+00 Ci/L (0.00)
Arrival Time	>= 12032 yr (0)	>= 12032 yr (0)
Cumulative Mass	0.000 Ci (0.059)	0.000 Ci (-)

(a) Numbers in parentheses indicate concentration ratio relative to base case.
(b) Numbers in parentheses indicate deviations in arrival time relative to base case.
(c) Numbers in parentheses indicate cumulative mass ratio relative to base case.

barrier recharge estimate and only 0.01 times the base-case prediction with the low degraded barrier recharge estimate. The percent of mass reaching the fenceline relative to the base-case scenario was so small that it is recorded as 0% in the low degraded barrier recharge case. By contrast, the U_0.20 mass reaching the fenceline in the high recharge case was more than 1000 times larger than the mass transported to the fenceline in the base case.

Arrival times were also accelerated by thousands of years for all species in the high recharge case. As shown in Figure E.22, the second ^{99}Tc peak was not only significantly increased, but accelerated as well relative to the base case (see Figure E.3). Shown in Figure E.27, the second peak was dampened by the lower estimate of recharge, and the first peak identified as the peak concentration. Hence, the arrival time for the peak concentration in the low case was also accelerated by thousands of years (~3500). For U_0.02, the arrival time was delayed by more than 4000 years because the second peak in the BTC was higher than the first. An evaluation of arrival times for ^{238}U species with $K_d \geq 0.10$ could not be performed for the lower degraded barrier recharge estimate because their concentrations were still increasing at the end of the simulation.

4.6.5 Aquifer Hydraulic Conductivity

The aquifer hydraulic conductivity sensitivity cases investigated the uncertainty in the estimate of the aquifer hydraulic conductivity and its impact on peak concentrations and arrival times at the groundwater table, fenceline and downstream compliance points. To evaluate impacts associated with the lower bound of the aquifer hydraulic conductivity, the median value of 3000 m/d was changed to 2000 m/d. Likewise, to examine the impact of the upper bound of the aquifer hydraulic conductivity, the median values was changed to 4000 m/d for both the steady-state and transient simulations.

For the upper bound of the aquifer saturated hydraulic conductivity (4000 m/d), the saturation distributions at year 2000, 2500 and 12032 are shown in Figure A.2a, A.4a and A.6a. Note that these saturations are the same as the base case. The concentration distributions of contaminants in 5714, the year the ^{99}Tc peak concentration occurs, are shown in Figure E.30 and the final concentration distributions (in 12032) in Figure E.31. The mass flux, cumulative mass, and BTCs for ^{99}Tc and U_0.20 are shown in Figures E.32 and E.33. No plots are shown for U_0.60 because it did not reach the fenceline by the end of the simulation. Only contaminants with a $K_d \leq 0.20$ mL/g reached the fenceline by the end of the simulation in 12032 (Table 4.25).

For the lower bound of the aquifer saturated hydraulic conductivity (2000 m/d), the saturation distributions at years 2000, 2500, and 12032 are shown in Figures A.2a, A.4a, and A.6a. These saturations are the same as the base case. The concentration distributions of the contaminants in 5717, when the ^{99}Tc peak concentration occurs, are shown in Figure E.34 and the final concentration distributions (in 12032) in Figure E.35. The mass flux, cumulative mass, and BTCs for ^{99}Tc and U_0.20 are shown in Figures E.36 and E.37. No plots are shown for U_0.60 because it did not reach the fenceline by the end of the simulation. Only contaminants with a $K_d \leq 0.20$ mL/g reached the fenceline by the end of the simulation in 12032 (Table 4.25).

The peak concentrations, arrival times, and cumulative mass for ^{99}Tc and ^{238}U with $K_d \leq 0.60$ mL/g are shown in Table 4.25, which also reports concentrations, arrival times, and cumulative mass relative to the base-case predictions. A graphical representation of relative concentrations and arrival times is shown in Figure 4.5, along with the results from the other sensitivity cases.

Results shown in Table 4.25 demonstrate that the uncertainty in the estimate of aquifer hydraulic conductivity had its largest impact on the peak concentrations at the fenceline. For the upper estimate of hydraulic conductivity, peak concentrations for all solutes were approximately 0.75 times lower than the base case because higher velocities increased dispersion. For the lower estimate, peak concentrations for all solutes were approximately 1.5 times higher due to less dispersion during transport.

Arrival times for both cases were close to the predictions in the base case, and differed by only one to three years. For the upper estimate, travel times were accelerated, and peak arrivals were earlier than in the base case. For the lower estimate, the ^{99}Tc peak concentration arrival time was the same as the base-case prediction, and delayed by three years for U_0.02. Given that ^{99}Tc required three years to reach the fenceline once it entered the water table in the base case, only small differences in arrival times were expected for both the upper and lower estimates of aquifer hydraulic conductivity.

Consistent with theoretical expectation, the amount of mass reaching the fenceline for both sensitivity cases were nearly the same as in the base case. Given the short residence time in the aquifer, the magnitude of the saturated hydraulic conductivity had little impact on the mass arriving at the fenceline.

Table 4.25. Peak Concentrations and Arrival Times at the WMA Fenceline for Case 4 for Different Aquifer Hydraulic Conductivity Estimates

Parameter	Upper Bound (4000 m/d)	Lower Bound (2000 m/d)
^{99}Tc		
Peak Concentration[(a)]	7.73E-10 Ci/L (0.75)	1.54E-09 Ci/L (1.50)
Arrival Time[(b)]	5714 yr (-3)	5717 yr (0)
Cumulative Mass[(c)]	0.990 Ci (1.000)	0.990 Ci (1.000)
U_0.02		
Peak Concentration	6.30E-10 Ci/L (0.75)	1.26E-09 Ci/L (1.50)
Arrival Time	7840 yr (-2)	7845 yr (3)
Cumulative Mass	0.892 Ci (1.000)	0.891 Ci (1.000)
U_0.10		
Peak Concentration	1.90E-10 Ci/L (0.75)	3.78E-10 Ci/L (1.49)
Arrival Time	>= 12032 yr (0)	>= 12032 yr (0)
Cumulative Mass	0.090 Ci (1.001)	0.090 Ci (0.999)
U_0.20		
Peak Concentration	2.34E-12 Ci/L (0.75)	4.65E-12 Ci/L (1.50)
Arrival Time	>= 12032 yr (0)	>= 12032 yr (0)
Cumulative Mass	0.001 Ci (1.000)	0.001 Ci (1.000)
U_0.60		
Peak Concentration	0.00E+00 Ci/L (0.00)	0.00E+00 Ci/L (0.00)
Arrival Time	>= 12032 yr (0)	>= 12032 yr (0)
Cumulative Mass	0.000 Ci (-)	0.000 Ci (-)

(a) Numbers in parentheses indicate concentration ratio relative to base case.
(b) Numbers in parentheses indicate deviations in arrival time relative to base case.
(c) Numbers in parentheses indicate cumulative mass ratio relative to base case.

4.6.6 Vadose Zone Saturated Hydraulic Conductivity

The vadose zone saturated hydraulic conductivity sensitivity cases investigated the uncertainty in the estimate of the saturated hydraulic conductivity for each strata in the vadose zone and its impact on peak concentrations and arrival times at the groundwater table, fenceline, and downstream compliance points. To evaluate impacts associated with the lower bound of the saturated hydraulic conductivities, the median value for the saturated hydraulic conductivity was decreased by an order of magnitude for each material type. Likewise, to examine the effect of the upper bound of the saturated hydraulic conductivities, the median values were increased by an order of magnitude for each material type.

For the upper bound on the estimated saturated hydraulic conductivity for all materials in the vadose zone (scale factor = 10.0), saturation distributions at years 2000, 2500, and 12032 are shown in Figures A.3a, A.5a, and A.7a, respectively. The concentration distributions of the contaminants in 2097, the

year the ^{99}Tc peak concentration occurs, are shown in Figure E.38 and the final concentration distributions (in 12032) in Figure E.39. The mass flux, cumulative mass, and BTCs for ^{99}Tc and U_0.20 are shown in Figures E.40 and E.41. No plots are shown for U_0.60 because it did not reach the fenceline by the end of the simulation. Only contaminants with a $K_d \leq 0.20$ mL/g reached the fenceline by the end of the simulation in 12032 (Table 4.26).

For the lower bound on the estimated saturated hydraulic conductivity for all materials in the vadose zone (scale factor = 0.10), saturation distributions at years 2000, 2500, and 12032 are shown in Figures A.3b, A.5c, and A.7c, respectively. The concentration distributions of the contaminants in 7158, when the ^{99}Tc peak concentration occurred, are shown in Figure E.42 and the final concentration distributions (in 12032) in Figure E.43. The mass flux, cumulative mass, and BTCs for ^{99}Tc and U_0.20 are shown in Figures E.44 and E.45. No plots are shown for U_0.60 because it did not reach the fenceline by the end of the simulation. Only contaminants with a $K_d \leq 0.20$ mL/g reached the fenceline by the end of the simulation in 12032 (Table 4.26).

The peak concentrations, arrival times and cumulative mass for ^{99}Tc and ^{238}U with $K_d \leq 0.60$ mL/g are shown in Table 4.26, which also reports concentrations, arrival times, and the cumulative mass relative to the base-case predictions. A graphical representation of relative concentrations and arrival times is shown in Figure 4.5, along with the results from the other sensitivity cases.

The results in Table 4.26 show that for the upper estimate of saturated hydraulic conductivity, arrival times were ~ 3600 years and ~900 years earlier for the conservative species, ^{99}Tc and U_0.02, respectively. The higher conductivities resulted in faster travel times but lower soil moisture content. For the lower estimate of saturated hydraulic conductivity, arrival times were delayed by thousands of years (~1400 years for both ^{99}Tc and U_0.02). The higher moisture content resulted in delays of the peak arrival times. No assessments of arrival times could be made with respect to ^{238}U species with higher distribution coefficients because their peaks occurred in the final year of simulation, when concentrations were still increasing.

Peak concentrations for the high saturated hydraulic conductivity case were 1.44, 1.25 and 1.17 times higher than the base-case predictions for ^{99}Tc, U_0.02, and U_0.10, respectively. The opposite trend occurred for the low case, where peak concentrations were 0.70, 0.72, and 0.75 times higher than the base-case predictions for the same species. The exception to these trends was the peak concentration for U_0.20. For the high case, the peak concentration was only ~50% of its base-case prediction. The amount of mass reaching the fenceline compliance point was also lower relative to the base-case prediction, whereas the more conservative solutes showed the opposite trend. However, because the peak concentration was reported in the final year of simulation, the true peak did not occur. It may be that the true peak for U_0.20 would show a similar trend as the more conservative species, or due to the lower moisture content, the delay in travel time might cause the true peak to be diluted with respect to the base-case prediction.

For the lower estimate of saturated hydraulic conductivity, the peak concentration was nearly twice the base-case value for U_0.20. Due to retardation, more U_0.20 mass was left in the domain relative to the conservative species when the high recharge period ended. The low recharge boundary condition due to the protective barrier essentially resulted in a system that was dominated by gravity drainage. For the

Table 4.26. Peak Concentrations and Arrival Times at the WMA Fenceline for Case for Different Vadose Zone Saturated Hydraulic Conductivity Estimates

Parameter	Upper Bound (10.0 scale factor)	Lower Bound (0.1 scale factor)
^{99}Tc		
Peak Concentration*	1.48E-09 Ci/L (1.44)	7.17E-10 Ci/L (0.70)
Arrival Time†	2097 yr (-3620)	7158 yr (1441)
Cumulative Mass‡	1.000 Ci (1.010)	0.892 Ci (0.901)
U_0.02		
Peak Concentration	1.05E-09 Ci/L (1.25)	6.08E-10 Ci/L (0.72)
Arrival Time	6959 yr (-883)	9235 yr (1393)
Cumulative Mass	0.967 Ci (1.085)	0.699 Ci (0.784)
U_0.10		
Peak Concentration	2.97E-10 Ci/L (1.17)	1.90E-10 Ci/L (0.75)
Arrival Time	>= 12032 yr (0)	>= 12032 yr (0)
Cumulative Mass	0.096 Ci (1.064)	0.079 Ci (0.878)
U_0.20		
Peak Concentration	1.64E-12 Ci/L (0.53)	5.92E-12 Ci/L (1.90)
Arrival Time	>= 12032 yr (0)	>= 12032 yr (0)
Cumulative Mass	0.000 Ci (0.500)	0.001 Ci (2.333)
U_0.60		
Peak Concentration	0.00E+00 Ci/L (0.00)	0.00E+00 Ci/L (0.00)
Arrival Time	>= 12032 yr (0)	>= 12032 yr (0)
Cumulative Mass	0.000 Ci (-)	0.000 Ci (-)

(a) Numbers in parentheses indicate concentration ratio relative to base case.
(b) Numbers in parentheses indicate deviations in arrival time relative to base case.
(c) Numbers in parentheses indicate cumulative mass ratio relative to base case.

lower estimate of saturated hydraulic conductivity, the higher soil moisture content accelerated solute transport. This caused the peak concentration for the low case to be higher than the peak predicted in the base-case scenario. More mass was also transported to the fenceline compliance point relative to the base case, whereas the opposite trend occurred for the more conservative species.

With the exception of U_0.20, less mass was transported to the fenceline for the lower estimate of saturated hydraulic conductivity, and more mass for the upper estimate. This is consistent with theoretical expectation because higher hydraulic conductivities should result in more mass being transported to the vadose zone to the groundwater table.

The dependence of the retardation factor on soil moisture content may have contributed to the different trends exhibited by U_0.20 for both the high and low cases. ^{238}U species with smaller distribution coefficients were not affected in the same way because more U_0.20 mass was left in the domain when the high recharge period ended and the low recharge boundary condition of the protective barrier resulted in a system dominated by gravity drainage.

4.6.7 Ancillary Equipment Summary

The effects of the preclosure recharge rate, barrier recharge rate, degraded barrier recharge rate, aquifer hydraulic conductivity, and saturated hydraulic conductivity of the vadose zone are shown in Figure 4.5 and summarized in this section.

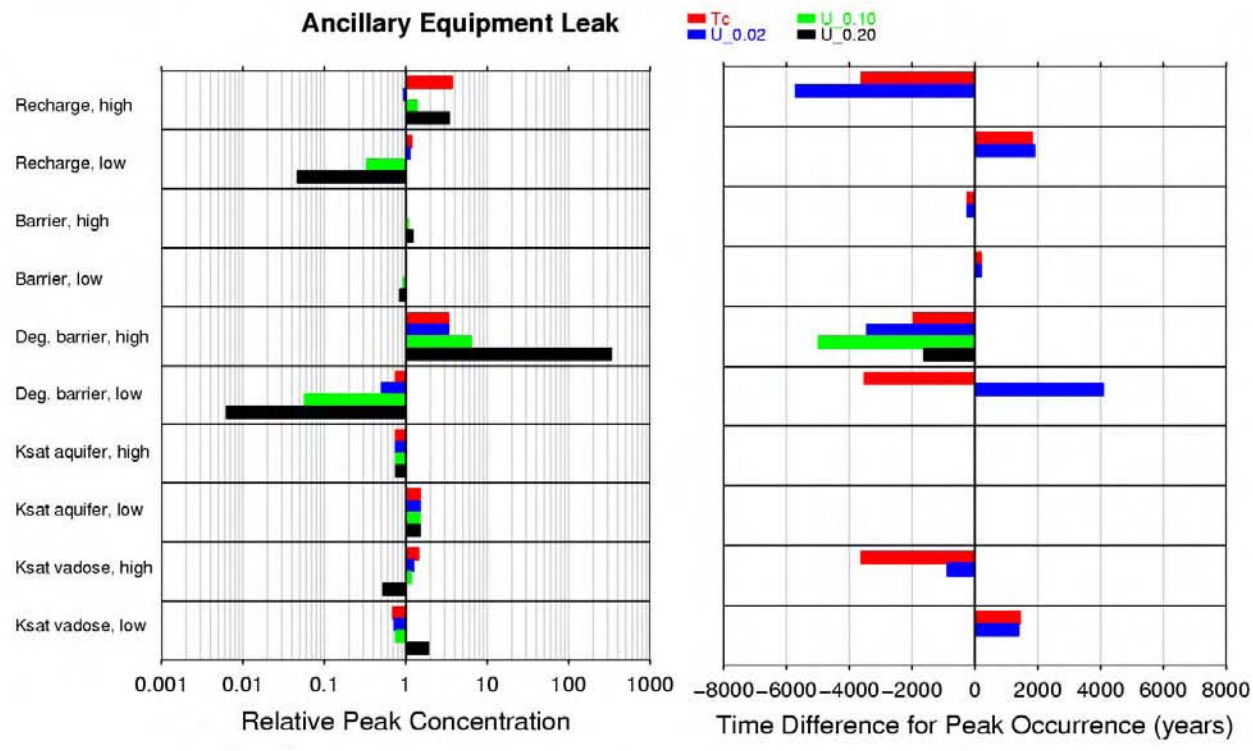

Figure 4.5. Relative Peak Concentrations and Arrival Times for Ancillary Equipment Sensitivity Cases

The system was sensitive to the magnitude of the preclosure recharge rate. Not only were the peak concentrations higher for the high recharge (140 mm/yr) case, but the arrival times were earlier. The peak concentrations and arrival times for the low recharge (40 mm/yr) case demonstrated opposite trends. Breakthroughs for the peak concentrations exhibited a more significant delay for the retarded species than the acceleration exhibited by the high recharge case. In general, the uncertainty in the barrier recharge estimate had only a small effect on contaminant transport predictions. Peak concentrations for both the high and low barrier recharge estimates were the same as those predicted for the base case.

The uncertainty in the degraded barrier recharge estimate affected peak concentrations, arrival times, and total mass reaching the fenceline compliance point. This effect increased with larger values of the distribution coefficient. For the upper estimate, arrival times were accelerated by thousands of years and peak concentrations increased. The reverse trend was demonstrated by the lower degraded barrier recharge estimate.

For the upper estimate of aquifer hydraulic conductivity, peak concentrations for all the solutes were ~0.75 of the base-case predictions because higher velocities increased dispersion. For the lower estimate, peak concentrations for all solutes were approximately ~1.5 times that in the base case due to less

dispersion during transport. For the upper estimate, travel times were accelerated and peak arrivals were earlier than in the base case and the opposite trend occurred for the lower estimate of hydraulic conductivity.

Distinct impacts resulted from scaling the saturated hydraulic conductivity in the vadose zone. For ^{99}Tc and U_0.02, arrival times were earlier for the upper estimate of saturated hydraulic conductivity and later for the lower estimate. Peak concentration for both ^{99}Tc and U_0.02 were higher than the base-case predictions for the upper estimates of saturated hydraulic conductivity. The opposite trends in peak concentrations were observed for the lower estimates of saturated hydraulic conductivity.

4.7 Comparison of Base-Case Sensitivities

In general, each of the base-case scenarios responded similarly to changes in recharge rates and estimates of hydraulic conductivities. Differences in responses were primarily due to the contaminant release rate and the position of the contaminant in the soil profile. For example, the retrieval leak (Case 3) and ancillary equipment leak (Case 4) behaved alike because of the initial release of the contaminants was at the same depth (~30 ft bgs). By contrast, the past leak scenario (Case 1) demonstrated similar trends, but the magnitude of the effect on peak concentrations and arrival times differed. In terms of arrival times, only U_0.20 was affected in Case 1 (see Figure 4.1). For the diffusion release case (Case 2), the slow contaminant release rate demonstrated different sensitivities than the other cases.

Increasing the preclosure recharge rate increased peak concentrations and accelerated their arrival times, while the reverse trend occurred when decreasing the preclosure recharge rate. However, the extent of the impact was most significant for the past leak, because the initial release of the contaminant was already close to the water table. Because this rate only represented a short period of time (~80 years) relative to the entire simulation, the impact on leaks initially positioned closer to the tanks was smaller because their peaks occurred much later in the simulations.

The barrier recharge rate, in general, had a relatively small impact when comparing changes in peak concentrations and arrival times amongst all of the sensitivity cases. All four of the base-case scenarios behaved similarly. The largest changes in peak concentrations arrival times occurred for the more retarded species (e.g., U_0.10 and U_0.20), while the more conservative species peaks and arrival times essentially remained unchanged by variations in the barrier recharge rate.

The degraded barrier recharge rate had its largest effect on the diffusion case (Case 2). Peak concentrations and arrival times were significantly impacted because the contaminants were still being released during the degraded barrier recharge period (2532–12032). By contrast, the other base cases simulated more rapid release scenarios, and all of the contaminants had been released into the profile by the time the degraded barrier recharge rate became effective. Similar effects, however, occurred among all of the cases. Peak concentrations increased with a higher recharge rate and decreased with the lower rate. Arrival times were also accelerated with the higher rate and delayed with the lower rate. Larger changes in peak concentrations and arrival times occurred with the more retarded species. For example, only U_0.20 was affected in the past leak scenario because more of its mass remained in the domain once the degraded barrier recharge rate became effective.

The magnitude of the effects on peak concentrations and arrival times for the estimates of aquifer hydraulic conductivity was the same in all of the cases. By contrast, changes in the saturated hydraulic conductivities of the vadose zone produced some dissimilar results. Results of Cases 2–4 showed that peak concentrations of ^{99}Tc, U_0.02, and U_0.10 increased with increasing hydraulic conductivity and decreased with the lower estimate. For U_0.20, the opposite trend occurred. For Case 1, this deviation from the general trend occurred for U_0.10 and not for U_0.20. The difference, however, is likely due to the arrival times for all cases except Case 1 occurring at the end of the simulation, when concentrations were still increasing.

4.8 Peak Concentrations at Compliance Points

As previously stated, solute concentrations at the groundwater table were scaled by the water flux at the fenceline (see Eq. 3.16, Section 3.6), and as a result, BTCs at the groundwater table and fenceline compliance points demonstrated similar behavior. A time shift, however, existed between the BTCs that was, on average, only a few years. For all cases, peak concentrations arrived later at the fenceline than at the groundwater table. Peak concentration values at the two compliance points were similar. The peak concentrations of the contaminants at the fenceline were slightly lower (≤1%) than those predicted at the groundwater table due to dilution.

Contaminant transport was simulated for two potential contaminant migration pathways from WMA C (see Section 5): a northerly path through the gap between Gable Butte and Gable Mountain to the northern reach of the Columbia River and an easterly path south of the gap to the Columbia River to the east of WMA C (see Figures 5.5 and 5.6). For both pathways, the peak concentrations of all contaminants at the exclusion boundary were 3–4 orders of magnitude lower than those at the fenceline for all cases. This large decrease in the peak concentration resulted due to dispersive transport. Although the streamtube model used to transport contaminants to the downstream compliance points simulated one-dimensional transport, dispersion was simulated in three dimensions. Hence, the sources at the fenceline from the two-dimensional cross section were considerably diluted by the time they reached the exclusion boundary.

By contrast, the decrease in peak concentrations was considerably smaller between the exclusion and the Columbia River boundaries because the initial dilution from a two- to a three-dimensional domain already occurred. For the base cases only, peak concentrations were ~4.1–5.1 times higher at the exclusion boundary than at the Columbia River along the northerly flow path. The peak arrival times were ~1–7 years later than the fenceline peak arrival time and ~75–189 years later for the exclusion boundary and Columbia River, respectively. The large variability in arrival times occurred because of the large range in distribution coefficients for the solutes. For higher distribution coefficients (e.g., U_0.20), the delay in peak arrival times was larger.

For the east flow path, peak concentrations for the base cases were ~7.8–9.4 times higher at the exclusion boundary than at the Columbia River. The peak arrival times were 21–28 years later than the fenceline peak arrival time and 104–266 years later for the exclusion boundary and Columbia River, respectively. Peak concentrations at the exclusion boundary were on average, ~2 times greater along the easterly flow path than on the northerly flow path and only ~10% higher at the Columbia River.

Because distances to the compliance points between the two pathways differ by less than 7%, differences in peak concentrations could be attributed to differences in velocities. This effect was greatest at the exclusion boundary, where the velocity along the northerly flow path was more than nine times higher than that for the east. Differences in velocities to the Columbia River, however, were much smaller. The northerly flow velocity was only 1.3 times higher than the easterly flow velocity. Although faster groundwater velocities generally predict higher peak concentrations, the reverse occurred along these two flow paths. This resulted due to the velocity component of the dispersion coefficient (Eq. 3.17). The higher the velocity, the higher the dispersion, which caused more spreading and dilution during transport.

4.9 Solute Mass Balance

Mass balance checks were performed on the eight solutes (^{99}Tc and ^{238}U with different values of K_d) for each simulation case at year 12032 using this expression:

$$m_{error} = \frac{m_{released} - m_{domain} - m_{exit}}{m_{released}} \times 100\% \tag{4.1}$$

where m_{error} is the mass balance error in percent, $m_{released}$ is the total amount of solute released in the system, m_{domain} is the solute inventory in the domain computed from the STOMP plot-file output at year 12032, and m_{exit} is the integrated solute inventory, leaving the computational domain computed from the STOMP surface-flux output. Mass balances were computed for three different domains: the vadose zone, the aquifer, and the entire domain (vadose zone and aquifer), and are shown in Tables F.65–F.96.

The amount of each solute released into the system was one curie. The solute mass leaving the computational domain through the aquifer was determined using surface-flux output on the eastern side of the domain. The solute mass leaving the vadose zone was determined using surface-flux output at the groundwater table. The surface-flux output provided both the solute-flux rate and cumulative mass. Other than solving the solute mass conservation equations, the STOMP simulator contains no algorithms for correcting local or global mass. Therefore, mass balance errors represent the actual mass balance errors from the conservation equations.

Mass balance errors were generally highest in Case 1 and lowest in Case 2. More mass was transported out of the domain for the past leak (Case 1) and the least amount of mass in the diffusion case (Case 2). Expressed as percent error, mass balance errors were small, no more than 1.02% for the vadose zone, 0.687% for the aquifer, and 0.417% for the vadose zone and aquifer combined (see Tables F.65 through F.96). .

5.0 Numerical Groundwater Transport Modeling Results

This section describes the two types of simulations performed with the three-dimensional numerical aquifer model of the Hanford Site. The first set of simulations was for a point source case that determined peak concentrations at the compliance boundaries and their respective travel times. This analysis was carried out to determine velocities needed as input to the analytical streamtube model (reported in Tables F.1 through F.64). A second set of simulations was performed to check the analytical groundwater transport results in Section 4. These simulations used a three-dimensional numerical aquifer model of the Hanford Site for Case 3, the 8000 gallon retrieval leak scenario. While the analytical model was used to predict concentrations of ^{238}U and ^{99}Tc, the numerical model simulations were conducted only for ^{99}Tc to yield the most conservative concentration estimates. Model comparisons were made at two locations that included the exclusion boundary and Columbia River.

The Hanford Site-wide Groundwater Model (SGM) is a three-dimensional finite element model based on the Coupled Fluid, Energy, and Solute Transport (CFEST-96) code (Gupta et al. 1987, Gupta 1996). This model and its conceptual basis are fully described in Wurstner et al. (1995) and Cole et al. (1997). It has been used in the Hanford Site Composite Analysis (Cole et al. 1997, Kincaid et al. 1998, Bergeron et al. 2001) and ILAW Performance Assessment (Bergeron and Wurstner 2000, Mann et al. 2001). Cole et al. (2001) contains a complete discussion of the uncertainties in the conceptual model as they are currently understood.

In the proceeding sections, the SGM implemented in this analysis is described. This is followed by a description of the point source simulation and how the results were used to obtain travel times (i.e., velocities) for the analytical streamtube model. In the final sections, numerical modeling results are presented and compared with the results obtained with the analytical streamtube model.

5.1 The Site-Wide Groundwater Model (SGM)

Although CFEST based SGMs have been used in tank farm field investigation reports (e.g., White et al. 2001, Zhang et al. 2004) and other closure assessments (e.g., Freedman et al. 2003, Zhang et al. 2004), important differences exist between these models and the one used in the current analysis. Important changes to the model calibrated in 2001 (Cole et al. 2001) include calibrating with well observations, river stage, and flux data through the year 2004 and incorporating changes to the geologic conceptual model based on recent data and interpretations (personal communication with Paul Thorne, PNNL). Re-calibrating the model brought the SGM up to date and improved its ability to simulate the groundwater mound dissipation.

For this SGM, a refined grid was used based on the 375-m transport grid that was developed for the Composite Analysis (CA) (Kincaid et al. 1998). This grid maintains 750-m spacing in the southern and western areas of the site (Figure 5.1), but the majority of the central plateau is discretized into 249-m units. The 200 West Area is further refined into 83-m nodal spacing.

Field data suggest that, for post-Hanford operations, the dissipation of the groundwater mounds in the 200 Areas will cause flow to be cut off through the gap between Gable Butte and Gable Mountain as the basalt outcrops above the water table. However, significant uncertainty (~ 15 m) exists in the elevation of

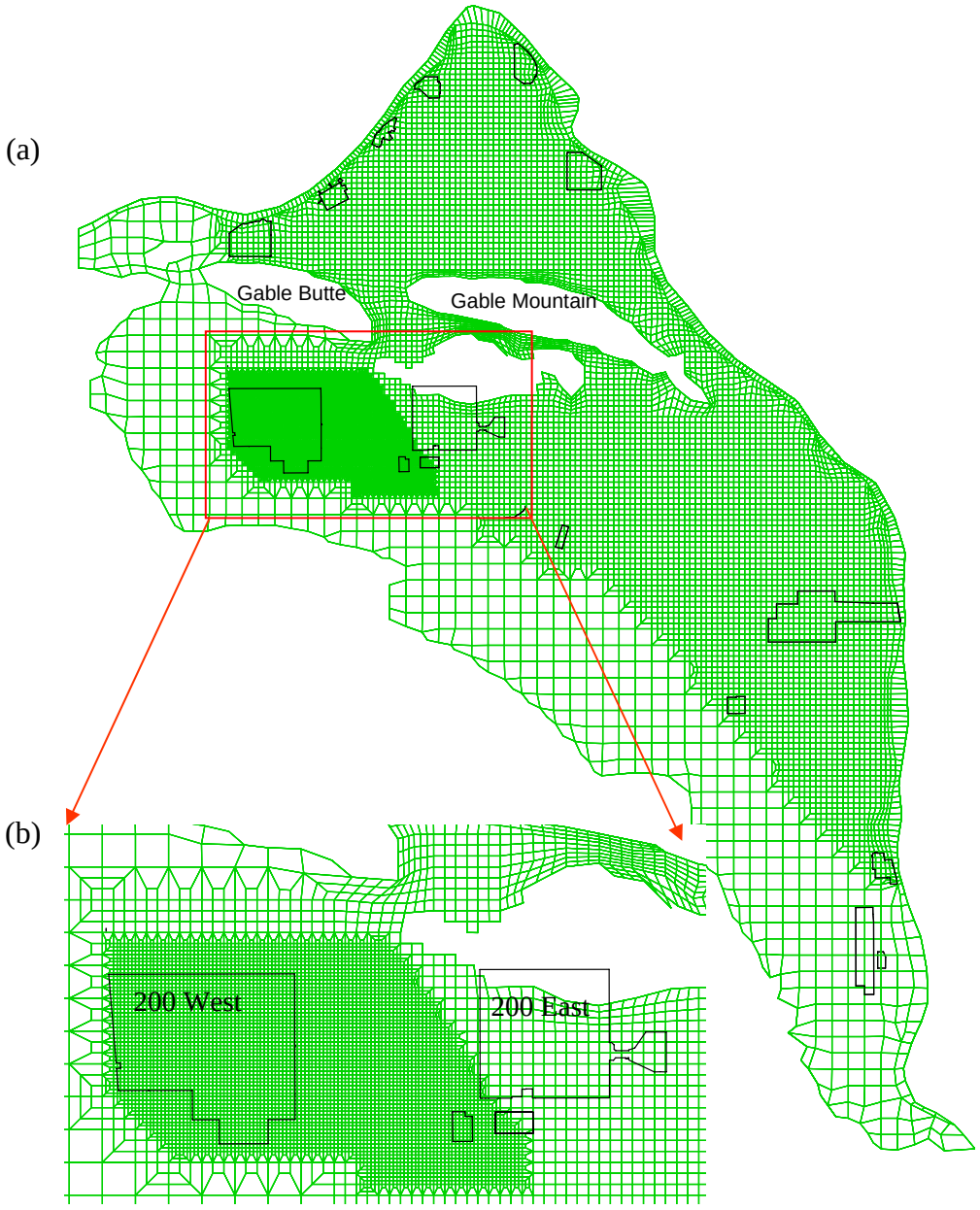

Figure 5.1. a) Refined Composite Analysis Grid (red square denotes area of smallest refinement); b) 200 Areas with 83 m Nodal Spacing in 200 West and 249 m in 200 East

the top of basalt in the gap. If the basalt outcrops above the water table, the easterly flow will predominate. If the elevation of the basalt is too low to impede flow through the gap, a northerly flow path is expected to predominate (personal communication with Paul Thorne, PNNL).

Because of the uncertainty in the top of basalt, two potential flow paths are investigated with this SGM. To simulate the northerly flow path, no modifications to the model were required. For the easterly flow path, nodes were deleted in the gap based on a new interpretation of the location of the basalt outcrops for post-Hanford conditions (Figure 5.2). Although the deletion of grid nodes significantly reduced northward flow, a small amount of groundwater still trickled through the gap. This analysis involved

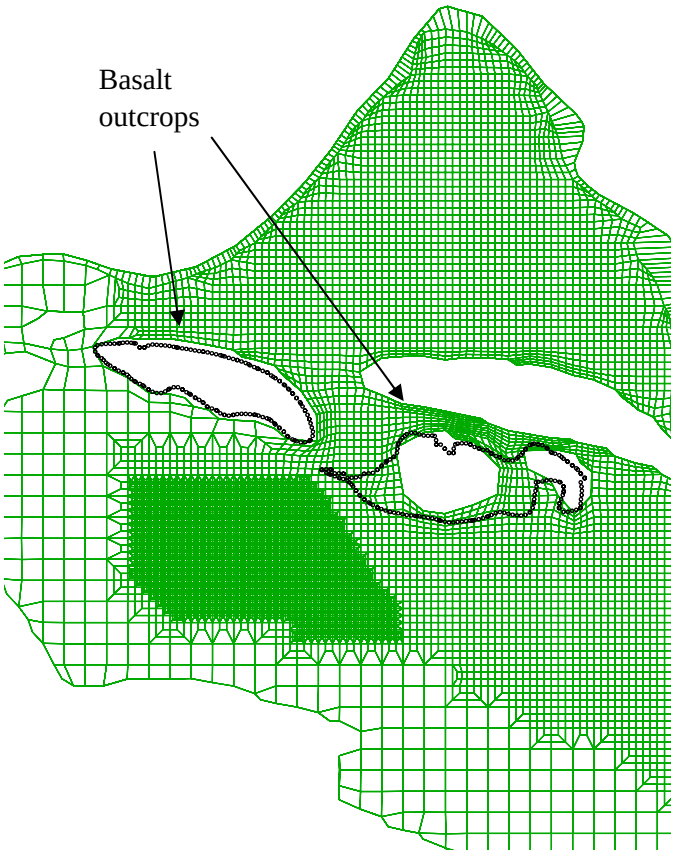

Figure 5.2. New Interpretation of Basalt Outcrop Locations for Post-Hanford Operation Flow Conditions (outlined in black) (nodes within black outlines were deleted from grid)

steady-state flow with transient transport. The setup represented future "Post-Hanford" conditions with no artificial recharge when the effects of the disposal mounds from Hanford operations have ceased.

5.2 Flow and Transport Parameters for the SGM

To model groundwater flow, the distribution of hydraulic properties, including both horizontal and vertical hydraulic conductivity and porosity, was required for each hydrogeologic unit defined in the model (Figure 5.3). The procedure used to calibrate the current detailed process model is based on Cole et al. (2001). The resulting hydraulic conductivity distribution determined for the upper part of the aquifer is provided in Figure 5.4.

To simulate movement of contaminant plumes, the required transport properties include contaminant-specific distribution coefficients, bulk density, effective porosity, and the longitudinal and transverse dispersivities (α_l and α_t) that are the components of the dispersion tensor generally used to represent dispersion in porous media that is isotropic with respect to dispersivity. As described in White et al. (2001), several difficulties are associated with determining appropriate values of dispersivity at the site-wide scale. Although dispersivity is often determined by inverse modeling of onsite tracer test BTCs, no field tests have been conducted at Hanford to develop an estimate for this parameter at the scale of transport appropriate for the SGM.

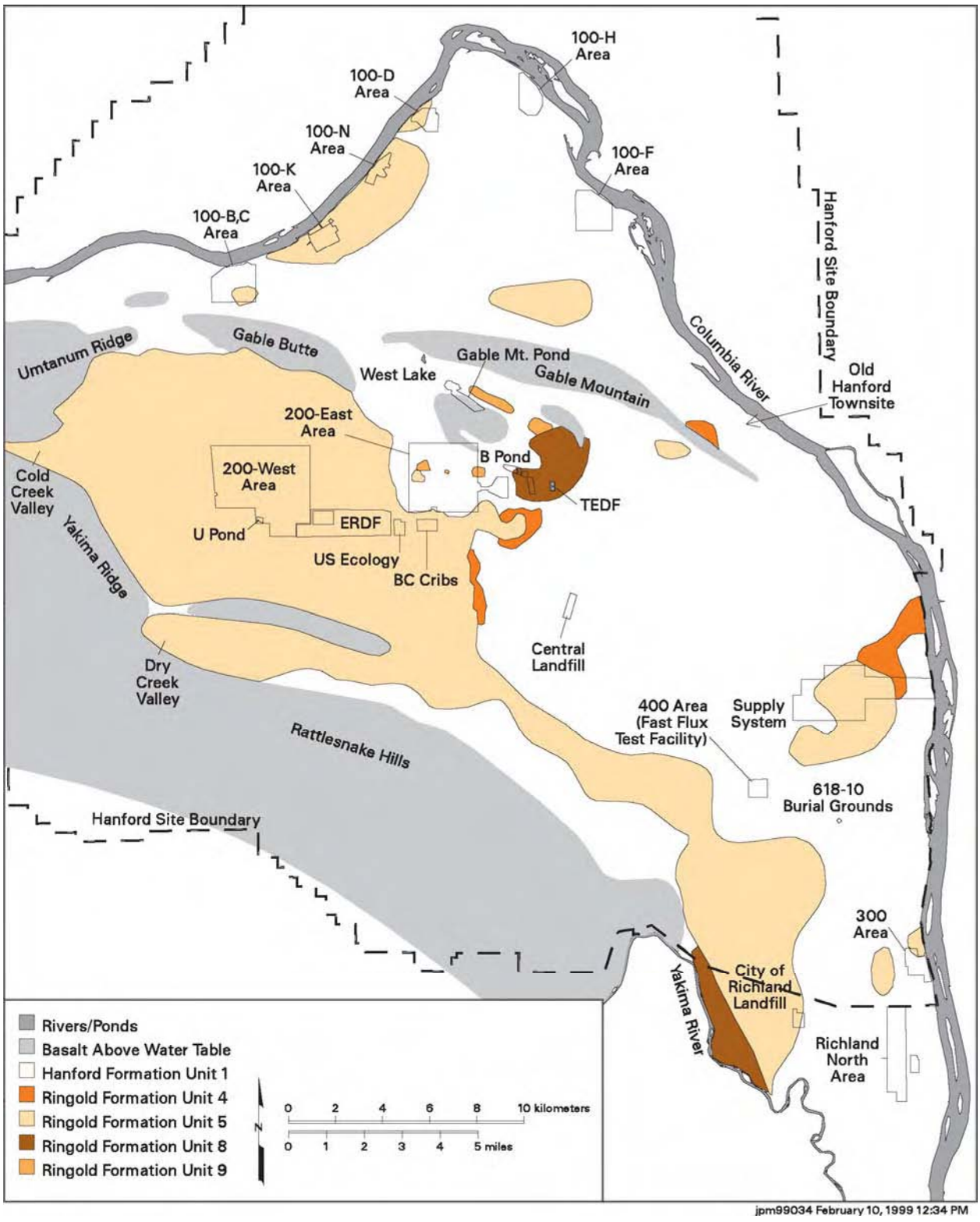

Figure 5.3. Map of SGM Hydrogeologic Units Containing the Water Table in March 1999 (Hartman 2000)

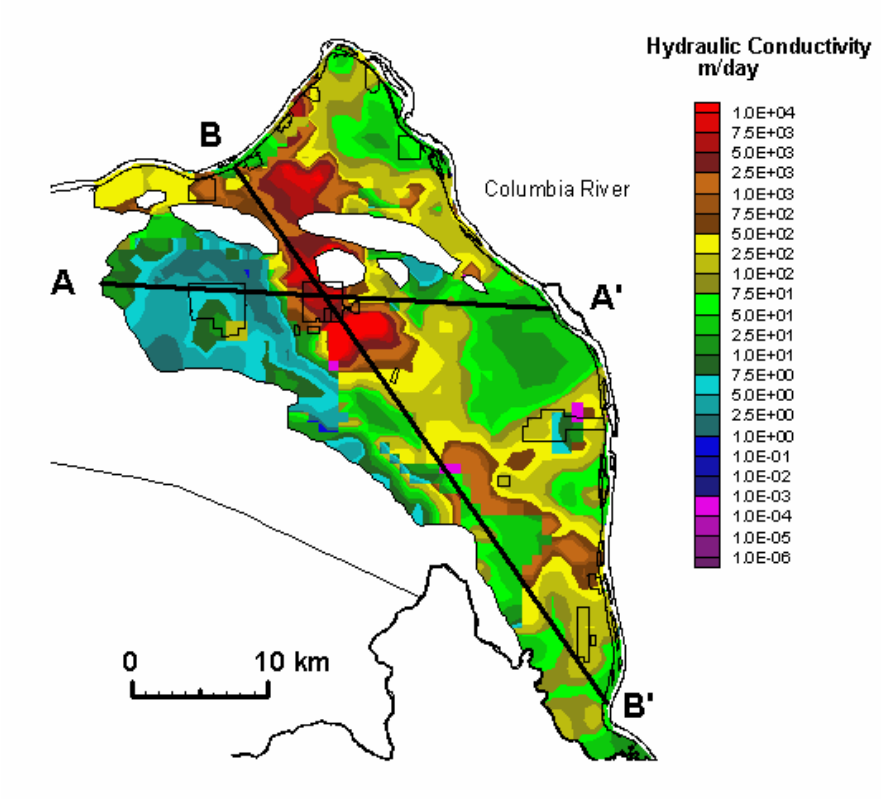

Figure 5.4. Hydraulic Conductivity Distribution (Cole et al. 2001)

Dispersivity is likely to vary across the Site depending on the degree of heterogeneity and the temporal variability of flow gradients. In the CA, uniform dispersivity values (e.g., longitudinal dispersivity, α_l = 95 m and transverse dispersivity, α_t = 19 m) were used. With the finer mesh used in the current model, dispersivities were reduced to satisfy the grid Peclet number. In 200 West, the area of greatest refinement, a longitudinal dispersivity of 30 m and a transverse dispersivity of 6 m were used for the Ringold Formation. For the other units, a 62.5 m longitudinal dispersivity and a 12.5 m transverse dispersivity were implemented.

5.3 Flow and Transport Parameters for the Streamtube Model

A CFEST simulation of the SGM was used to determine solute transport velocities for the analytical streamtube model described in Section 3.7. A unit point source (1 Ci) simulation was performed to determine velocities, dispersivities, and travel distances to the downstream compliance points (the exclusion boundary and the Columbia River). Because of the uncertainty in the top of the basalt surface in the gap between Gable Mountain and Gable Butte, simulations were performed with two steady-state flow fields representing post-Hanford conditions; one predicting northward flow through the gap, and one predicting eastward flow. A unit source was injected as a pulse over a single time step into four surface nodes at the C Tank Farm. Transient transport based on each flow field was simulated for 500 years, using one-year time steps. Figures 5.5 and 5.6 show the resulting streamlines based on the easterly and northerly flow fields, respectively.

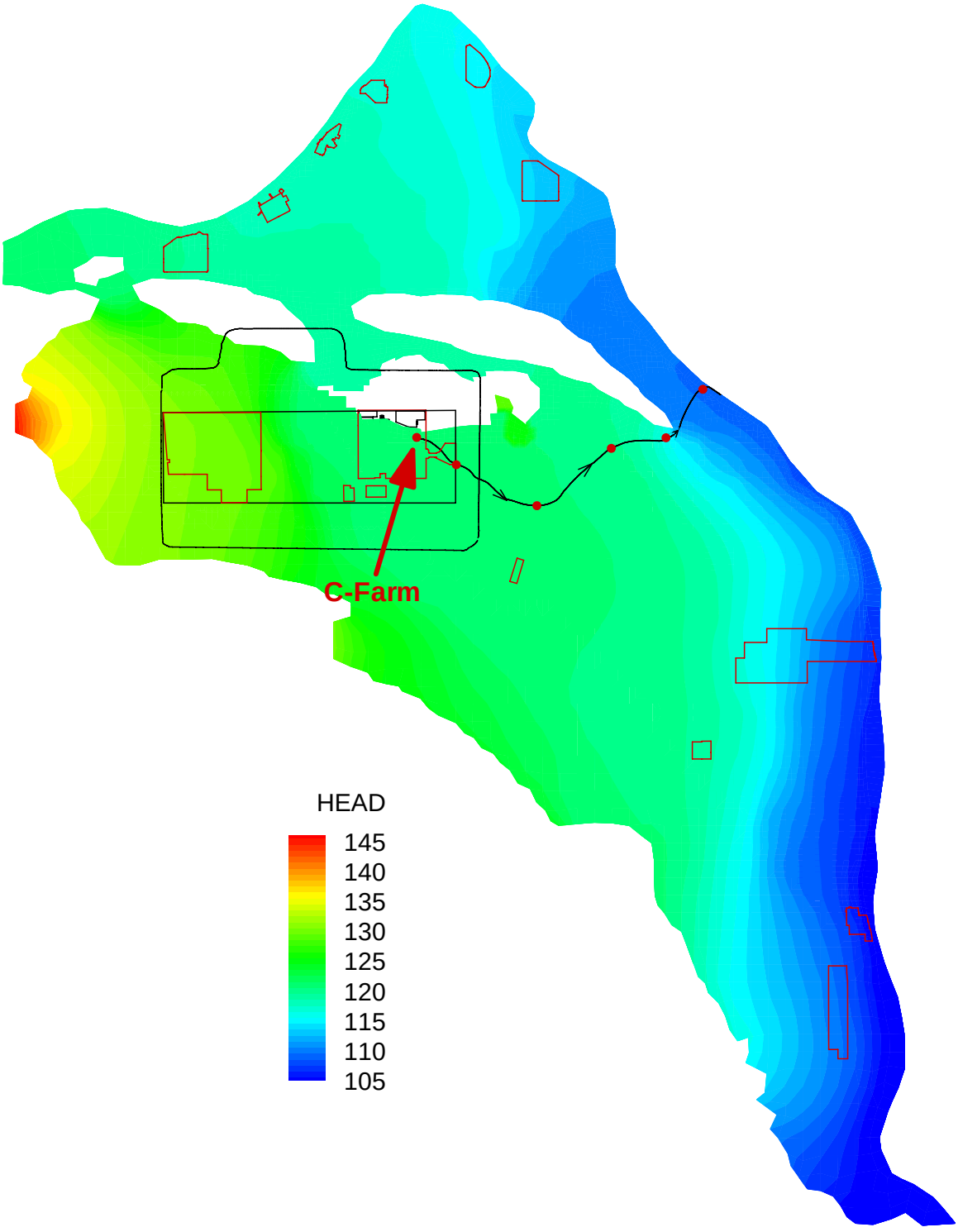

Figure 5.5. Post-Hanford Operations, Steady-State Potentiometric Surface for the SGM Based on an Easterly Flow Assumption and a Streamtrace Along the Peak Concentration Pathway. Red markers on the streamtrace indicate points along which the travel distances were computed.

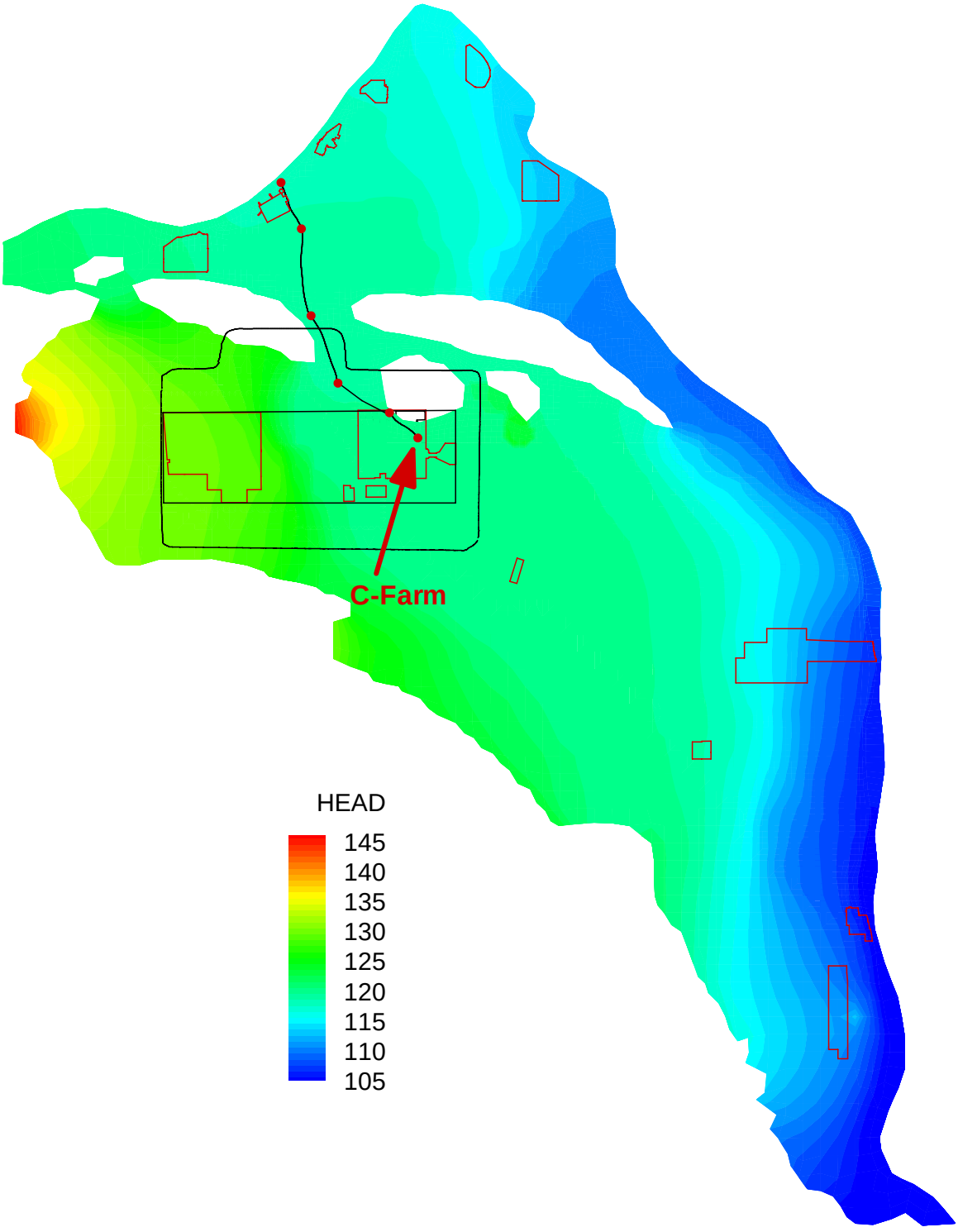

Figure 5.6. Post-Hanford Operations, Steady-State Potentiometric Surface for the SGM Based on a Northerly Flow Assumption and a Streamtrace Along the Peak Concentration Pathway. Red markers on the streamtrace indicate points along which the travel distances were computed.

To determine average flow velocities, the peak concentrations were determined at each of the downstream compliance boundaries based on the unit source simulations. The arrival time of the peak concentrations at the compliance boundaries was assumed to be the travel time from the source. The travel distance was then determined using streamlines generated by Tecplot.(a) Figures 5.5 and 5.6 show the red markers on the streamtrace that were used to calculate travel distances. Because of the circuitous nature of flow, the flow path distance was greater than the straight line distance. Therefore, straight line segments were used to approximate the flow path. The flow velocity was then calculated using the time and distance data for each flow field.

Table 5.1 shows the peak concentrations and arrival times resulting from the unit source simulations using both flow fields. The corresponding BTCs for the exclusion boundary and the Columbia River are shown in Figure 5.7. The shorter distances along the northern pathway to both compliance points resulted in earlier arrival times and higher peak concentrations than the easterly flow path.

Table 5.2 shows the travel distances and velocities determined from the unit source analysis. Also shown are the CFEST dispersivities that were used as inputs to the streamtube model. Because of the shorter distances and arrival times, higher flow velocities result for the northerly flow path.

A test of the analytical model's ability to emulate the transport behavior of the CFEST-based SGM, was conducted using MATHCAD(b) software. This verification is presented in Zhang et al. (2004).

Table 5.1. Arrival Times for a Unit Point Source; Simulated Based on Easterly and Northerly Flow Paths Using the CFEST-Based SGM

Flow	Exclusion Boundary		Columbia River	
	Time (yr)	Conc. (pCi/L)	Time (yr)	Conc. (pCi/L)
Easterly Flow Field	23	7.085	107	1.077E-3
Northerly Flow Field	4	185.359	78	1.804E-2

Table 5.2. Travel Distances, Dispersivities, and Average Velocities for the Streamtube Model

Flow Field	Compliance Points	Distance (km)	Velocity (m/yr)	Longitudinal Dispersivity (m)	Transverse Dispersivity (m)	Vertical Dispersivity (m)
Easterly Flow Field	Exclusion Boundary	2.458	106.87	62.5	12.5	0.0002
	Columbia River	15.829	147.94	62.5	12.5	0.0002
Northerly Flow Field	Exclusion Boundary	1.904	476.04	62.5	12.5	0.0002
	Columbia River	14.950	191.67	62.5	12.5	0.0002

(a) Tecplot Version 10.0, Tecplot, Inc., Bellevue, WA.
(b) MATHCAD 2001i, Mathsoft Engineering & Education, Inc., Cambridge, MA.

a)

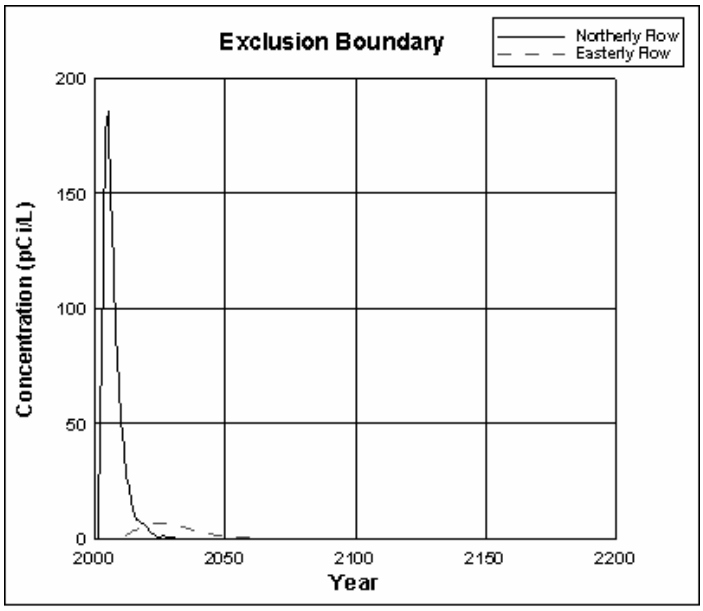

b)

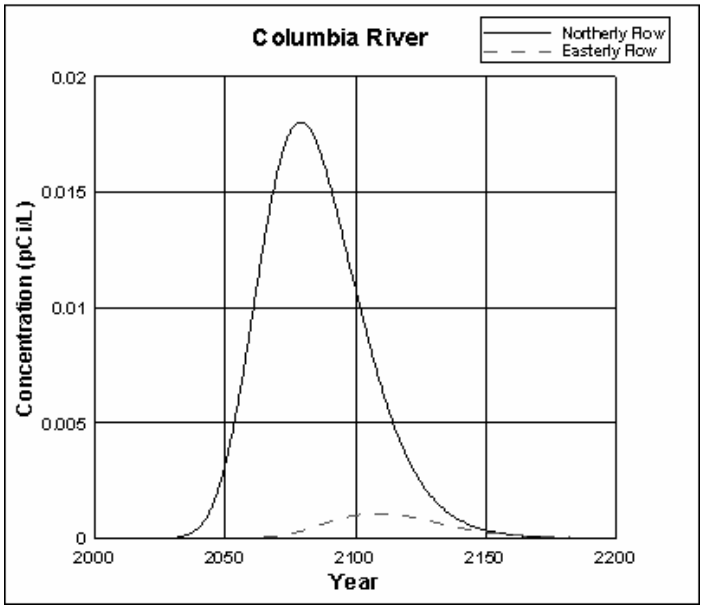

Figure 5.7. Breakthrough Curves for Unit Point Source Release (1 Ci) at a) Exclusion and b) Columbia River Boundaries for the Easterly and Northerly Flow Fields

5.3.1 Modeling Results

Transport of ^{99}Tc through the groundwater was simulated for Case 3 using both the easterly and northerly flow fields. Results of each of these simulations are presented separately, followed by a comparison of results for the two flow pathways.

To simulate the contaminant release in the 14-day, 8,000-gallon potential retrieval leak of Case 3, STOMP mass fluxes were used as input into the CFEST SGM beginning in 2021, the year the fluxes arrived at the water table in the vadose zone simulation. The annual mass fluxes from STOMP were injected as dry mass into four surface nodes at the C Tank Farm. ^{99}Tc transport was simulated for ~500 years using one-year time steps.

5.3.2 Easterly Flow Field Transport Results

The peak concentration and arrival time were identified for the easterly flow path at both the exclusion and Columbia River boundaries. Figure 5.8 shows the BTCs predicted by the CFEST SGM at these boundaries, and Figure 5.9 illustrates the plan view concentration contours at the water table when the peak concentration occurred at the exclusion boundary and the Columbia River. At the downstream compliance points, dilution occurred for both models. As shown in Table 5.3, the peak concentration predicted by the analytical model was only 1.1 times higher at the exclusion boundary than the peak predicted by the SGM. The same was true for the Columbia River (1.1 times). At the Columbia River, both the SGM and the analytical model predicted a ~87% reduction in the peak concentration relative to its peak at the exclusion boundary.

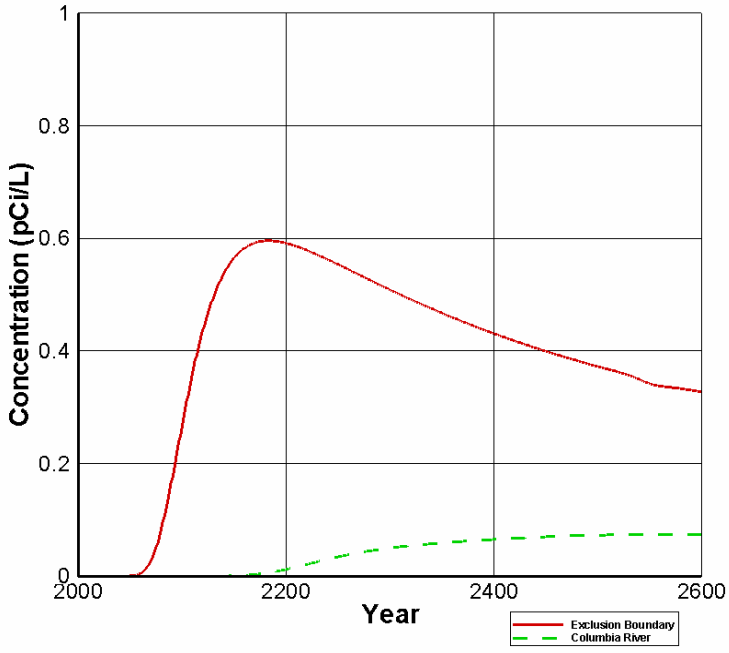

Figure 5.8. Breakthrough Curves Simulated by CFEST SGM Based on Easterly Flow Field at Both Exclusion and Columbia River Compliance Boundaries

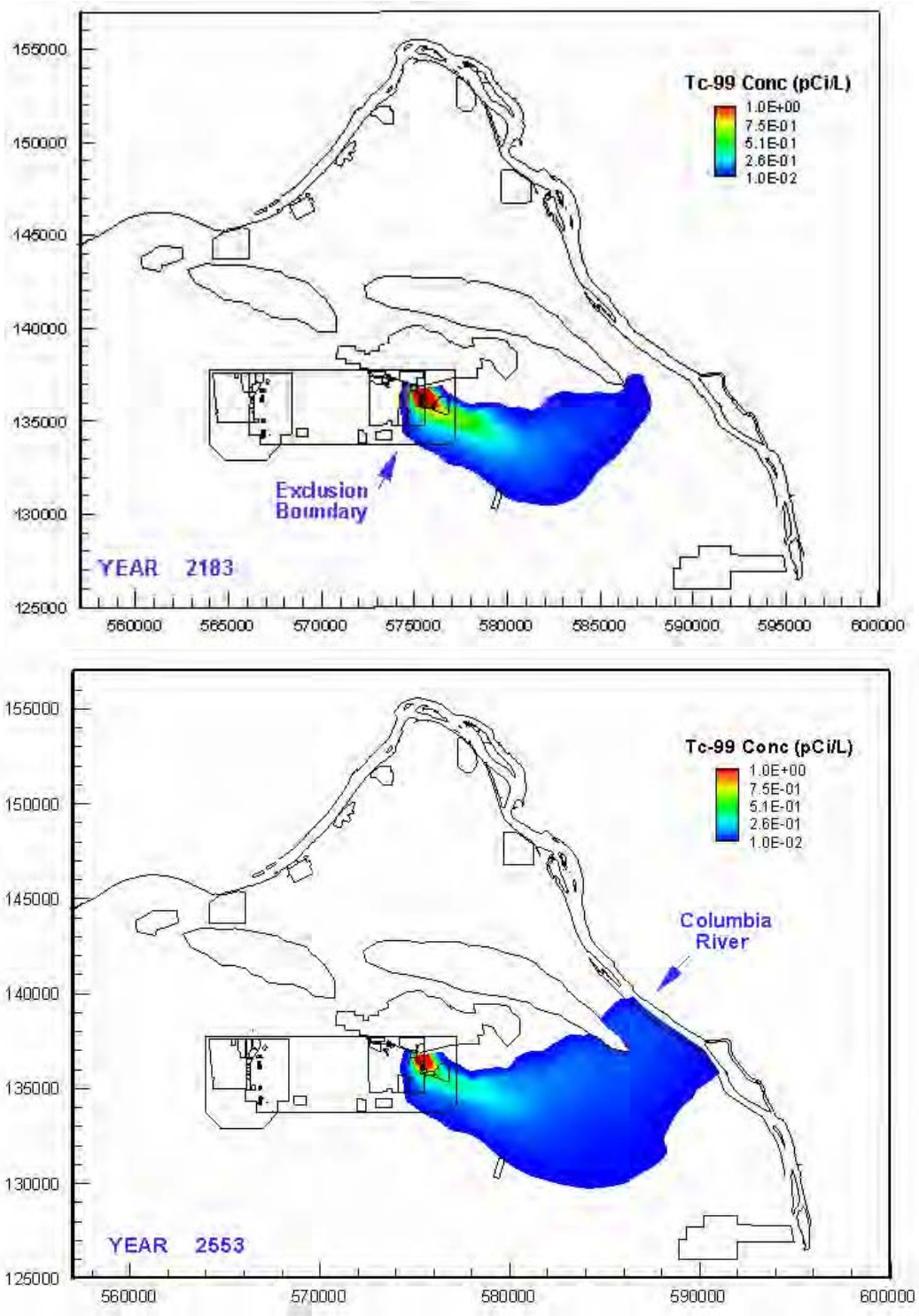

Figure 5.9. Composite SGM Results for Case 3, Easterly Flow Field, Illustrating Plan View Concentration Contours when Peak Concentrations Occurred at Exclusion Boundary (top) and Columbia River (bottom)

Table 5.3. Peak ^{99}Tc Concentrations (pCi/L) at Compliance Points for Case 3, Easterly Flow Field

Models	Exclusion Boundary		Columbia River	
	Time (yr)	Conc (pCi/L)	Time (yr)	Conc. (pCi/L)
Streamtube	2144	0.659	2229	0.083
SGM (CFEST)	2183	0.596	2553	0.074

Because the streamtube model was calibrated with parameters from the SGM, its predictions of peak concentrations were fairly similar to those by CFEST but represented slightly more conservative estimates of the peaks. At the exclusion boundary, the streamtube model predicted that the peak concentration would arrive 39 years earlier than the CFEST based SGM. At the Columbia River boundary, however, the numerical model predicted a much longer delay in the peak concentration arrival time (324 yr). Unlike the streamtube model, the CFEST based SGM simulates vertical transport and transport through geologic heterogeneities. These factors caused more spreading of the contaminant, and therefore delayed the peak arrival time relative to the streamtube prediction.

5.3.3 Northerly Flow Field Transport Results

The peak concentration and arrival time were identified for the northerly flow path at both the exclusion and Columbia River boundaries. Figure 5.10 shows BTCs predicted by the CFEST SGM at both boundaries. The peak concentration at the exclusion boundary occurred near a basalt outcrop where the thickness of the aquifer was only ~3 m (Figure 5.11). Oscillations shown on the rising limb of the breakthrough curve were likely due to these factors.

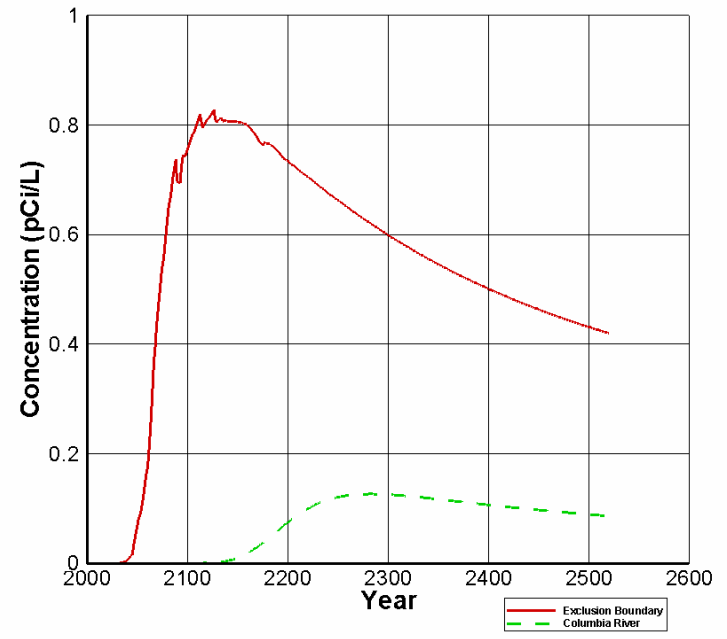

Figure 5.10. BTCs Simulated by CFEST SGM Based on Northerly Flow Field at Both Exclusion and Columbia River Compliance Boundaries

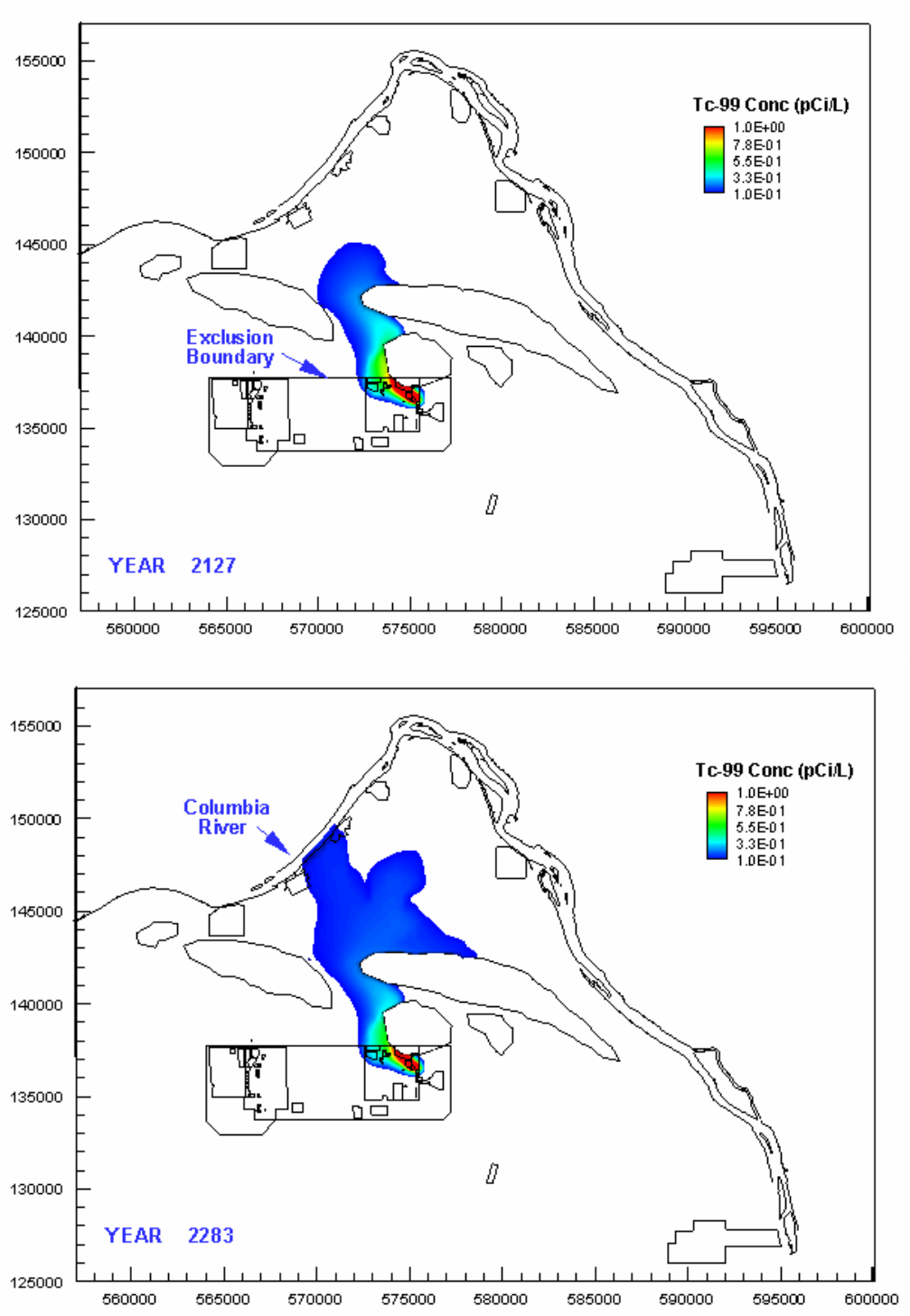

Figure 5.11. Composite SGM Results for Case 3 Northerly Flow Field, Illustrating Plan-View Concentration Contours when Peak Concentrations Occurred at Exclusion Boundary (top) and Columbia River (bottom)

Figure 5.11 illustrates the plan view concentration contours at the water table when the peak concentration occurs at the exclusion boundary and the Columbia River. At the downstream compliance points, dilution occurred in both models. As shown in Table 5.4, the peak concentration predicted by the analytical model was 2.7 times less at the exclusion boundary than predicted by the SGM. At the Columbia River, the peak predicted by the analytical model was also 2.7 times lower than predicted by the SGM.

At the Columbia River, the analytical model predicted a ~75% reduction in the peak concentration relative to the exclusion boundary. The SGM predicted a larger reduction (~91%) because it can simulate three-dimensional transport. Estimates of the arrival times were more conservative in the streamtube model but differed only by three years at the exclusion boundary and 84 years at the Columbia River.

Table 5.4. Peak ^{99}Tc Concentrations (pCi/L) at Compliance Points for Case 3, Northerly Flow Field

Models	Exclusion Boundary		Columbia River	
	Time (yr)	Conc (pCi/L)	Time (yr)	Conc. (pCi/L)
Streamtube	2124	0.306	2199	0.075
SGM (CFEST)	2127	0.828	2283	0.126

5.3.4 Comparison of Northerly and Easterly Flow Paths

The results of both the unit release and retrieval leak simulations demonstrate that the SGM predicts earlier arrival times and higher peak concentrations along the northerly flow path than on the easterly path. For example, the retrieval leak simulation predicted peak concentrations that were approximately 40% higher at the exclusion boundary and more than 70% higher at the Columbia River along the northern flow path. Arrival times were more than 50 years earlier at the northern exclusion boundary and nearly 250 years earlier at the Columbia River. Differences in arrival times for the unit release simulation were less dramatic, differing by ~20 years at the exclusion boundary and ~30 years at the Columbia River. Peak concentrations, however, were much higher along the northern flow path, with peaks that were 26 times and 17 times higher at the exclusion and Columbia River boundaries, respectively.

The continuous release simulated with the retrieval leak sources showed that contaminant loading had a significant effect on both peak concentrations and arrival times. With the unit release simulation, contaminants tended to move along pathways of higher conductivity that reduced travel times along both flow paths. In the retrieval leak simulation, more spreading occurred with higher contaminant load, causing more dilution of peak concentrations and a longer delay at the downstream compliance boundaries.

An important difference in the predictions of the numerical and analytical models is the relative magnitude in the peak concentrations predicted along both of the flow paths. Although for both models the peak arrival times are earlier along the northerly flow path, the peak concentrations predicted by the streamtube model are higher along the easterly flow path. In the SGM, peak concentrations are lower on the easterly flow path than they are to the north. This latter result is consistent with theoretical expectation as faster groundwater velocities generally predict higher concentrations. The results of the analytical model are contrary to this expectation due to a limitation in its ability to predict contaminant spreading. In the streamtube model, the higher the velocity, the higher the dispersion (Eq. 3.17). This higher dispersivity over-predicted contaminant spreading and dilution relative to the SGM.

6.0 Electronic Files

The principal objectives of this investigation were to conduct the simulations and analyses using an open scientific approach and to provide modeling results that could be verified and repeated. In partial fulfillment of these objectives, the source coding for the STOMP simulator, ancillary utilities coding, input files, simulation output files, and converted result files is provided in electronic form with enough detail to enable the reported calculations to be repeated. This section describes the directory structure and contents of the files stored in electronic format.

6.1 Source Coding

Source code for the STOMP simulator is stored in the "stomp_src" directory. Ancillary utilities are stored in the "source" directory. The STOMP source code is in the file "stomp1_sp.f" and comprises a main calling routine and subroutines listed in alphabetical order. The STOMP source code can be compiled with a FORTRAN 77 compiler, which includes the files "parameters" and "commons." The "parameters" file was dimensioned for all of the simulations. Once compiled, the STOMP simulator must be linked with the "splib.a" library configured for a particular compiler. Files and instructions needed to create the "splib.a" library are included in the file "splib.tar.gz." The location of source coding for the various conversion and translations utilities used during these investigations is shown in Table 6.1.

Table 6.1. Source Code Directory

Program Name	Source Code File	Auxiliary Files	Functions
STOMP	stomp1_sp.f	commons, parameters	Simulate both flow and transport in the vadose zone and unconfined aquifer below the tank farm
Complinkit			Shell script to compile stomp1_sp.f and statically link it to splib.a, libblas.a
Total_flux	total_flux.f90		Modify STOMP surface file so that cumulative flux is continuous between stages 1 and 2
Surfcalc	surfcalc.c		Calculate solute concentration at the water table and fenceline
PlotTec	plot_tec.f		Convert the STOMP plot files to TecPlot readable format
Point3d_disp	point3d_disp.f		Simulate transport in an aquifer, point3d_disp_slib.x.2d, point3d_disp_slib.x.3d
Mass_bal	mass_bal.f90		Calculate and tabularize mass balance of each simulation
Peak_conc	peak_conc.f90		Tabularize peak concentrations at each of the compliance points
Peak_flux	peak_flux.f90		Tabularize peak fluxes at each of the water table and the fenceline

6.2 Geology

Zonation files to define the rock/soil-type and inactive-node distributions were provided with the MDP (Khaleel et al. 2003). These lithologic descriptions were based on inferences drawn from groundwater monitoring wells near the C Tank Farm and from grain size data and supplemented by information from tank farm drywells and excavation (e.g., Price and Fecht 1976a, 1976b). Zonation files are stored in the individual case directories as well as the geology directory. Within the zonation file is information on the inactive nodes that define the tanks and cross-section boundaries. Rock/soil zonation files can be visualized as two-dimensional color-scaled images with Tecplot by opening the layout file for the cross section.

6.3 Steady Flow Simulations

A steady flow simulation was executed to generate initial condition flow fields for each of the transient solute transport simulations. This simulation is found in the "case00" directory and was executed with the STOMP simulator, which produced a "restart" file that described the steady flow field. The input, output, and restart files are catalogued in Table 6.2.

Table 6.2. Steady Flow Initial Condition Files

File Name	Description	File Type
input	STOMP input file	Text
output	STOMP reference-node output file	Text
plot	STOMP plot-file output file	Text
restart	STOMP restart file	Text

6.4 Coupled Vadose Zone and Unconfined Aquifer Modeling

Coupled vadose zone and unconfined aquifer modeling files are stored in directories named according to case number (e.g., directory "case01" holds files associated with the Case 1 simulations). Within the case directories, a subdirectory named base contains the base-case simulation. Also within the case directories, at the same level as the base directory, subdirectories exist for each of the sensitivity cases investigated. A high and low subdirectory exists within each sensitivity subdirectory for the upper and lower bounds simulations. Table 6.3 identifies the directory name for each of the sensitivity cases.

Table 6.3. Case Directory Names Used for the Sensitivity Cases

Directory Name	Sensitivity Cases
Recharge	Preclosure Recharge Rate
Barrier	Barrier Recharge Rate
barrier_deg	Degraded Barrier Recharge Rate
ksat_aq	Aquifer Hydraulic Conductivity
ksat_vz	Vadose Zone Saturated Hydraulic Conductivity
Plume	Initial Plume Depth for Past Leak Scenario
Diffusion	Diffusion coefficient for Diffusion Release Scenario

Within the base and high and low directories is a run directory named "2000to12032." This subdirectory holds the input files, zonation files, reference-node output files, plot-file output files, and surface-flux output files. Also within the case directories are subdirectories containing converted plot-file output, Tecplot layout files, solute concentration and mass flux data files, and images. Flux and concentration time series data are contained in the "btc" subdirectory, whereas the "tecplot" subdirectory contains encapsulated postscript (eps) and portable network graphics (*.png) images of concentration and saturation distributions in the cross section for distinct points in time. Table 6.4 summarizes the naming conventions for the files stored under each of these directories.

To distinguish concentration data for ^{238}U with a source at Tank C-112, the notation u_K_d was used; e.g., for files containing data on ^{238}U with K_d = 0.01 mL/g, u_0.01 was used in the filename (Table 6.4).

Table 6.4. Coupled Vadose Zone and Unconfined Aquifer Modeling Files

File Name	Description	File Type	Subdirectory
Input	STOMP simulator input	Text	2000to12032
Output	STOMP simulator reference-node output	Text	2000to12032
fn.srf(a)	STOMP simulator surface-flux output	Text	2000to12032
p#.plt(b)	Tecplot data file for color-scale images of plot-file output	Tecplot binary	tecplot
yr_type_*.eps(c,d)	Image file showing concentration or saturation profiles at distinct points in time	Text/Image	tecplot/eps
yr_type_*.png(c,d)	Image file showing concentration or saturation profiles at distinct points in time	Image	tecplot/png
prepsurf_fenceline.csh	C-Shell script for computing BTCs at the fenceline	Text	2_btc/scripts
prepsurf_gwtable.csh	C-Shell script for computing BTCs at the groundwater table	Text	2_btc/scripts
*_location_mf.dat(d)	Solute mass flux breakthrough data at the fenceline	Text	btc
*_location_c.dat(d)	Solute concentration breakthrough data at the fenceline	Text	btc
*_c.btc(d)	Solute concentration and mass flux breakthrough data at the water table, fenceline and downstream compliance points	Text	btc
*_location_mf.eps(d,e)	Mass flux breakthrough curve (encapsulated postscript file) generated using rungnu.csh	Text/Image	btc
*_location_mf.eps(d,e)	Image file containing mass flux breakthrough curves (generated using rungnu.csh)	Text/Image	btc
*_direction_c.dat(d,f)	Solute concentration breakthrough data 4 m from the source release	Text	btc

(a) *fn* is the user-defined filename.
(b) *#* is the plot file number indicator (e.g., plot.175, plot.3462).
(c) *yr* represents the calendar year plotted in the image file.
(d) * is the plot variable [e.g., sat (saturation), ac_tc (aqueous conc tc), vc_U_0.10 (u total conc w/ K_d =0.10].
(e) *Location* represents the fenceline or the gwtable (groundwater table) locations.
(f) *Direction* is north, south, east or west.

For each transient flow and solute transport simulation, the STOMP simulator read an input file, restart file, zonation file, and solute inventory file and generated one reference-node output file, one or more plot-file output files, and one or more surface-flux output files. The STOMP-generated plot-file output files were converted to Tecplot ASCII format using the PlotTec utility. These ASCII files, when visualized through Tecplot, were used to generate color-scaled images of saturation and solute concentration for selected points in time.

The STOMP-generated surface-flux output files were translated to ASCII mass flux and concentration text format using prepsurf.c and combobtc.c utilities. These programs are archived in the "source" directory. The files generated from execution of these utilities contain aqueous volumetric flux and solute mass flux at the groundwater and fenceline boundaries with the groundwater for each simulation year.

Plot-file output can be viewed as color-scaled, two-dimensional images by viewing the encapsulated postscript file. Surface-flux output and breakthrough curves can be viewed as plots using standard graphing software (e.g., gnuplot, Excel) for the cross section of interest. Reference-node data can be viewed by editing the reference-node output file.

6.5 Analytical Groundwater Transport Modeling

C-Shell scripts for running the analytical model and generating plots are archived in the "2_btc" directory and listed in Table 6.5. The master script (runallmodels.csh) executes a series of C-Shell scripts to generate breakthrough curves at the downstream compliance points. These scripts (runpoint.csh) contain flow-path length, velocity, and hydraulic parameters. The analytical model script creates output files for each species that contains the time and calculated concentrations at each compliance point in columns. Additional scripts were developed and archived in the case directories for generating plots from the analytical results (runcombo.csh and rungnu.csh). These scripts were executed for each case directory to generate the encapsulated postscript files for the plots found in the appendixes of this report.

6.6 Appendixes

STOMP runs and all of the post processing steps can be executed using the shell scripts described in this section, and each of these steps may be executed individually at the command line to obtain the vadose zone and streamtube modeling results and graphics. To provide further automation to the processing, R scripts were developed to provide a "wrapper" to the existing programs. R was used to simplify and generalize the selection of specific steps and cases for execution and provide all necessary intermediate steps with a single command line execution. The actual computations at each of the processing steps described previously were accomplished with the existing C and FORTRAN programs and shell, Tecplot, and Gnuplot scripts. A few additional processing steps were included in the R scripts, such as restart simulations to capture spatial output in the year the peak concentration occurred and generating appendixes.

Once simulations were completed, the R script run_cases.r was executed to restart the STOMP simulations to capture spatial concentration distributions for the year ^{99}Tc peak concentrations occurred. The script each_case.r was called by run_cases.r to execute the following steps: 1) convert the surface flux output file format using the surfaceTo.pl and outputTo.pl Perl scripts; 2) read the surface flux files

Table 6.5. Analytical Groundwater Transport Modeling Files

File Name[(a)]	Description	File Type	Subdirectory
runallmodels.csh	C-Shell script for executing series of C-Shell scripts used to generate breakthrough curves	C-Shell (text)	2_btc
runpoint.csh	C-Shell script for executing the analytical model (includes model parameters)	C-Shell (text)	2_btc/scripts
runcombo.csh	C-Shell script for combining breakthrough data at the groundwater table, fenceline, exclusion boundary, and Columbia River into one file	C-Shell (text)	2_btc/scripts
run_gnu.csh	C-Shell script for generating breakthrough curve plot files	C-Shell (text)	2_btc/scripts
riv_thrugap_*.btc	Solute-concentration breakthrough data at the Columbia River for the flow path through the gap	Text	btc
exc_thrugap_*.btc	Solute-concentration breakthrough data at the exclusion boundary for the flow path through the gap	Text	btc
riv_sgap_*.btc	Solute-concentration breakthrough data at the Columbia River for the flow path south of the gap	Text	btc
exc_sgap_*.btc	Solute-concentration breakthrough data at the exclusion boundary for the flow path south of the gap	Text	btc
all_*_thrugap.dat	Solute-concentration breakthrough data at all compliance points for the groundwater flow path north and thru the gap	Text	btc
all_*_sgap.dat	Solute-concentration breakthrough data at all compliance points for the groundwater flow path south of the gap	Text	btc
*_thrugap_c.eps	Image file containing concentration breakthrough curve data at the groundwater, fenceline, exclusion boundary, and Columbia River for the flow path through the gap	Text/image	btc
*_sgap_c.eps	Image file containing concentration breakthrough curve data at the groundwater, fenceline, exclusion boundary, and Columbia River for the flow path south of the gap	Text/Image	btc
(a) * indicates the solute species (e.g., u_K_d, tc).			

and determine the year of maximum ^{99}Tc concentration at the fenceline; 3) identify the appropriate STOMP restart file; 4) create new STOMP input files; 5) run STOMP; 6) convert plot files to Tecplot format and create a batch file to run tecplot to produce the concentration distribution plots near and at the year the peak occurred. Script each_case.r also has additional functions such as checking and waiting, if necessary, for an available Tecplot license, timing the processing, and recording progress in a log file.

The third R script, create_appendixes2.r, was used to assemble graphics and create the appendixes as a single .pdf file. This script starts with a section for initialization, including switches for selecting different plots, and concludes with a loop for generating a separate appendix for each case. Most of the processing in this script sets up the figure callouts and captions in the document LaTeX file, *appendix_all.tex*.

The LaTeX processing and conversion to .pdf format is also handled in the script. A nice feature of LaTeX is the availability of automated, hyperlinked contents lists. The reader may use these hyperlinks in the .pdf file to conveniently navigate onscreen.

R is essentially an expanded and open source version of the commercially distributed S-plus, the statistics, graphing, and general purpose programming environment. R is a mature, well-supported, and documented product available at no cost for all of the usual operating systems (http://www.R-project.org). Help in using R can be found within the program and in Venables and Smith (2001), Krause and Olson (2000), and Venables and Ripley (1999, 2000). The R script can be executed two ways: 1) from the R shell or 2) direct from the command line. For method 1, start R by entering R at the command line, then enter 'source ("run_cases.r").' For method 2, enter the following at the command line: 'R –slave –no-save < run_cases.r.'

C-Shell scripts for generating the tabularized data found in the appendixes in this report are archived in the "3_tables" directory and listed in Table 6.6. The master script (runtables.csh) executes a series of C-Shell scripts that execute FORTRAN 90 programs (see Table 6.1) for tabularizing data. These scripts (peakconc.csh, peakflux.csh and massbal.csh) generate peak concentration, peak mass flux, and mass balance tables to be imported into excel spreadsheets.

Table 6.6. Post-Processing Scripts

File Name	Description	File Type	Subdirectory
run_cases.r	Loop through subcases requiring processing	R (text)	scripts
each_case.r	Perform desired processing on each subcase, including running of STOMP around the year of peak concentration and generating color contour plots of concentration	R (text)	scripts
create_appendixes2.r	Assemble desired figures, generate call-outs and captions, run LaTeX, and create final PDF file	R (text)	scripts
surfaceTo.pl	C-Shell script for generating BTC plot files	Perl (text)	scripts
outputTo.pl	Solute-concentration breakthrough data at the Columbia River for the flow path through the gap	Perl (text)	scripts
runtables.csh	C-Shell script for executing series of C-Shell scripts used to generate tabular data	C-Shell (text)	3_tables
peakconc.csh	C-Shell script that tabularizes peak concentration data	C-Shell (text)	3_tables
peakflux.csh	C-Shell script that tabularizes peak mass flux data	C-Shell (text)	3_tables
massbal.csh	C-Shell script that tabularizes mass balance data	C-Shell (text)	3_tables

7.0 References

Baetslé LH. 1969. "Migration of radionuclides in porous media." *Progress in Nuclear Energy Series XII, Health Physics*, AMF Duhamel, ed. Pergamon Press, Elmsford, New York, pp. 707–730.

Bergeron MP and SK Wurstner. 2000. *Groundwater Calculations Supporting the 2001 Immobilized Low-Activity Waste Disposal Facility Performance Assessment at the Hanford Site in Southeastern Washington*. PNNL-13400, Pacific Northwest National Laboratory, Richland, Washington.

Bergeron MP, E Freeman, S Wurstner, CT Kincaid, FM Coony, D Strenge, R Aaberg, and P Eslinger. 2001. *Addendum to Composite Analysis for Low-Level Waste Disposal in the 200 Area Plateau of the Hanford Site*. PNNL-11800-Addendum 1, Pacific Northwest National Laboratory, Richland, Washington.

Bramley R and X Wang. 1995. *SPLIB: A Library of Iterative Methods for Sparse Linear Systems*. Indiana University, Bloomington.

Cole CR, MP Bergeron, SK Wurstner, PD Thorne, S. Orr, and MI McKinley. 2001. *Transient Inverse Calibration of Hanford Site-Wide Groundwater Model to Hanford Operational Impacts—1943 to 1996*. PNNL-13447, Pacific Northwest National Laboratory, Richland, Washington.

Cole CR, SK Wurstner, MP Bergeron, MD Williams, and PD Thorne. 1997. *Three-Dimensional Analysis of Future Groundwater Flow Conditions and Contaminant Plume Transport in the Hanford Site Unconfined Aquifer System: FY 1996 and 1997 Status Report.* PNNL-11801, Pacific Northwest National Laboratory, Richland, Washington.

Domenico PA and FW Schwartz. 1990. *Physical and Chemical Hydrogeology*. John Wiley & Sons, New York, pp. 824.

Freedman, VL, MW Williams, CR Cole , MD White, and MP Bergeron. 2002. *2002 Initial Assessments for B-BX-BY Field Investigation Report (FIR): Numerical Simulations*. PNNL-13949, Pacific Northwest National Laboratory, Richland, Washington.

Gardner WR. 1958. "Some Steady-State Solutions of the Unsaturated Moisture Flow Equation with Applications to Evaporation from a Water Table." *Soil Science*, 85:228-232.

Gelhar LW. 1993. *Stochastic Subsurface Hydrology*. Prentice Hall, Englewood Cliffs, New Jersey.

Gelhar, LW and CL Axness. 1983. "Three-dimensional stochastic analysis of macrodispersion in aquifers." *Water Resources Research*, 19:161–180.

Gelhar LW, C Welty, and KR Rehfeldt. 1992. "A critical review of data on fieldscale dispersion in aquifers." *Water Resources Research*, 28:1955–1974.

Gupta SK, CR Cole, CT Kincaid, and AM Monti. 1987. *Coupled Fluid, Energy, and Solute Transport (CFEST) Model: Formulation and User's Manual.* BMI/ONWI-660, Battelle Memorial Institute, Columbus, Ohio.

Gupta SK. 1996. *Draft User's Manual, CFEST-96 Flow and Solute Transport, Constant/Variable Density, Computationally Efficient, and Low Disk PC/Unix Version.* Environmental System Technologies, Irvine, California.

Hartman MJ. 2000. *Hanford Site Groundwater Monitoring: Setting, Sources and Methods*. PNNL-13080, Pacific Northwest National Laboratory, Richland, Washington.

Kaplan DI, J Conca, RJ Serne, TW Wietsma, AT Owen, and TL Gervais. 1996. *Radionuclide Adsorption Distribution Coefficients Measured in Hanford Sediments for the Low Level Waste Performance Assessment Project*. PNNL-11485, Pacific Northwest National Laboratory, Richland, Washington.

Khaleel R, JF Relyea, and JL Conca. 1995. "Evaluation of van-Genuchten-Mualem relationships to estimate unsaturated conductivity at low water contents." *Water Resources Research*, 31:2659-2668.

Khaleel R and JF Relyea. 1997. "Correcting laboratory-measured moisture retention data for gravels." *Water Resources Research*, 33:1875-1878.

Khaleel R and MP Connelly. 2003. *Modeling Data Package for an Initial Assessment of Closure for S-SX Tank Farm.* RPP-17209 Rev. 0, CH2M HILL Hanford Group, Inc., Richland, Washington.

Kincaid CT, JW Shade, GA Whyatt, MG Piepho, K Rhoads, JA Voogd, JH Westsik Jr, MD Freshley, KA Blanchard, and BG Lauzon. 1995. *Performance Assessment of Grouted Double-Shell Tank Waste Disposal at Hanford*. WHC-SD-WM-EE-004 Rev. 1, Westinghouse Hanford Company, Richland, Washington.

Kincaid CT, MP Bergeron, CR Cole, MD Freshley, NL Hassig, VG Johnson, DI Kaplan, RJ Serne, GP Streile, DL Strenge, PD Thorne, LW Vail, GA Whyatt, and SK Wurster. 1998. *Composite Analysis for Low-Level Waste Disposal in the 200-Area Plateau of the Hanford Site.* PNNL-11800, Pacific Northwest National Laboratory, Richland, Washington.

Krause A and M Olson. 2000. T*he Basics of S and S-plus*, 2nd edition. Springer, New York.

Lindsey KA and KD Reynolds. 2001. *Vadose Zone Geology of Boreholes 299-E33-45 and 299-E33-46 B-BX-BY Waste Management Area, Hanford Site, South-Central Washington.* RPP-8681 Rev. 0, CH2M HILL Hanford Group, Inc., Richland, Washington.

Mann FM, RJ Puigh II, SH Finfrock, EJ Freeman, R Khaleel, DH Bacon, MP Bergeron, BP McGrail, and SK Wurstner. 2001. *Hanford Immobilized Low-Activity Tank Waste Performance Assessment, 2001 Version*. DOE/ORP-2000-24, U.S. Department of Energy Office of River Protection, Richland, Washington

Millington RJ and JP Quirk. 1961. "Permeability of Porous Media." *Nature*, 183:387-388.

Mualem Y. 1976. "A New Model for Predicting the Hydraulic Conductivity of Unsaturated Porous Media." *Water Resources Research*, 12:513-522.

Polmann DJ. 1990. *Application of Stochastic Methods to Transient Flow and Transport in Heterogeneous Unsaturated Soils*. Ph.D. Thesis, Massachusetts Institute of Technology, Cambridge.

Price WH and KR Fecht. 1976a. *Geology of the 241-S Tank Farm*. ARH-LD-133, Atlantic Richfield Hanford Company, Richland, Washington.

Price WH and KR Fecht. 1976b. *Geology of the 241-SX Tank Farm*. ARH-LD-134, Atlantic Richfield Hanford Company, Richland, Washington.

Russo D. 1993. "Stochastic modeling of macrodispersion for solute transporting a heterogeneous unsaturated porous formation." *Water Resources Research*, 29:383–397.

Talbott ME and LW Gelhar. 1994. *Performance Assessment of a Hypothetical Low-Level Waste Facility: Groundwater Flow and Transport Simulation.* NUREG/CR-6114 Vol. 3, U.S. Nuclear Regulatory Commission, Washington, D.C.

van Genuchten MT. 1980. "A Closed-Form Equation for Predicting the Hydraulic Conductivity of Unsaturated Soils." *Soil Science Society of America Journal*, 44:892-898.

Venables W and B Ripley. 1999. *Modern Applied Statistics with S-plus*, 3rd edition. Springer, New York.

Venables W and B Ripley. 2000. *S Programming*. Springer, New York.

Venables W and D Smith. 2001. *An Introduction to R.* Network Theory Limited, Bristol, UK.

Ward AL, RE Clayton, and JC Ritter. September 1998. *Hanford Low-Activity Tank Waste Performance Assessment Activity: Determination of In Situ Hydraulic Parameters of Hanford Sediments.* A letter report for activity Task 4b submitted to the Lockheed Martin Hanford Company, Richland, Washington.

Washington State Department of Ecology, U.S.Environmental Protection Agency, and U.S. Department of Energy. 1989, as Amended Through December 31, 1998. *Hanford Federal Facility Agreement and Consent Order*. 89-10 Rev. 5, Ecology, EPA, and DOE, Olympia, Washington.

White MD and M Oostrom. 2000a. *STOMP Subsurface Transport Over Multiple Phases, Version 2.0, Theory Guide*. PNNL-12030, Pacific Northwest National Laboratory, Richland, Washington.

White MD and M Oostrom. 2000b. *STOMP Subsurface Transport Over Multiple Phases, Version 2.0, User's Guide*. PNNL-12034, Pacific Northwest National Laboratory, Richland, Washington.

White MD, M Oostrom, MD Williams, CR Cole and MP Bergeron. 2001. *FY00 Initial Assessments for S-SX Field Investigation Report (FIR): Simulations of Contaminant Migration with Surface Barriers*. PNWD-3111, Pacific Northwest National Laboratory, Richland, Washington.

Wurstner SK, PD Thorne, MA Chamness, MD Freshley, and MD Williams. 1995. *Development of a Three-Dimensional Groundwater Model of the Hanford Site Unconfined Aquifer System: FY 1995 Status Report*. PNL-10886, Pacific Northwest Laboratory, Richland, Washington.

Yeh TCJ, LW Gelhar and AL Gutjahr. 1985. "Stochastic Analysis of Unsaturated Flow in Heterogeneous Soils, 2. Statistically Anisotropic Media with Variable α." *Water Resources Research*, 21:457-464.

Zhang ZF, VL Freedman, and MD White. 2003. *2003 Initial Assessments of Closure for the C Tank Farm: Numerical Simulations.* PNNL-14334. Pacific Northwest National Laboratory, Richland, Washington.

Zhang ZF, VL Freedman, SR Waichler, and MD White. 2004. *Initial Assessments of Closure for S-SX Tank Farm: Numerical Simulations*. PNNL-14604, Pacific Northwest National Laboratory, Richland, Washington.

C Tank Farm Simulations
Contour and BTC Plots

List of Figures

Appendix A

C Farm Saturation Contour Plots

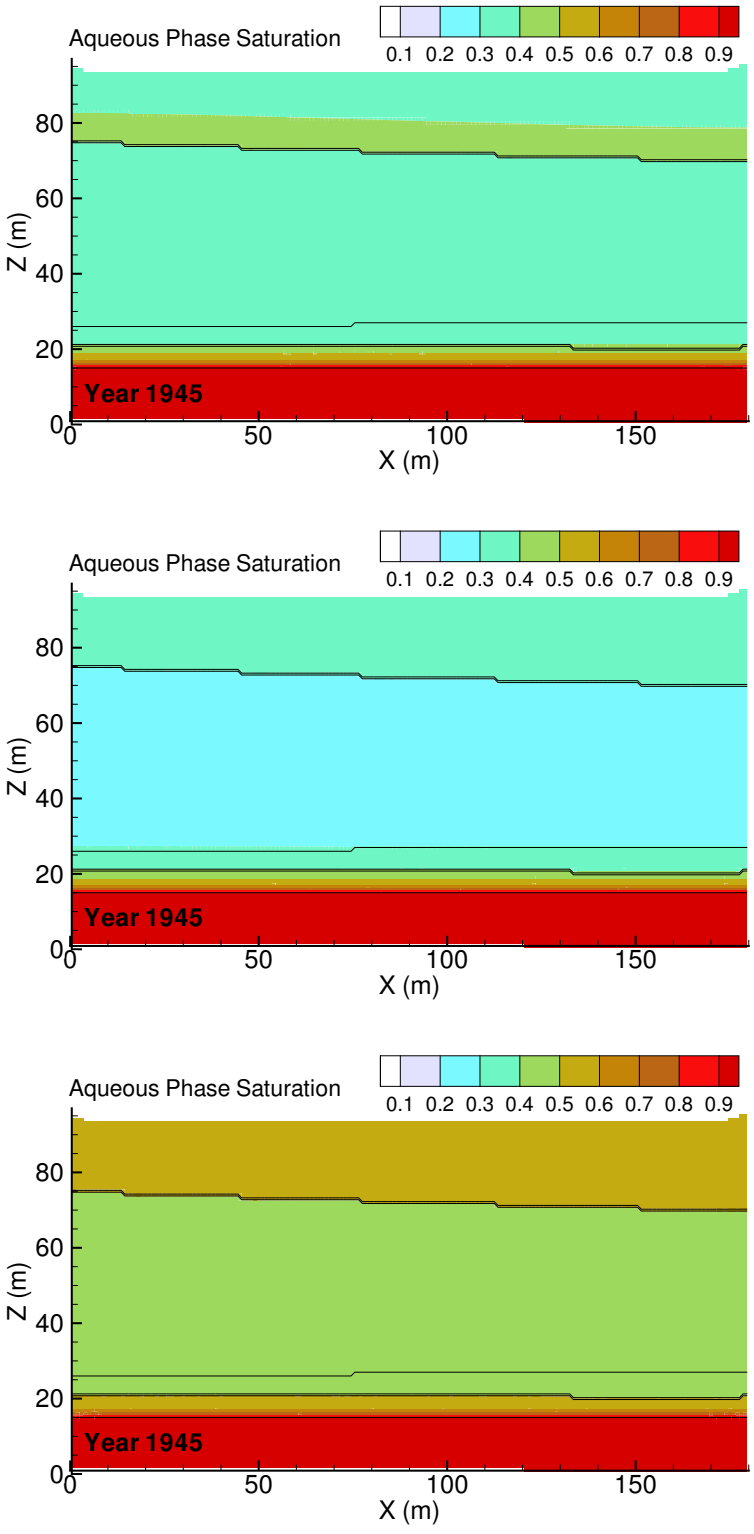

Figure A.1. Pre-Hanford operations saturation distribution at year 1945 for (a) Base Case, (b) High Vadose Zone Hydraulic Conductivity ($K_{sat} \times 10$) and (c) Low Vadose Zone Hydraulic Conductivity ($K_{sat} \times 0.1$).

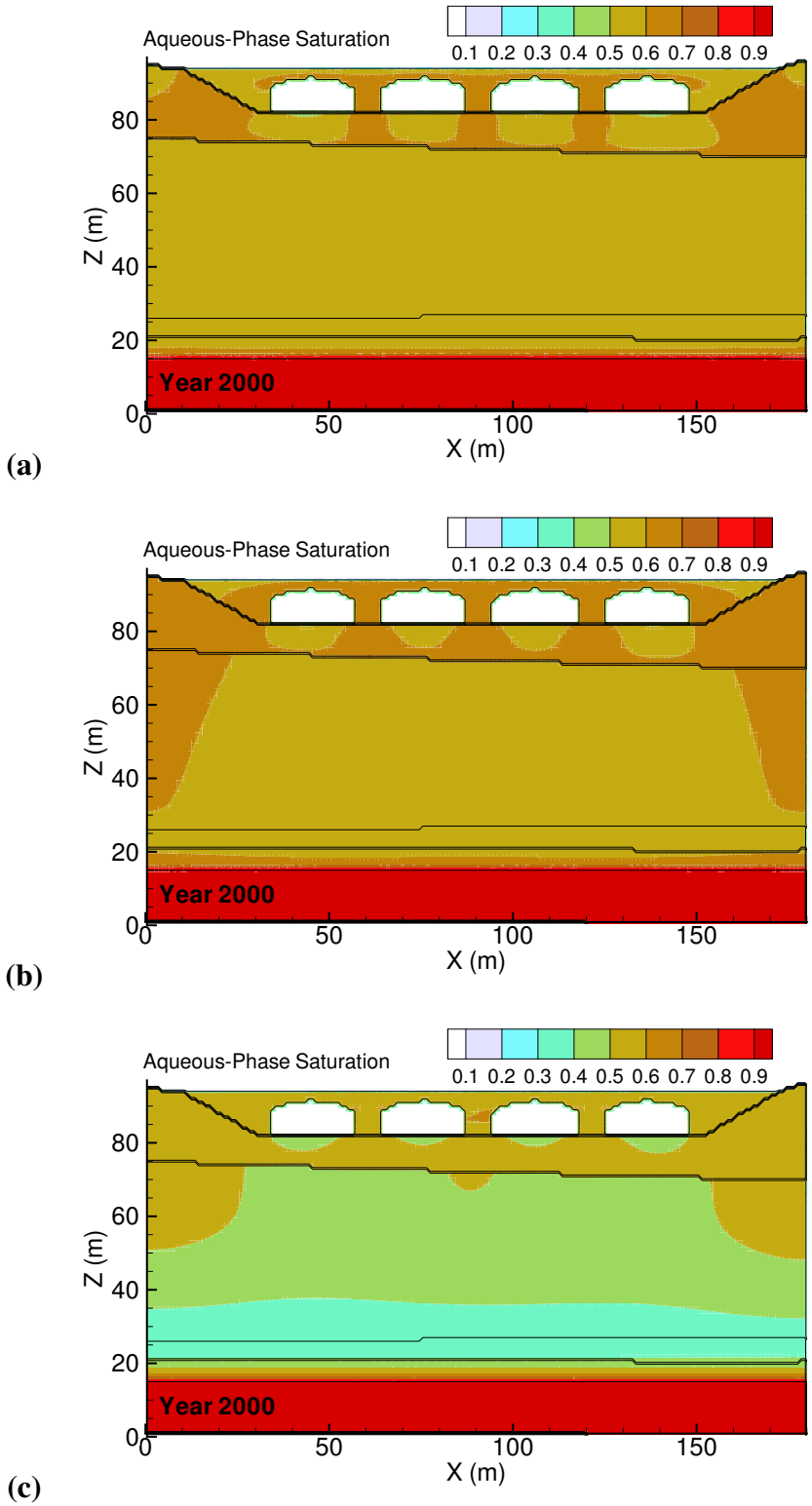

Figure A.2. Preclosure saturation distribution at year 2000 for (a) Base Case, (b) High Preclosure Recharge Rate (140 mm/yr) and (c) Low Preclosure Recharge Rate (40 mm/yr).

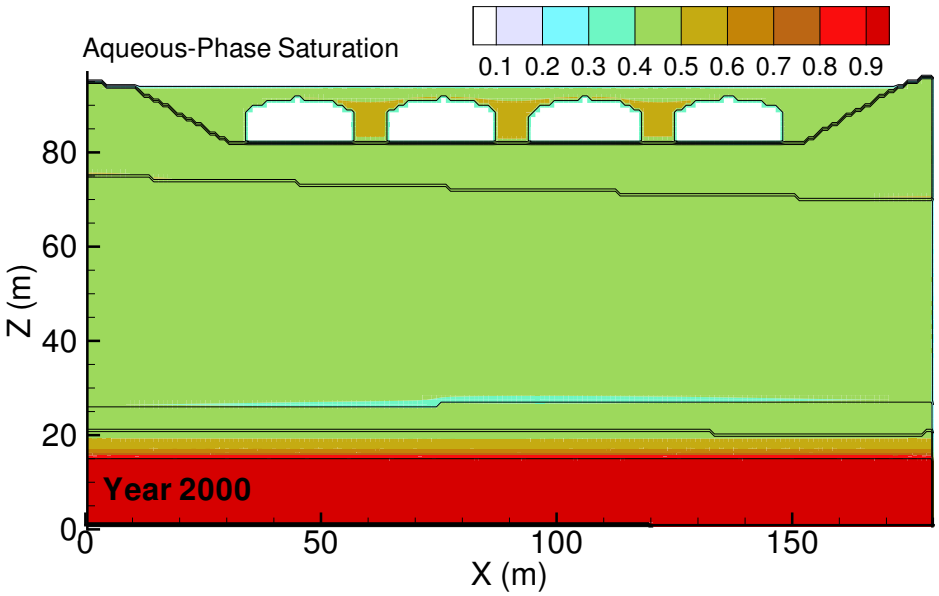

(a)

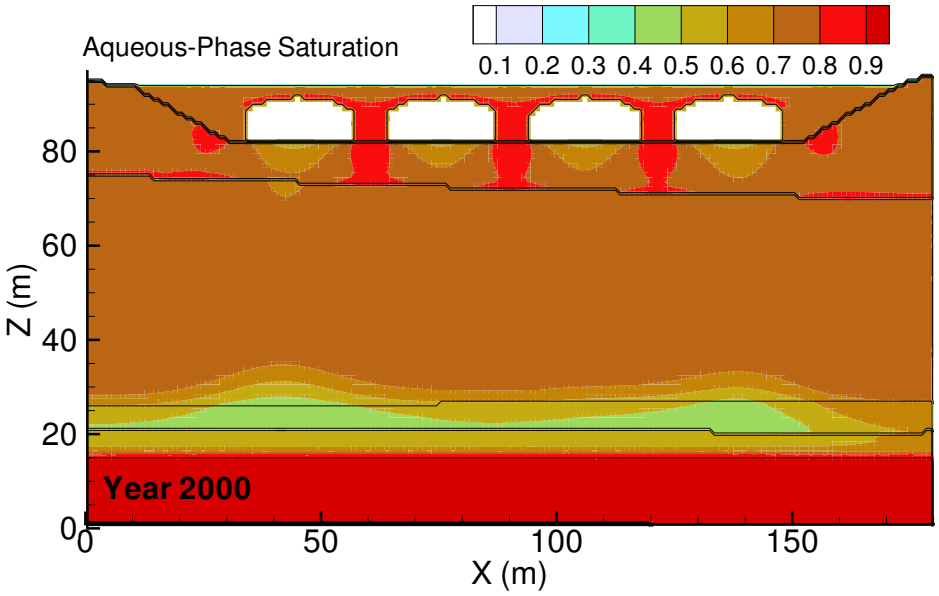

(b)

Figure A.3. Preclosure saturation distribution at year 2000 for (a) High Vadose Zone Hydraulic Conductivity ($K_{sat} \times 10$) and (b) Low Vadose Zone Hydraulic Conductivity ($K_{sat} \times 0.1$).

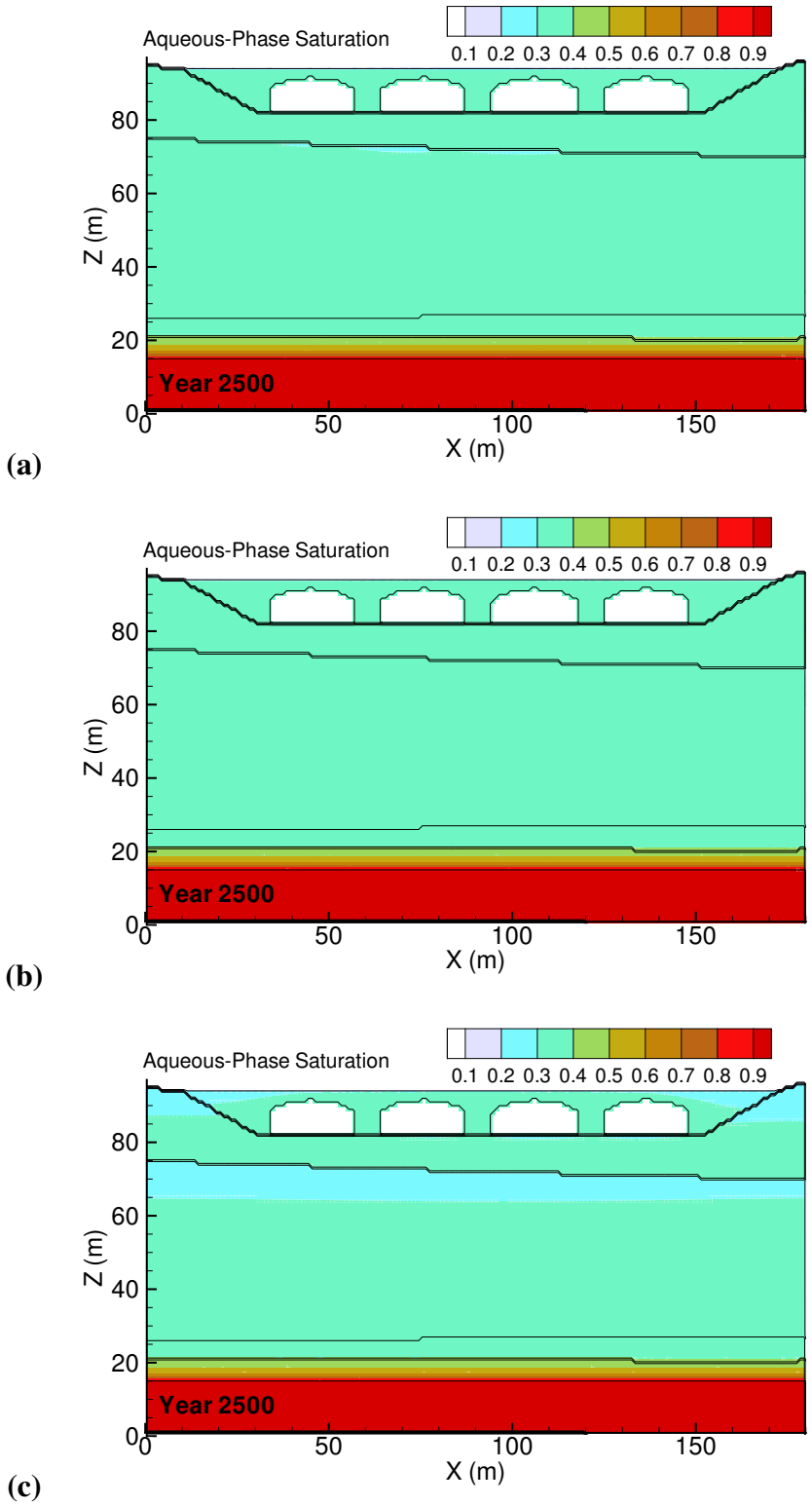

Figure A.4. Barrier saturation distribution at year 2500 for (a) Base Case, (b) High Barrier Recharge Rate (1.0 mm/yr) and (c) Low Barrier Recharge Rate (0.1 mm/yr).

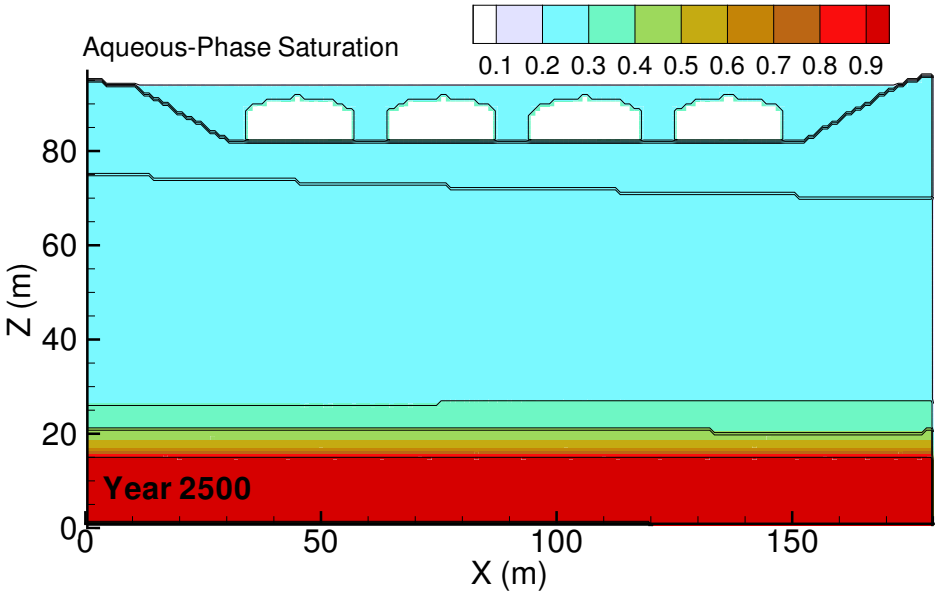

(a)

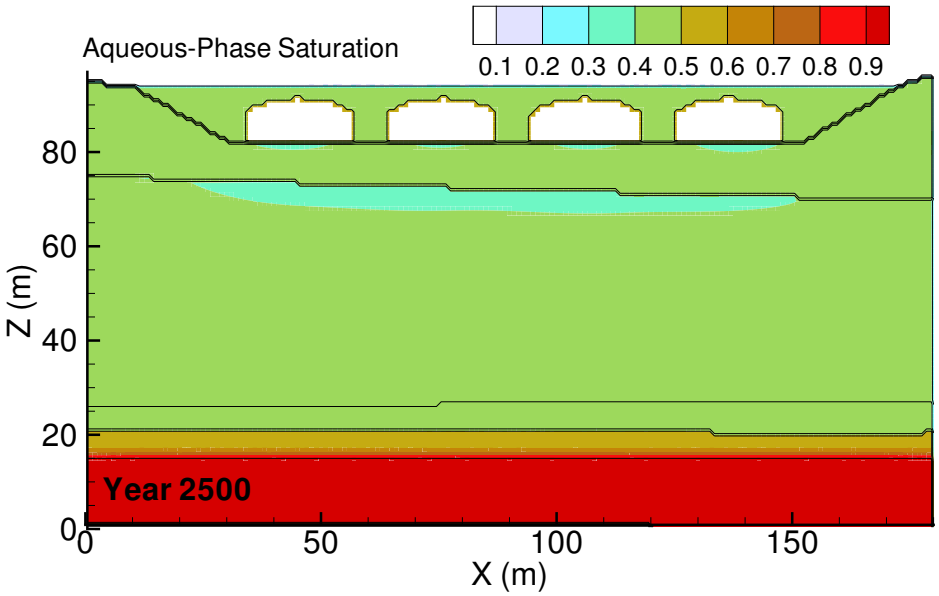

(b)

Figure A.5. Barrier saturation distribution at year 2500 for (a) High Vadose Zone Hydraulic Conductivity ($K_{\text{sat}} \times 10$) and (b) Low Vadose Zone Hydraulic Conductivity ($K_{\text{sat}} \times 0.1$).

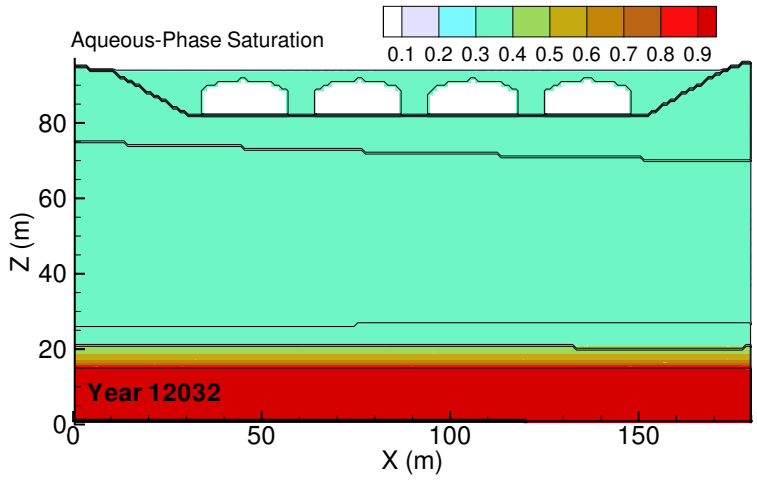

(a)

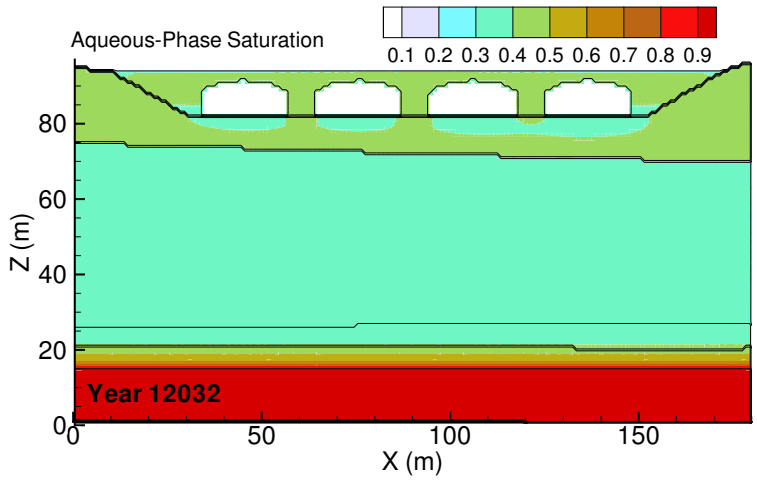

(b)

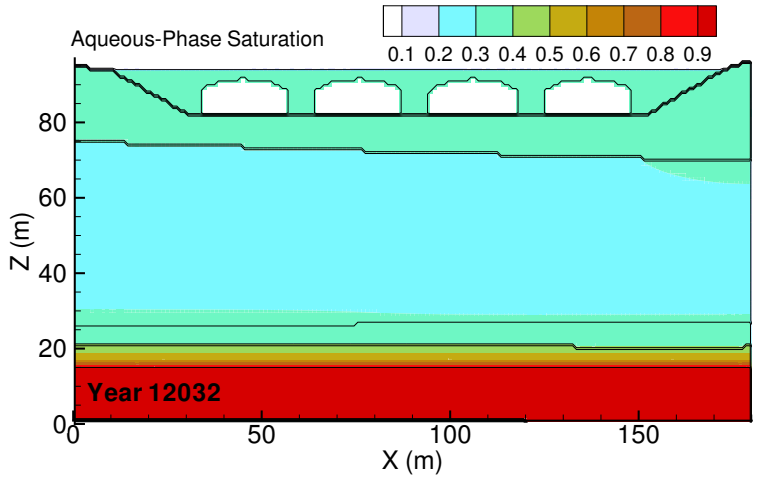

(c)

Figure A.6. Degraded Barrier saturation distribution at year 12032 for (a) Base Case, (b) High Degraded-Barrier Recharge Rate (3.5 mm/yr) and (c) Low Degraded-Barrier Recharge Rate (0.5 mm/yr).

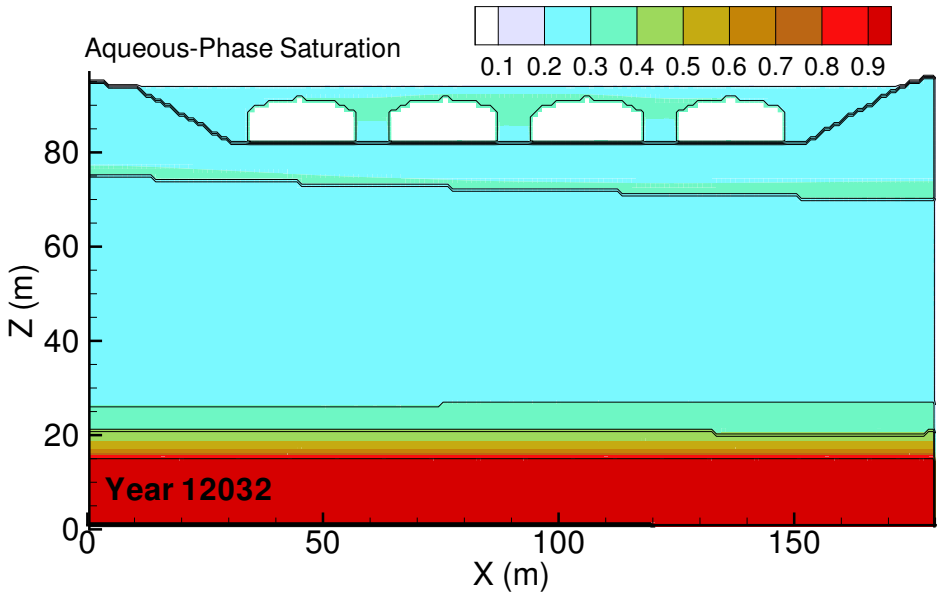

(a)

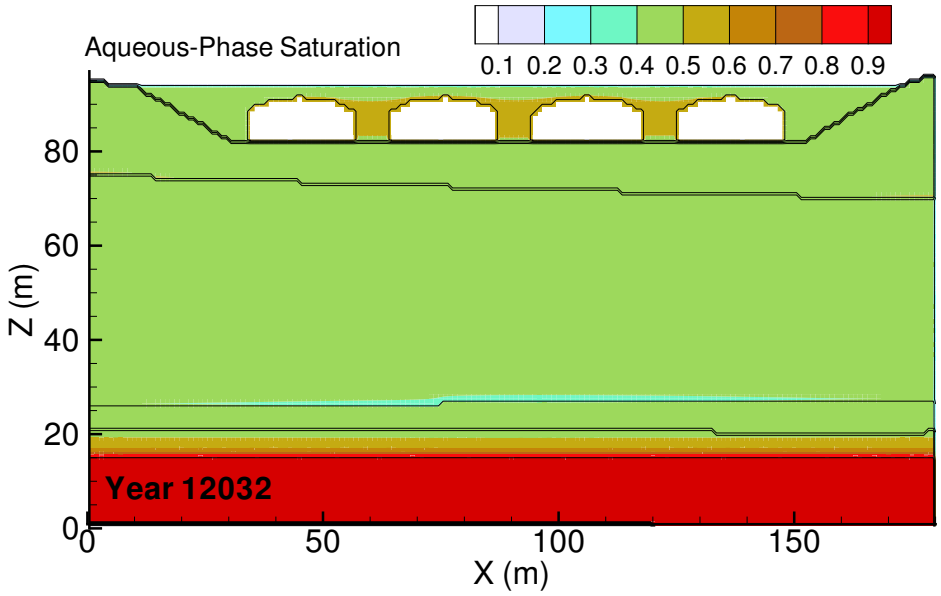

(b)

Figure A.7. Degraded Barrier saturation distribution at year 12032 for (a) High Vadose Zone Hydraulic Conductivity ($K_{sat} \times 10$) and (b) Low Vadose Zone Hydraulic Conductivity ($K_{sat} \times 0.1$).

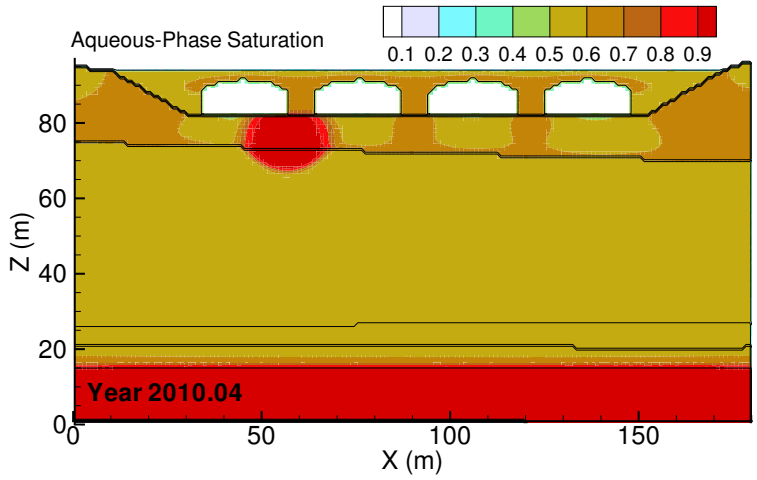

(a)

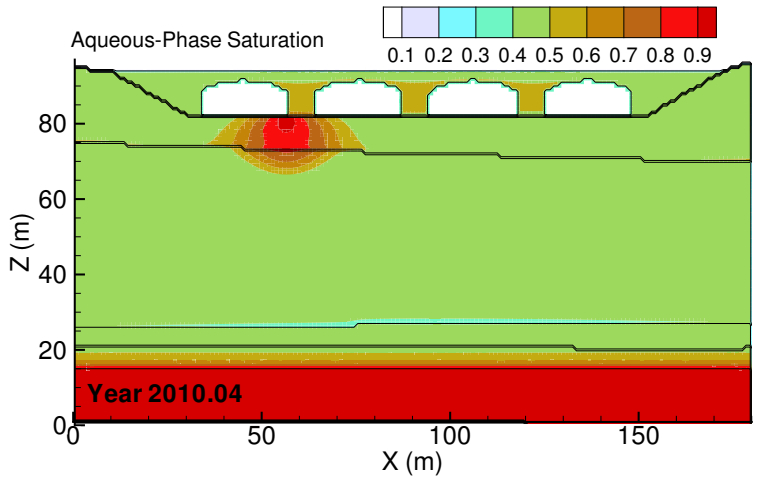

(b)

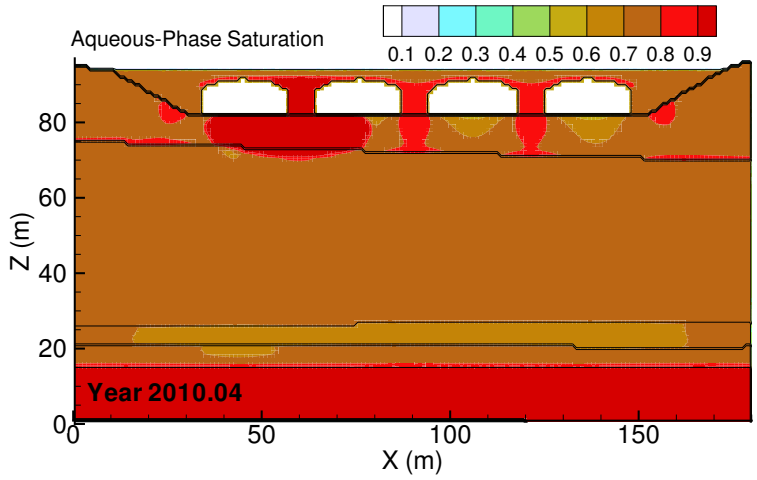

(c)

Figure A.8. Preclosure saturation distribution after retrieval leak at year 2010.04 for (a) Base Case, (b) High Vadose Zone Hydraulic Conductivity ($K_{\text{sat}} \times 10$) and (c) Low Vadose Zone Hydraulic Conductivity ($K_{\text{sat}} \times 0.1$).

Appendix B

C Farm Past Leak

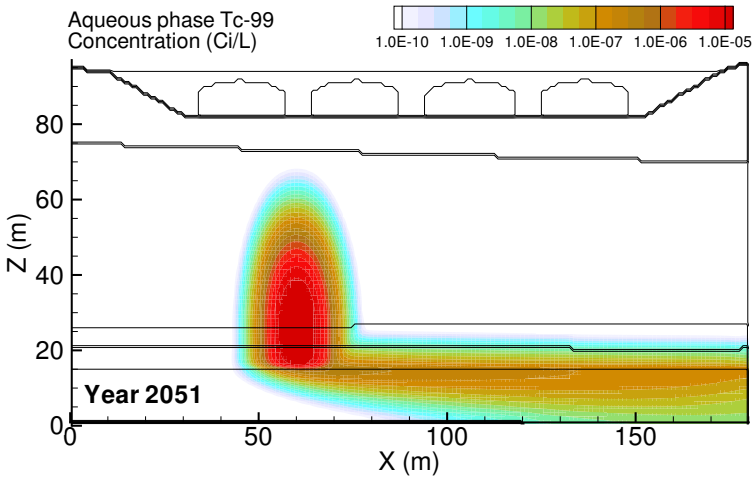

(a)

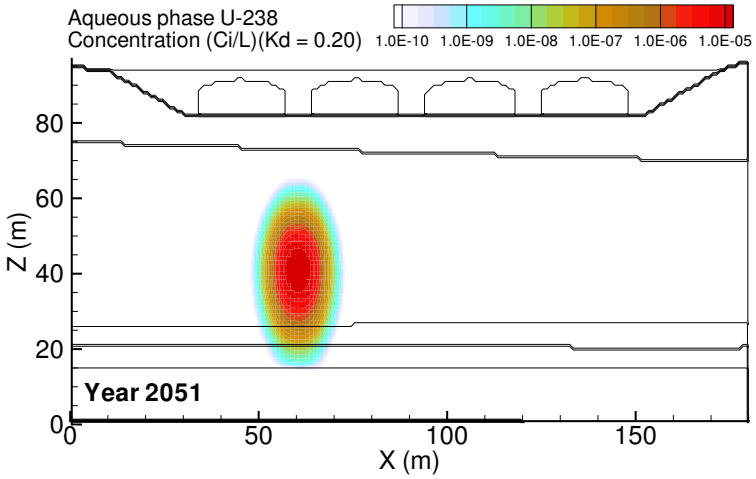

(b)

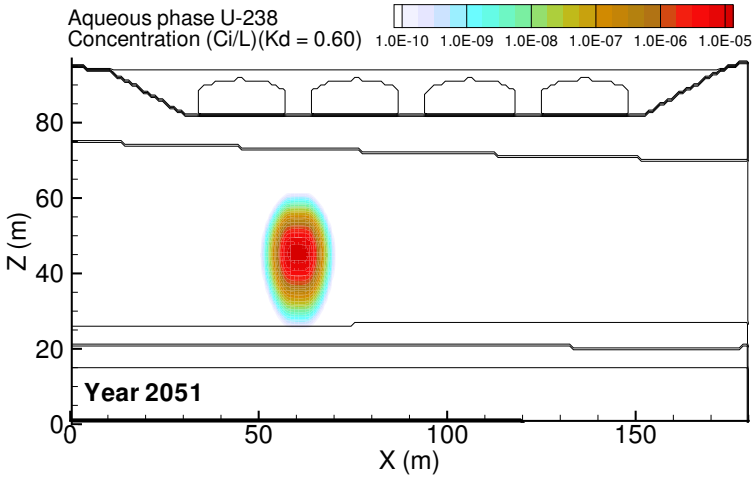

(c)

Figure B.1. Past Leak: Base Case aqueous concentration distributions at year 2051 for (a) Tc-99, (b) U_0.20 and (c) U_0.60. Year of Tc-99 peak concentration at fenceline was 2051.

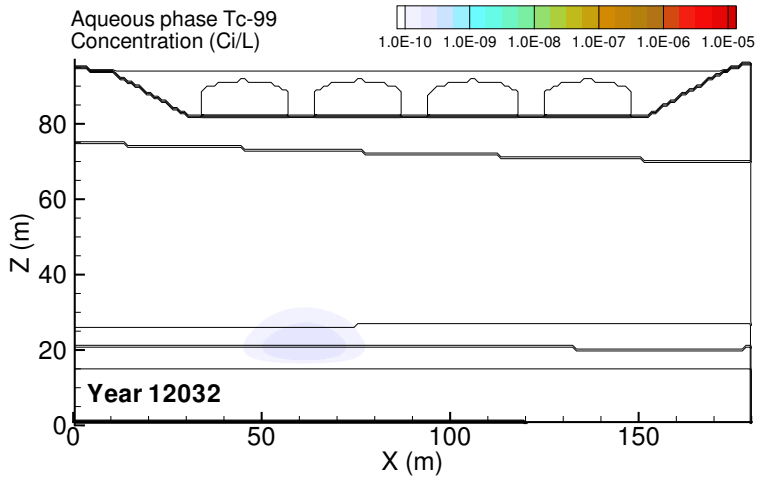

(a)

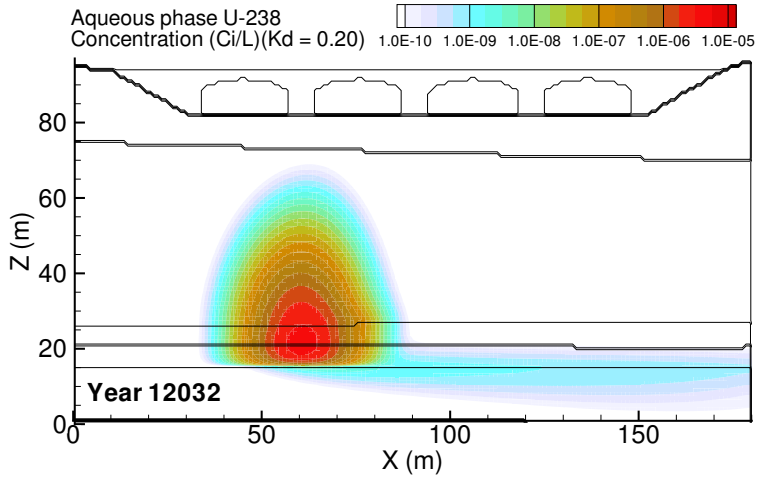

(b)

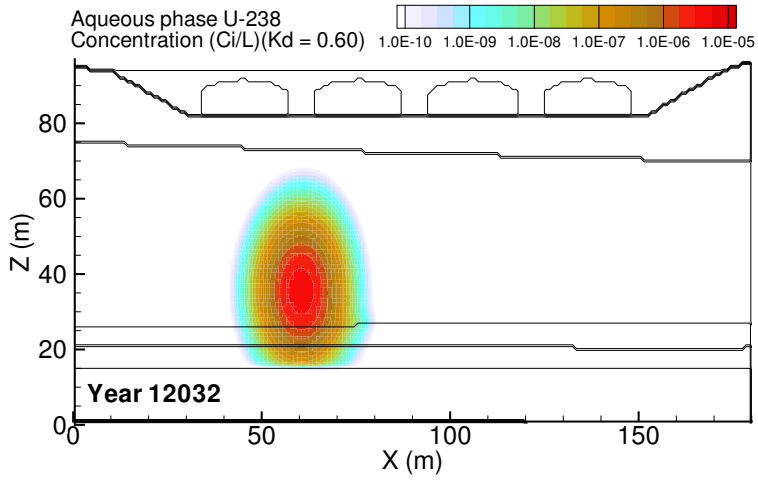

(c)

Figure B.2. Past Leak: Base Case aqueous concentration distributions at year 12032 for (a) Tc-99, (b) U_0.20 and (c) U_0.60.

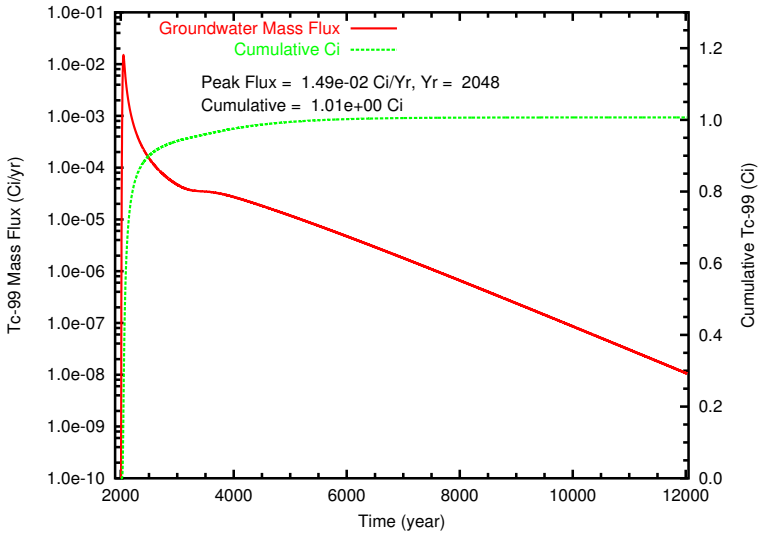

(a)

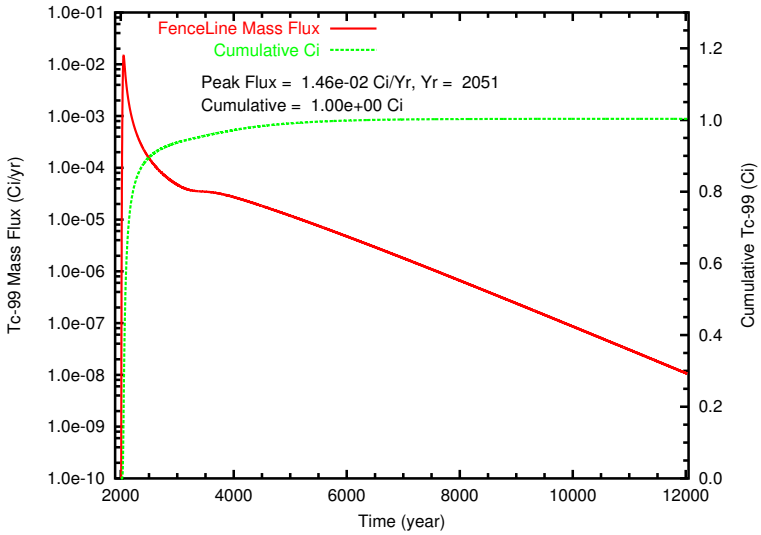

(b)

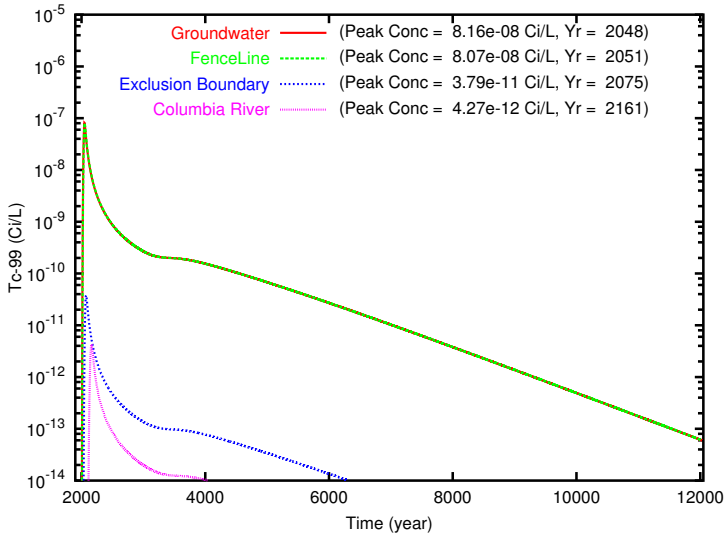

(c)

Figure B.3. Past Leak: Base Case Tc-99 mass flux at (a) the groundwater table and (b) the fenceline; and (c) the Tc-99 concentration at groundwater, fenceline, and easterly downstream compliance points.

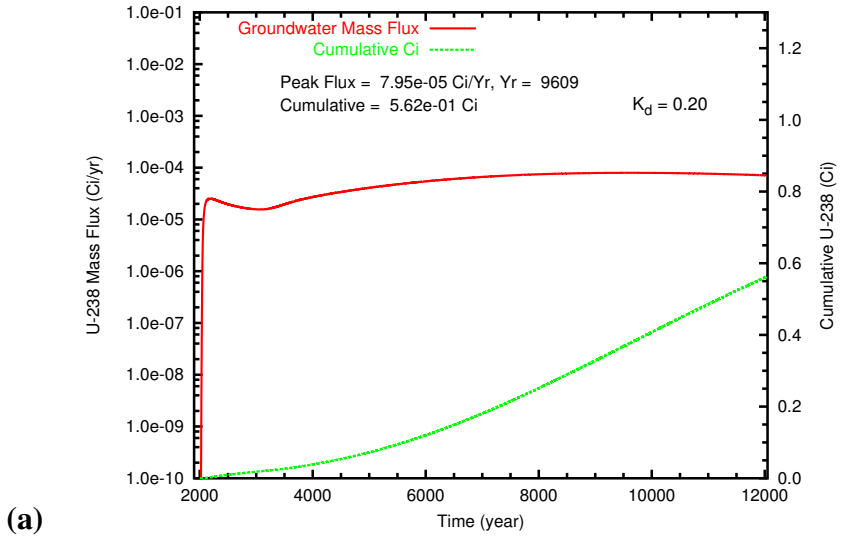

(a)

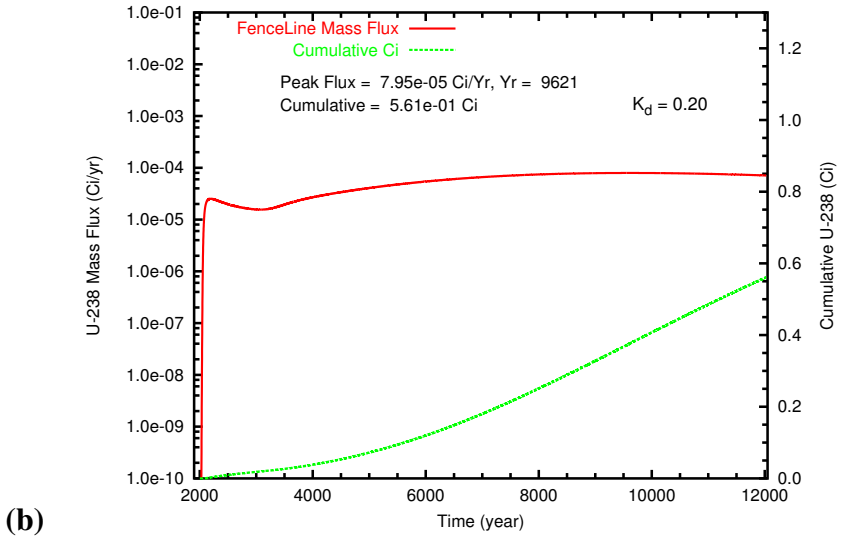

(b)

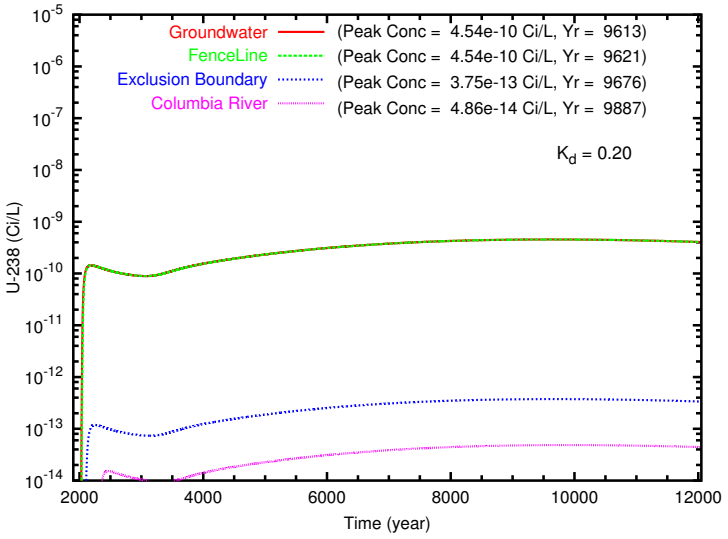

(c)

Figure B.4. Past Leak: Base Case U_0.20 mass flux at (a) the groundwater table and (b) the fenceline; and (c) the Tc-99 concentration at groundwater, fenceline, and easterly downstream compliance points.

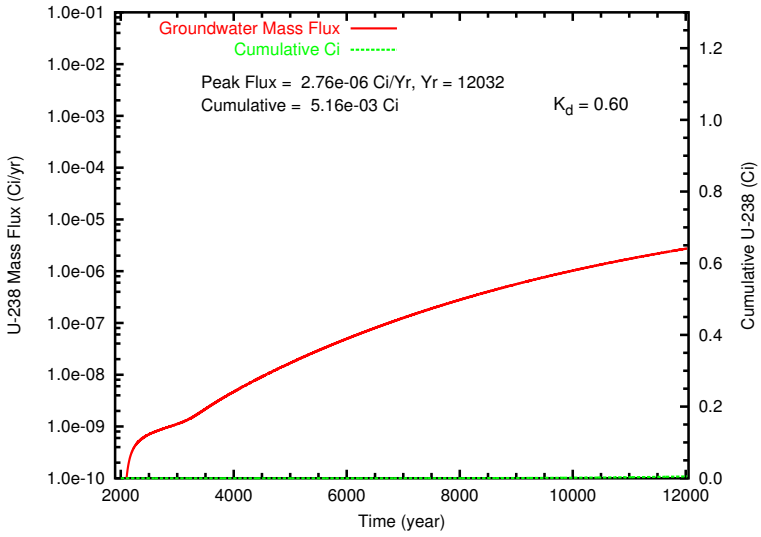

(a)

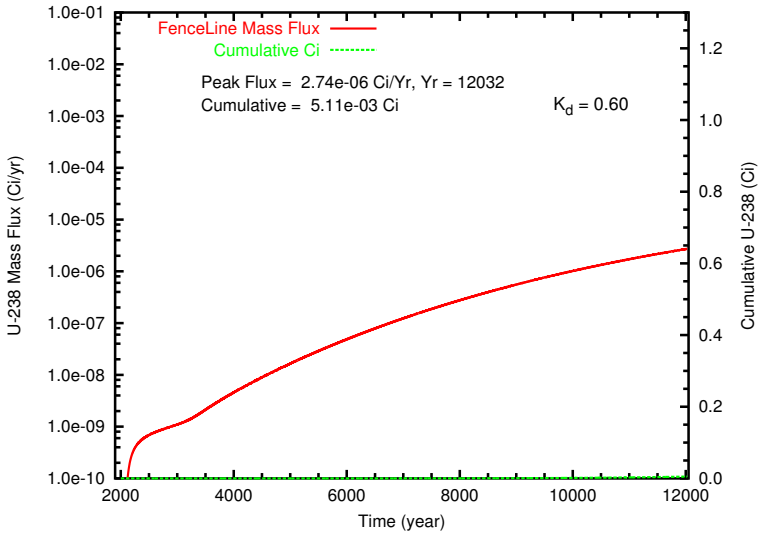

(b)

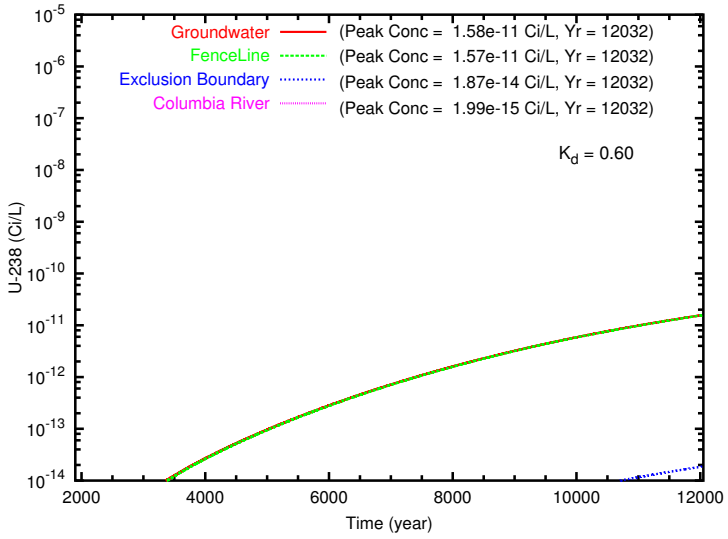

(c)

Figure B.5. Past Leak: Base Case U_0.60 mass flux at (a) the groundwater table and (b) the fenceline; and (c) the Tc-99 concentration at groundwater, fenceline, and easterly downstream compliance points.

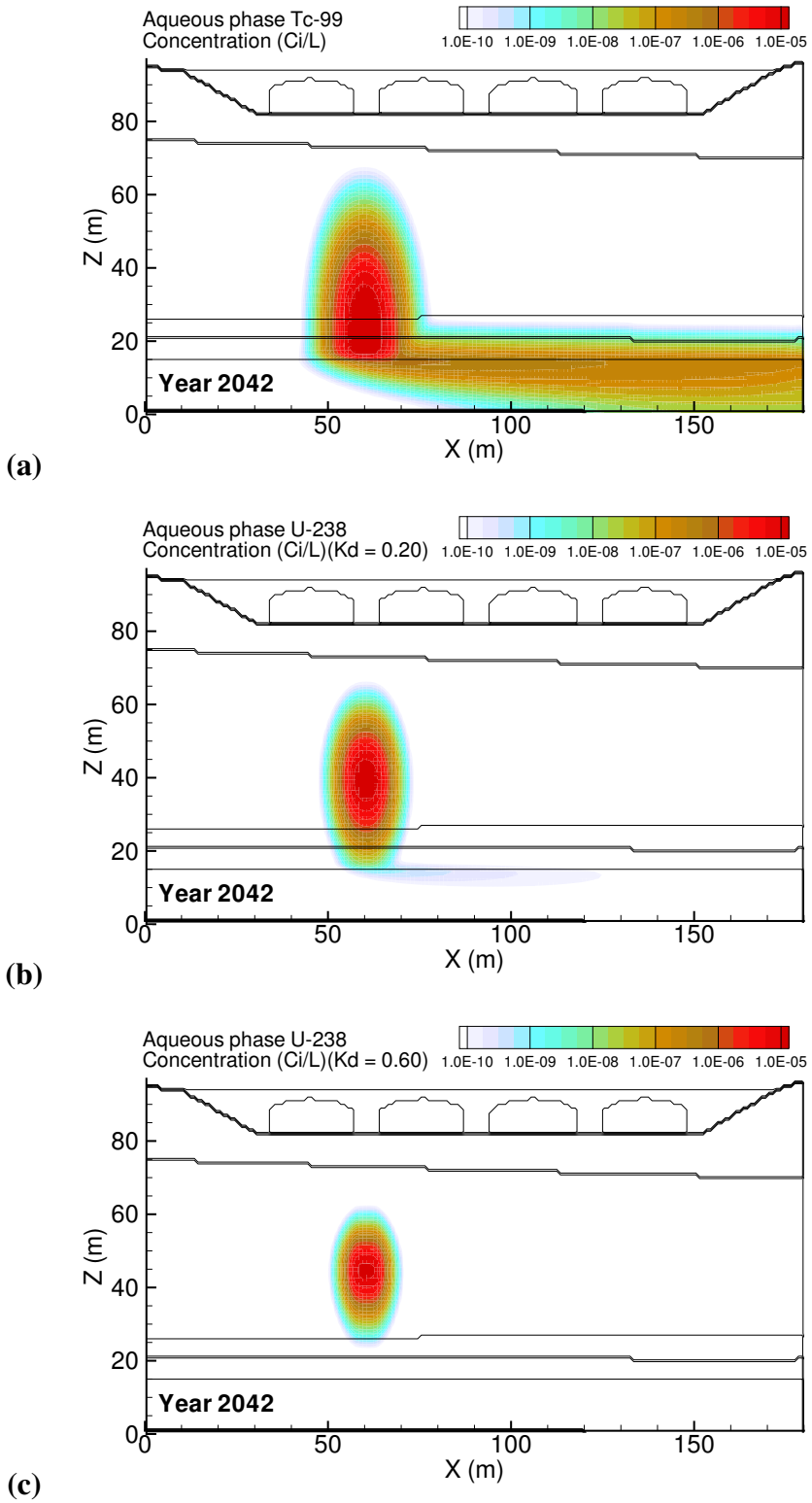

Figure B.6. Past Leak: High Preclosure Recharge Rate (140 mm/yr) aqueous concentration distributions at year 2042 for (a) Tc-99, (b) U_0.20 and (c) U_0.60. Year of Tc-99 peak concentration at fenceline was 2042.

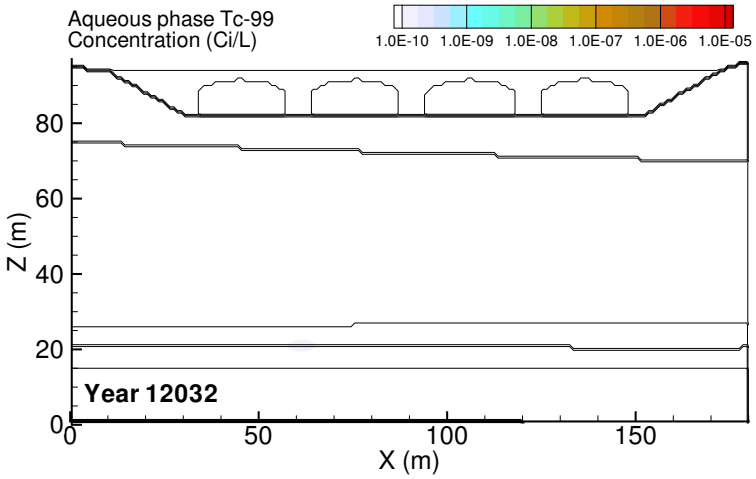

(a)

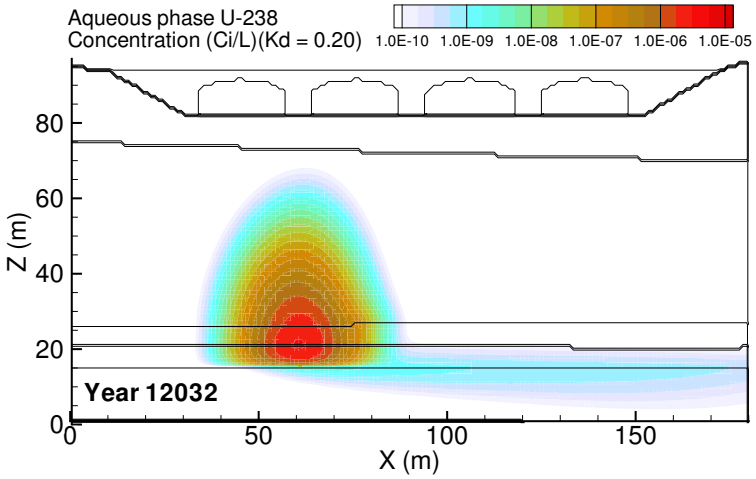

(b)

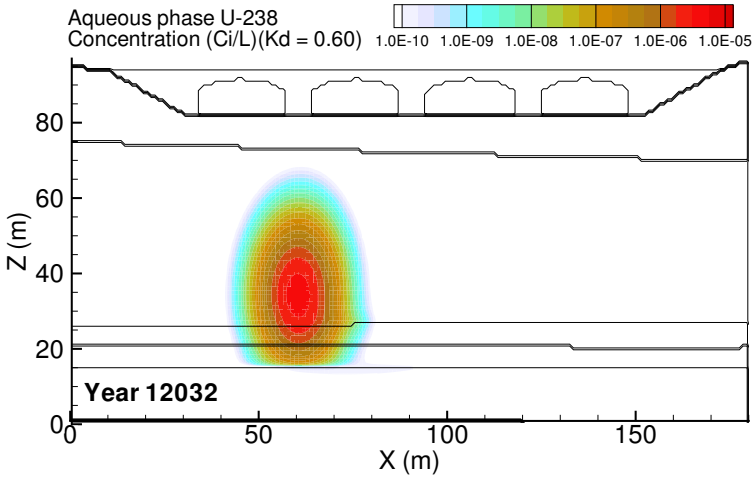

(c)

Figure B.7. Past Leak: High Preclosure Recharge Rate (140 mm/yr) aqueous concentration distributions at year 12032 for (a) Tc-99, (b) U_0.20 and (c) U_0.60.

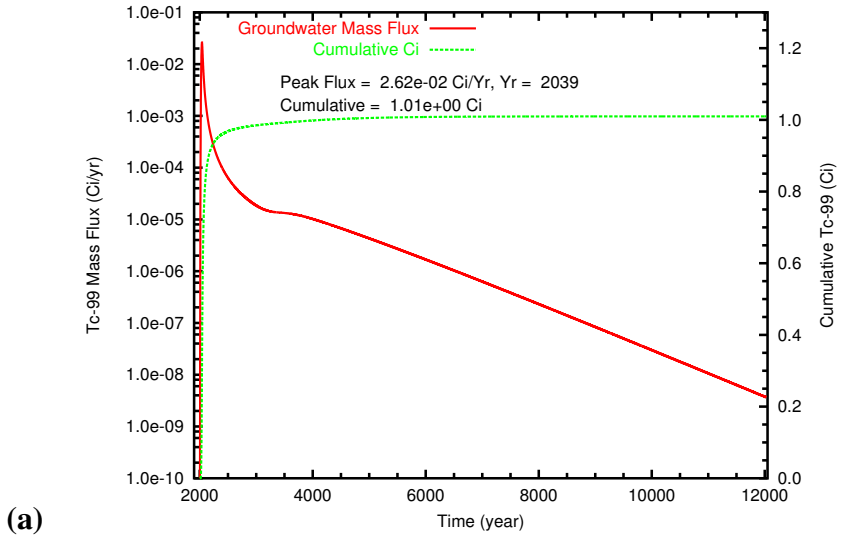

(a)

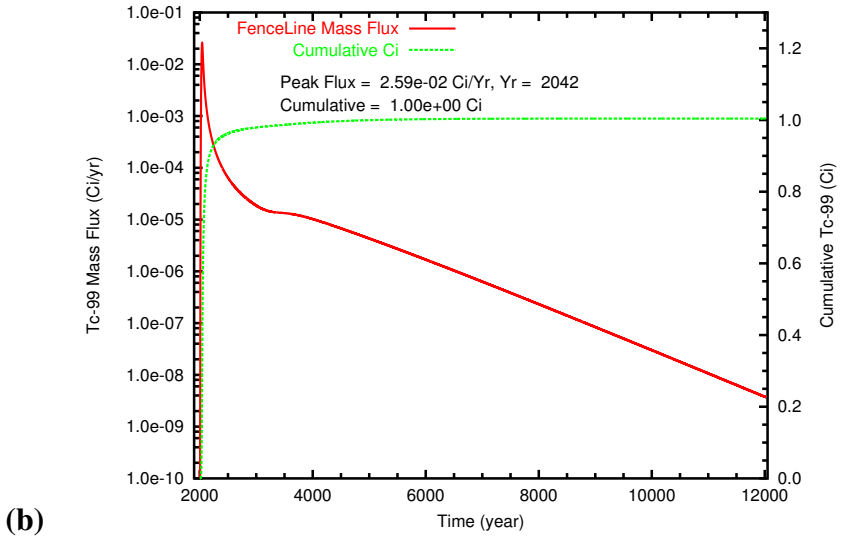

(b)

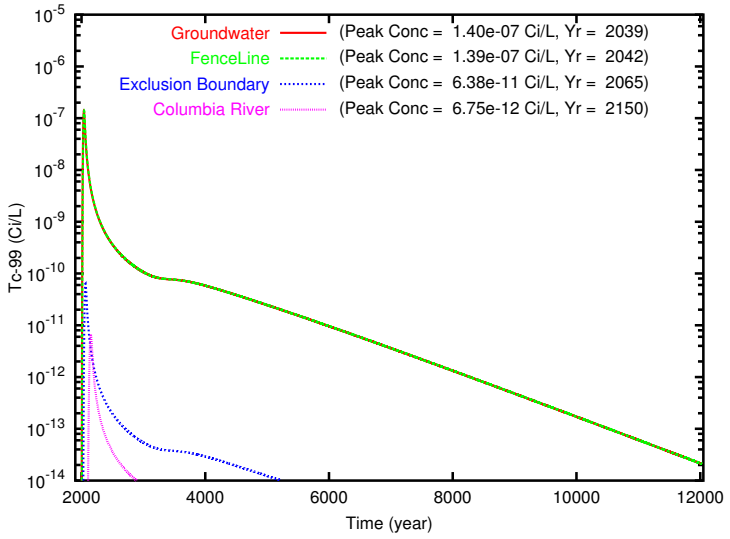

(c)

Figure B.8. Past Leak: High Preclosure Recharge Rate (140 mm/yr) Tc-99 mass flux at (a) the groundwater table and (b) the fenceline; and (c) the Tc-99 concentration at groundwater, fenceline, and easterly downstream compliance points.

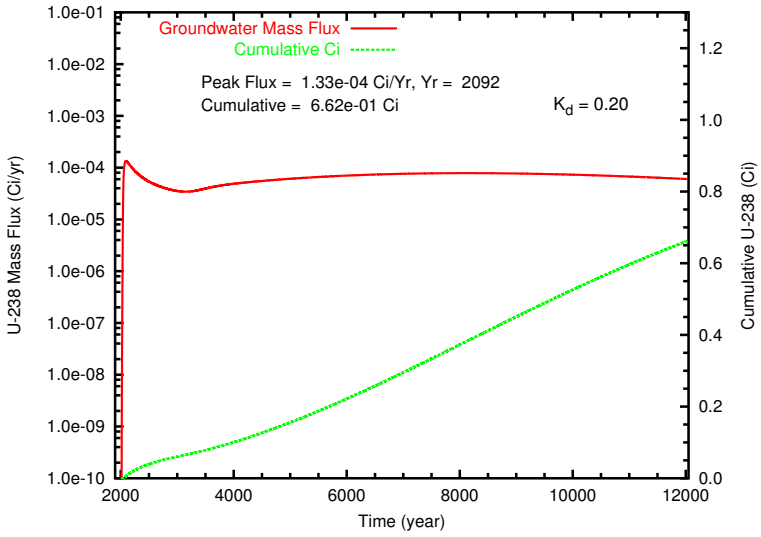

(a)

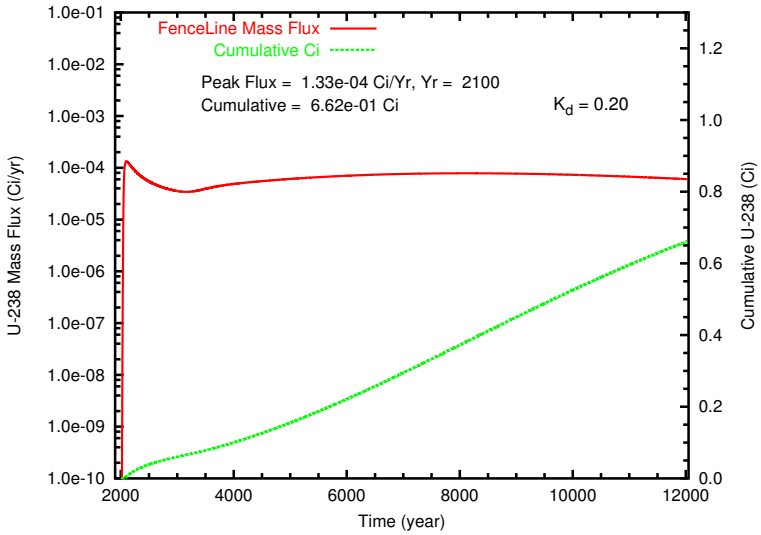

(b)

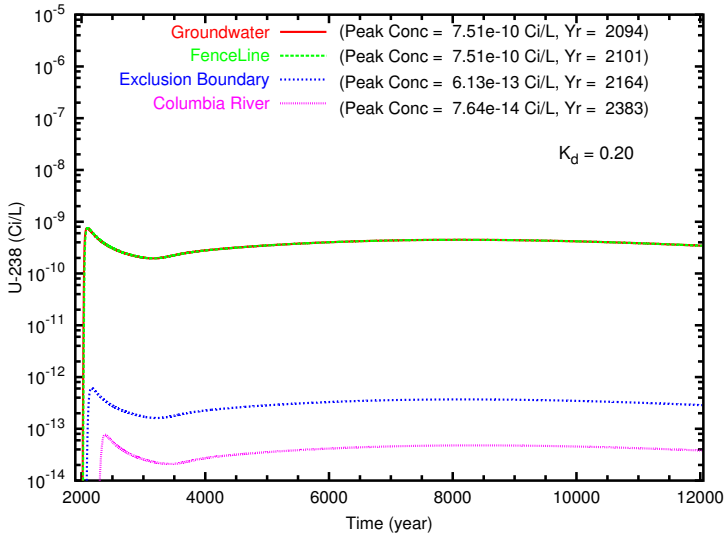

(c)

Figure B.9. Past Leak: High Preclosure Recharge Rate (140 mm/yr) U_0.20 mass flux at (a) the groundwater table and (b) the fenceline; and (c) the Tc-99 concentration at groundwater, fenceline, and easterly downstream compliance points.

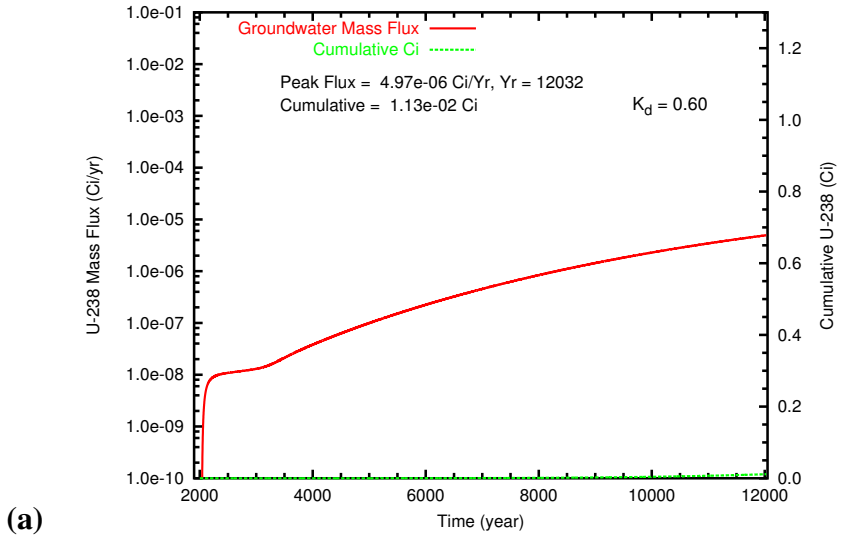

(a)

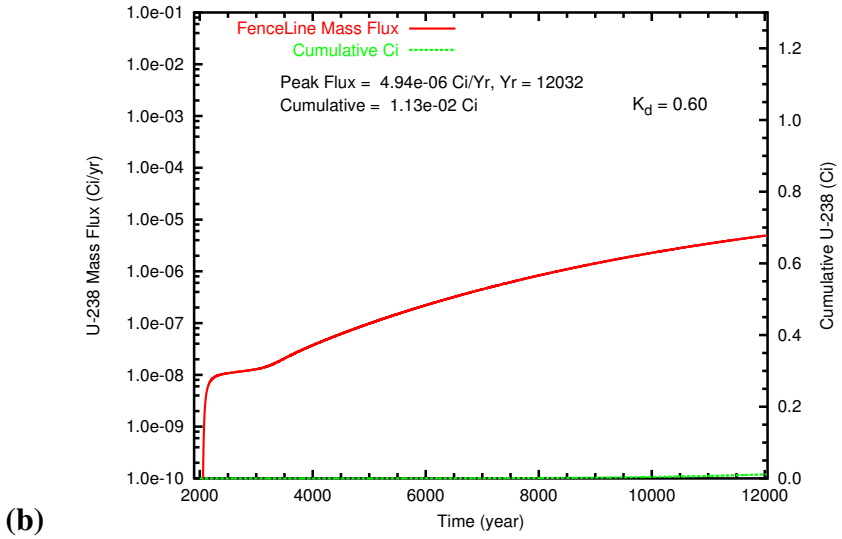

(b)

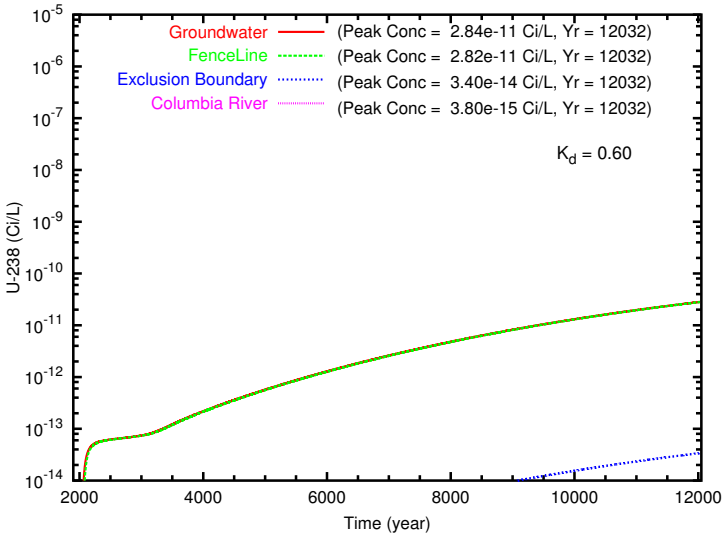

(c)

Figure B.10. Past Leak: High Preclosure Recharge Rate (140 mm/yr) U_0.60 mass flux at (a) the groundwater table and (b) the fenceline; and (c) the Tc-99 concentration at groundwater, fenceline, and easterly downstream compliance points.

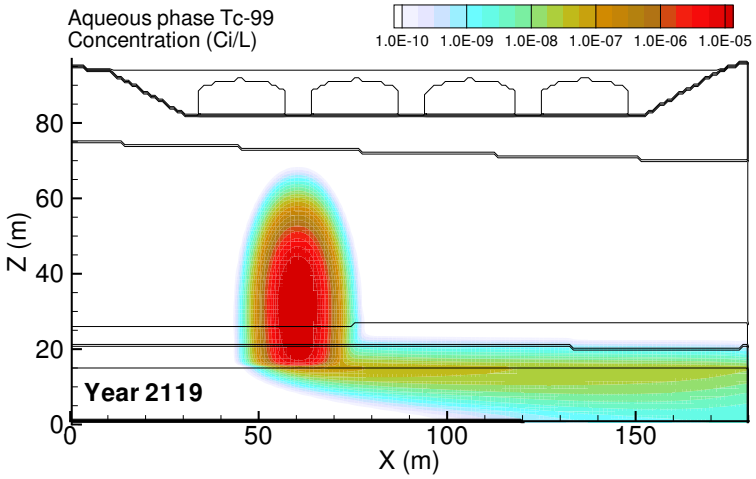

(a)

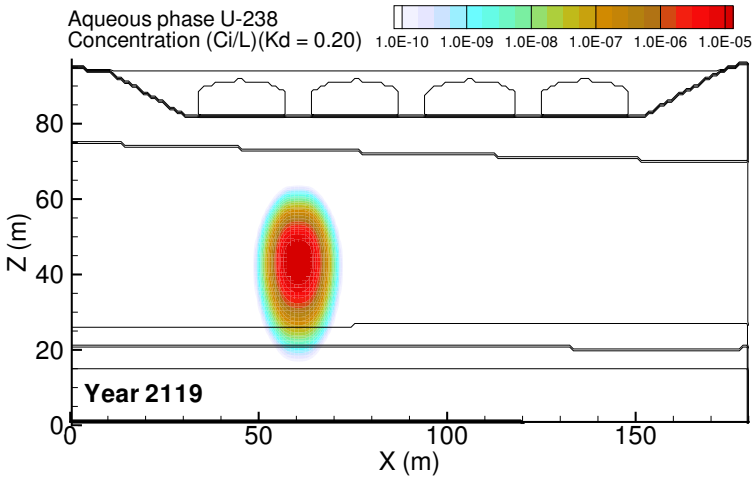

(b)

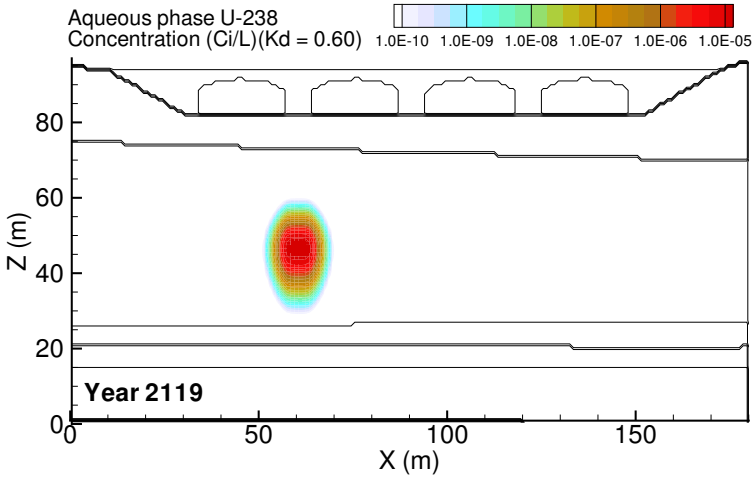

(c)

Figure B.11. Past Leak: Low Preclosure Recharge Rate (40 mm/yr) aqueous concentration distributions at year 2119 for (a) Tc-99, (b) U_0.20 and (c) U_0.60. Year of Tc-99 peak concentration at fenceline was 2119.

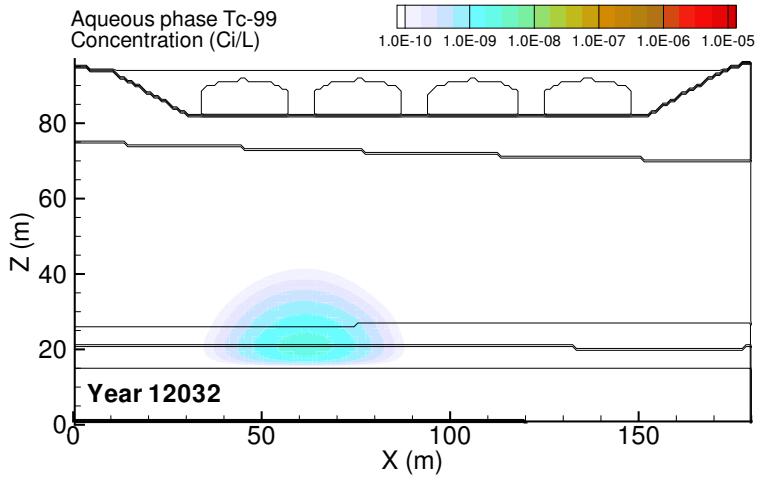

(a)

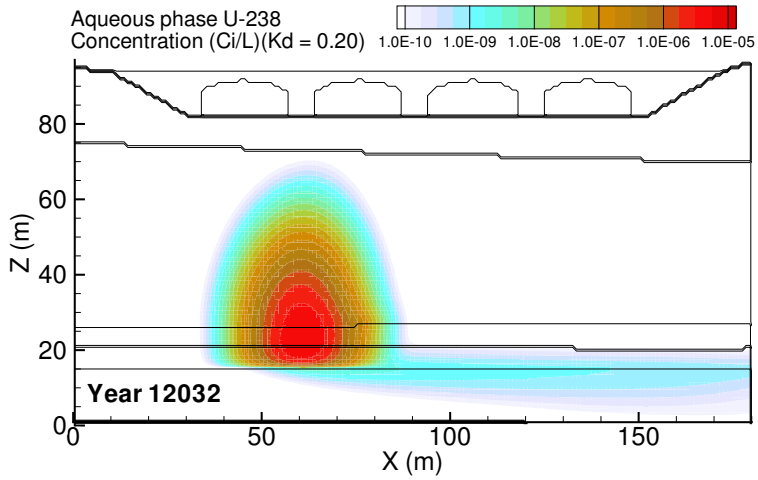

(b)

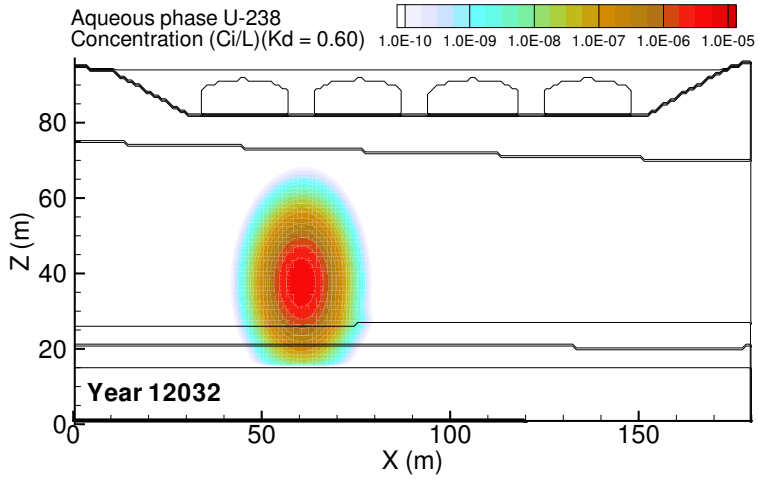

(c)

Figure B.12. Past Leak: Low Preclosure Recharge Rate (40 mm/yr) aqueous concentration distributions at year 12032 for (a) Tc-99, (b) U_0.20 and (c) U_0.60.

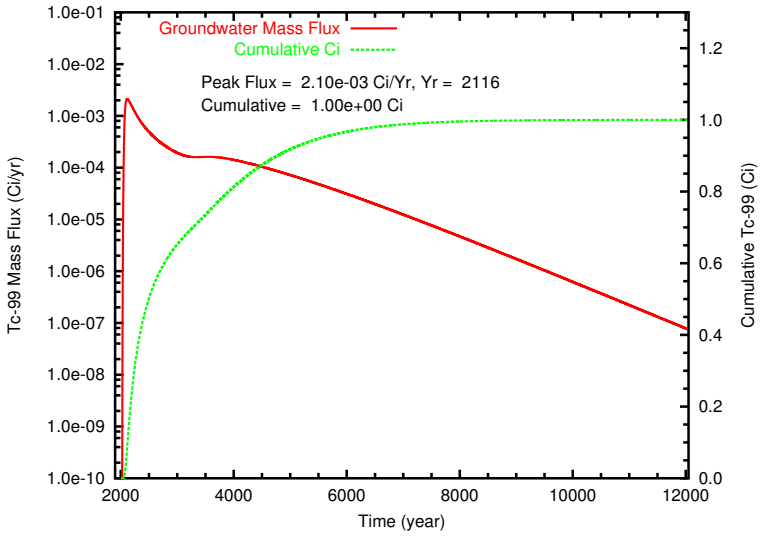

(a)

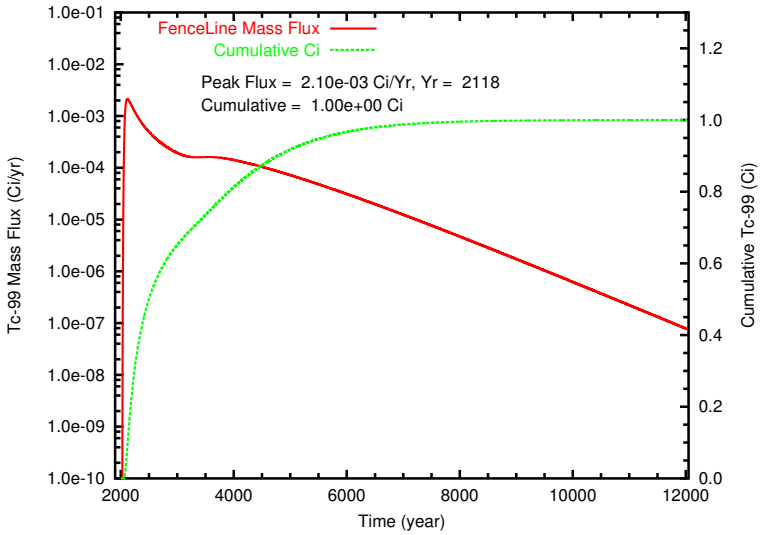

(b)

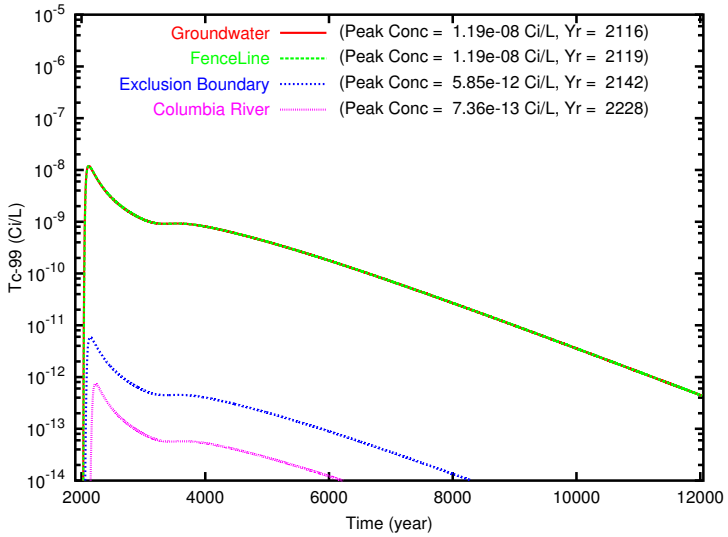

(c)

Figure B.13. Past Leak: Low Preclosure Recharge Rate (40 mm/yr) Tc-99 mass flux at (a) the groundwater table and (b) the fenceline; and (c) the Tc-99 concentration at groundwater, fenceline, and easterly downstream compliance points.

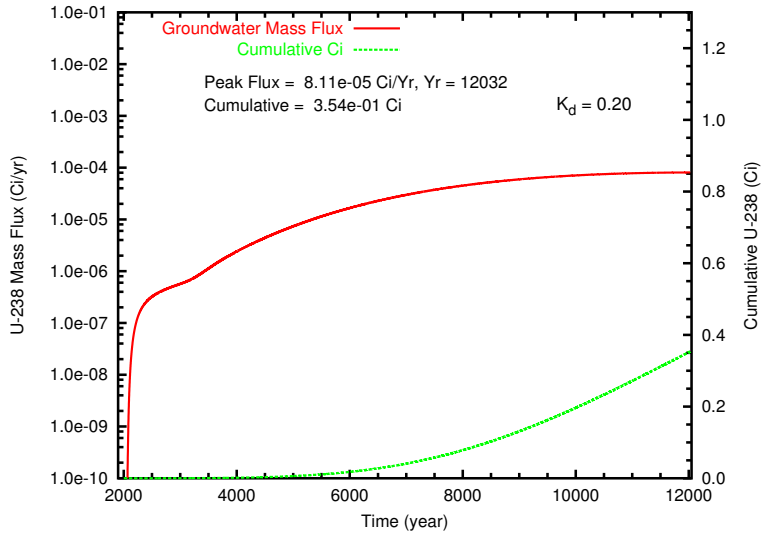

(a)

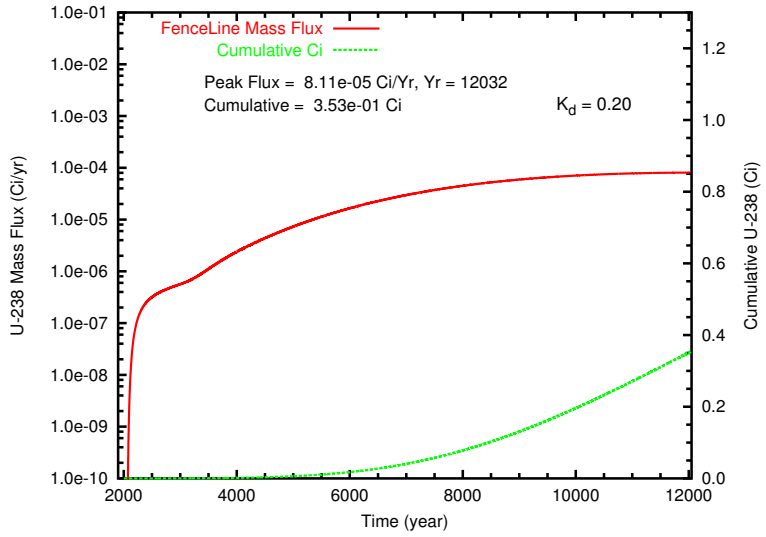

(b)

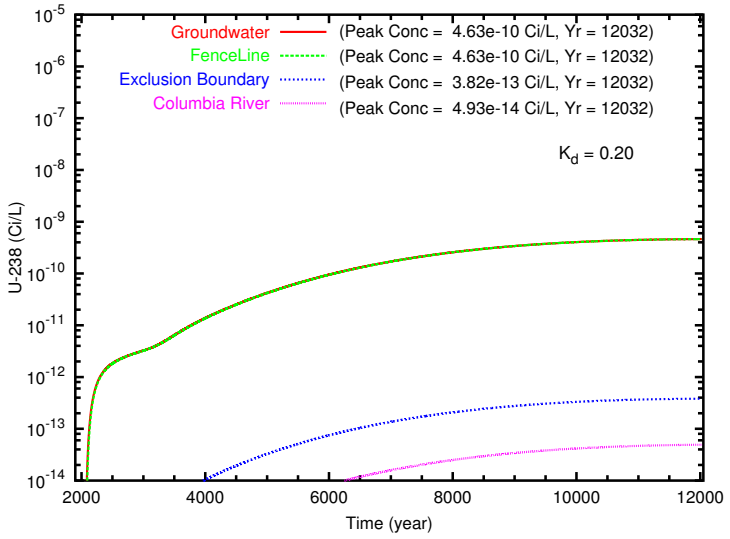

(c)

Figure B.14. Past Leak: Low Preclosure Recharge Rate (40 mm/yr) U_0.20 mass flux at (a) the groundwater table and (b) the fenceline; and (c) the Tc-99 concentration at groundwater, fenceline, and easterly downstream compliance points.

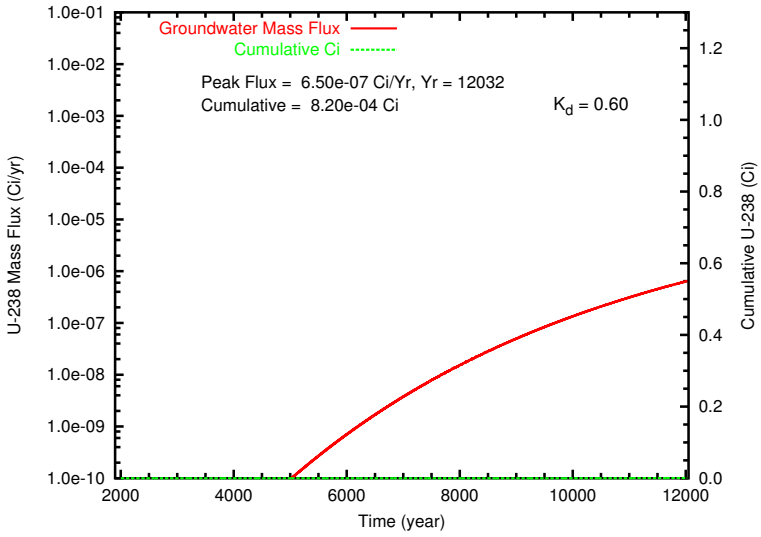

(a)

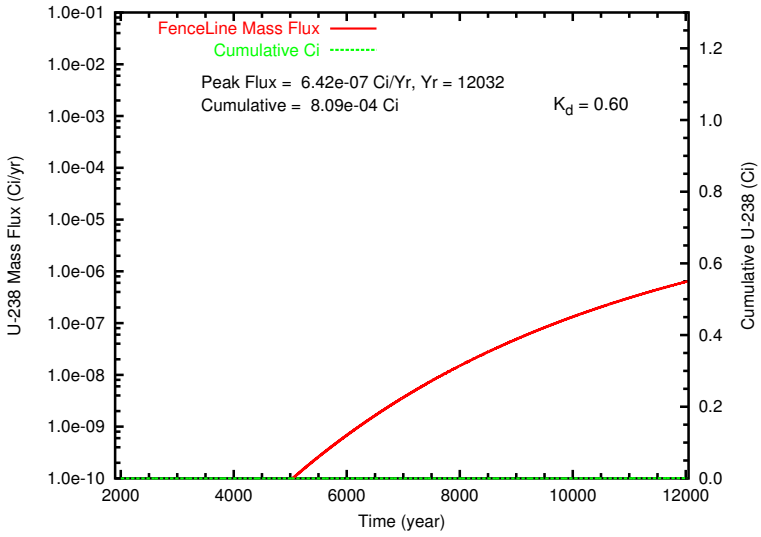

(b)

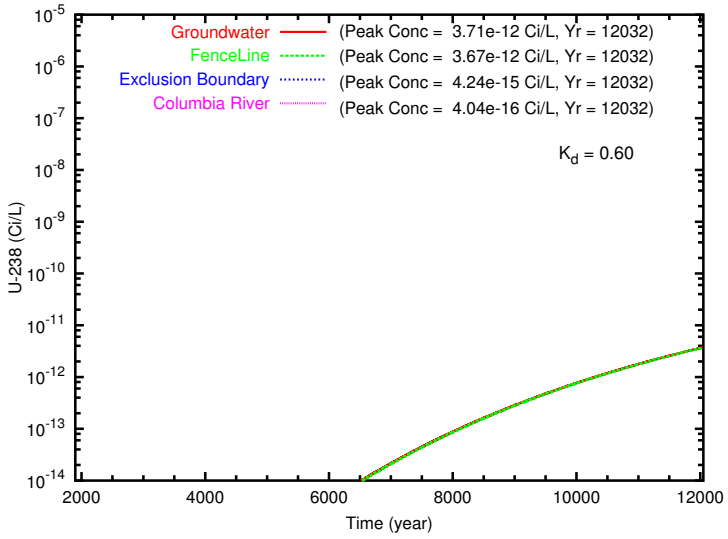

(c)

Figure B.15. Past Leak: Low Preclosure Recharge Rate (40 mm/yr) U_0.60 mass flux at (a) the groundwater table and (b) the fenceline; and (c) the Tc-99 concentration at groundwater, fenceline, and easterly downstream compliance points.

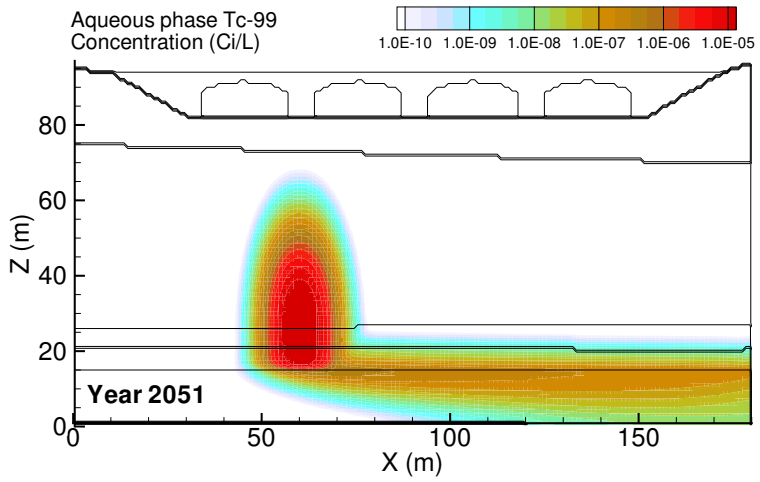

(a)

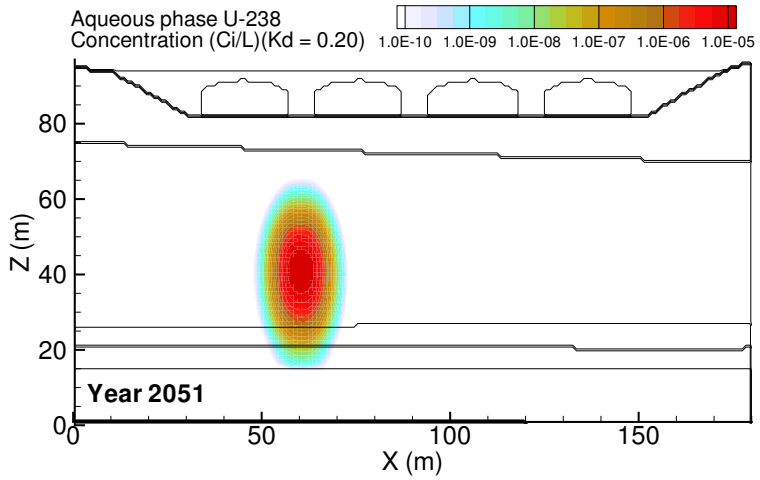

(b)

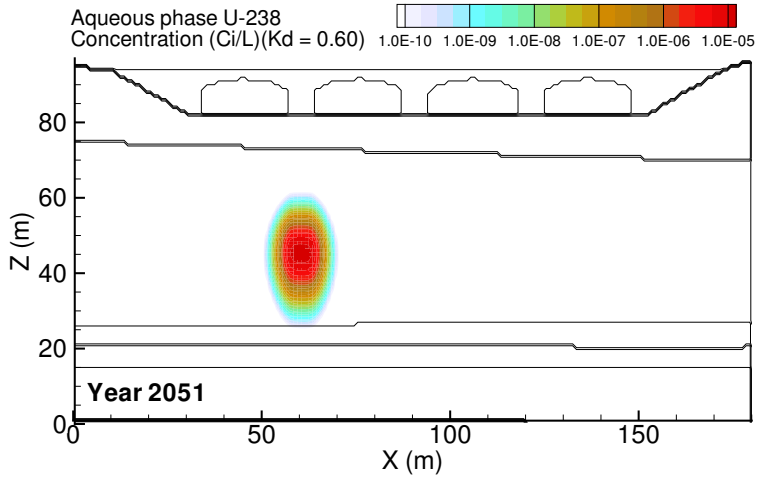

(c)

Figure B.16. Past Leak: High Barrier Recharge Rate (1.0 mm/yr) aqueous concentration distributions at year 2051 for (a) Tc-99, (b) U_0.20 and (c) U_0.60. Year of Tc-99 peak concentration at fenceline was 2051.

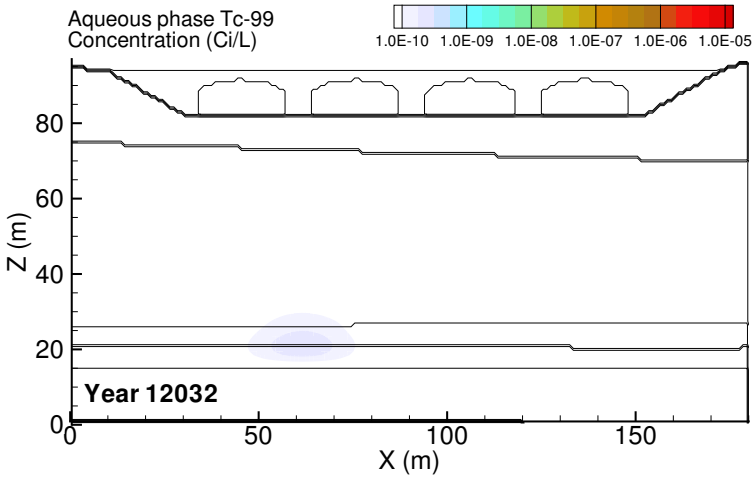

(a)

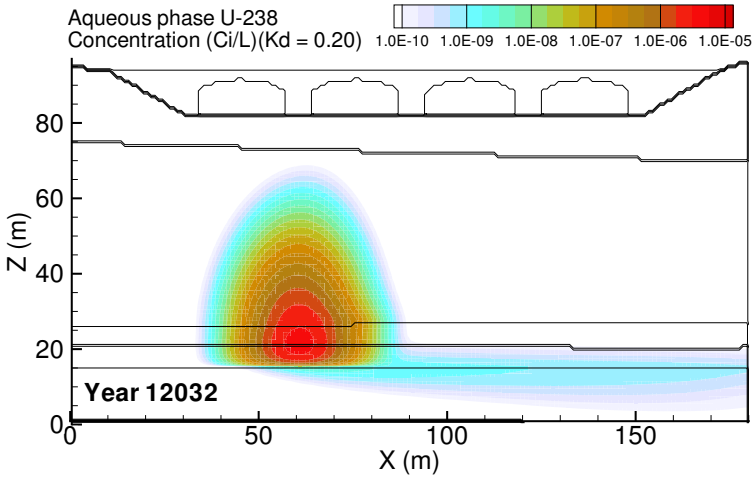

(b)

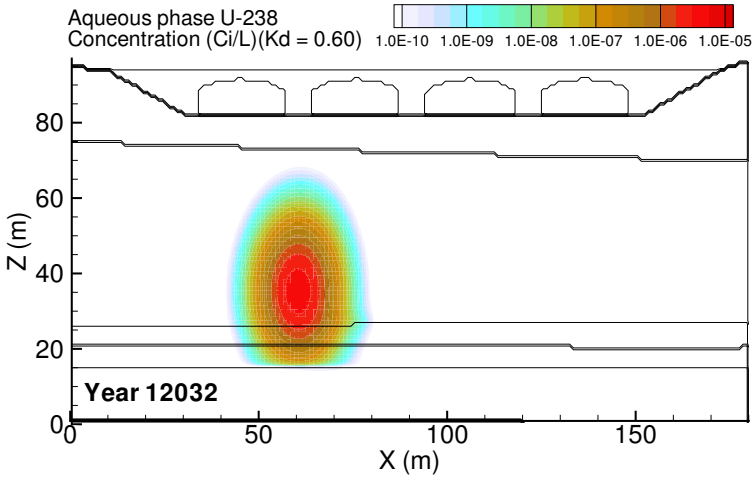

(c)

Figure B.17. Past Leak: High Barrier Recharge Rate (1.0 mm/yr) aqueous concentration distributions at year 12032 for (a) Tc-99, (b) U_0.20 and (c) U_0.60.

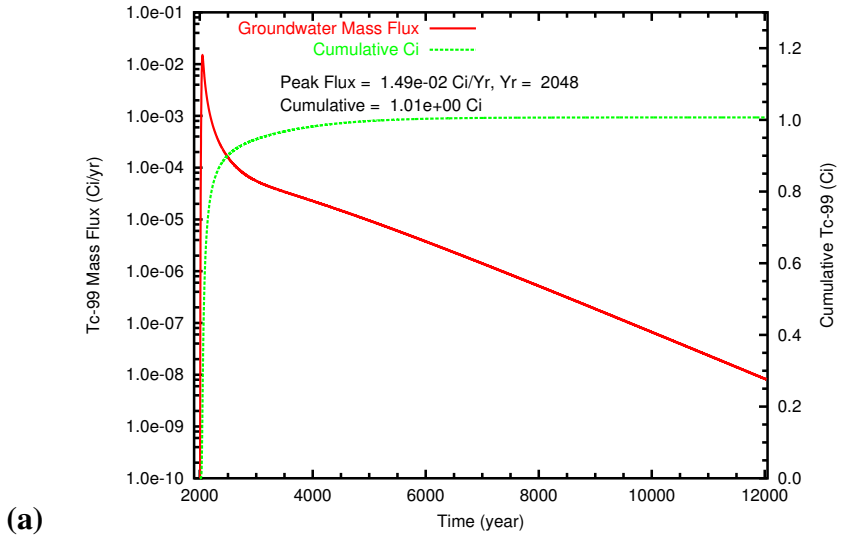

(a)

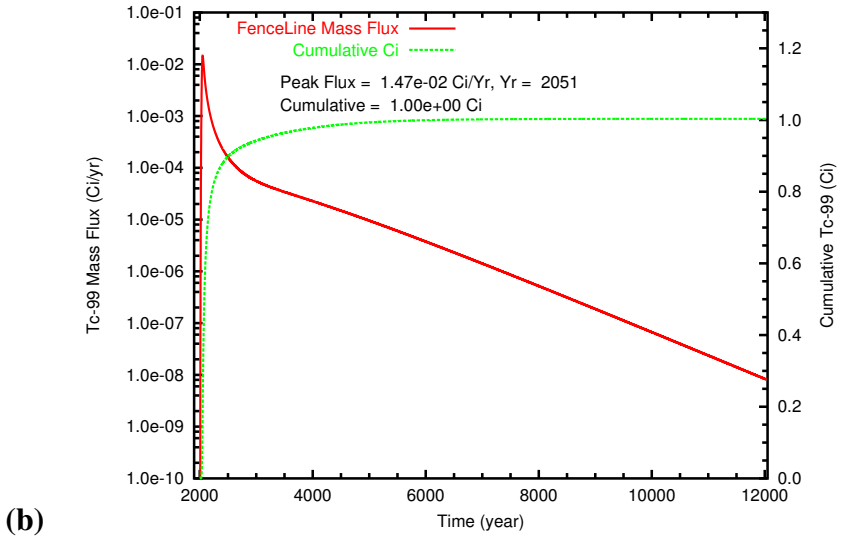

(b)

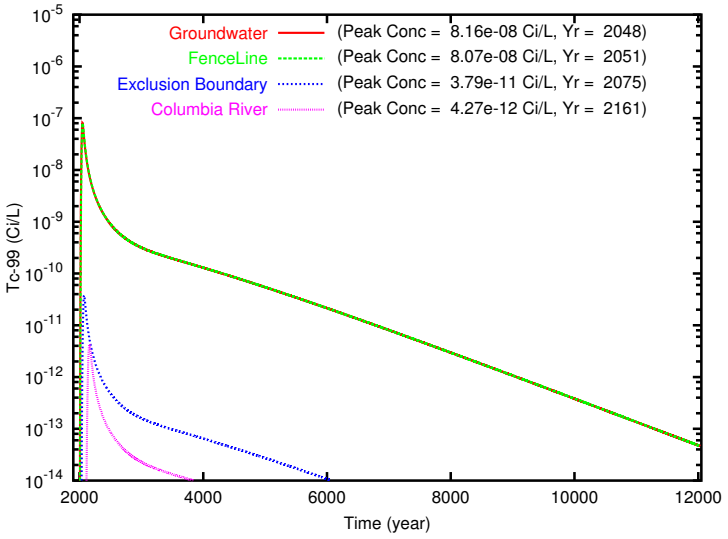

(c)

Figure B.18. Past Leak: High Barrier Recharge Rate (1.0 mm/yr) Tc-99 mass flux at (a) the groundwater table and (b) the fenceline; and (c) the Tc-99 concentration at groundwater, fenceline, and easterly downstream compliance points.

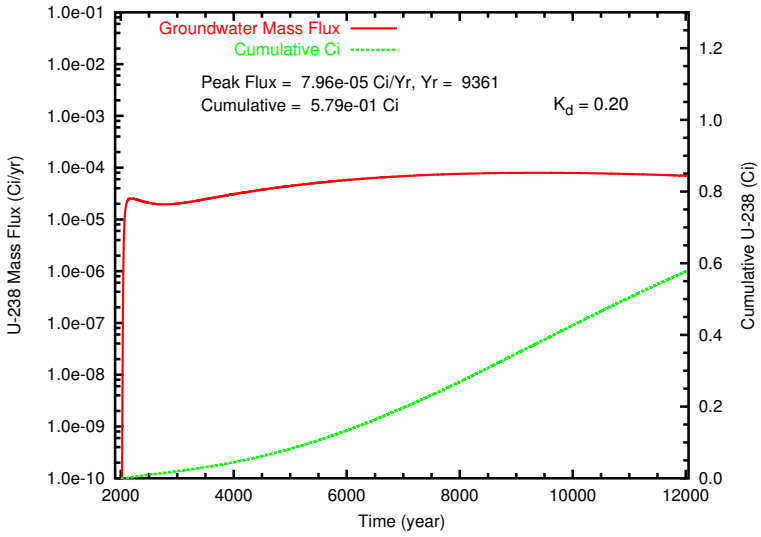

(a)

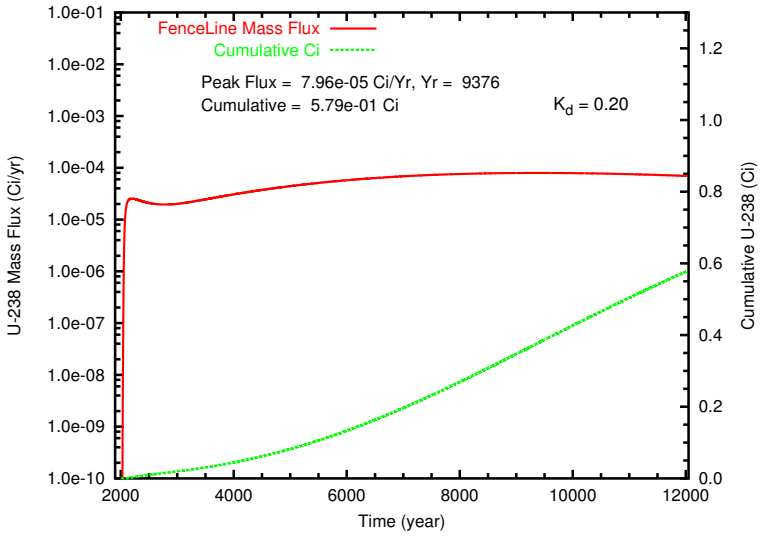

(b)

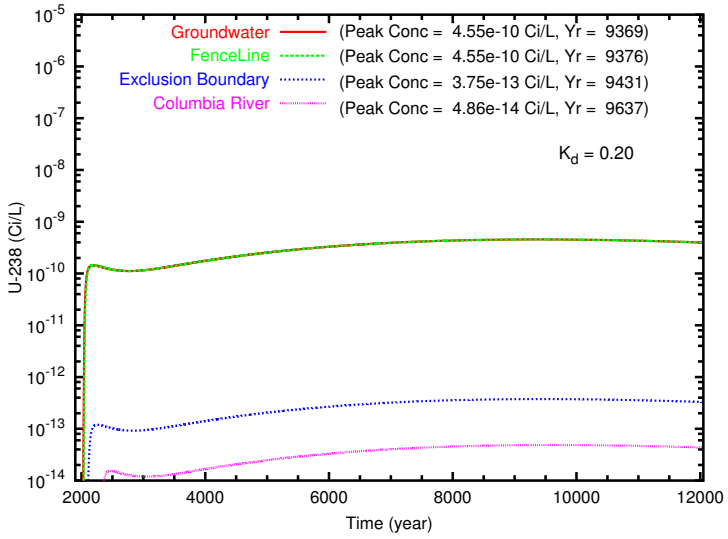

(c)

Figure B.19. Past Leak: High Barrier Recharge Rate (1.0 mm/yr) U_0.20 mass flux at (a) the groundwater table and (b) the fenceline; and (c) the Tc-99 concentration at groundwater, fenceline, and easterly downstream compliance points.

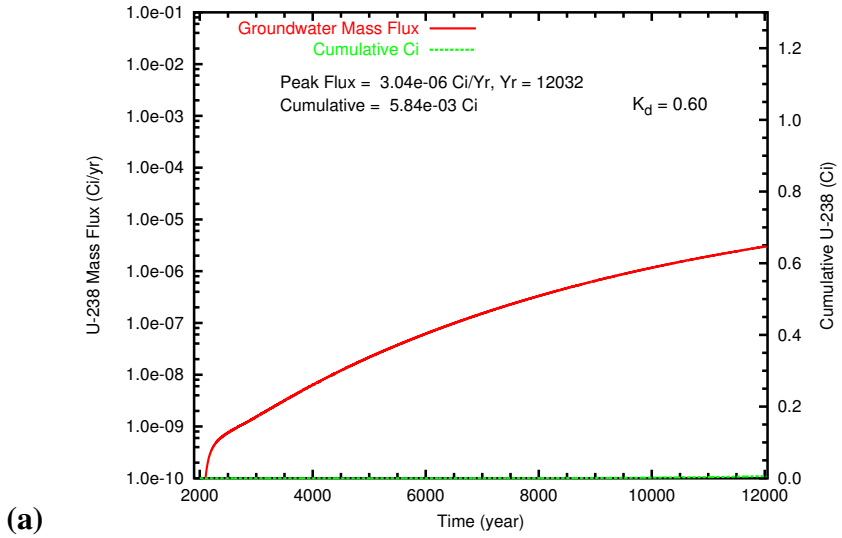

(a)

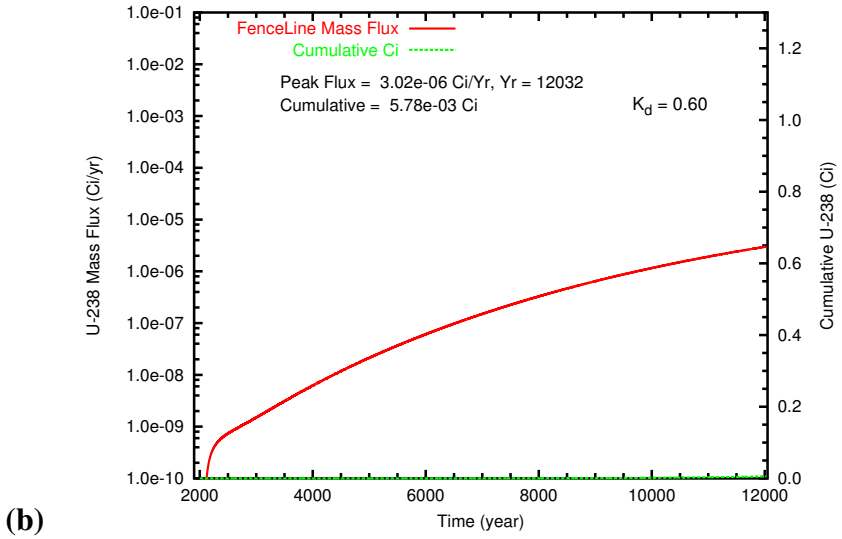

(b)

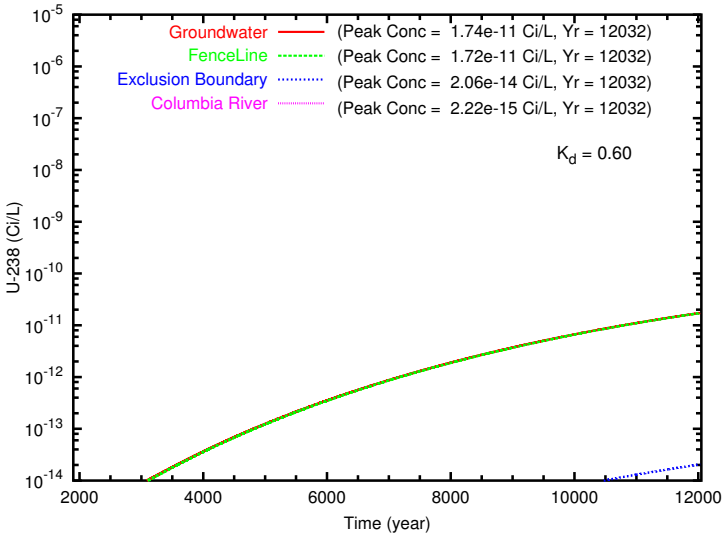

(c)

Figure B.20. Past Leak: High Barrier Recharge Rate (1.0 mm/yr) U_0.60 mass flux at (a) the groundwater table and (b) the fenceline; and (c) the Tc-99 concentration at groundwater, fenceline, and easterly downstream compliance points.

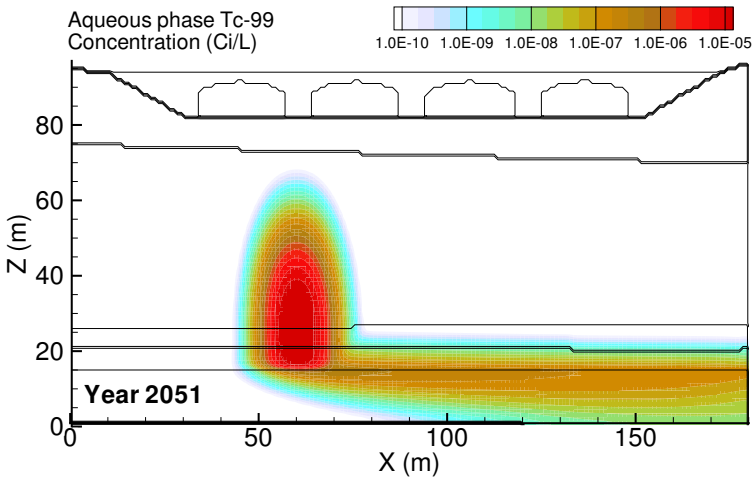

(a)

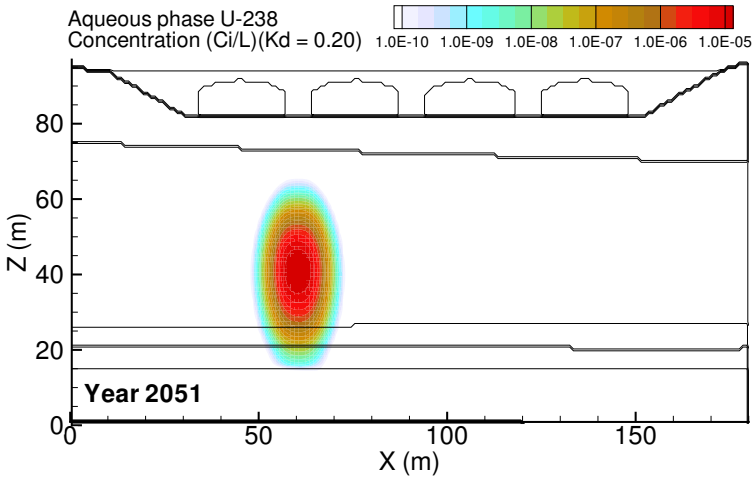

(b)

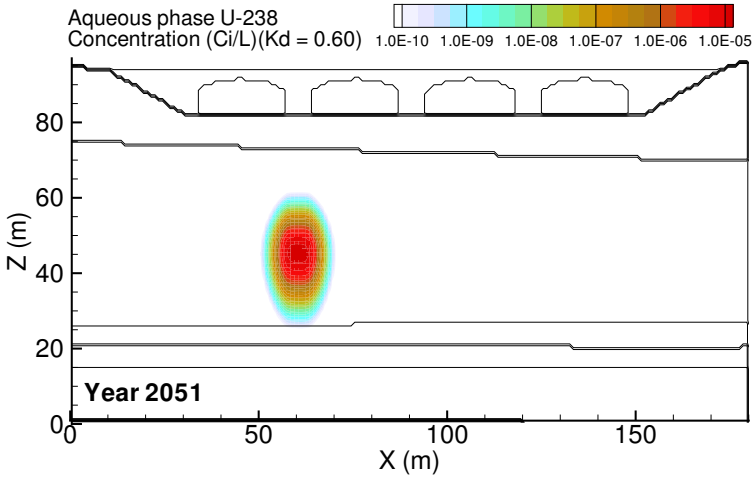

(c)

Figure B.21. Past Leak: Low Barrier Recharge Rate (0.1 mm/yr) aqueous concentration distributions at year 2051 for (a) Tc-99, (b) U_0.20 and (c) U_0.60. Year of Tc-99 peak concentration at fenceline was 2051.

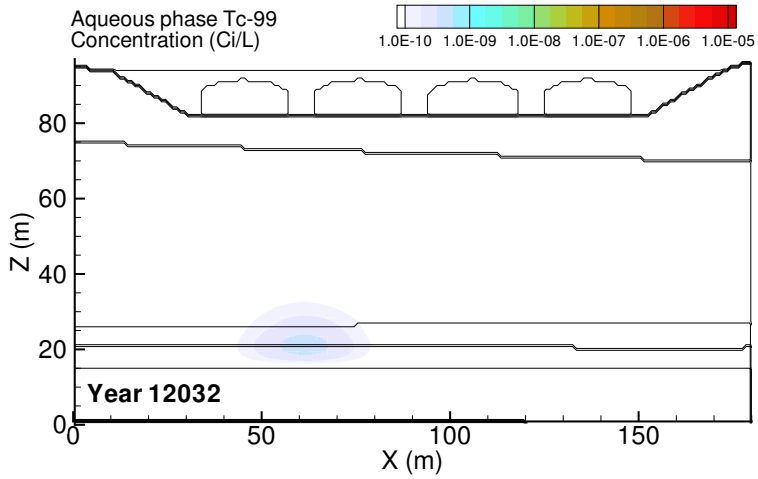

(a)

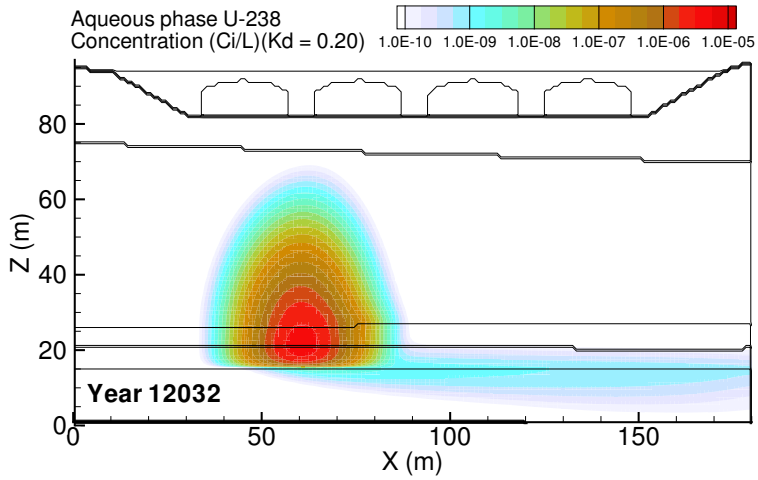

(b)

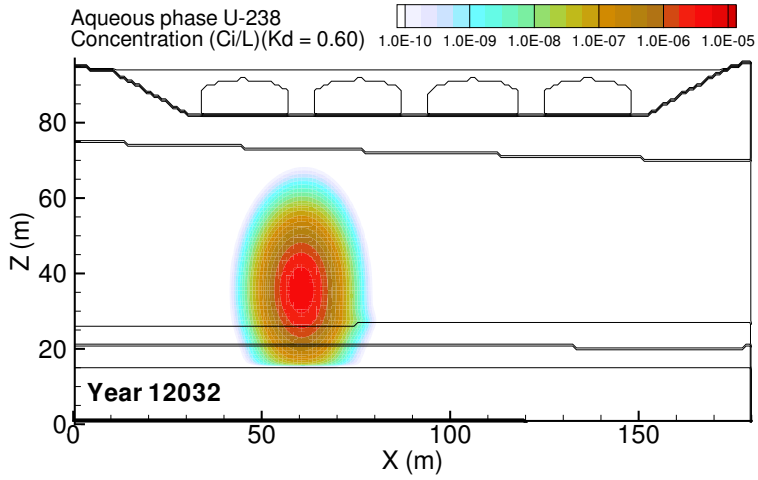

(c)

Figure B.22. Past Leak: Low Barrier Recharge Rate (0.1 mm/yr) aqueous concentration distributions at year 12032 for (a) Tc-99, (b) U_0.20 and (c) U_0.60.

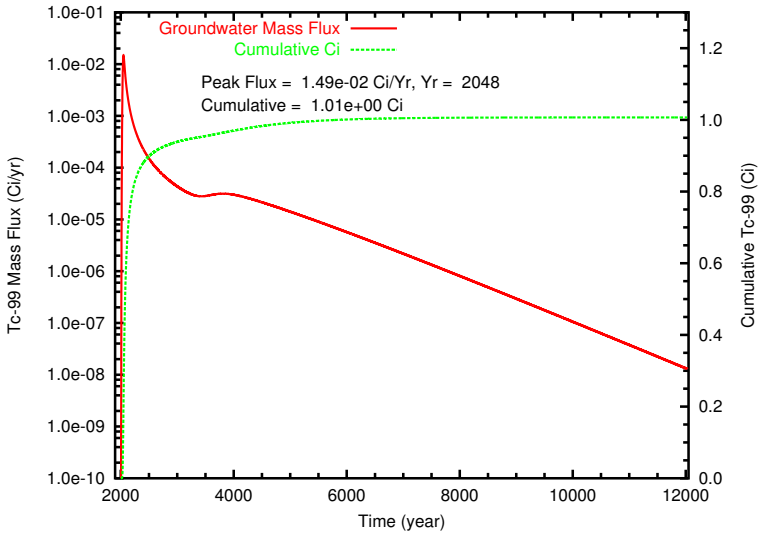

(a)

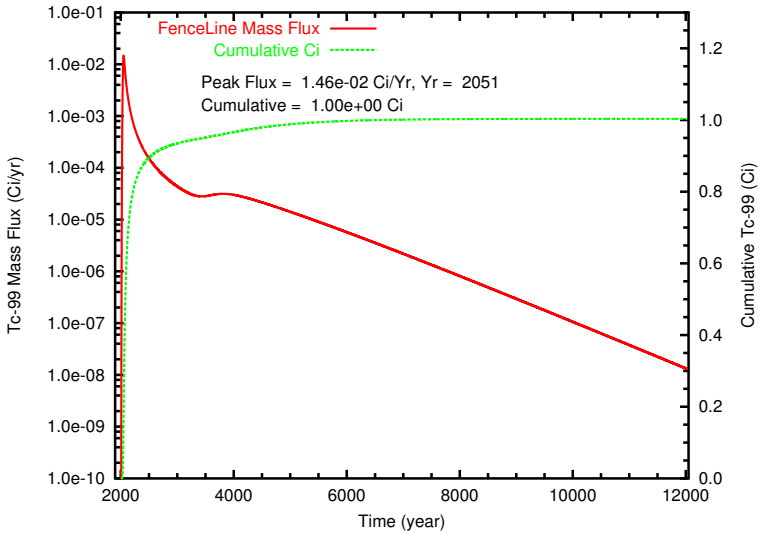

(b)

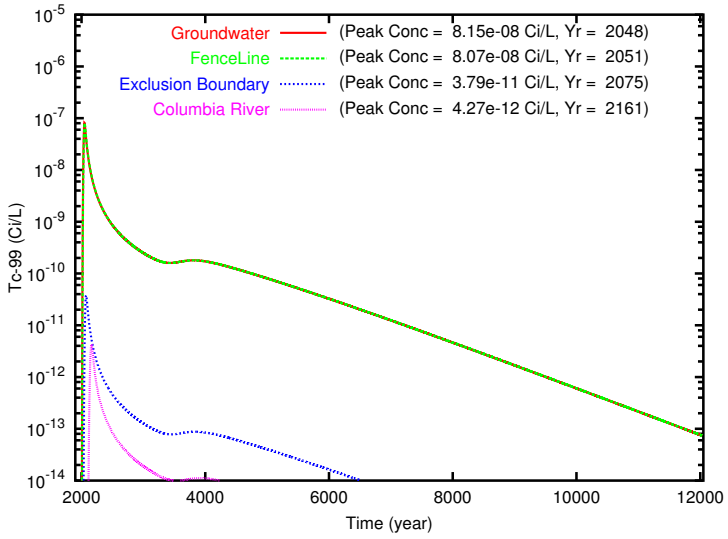

(c)

Figure B.23. Past Leak: Low Barrier Recharge Rate (0.1 mm/yr) Tc-99 mass flux at (a) the groundwater table and (b) the fenceline; and (c) the Tc-99 concentration at groundwater, fenceline, and easterly downstream compliance points.

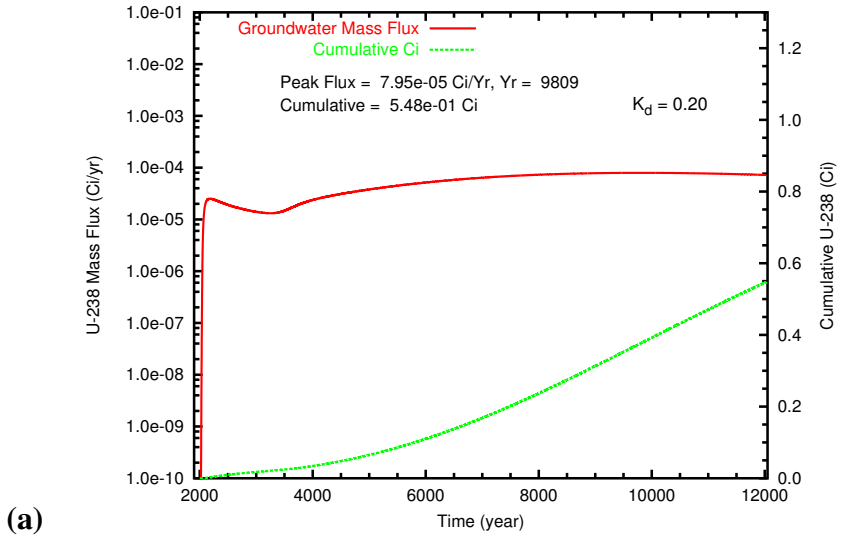

(a)

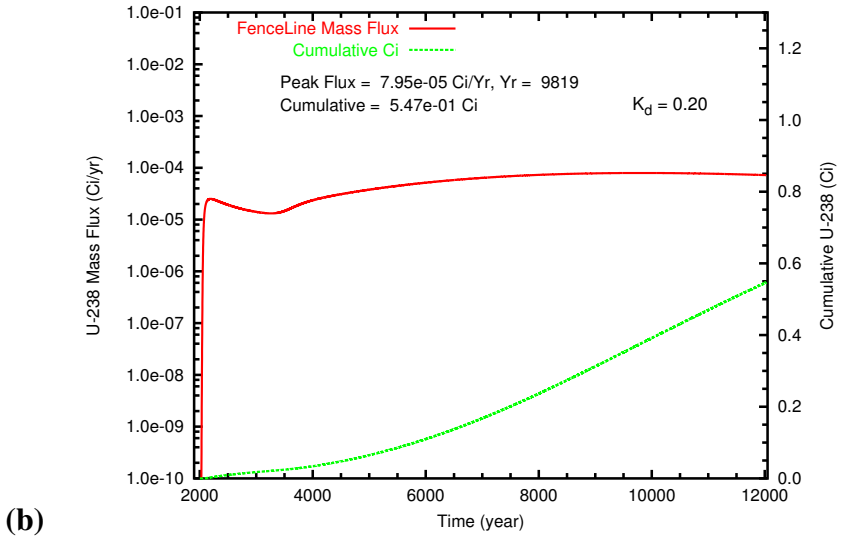

(b)

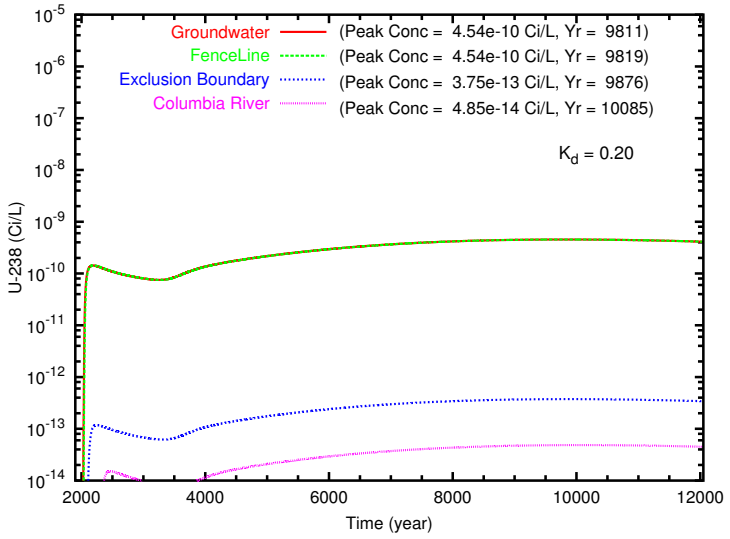

(c)

Figure B.24. Past Leak: Low Barrier Recharge Rate (0.1 mm/yr) U_0.20 mass flux at (a) the groundwater table and (b) the fenceline; and (c) the Tc-99 concentration at groundwater, fenceline, and easterly downstream compliance points.

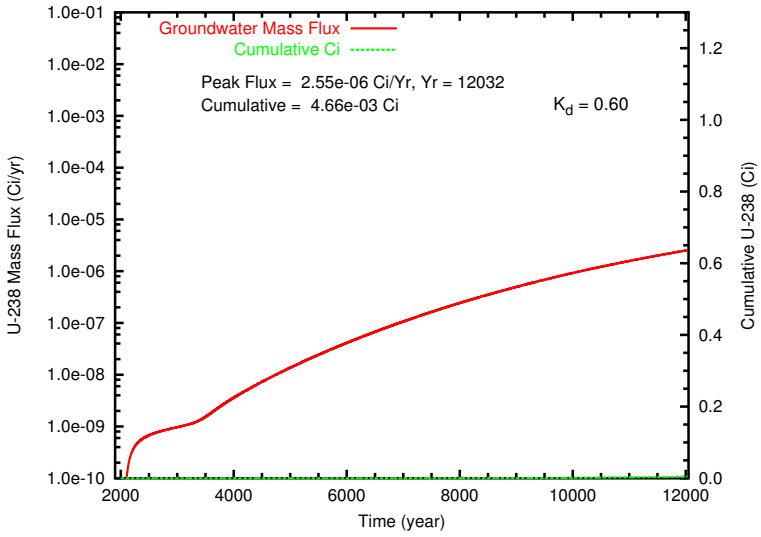

(a)

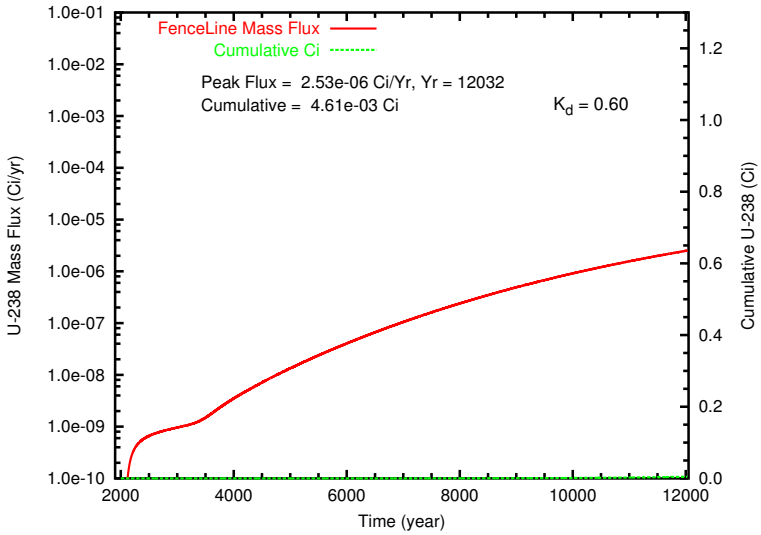

(b)

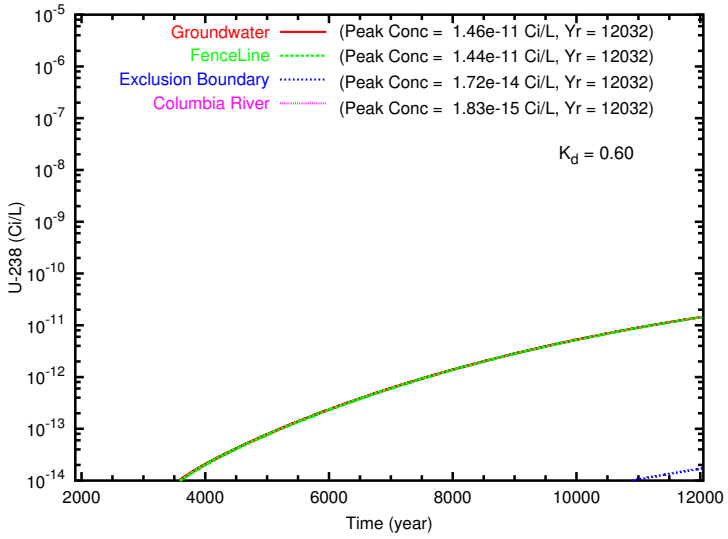

(c)

Figure B.25. Past Leak: Low Barrier Recharge Rate (0.1 mm/yr) U_0.60 mass flux at (a) the groundwater table and (b) the fenceline; and (c) the Tc-99 concentration at groundwater, fenceline, and easterly downstream compliance points.

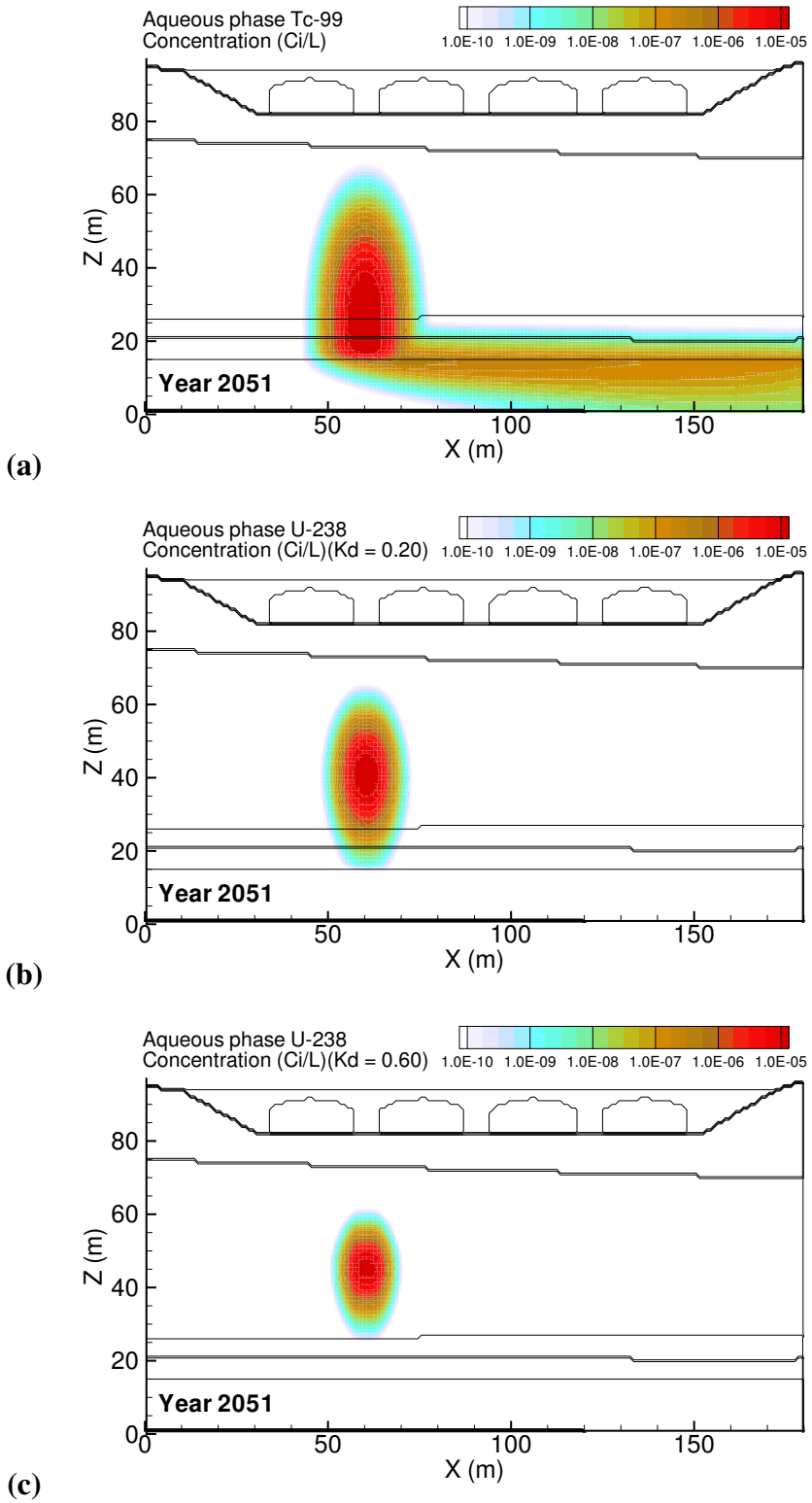

Figure B.26. Past Leak: High Degraded-Barrier Recharge Rate (3.5 mm/yr) aqueous concentration distributions at year 2051 for (a) Tc-99, (b) U_0.20 and (c) U_0.60. Year of Tc-99 peak concentration at fenceline was 2051.

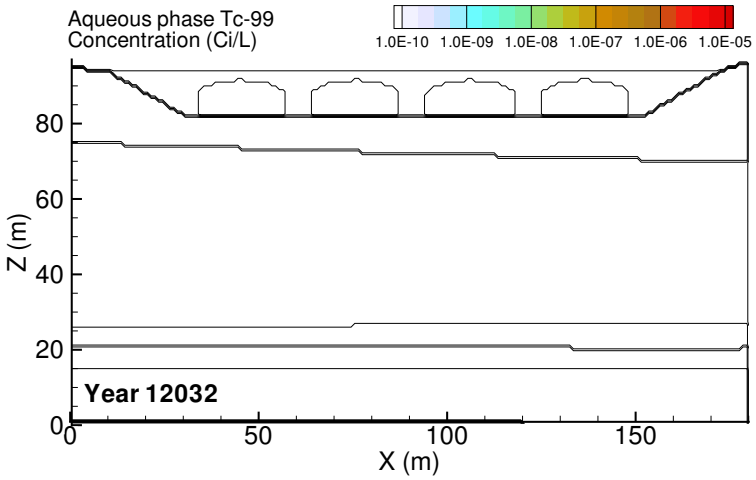

(a)

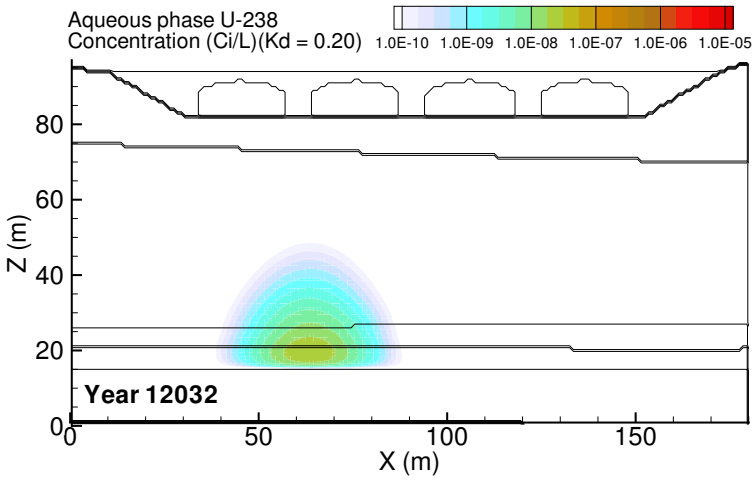

(b)

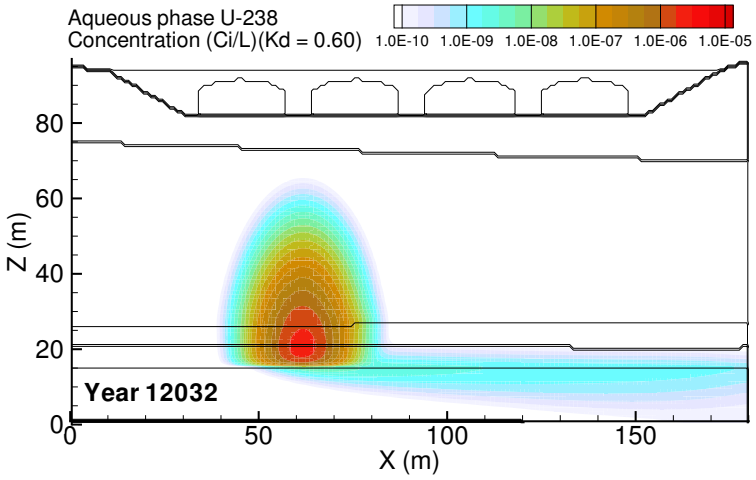

(c)

Figure B.27. Past Leak: High Degraded-Barrier Recharge Rate (3.5 mm/yr) aqueous concentration distributions at year 12032 for (a) Tc-99, (b) U_0.20 and (c) U_0.60.

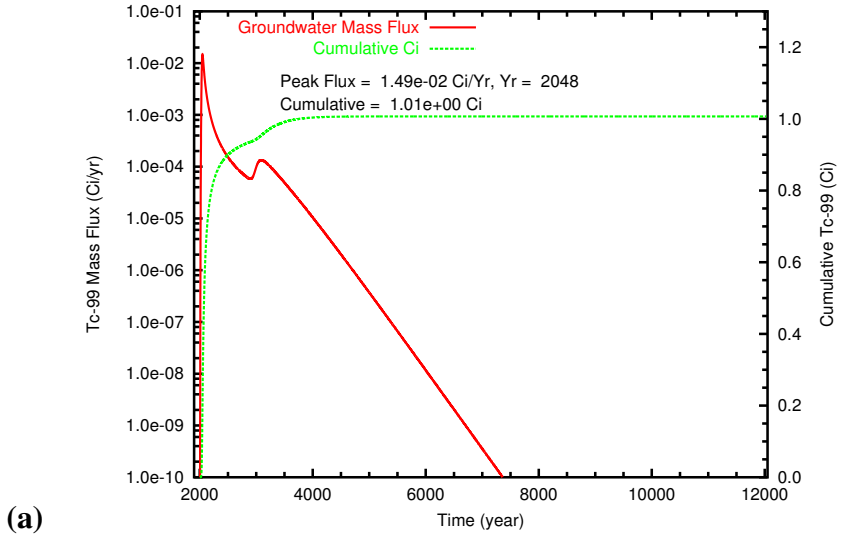

(a)

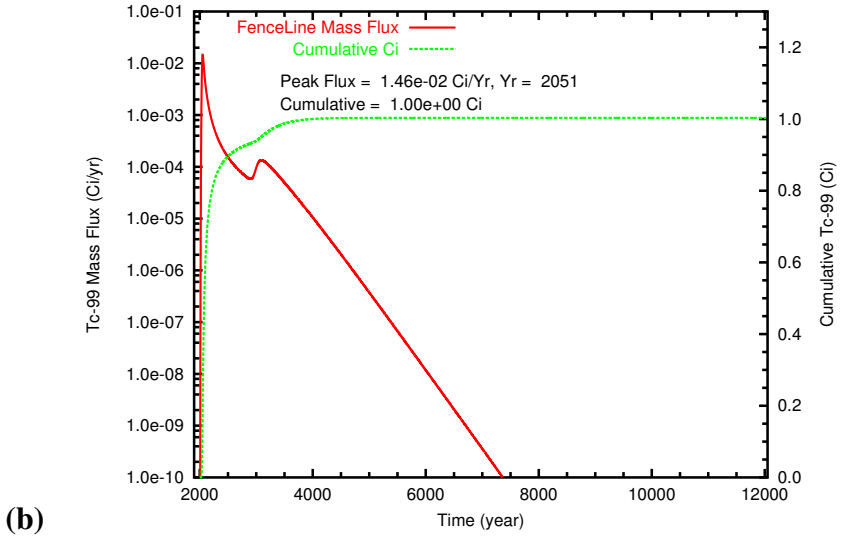

(b)

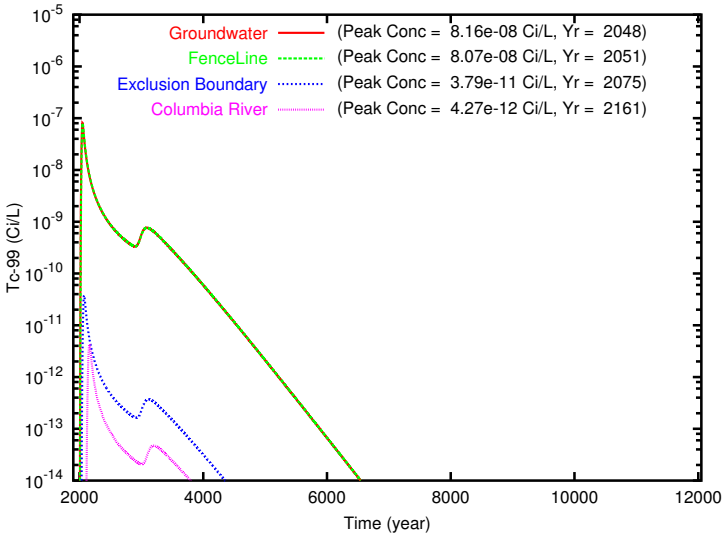

(c)

Figure B.28. Past Leak: High Degraded-Barrier Recharge Rate (3.5 mm/yr) Tc-99 mass flux at (a) the groundwater table and (b) the fenceline; and (c) the Tc-99 concentration at groundwater, fenceline, and easterly downstream compliance points.

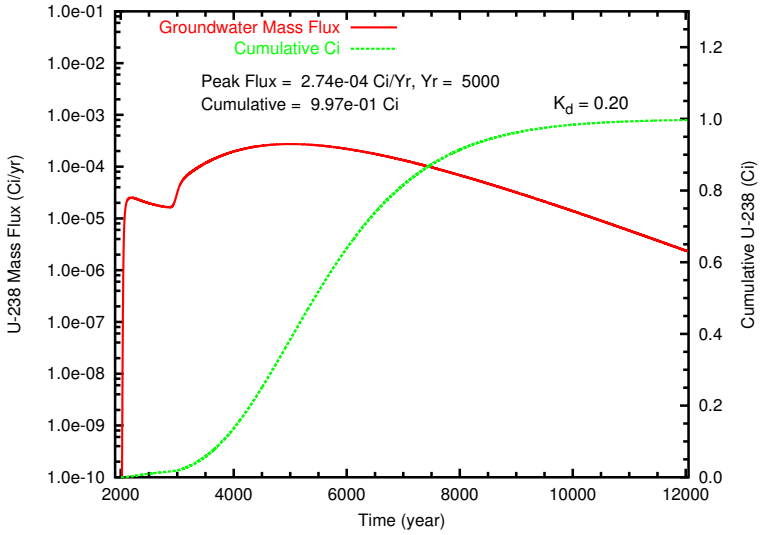

(a)

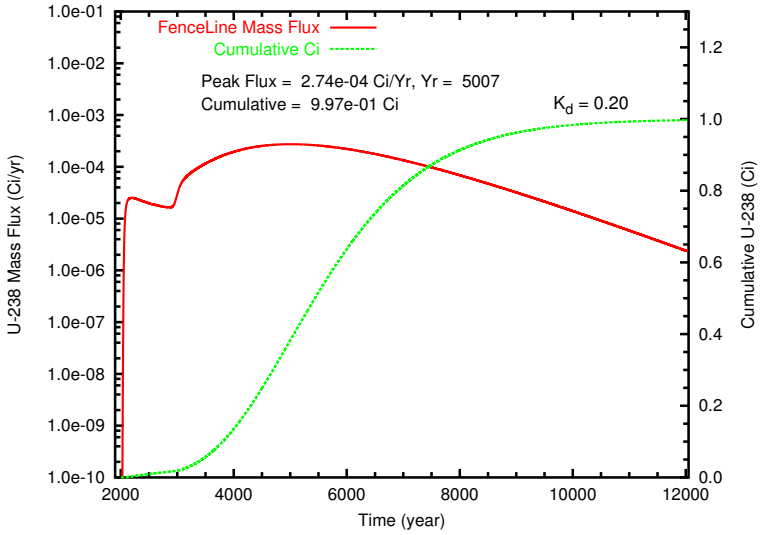

(b)

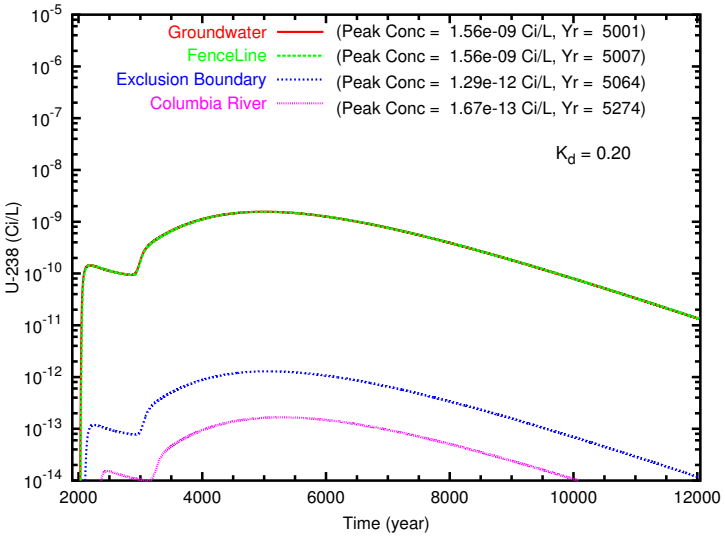

(c)

Figure B.29. Past Leak: High Degraded-Barrier Recharge Rate (3.5 mm/yr) U_0.20 mass flux at (a) the groundwater table and (b) the fenceline; and (c) the Tc-99 concentration at groundwater, fenceline, and easterly downstream compliance points.

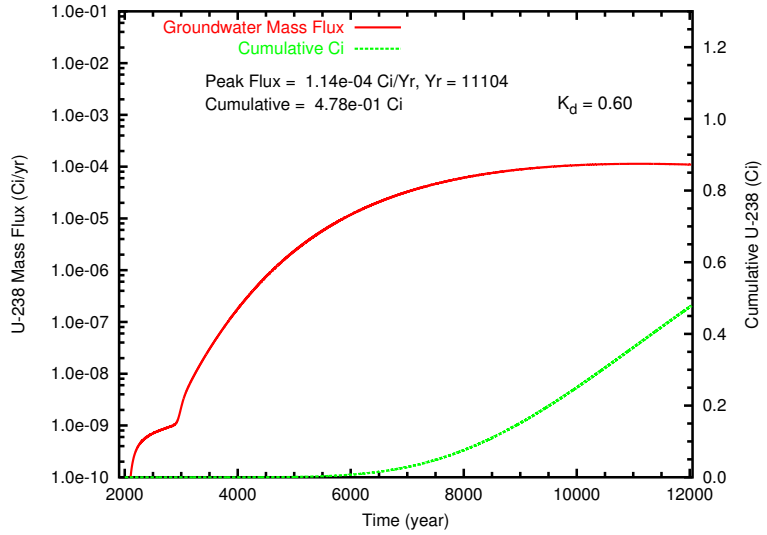

(a)

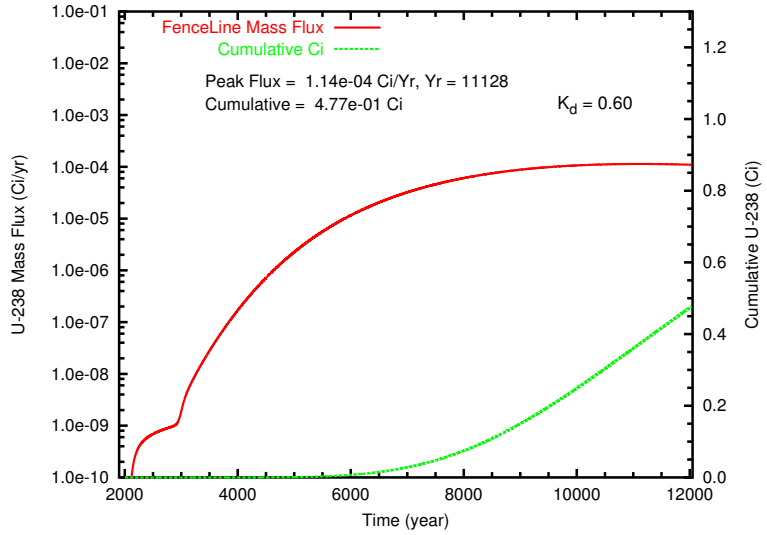

(b)

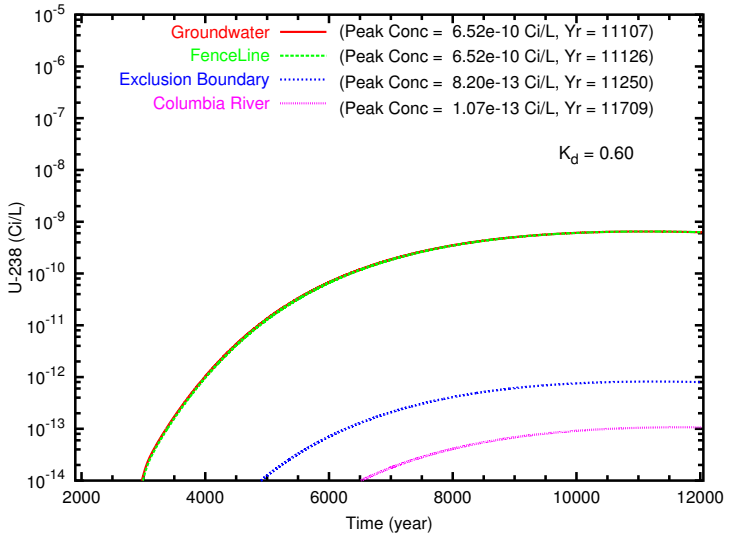

(c)

Figure B.30. Past Leak: High Degraded-Barrier Recharge Rate (3.5 mm/yr) U_0.60 mass flux at (a) the groundwater table and (b) the fenceline; and (c) the Tc-99 concentration at groundwater, fenceline, and easterly downstream compliance points.

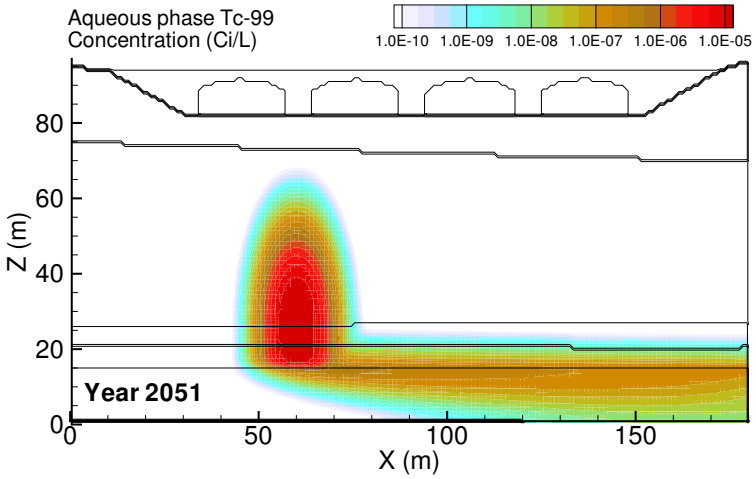

(a)

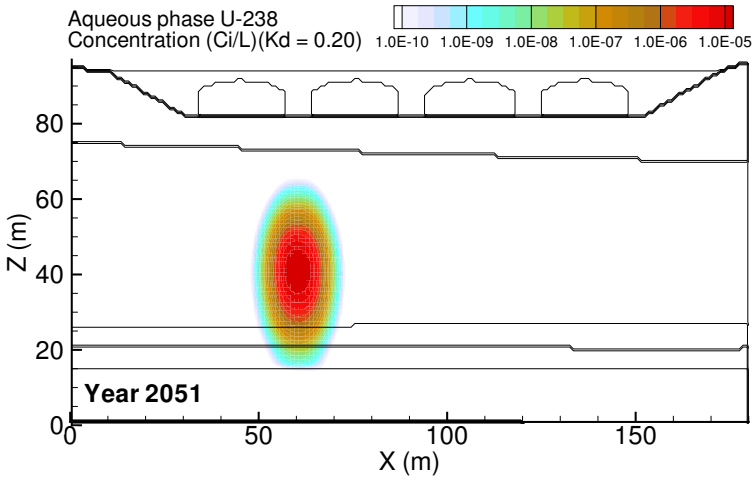

(b)

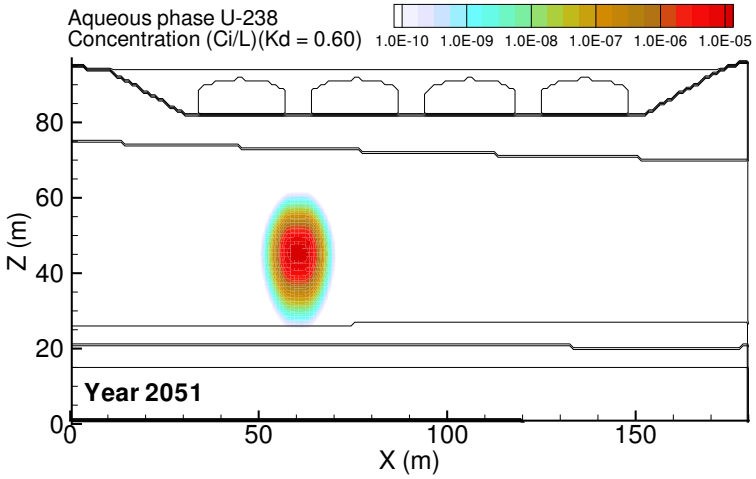

(c)

Figure B.31. Past Leak: Low Degraded-Barrier Recharge Rate (0.5 mm/yr) aqueous concentration distributions at year 2051 for (a) Tc-99, (b) U_0.20 and (c) U_0.60. Year of Tc-99 peak concentration at fenceline was 2051.

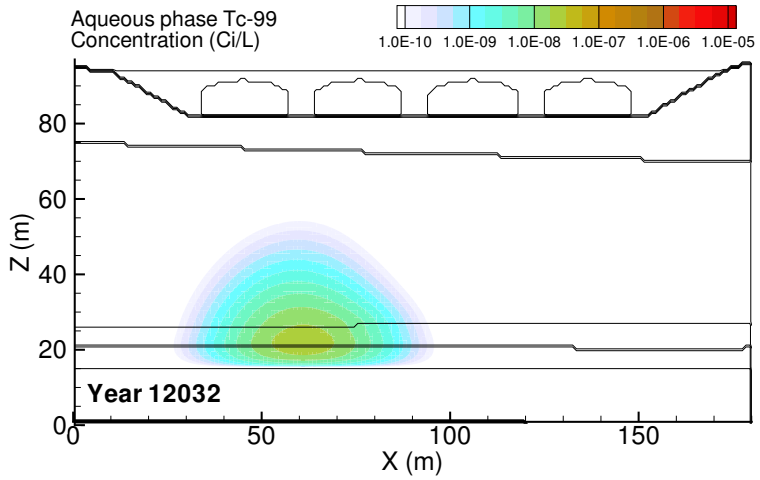

(a)

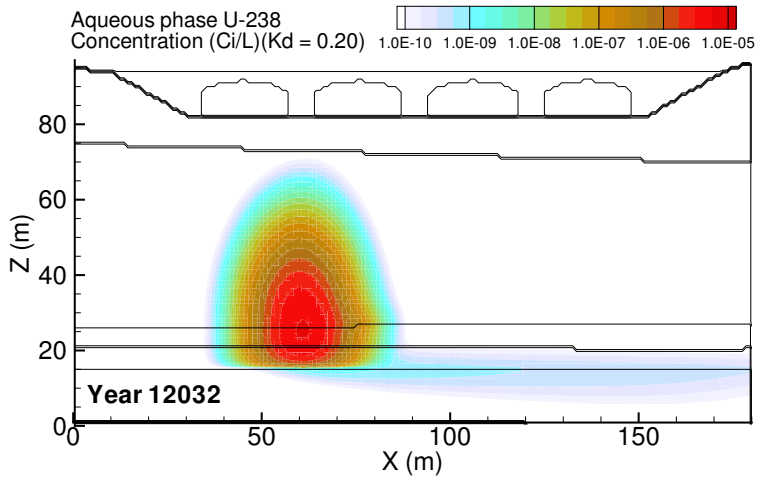

(b)

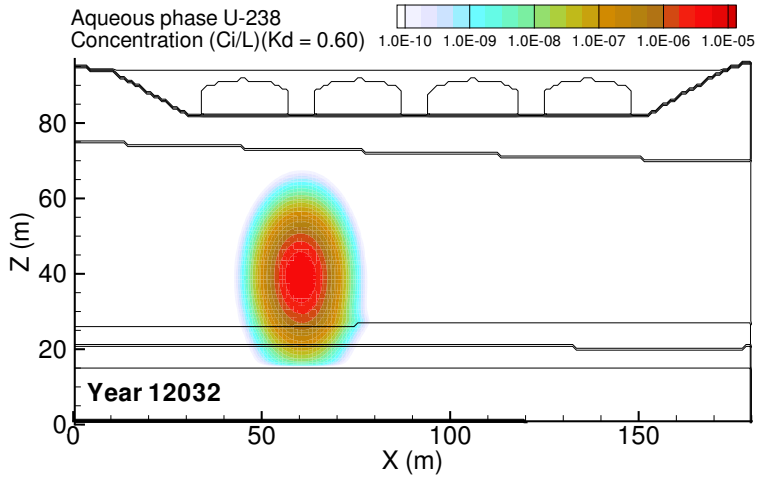

(c)

Figure B.32. Past Leak: Low Degraded-Barrier Recharge Rate (0.5 mm/yr) aqueous concentration distributions at year 12032 for (a) Tc-99, (b) U_0.20 and (c) U_0.60.

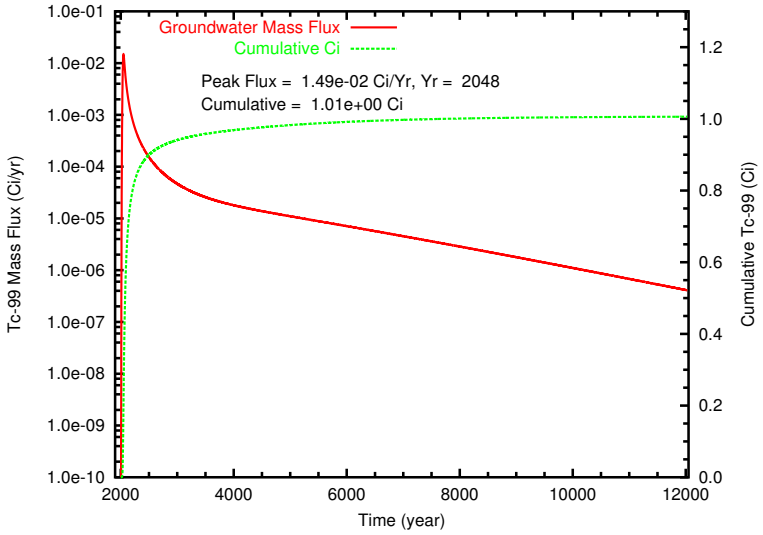

(a)

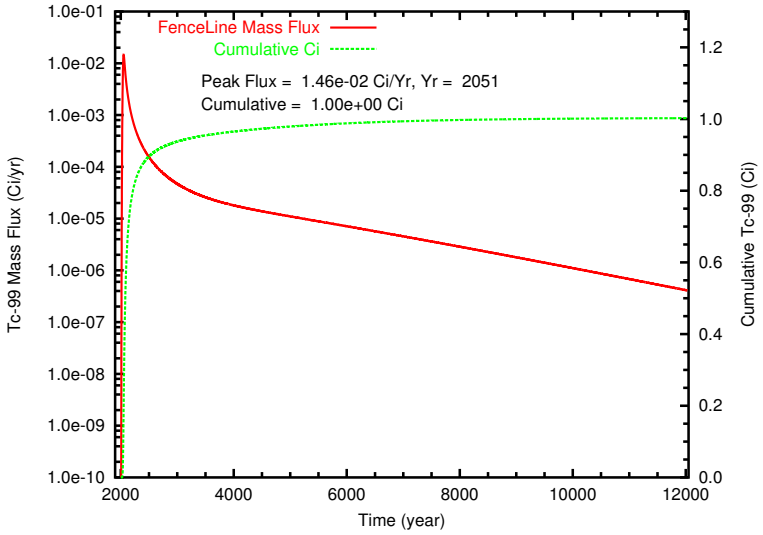

(b)

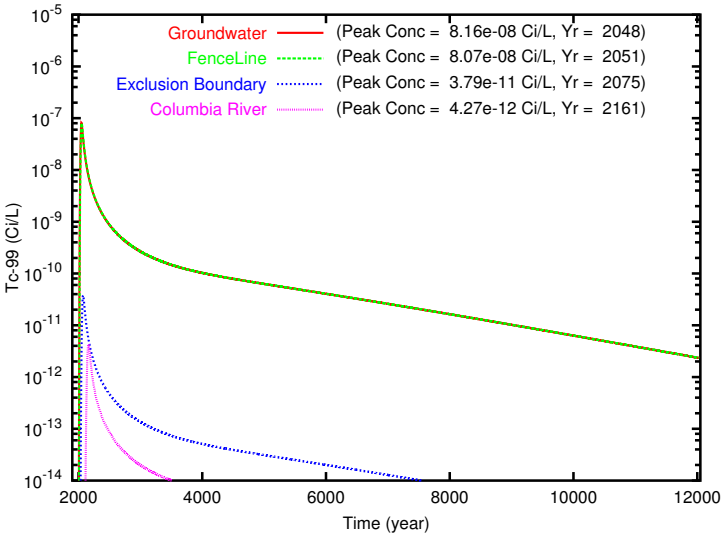

(c)

Figure B.33. Past Leak: Low Degraded-Barrier Recharge Rate (0.5 mm/yr) Tc-99 mass flux at (a) the groundwater table and (b) the fenceline; and (c) the Tc-99 concentration at groundwater, fenceline, and easterly downstream compliance points.

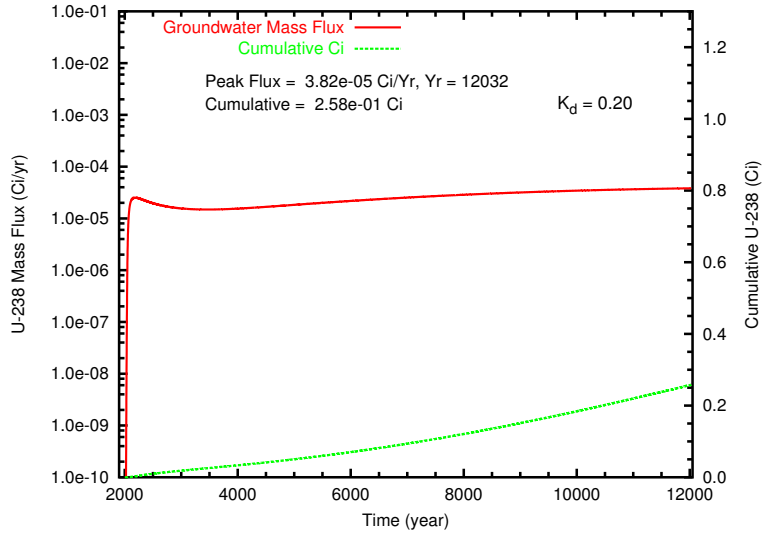

(a)

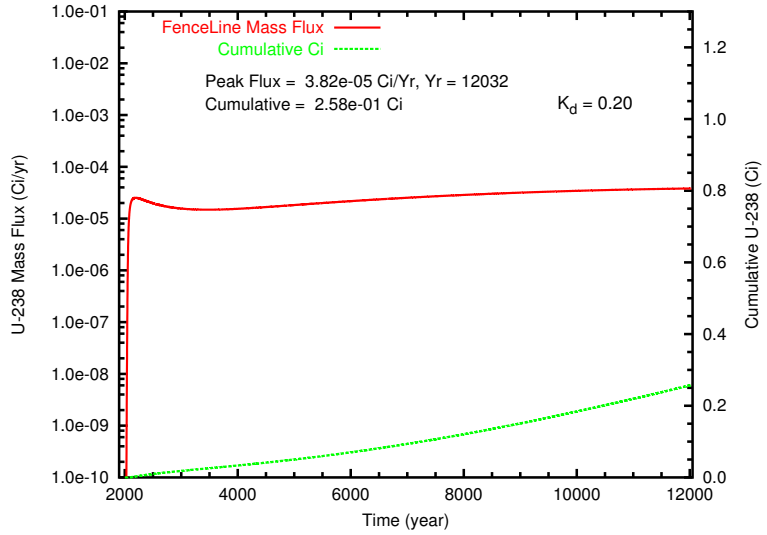

(b)

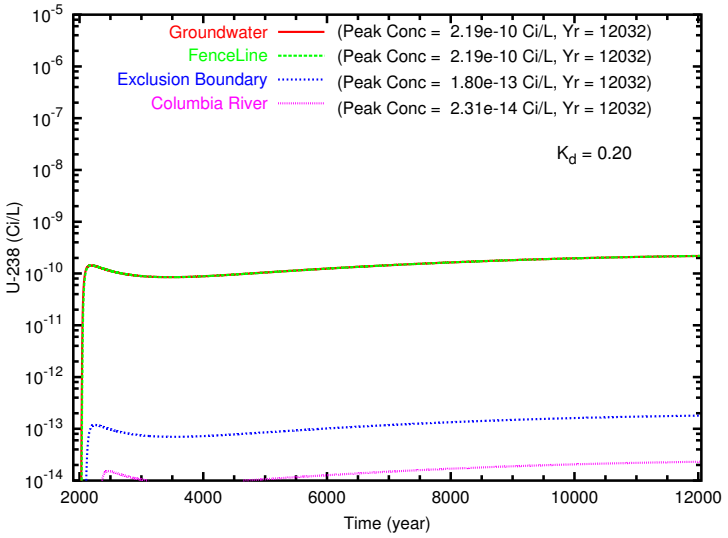

(c)

Figure B.34. Past Leak: Low Degraded-Barrier Recharge Rate (0.5 mm/yr) U_0.20 mass flux at (a) the groundwater table and (b) the fenceline; and (c) the Tc-99 concentration at groundwater, fenceline, and easterly downstream compliance points.

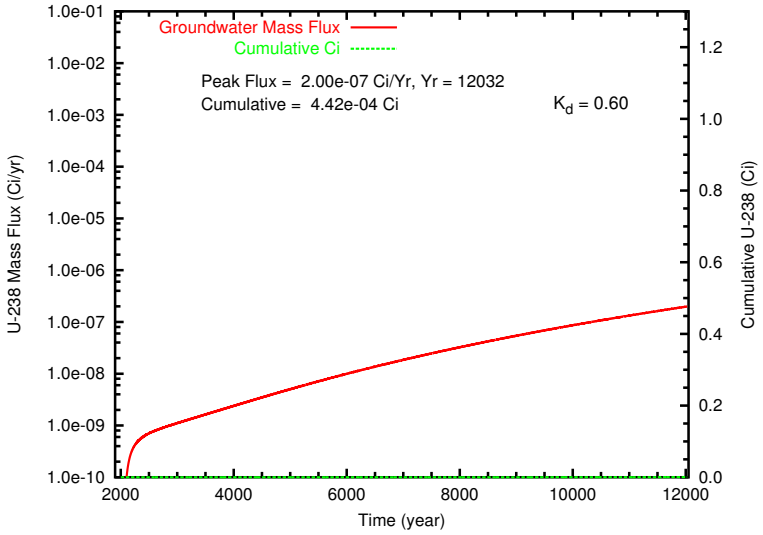

(a)

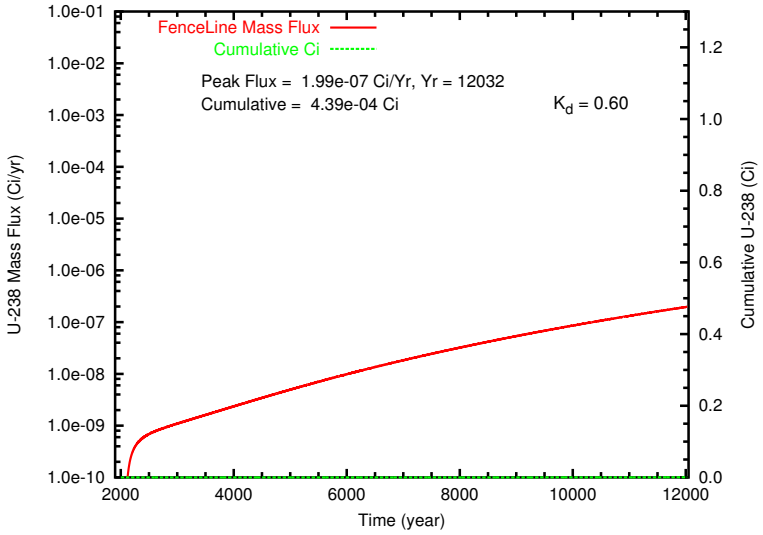

(b)

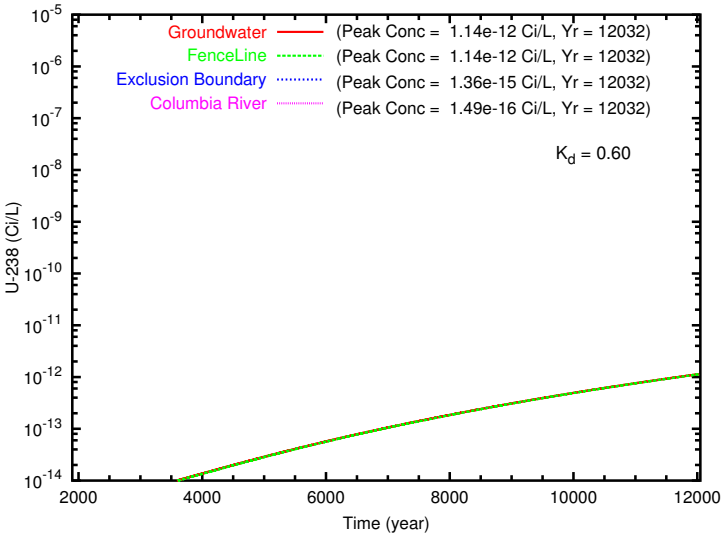

(c)

Figure B.35. Past Leak: Low Degraded-Barrier Recharge Rate (0.5 mm/yr) U_0.60 mass flux at (a) the groundwater table and (b) the fenceline; and (c) the Tc-99 concentration at groundwater, fenceline, and easterly downstream compliance points.

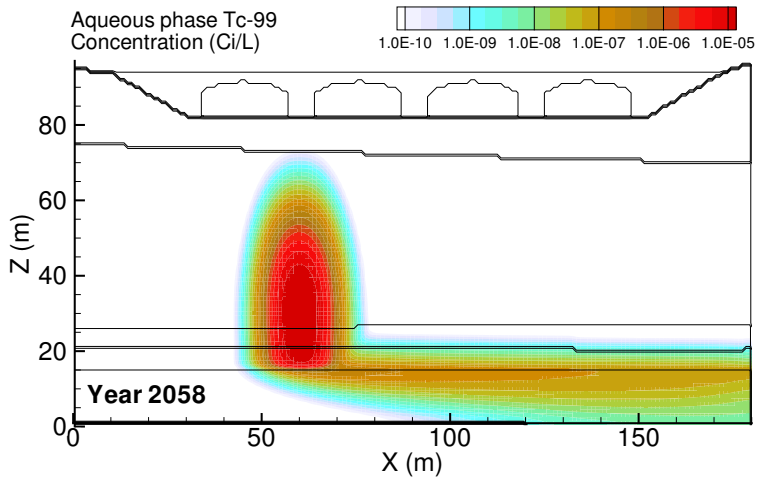

(a)

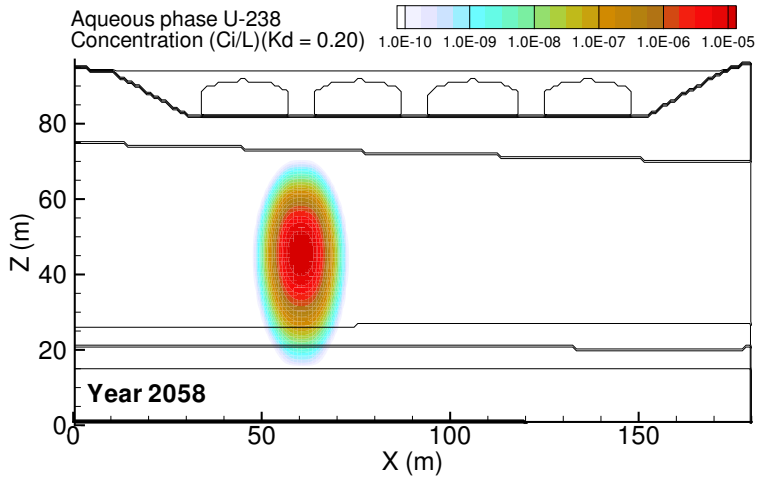

(b)

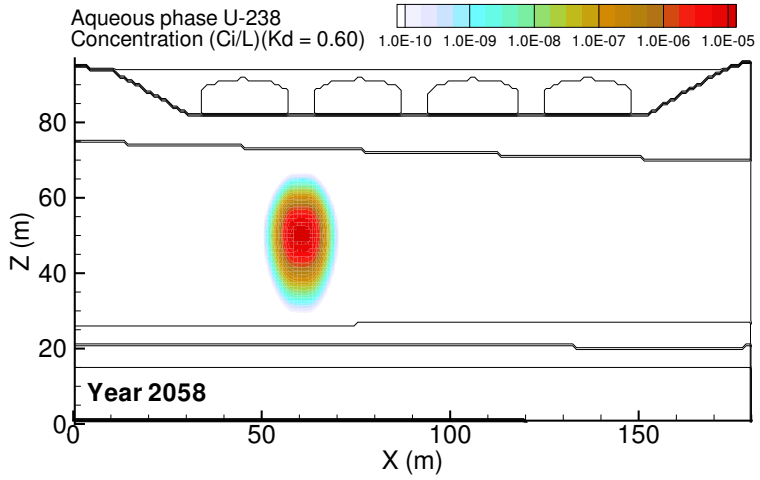

(c)

Figure B.36. Past Leak: High Plume Placement (170 ft bgs) aqueous concentration distributions at year 2058 for (a) Tc-99, (b) U_0.20 and (c) U_0.60. Year of Tc-99 peak concentration at fenceline was 2058.

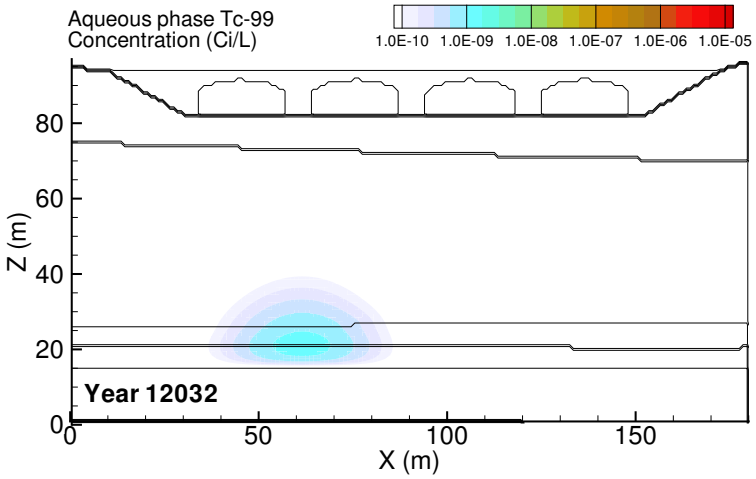

(a)

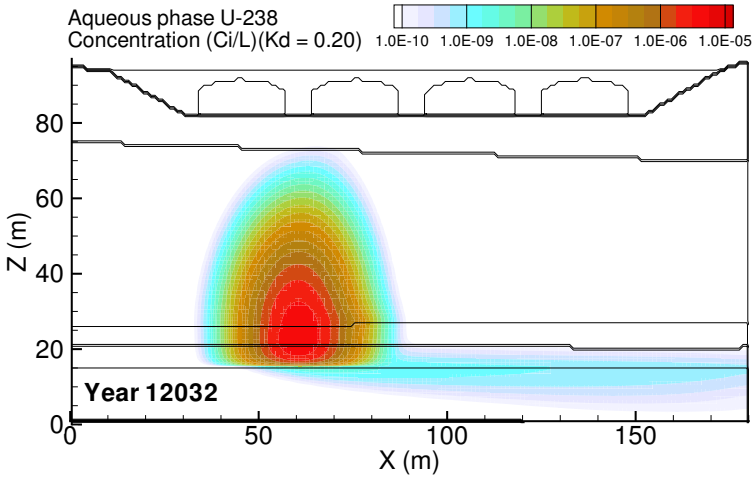

(b)

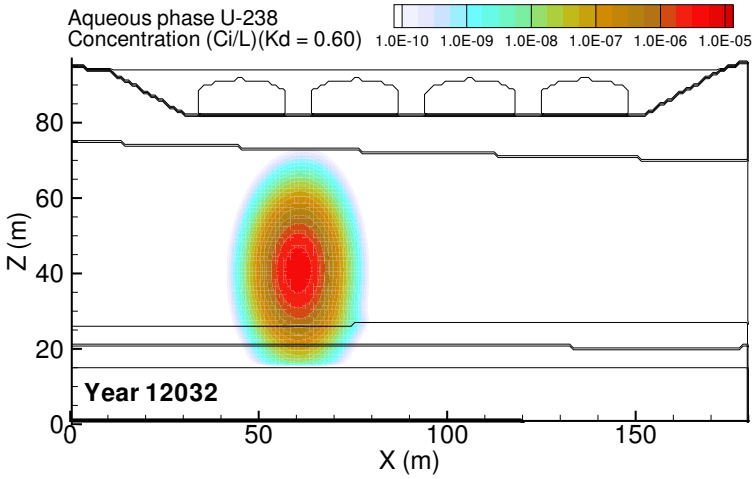

(c)

Figure B.37. Past Leak: High Plume Placement (170 ft bgs) aqueous concentration distributions at year 12032 for (a) Tc-99, (b) U_0.20 and (c) U_0.60.

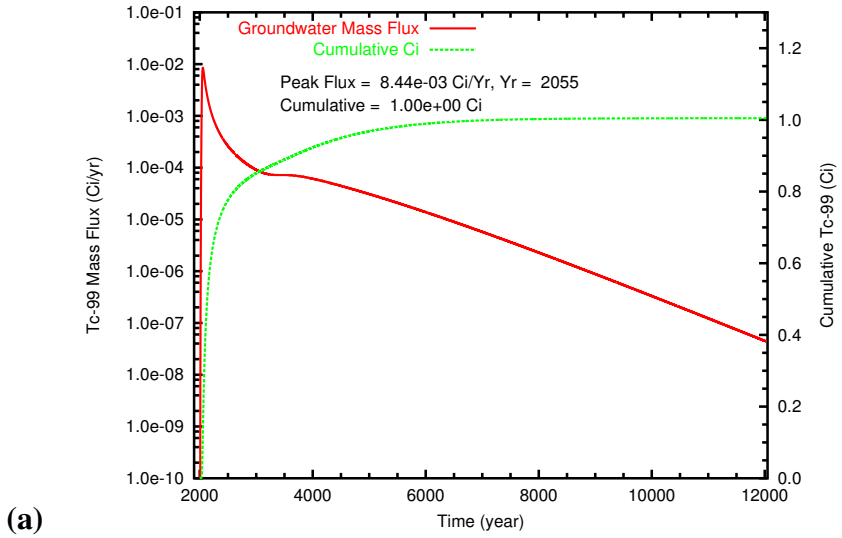

(a)

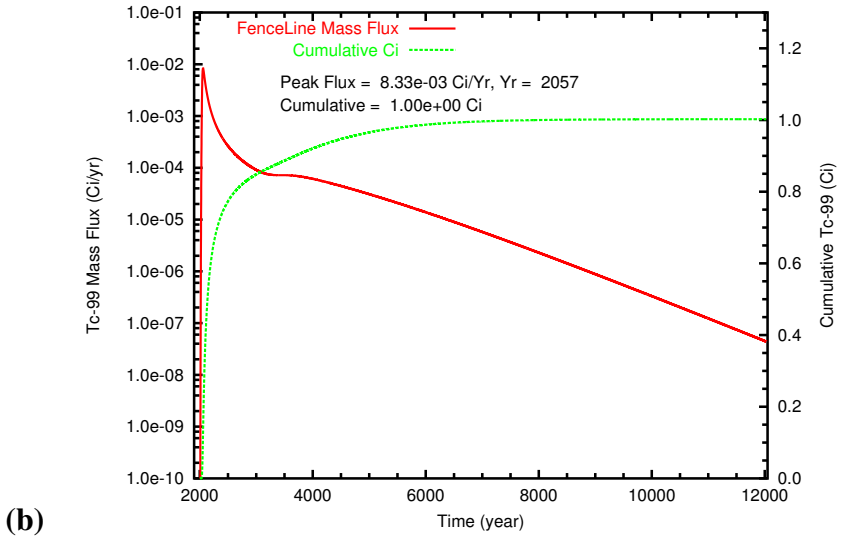

(b)

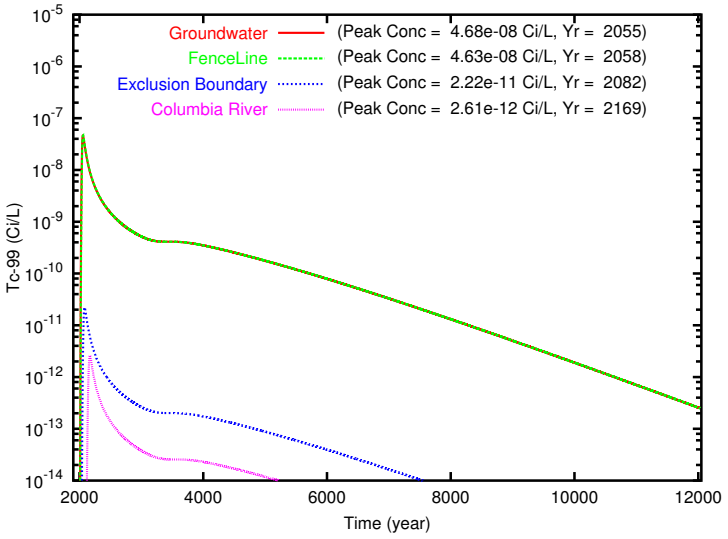

(c)

Figure B.38. Past Leak: High Plume Placement (170 ft bgs) Tc-99 mass flux at (a) the groundwater table and (b) the fenceline; and (c) the Tc-99 concentration at groundwater, fenceline, and easterly downstream compliance points.

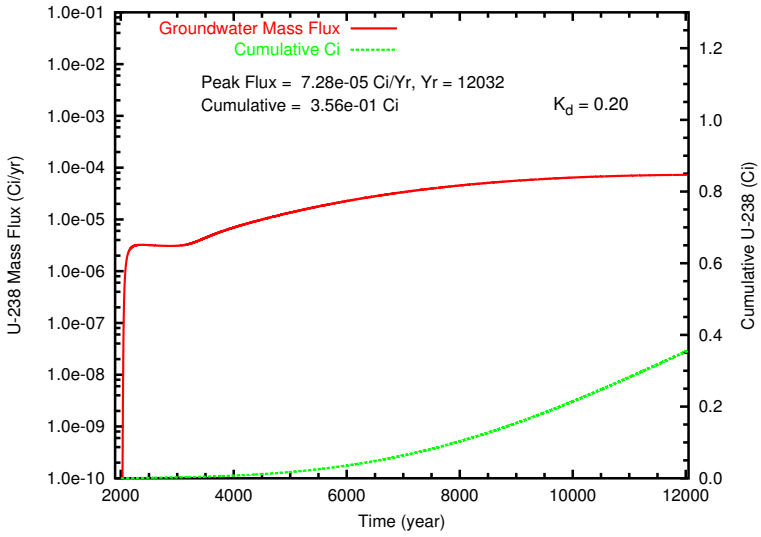

(a)

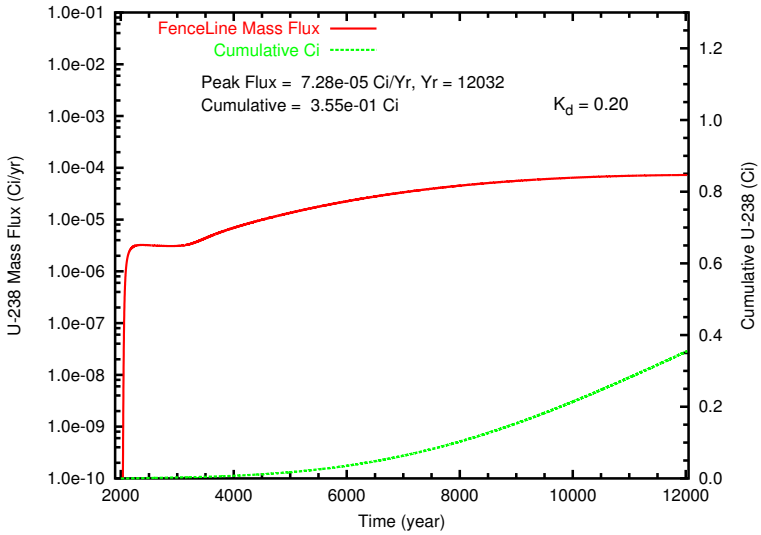

(b)

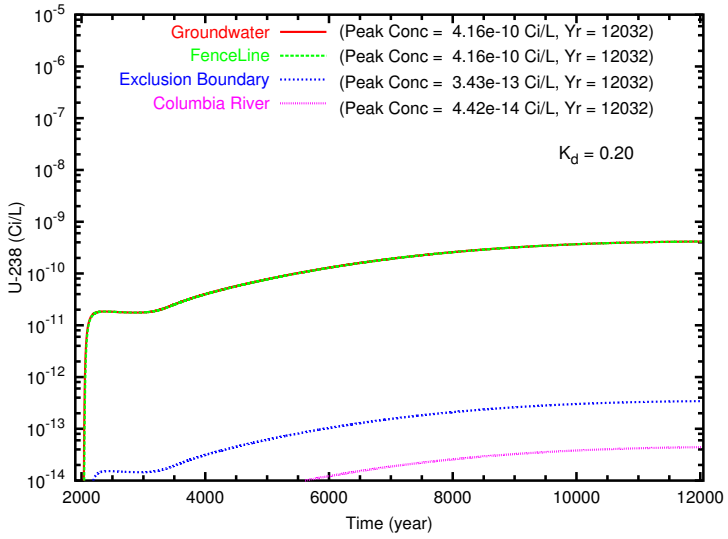

(c)

Figure B.39. Past Leak: High Plume Placement (170 ft bgs) U_0.20 mass flux at (a) the groundwater table and (b) the fenceline; and (c) the Tc-99 concentration at groundwater, fenceline, and easterly downstream compliance points.

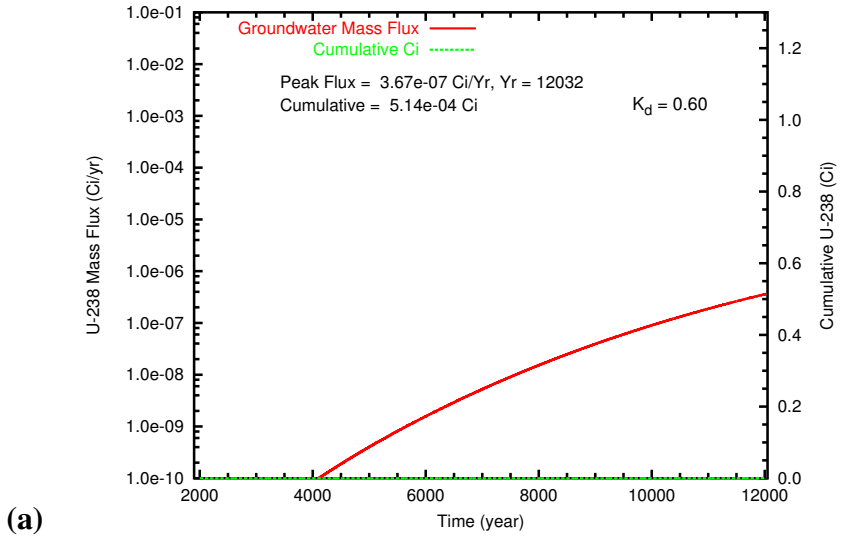

(a)

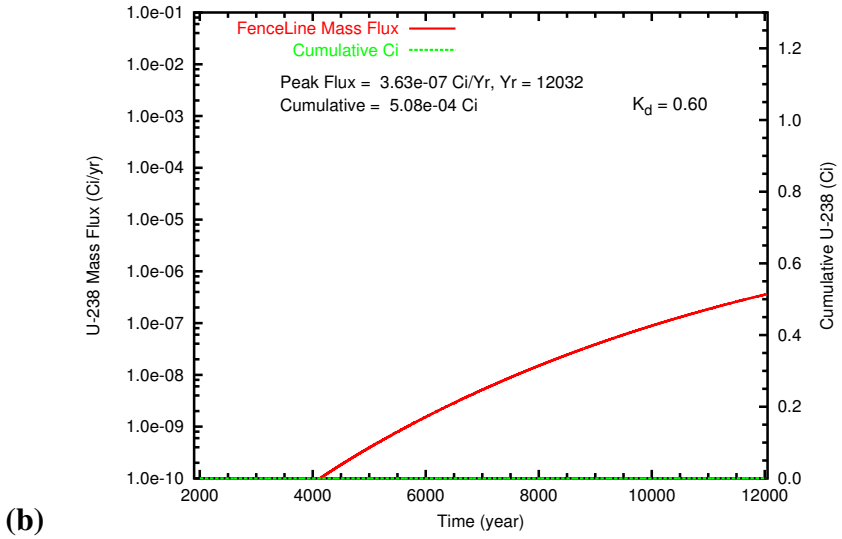

(b)

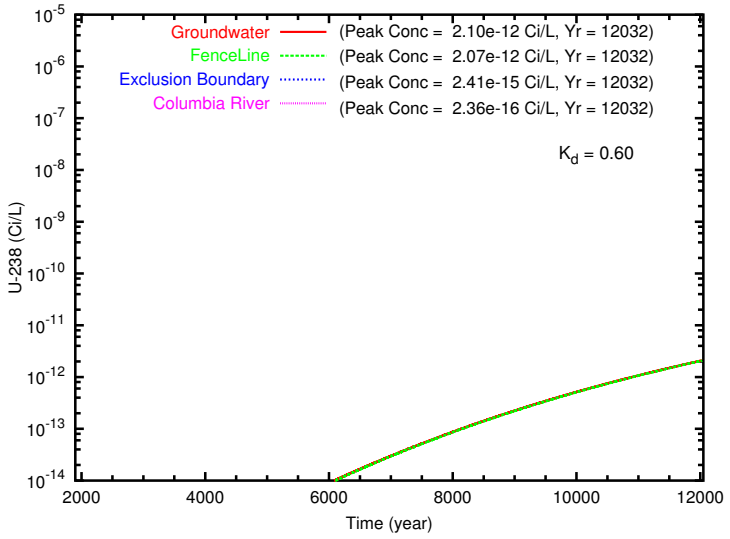

(c)

Figure B.40. Past Leak: High Plume Placement (170 ft bgs) U_0.60 mass flux at (a) the groundwater table and (b) the fenceline; and (c) the Tc-99 concentration at groundwater, fenceline, and easterly downstream compliance points.

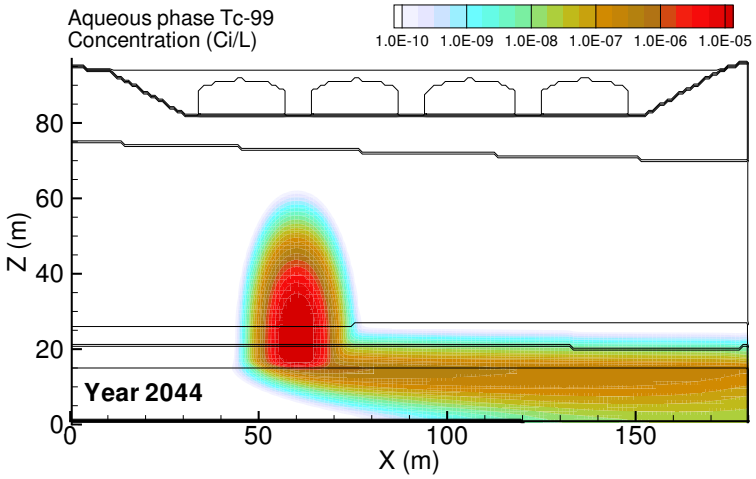

(a)

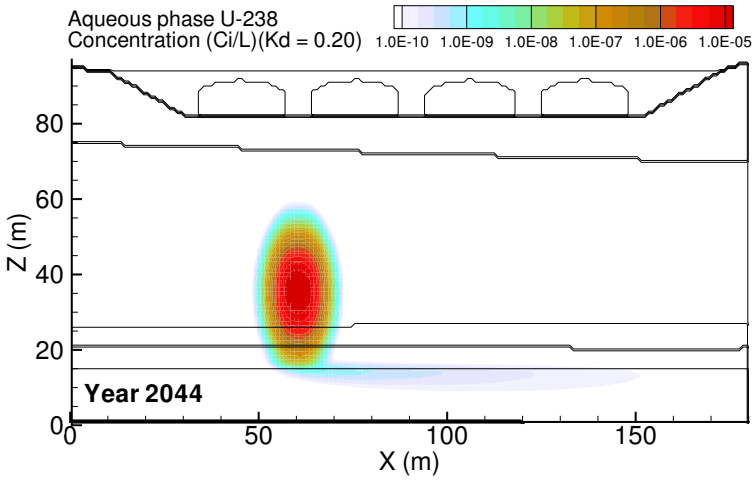

(b)

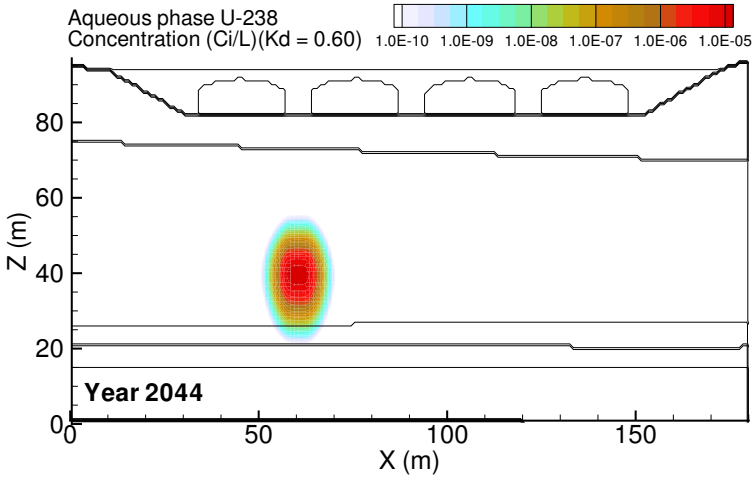

(c)

Figure B.41. Past Leak: Low Plume Placement (130 ft bgs) aqueous concentration distributions at year 2044 for (a) Tc-99, (b) U_0.20 and (c) U_0.60. Year of Tc-99 peak concentration at fenceline was 2044.

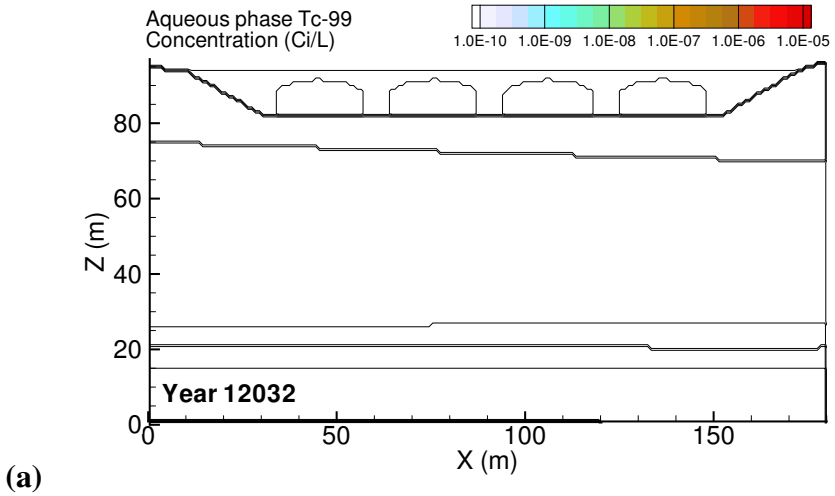

(a)

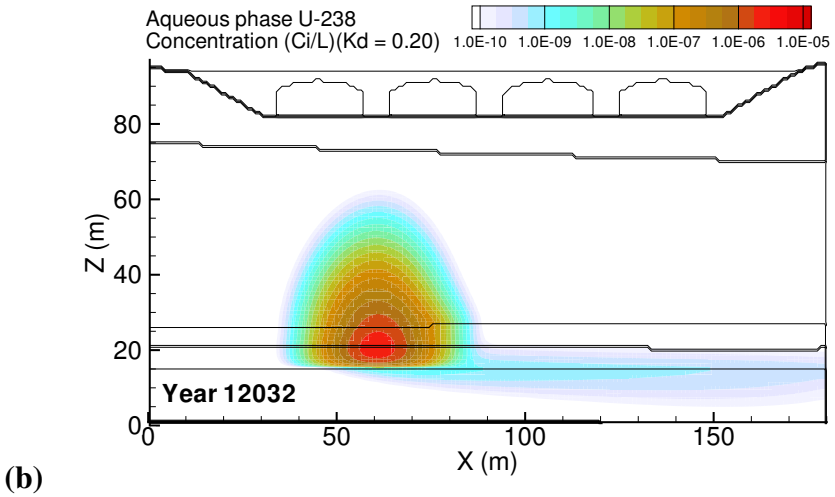

(b)

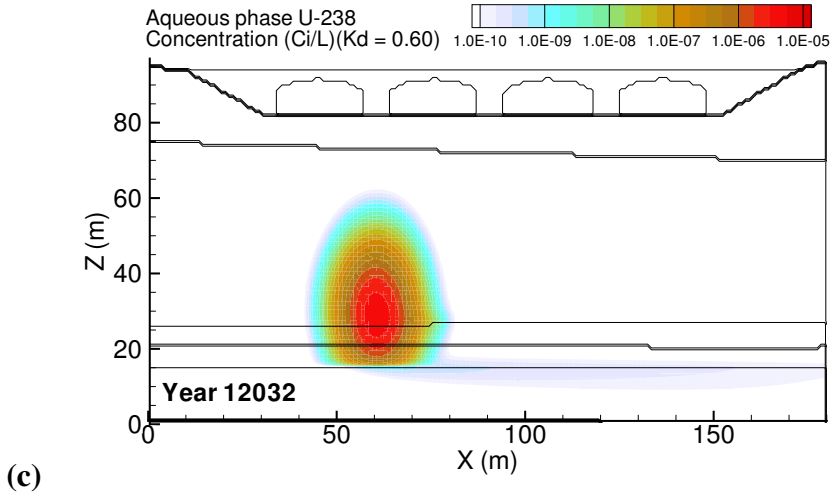

(c)

Figure B.42. Past Leak: Low Plume Placement (130 ft bgs) aqueous concentration distributions at year 12032 for (a) Tc-99, (b) U_0.20 and (c) U_0.60.

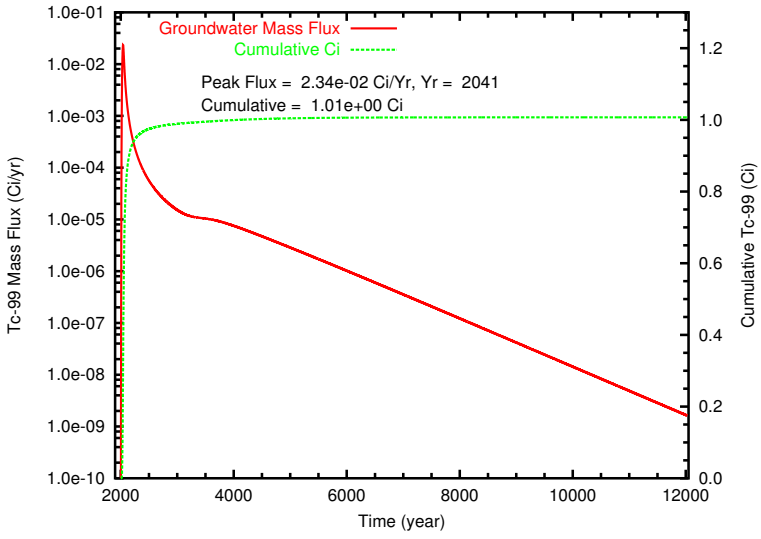

(a)

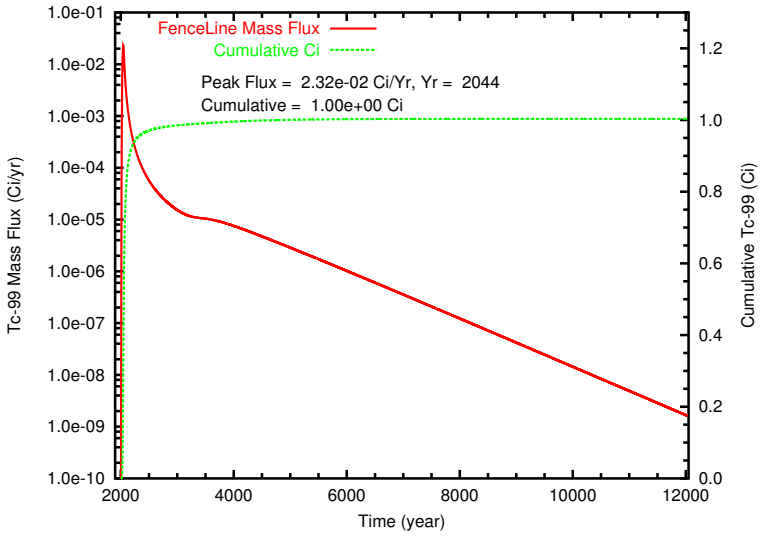

(b)

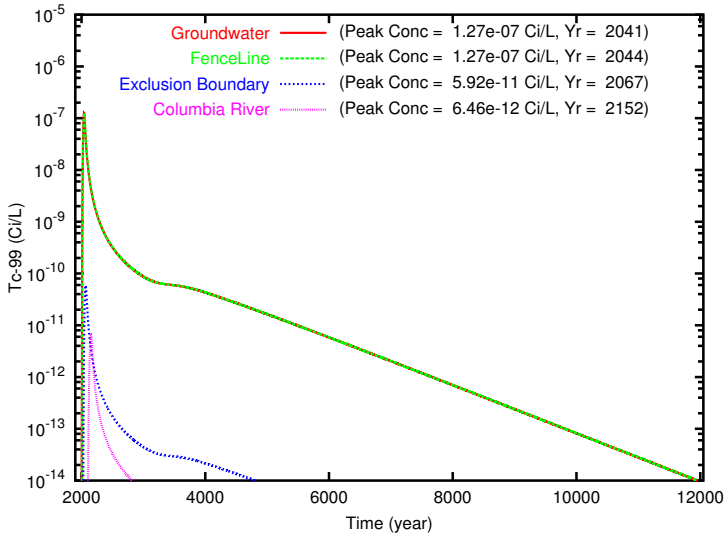

(c)

Figure B.43. Past Leak: Low Plume Placement (130 ft bgs) Tc-99 mass flux at (a) the groundwater table and (b) the fenceline; and (c) the Tc-99 concentration at groundwater, fenceline, and easterly downstream compliance points.

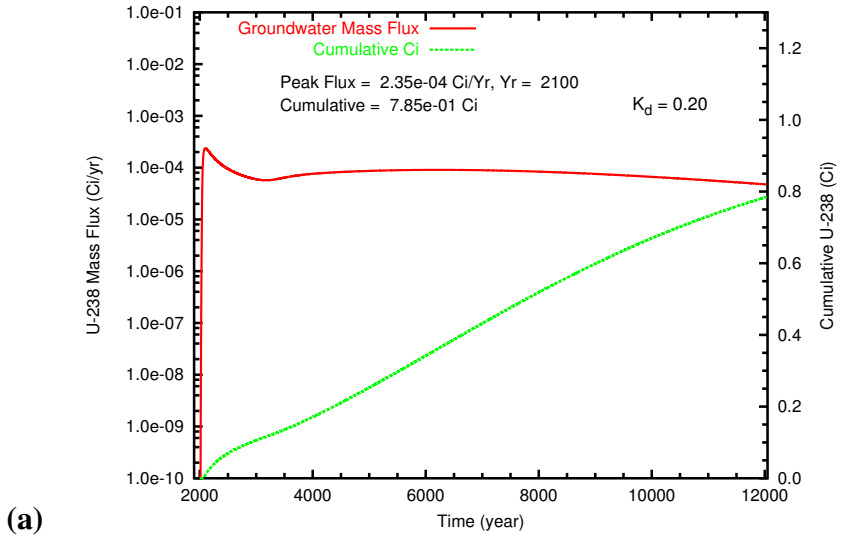

(a)

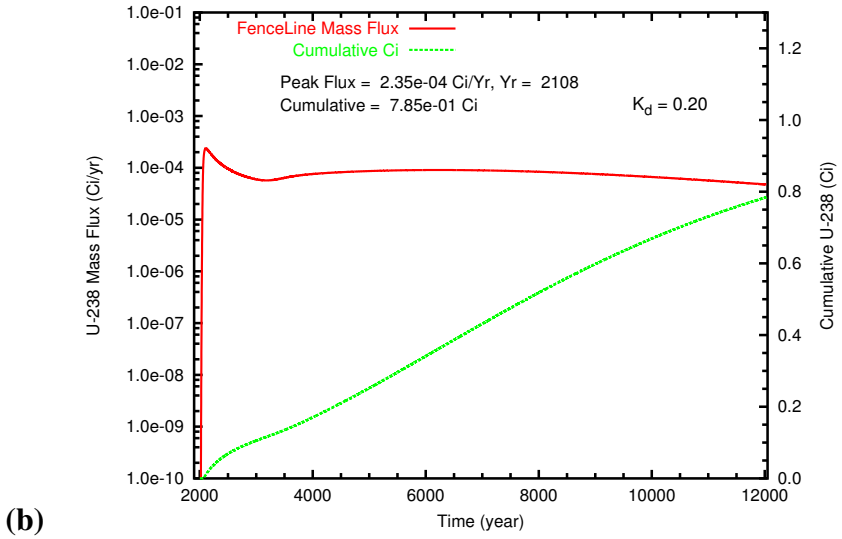

(b)

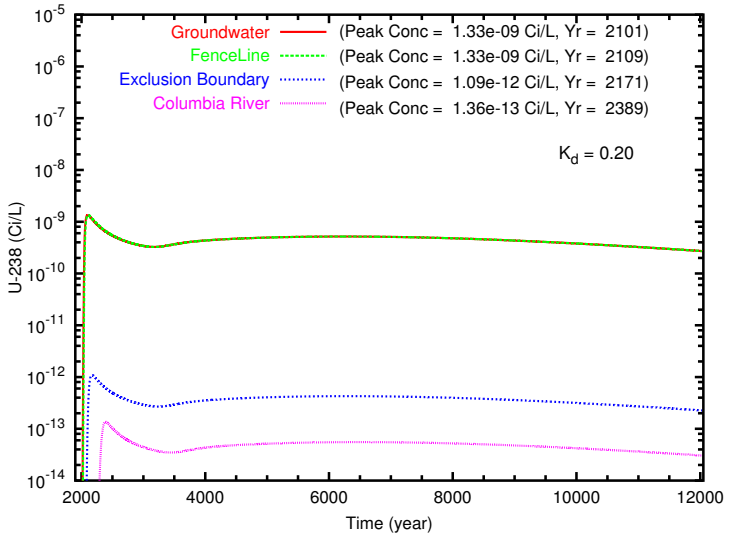

(c)

Figure B.44. Past Leak: Low Plume Placement (130 ft bgs) U_0.20 mass flux at (a) the groundwater table and (b) the fenceline; and (c) the Tc-99 concentration at groundwater, fenceline, and easterly downstream compliance points.

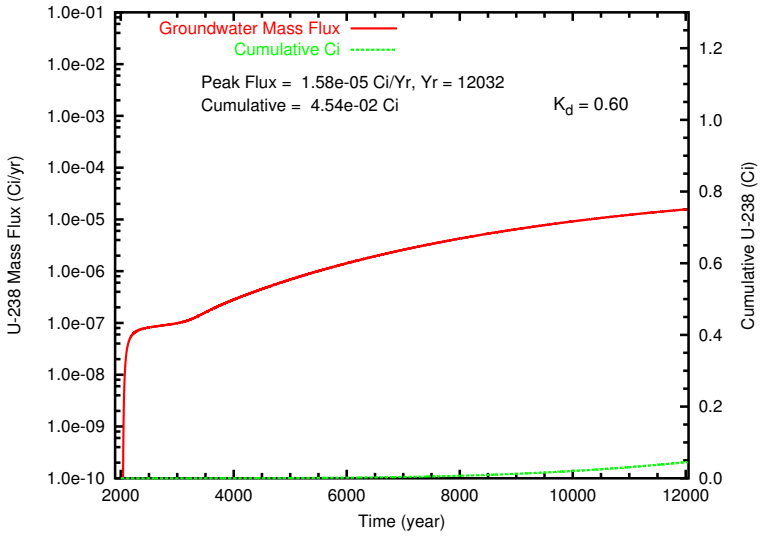

(a)

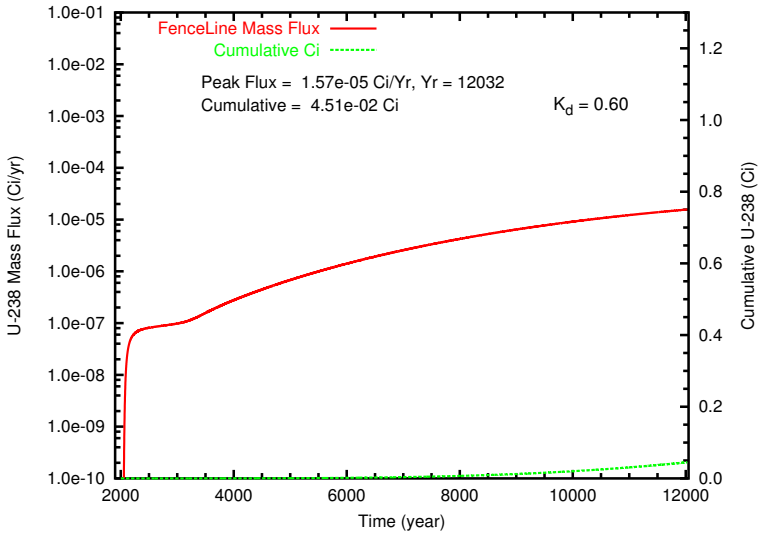

(b)

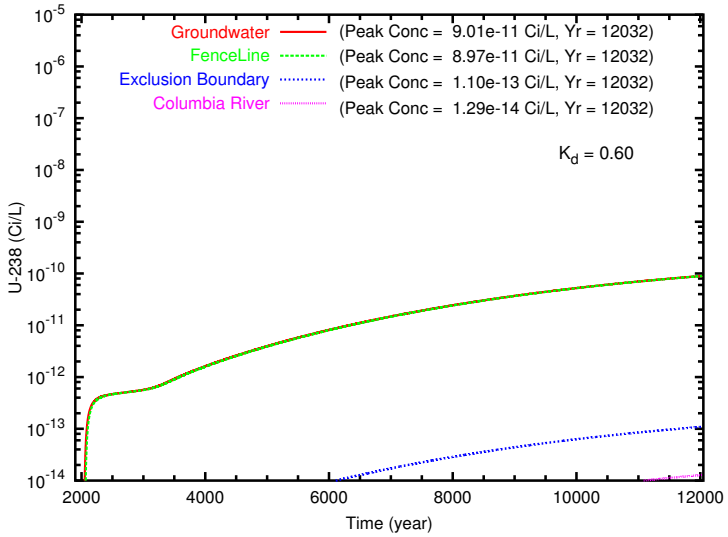

(c)

Figure B.45. Past Leak: Low Plume Placement (130 ft bgs) U_0.60 mass flux at (a) the groundwater table and (b) the fenceline; and (c) the Tc-99 concentration at groundwater, fenceline, and easterly downstream compliance points.

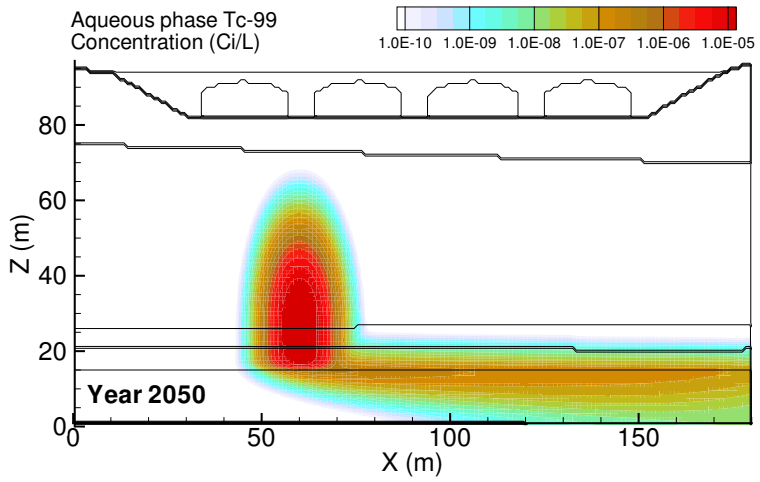

(a)

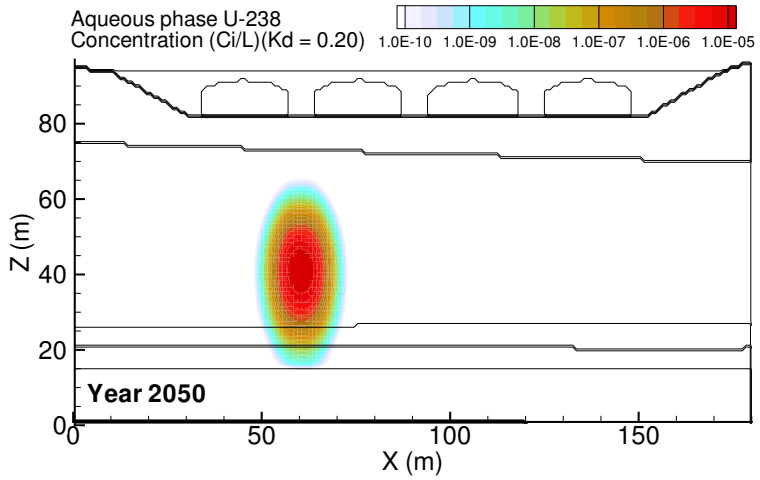

(b)

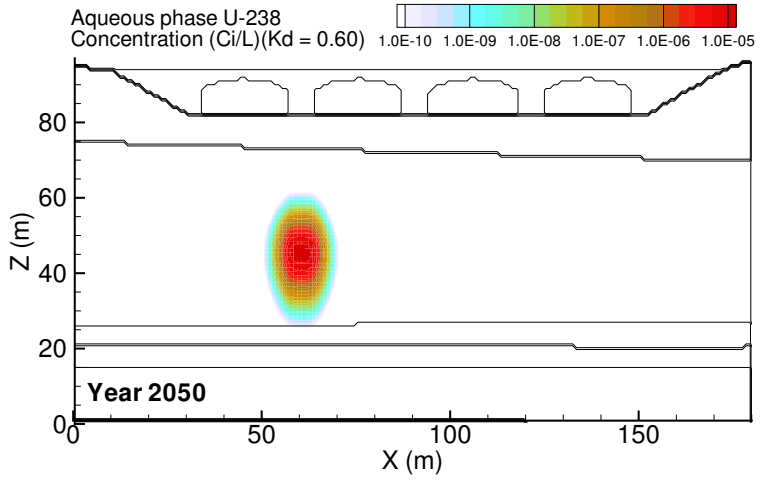

(c)

Figure B.46. Past Leak: High Aquifer Hydraulic Conductivity (4000 m/d) aqueous concentration distributions at year 2050 for (a) Tc-99, (b) U_0.20 and (c) U_0.60. Year of Tc-99 peak concentration at fenceline was 2050.

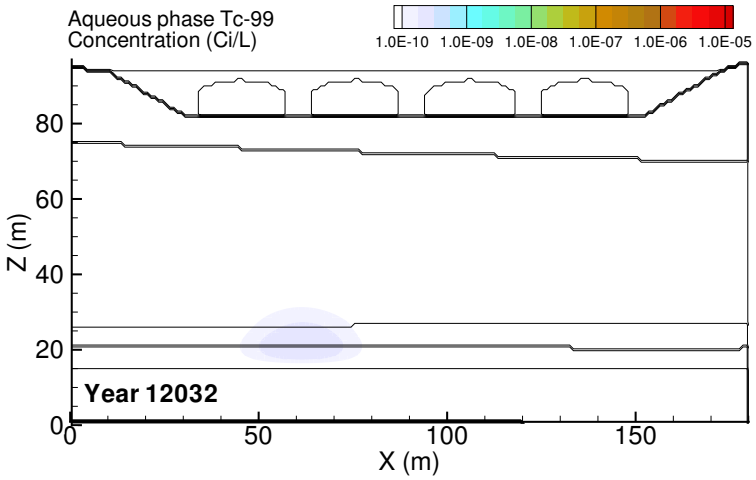

(a)

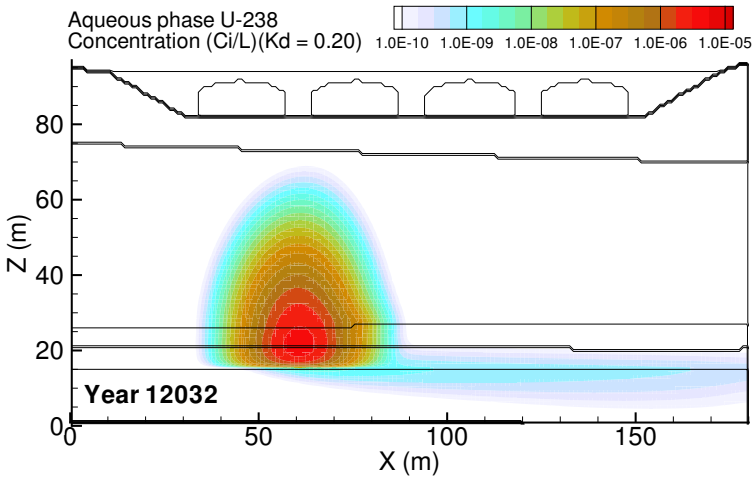

(b)

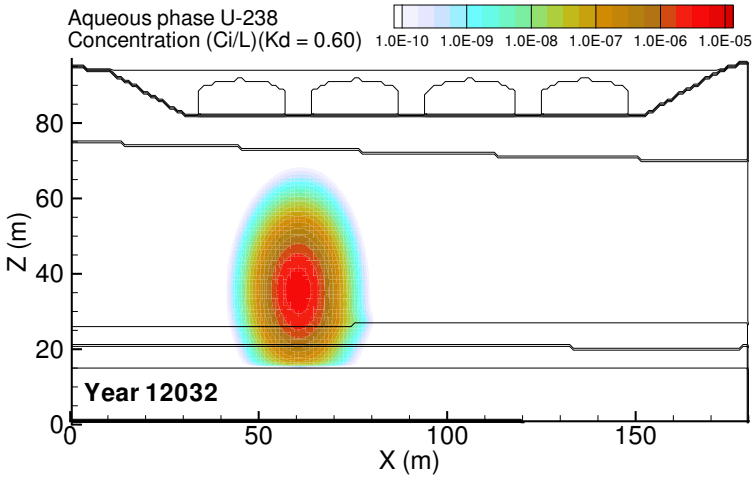

(c)

Figure B.47. Past Leak: High Aquifer Hydraulic Conductivity (4000 m/d) aqueous concentration distributions at year 12032 for (a) Tc-99, (b) U_0.20 and (c) U_0.60.

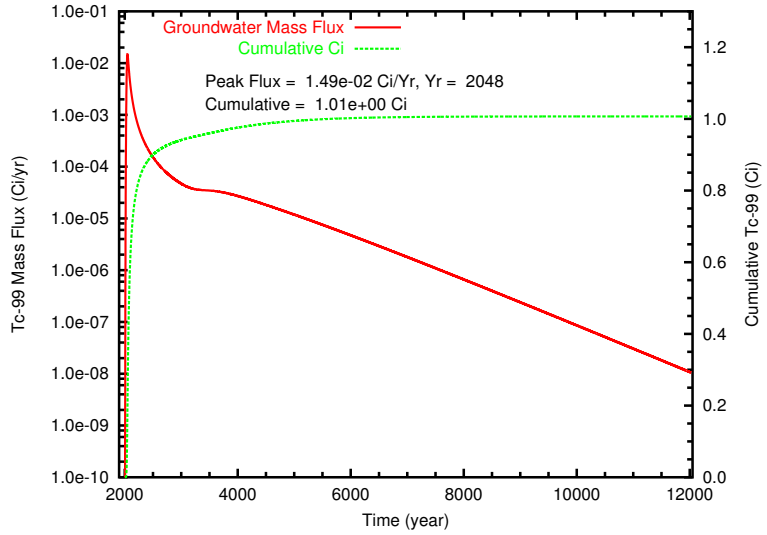

(a)

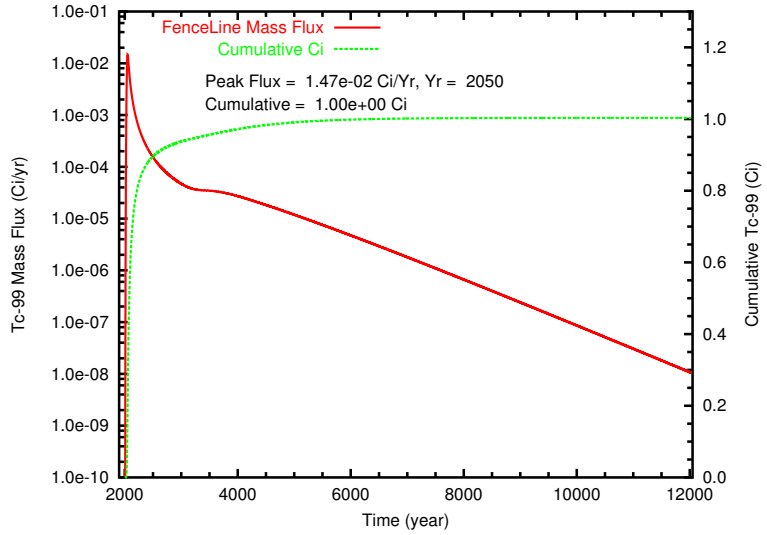

(b)

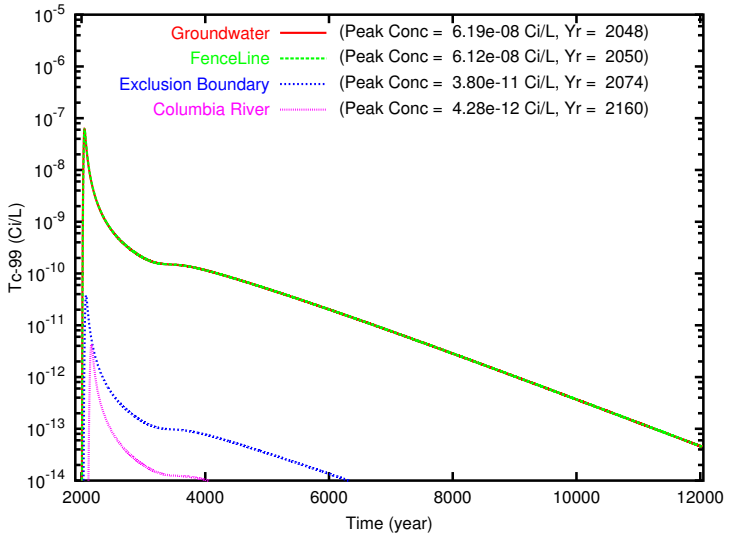

(c)

Figure B.48. Past Leak: High Aquifer Hydraulic Conductivity (4000 m/d) Tc-99 mass flux at (a) the groundwater table and (b) the fenceline; and (c) the Tc-99 concentration at groundwater, fenceline, and easterly downstream compliance points.

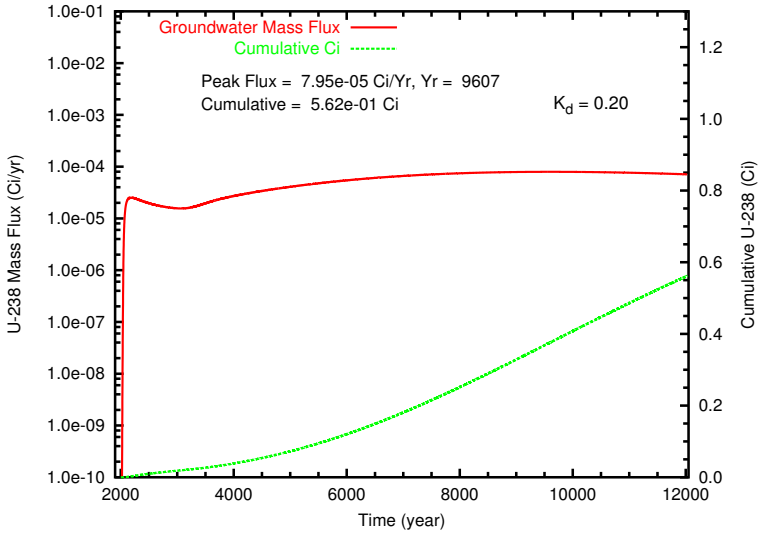

(a)

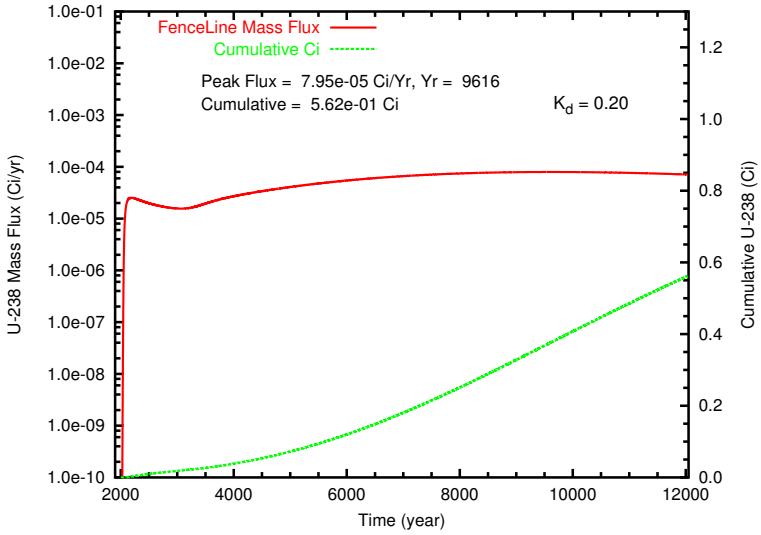

(b)

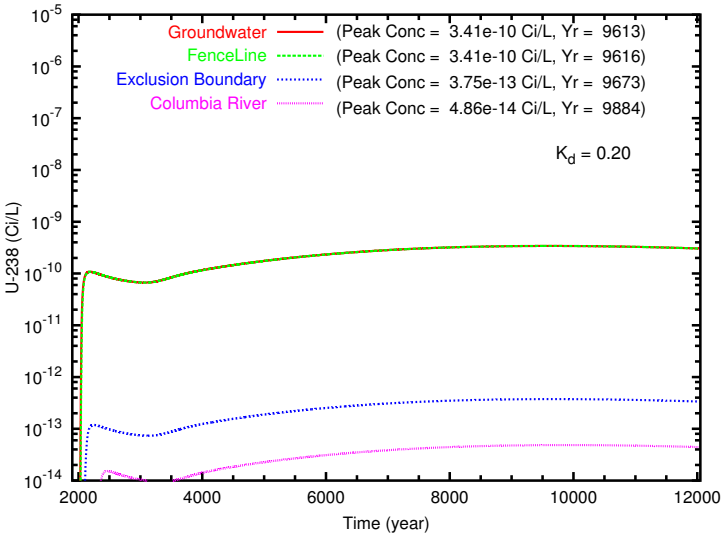

(c)

Figure B.49. Past Leak: High Aquifer Hydraulic Conductivity (4000 m/d) U_0.20 mass flux at (a) the groundwater table and (b) the fenceline; and (c) the Tc-99 concentration at groundwater, fenceline, and easterly downstream compliance points.

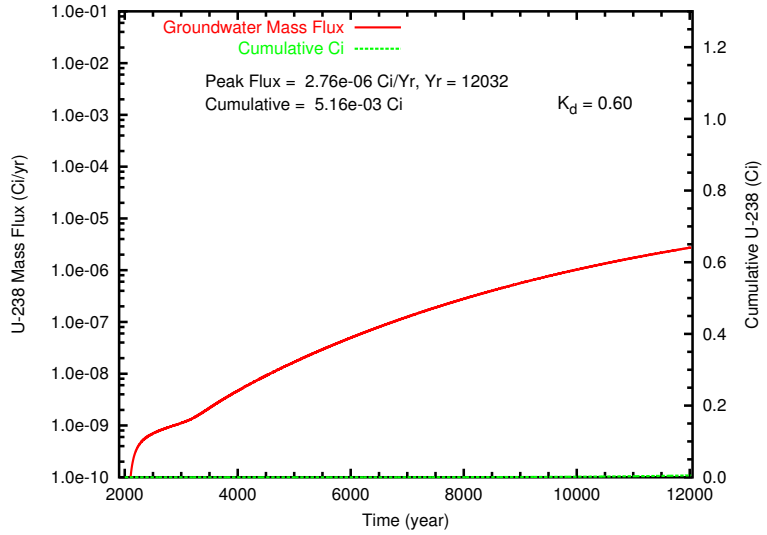

(a)

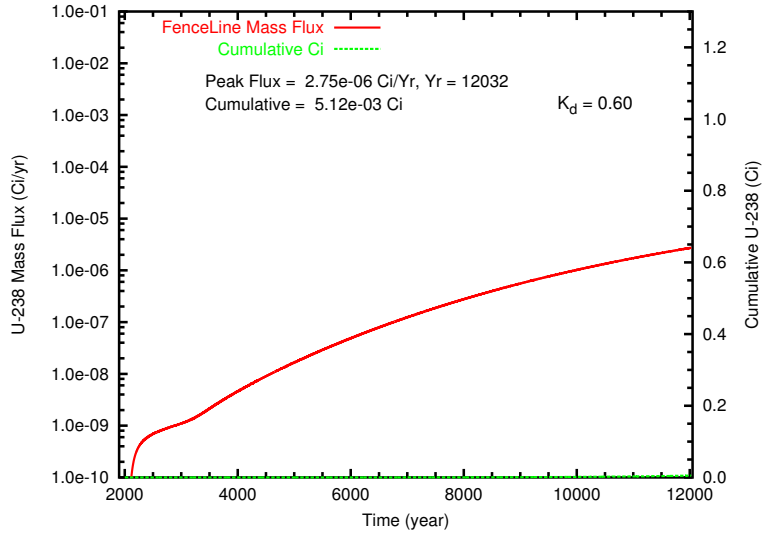

(b)

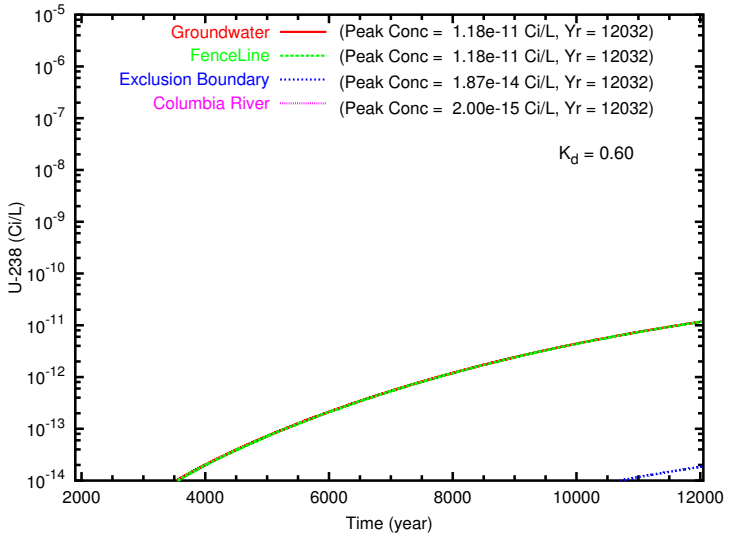

(c)

Figure B.50. Past Leak: High Aquifer Hydraulic Conductivity (4000 m/d) U_0.60 mass flux at (a) the groundwater table and (b) the fenceline; and (c) the Tc-99 concentration at groundwater, fenceline, and easterly downstream compliance points.

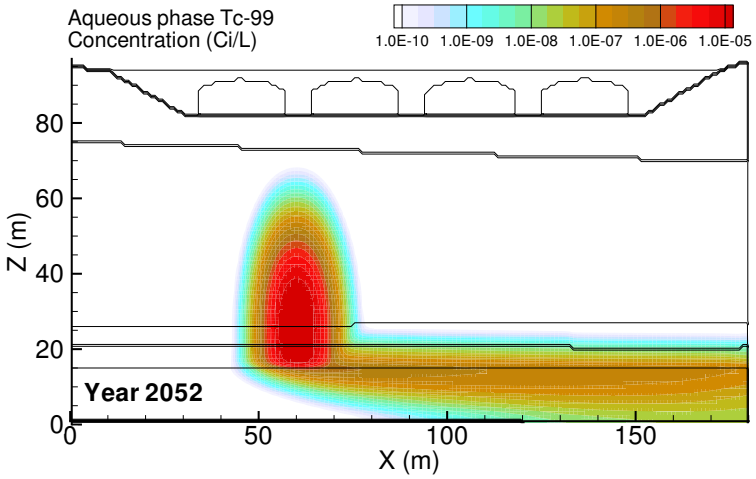

(a)

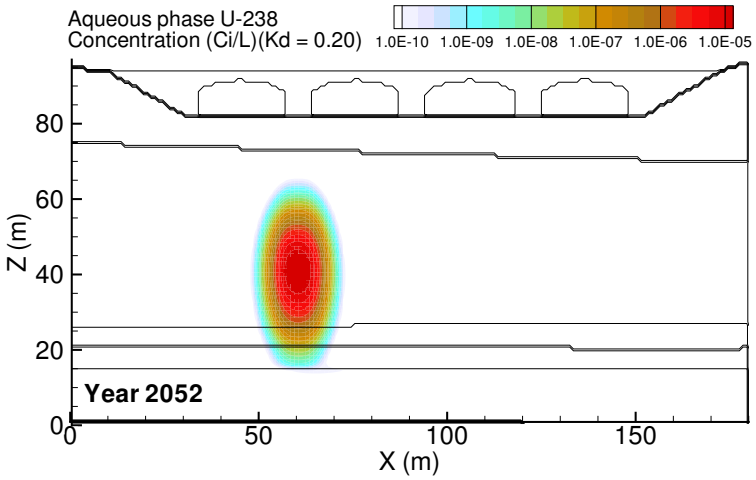

(b)

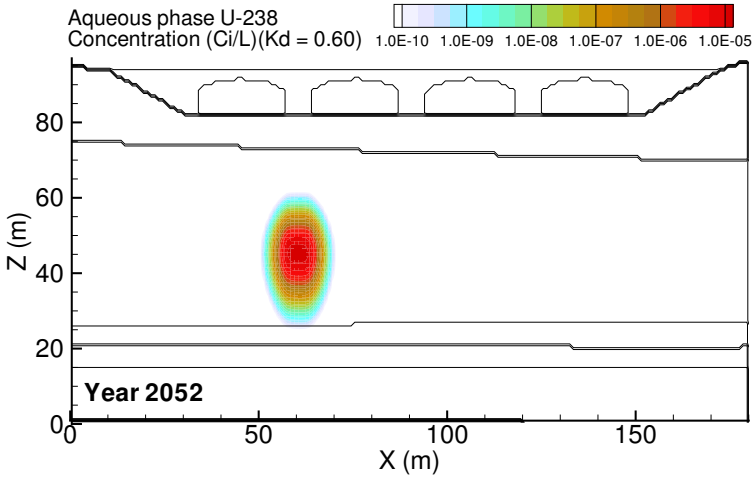

(c)

Figure B.51. Past Leak: Low Aquifer Hydraulic Conductivity (2000 m/d) aqueous concentration distributions at year 2052 for (a) Tc-99, (b) U_0.20 and (c) U_0.60. Year of Tc-99 peak concentration at fenceline was 2052.

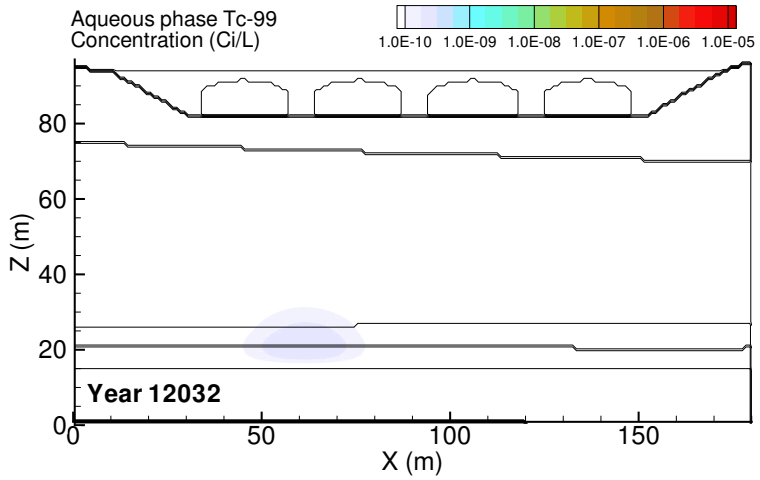

(a)

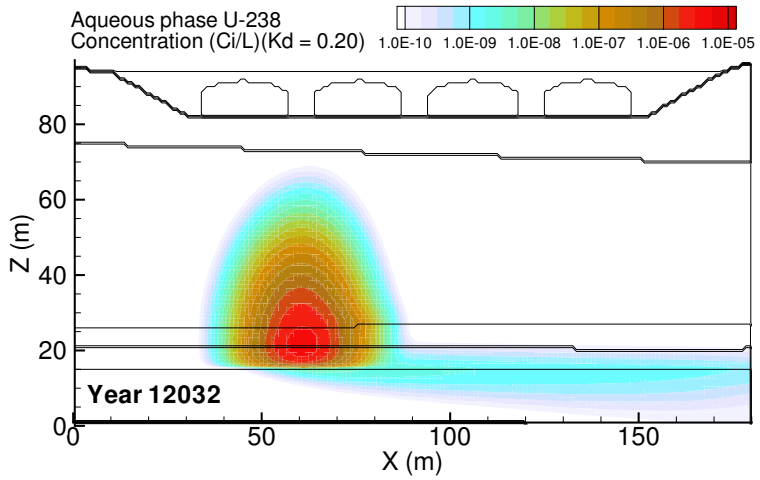

(b)

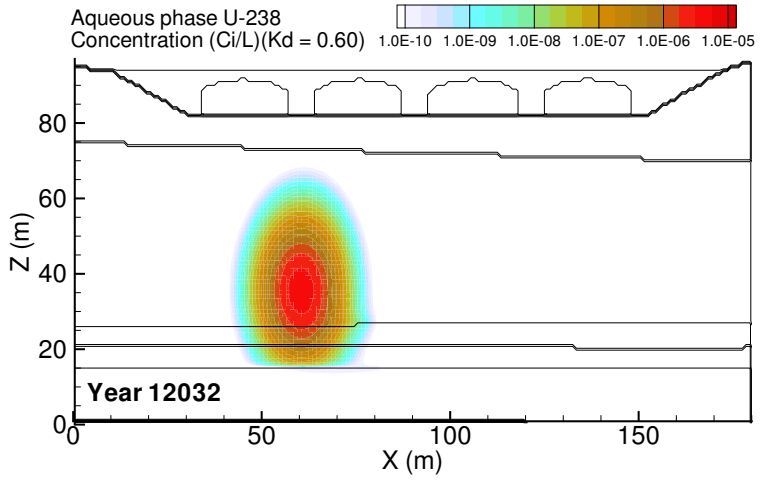

(c)

Figure B.52. Past Leak: Low Aquifer Hydraulic Conductivity (2000 m/d) aqueous concentration distributions at year 12032 for (a) Tc-99, (b) U_0.20 and (c) U_0.60.

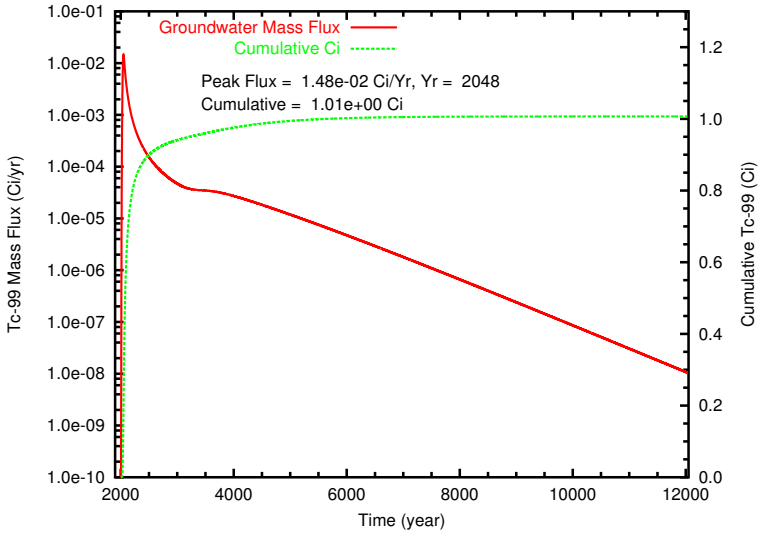

(a)

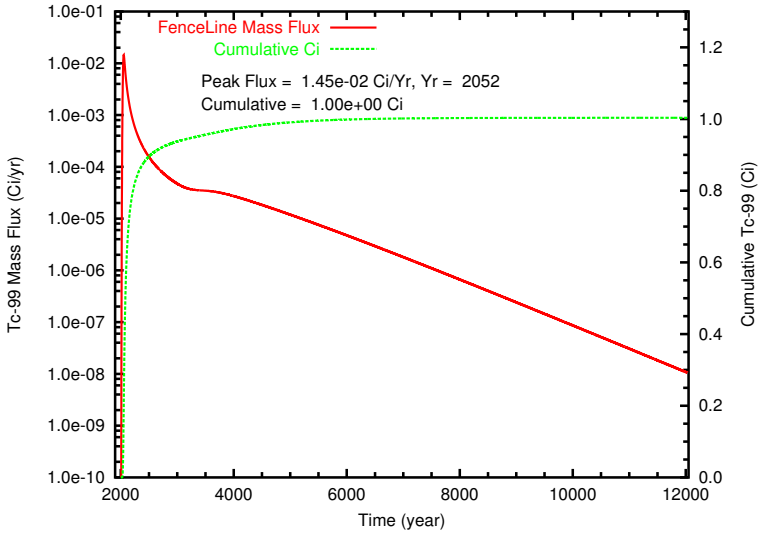

(b)

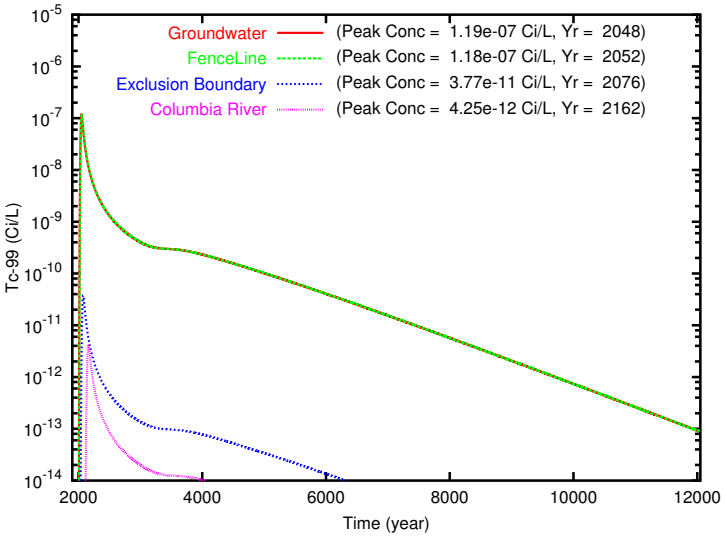

(c)

Figure B.53. Past Leak: Low Aquifer Hydraulic Conductivity (2000 m/d) Tc-99 mass flux at (a) the groundwater table and (b) the fenceline; and (c) the Tc-99 concentration at groundwater, fenceline, and easterly downstream compliance points.

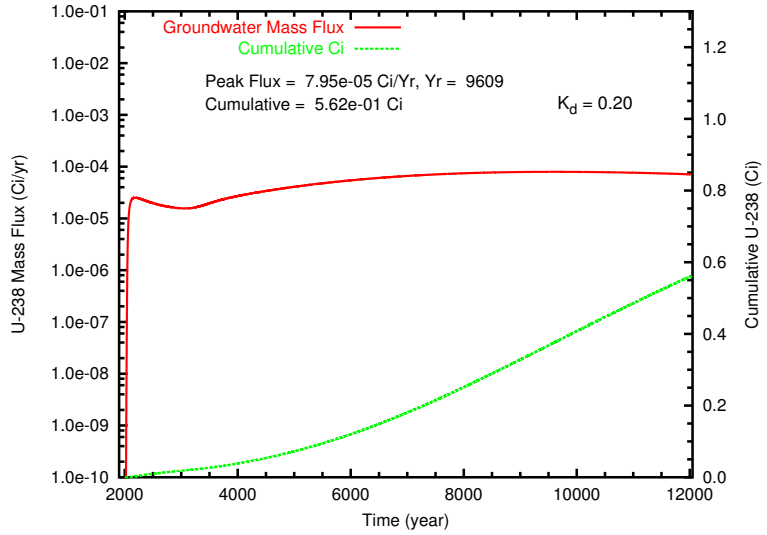

(a)

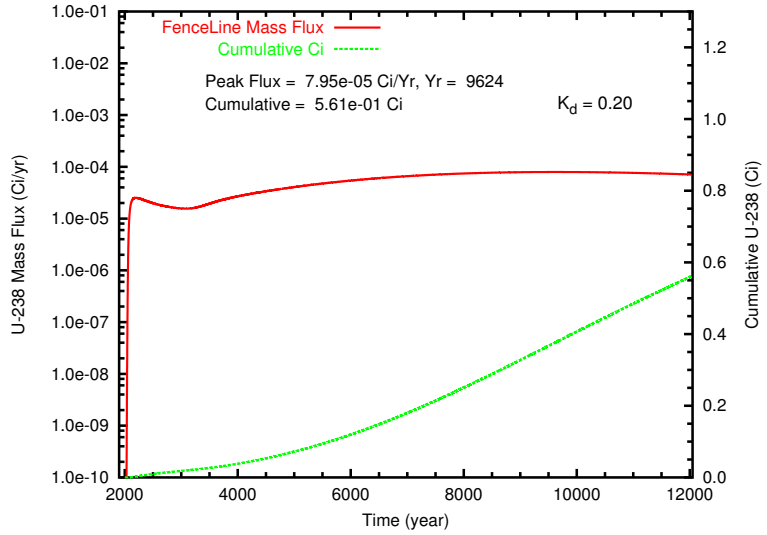

(b)

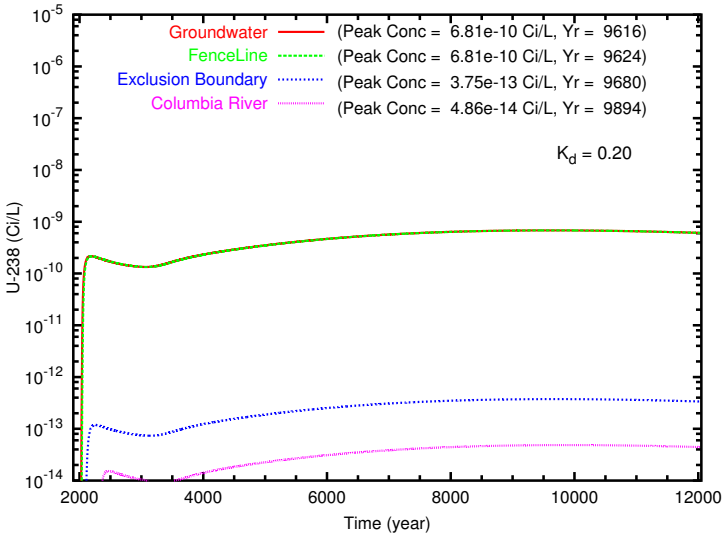

(c)

Figure B.54. Past Leak: Low Aquifer Hydraulic Conductivity (2000 m/d) U_0.20 mass flux at (a) the groundwater table and (b) the fenceline; and (c) the Tc-99 concentration at groundwater, fenceline, and easterly downstream compliance points.

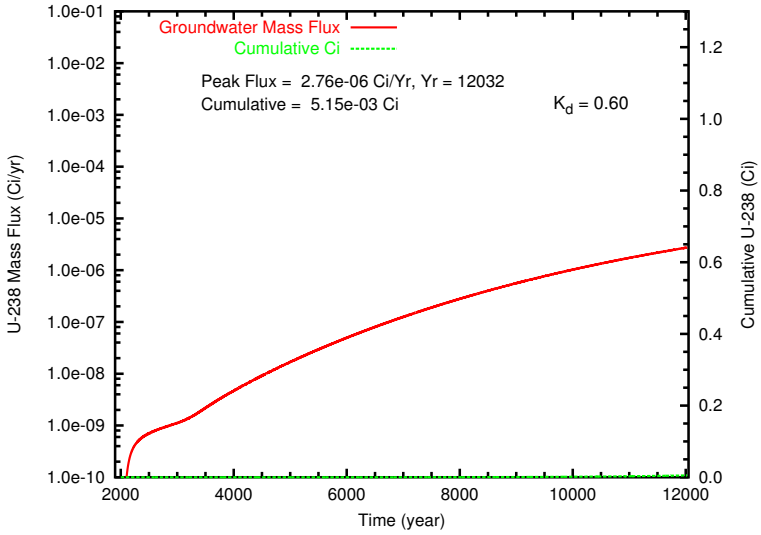

(a)

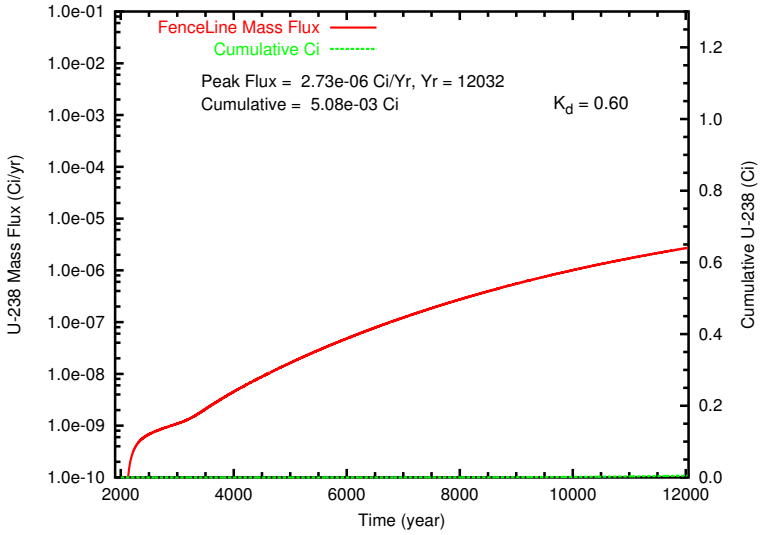

(b)

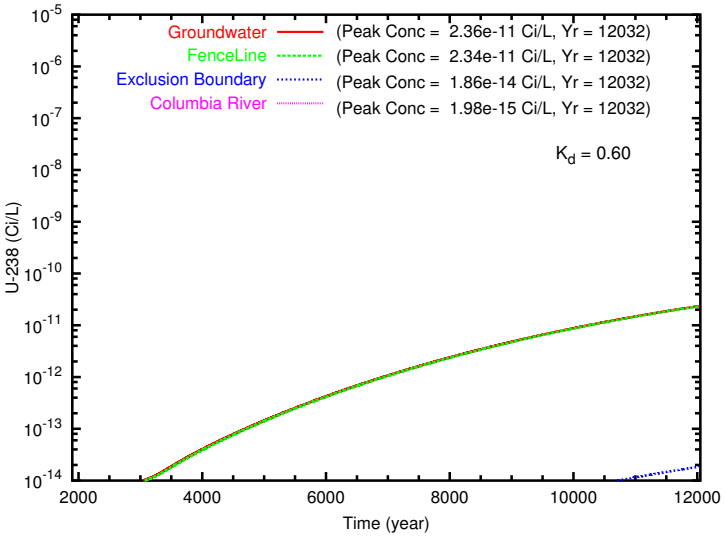

(c)

Figure B.55. Past Leak: Low Aquifer Hydraulic Conductivity (2000 m/d) U_0.60 mass flux at (a) the groundwater table and (b) the fenceline; and (c) the Tc-99 concentration at groundwater, fenceline, and easterly downstream compliance points.

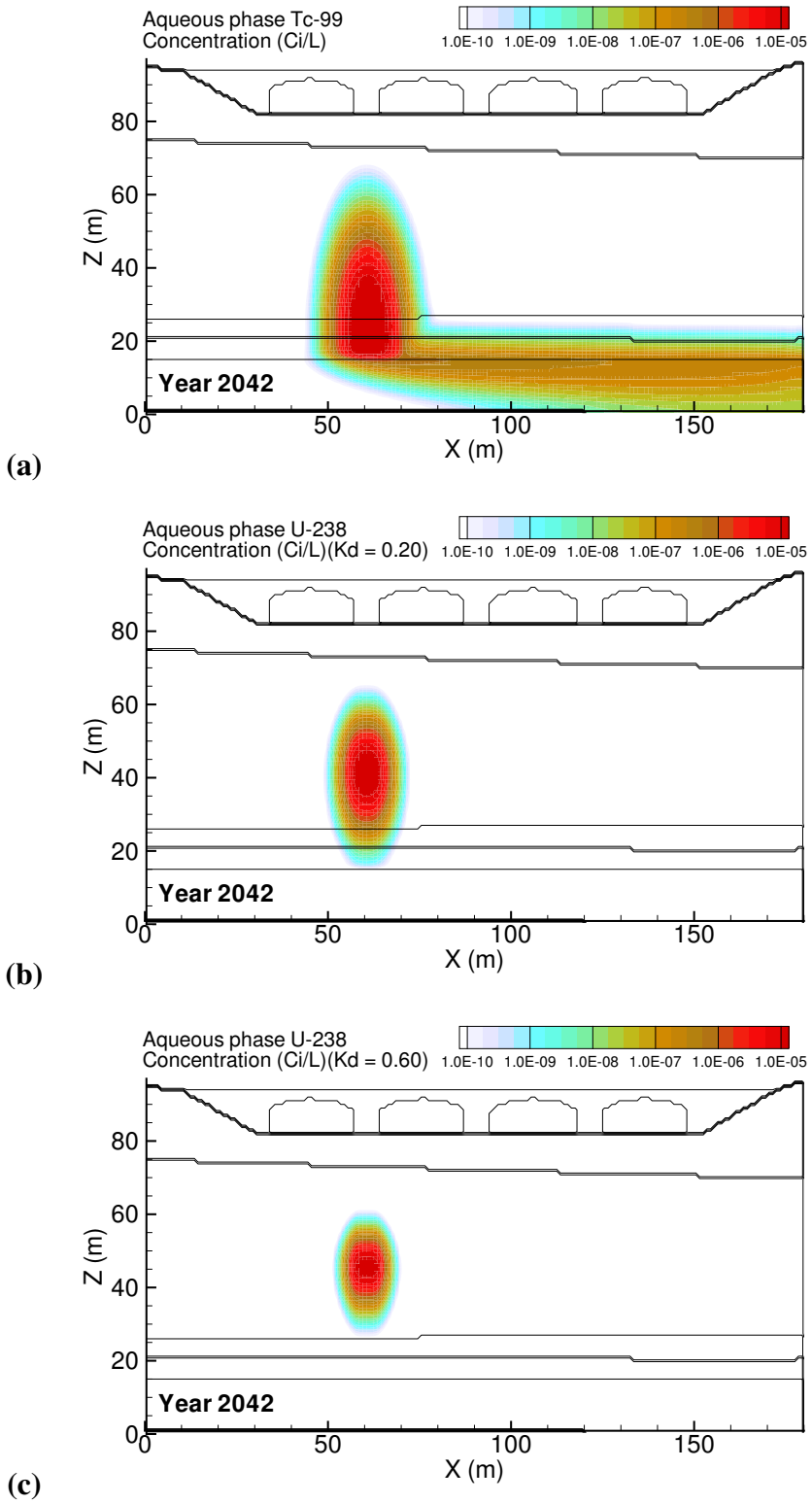

Figure B.56. Past Leak: High Vadose Zone Hydraulic Conductivity ($K_{sat} \times 10$) aqueous concentration distributions at year 2042 for (a) Tc-99, (b) U_0.20 and (c) U_0.60. Year of Tc-99 peak concentration at fenceline was 2042.

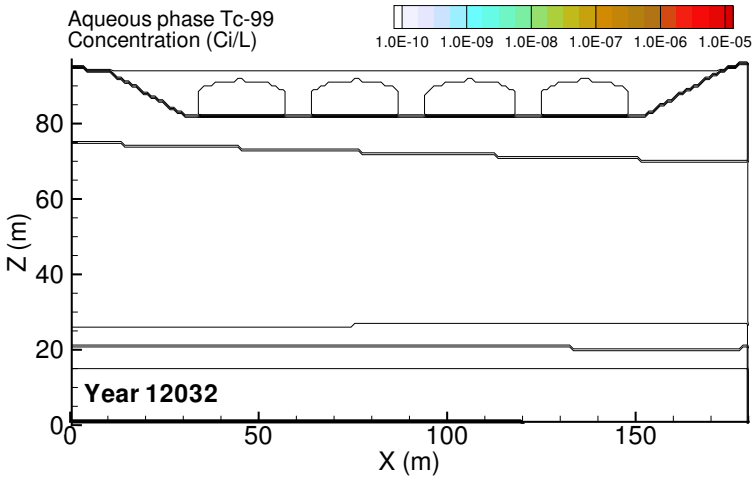

(a)

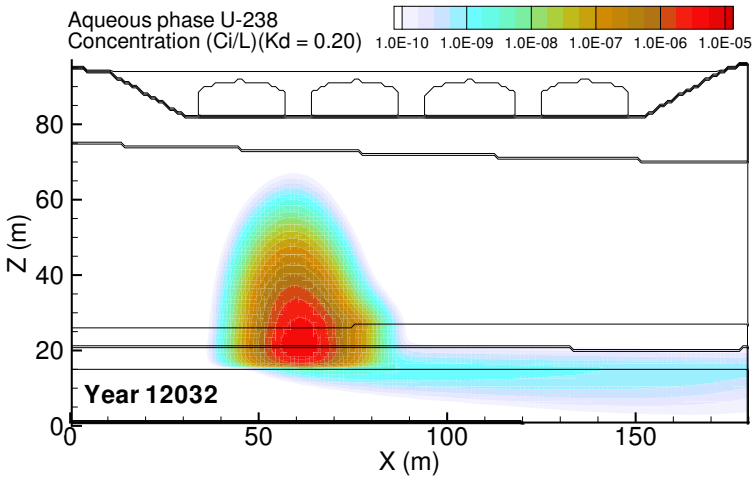

(b)

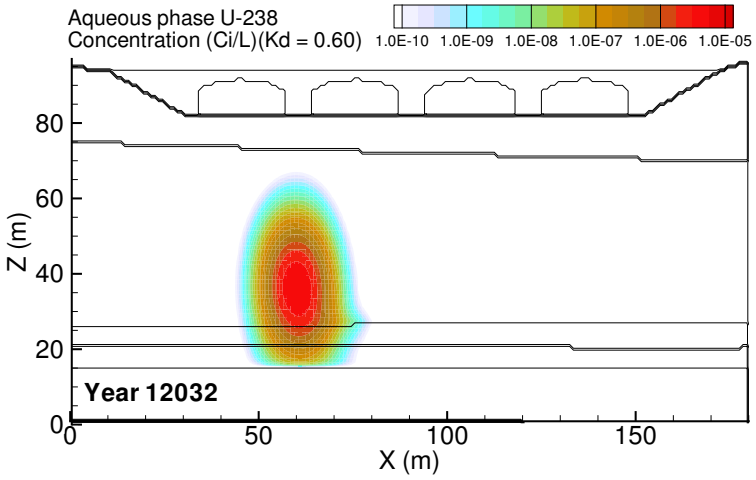

(c)

Figure B.57. Past Leak: High Vadose Zone Hydraulic Conductivity ($K_{sat} \times 10$) aqueous concentration distributions at year 12032 for (a) Tc-99, (b) U_0.20 and (c) U_0.60.

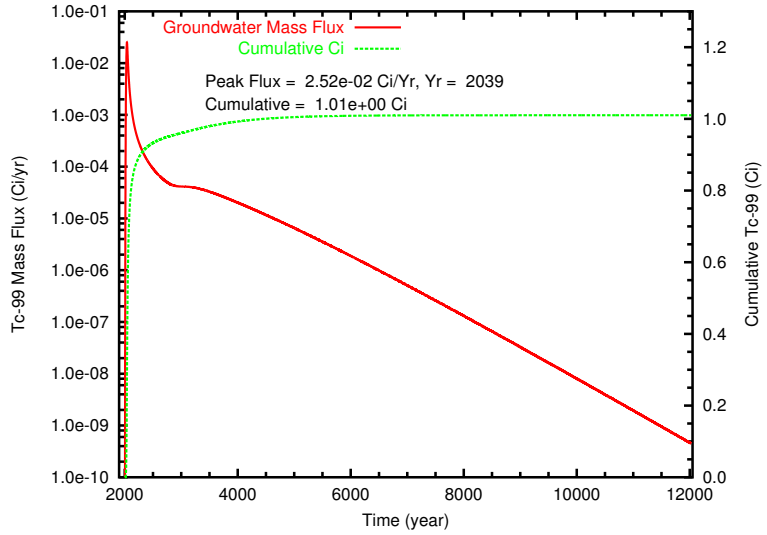

(a)

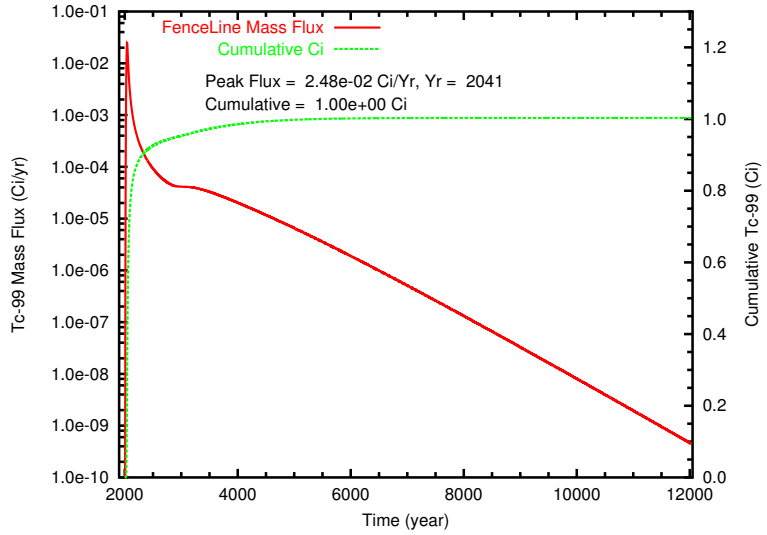

(b)

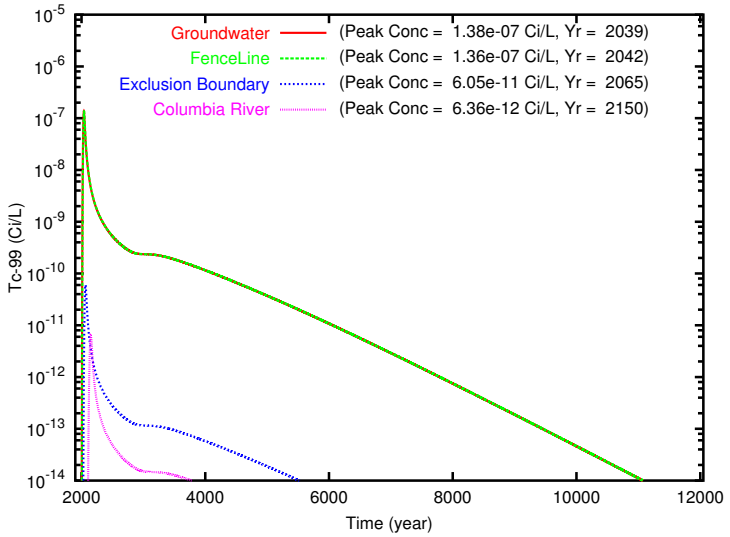

(c)

Figure B.58. Past Leak: High Vadose Zone Hydraulic Conductivity ($K_{sat} \times 10$) Tc-99 mass flux at (a) the groundwater table and (b) the fenceline; and (c) the Tc-99 concentration at groundwater, fenceline, and easterly downstream compliance points.

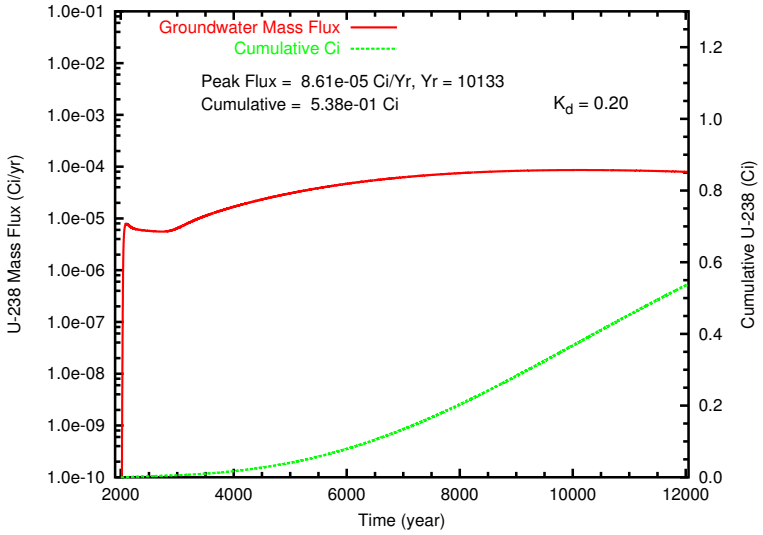

(a)

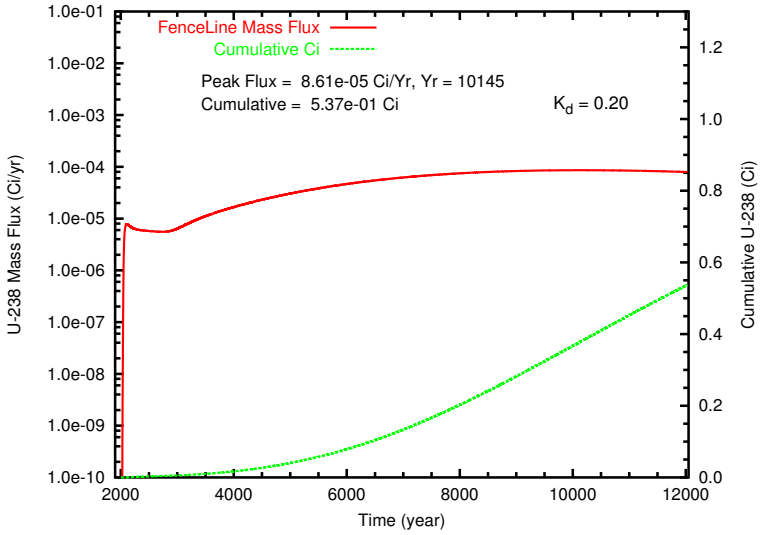

(b)

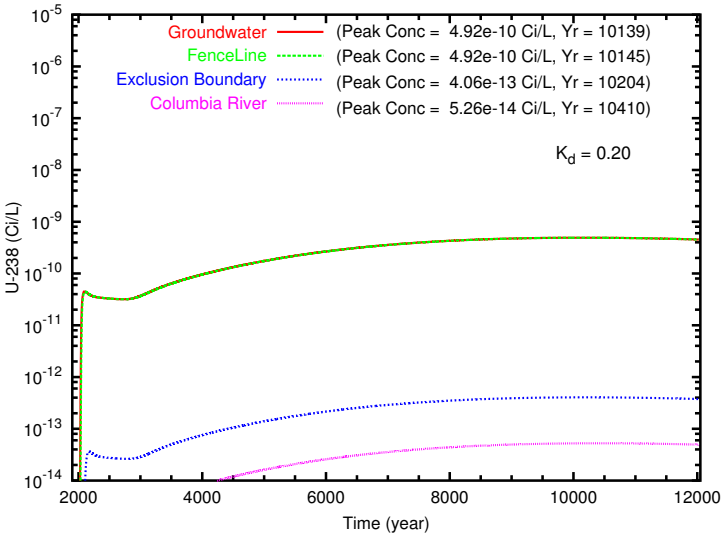

(c)

Figure B.59. Past Leak: High Vadose Zone Hydraulic Conductivity ($K_{sat} \times 10$) U_0.20 mass flux at (a) the groundwater table and (b) the fenceline; and (c) the Tc-99 concentration at groundwater, fenceline, and easterly downstream compliance points.

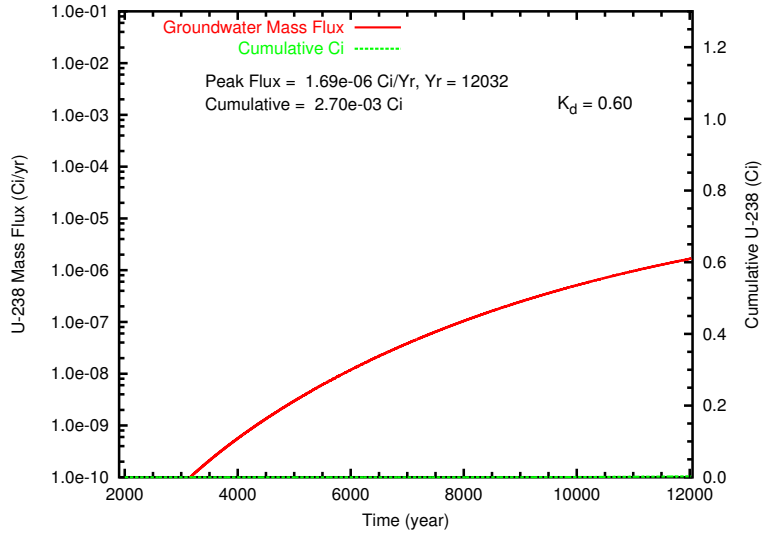

(a)

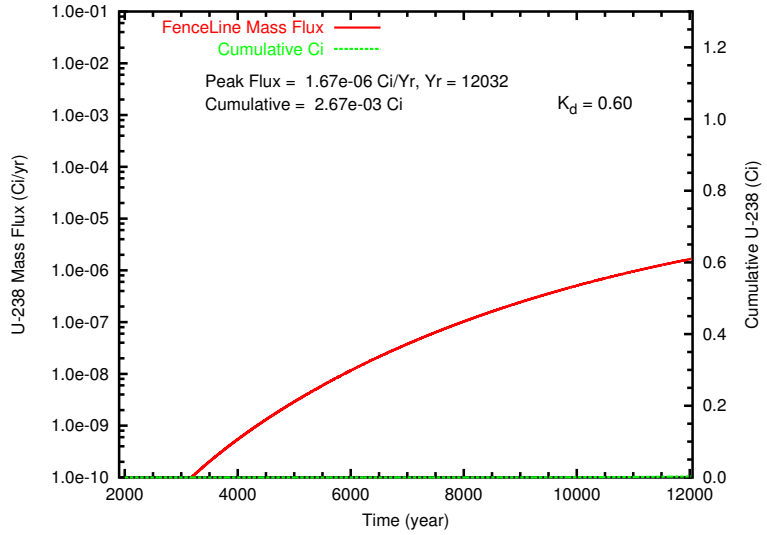

(b)

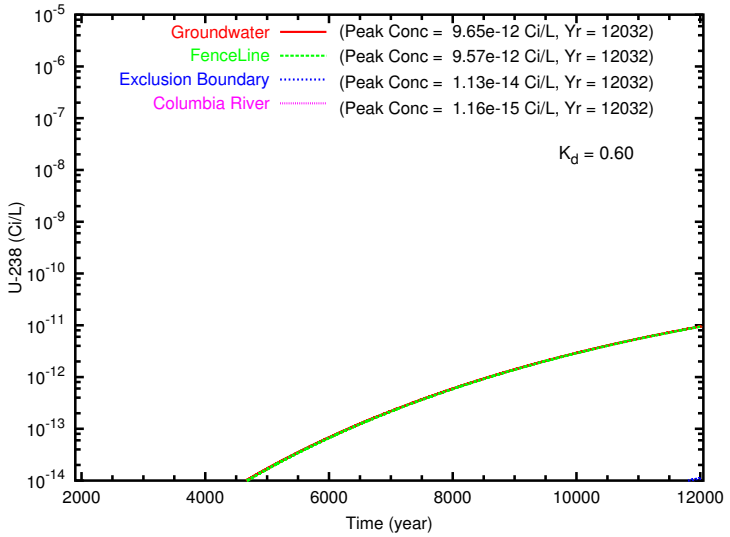

(c)

Figure B.60. Past Leak: High Vadose Zone Hydraulic Conductivity ($K_{sat} \times 10$) U_0.60 mass flux at (a) the groundwater table and (b) the fenceline; and (c) the Tc-99 concentration at groundwater, fenceline, and easterly downstream compliance points.

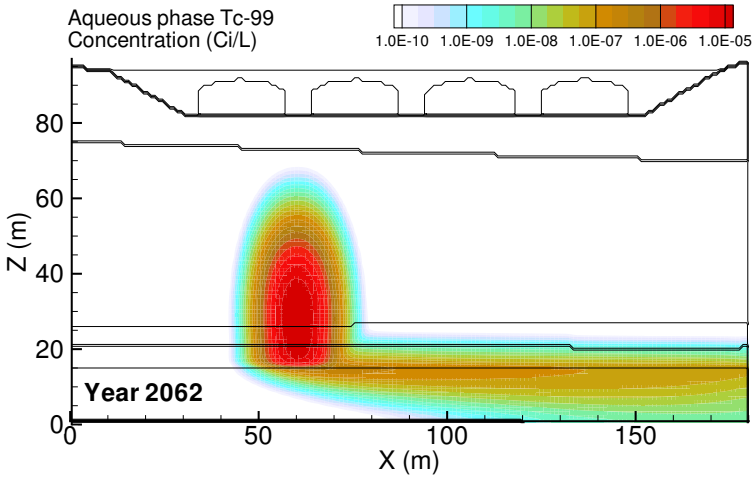

(a)

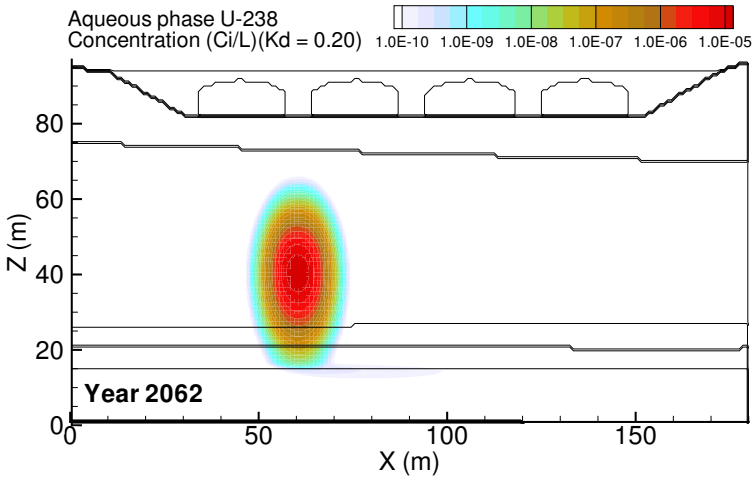

(b)

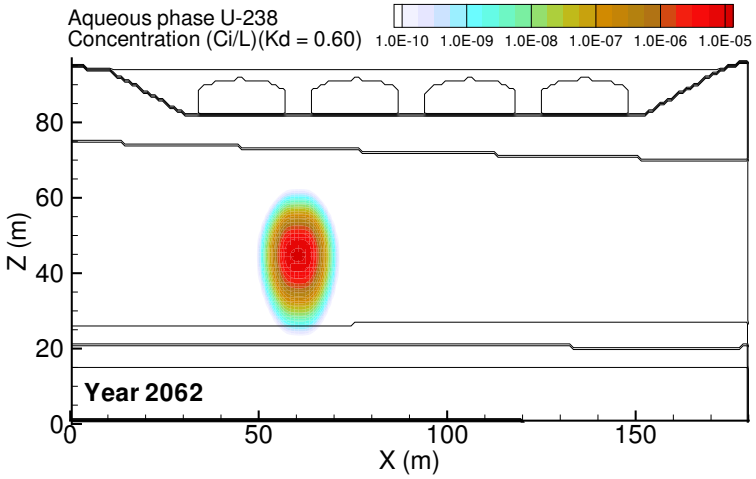

(c)

Figure B.61. Past Leak: Low Vadose Zone Hydraulic Conductivity ($K_{sat} \times 0.1$) aqueous concentration distributions at year 2062 for (a) Tc-99, (b) U_0.20 and (c) U_0.60. Year of Tc-99 peak concentration at fenceline was 2062.

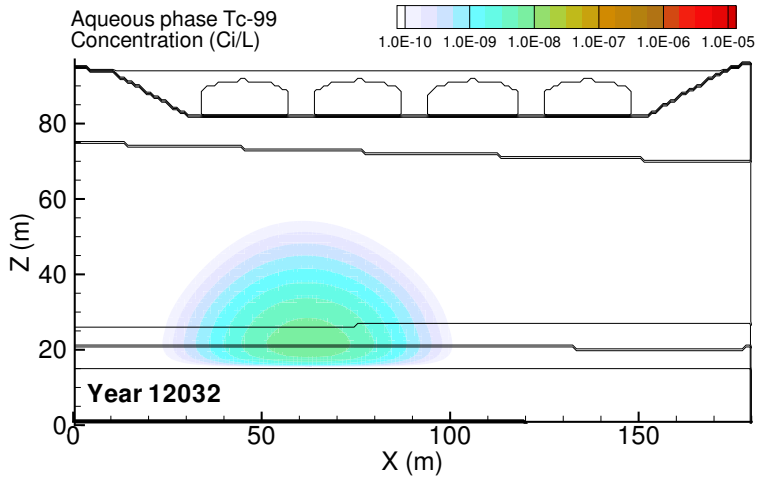

(a)

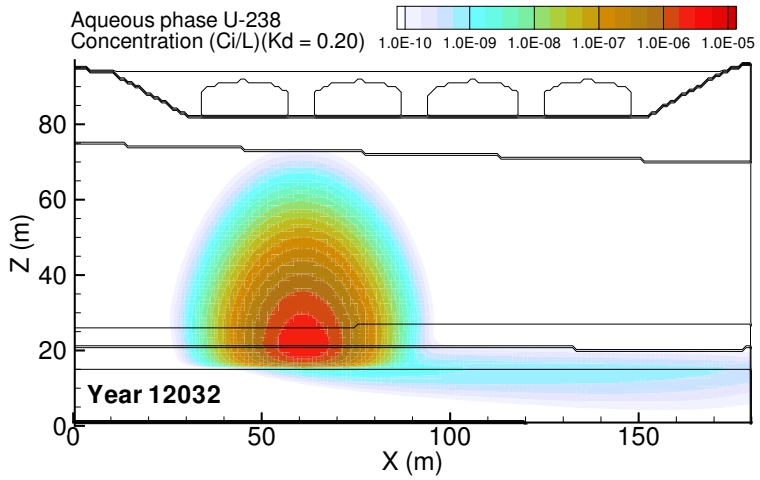

(b)

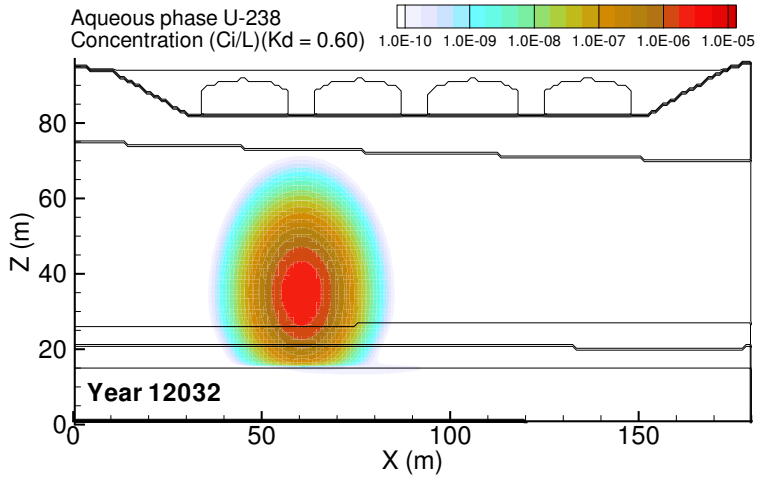

(c)

Figure B.62. Past Leak: Low Vadose Zone Hydraulic Conductivity ($K_{sat} \times 0.1$) aqueous concentration distributions at year 12032 for (a) Tc-99, (b) U_0.20 and (c) U_0.60.

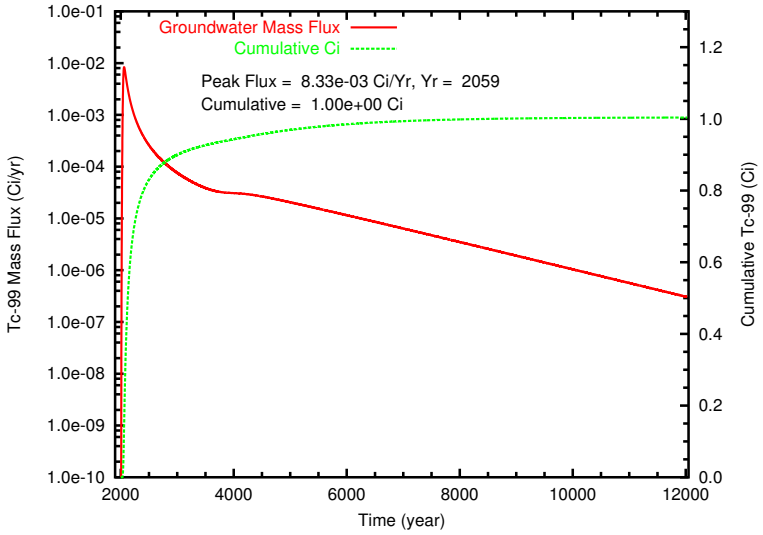

(a)

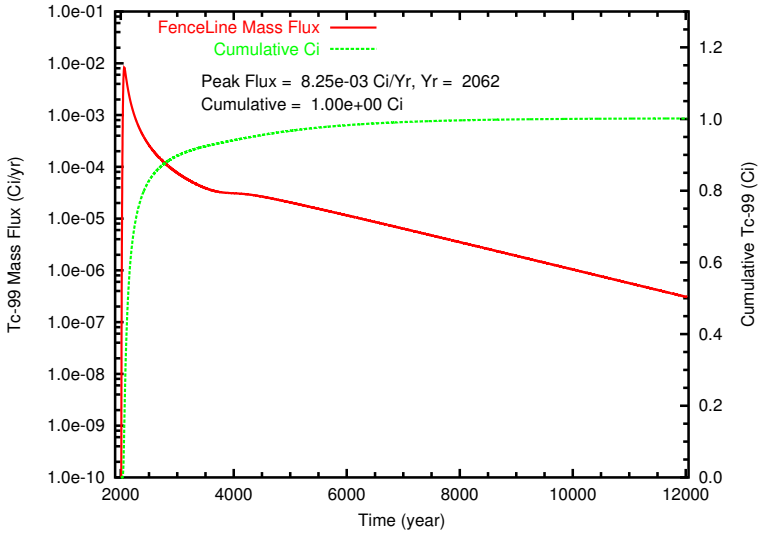

(b)

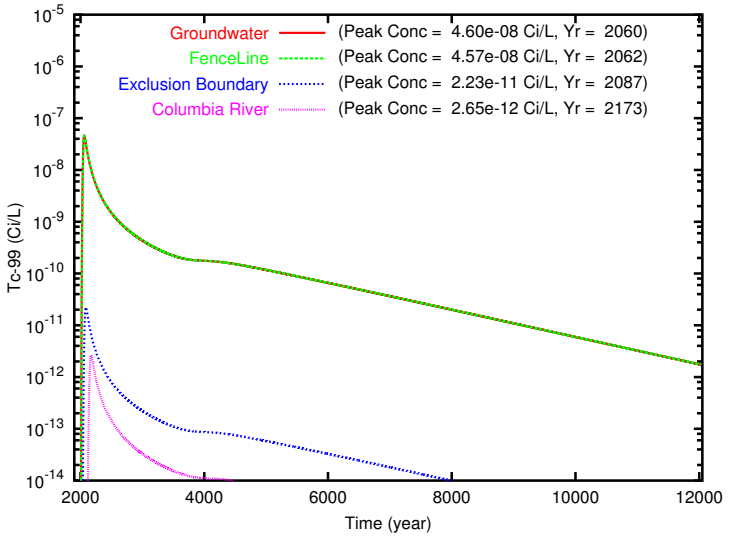

(c)

Figure B.63. Past Leak: Low Vadose Zone Hydraulic Conductivity ($K_{sat} \times 0.1$) Tc-99 mass flux at (a) the groundwater table and (b) the fenceline; and (c) the Tc-99 concentration at groundwater, fenceline, and easterly downstream compliance points.

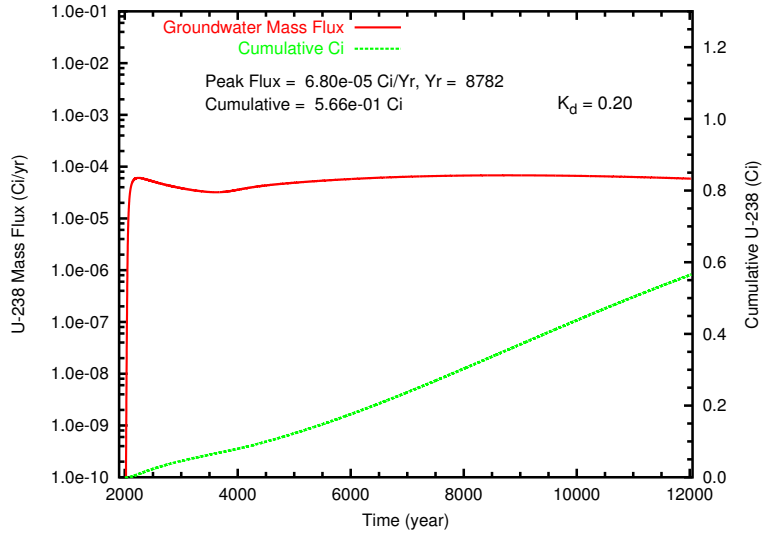

(a)

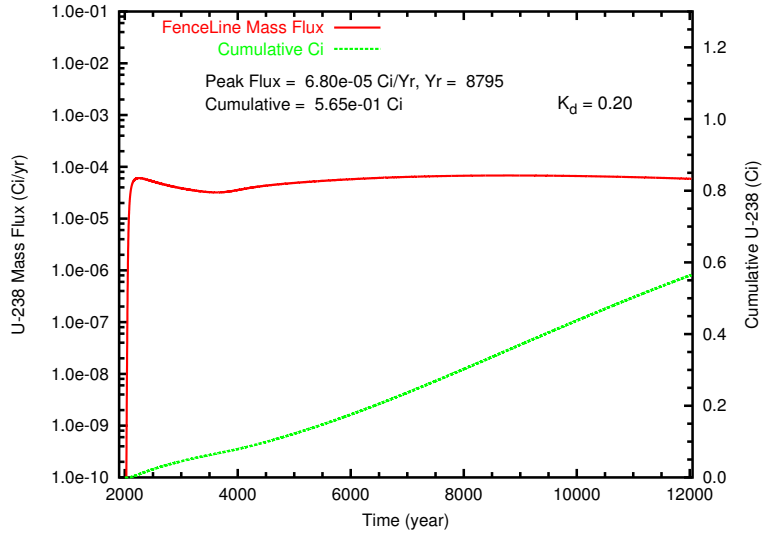

(b)

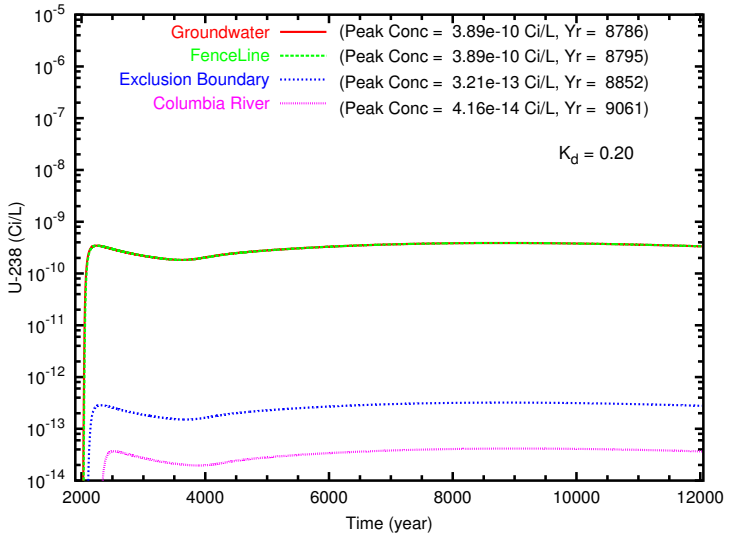

(c)

Figure B.64. Past Leak: Low Vadose Zone Hydraulic Conductivity ($K_{sat} \times 0.1$) U_0.20 mass flux at (a) the groundwater table and (b) the fenceline; and (c) the Tc-99 concentration at groundwater, fenceline, and easterly downstream compliance points.

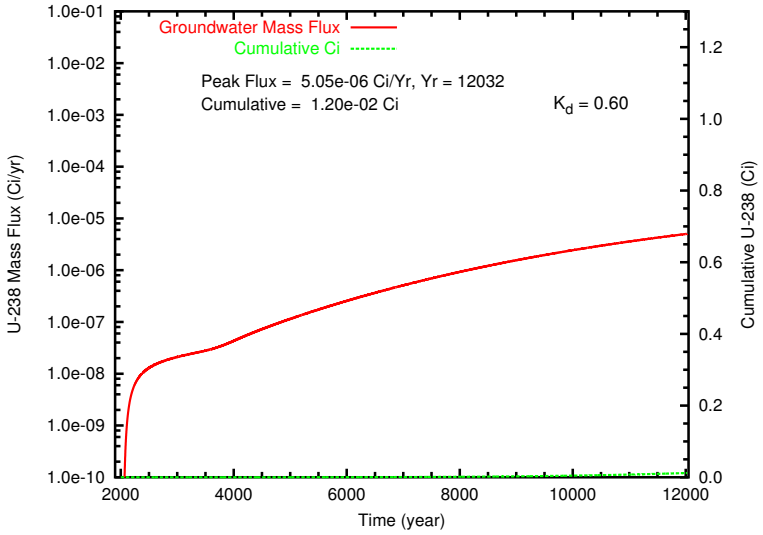

(a)

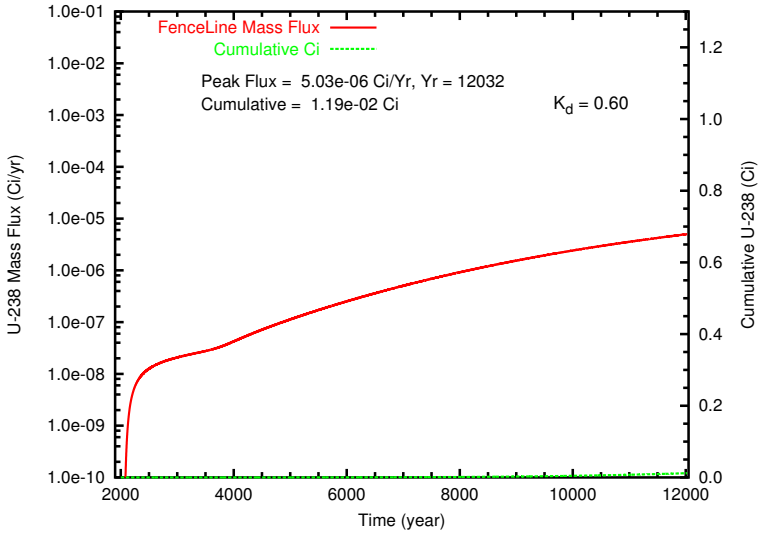

(b)

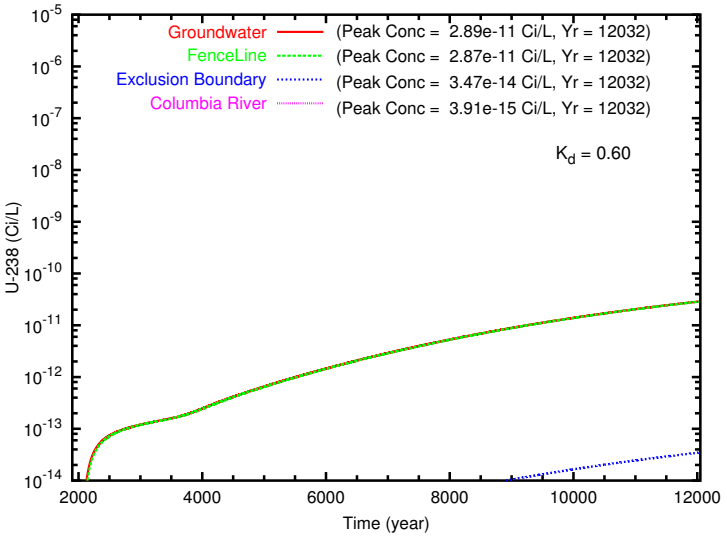

(c)

Figure B.65. Past Leak: Low Vadose Zone Hydraulic Conductivity ($K_{sat} \times 0.1$) U_0.60 mass flux at (a) the groundwater table and (b) the fenceline; and (c) the Tc-99 concentration at groundwater, fenceline, and easterly downstream compliance points.

Appendix C

C Farm Diffusion Release

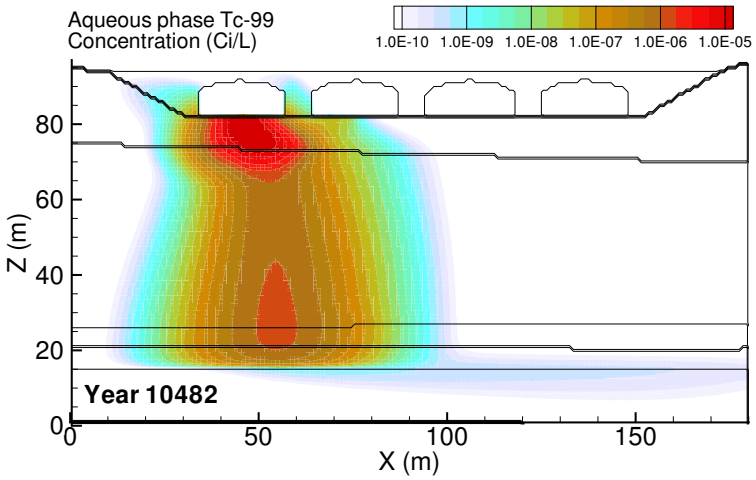

(a)

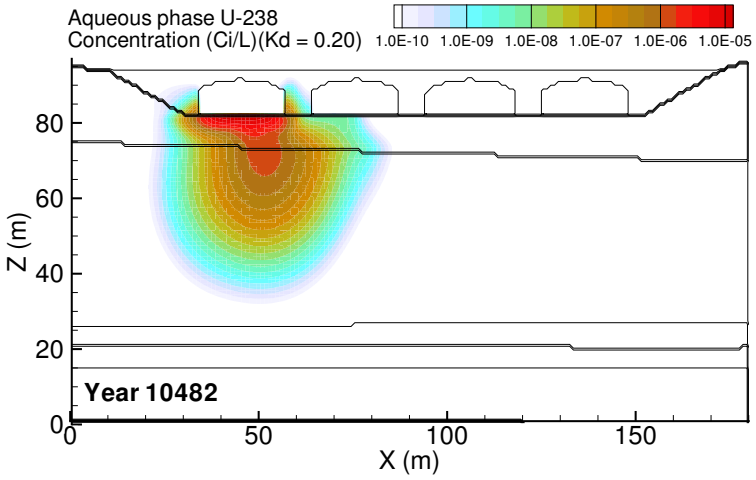

(b)

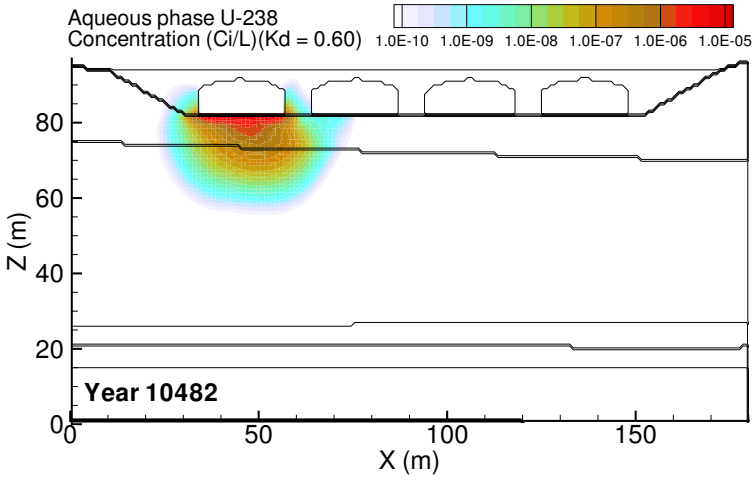

(c)

Figure C.1. Diffusion Release: Base Case aqueous concentration distributions at year 10482 for (a) Tc-99, (b) U_0.20 and (c) U_0.60. Year of Tc-99 peak concentration at fenceline was 10482.

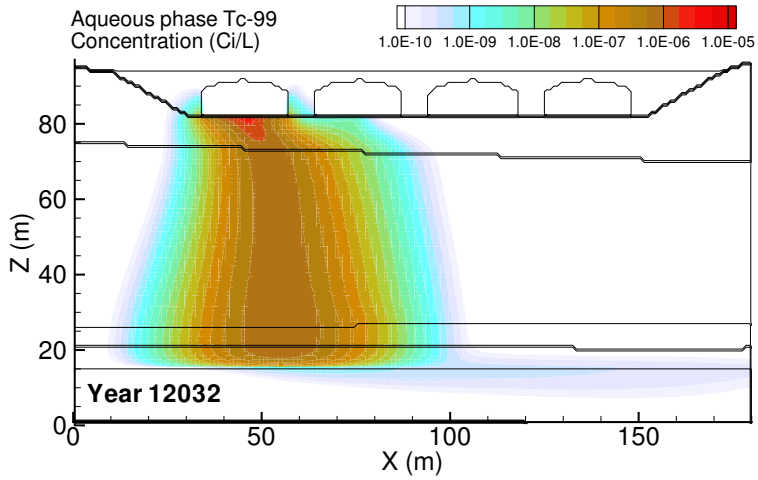

(a)

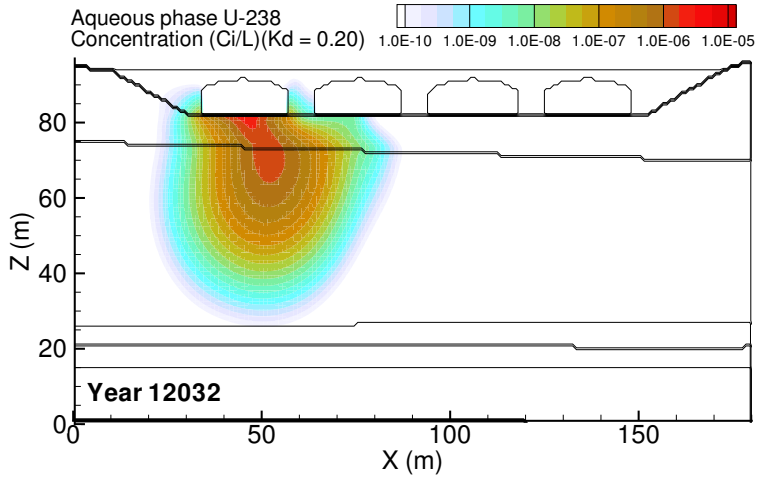

(b)

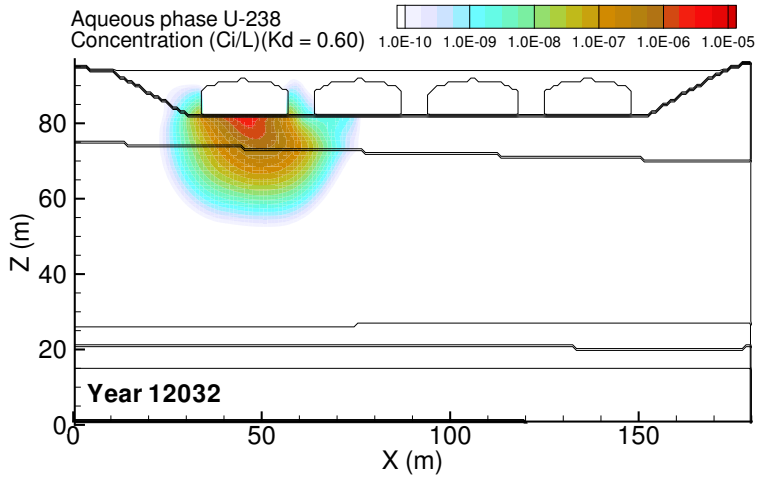

(c)

Figure C.2. Diffusion Release: Base Case aqueous concentration distributions at year 12032 for (a) Tc-99, (b) U_0.20 and (c) U_0.60.

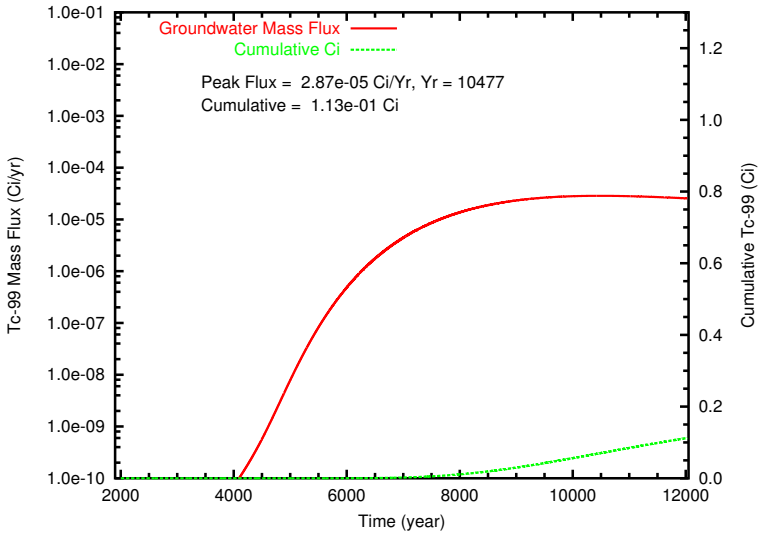

(a)

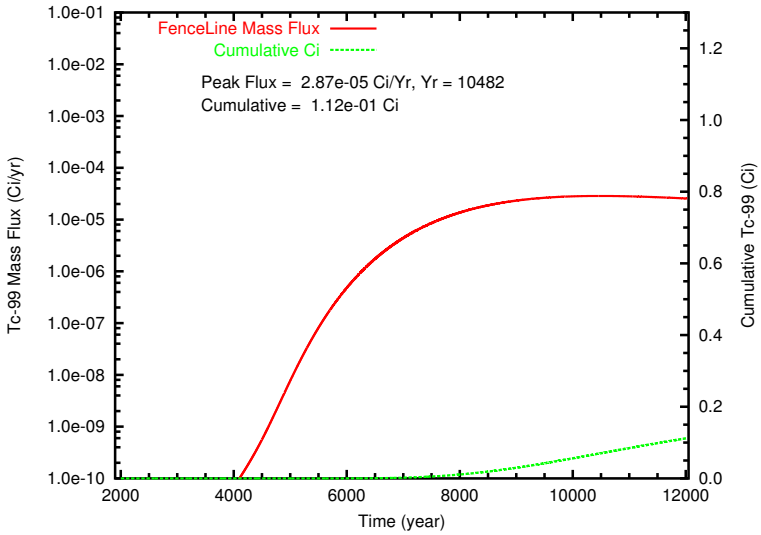

(b)

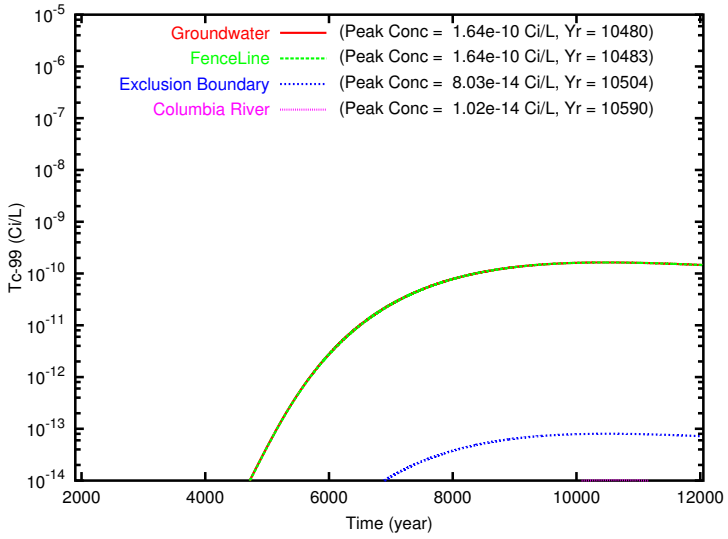

(c)

Figure C.3. Diffusion Release: Base Case Tc-99 mass flux at (a) the groundwater table and (b) the fenceline; and (c) the Tc-99 concentration at groundwater, fenceline, and easterly downstream compliance points.

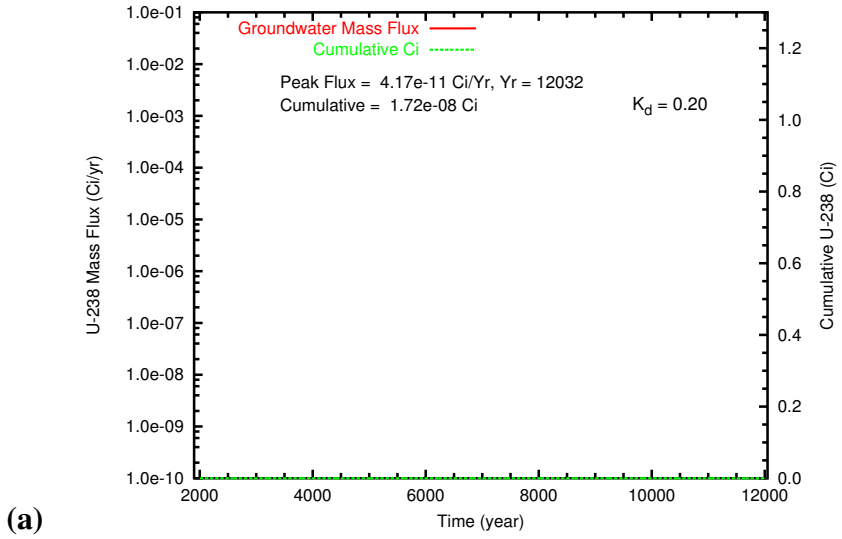

(a)

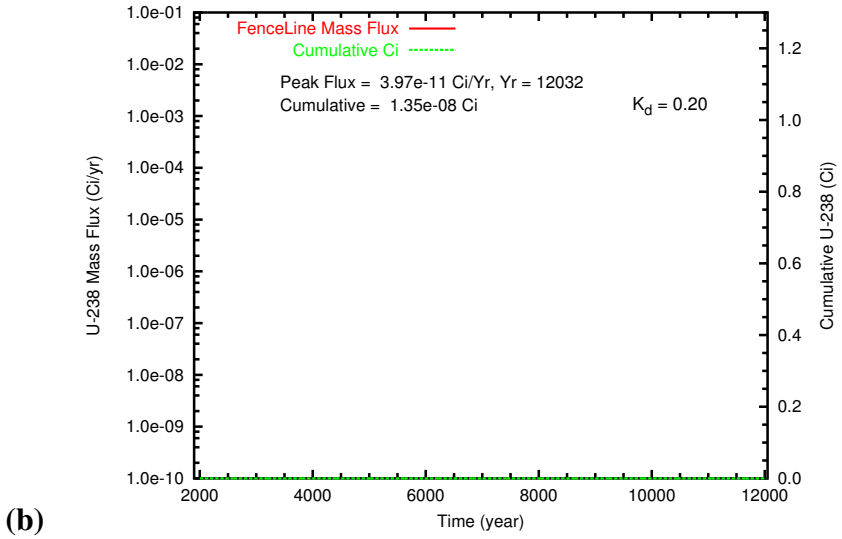

(b)

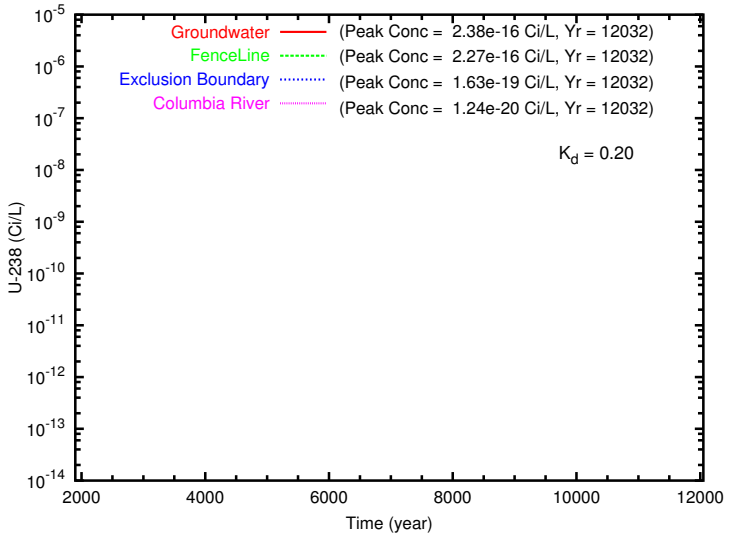

(c)

Figure C.4. Diffusion Release: Base Case U_0.20 mass flux at (a) the groundwater table and (b) the fenceline; and (c) the Tc-99 concentration at groundwater, fenceline, and easterly downstream compliance points.

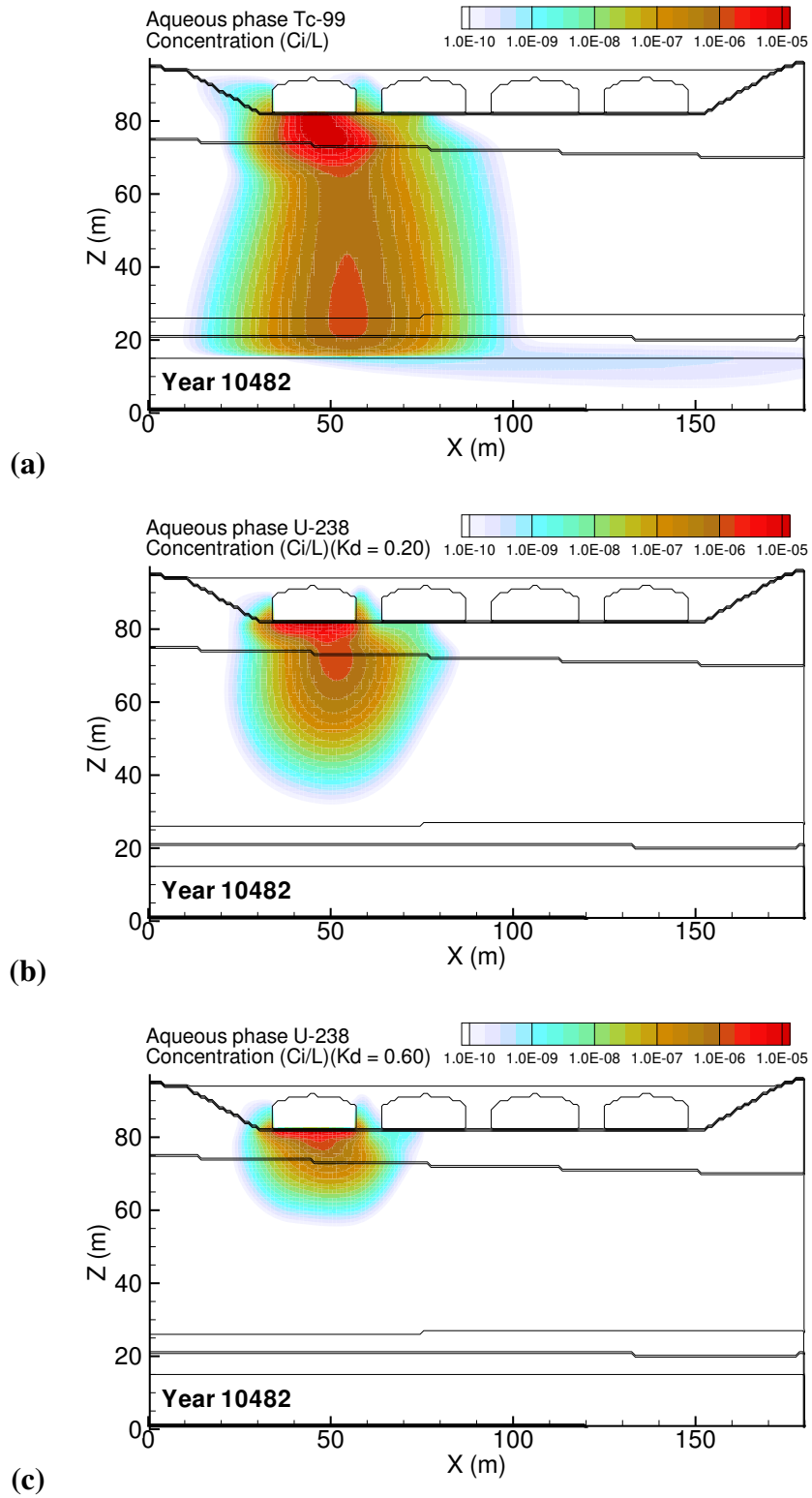

Figure C.5. Diffusion Release: High Preclosure Recharge Rate (140 mm/yr) aqueous concentration distributions at year 10482 for (a) Tc-99, (b) U_0.20 and (c) U_0.60. Year of Tc-99 peak concentration at fenceline was 10482.

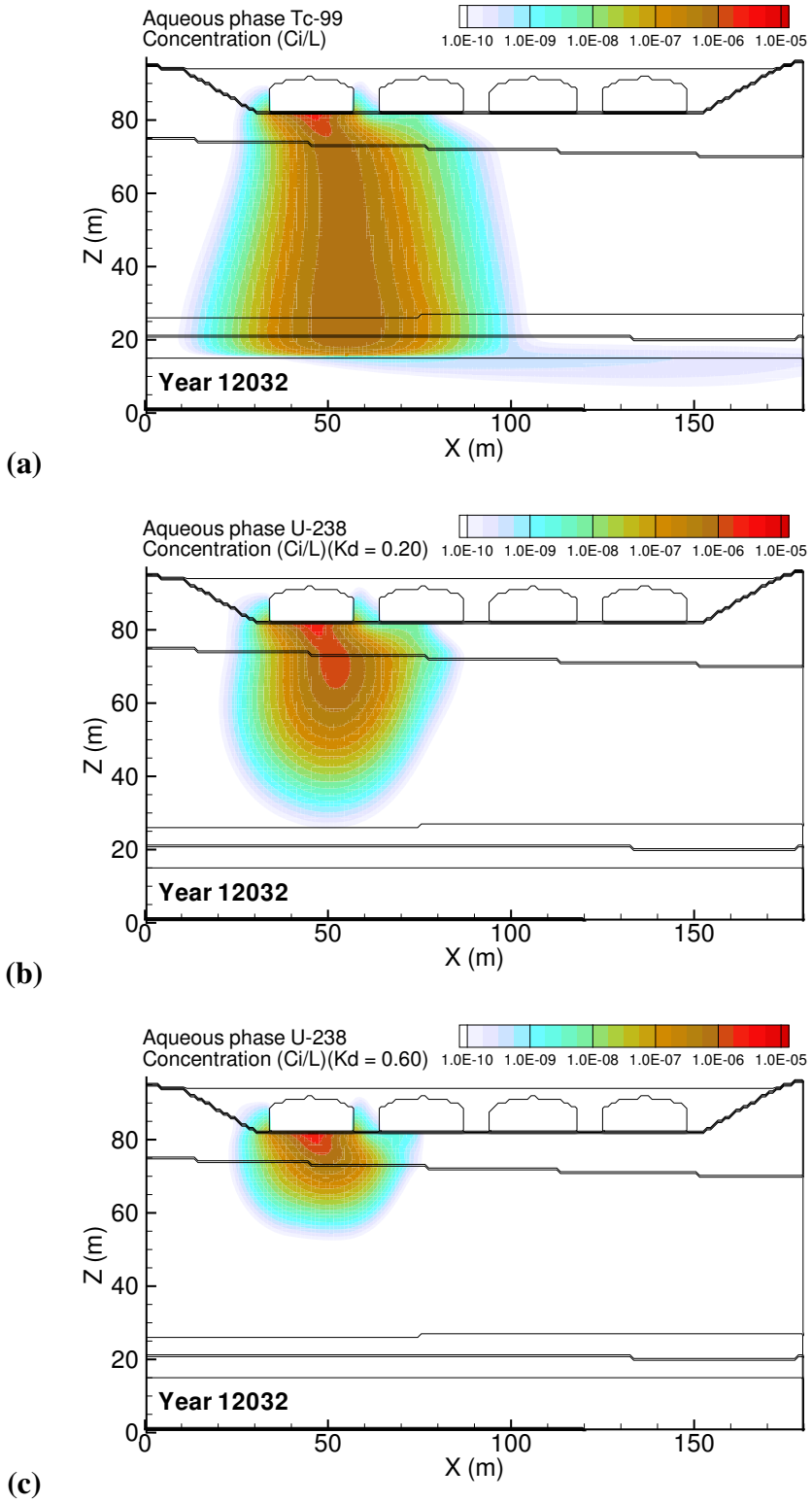

Figure C.6. Diffusion Release: High Preclosure Recharge Rate (140 mm/yr) aqueous concentration distributions at year 12032 for (a) Tc-99, (b) U_0.20 and (c) U_0.60.

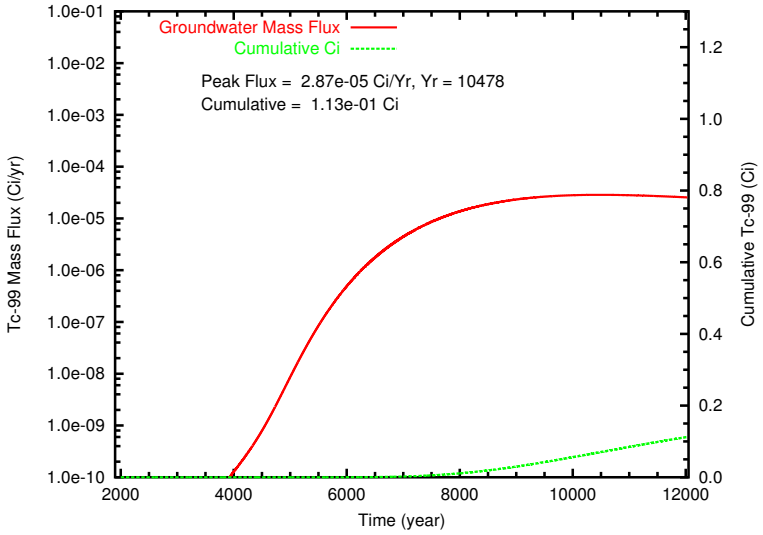

(a)

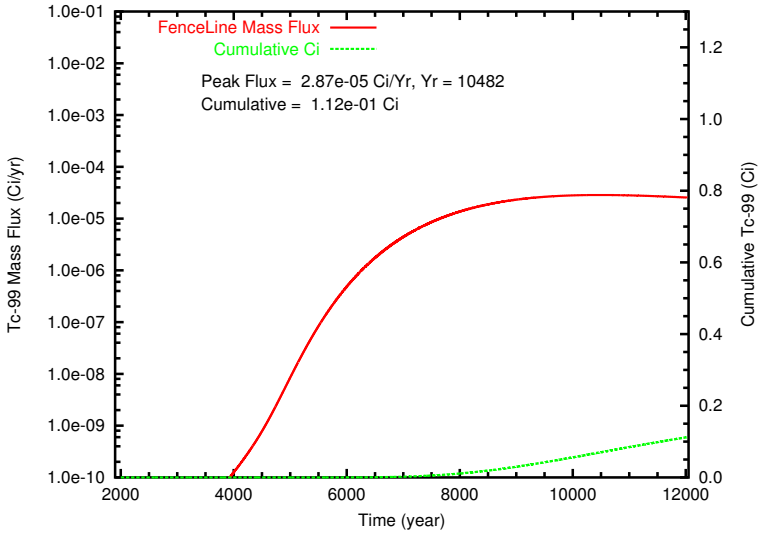

(b)

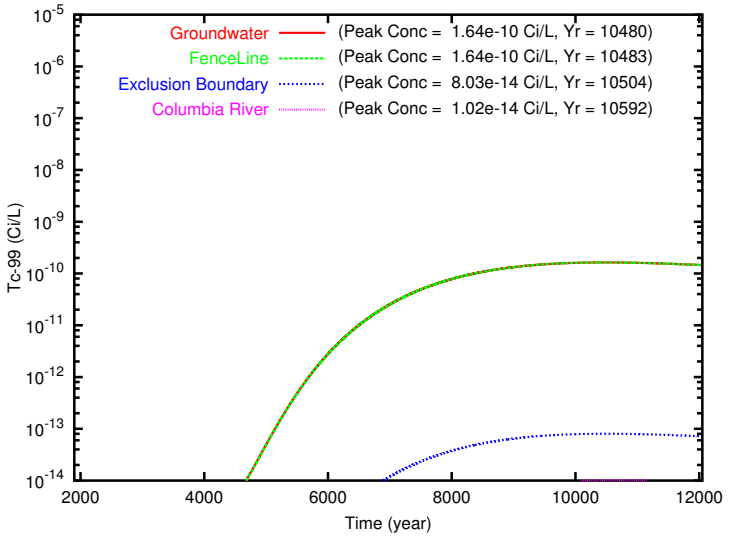

(c)

Figure C.7. Diffusion Release: High Preclosure Recharge Rate (140 mm/yr) Tc-99 mass flux at (a) the groundwater table and (b) the fenceline; and (c) the Tc-99 concentration at groundwater, fenceline, and easterly downstream compliance points.

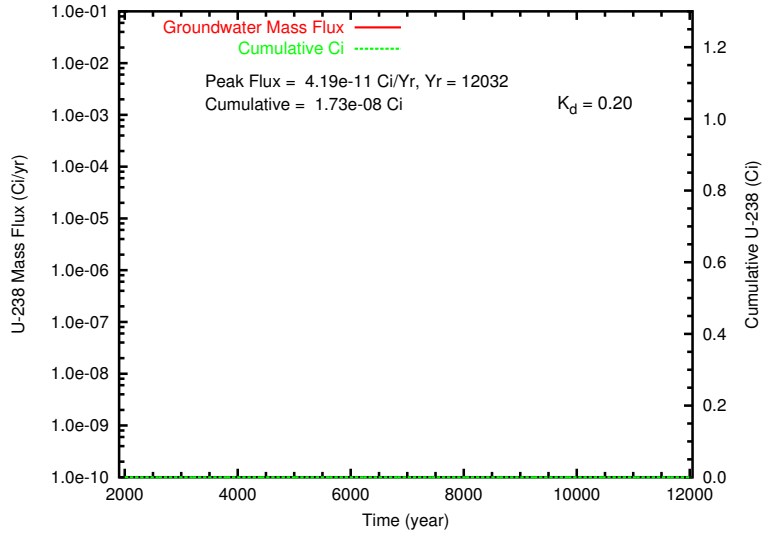

(a)

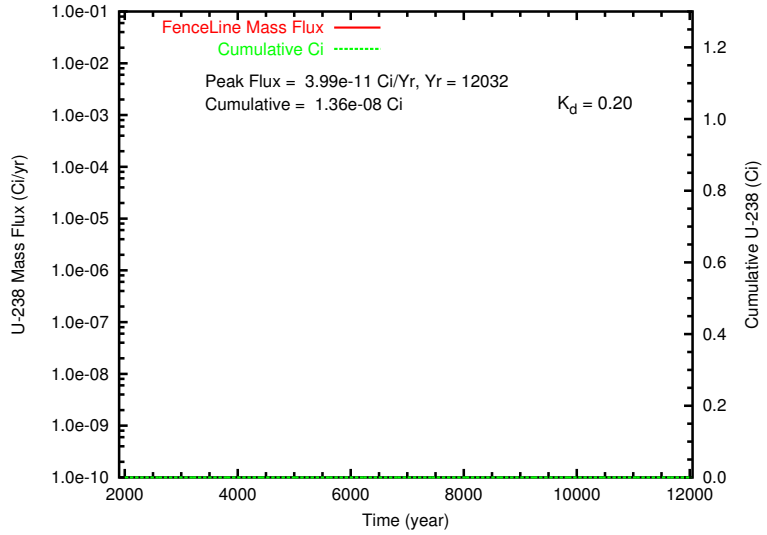

(b)

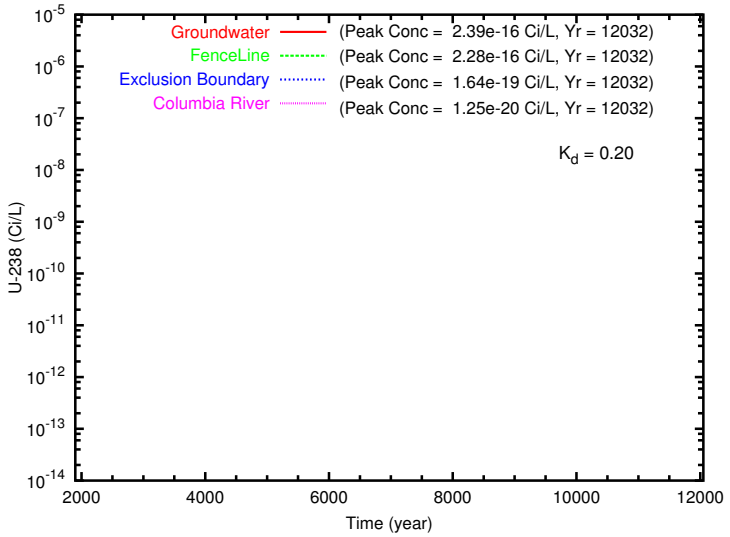

(c)

Figure C.8. Diffusion Release: High Preclosure Recharge Rate (140 mm/yr) U_0.20 mass flux at (a) the groundwater table and (b) the fenceline; and (c) the Tc-99 concentration at groundwater, fenceline, and easterly downstream compliance points.

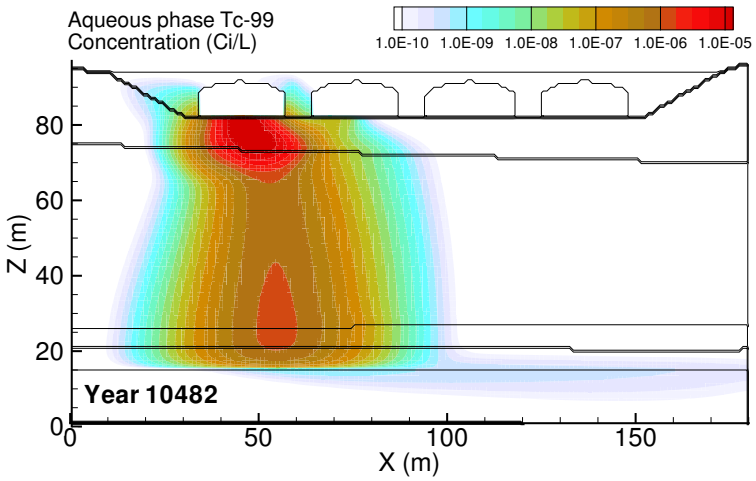

(a)

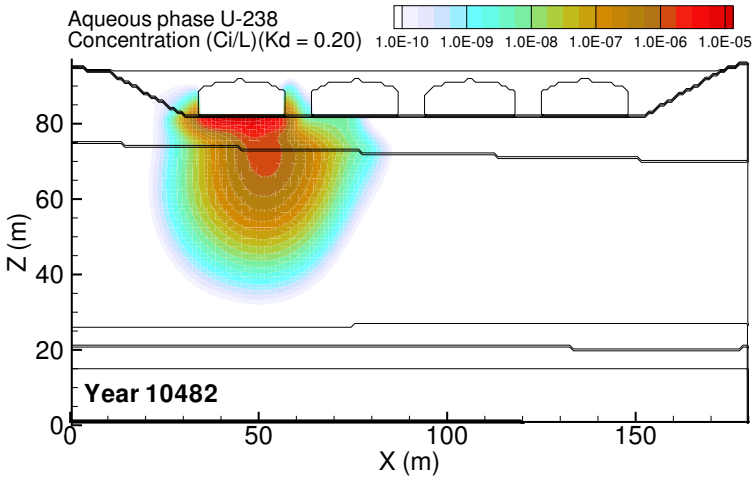

(b)

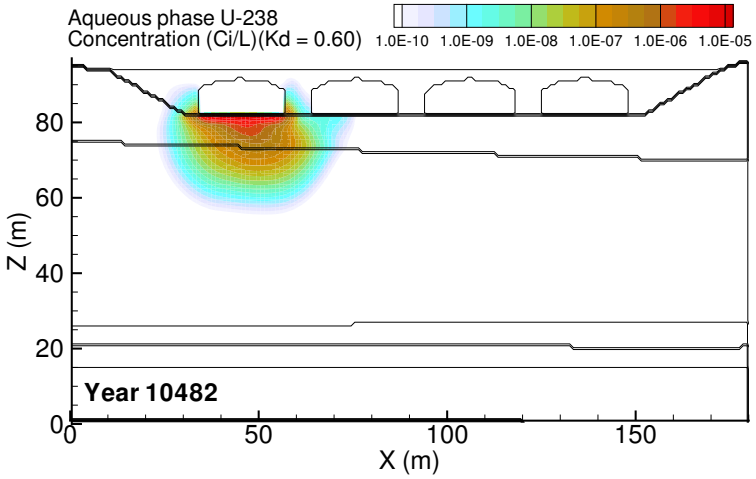

(c)

Figure C.9. Diffusion Release: Low Preclosure Recharge Rate (40 mm/yr) aqueous concentration distributions at year 10482 for (a) Tc-99, (b) U_0.20 and (c) U_0.60. Year of Tc-99 peak concentration at fenceline was 10482.

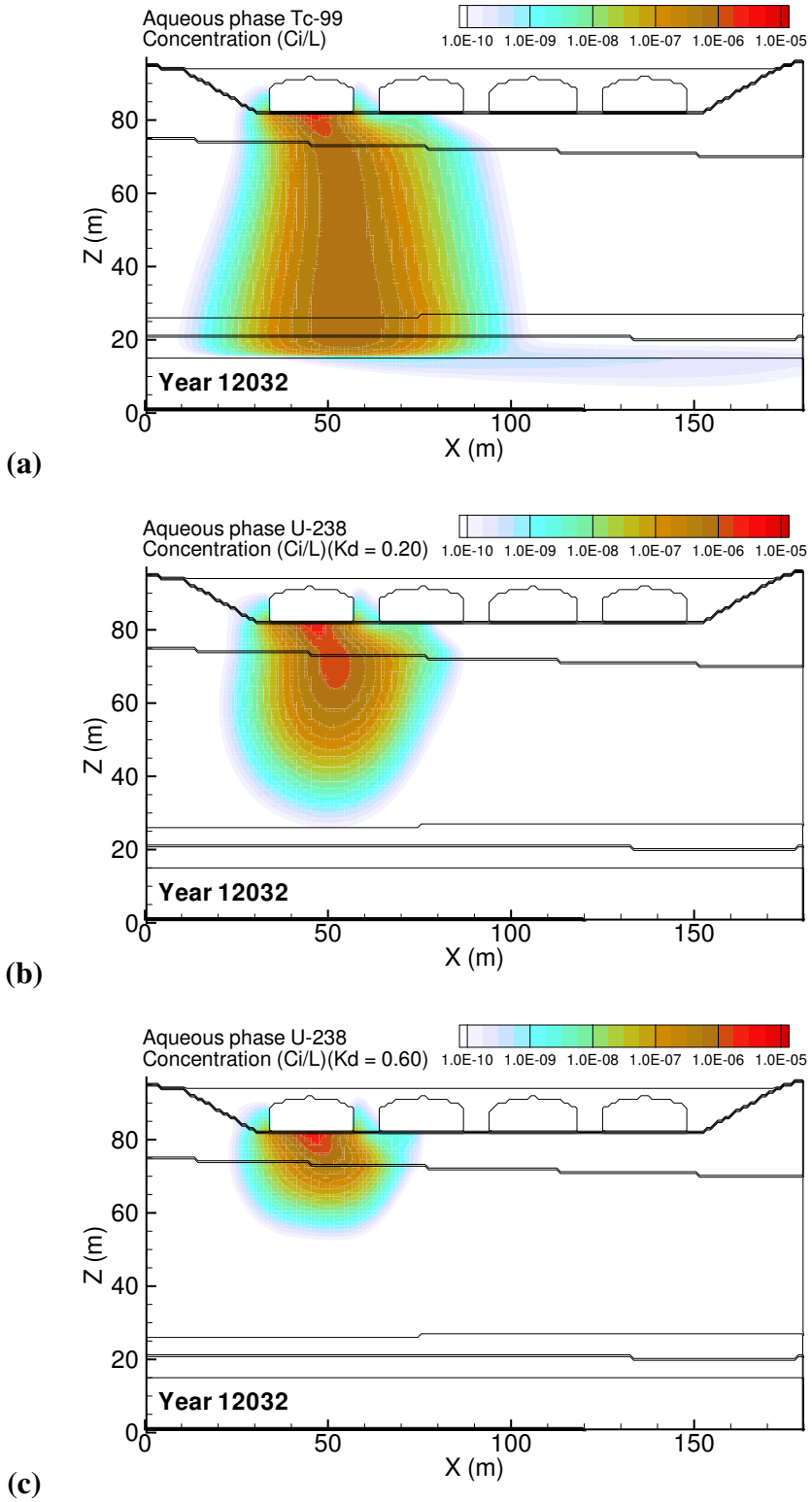

Figure C.10. Diffusion Release: Low Preclosure Recharge Rate (40 mm/yr) aqueous concentration distributions at year 12032 for (a) Tc-99, (b) U_0.20 and (c) U_0.60.

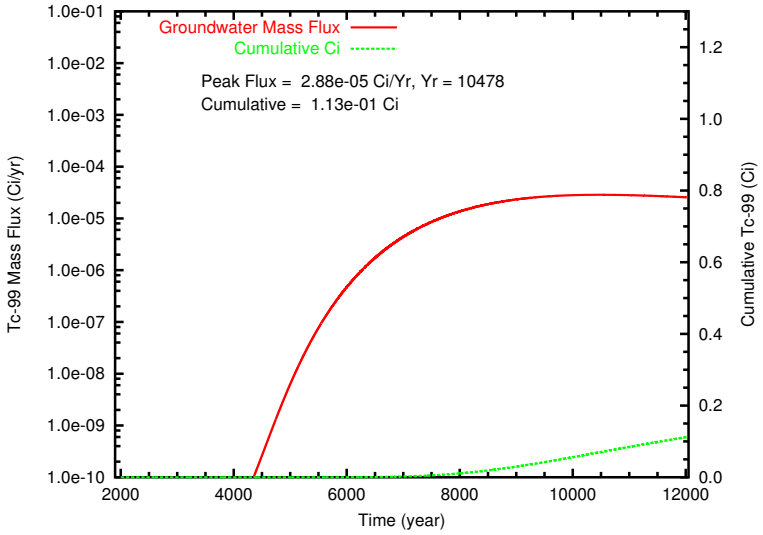

(a)

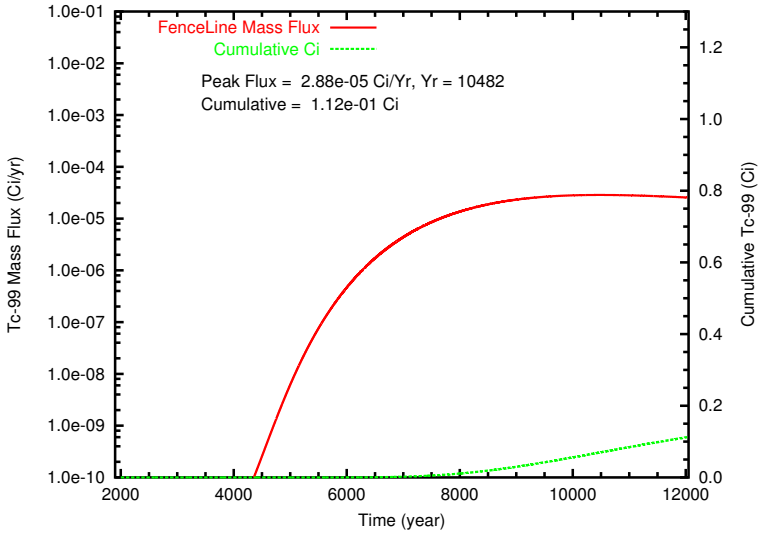

(b)

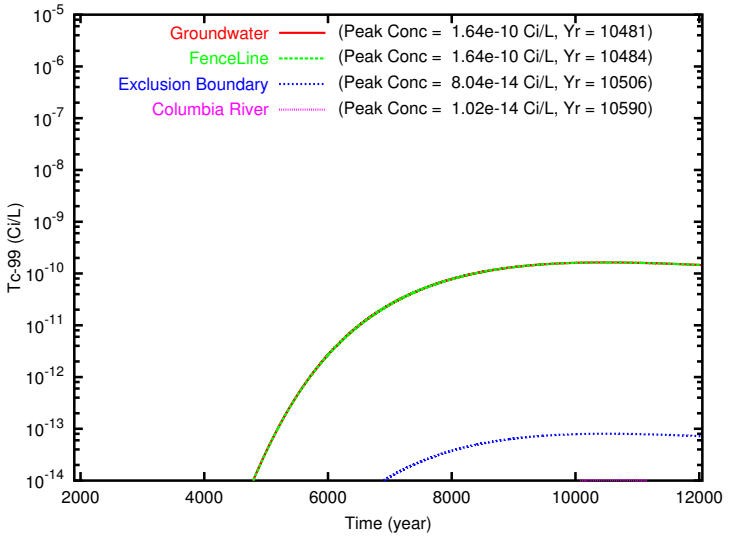

(c)

Figure C.11. Diffusion Release: Low Preclosure Recharge Rate (40 mm/yr) Tc-99 mass flux at (a) the groundwater table and (b) the fenceline; and (c) the Tc-99 concentration at groundwater, fenceline, and easterly downstream compliance points.

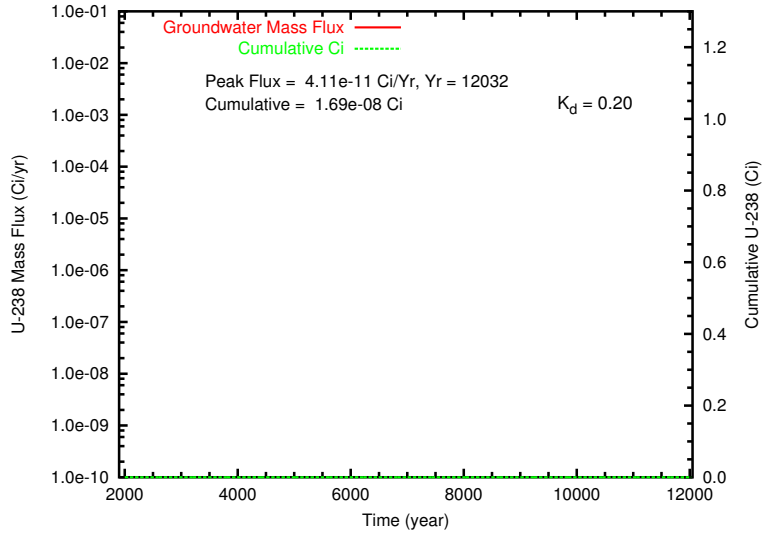

(a)

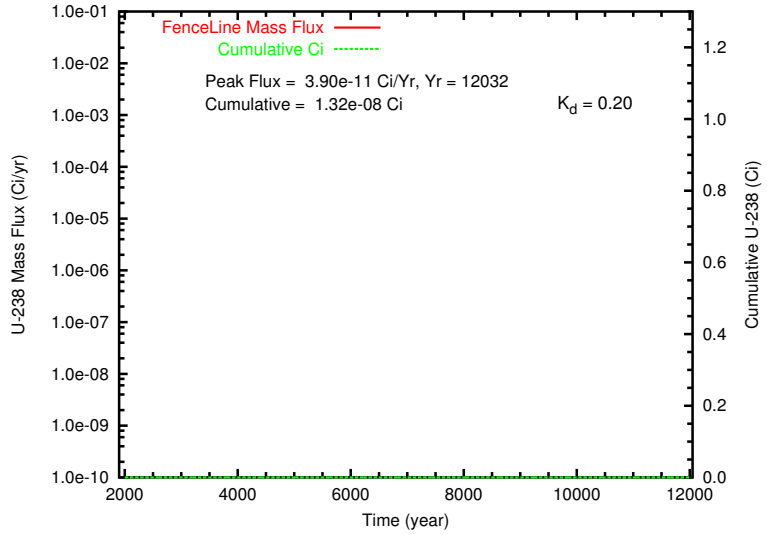

(b)

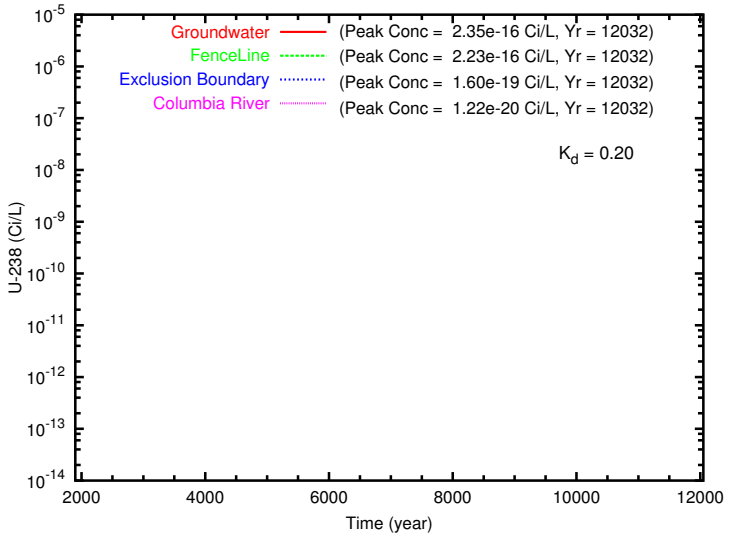

(c)

Figure C.12. Diffusion Release: Low Preclosure Recharge Rate (40 mm/yr) U_0.20 mass flux at (a) the groundwater table and (b) the fenceline; and (c) the Tc-99 concentration at groundwater, fenceline, and easterly downstream compliance points.

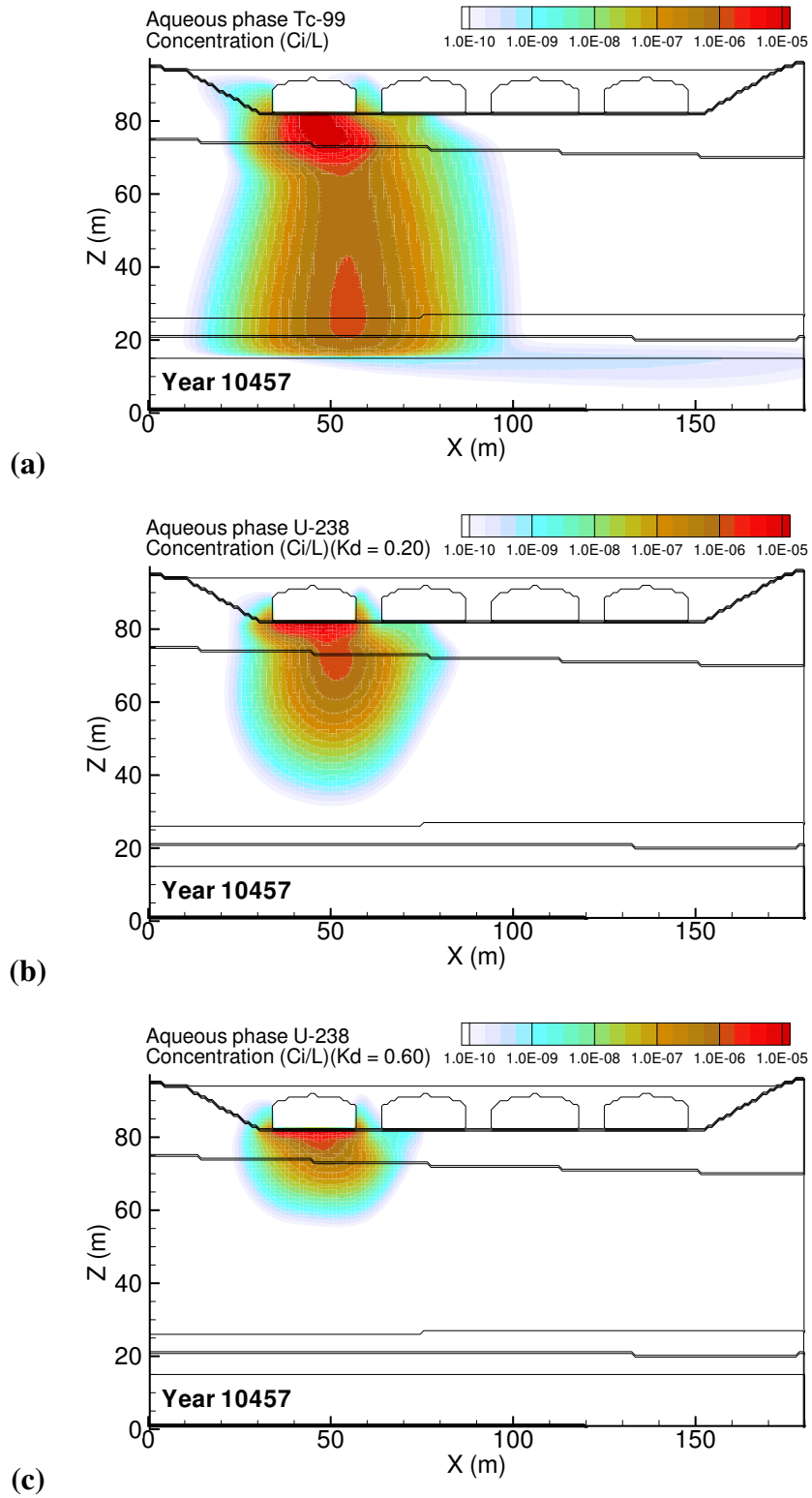

Figure C.13. Diffusion Release: High Barrier Recharge Rate (1.0 mm/yr) aqueous concentration distributions at year 10457 for (a) Tc-99, (b) U_0.20 and (c) U_0.60. Year of Tc-99 peak concentration at fenceline was 10457.

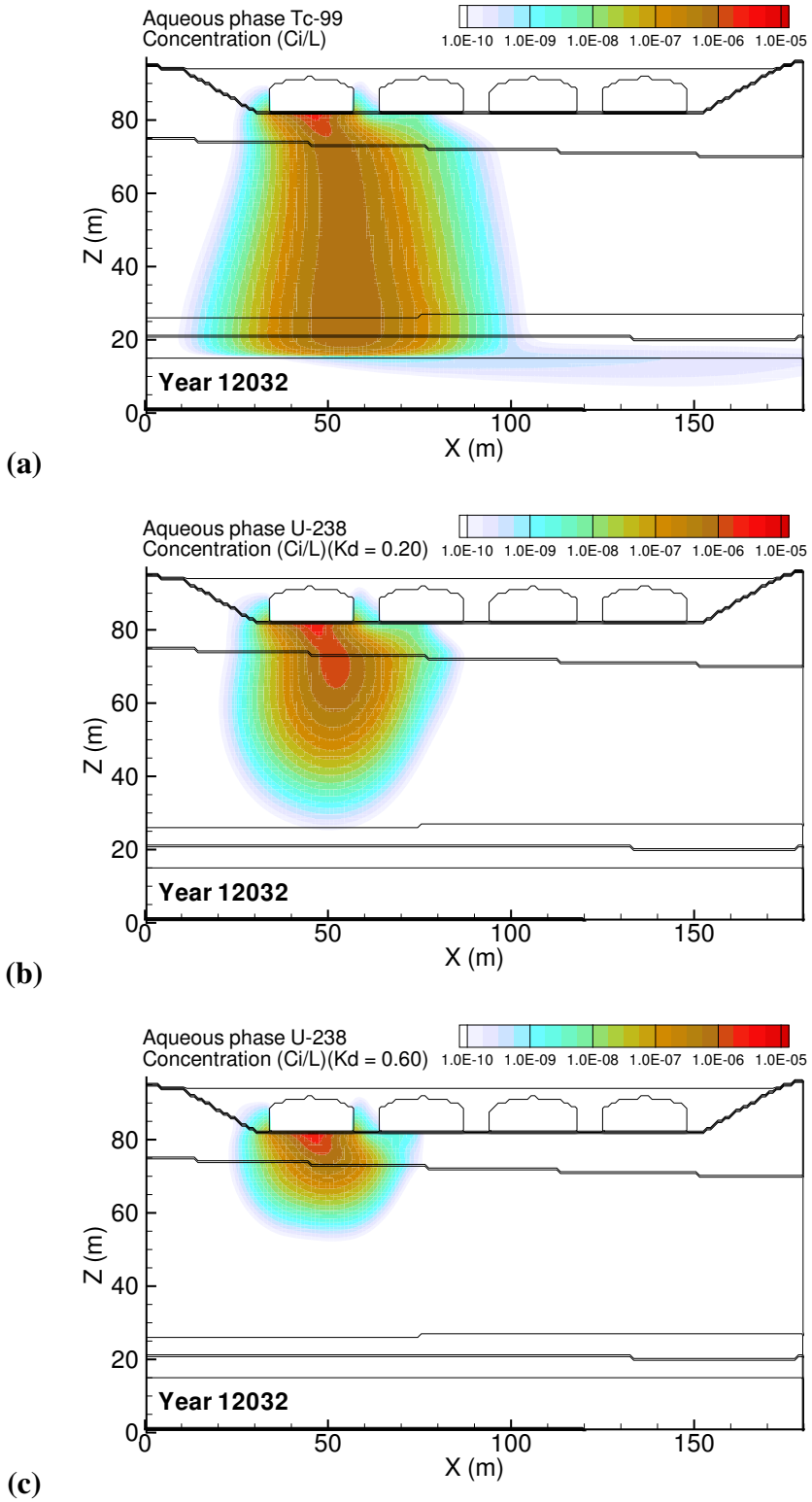

Figure C.14. Diffusion Release: High Barrier Recharge Rate (1.0 mm/yr) aqueous concentration distributions at year 12032 for (a) Tc-99, (b) U_0.20 and (c) U_0.60.

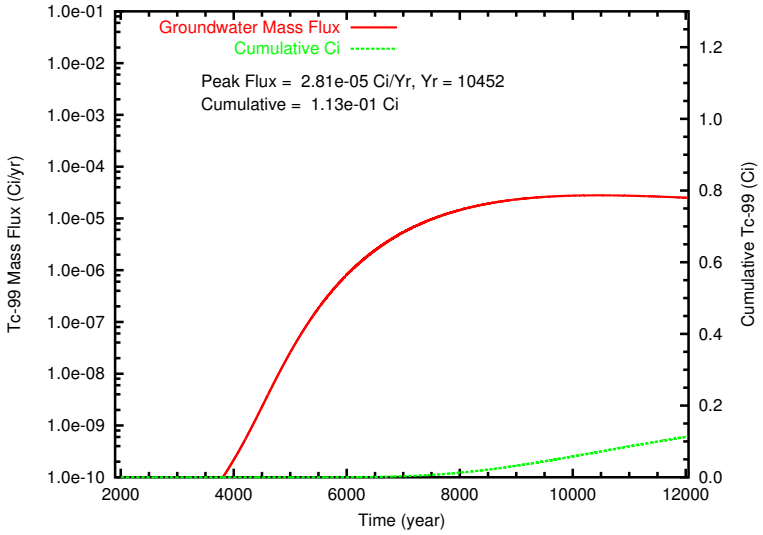

(a)

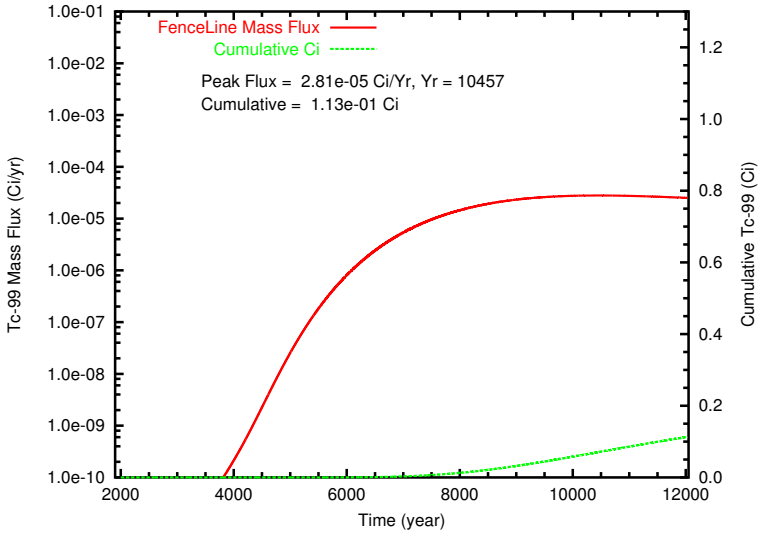

(b)

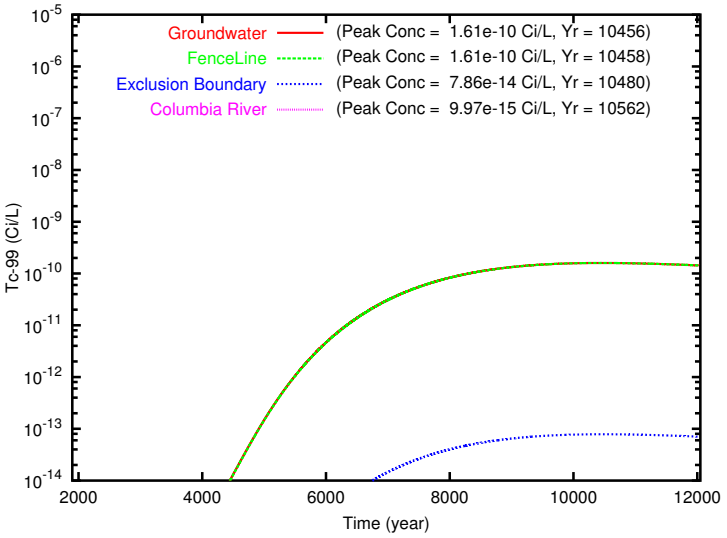

(c)

Figure C.15. Diffusion Release: High Barrier Recharge Rate (1.0 mm/yr) Tc-99 mass flux at (a) the groundwater table and (b) the fenceline; and (c) the Tc-99 concentration at groundwater, fenceline, and easterly downstream compliance points.

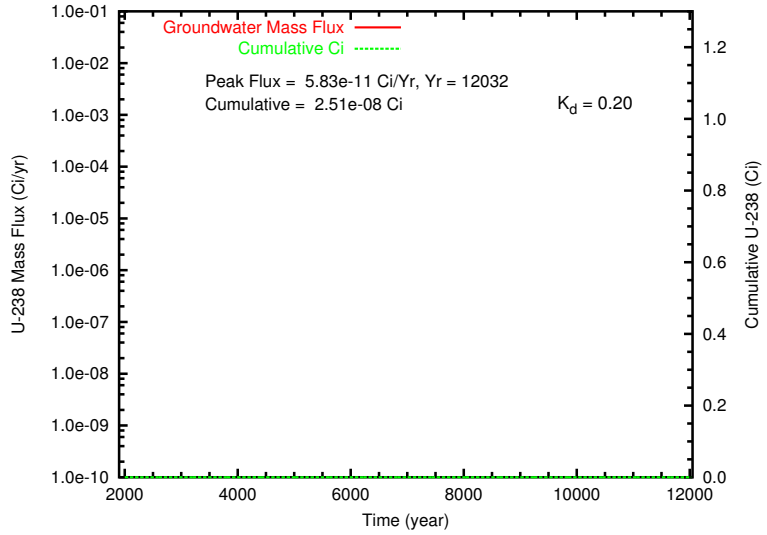

(a)

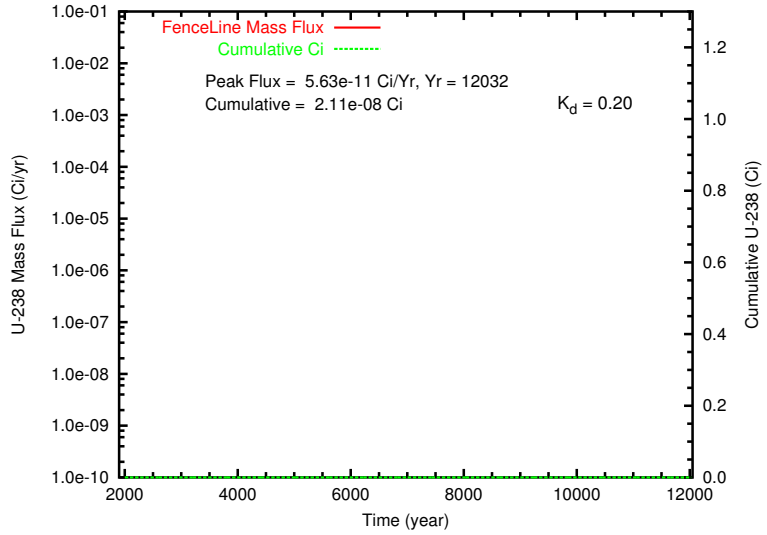

(b)

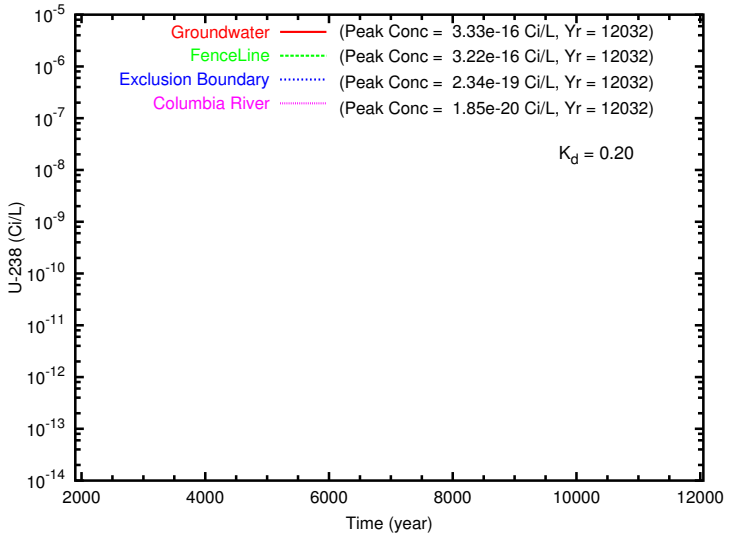

(c)

Figure C.16. Diffusion Release: High Barrier Recharge Rate (1.0 mm/yr) U_0.20 mass flux at (a) the groundwater table and (b) the fenceline; and (c) the Tc-99 concentration at groundwater, fenceline, and easterly downstream compliance points.

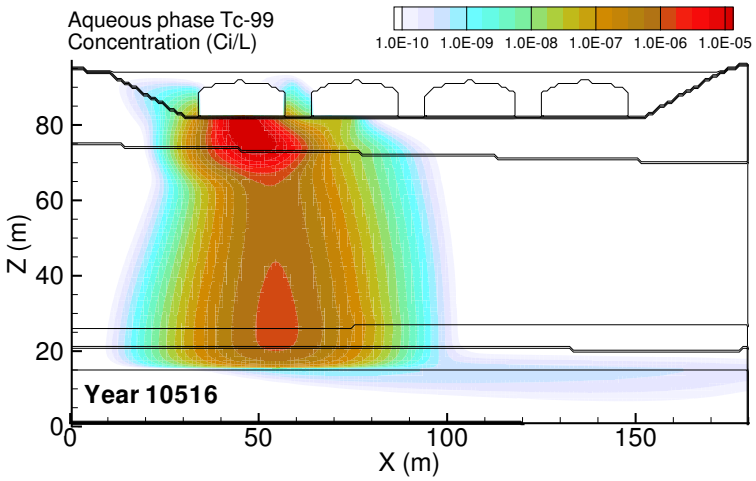

(a)

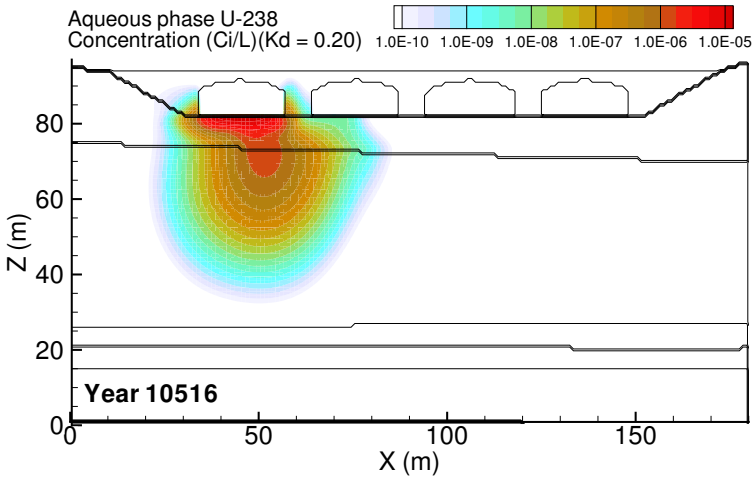

(b)

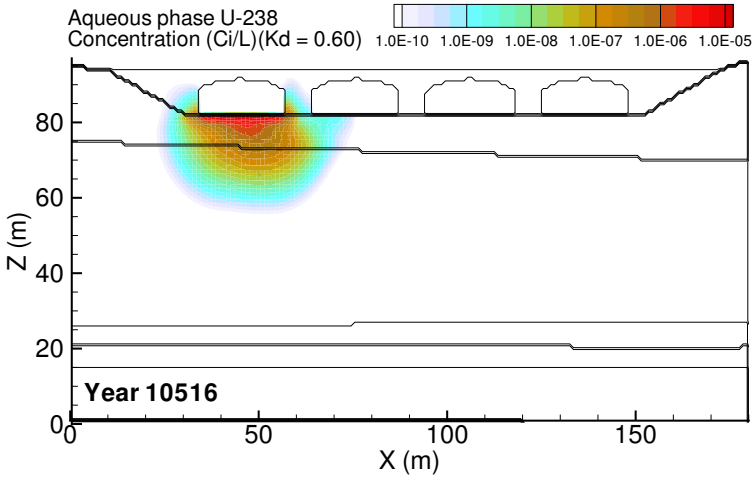

(c)

Figure C.17. Diffusion Release: Low Barrier Recharge Rate (0.1 mm/yr) aqueous concentration distributions at year 10516 for (a) Tc-99, (b) U_0.20 and (c) U_0.60. Year of Tc-99 peak concentration at fenceline was 10516.

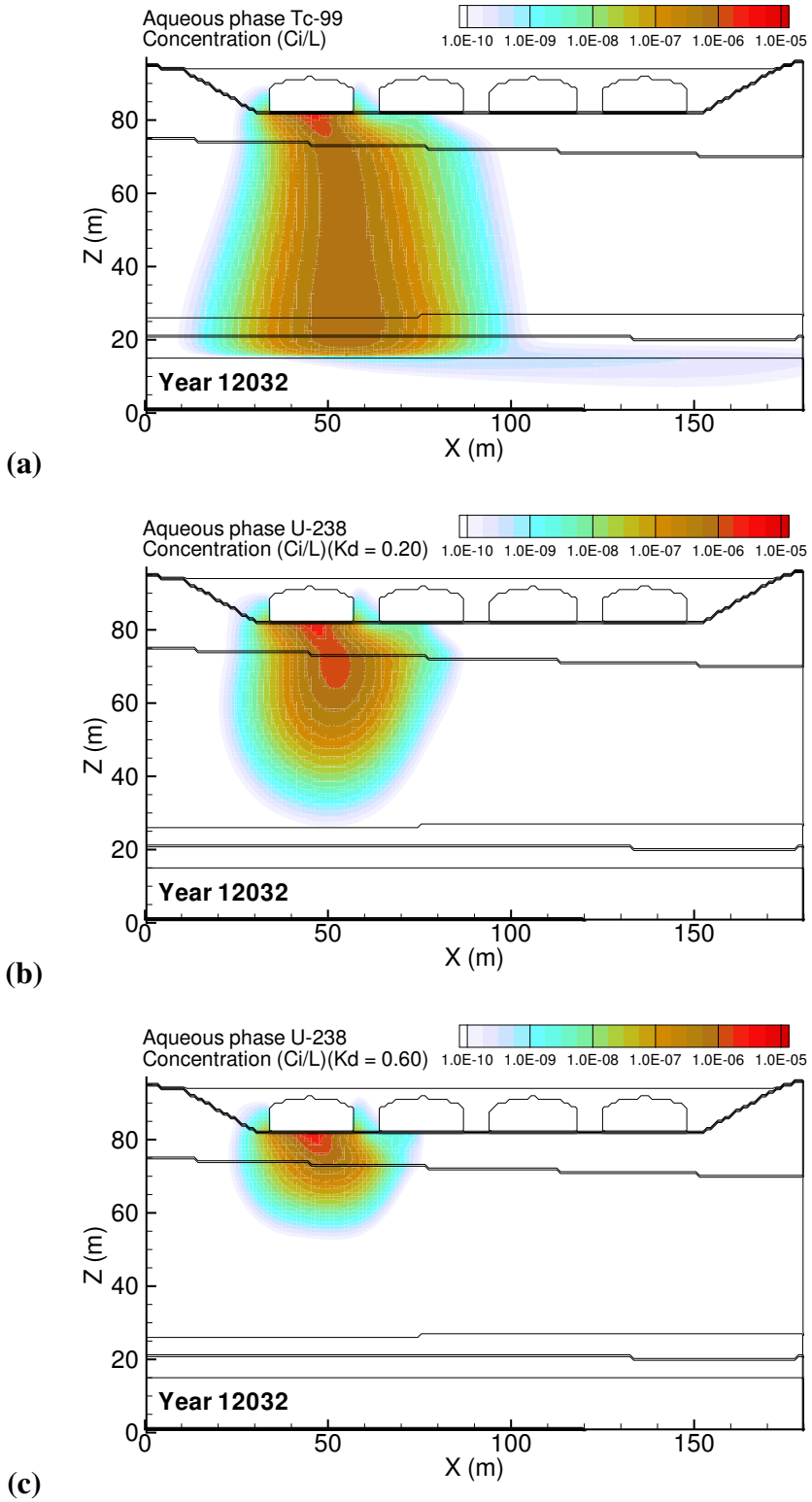

Figure C.18. Diffusion Release: Low Barrier Recharge Rate (0.1 mm/yr) aqueous concentration distributions at year 12032 for (a) Tc-99, (b) U_0.20 and (c) U_0.60.

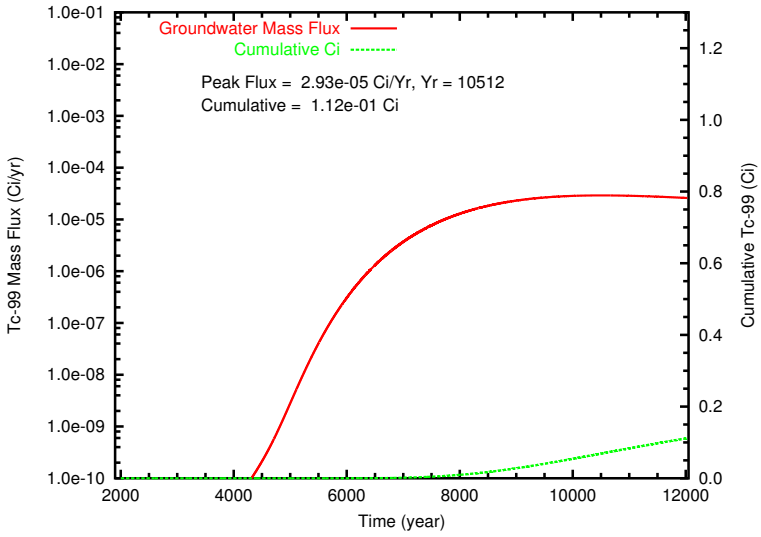

(a)

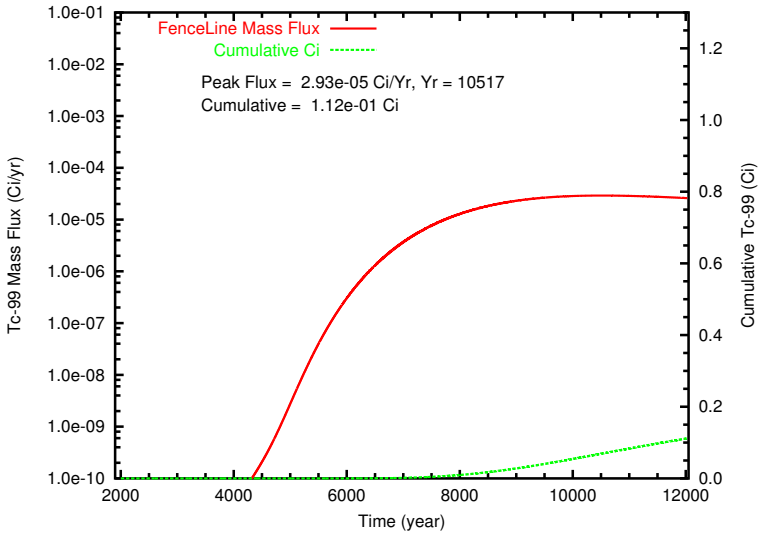

(b)

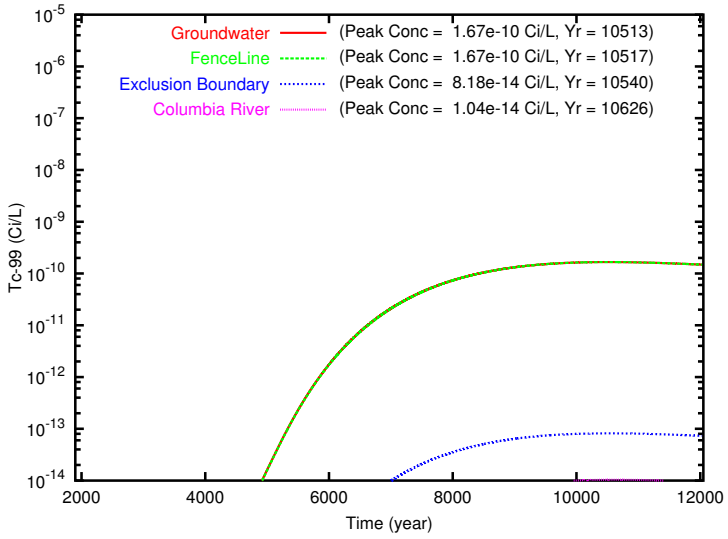

(c)

Figure C.19. Diffusion Release: Low Barrier Recharge Rate (0.1 mm/yr) Tc-99 mass flux at (a) the groundwater table and (b) the fenceline; and (c) the Tc-99 concentration at groundwater, fenceline, and easterly downstream compliance points.

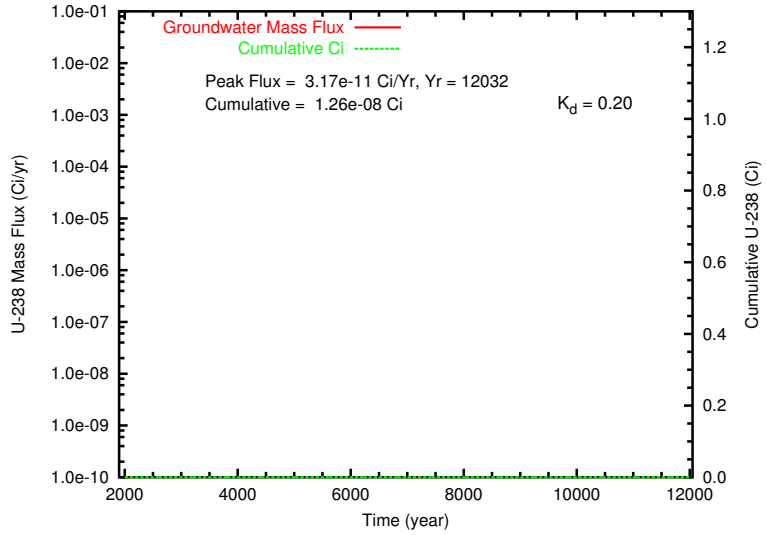

(a)

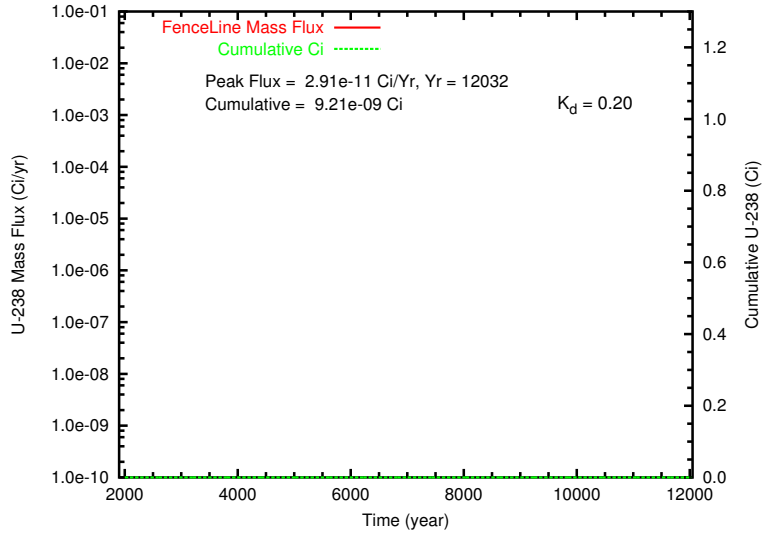

(b)

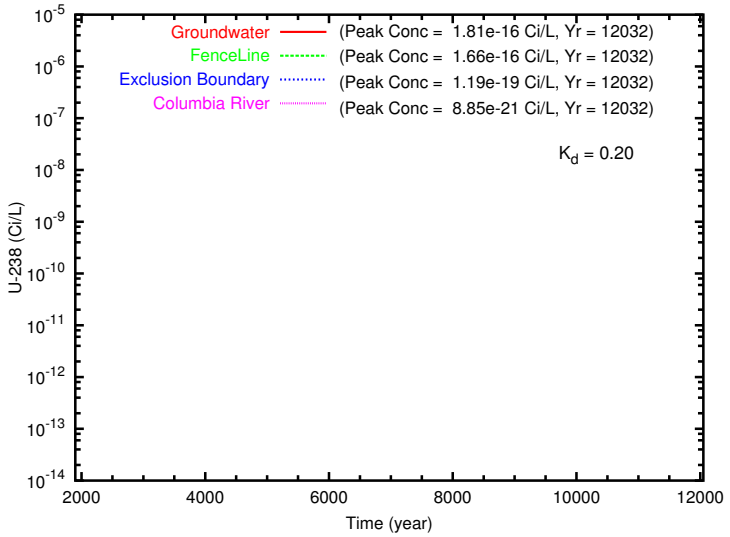

(c)

Figure C.20. Diffusion Release: Low Barrier Recharge Rate (0.1 mm/yr) U_0.20 mass flux at (a) the groundwater table and (b) the fenceline; and (c) the Tc-99 concentration at groundwater, fenceline, and easterly downstream compliance points.

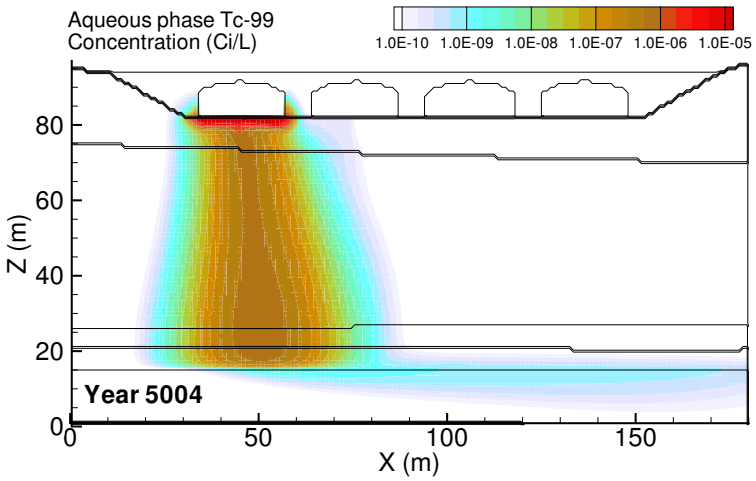

(a)

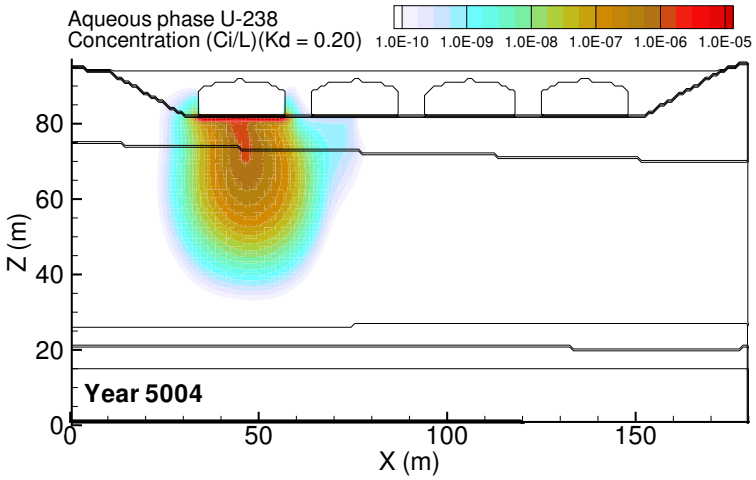

(b)

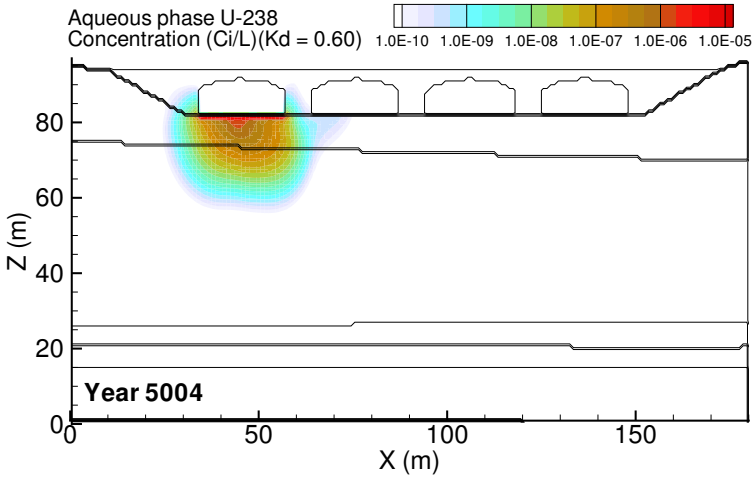

(c)

Figure C.21. Diffusion Release: High Degraded-Barrier Recharge Rate (3.5 mm/yr) aqueous concentration distributions at year 5004 for (a) Tc-99, (b) U_0.20 and (c) U_0.60. Year of Tc-99 peak concentration at fenceline was 5004.

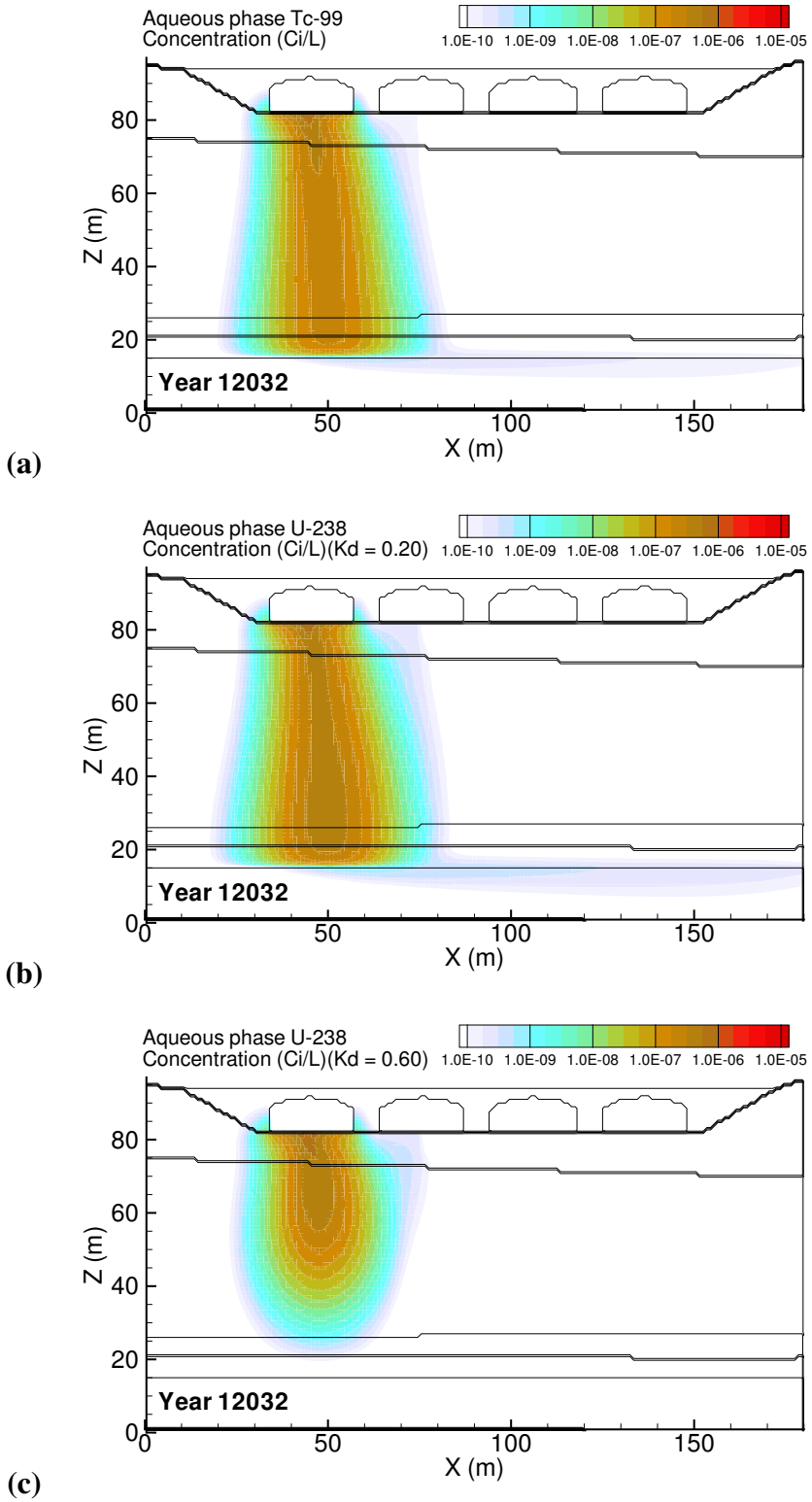

Figure C.22. Diffusion Release: High Degraded-Barrier Recharge Rate (3.5 mm/yr) aqueous concentration distributions at year 12032 for (a) Tc-99, (b) U_0.20 and (c) U_0.60.

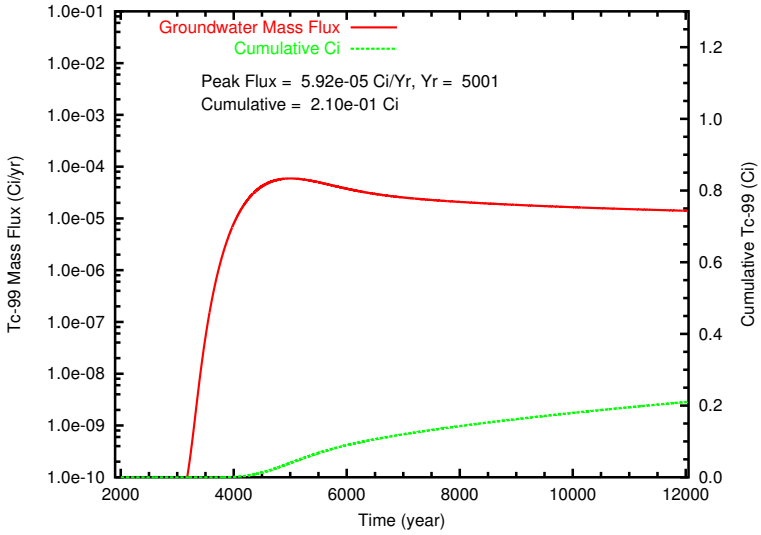

(a)

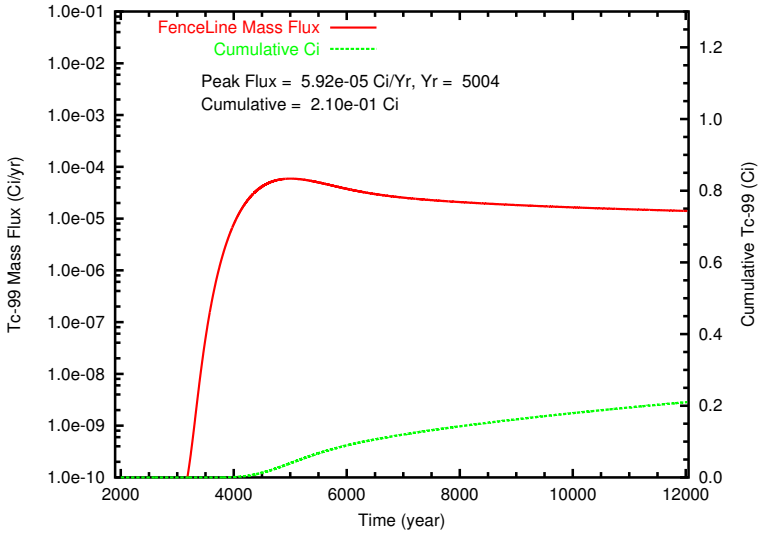

(b)

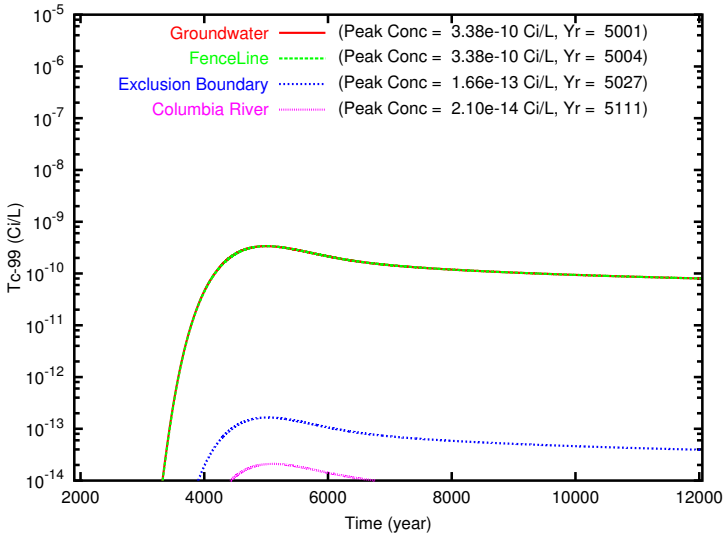

(c)

Figure C.23. Diffusion Release: High Degraded-Barrier Recharge Rate (3.5 mm/yr) Tc-99 mass flux at (a) the groundwater table and (b) the fenceline; and (c) the Tc-99 concentration at groundwater, fenceline, and easterly downstream compliance points.

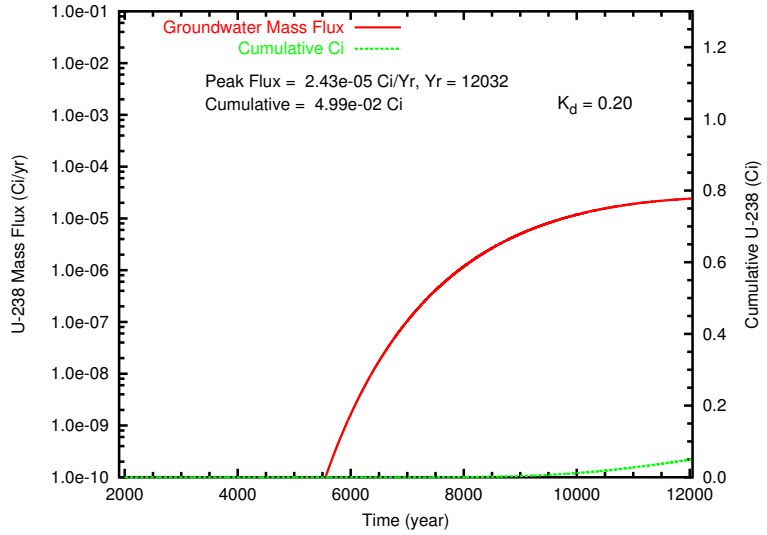

(a)

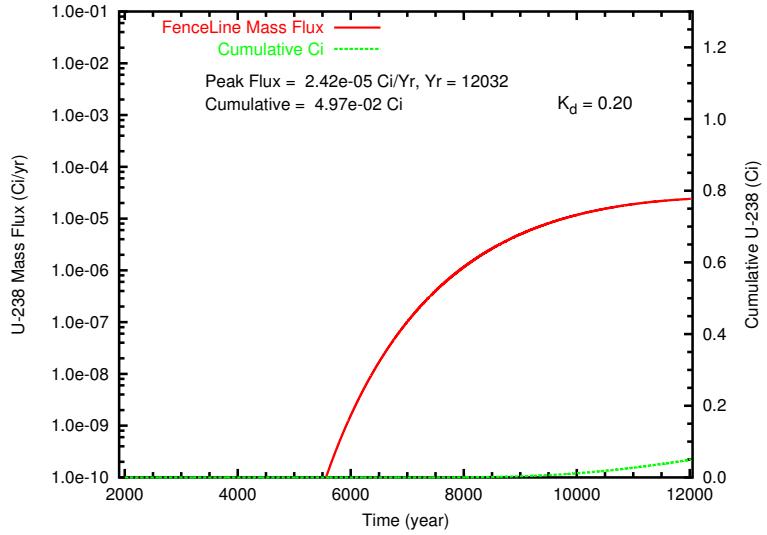

(b)

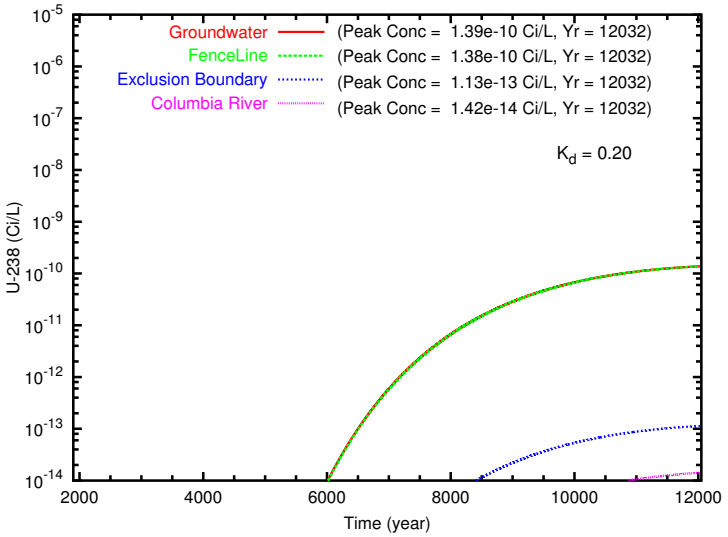

(c)

Figure C.24. Diffusion Release: High Degraded-Barrier Recharge Rate (3.5 mm/yr) U_0.20 mass flux at (a) the groundwater table and (b) the fenceline; and (c) the Tc-99 concentration at groundwater, fenceline, and easterly downstream compliance points.

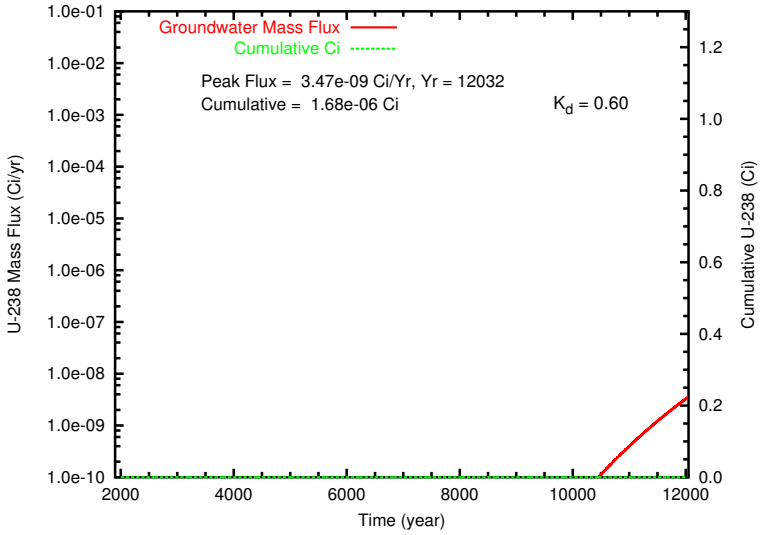

(a)

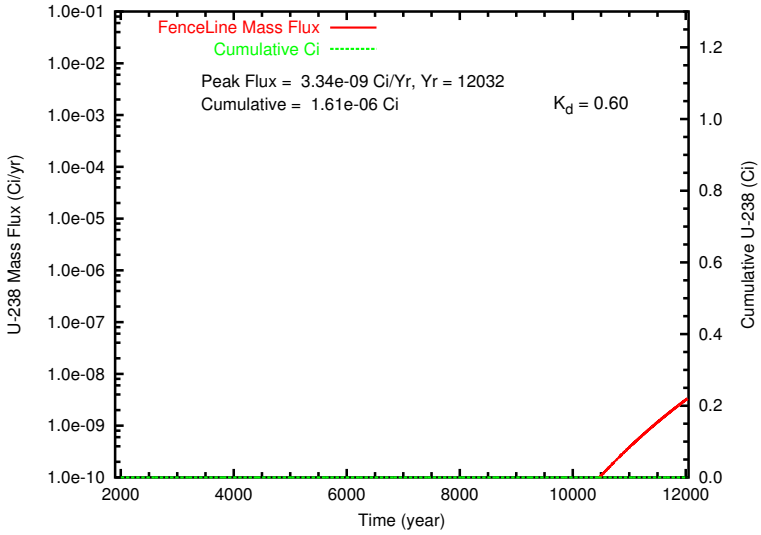

(b)

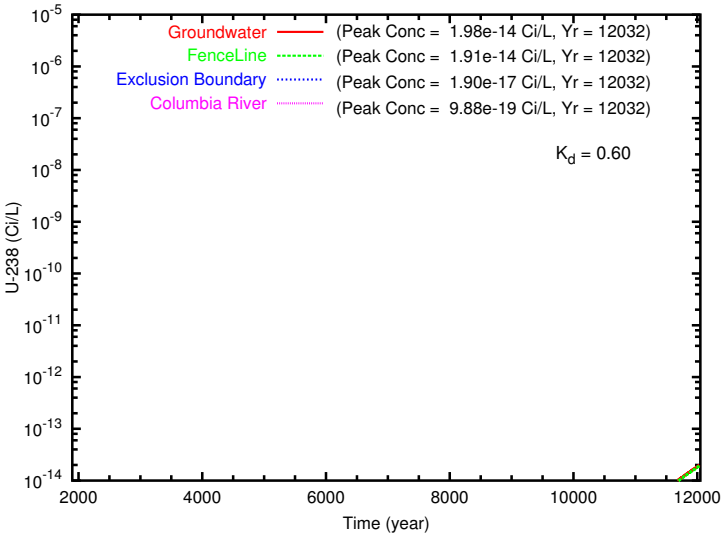

(c)

Figure C.25. Diffusion Release: High Degraded-Barrier Recharge Rate (3.5 mm/yr) U_0.60 mass flux at (a) the groundwater table and (b) the fenceline; and (c) the Tc-99 concentration at groundwater, fenceline, and easterly downstream compliance points.

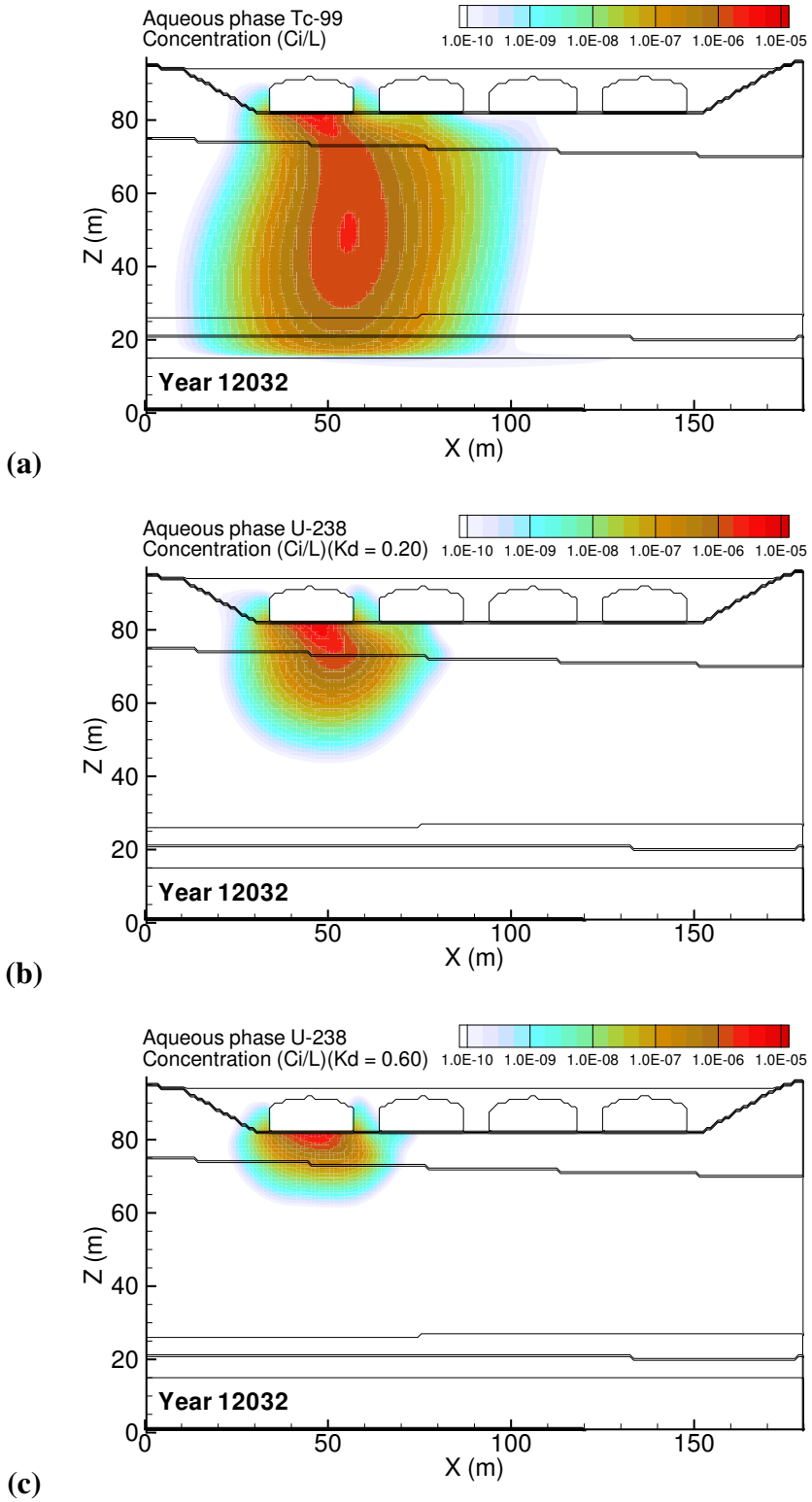

Figure C.26. Diffusion Release: Low Degraded-Barrier Recharge Rate (0.5 mm/yr) aqueous concentration distributions at year 12032 for (a) Tc-99, (b) U_0.20 and (c) U_0.60.

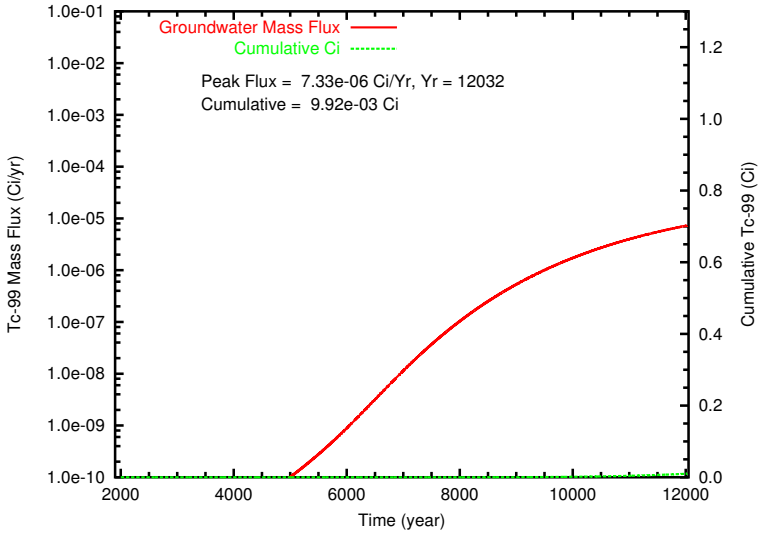

(a)

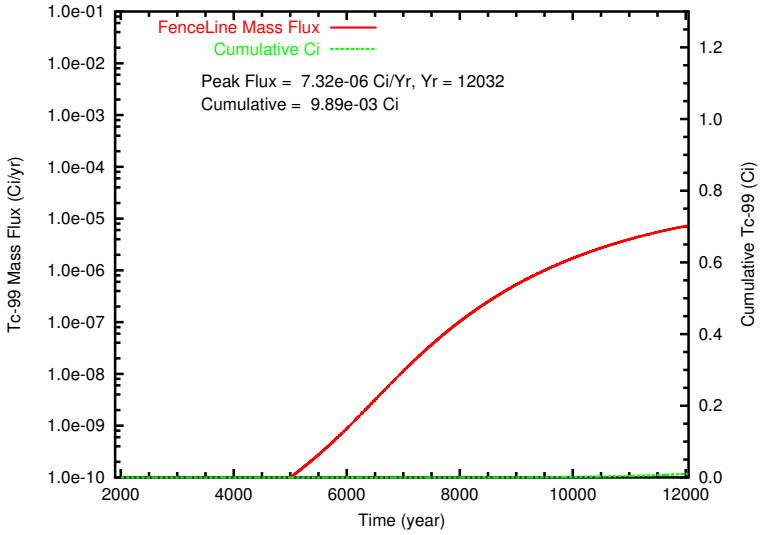

(b)

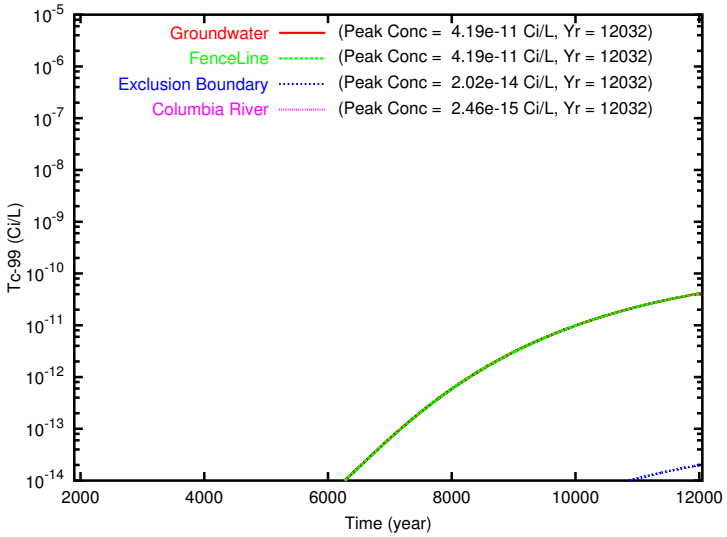

(c)

Figure C.27. Diffusion Release: Low Degraded-Barrier Recharge Rate (0.5 mm/yr) Tc-99 mass flux at (a) the groundwater table and (b) the fenceline; and (c) the Tc-99 concentration at groundwater, fenceline, and easterly downstream compliance points.

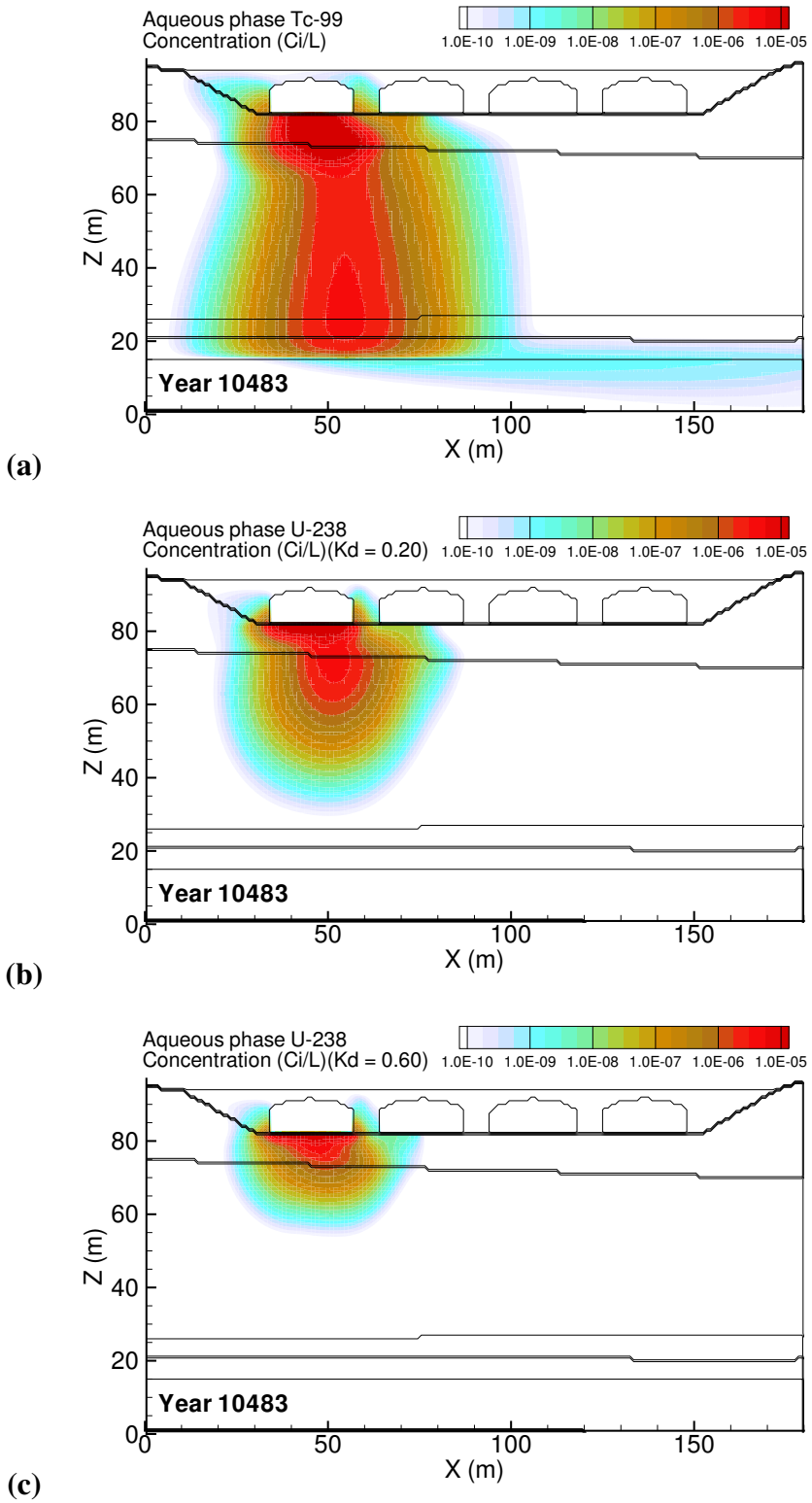

Figure C.28. Diffusion Release: High Diffusion Release (1e-8 cm2/s) aqueous concentration distributions at year 10483 for (a) Tc-99, (b) U_0.20 and (c) U_0.60. Year of Tc-99 peak concentration at fenceline was 10483.

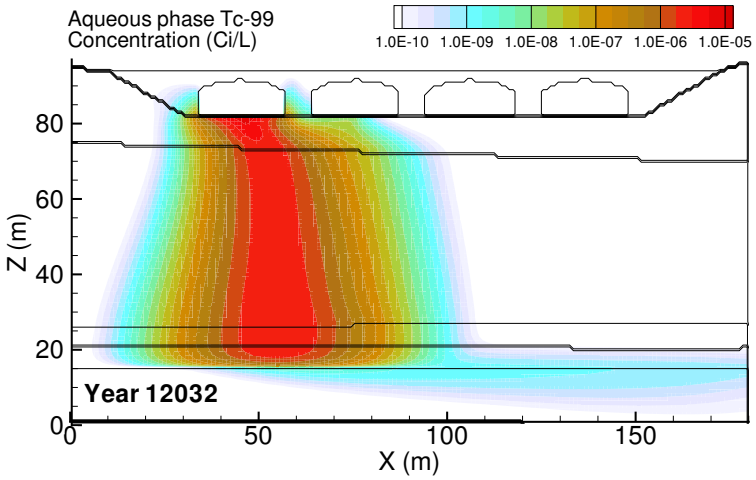

(a)

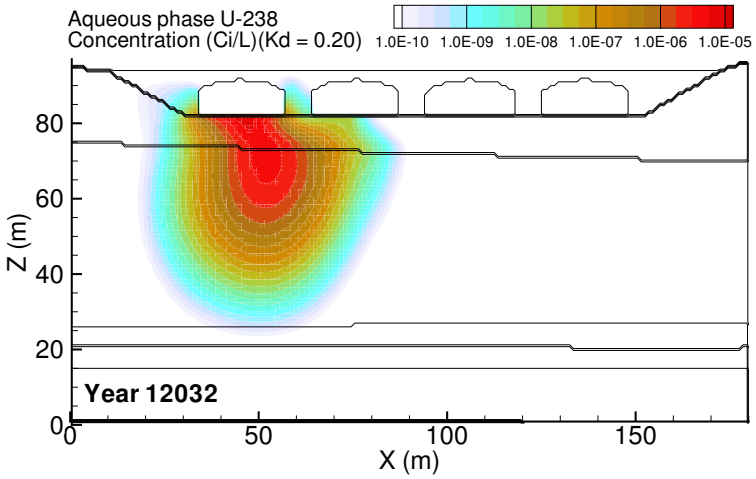

(b)

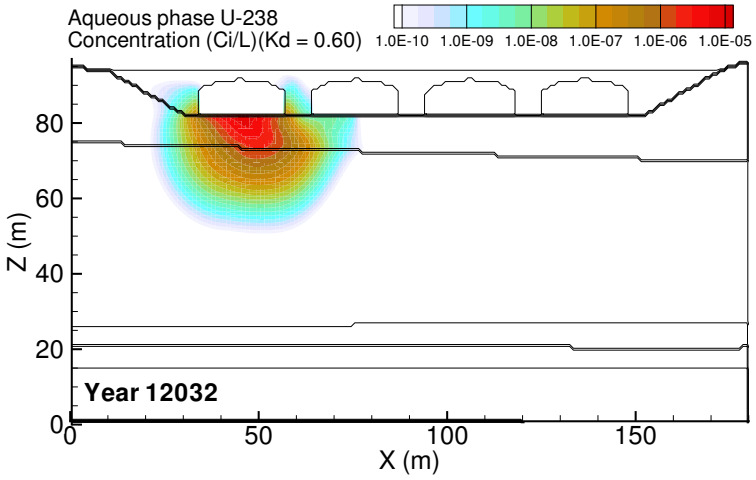

(c)

Figure C.29. Diffusion Release: High Diffusion Release (1e-8 cm2/s) aqueous concentration distributions at year 12032 for (a) Tc-99, (b) U_0.20 and (c) U_0.60.

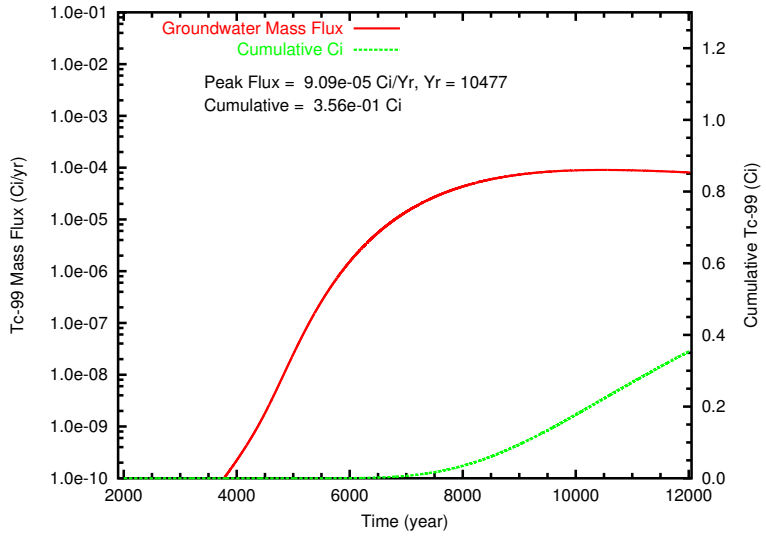

(a)

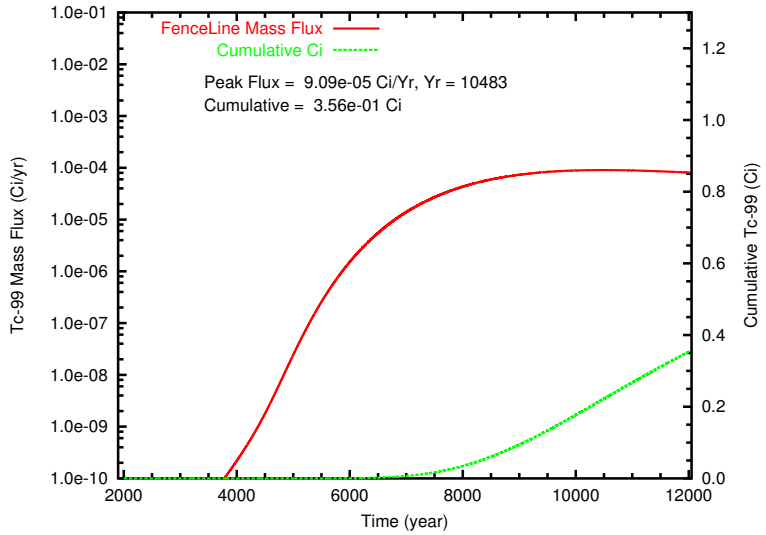

(b)

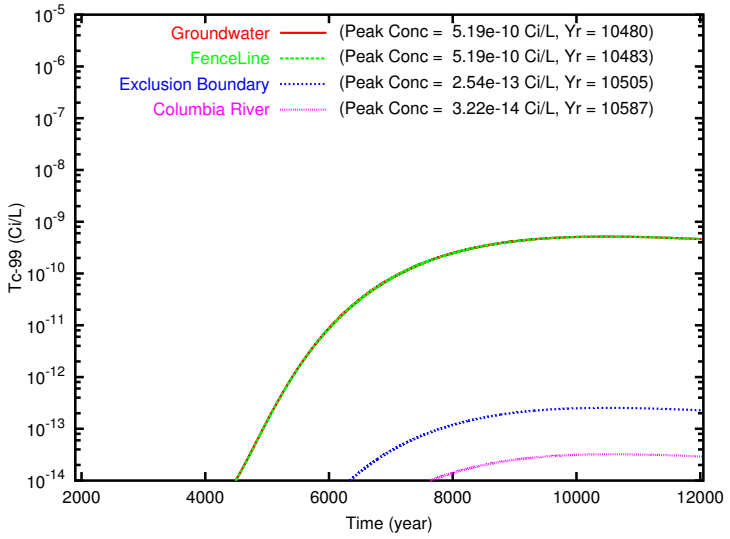

(c)

Figure C.30. Diffusion Release: High Diffusion Release (1e-8 cm2/s) Tc-99 mass flux at (a) the groundwater table and (b) the fenceline; and (c) the Tc-99 concentration at groundwater, fenceline, and easterly downstream compliance points.

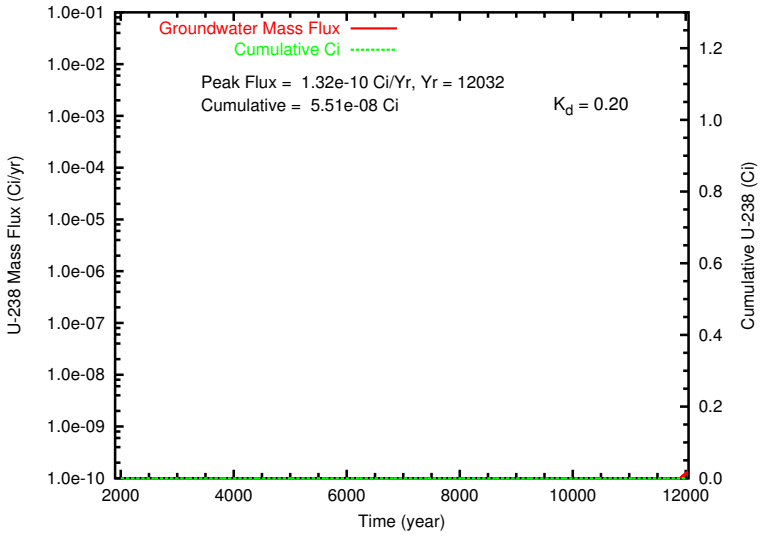

(a)

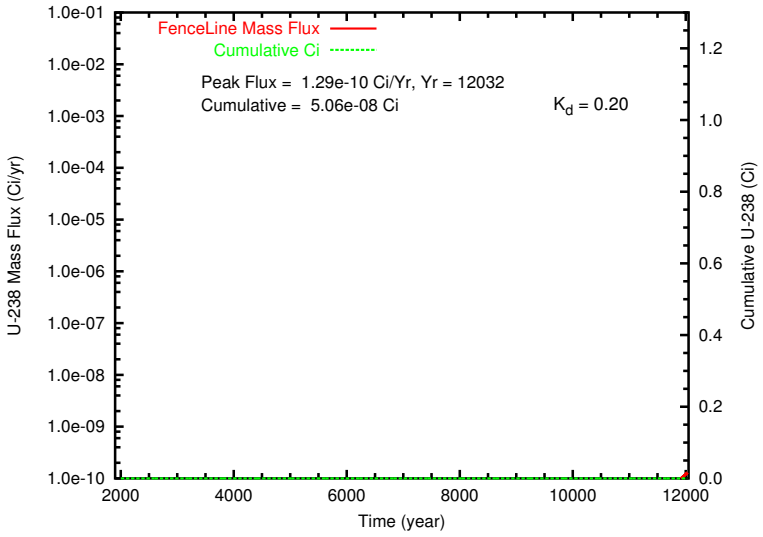

(b)

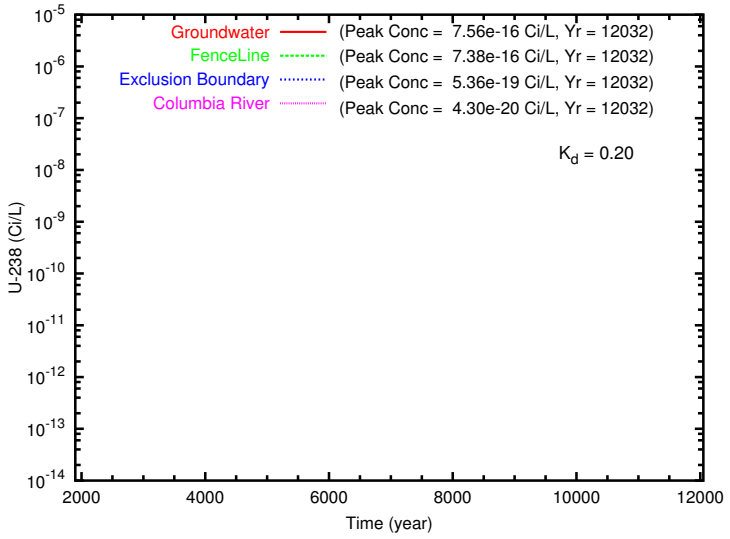

(c)

Figure C.31. Diffusion Release: High Diffusion Release (1e-8 cm2/s) U_0.20 mass flux at (a) the groundwater table and (b) the fenceline; and (c) the Tc-99 concentration at groundwater, fenceline, and easterly downstream compliance points.

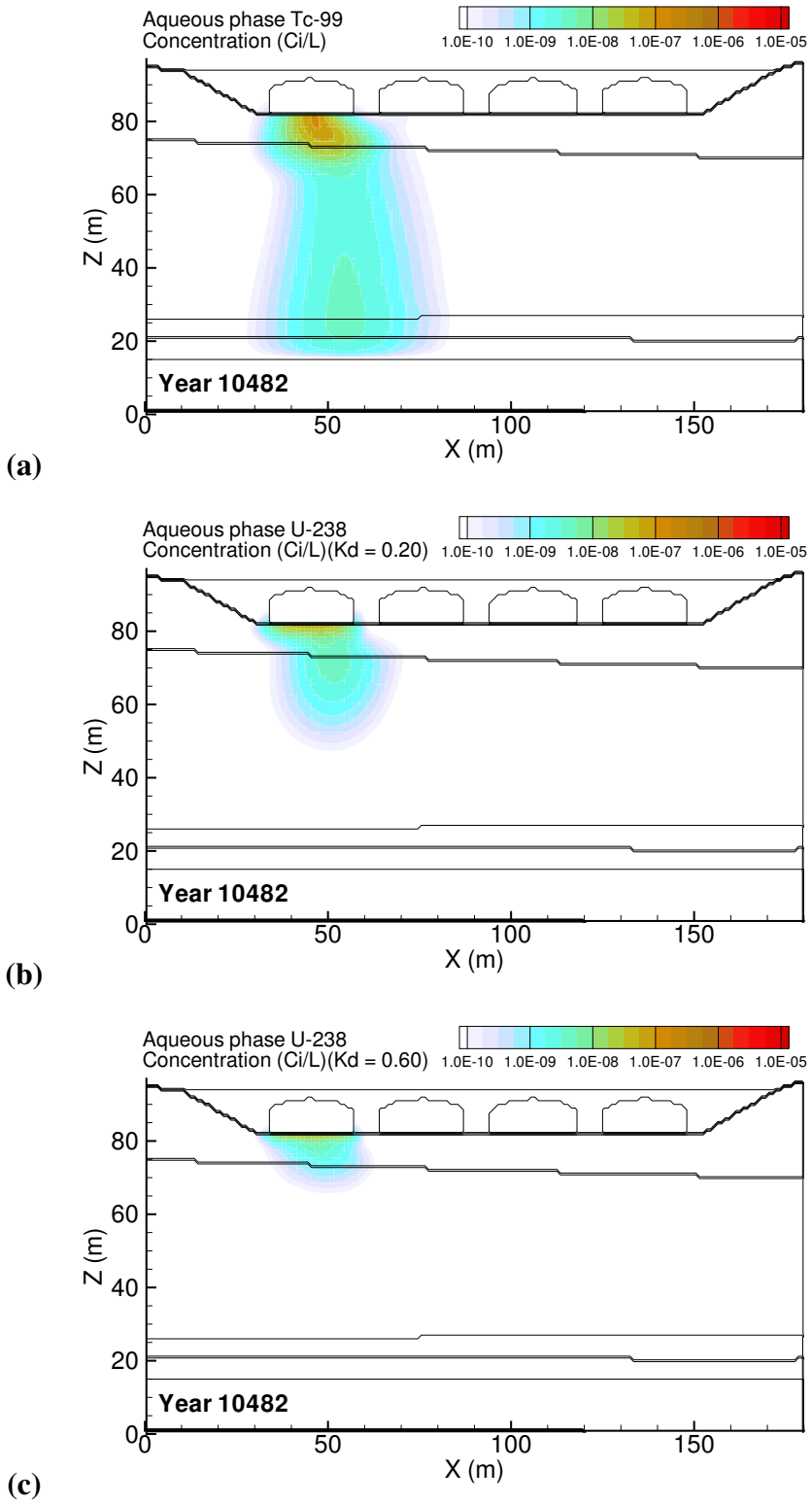

Figure C.32. Diffusion Release: Low Diffusion Release (1e-14 cm2/s) aqueous concentration distributions at year 10482 for (a) Tc-99, (b) U_0.20 and (c) U_0.60. Year of Tc-99 peak concentration at fenceline was 10482.

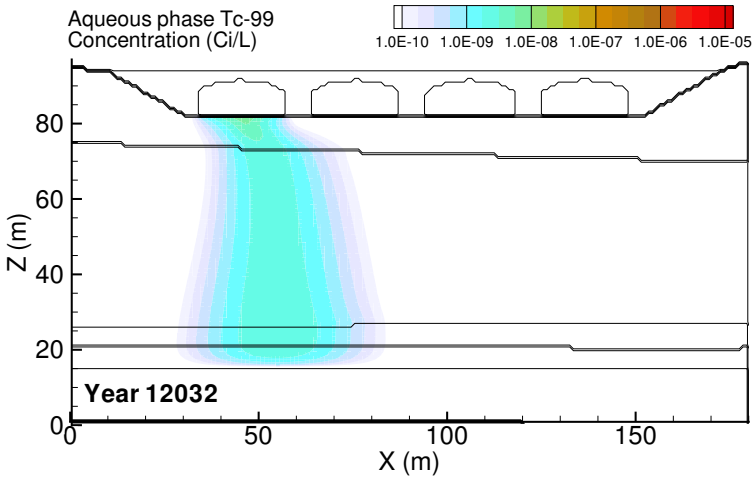

(a)

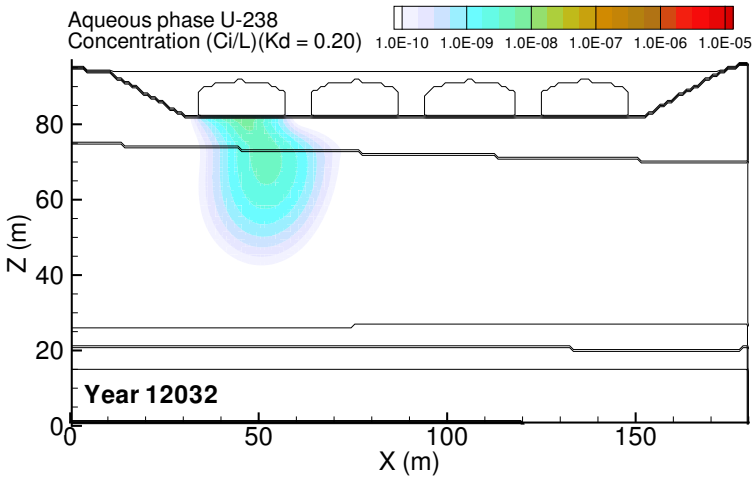

(b)

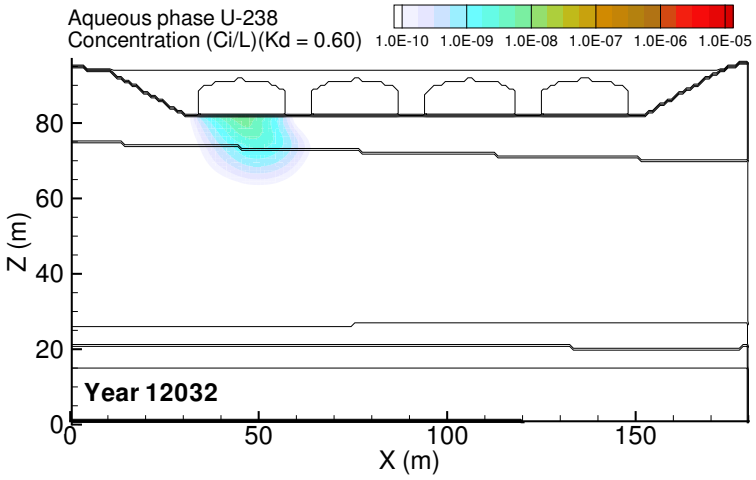

(c)

Figure C.33. Diffusion Release: Low Diffusion Release (1e-14 cm2/s) aqueous concentration distributions at year 12032 for (a) Tc-99, (b) U_0.20 and (c) U_0.60.

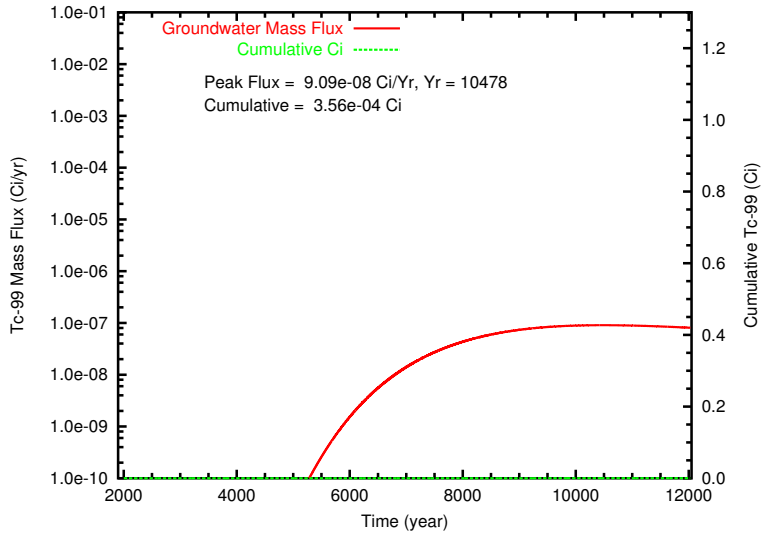

(a)

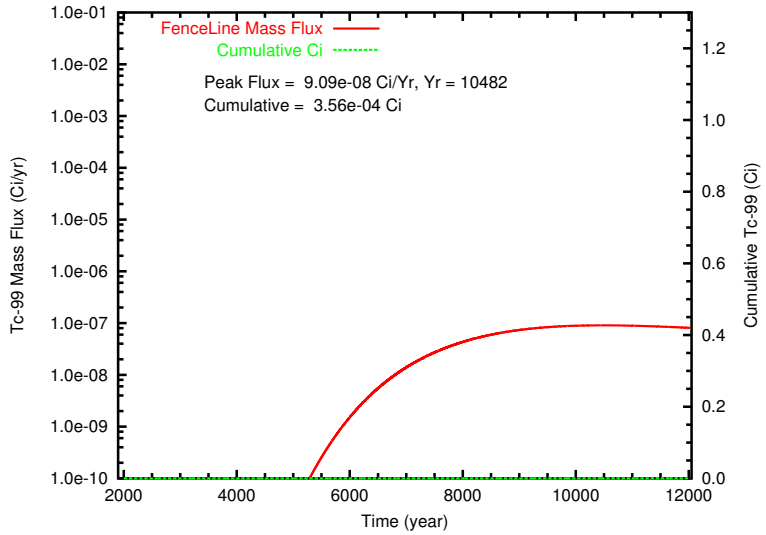

(b)

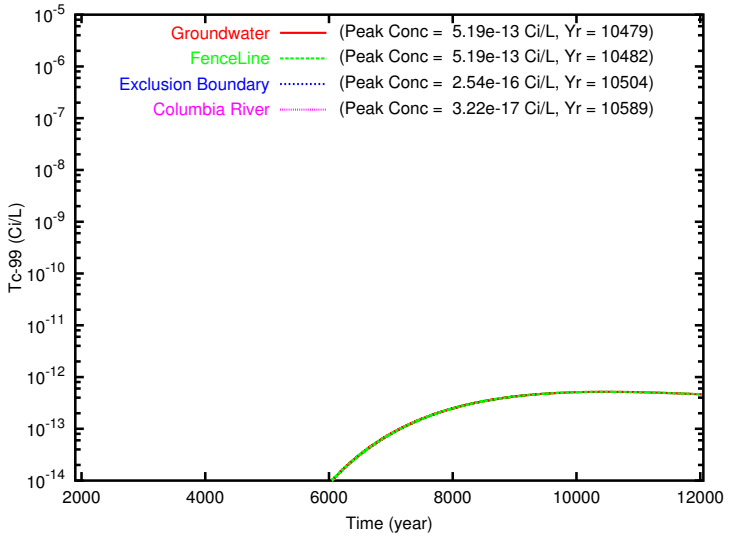

(c)

Figure C.34. Diffusion Release: Low Diffusion Release (1e-14 cm2/s) Tc-99 mass flux at (a) the groundwater table and (b) the fenceline; and (c) the Tc-99 concentration at groundwater, fenceline, and easterly downstream compliance points.

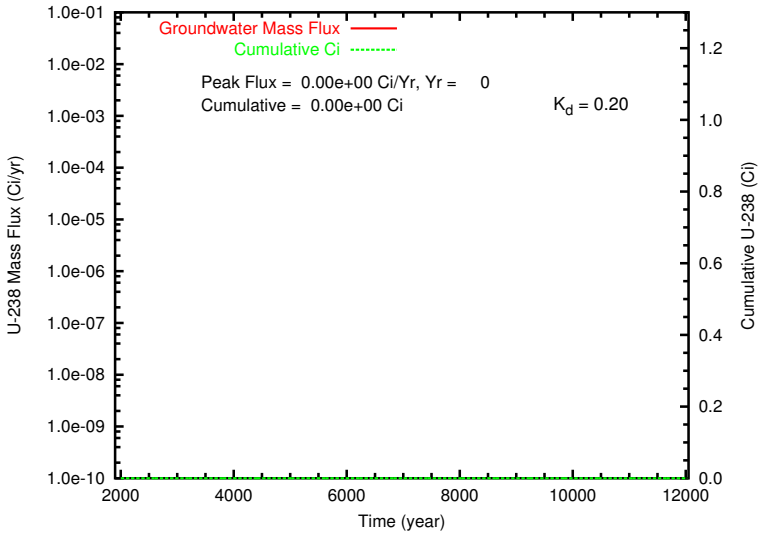

(a)

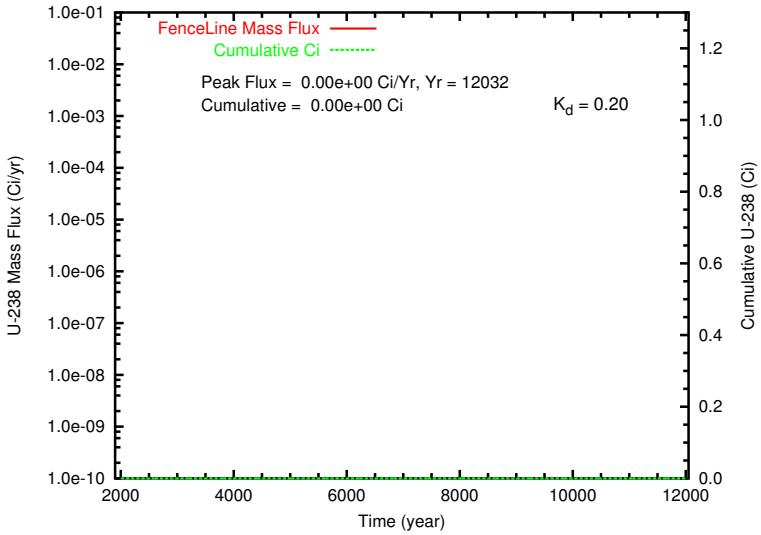

(b)

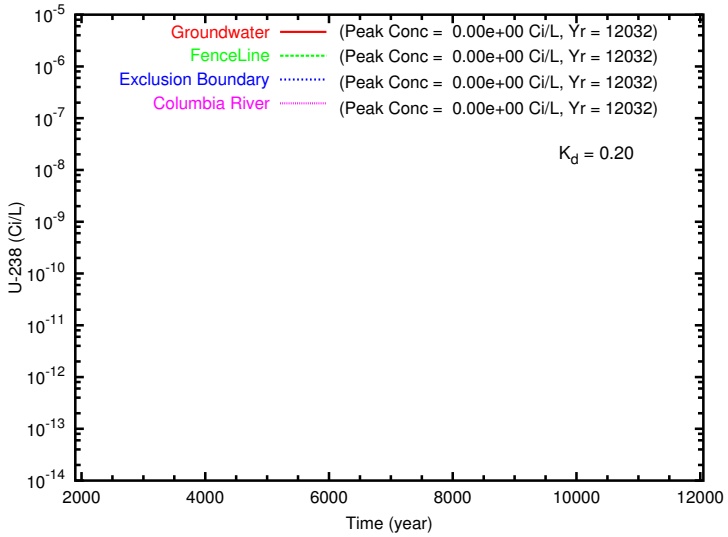

(c)

Figure C.35. Diffusion Release: Low Diffusion Release (1e-14 cm2/s) U_0.20 mass flux at (a) the groundwater table and (b) the fenceline; and (c) the Tc-99 concentration at groundwater, fenceline, and easterly downstream compliance points.

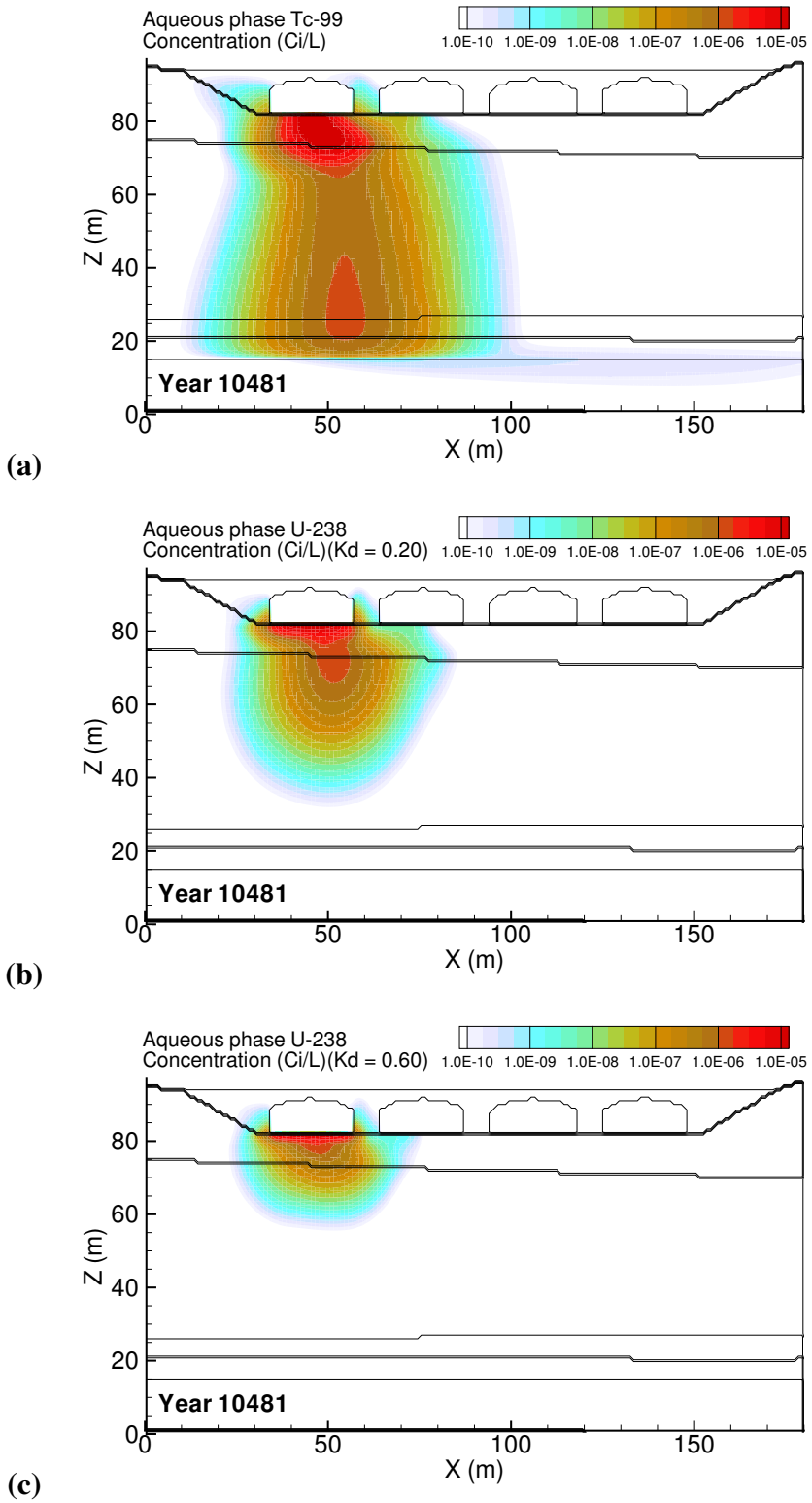

Figure C.36. Diffusion Release: High Aquifer Hydraulic Conductivity (4000 m/d) aqueous concentration distributions at year 10481 for (a) Tc-99, (b) U_0.20 and (c) U_0.60. Year of Tc-99 peak concentration at fenceline was 10481.

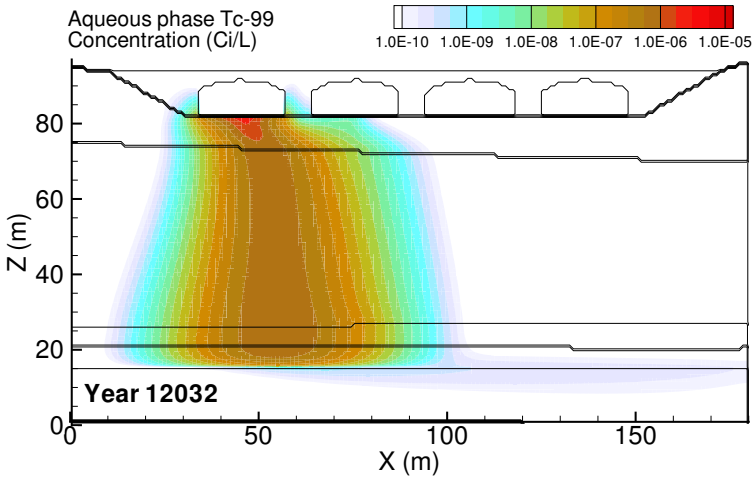

(a)

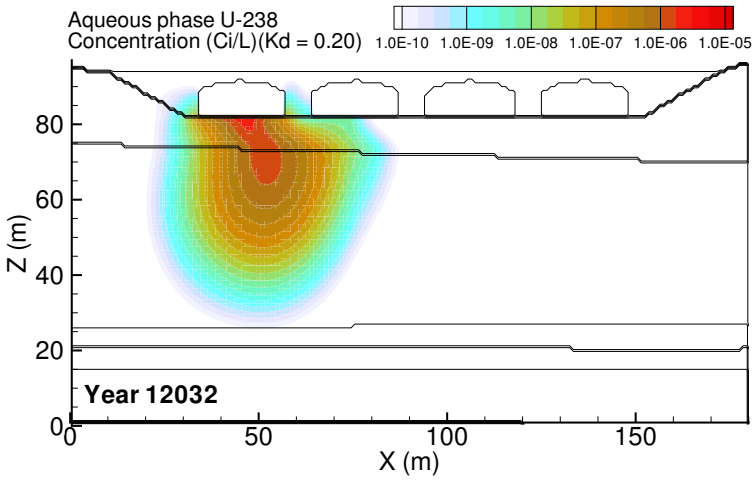

(b)

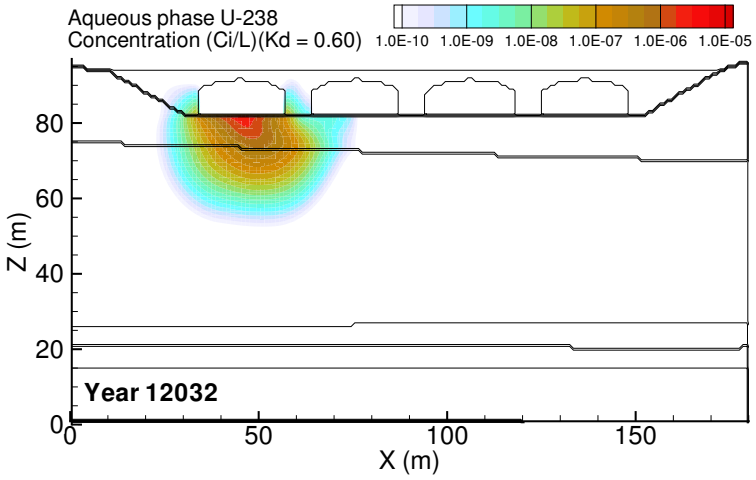

(c)

Figure C.37. Diffusion Release: High Aquifer Hydraulic Conductivity (4000 m/d) aqueous concentration distributions at year 12032 for (a) Tc-99, (b) U_0.20 and (c) U_0.60.

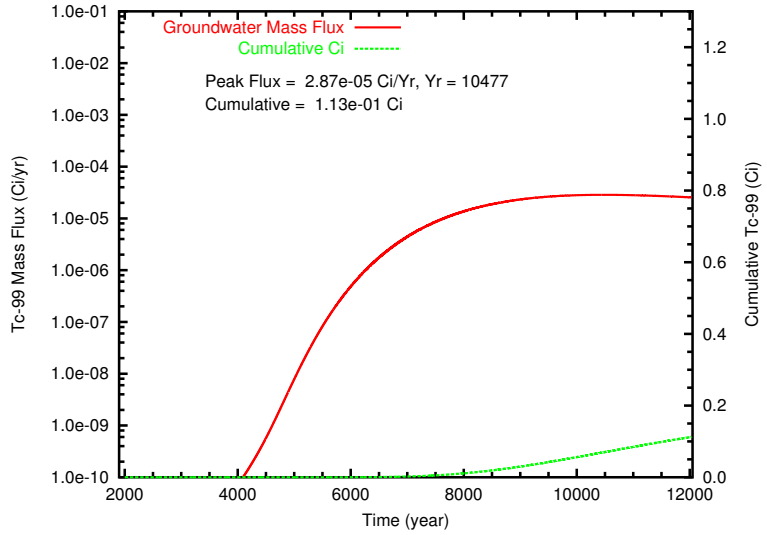

(a)

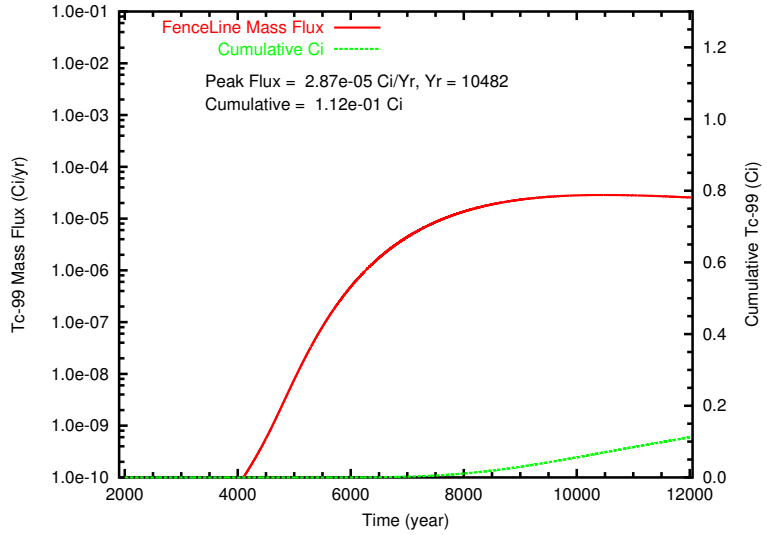

(b)

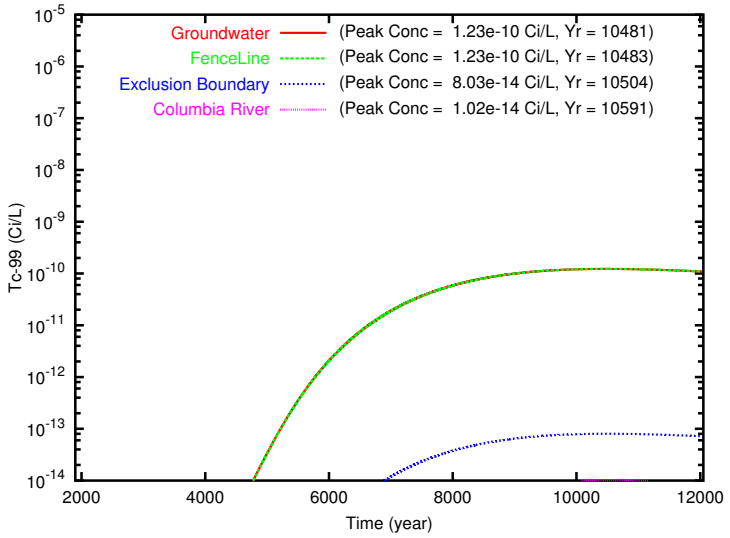

(c)

Figure C.38. Diffusion Release: High Aquifer Hydraulic Conductivity (4000 m/d) Tc-99 mass flux at (a) the groundwater table and (b) the fenceline; and (c) the Tc-99 concentration at groundwater, fenceline, and easterly downstream compliance points.

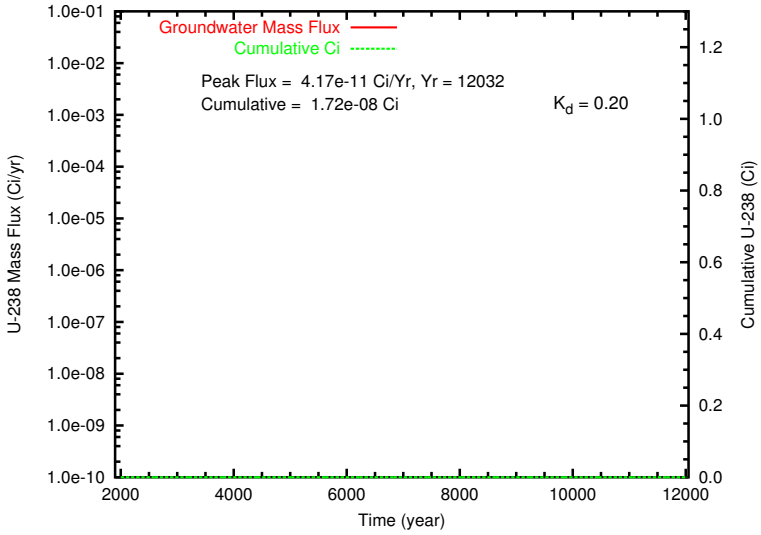

(a)

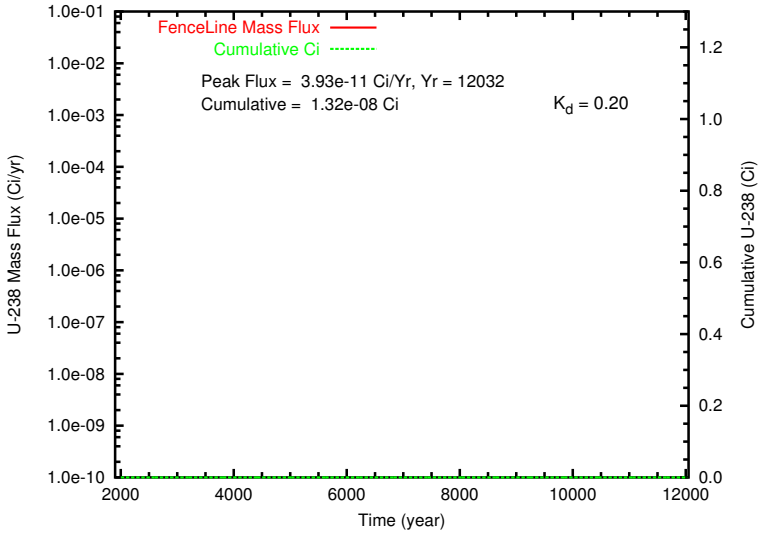

(b)

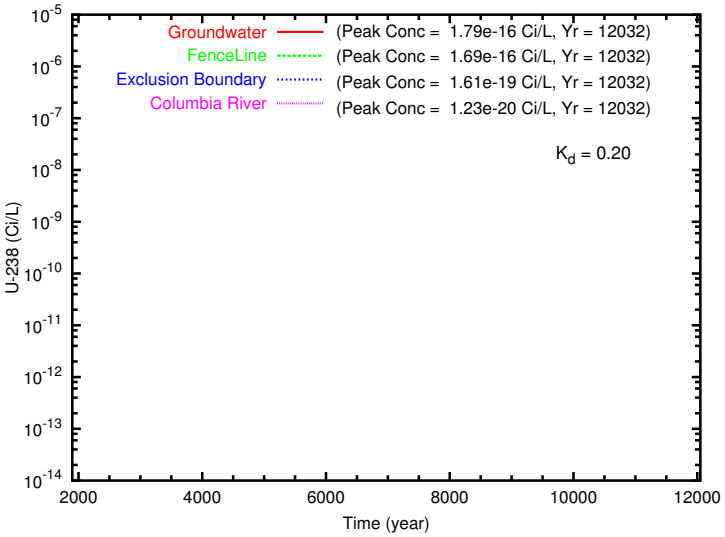

(c)

Figure C.39. Diffusion Release: High Aquifer Hydraulic Conductivity (4000 m/d) U_0.20 mass flux at (a) the groundwater table and (b) the fenceline; and (c) the Tc-99 concentration at groundwater, fenceline, and easterly downstream compliance points.

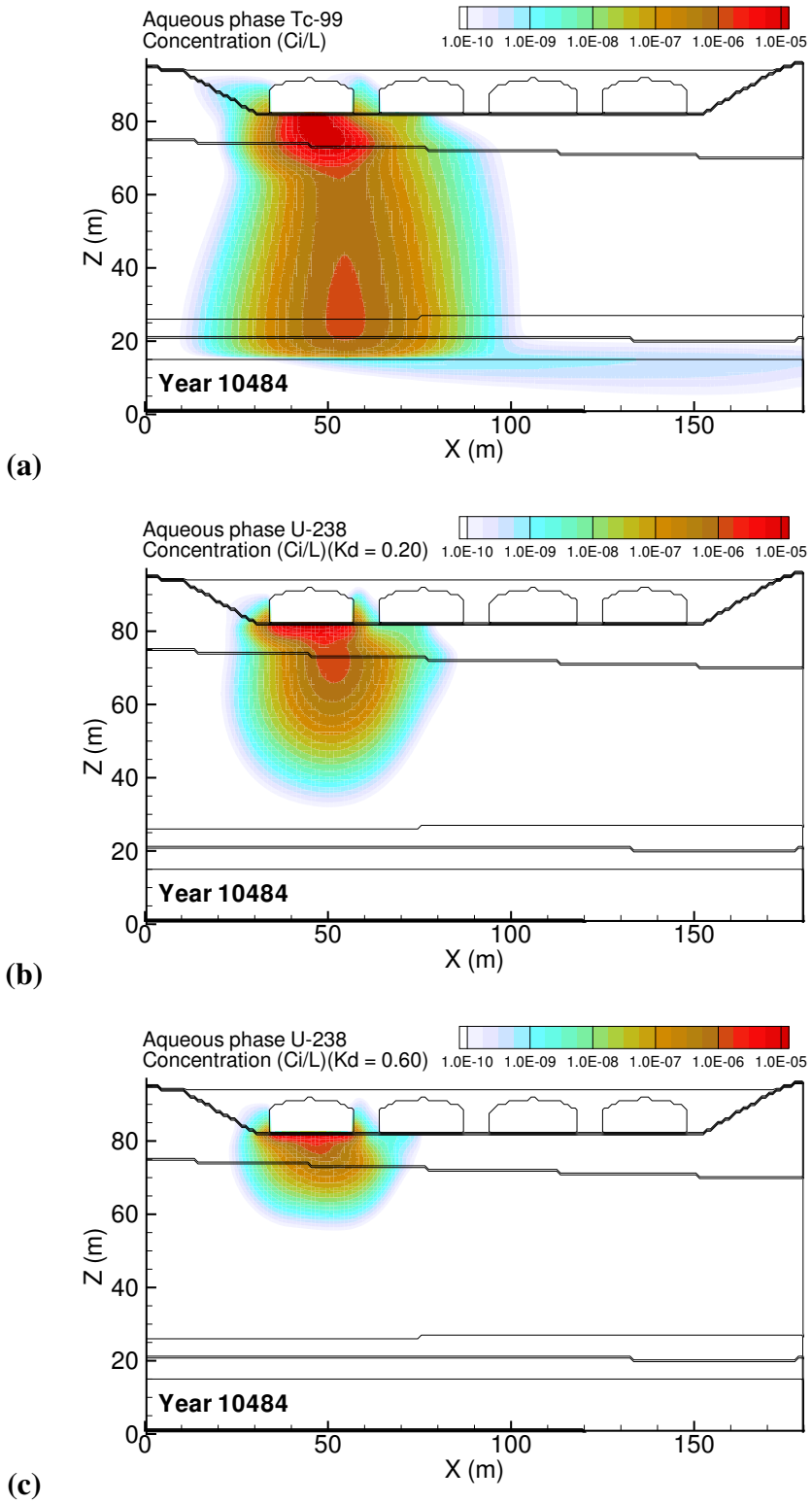

Figure C.40. Diffusion Release: Low Aquifer Hydraulic Conductivity (2000 m/d) aqueous concentration distributions at year 10484 for (a) Tc-99, (b) U_0.20 and (c) U_0.60. Year of Tc-99 peak concentration at fenceline was 10484.

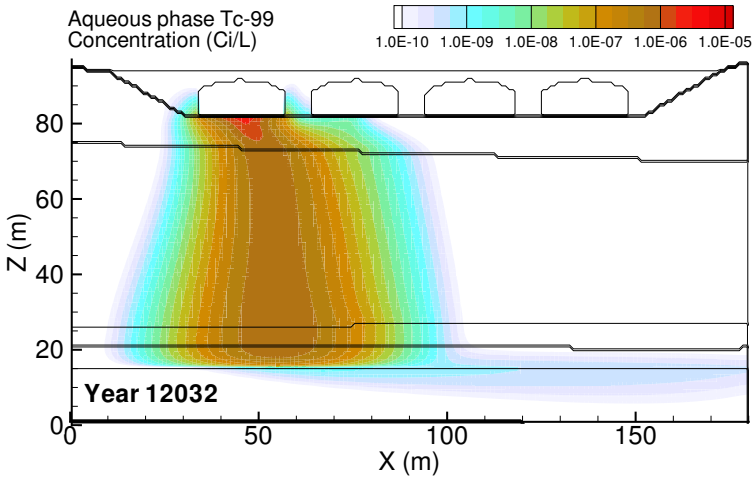

(a)

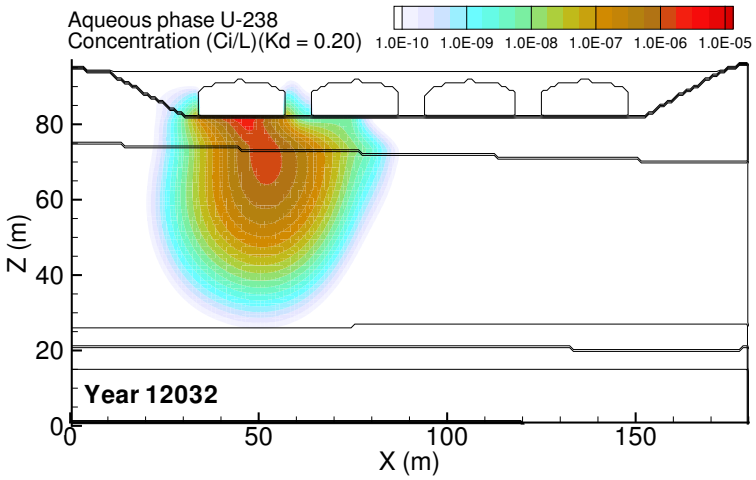

(b)

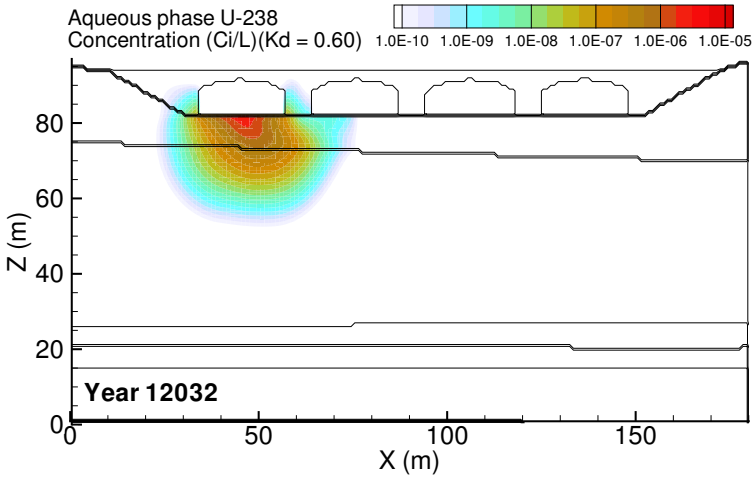

(c)

Figure C.41. Diffusion Release: Low Aquifer Hydraulic Conductivity (2000 m/d) aqueous concentration distributions at year 12032 for (a) Tc-99, (b) U_0.20 and (c) U_0.60.

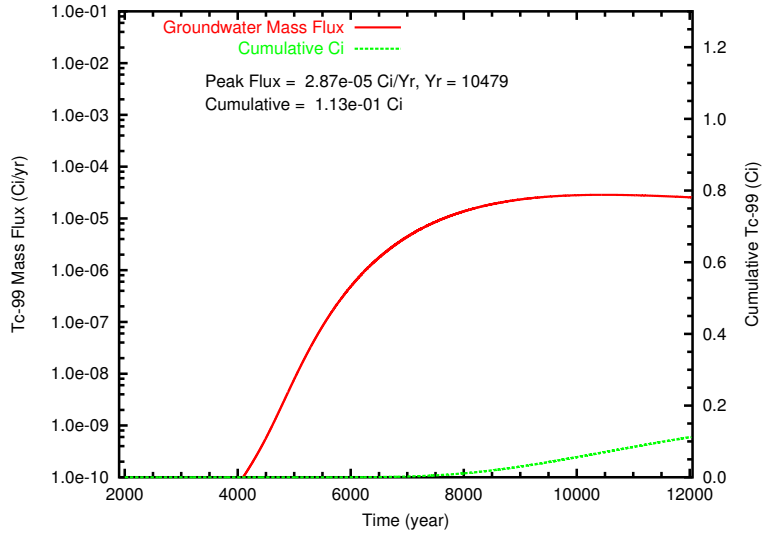

(a)

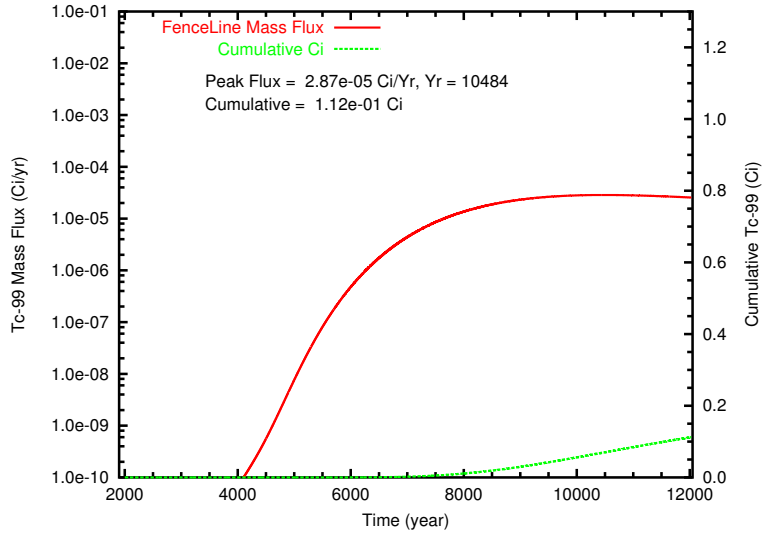

(b)

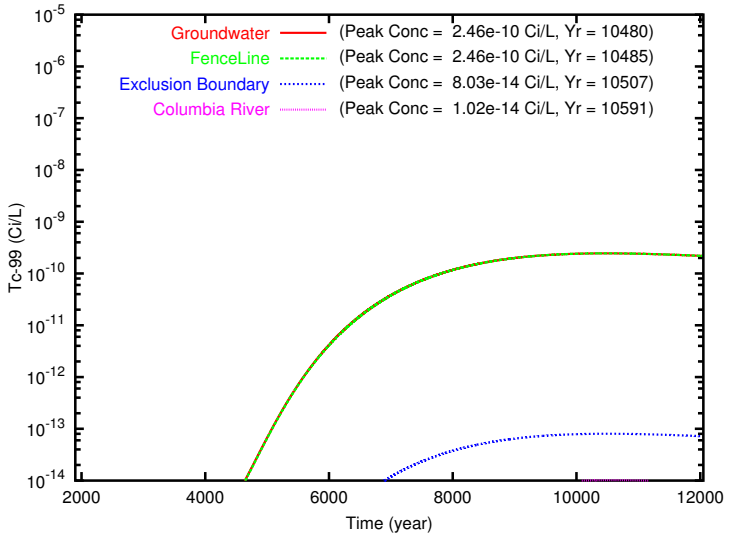

(c)

Figure C.42. Diffusion Release: Low Aquifer Hydraulic Conductivity (2000 m/d) Tc-99 mass flux at (a) the groundwater table and (b) the fenceline; and (c) the Tc-99 concentration at groundwater, fenceline, and easterly downstream compliance points.

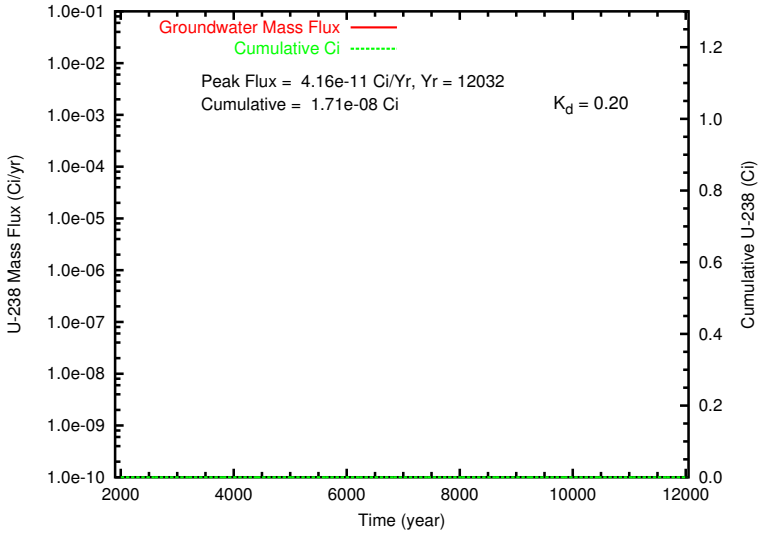

(a)

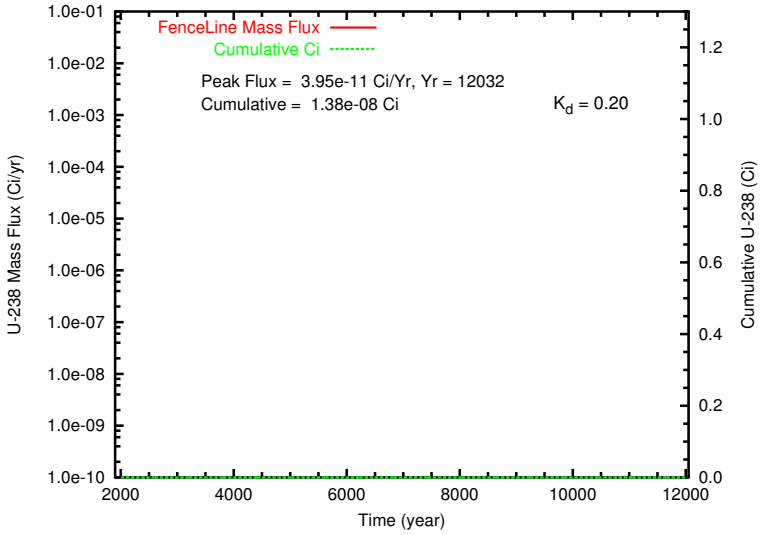

(b)

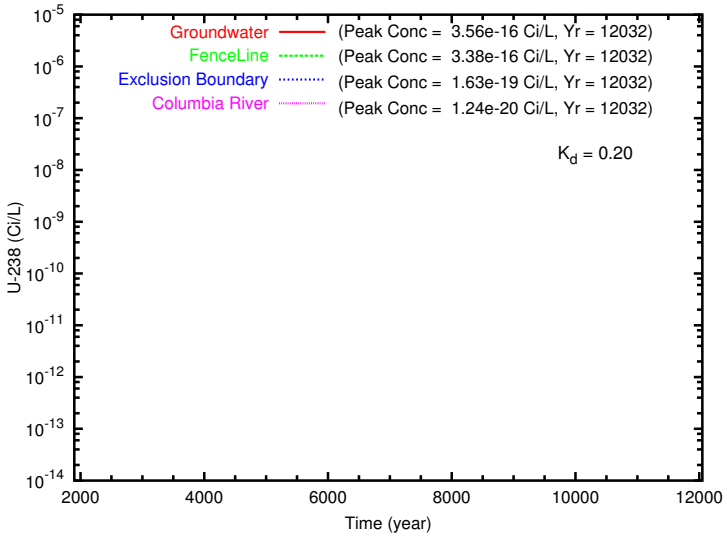

(c)

Figure C.43. Diffusion Release: Low Aquifer Hydraulic Conductivity (2000 m/d) U_0.20 mass flux at (a) the groundwater table and (b) the fenceline; and (c) the Tc-99 concentration at groundwater, fenceline, and easterly downstream compliance points.

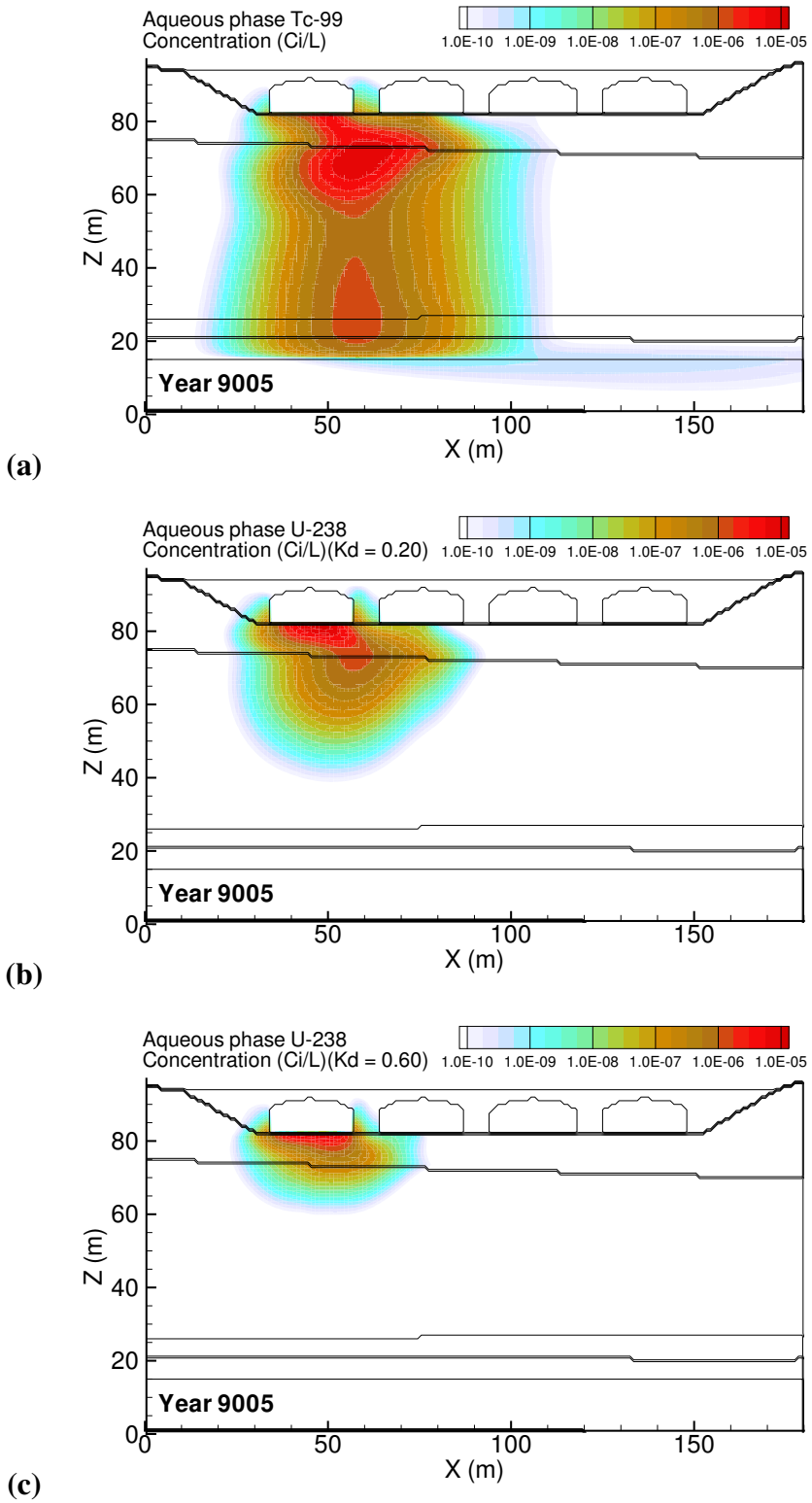

Figure C.44. Diffusion Release: High Vadose Zone Hydraulic Conductivity ($K_{sat} \times 10$) aqueous concentration distributions at year 9005 for (a) Tc-99, (b) U_0.20 and (c) U_0.60. Year of Tc-99 peak concentration at fenceline was 9005.

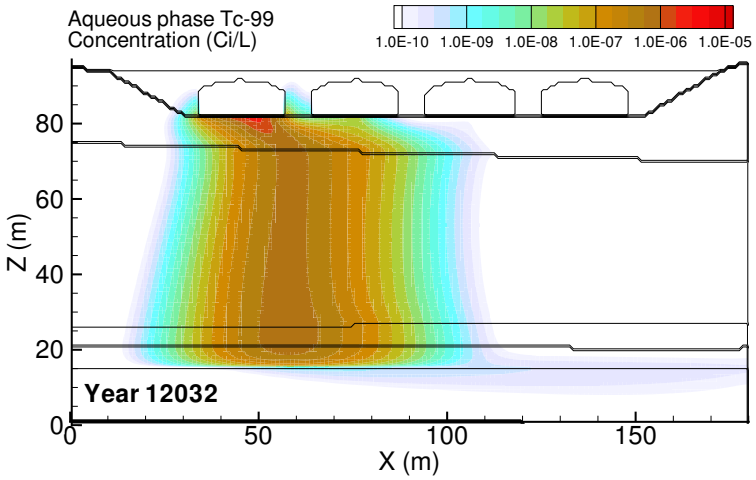

(a)

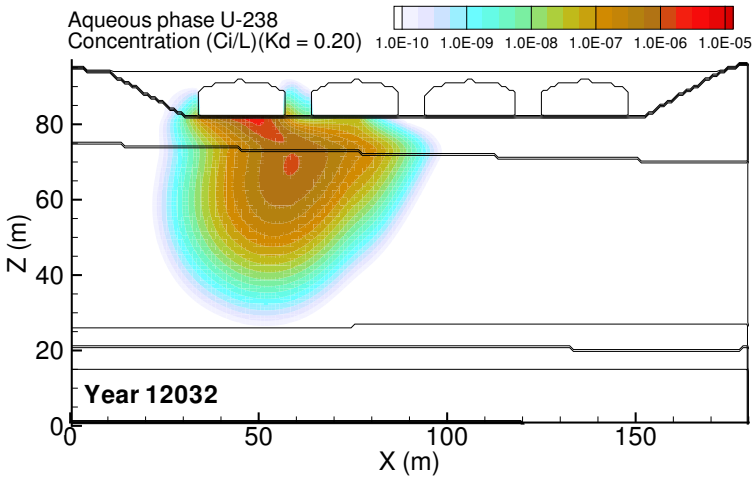

(b)

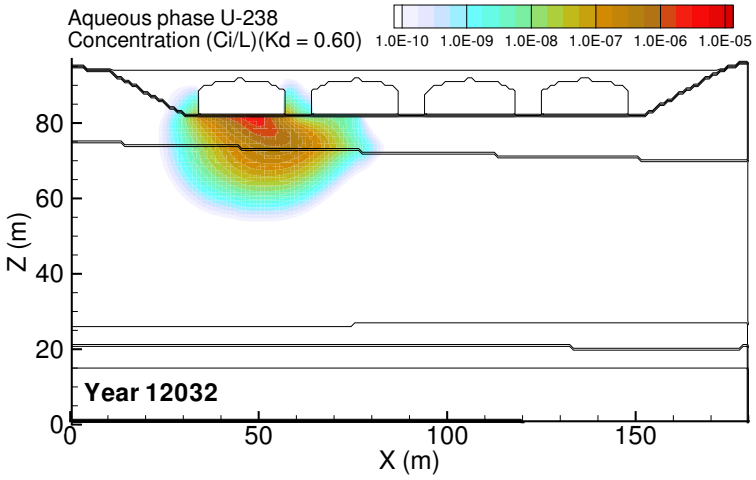

(c)

Figure C.45. Diffusion Release: High Vadose Zone Hydraulic Conductivity ($K_{sat} \times 10$) aqueous concentration distributions at year 12032 for (a) Tc-99, (b) U_0.20 and (c) U_0.60.

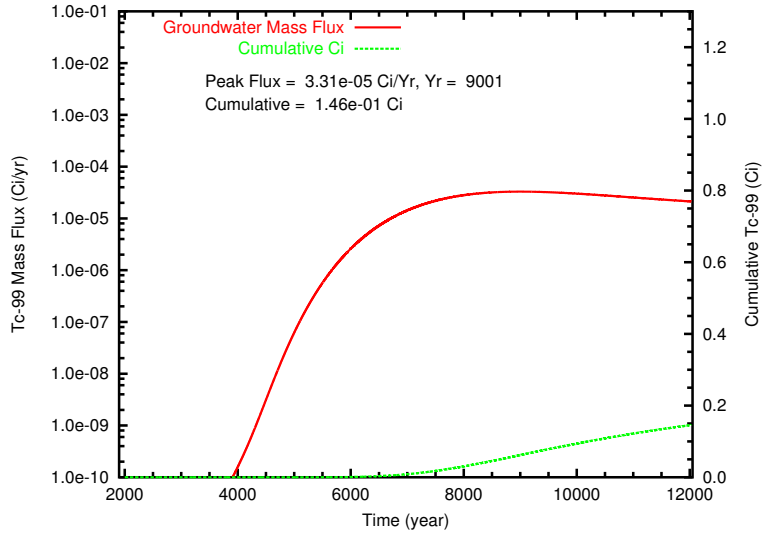

(a)

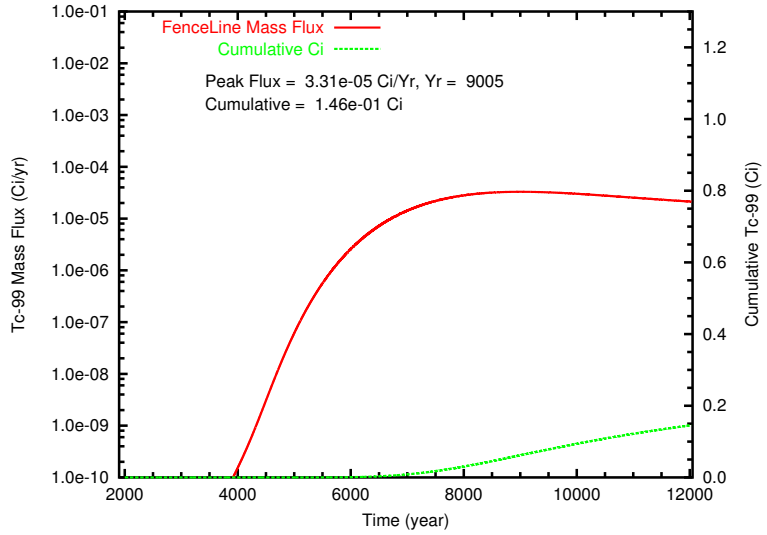

(b)

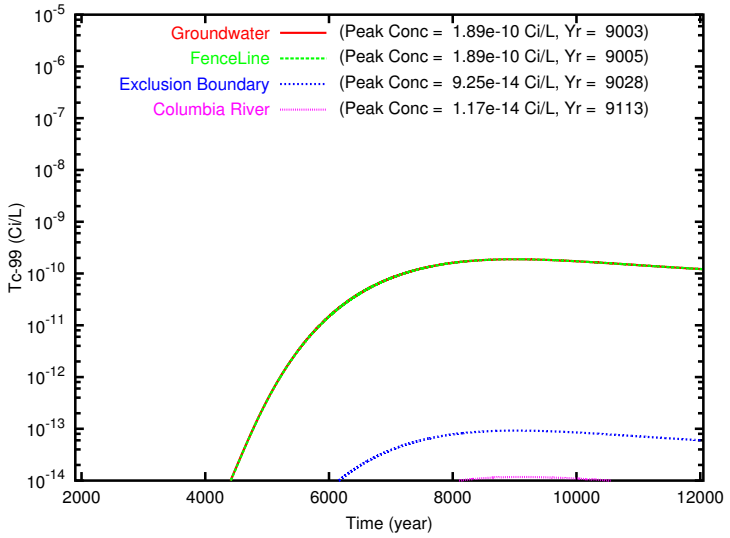

(c)

Figure C.46. Diffusion Release: High Vadose Zone Hydraulic Conductivity ($K_{sat} \times 10$) Tc-99 mass flux at (a) the groundwater table and (b) the fenceline; and (c) the Tc-99 concentration at groundwater, fenceline, and easterly downstream compliance points.

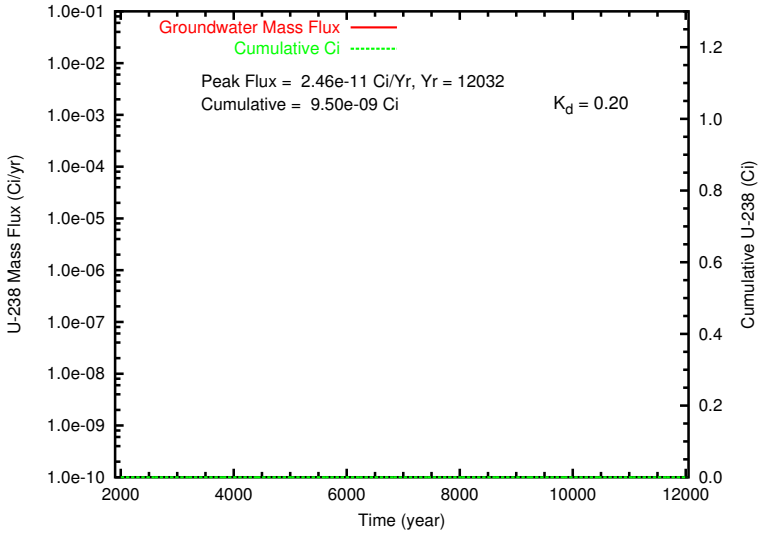

(a)

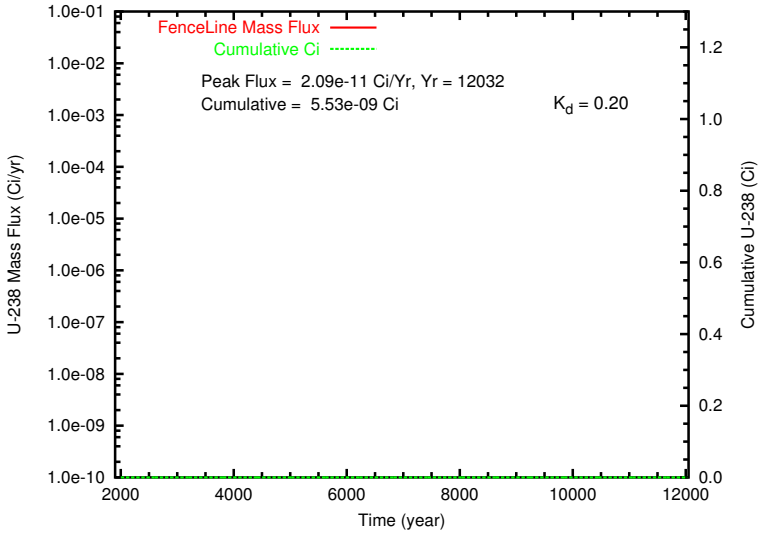

(b)

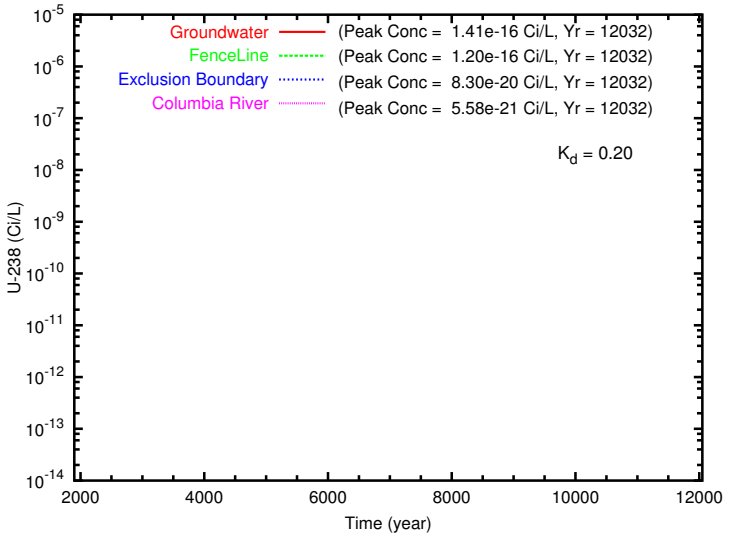

(c)

Figure C.47. Diffusion Release: High Vadose Zone Hydraulic Conductivity ($K_{sat} \times 10$) U_0.20 mass flux at (a) the groundwater table and (b) the fenceline; and (c) the Tc-99 concentration at groundwater, fenceline, and easterly downstream compliance points.

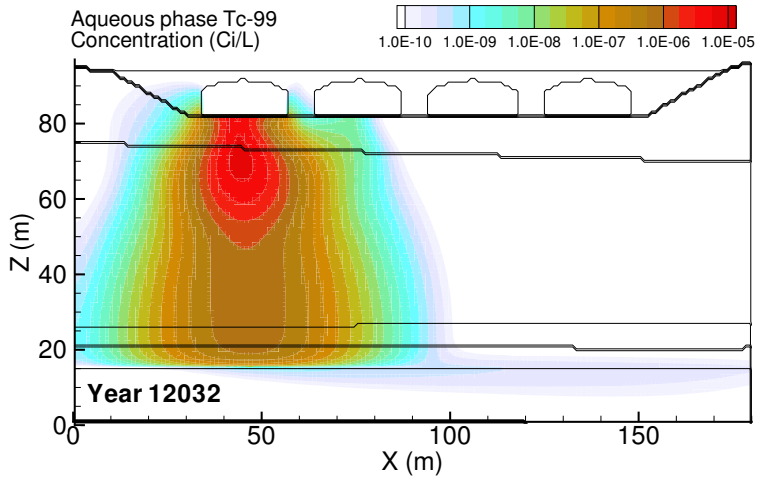

(a)

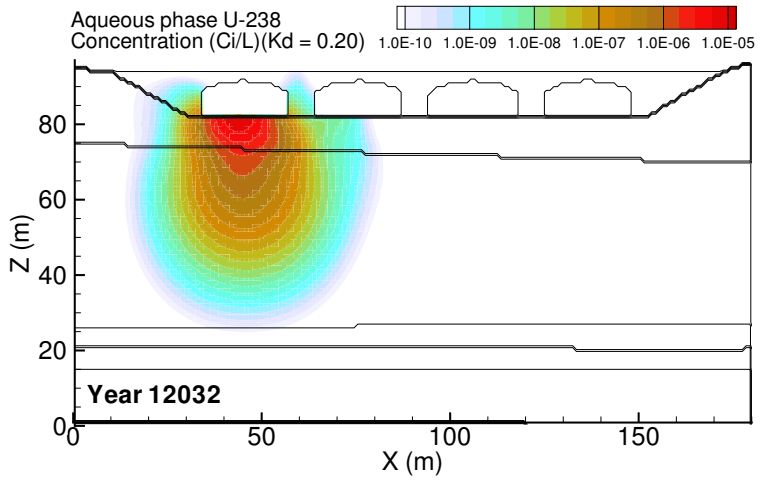

(b)

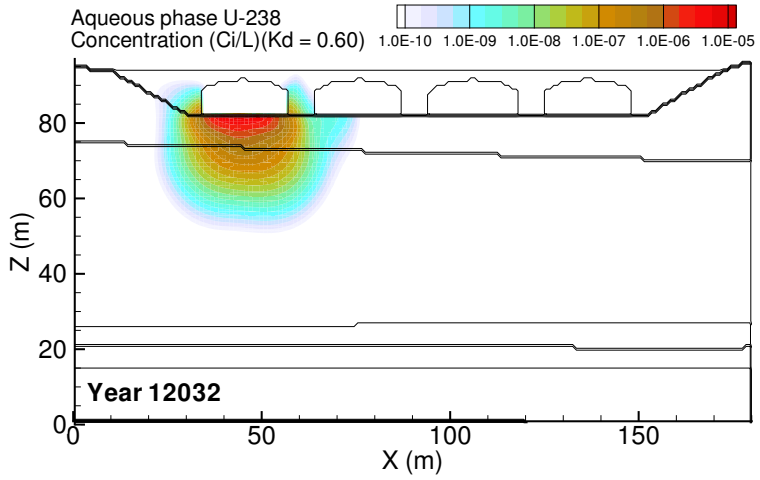

(c)

Figure C.48. Diffusion Release: Low Vadose Zone Hydraulic Conductivity ($K_{sat} \times 0.1$) aqueous concentration distributions at year 12032 for (a) Tc-99, (b) U_0.20 and (c) U_0.60.

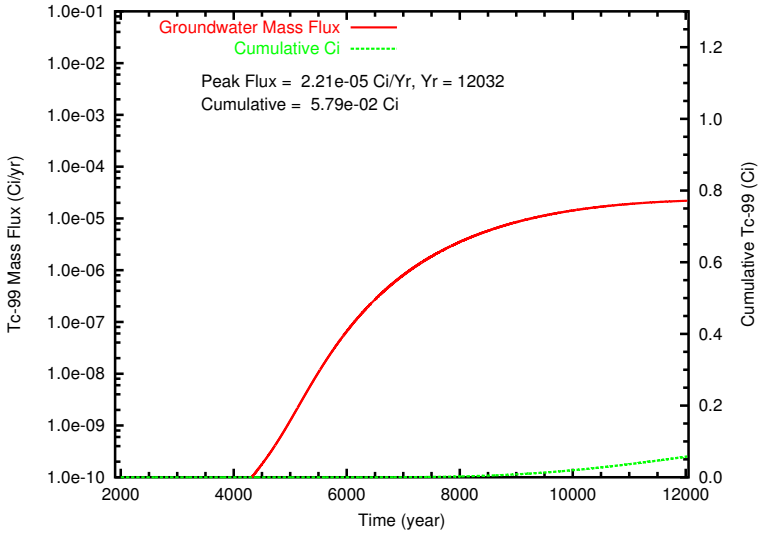

(a)

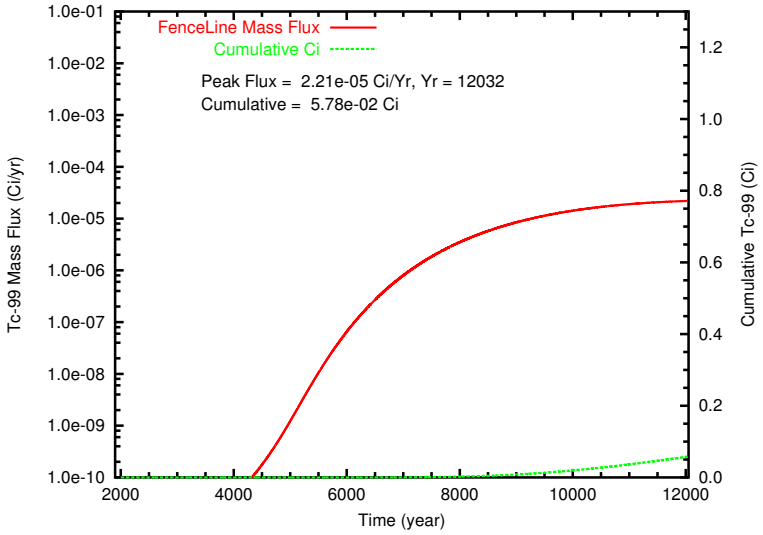

(b)

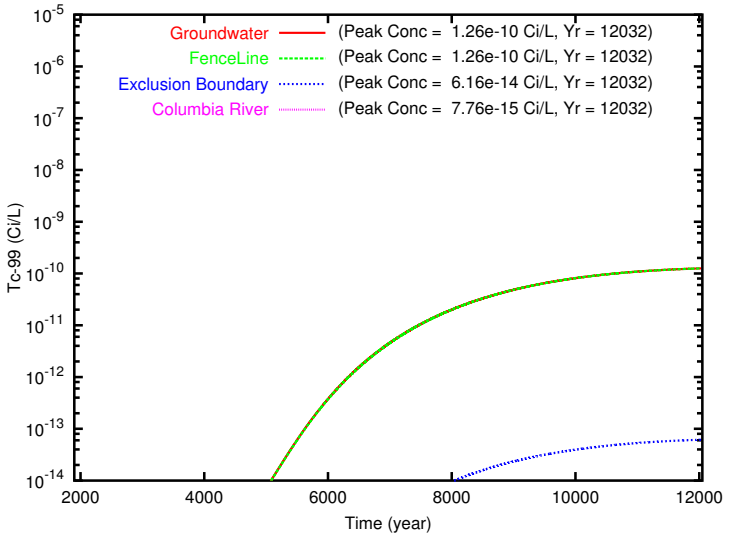

(c)

Figure C.49. Diffusion Release: Low Vadose Zone Hydraulic Conductivity ($K_{sat} \times 0.1$) Tc-99 mass flux at (a) the groundwater table and (b) the fenceline; and (c) the Tc-99 concentration at groundwater, fenceline, and easterly downstream compliance points.

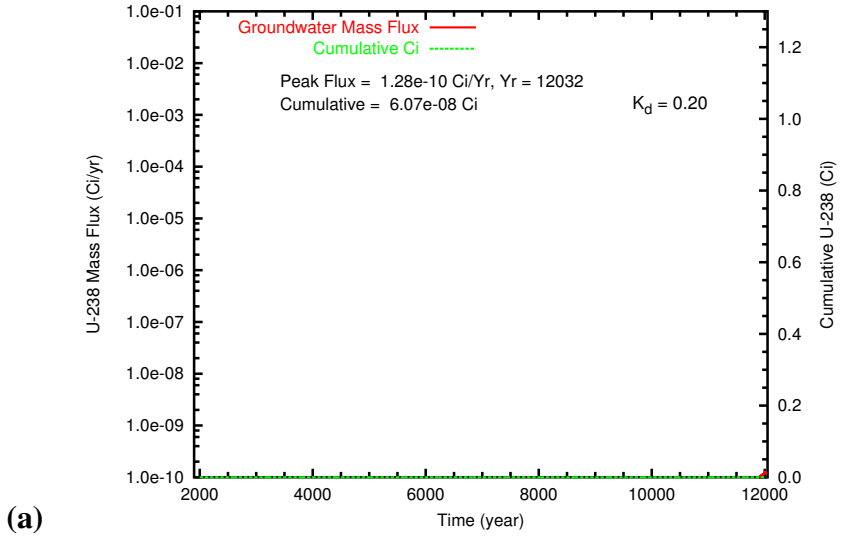

(a)

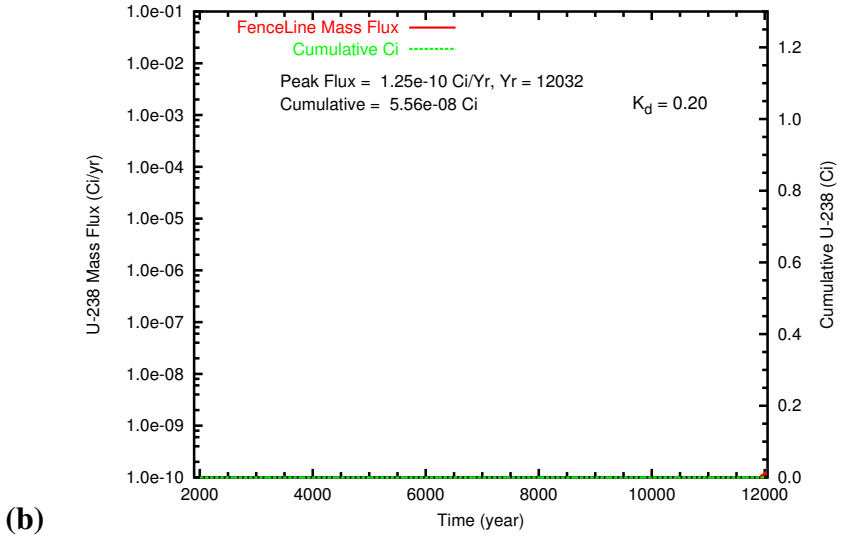

(b)

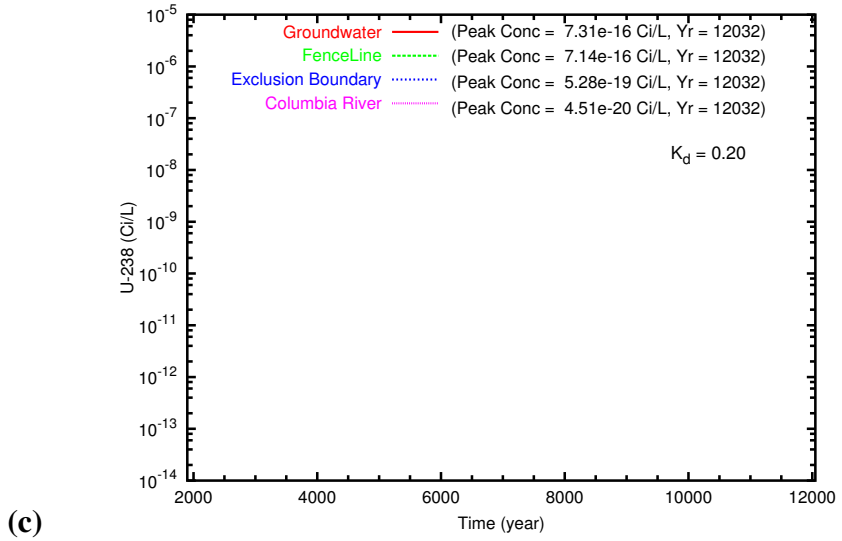

(c)

Figure C.50. Diffusion Release: Low Vadose Zone Hydraulic Conductivity ($K_{sat} \times 0.1$) U_0.20 mass flux at (a) the groundwater table and (b) the fenceline; and (c) the Tc-99 concentration at groundwater, fenceline, and easterly downstream compliance points.

Appendix D

C Farm Retrieval Leak

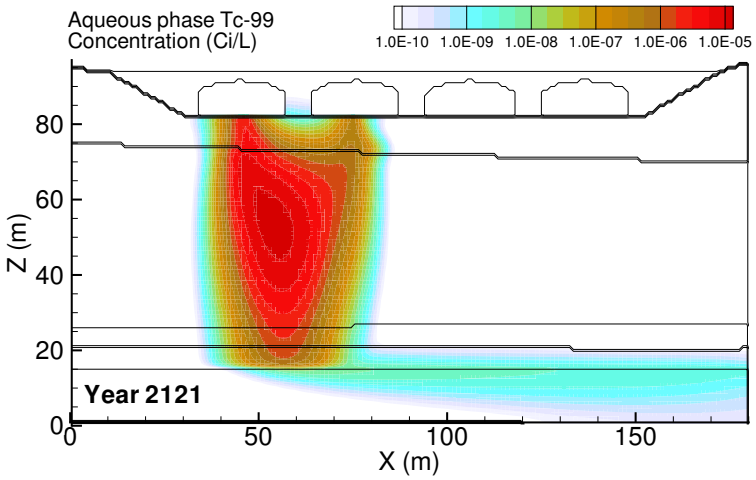

(a)

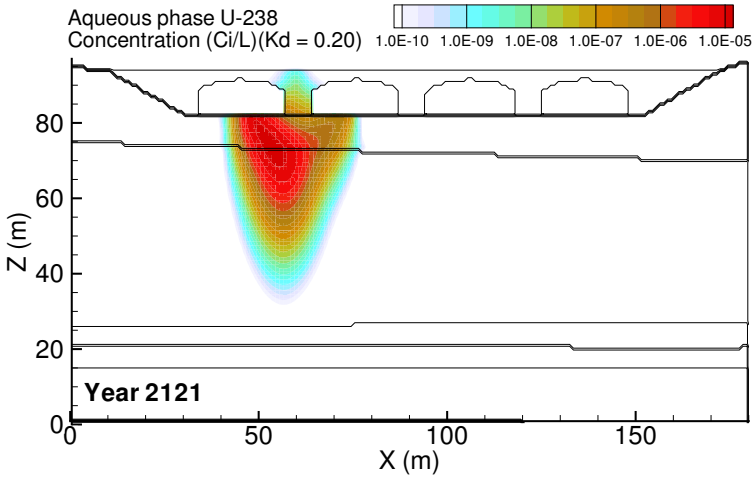

(b)

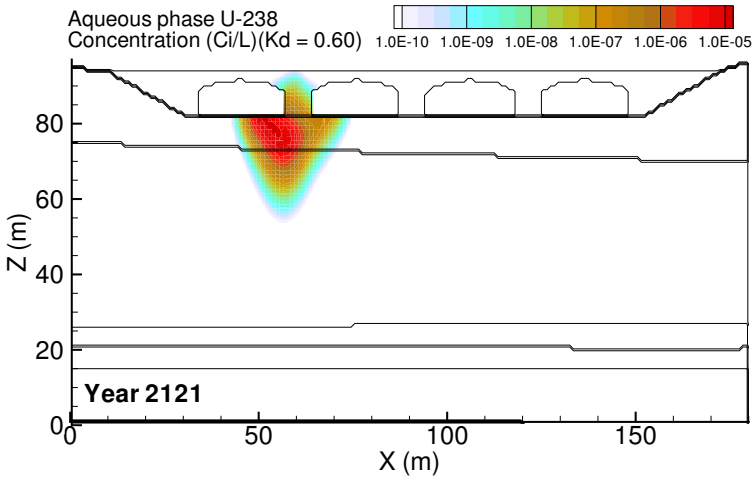

(c)

Figure D.1. Retrieval Leak: Base Case aqueous concentration distributions at year 2121 for (a) Tc-99, (b) U_0.20 and (c) U_0.60. Year of Tc-99 peak concentration at fenceline was 2121.

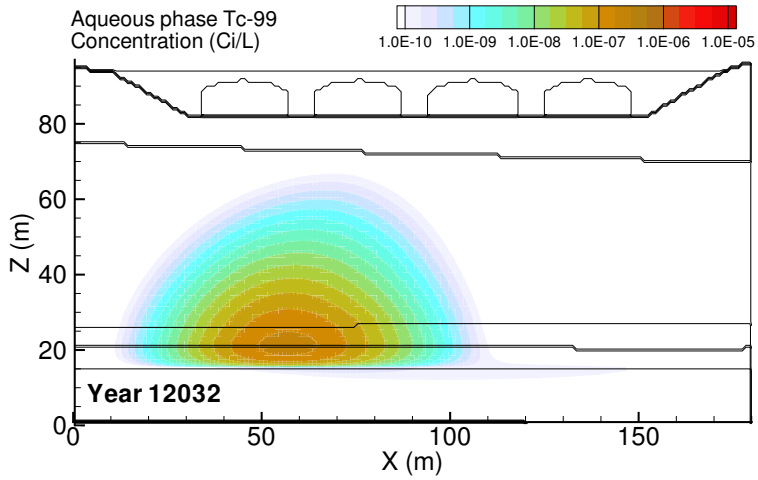

(a)

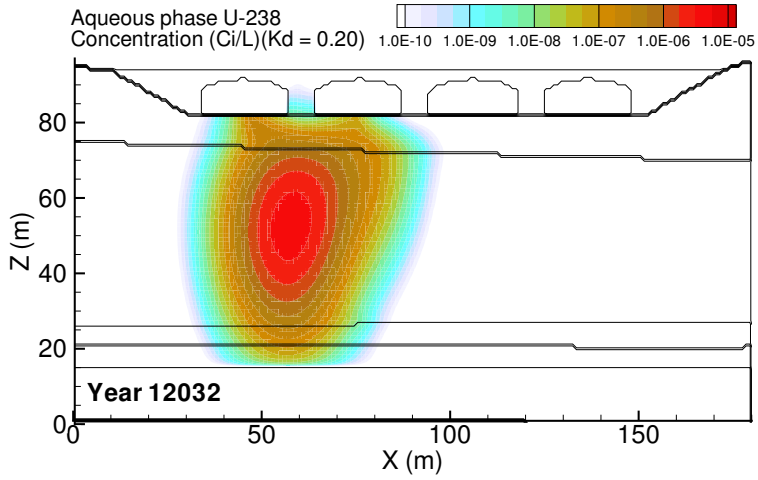

(b)

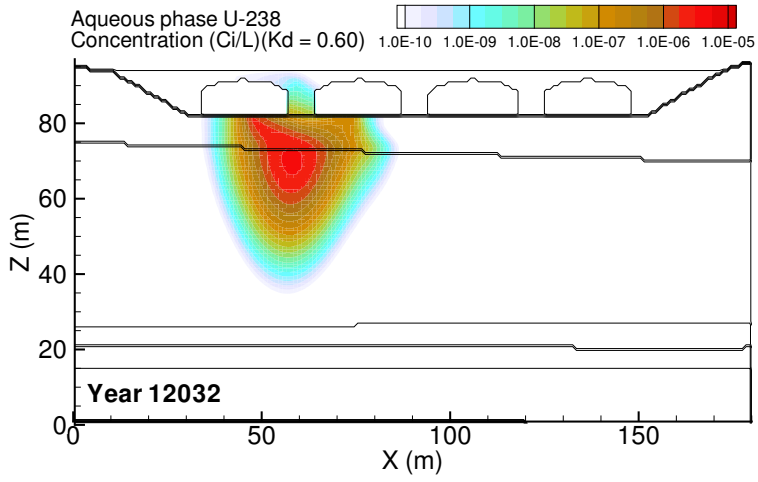

(c)

Figure D.2. Retrieval Leak: Base Case aqueous concentration distributions at year 12032 for (a) Tc-99, (b) U_0.20 and (c) U_0.60.

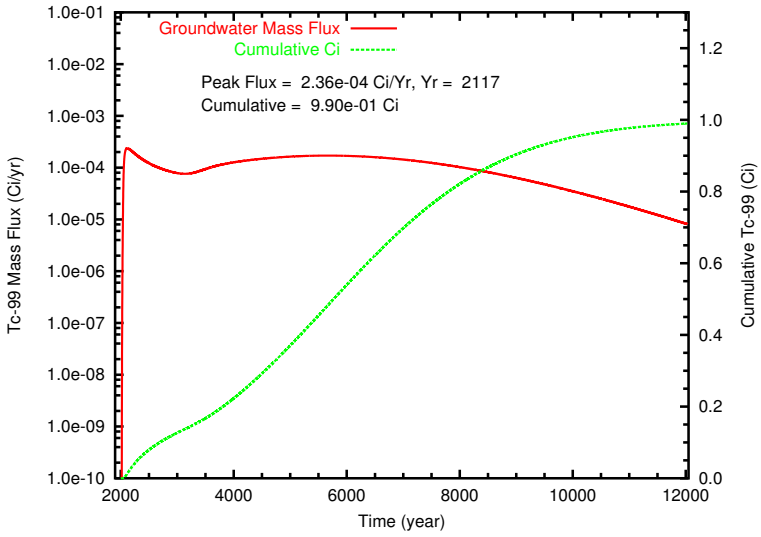

(a)

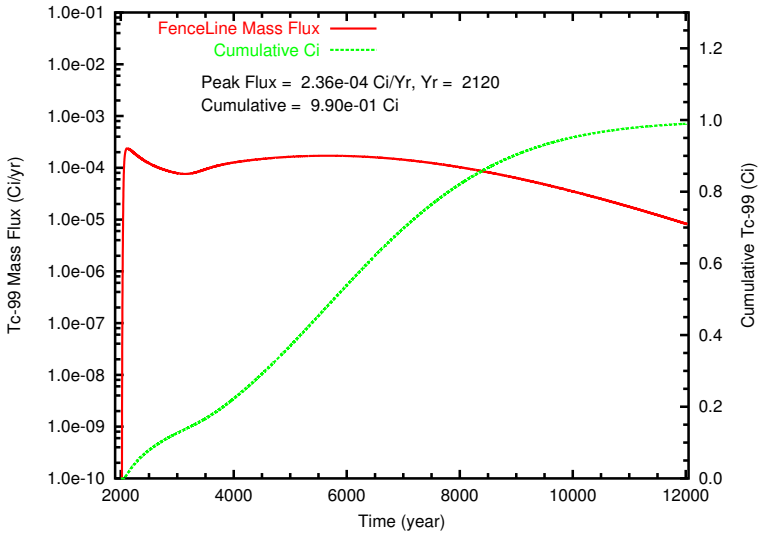

(b)

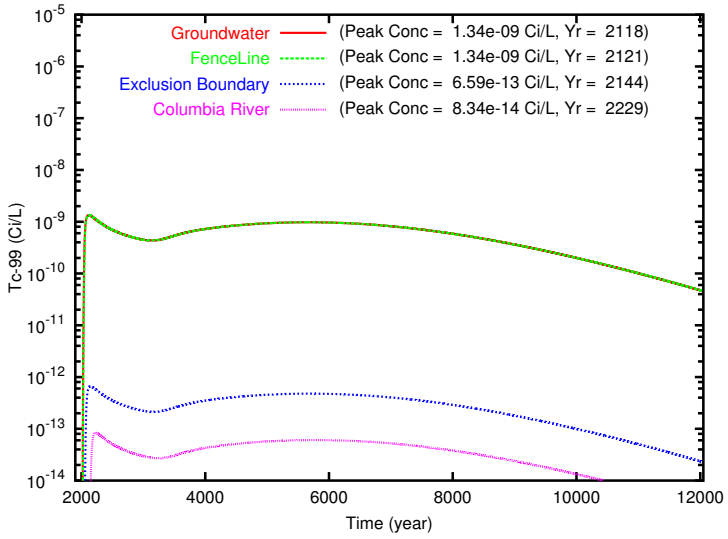

(c)

Figure D.3. Retrieval Leak: Base Case Tc-99 mass flux at (a) the groundwater table and (b) the fenceline; and (c) the Tc-99 concentration at groundwater, fenceline, and easterly downstream compliance points.

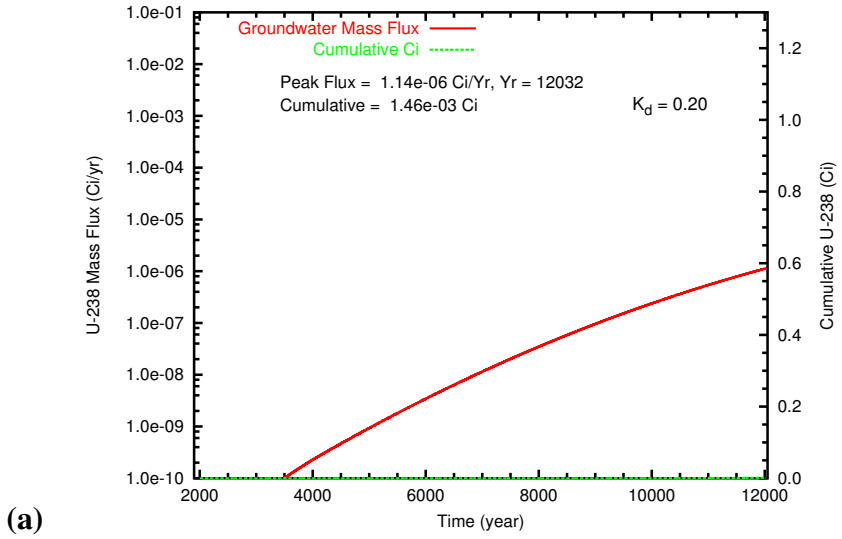

(a)

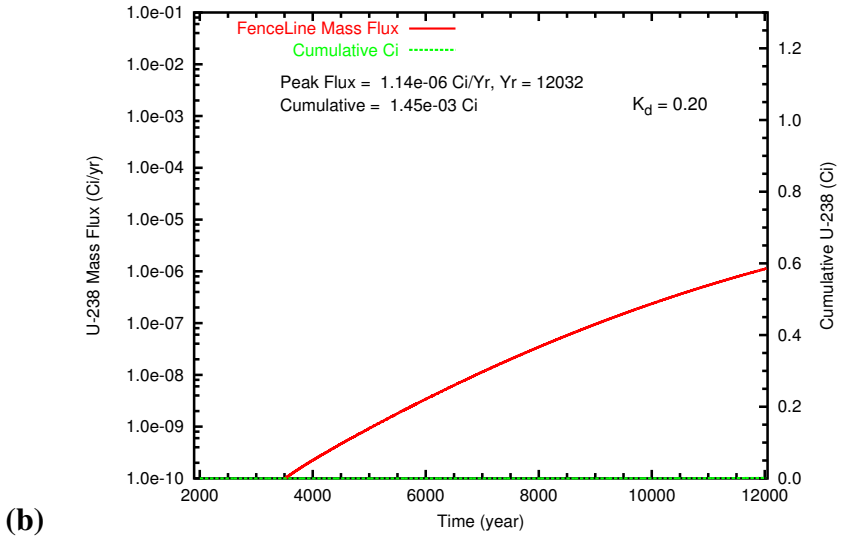

(b)

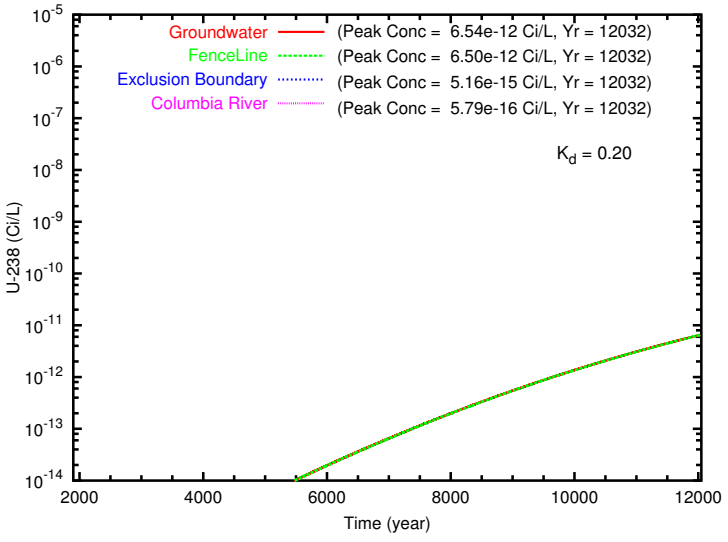

(c)

Figure D.4. Retrieval Leak: Base Case U_0.20 mass flux at (a) the groundwater table and (b) the fenceline; and (c) the Tc-99 concentration at groundwater, fenceline, and easterly downstream compliance points.

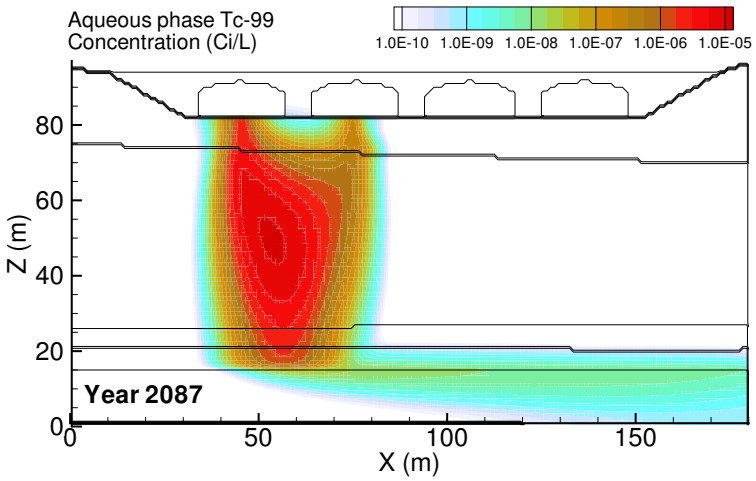

(a)

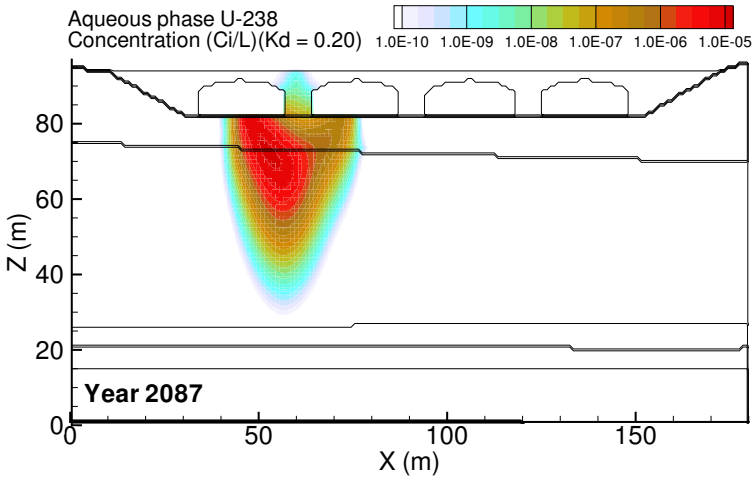

(b)

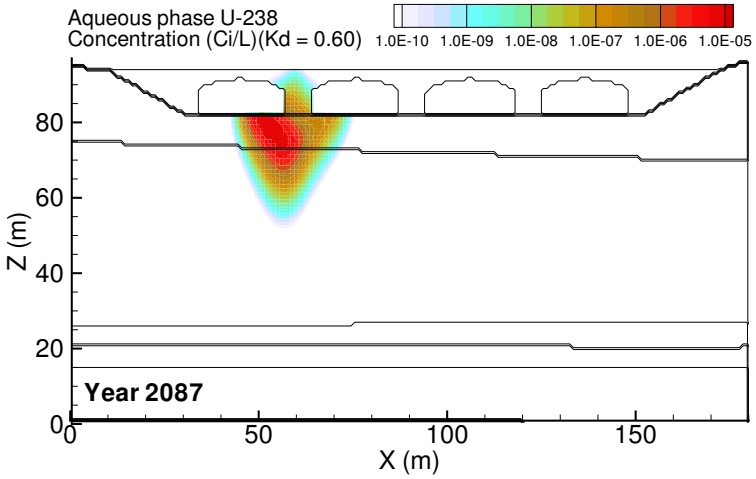

(c)

Figure D.5. Retrieval Leak: High Preclosure Recharge Rate (140 mm/yr) aqueous concentration distributions at year 2087 for (a) Tc-99, (b) U_0.20 and (c) U_0.60. Year of Tc-99 peak concentration at fenceline was 2087.

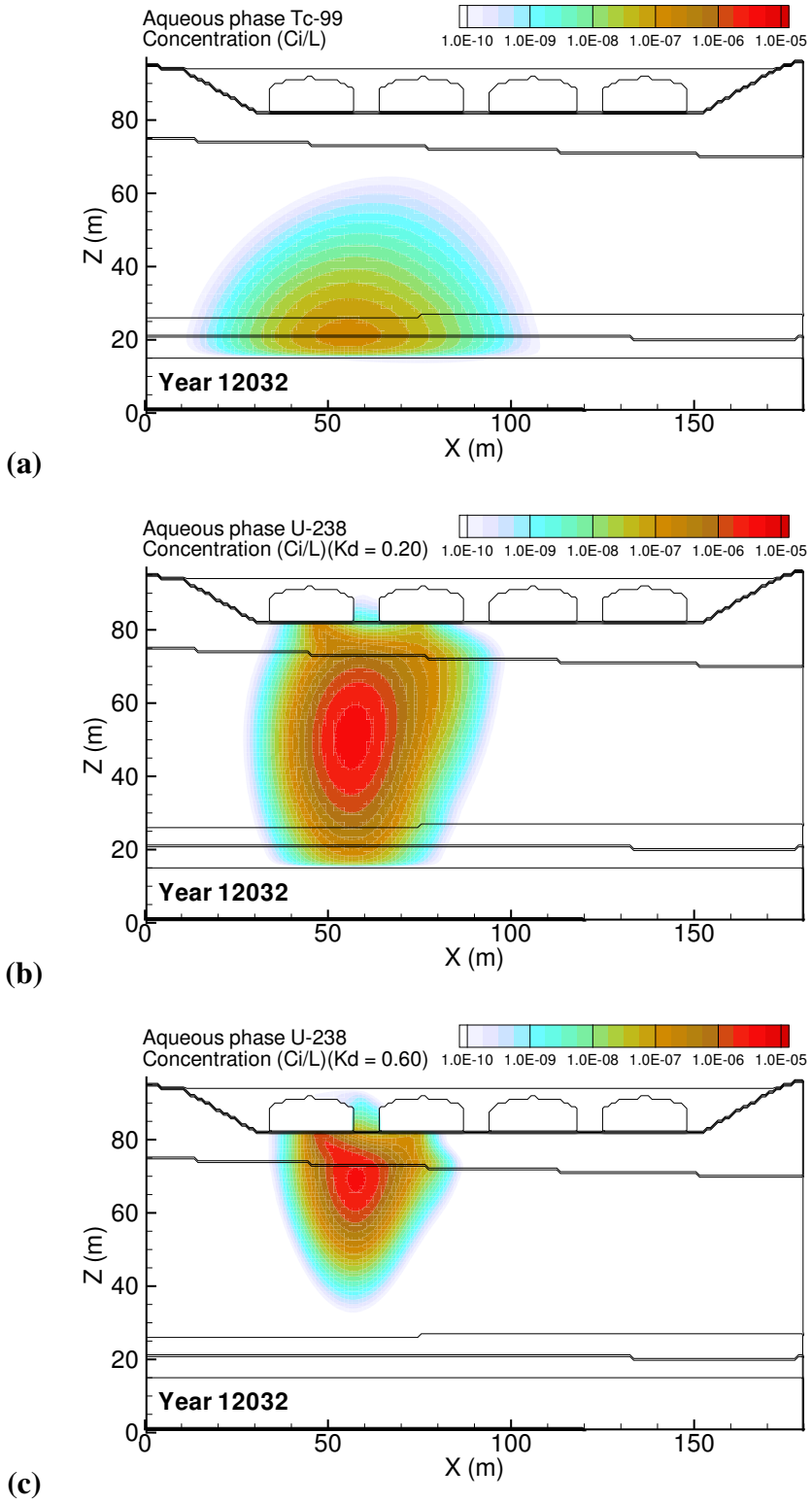

Figure D.6. Retrieval Leak: High Preclosure Recharge Rate (140 mm/yr) aqueous concentration distributions at year 12032 for (a) Tc-99, (b) U_0.20 and (c) U_0.60.

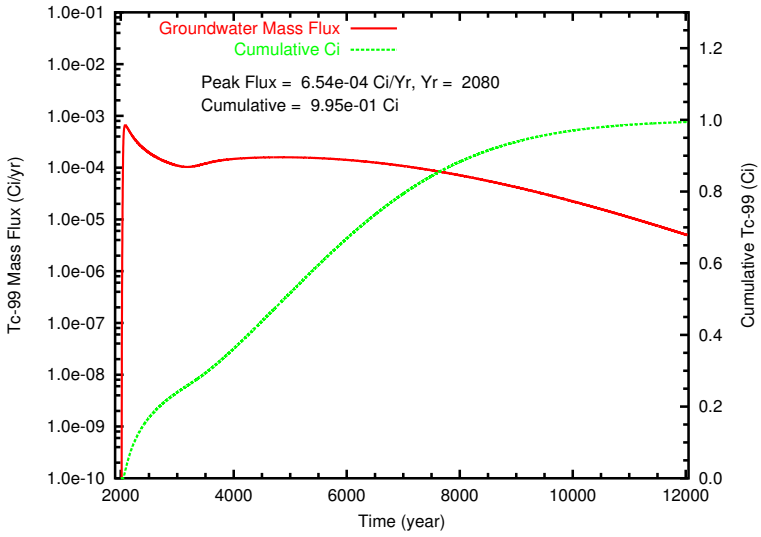

(a)

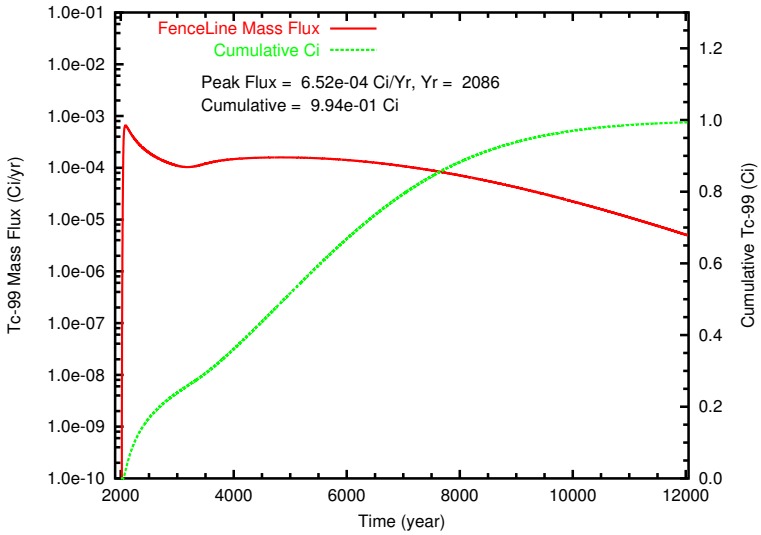

(b)

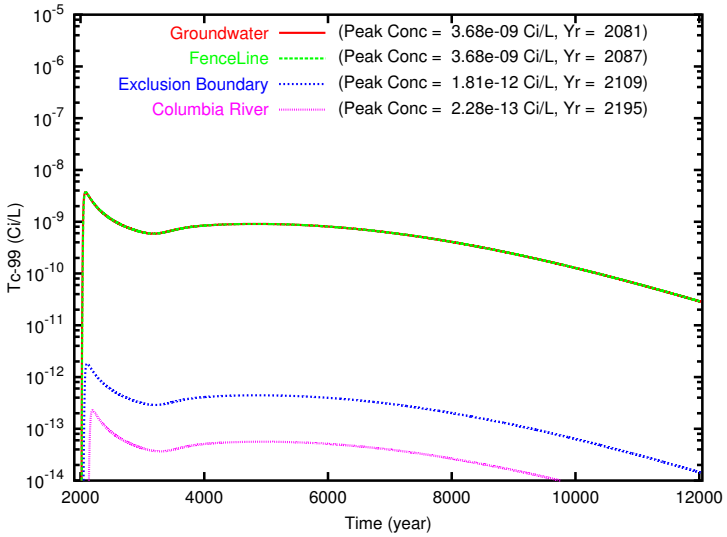

(c)

Figure D.7. Retrieval Leak: High Preclosure Recharge Rate (140 mm/yr) Tc-99 mass flux at (a) the groundwater table and (b) the fenceline; and (c) the Tc-99 concentration at groundwater, fenceline, and easterly downstream compliance points.

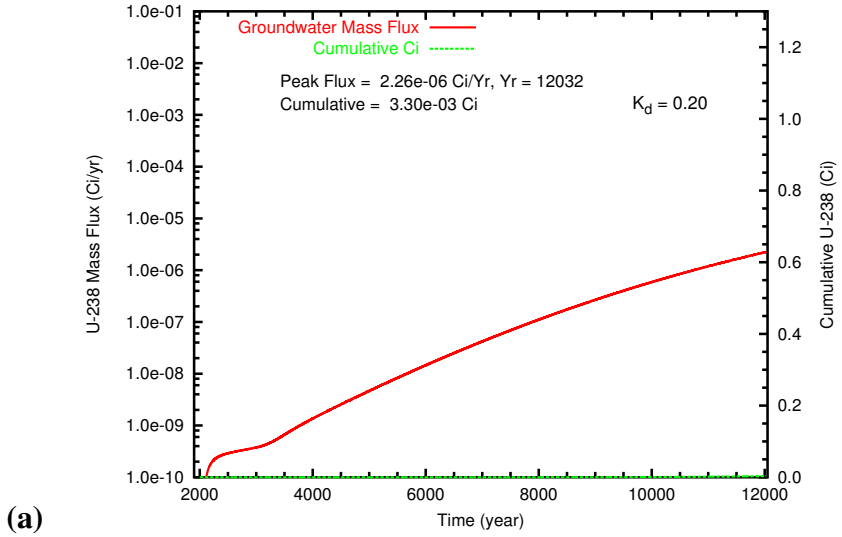

(a)

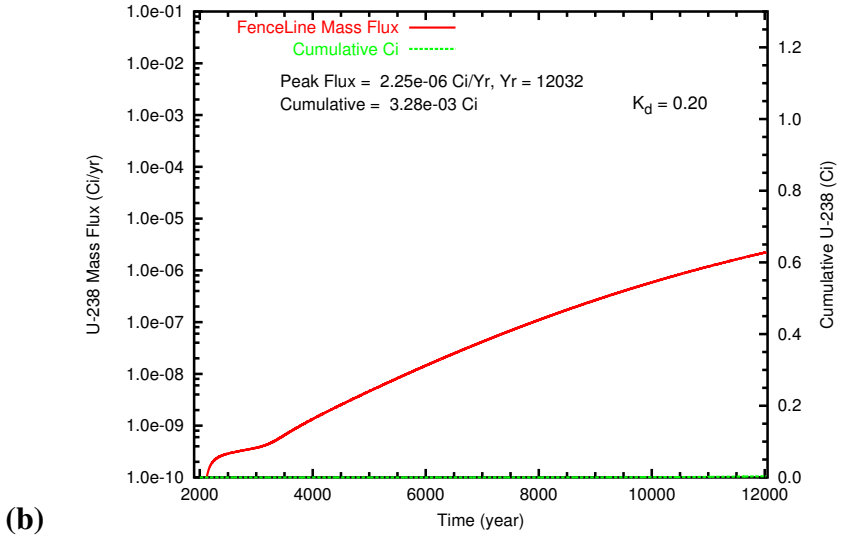

(b)

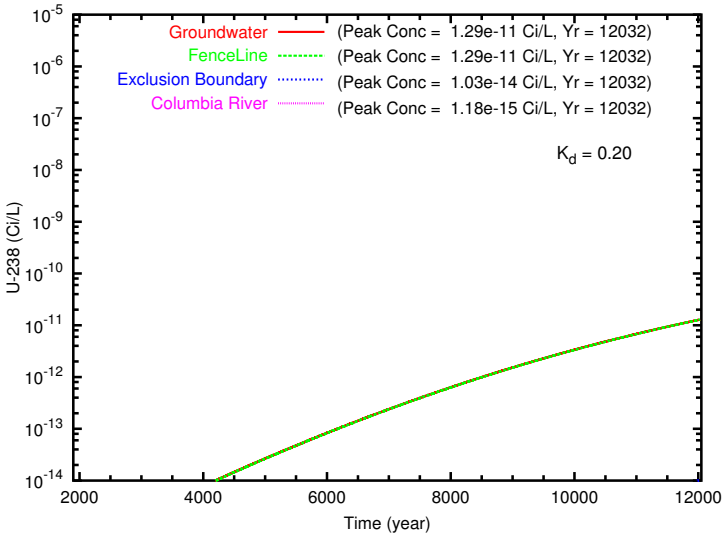

(c)

Figure D.8. Retrieval Leak: High Preclosure Recharge Rate (140 mm/yr) U_0.20 mass flux at (a) the groundwater table and (b) the fenceline; and (c) the Tc-99 concentration at groundwater, fenceline, and easterly downstream compliance points.

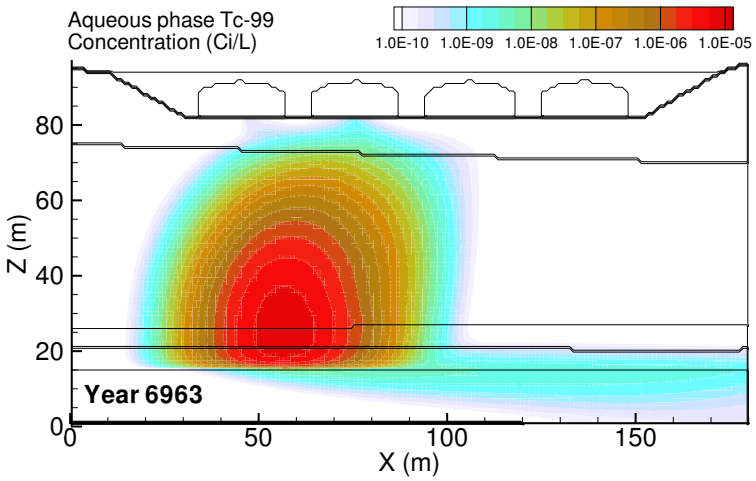

(a)

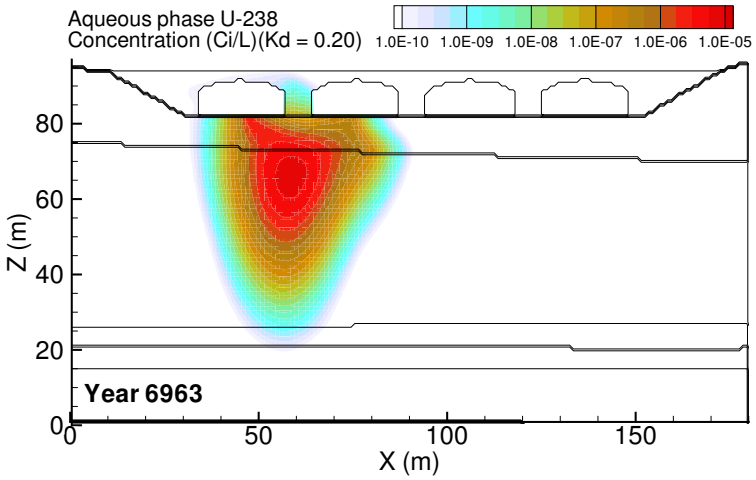

(b)

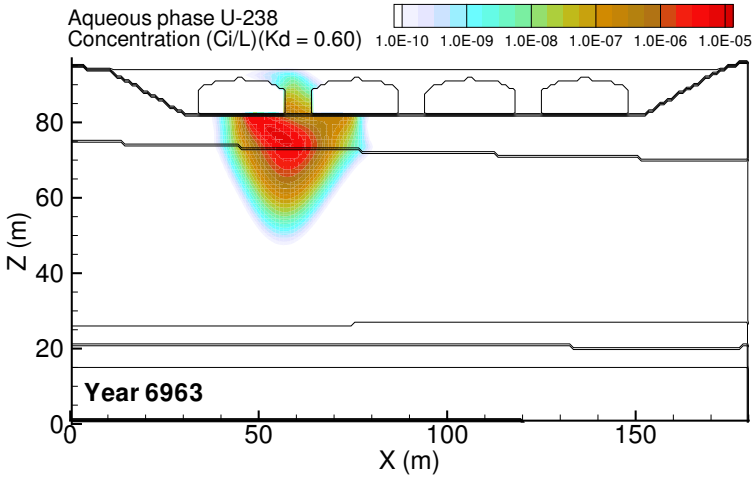

(c)

Figure D.9. Retrieval Leak: Low Preclosure Recharge Rate (40 mm/yr) aqueous concentration distributions at year 6963 for (a) Tc-99, (b) U_0.20 and (c) U_0.60. Year of Tc-99 peak concentration at fenceline was 6963.

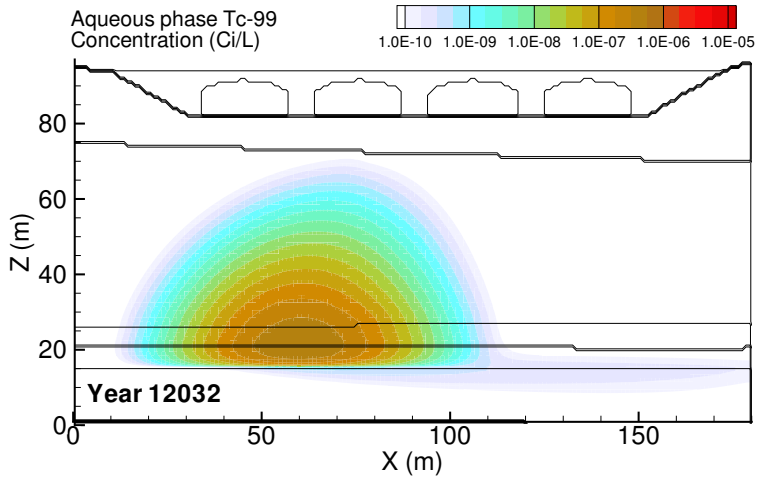

(a)

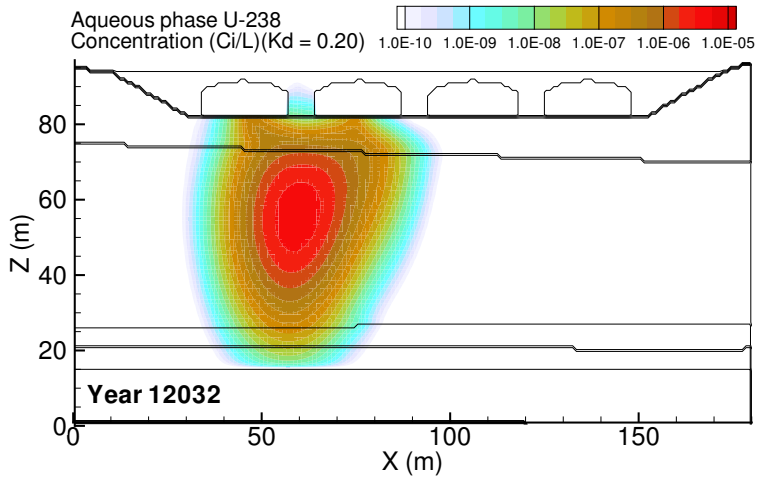

(b)

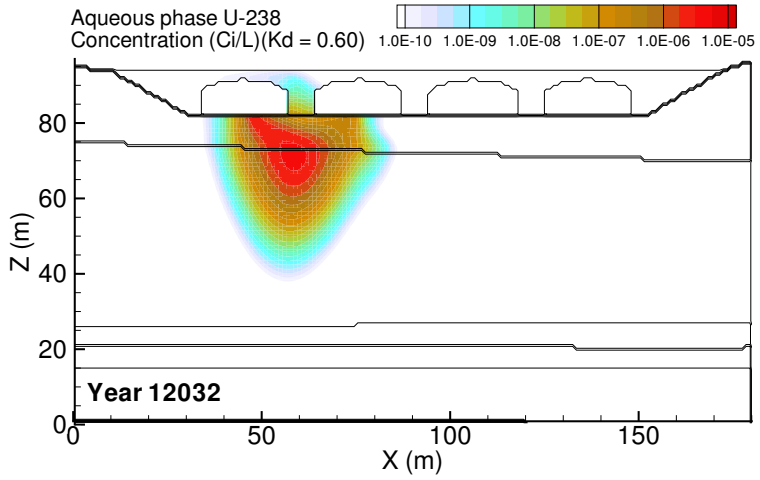

(c)

Figure D.10. Retrieval Leak: Low Preclosure Recharge Rate (40 mm/yr) aqueous concentration distributions at year 12032 for (a) Tc-99, (b) U_0.20 and (c) U_0.60.

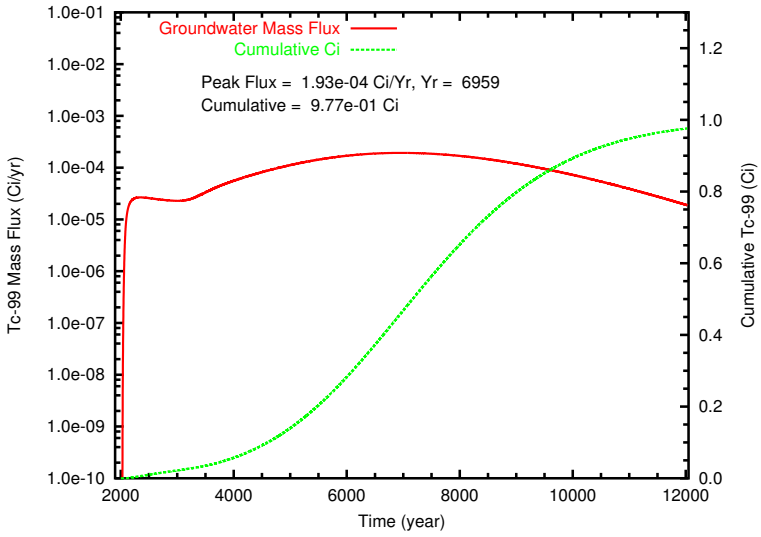

(a)

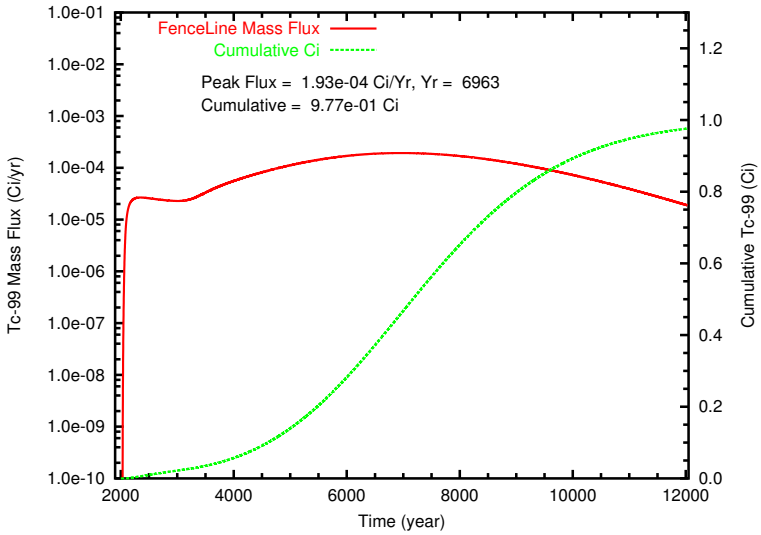

(b)

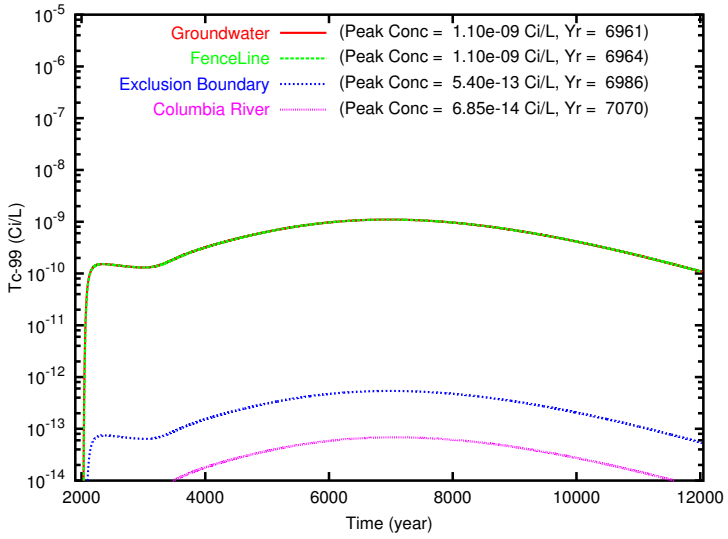

(c)

Figure D.11. Retrieval Leak: Low Preclosure Recharge Rate (40 mm/yr) Tc-99 mass flux at (a) the groundwater table and (b) the fenceline; and (c) the Tc-99 concentration at groundwater, fenceline, and easterly downstream compliance points.

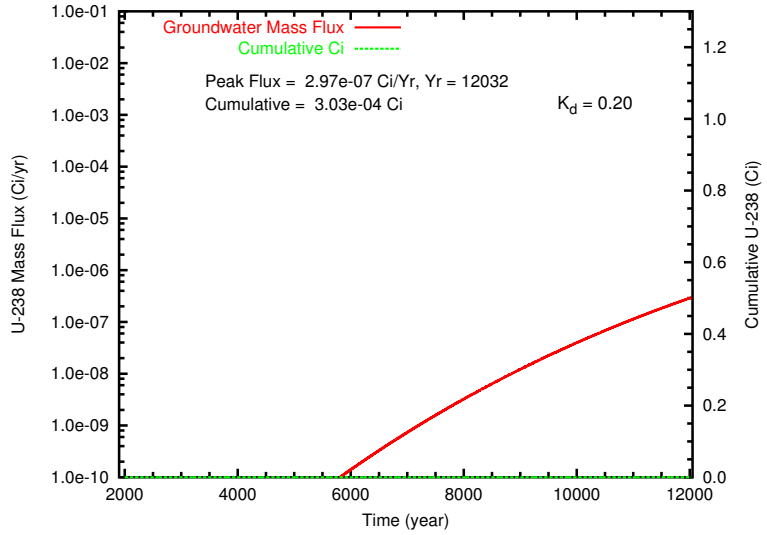

(a)

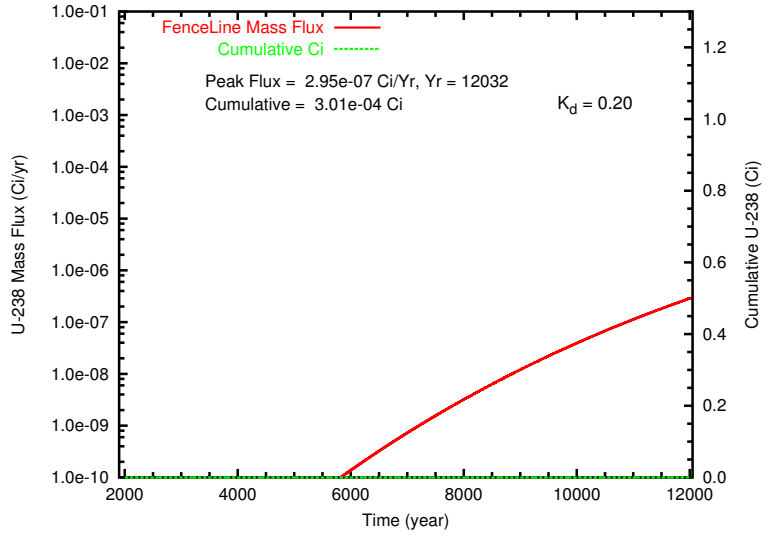

(b)

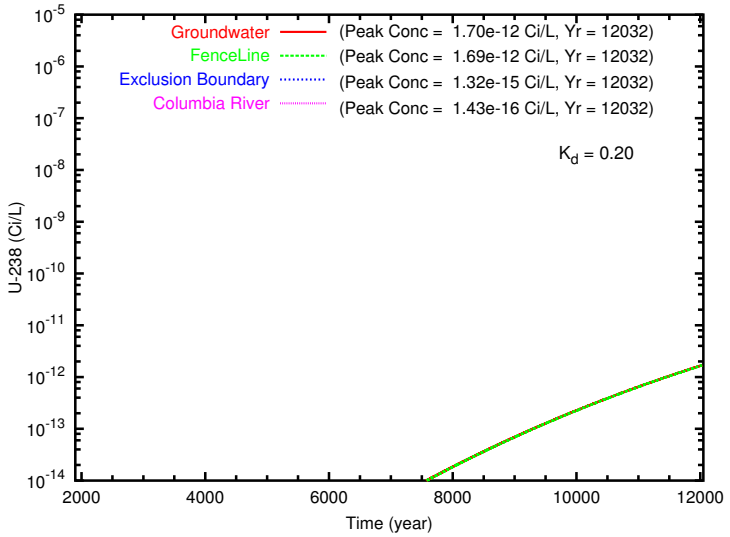

(c)

Figure D.12. Retrieval Leak: Low Preclosure Recharge Rate (40 mm/yr) U_0.20 mass flux at (a) the groundwater table and (b) the fenceline; and (c) the Tc-99 concentration at groundwater, fenceline, and easterly downstream compliance points.

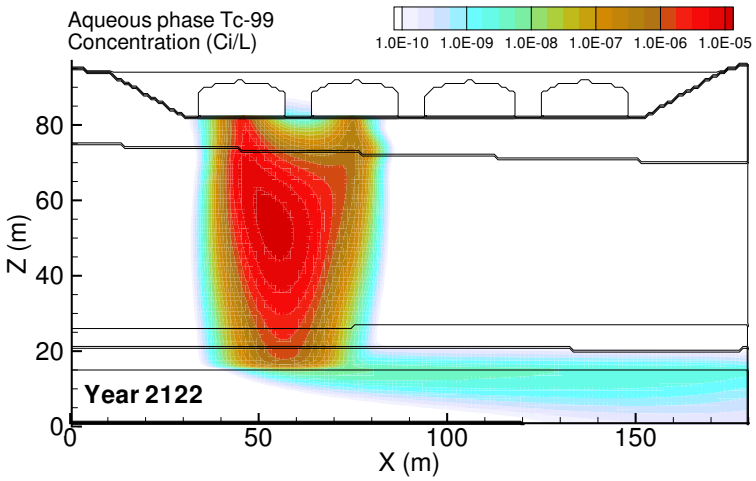

(a)

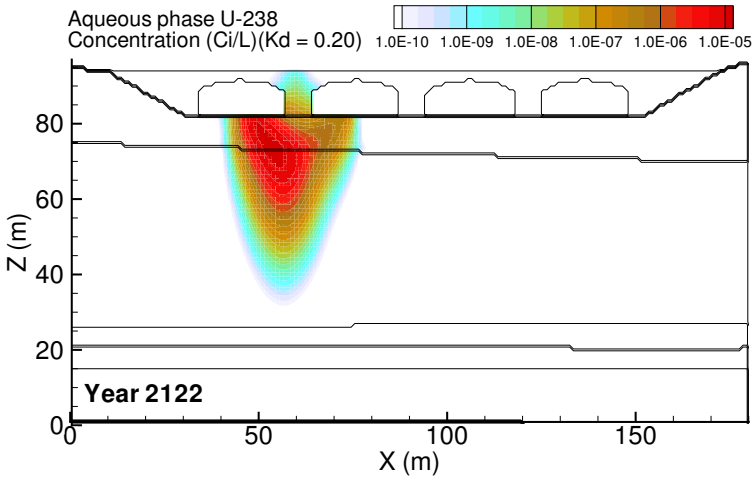

(b)

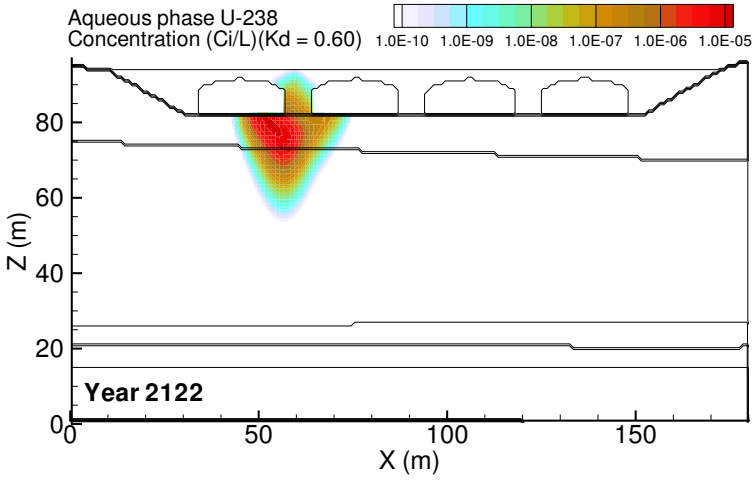

(c)

Figure D.13. Retrieval Leak: High Barrier Recharge Rate (1.0 mm/yr) aqueous concentration distributions at year 2122 for (a) Tc-99, (b) U_0.20 and (c) U_0.60. Year of Tc-99 peak concentration at fenceline was 2122.

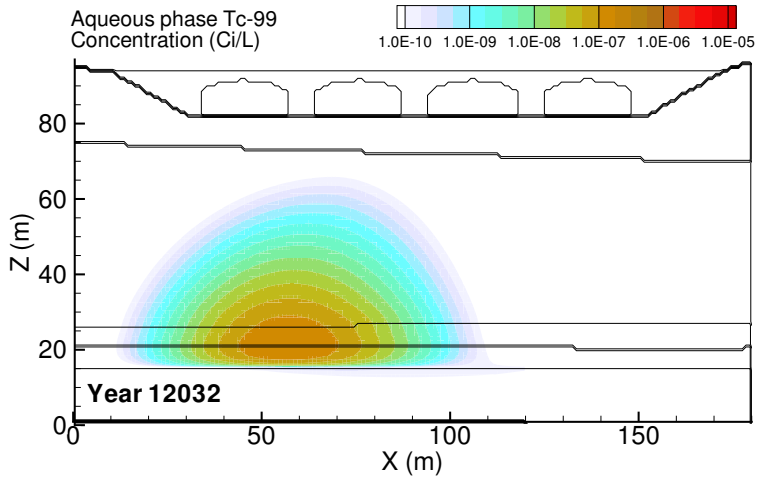

(a)

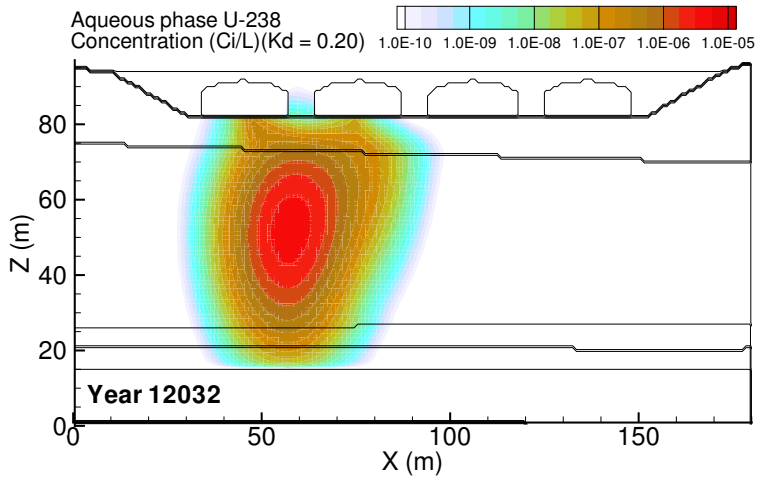

(b)

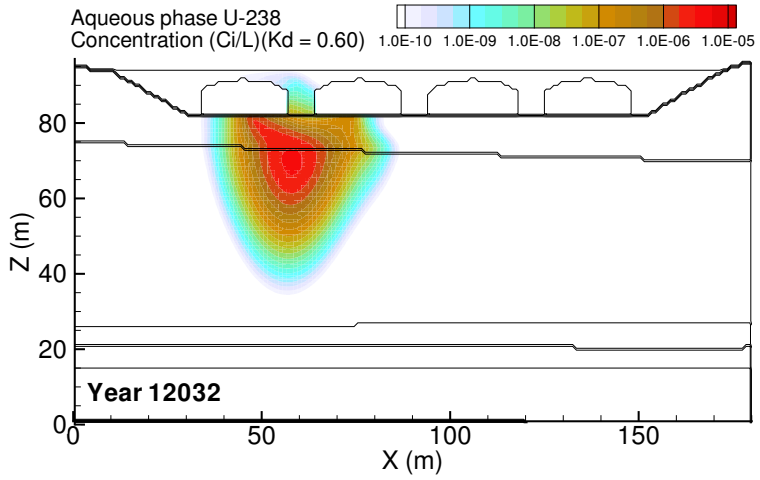

(c)

Figure D.14. Retrieval Leak: High Barrier Recharge Rate (1.0 mm/yr) aqueous concentration distributions at year 12032 for (a) Tc-99, (b) U_0.20 and (c) U_0.60.

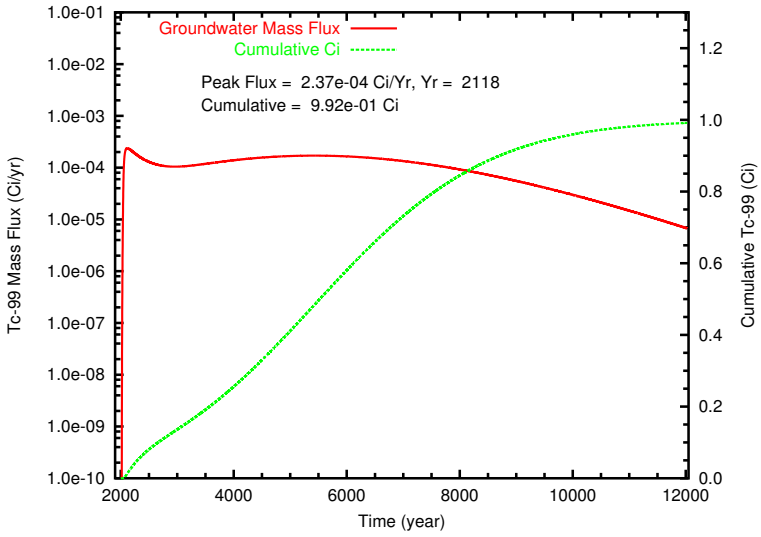

(a)

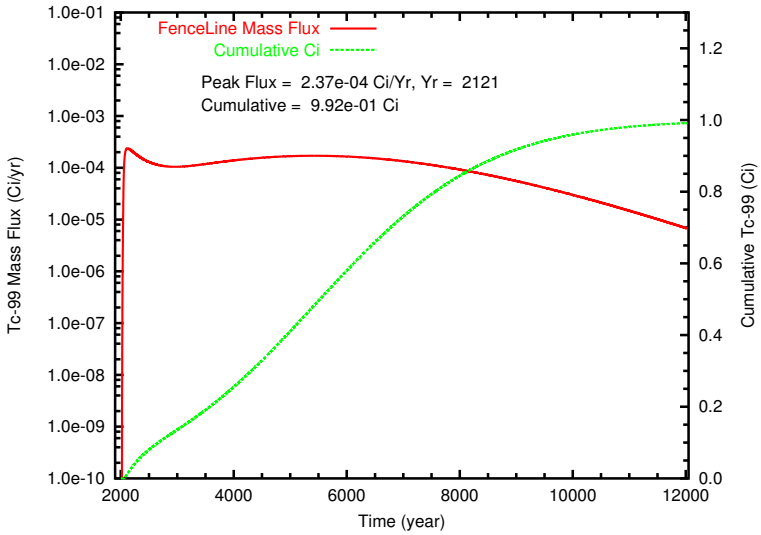

(b)

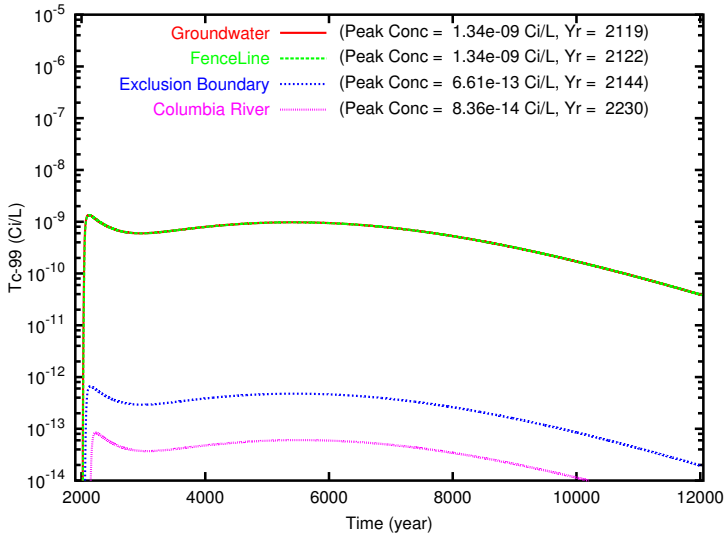

(c)

Figure D.15. Retrieval Leak: High Barrier Recharge Rate (1.0 mm/yr) Tc-99 mass flux at (a) the groundwater table and (b) the fenceline; and (c) the Tc-99 concentration at groundwater, fenceline, and easterly downstream compliance points.

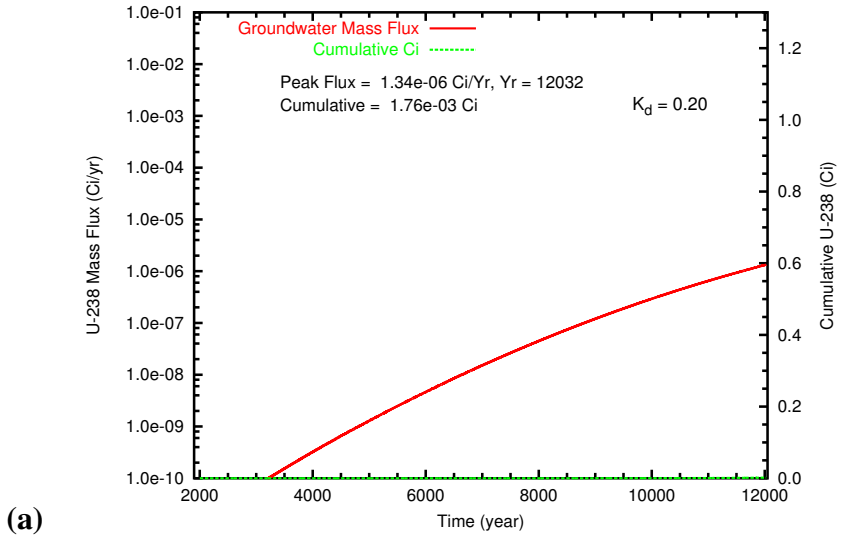

(a)

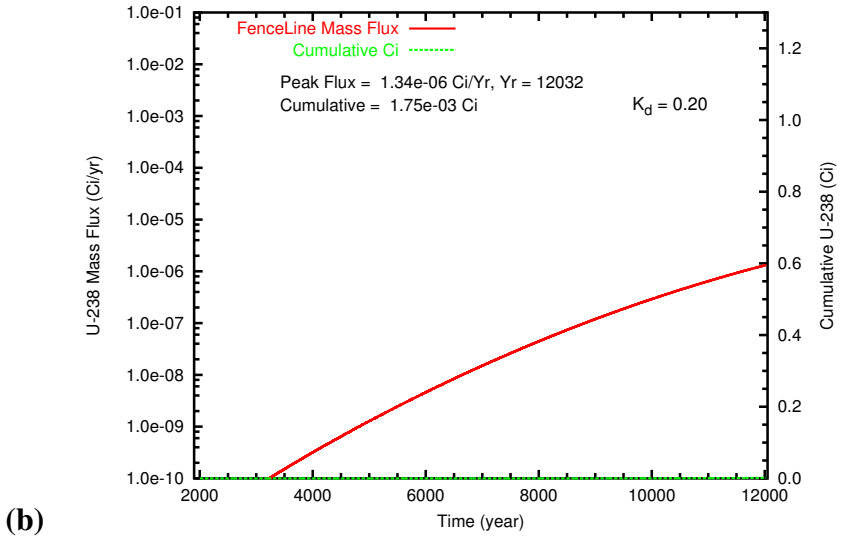

(b)

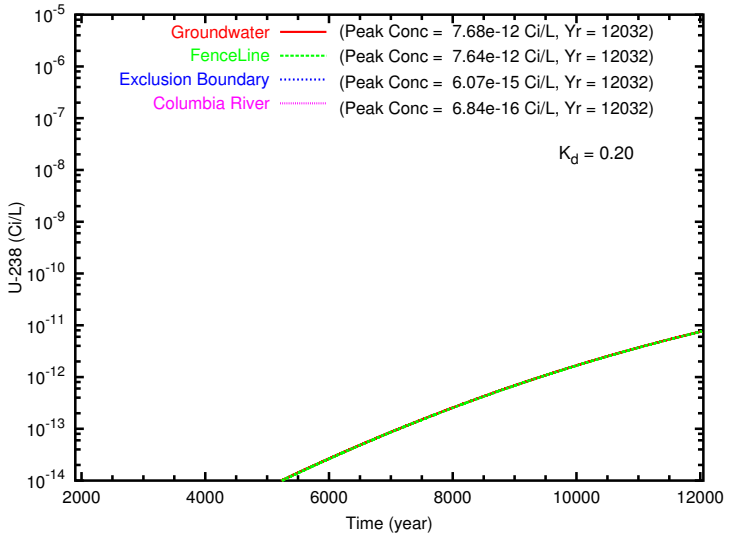

(c)

Figure D.16. Retrieval Leak: High Barrier Recharge Rate (1.0 mm/yr) U_0.20 mass flux at (a) the groundwater table and (b) the fenceline; and (c) the Tc-99 concentration at groundwater, fenceline, and easterly downstream compliance points.

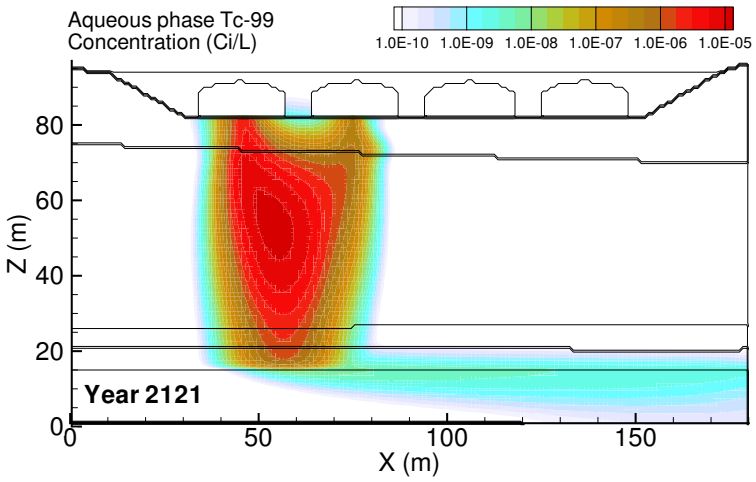

(a)

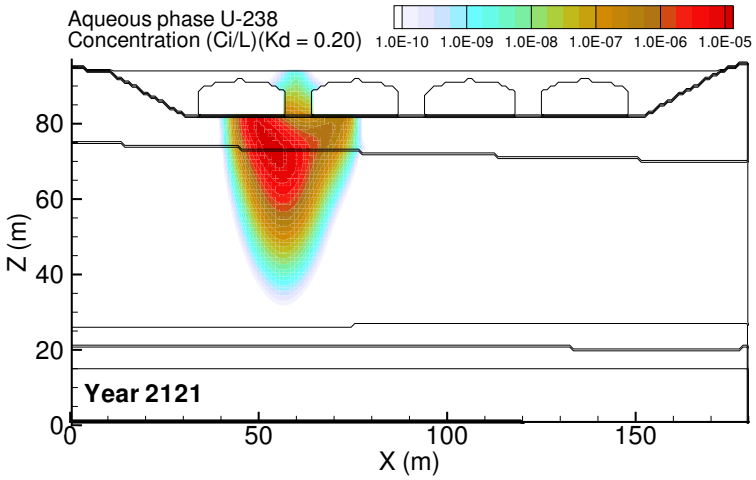

(b)

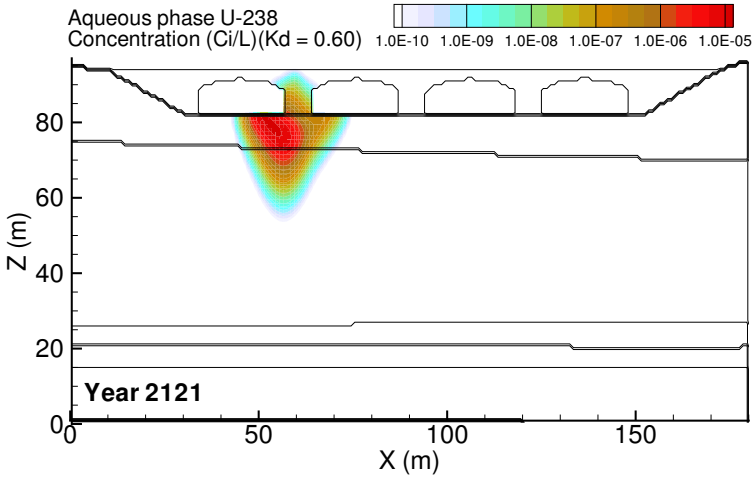

(c)

Figure D.17. Retrieval Leak: Low Barrier Recharge Rate (0.1 mm/yr) aqueous concentration distributions at year 2121 for (a) Tc-99, (b) U_0.20 and (c) U_0.60. Year of Tc-99 peak concentration at fenceline was 2121.

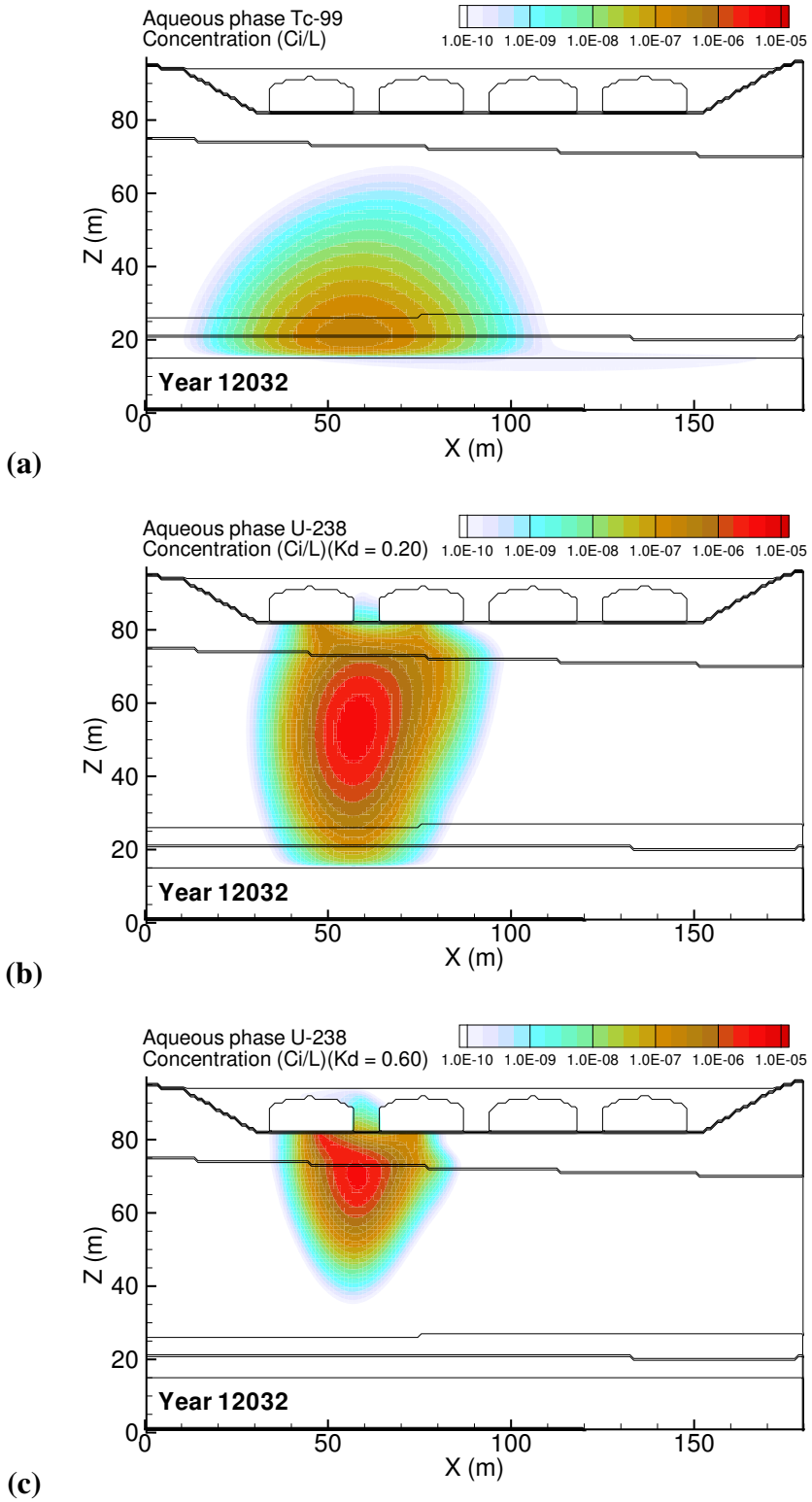

Figure D.18. Retrieval Leak: Low Barrier Recharge Rate (0.1 mm/yr) aqueous concentration distributions at year 12032 for (a) Tc-99, (b) U_0.20 and (c) U_0.60.

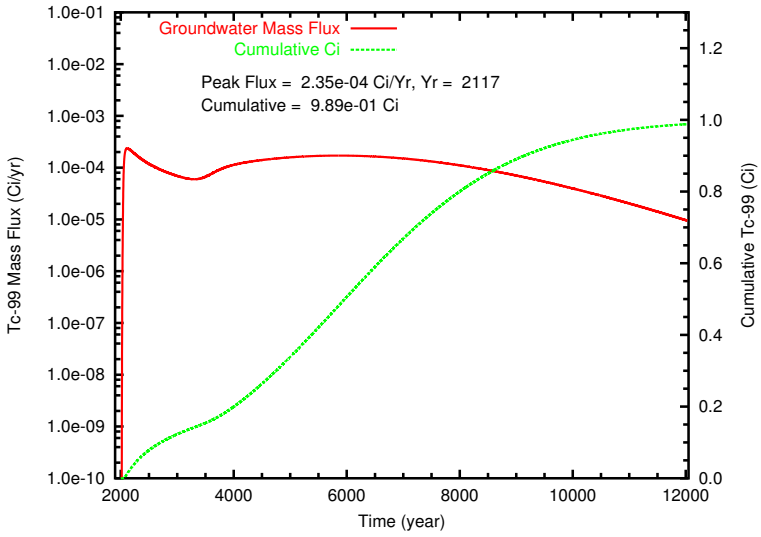

(a)

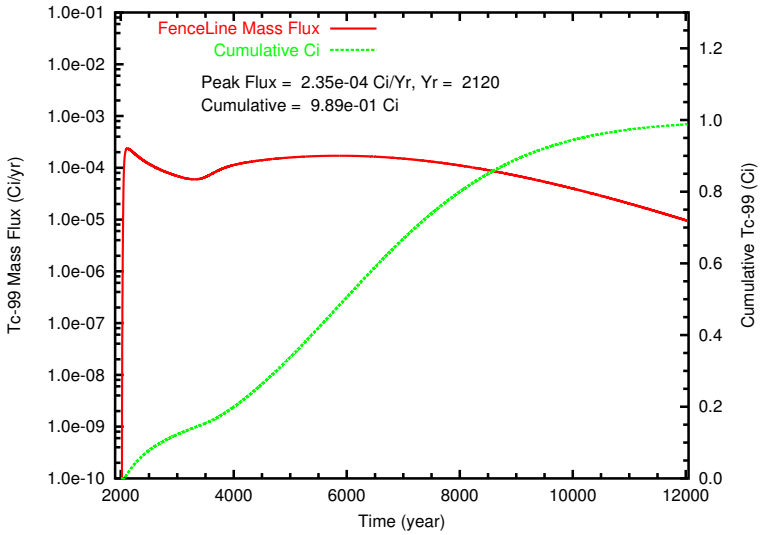

(b)

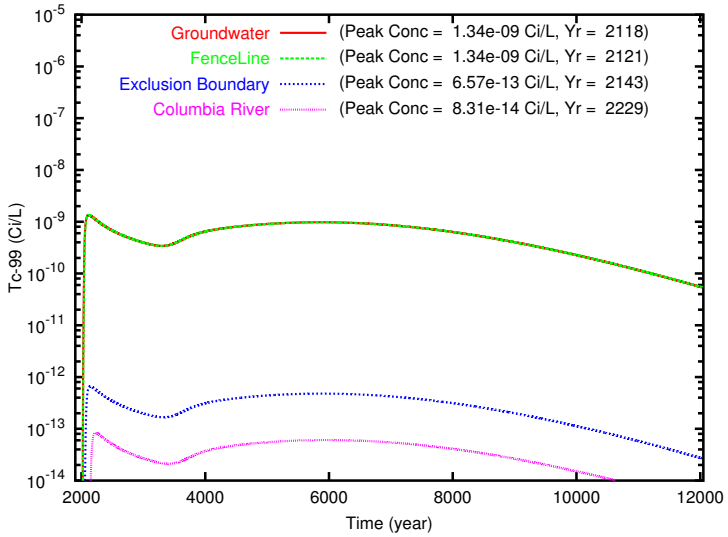

(c)

Figure D.19. Retrieval Leak: Low Barrier Recharge Rate (0.1 mm/yr) Tc-99 mass flux at (a) the groundwater table and (b) the fenceline; and (c) the Tc-99 concentration at groundwater, fenceline, and easterly downstream compliance points.

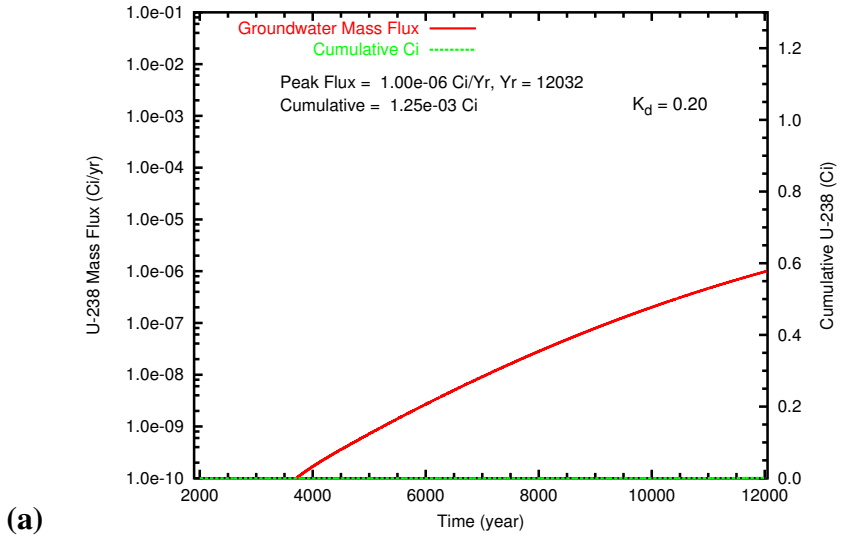

(a)

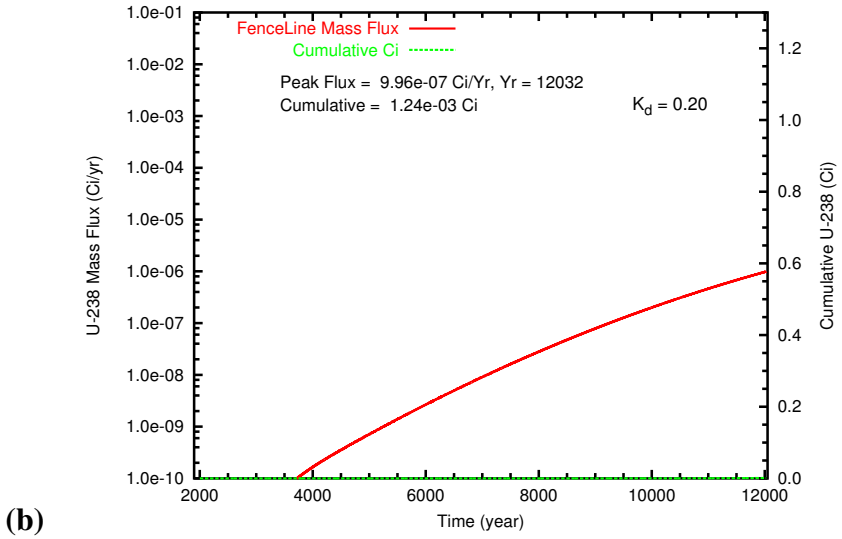

(b)

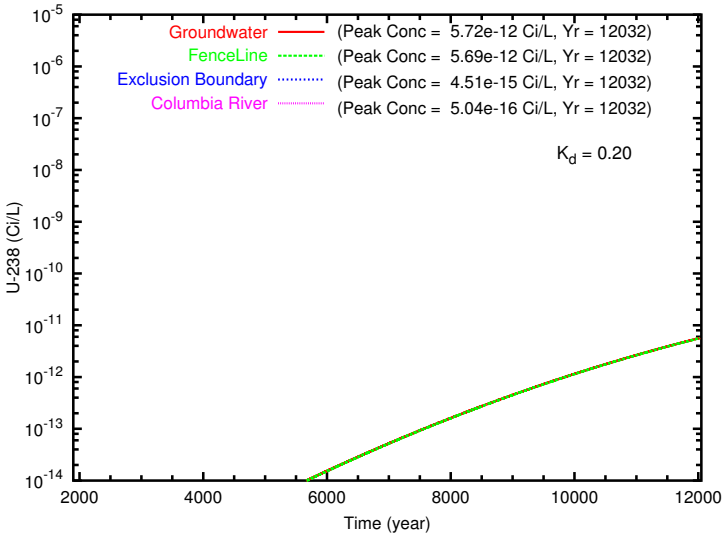

(c)

Figure D.20. Retrieval Leak: Low Barrier Recharge Rate (0.1 mm/yr) U_0.20 mass flux at (a) the groundwater table and (b) the fenceline; and (c) the Tc-99 concentration at groundwater, fenceline, and easterly downstream compliance points.

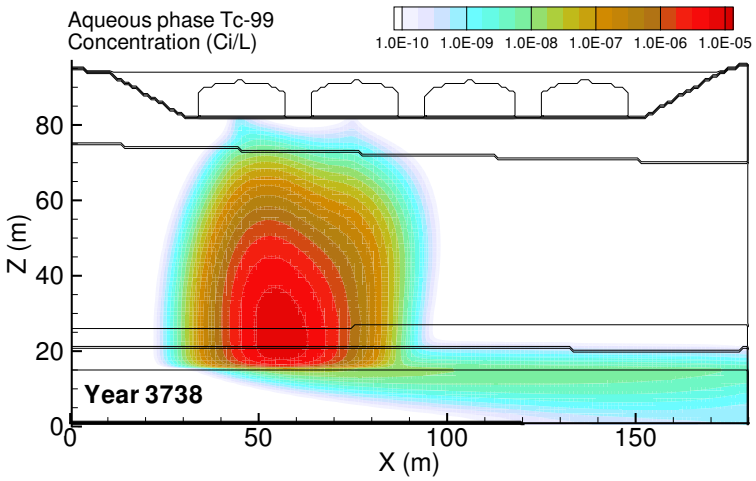

(a)

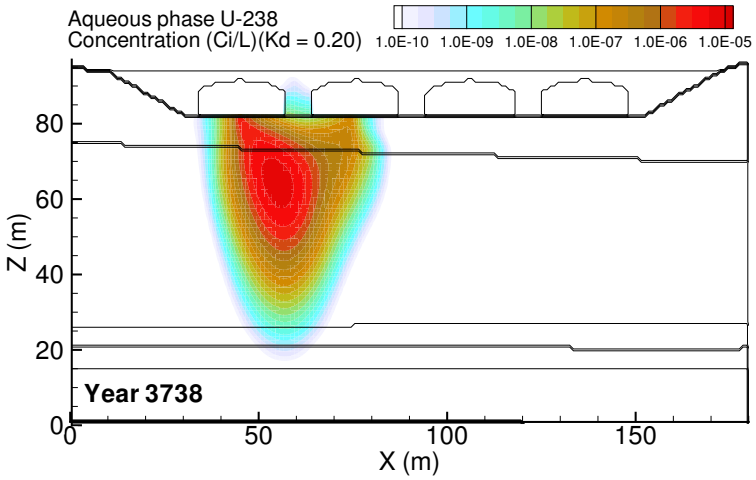

(b)

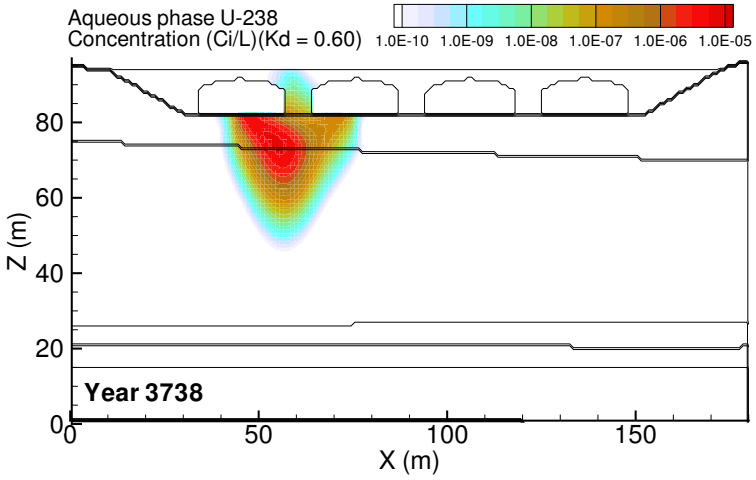

(c)

Figure D.21. Retrieval Leak: High Degraded-Barrier Recharge Rate (3.5 mm/yr) aqueous concentration distributions at year 3738 for (a) Tc-99, (b) U_0.20 and (c) U_0.60. Year of Tc-99 peak concentration at fenceline was 3738.

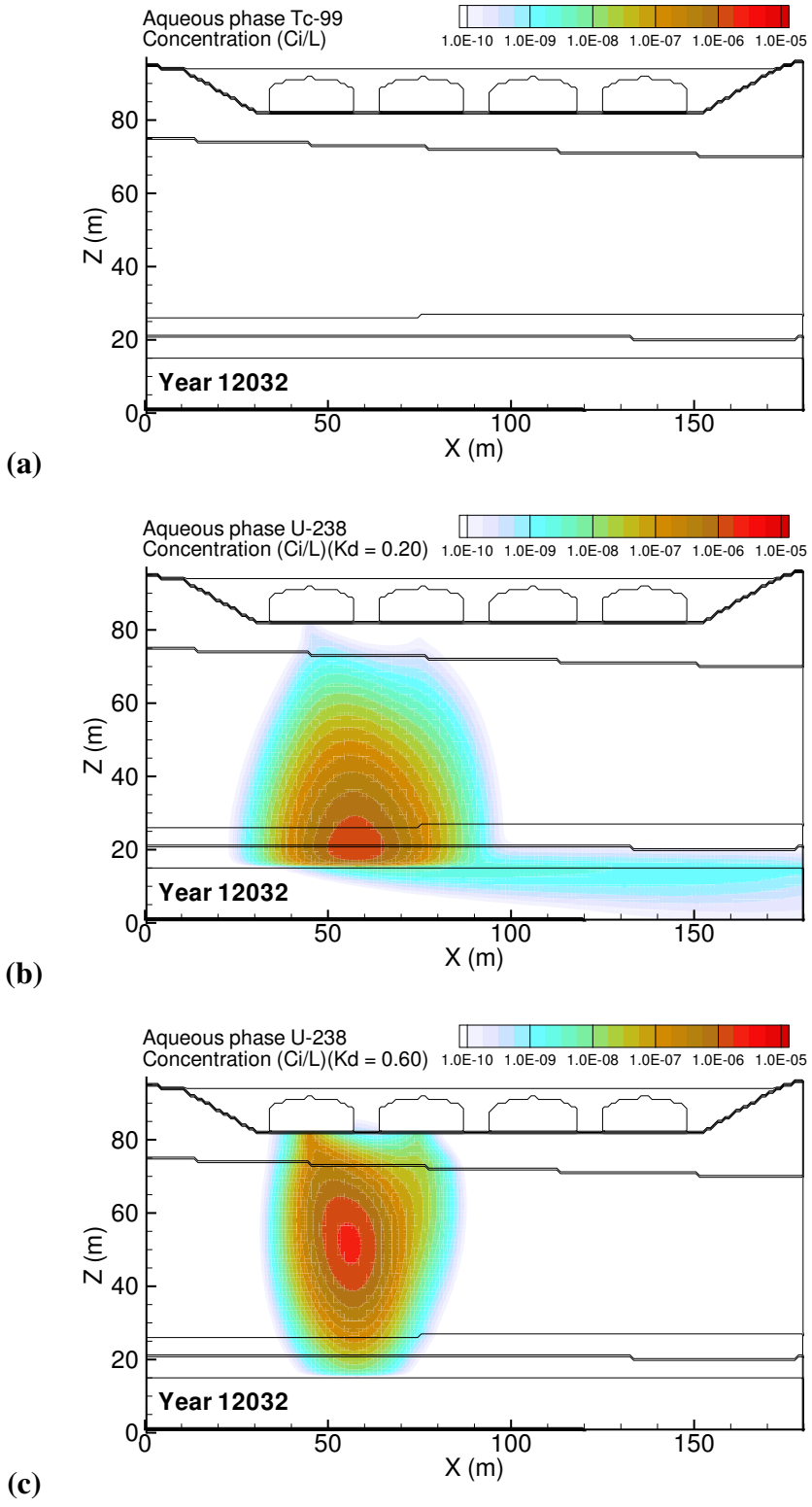

Figure D.22. Retrieval Leak: High Degraded-Barrier Recharge Rate (3.5 mm/yr) aqueous concentration distributions at year 12032 for (a) Tc-99, (b) U_0.20 and (c) U_0.60.

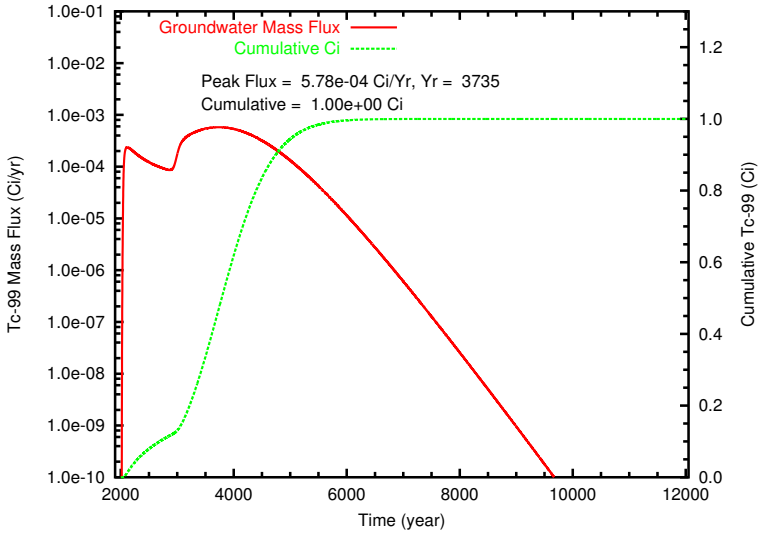

(a)

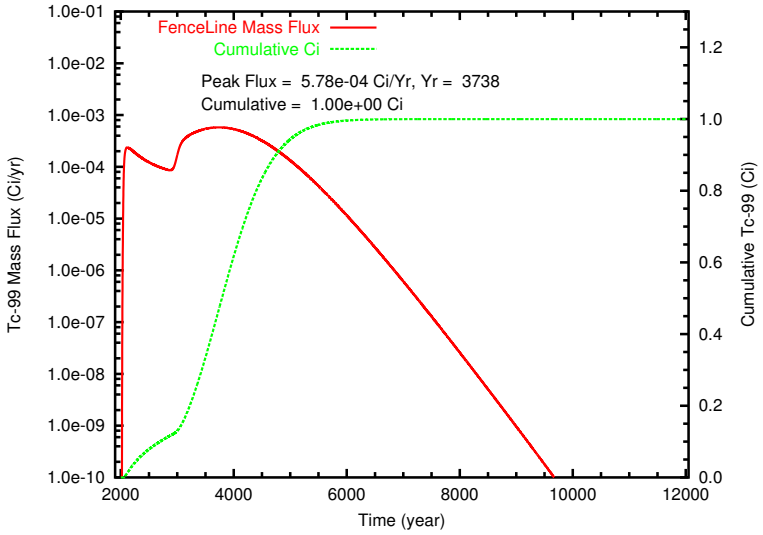

(b)

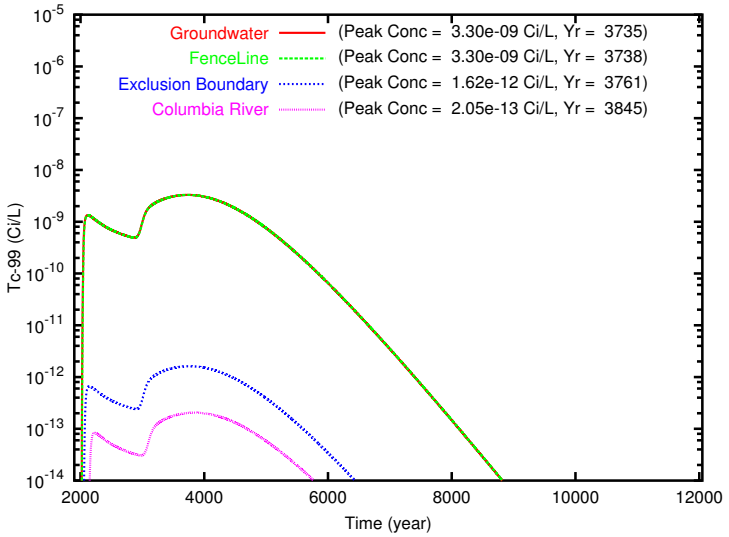

(c)

Figure D.23. Retrieval Leak: High Degraded-Barrier Recharge Rate (3.5 mm/yr) Tc-99 mass flux at (a) the groundwater table and (b) the fenceline; and (c) the Tc-99 concentration at groundwater, fenceline, and easterly downstream compliance points.

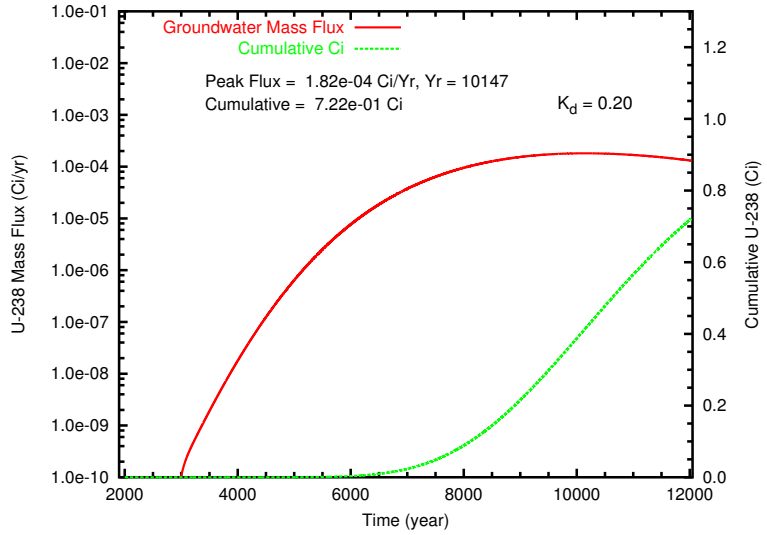

(a)

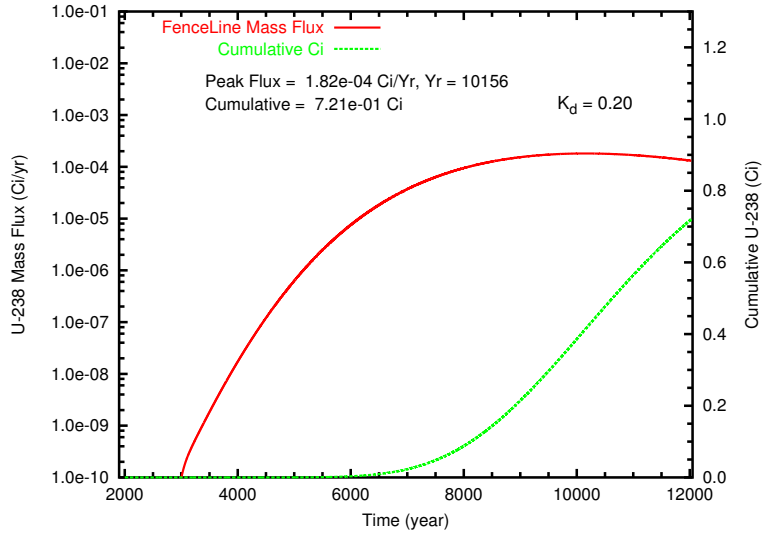

(b)

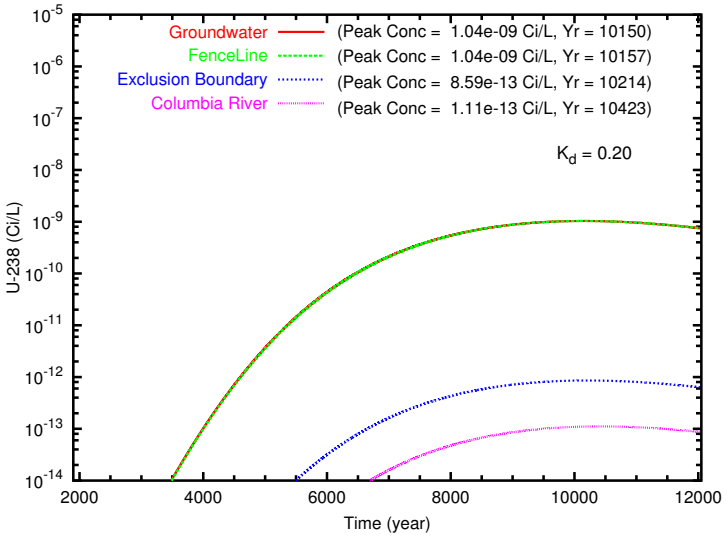

(c)

Figure D.24. Retrieval Leak: High Degraded-Barrier Recharge Rate (3.5 mm/yr) U_0.20 mass flux at (a) the groundwater table and (b) the fenceline; and (c) the Tc-99 concentration at groundwater, fenceline, and easterly downstream compliance points.

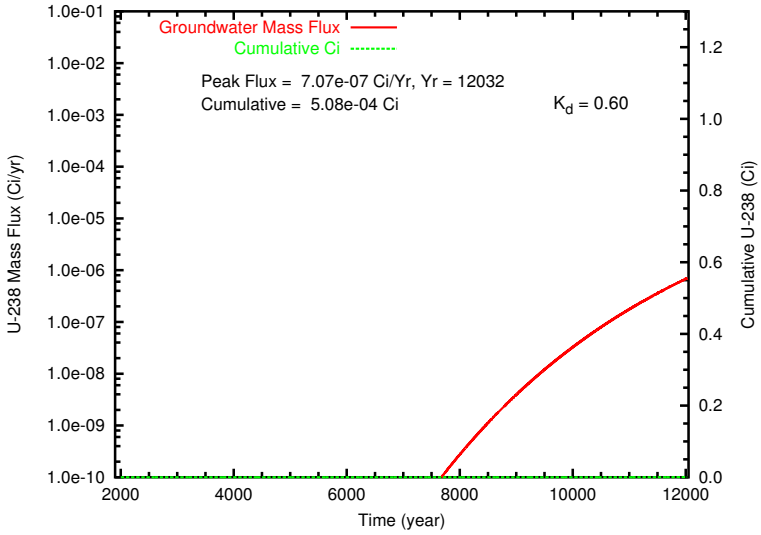

(a)

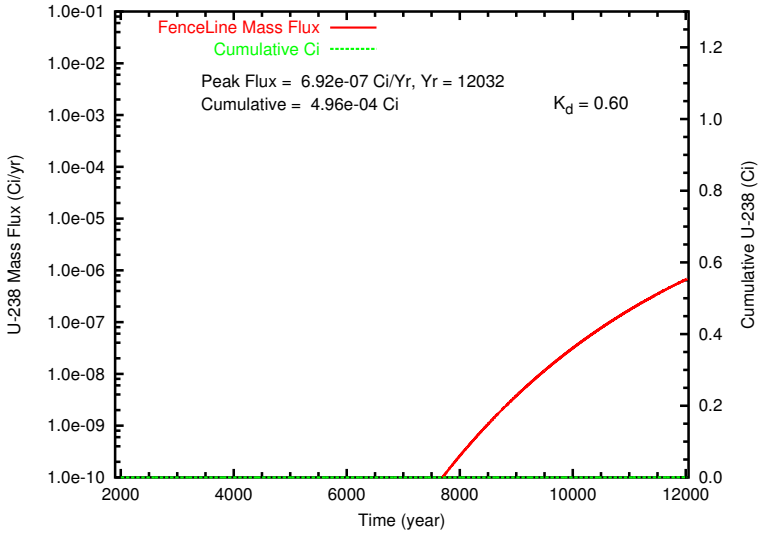

(b)

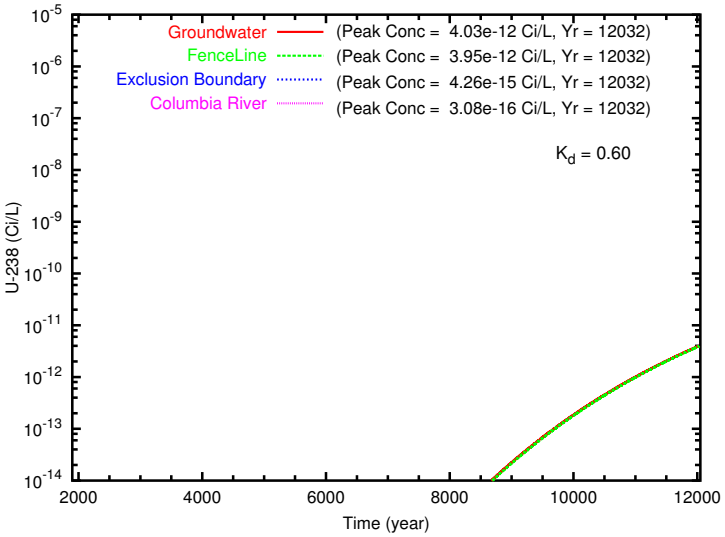

(c)

Figure D.25. Retrieval Leak: High Degraded-Barrier Recharge Rate (3.5 mm/yr) U_0.60 mass flux at (a) the groundwater table and (b) the fenceline; and (c) the Tc-99 concentration at groundwater, fenceline, and easterly downstream compliance points.

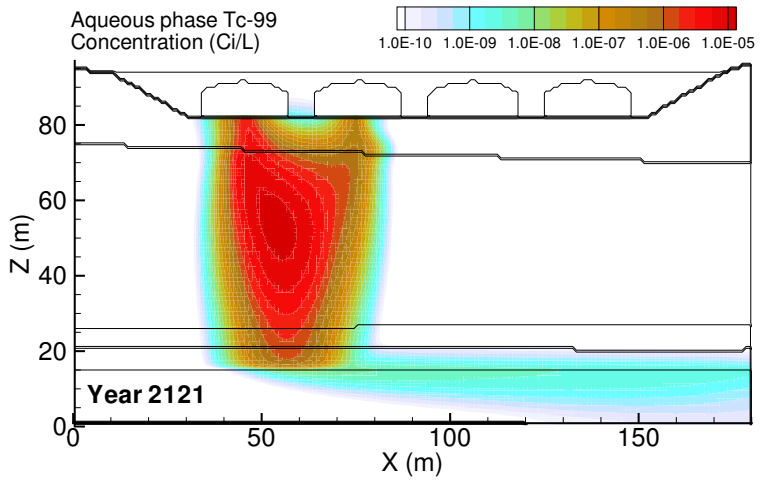

(a)

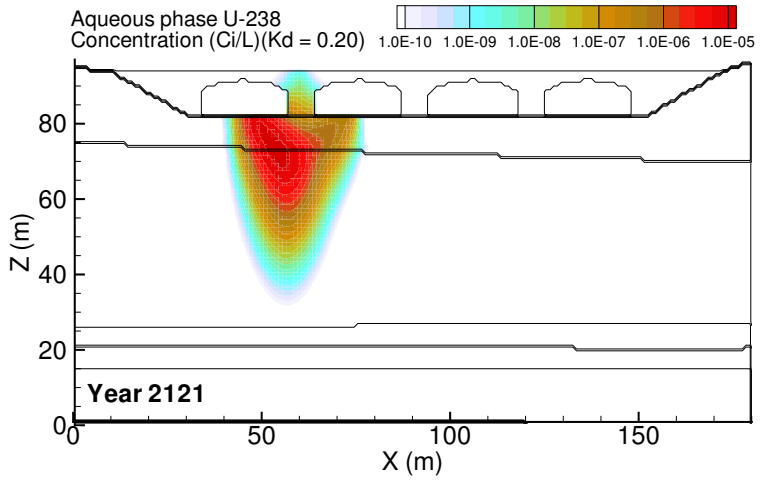

(b)

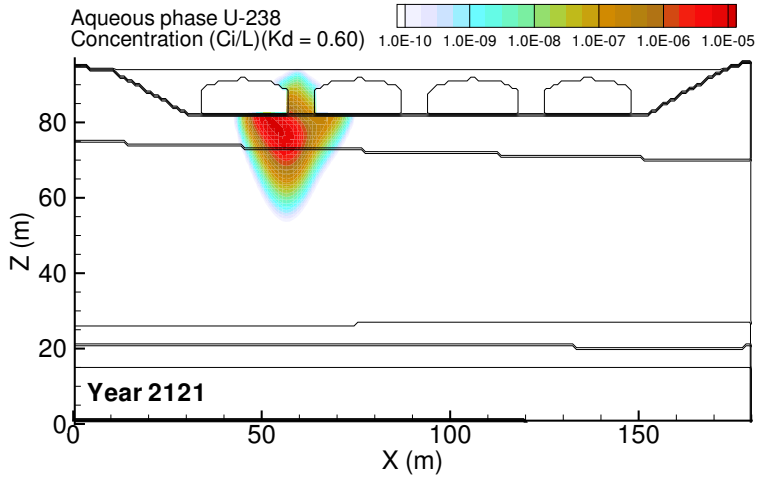

(c)

Figure D.26. Retrieval Leak: Low Degraded-Barrier Recharge Rate (0.5 mm/yr) aqueous concentration distributions at year 2121 for (a) Tc-99, (b) U_0.20 and (c) U_0.60. Year of Tc-99 peak concentration at fenceline was 2121.

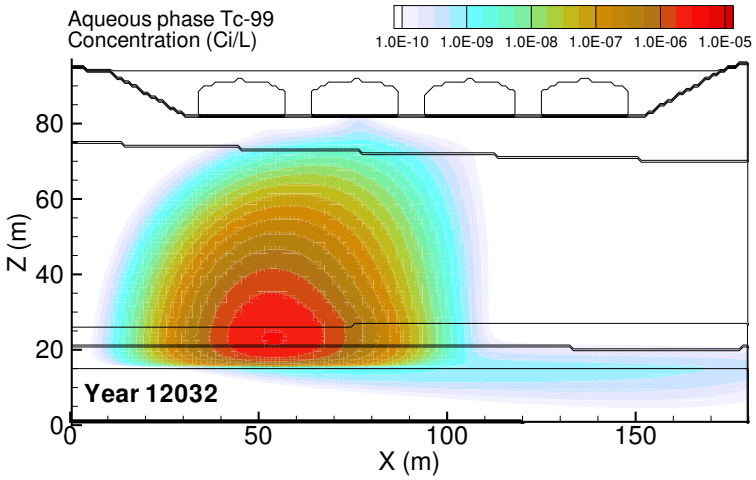

(a)

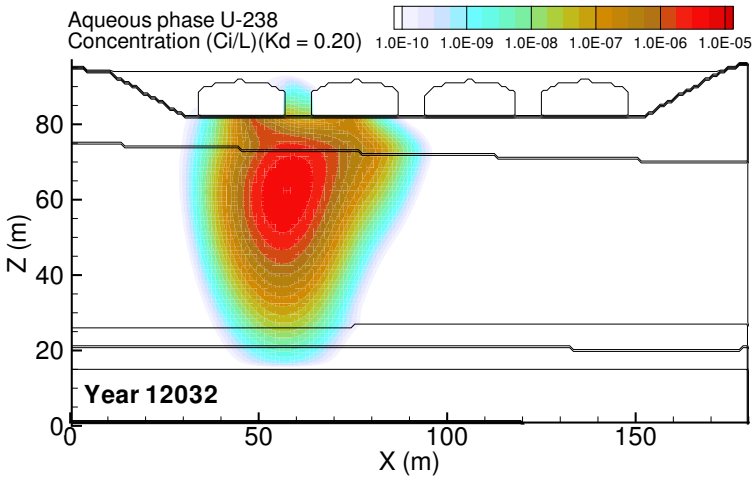

(b)

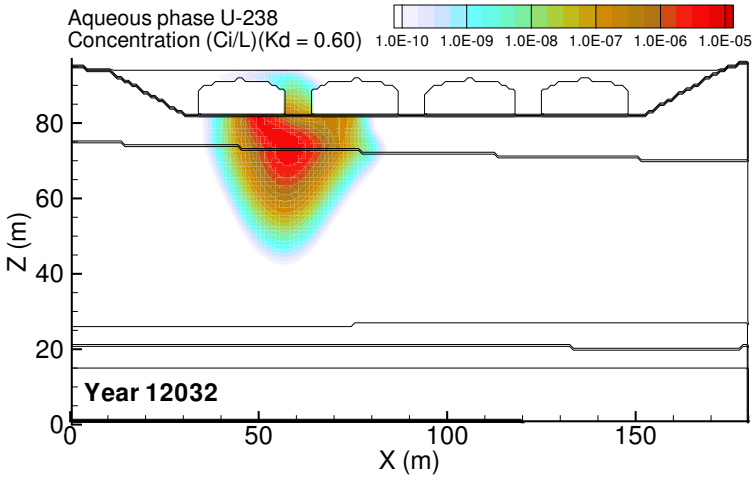

(c)

Figure D.27. Retrieval Leak: Low Degraded-Barrier Recharge Rate (0.5 mm/yr) aqueous concentration distributions at year 12032 for (a) Tc-99, (b) U_0.20 and (c) U_0.60.

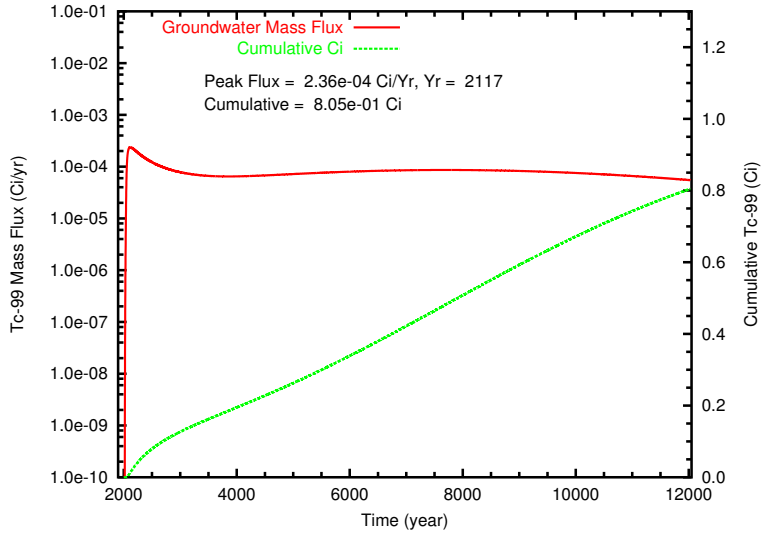

(a)

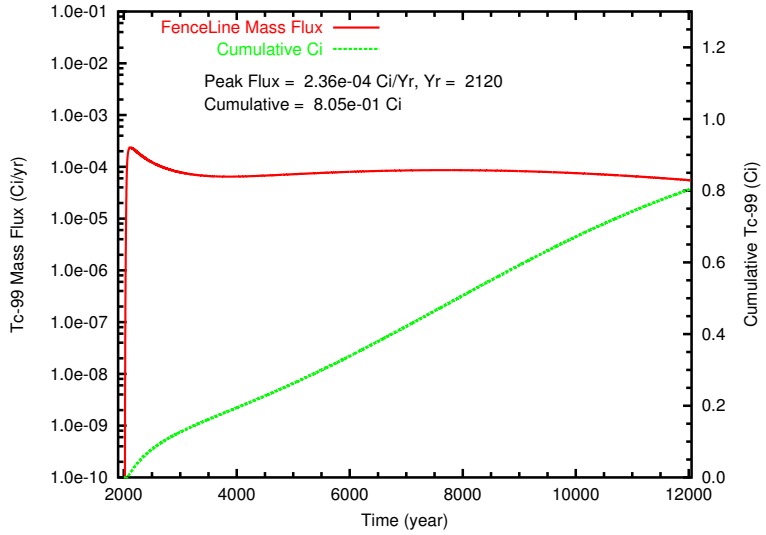

(b)

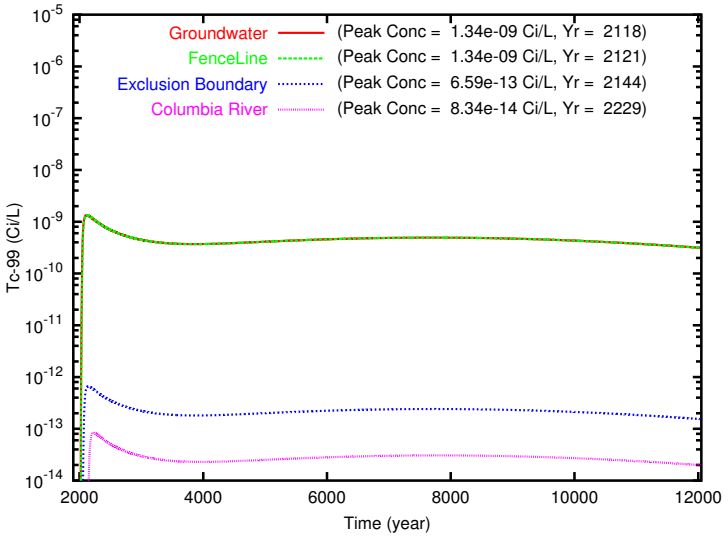

(c)

Figure D.28. Retrieval Leak: Low Degraded-Barrier Recharge Rate (0.5 mm/yr) Tc-99 mass flux at (a) the groundwater table and (b) the fenceline; and (c) the Tc-99 concentration at groundwater, fenceline, and easterly downstream compliance points.

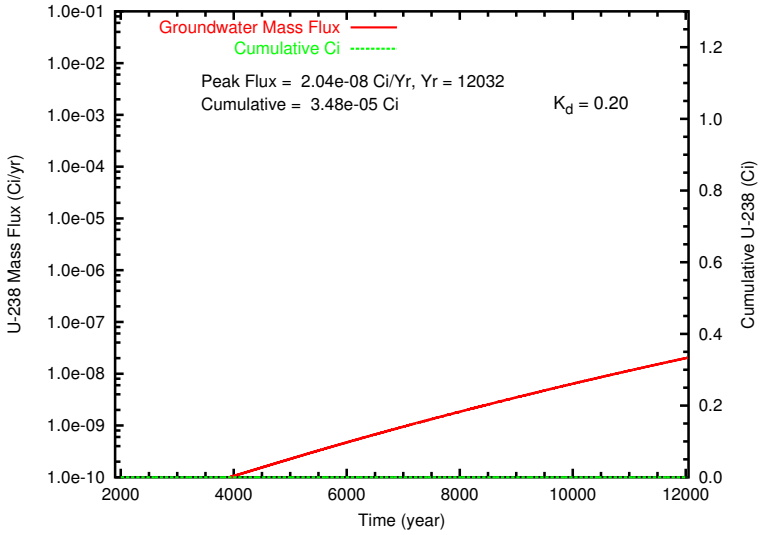

(a)

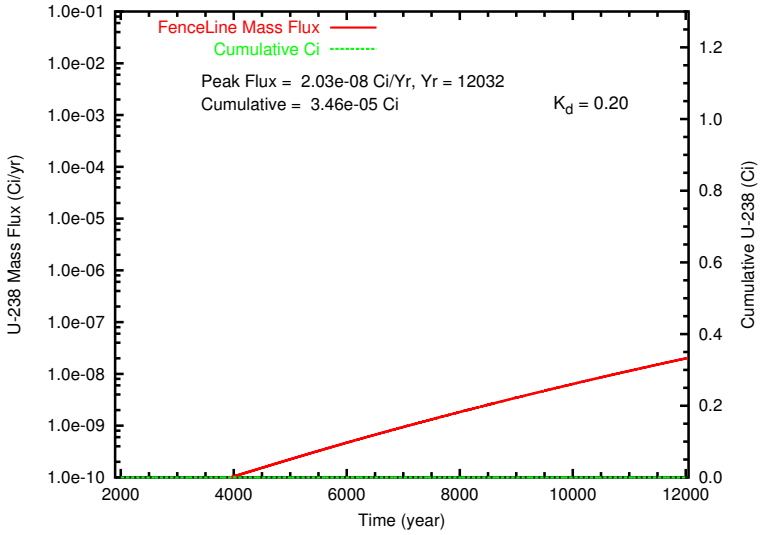

(b)

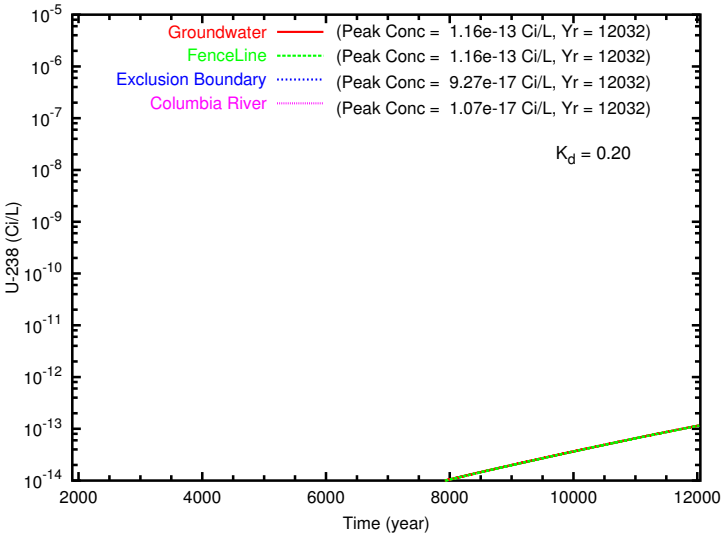

(c)

Figure D.29. Retrieval Leak: Low Degraded-Barrier Recharge Rate (0.5 mm/yr) U_0.20 mass flux at (a) the groundwater table and (b) the fenceline; and (c) the Tc-99 concentration at groundwater, fenceline, and easterly downstream compliance points.

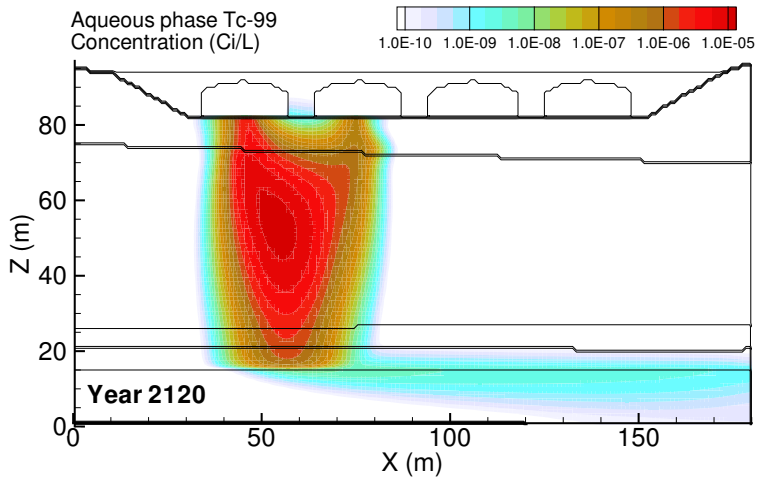

(a)

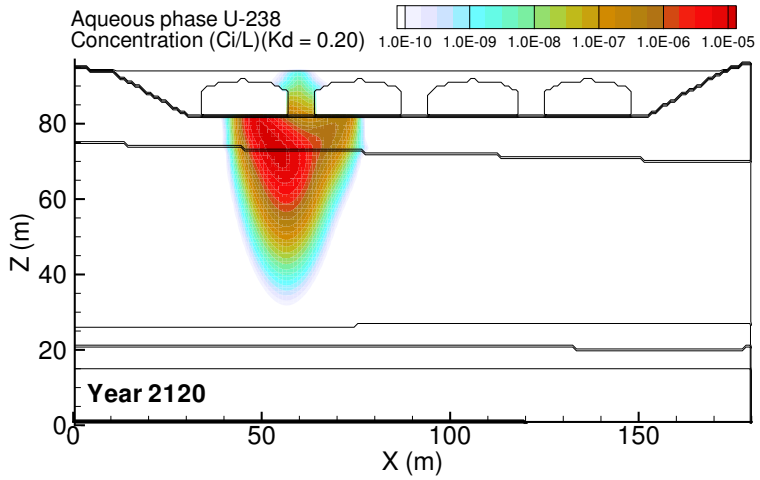

(b)

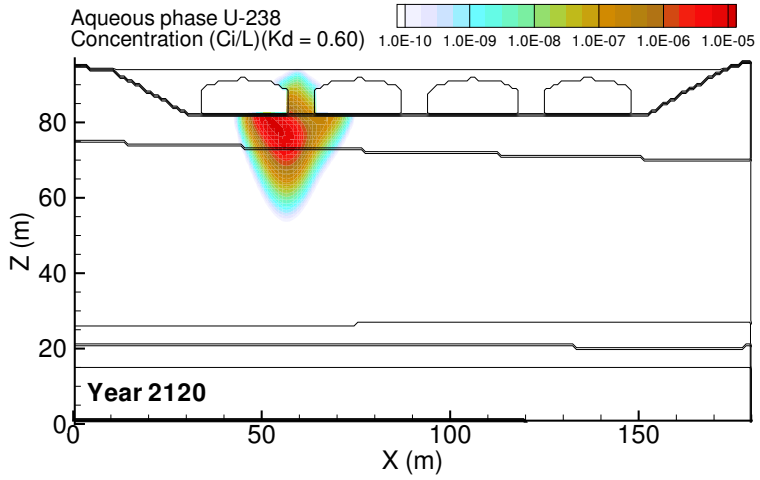

(c)

Figure D.30. Retrieval Leak: High Aquifer Hydraulic Conductivity (4000 m/d) aqueous concentration distributions at year 2120 for (a) Tc-99, (b) U_0.20 and (c) U_0.60. Year of Tc-99 peak concentration at fenceline was 2120.

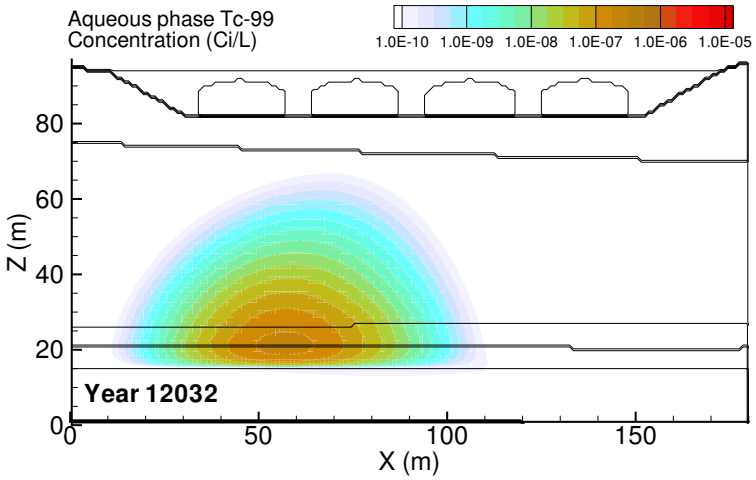

(a)

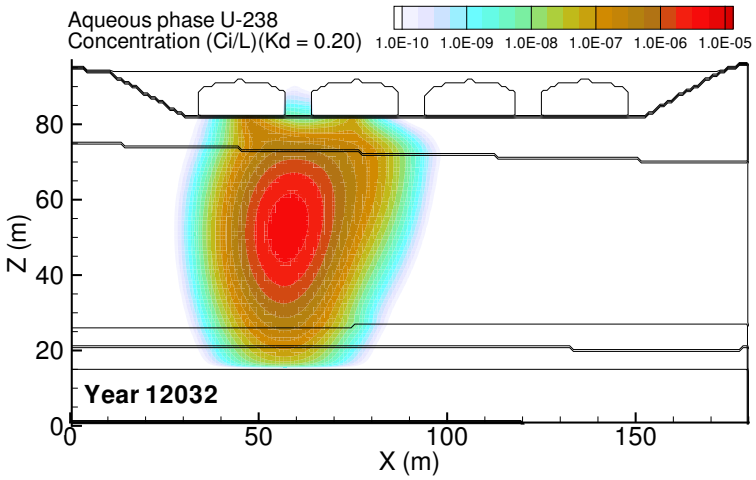

(b)

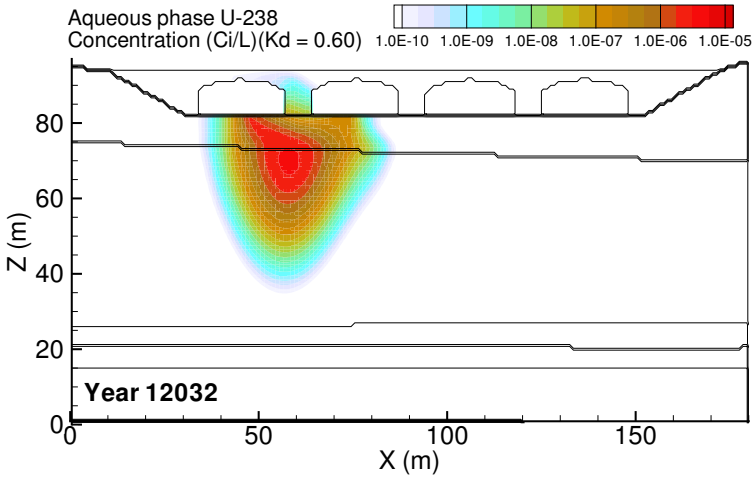

(c)

Figure D.31. Retrieval Leak: High Aquifer Hydraulic Conductivity (4000 m/d) aqueous concentration distributions at year 12032 for (a) Tc-99, (b) U_0.20 and (c) U_0.60.

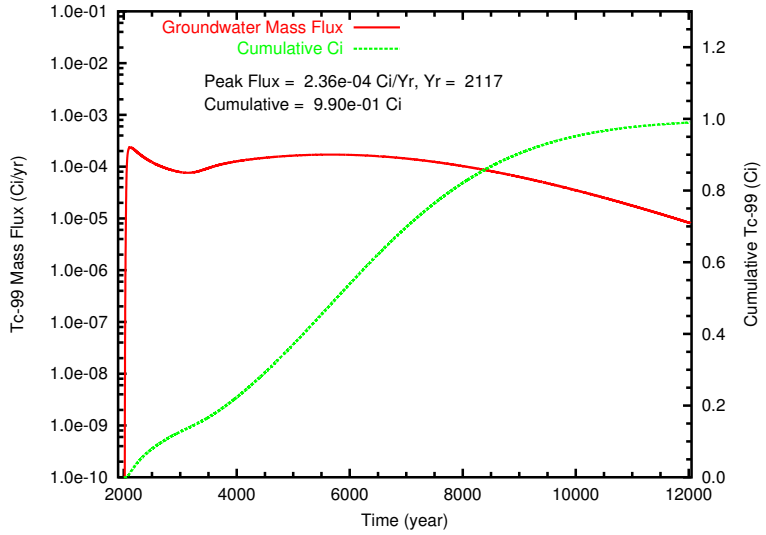

(a)

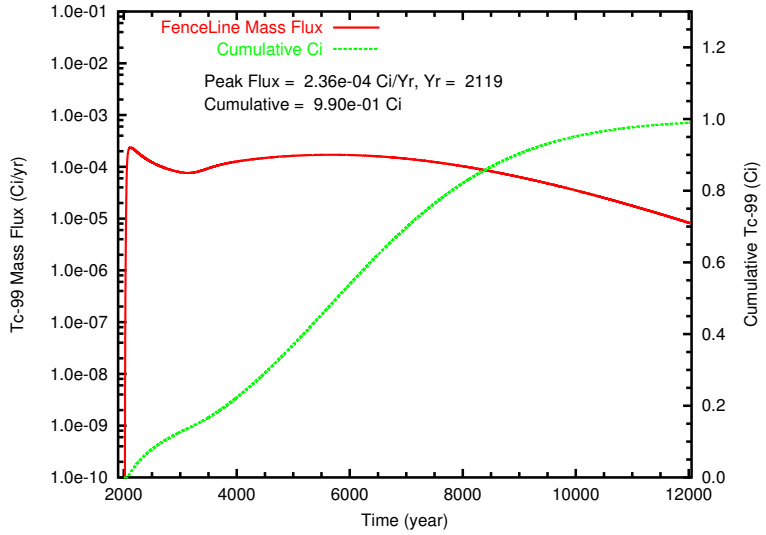

(b)

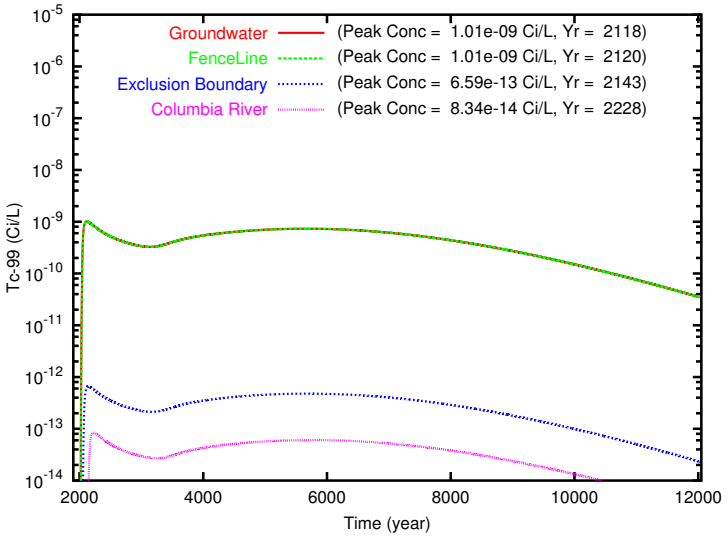

(c)

Figure D.32. Retrieval Leak: High Aquifer Hydraulic Conductivity (4000 m/d) Tc-99 mass flux at (a) the groundwater table and (b) the fenceline; and (c) the Tc-99 concentration at groundwater, fenceline, and easterly downstream compliance points.

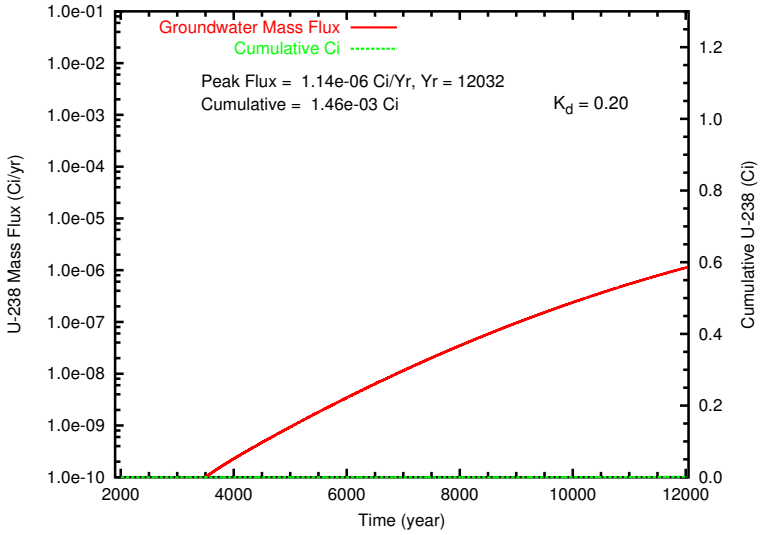

(a)

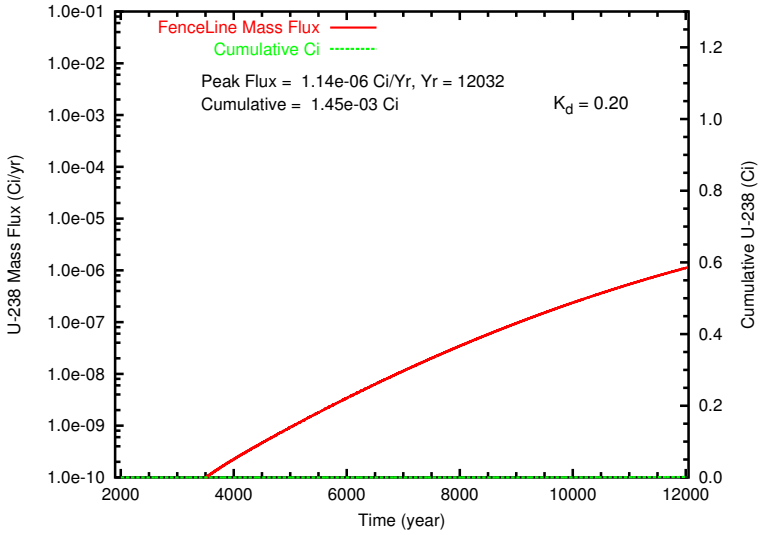

(b)

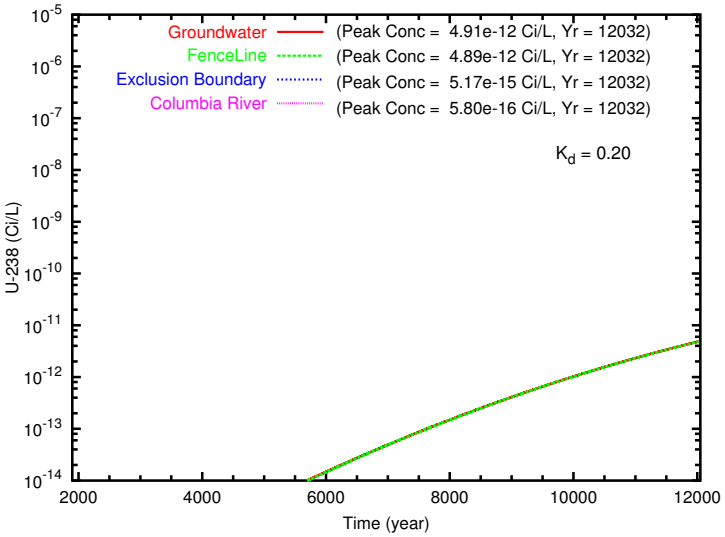

(c)

Figure D.33. Retrieval Leak: High Aquifer Hydraulic Conductivity (4000 m/d) U_0.20 mass flux at (a) the groundwater table and (b) the fenceline; and (c) the Tc-99 concentration at groundwater, fenceline, and easterly downstream compliance points.

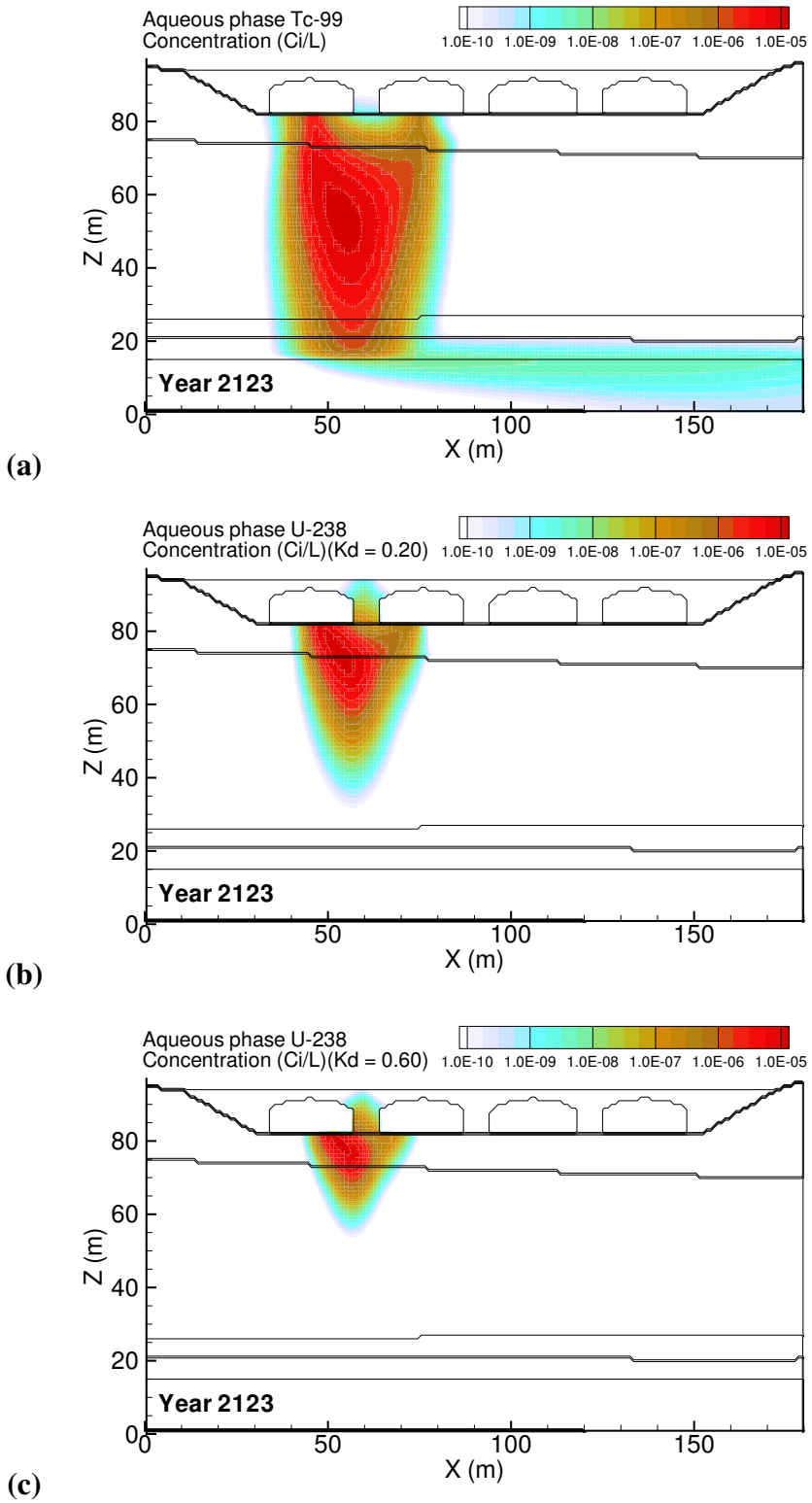

Figure D.34. Retrieval Leak: Low Aquifer Hydraulic Conductivity (2000 m/d) aqueous concentration distributions at year 2123 for (a) Tc-99, (b) U_0.20 and (c) U_0.60. Year of Tc-99 peak concentration at fenceline was 2123.

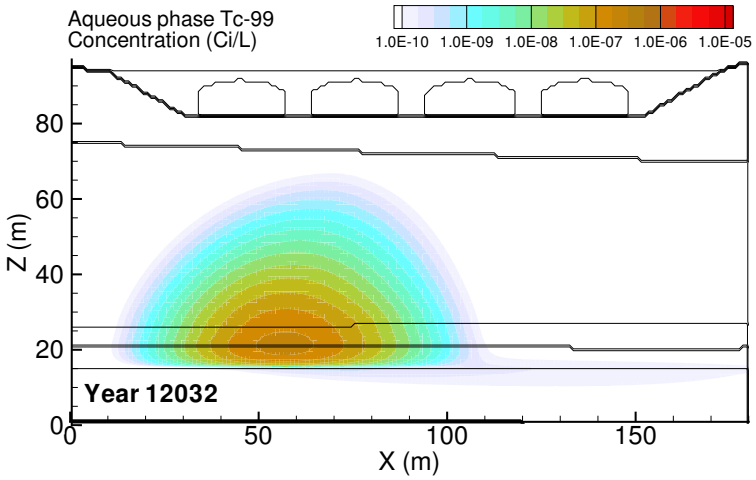

(a)

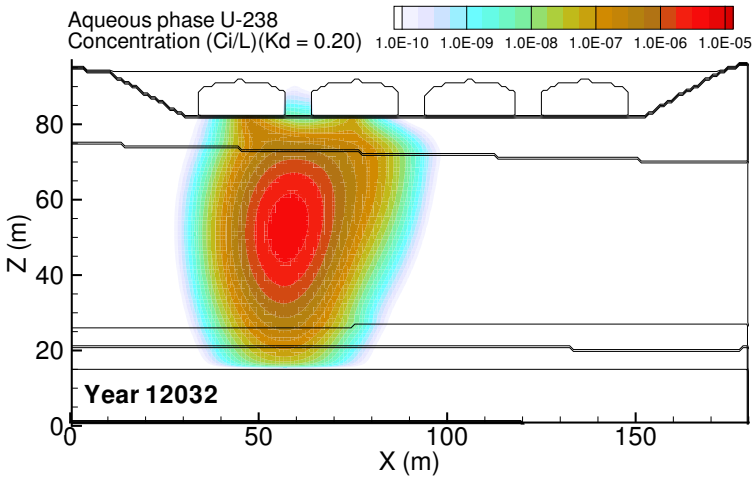

(b)

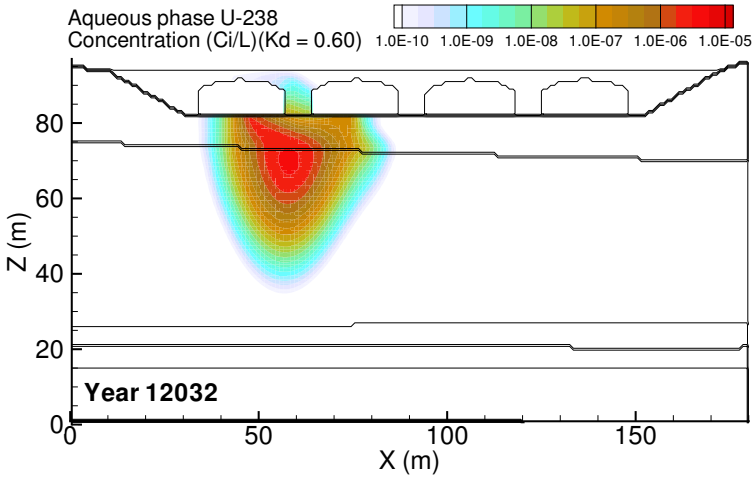

(c)

Figure D.35. Retrieval Leak: Low Aquifer Hydraulic Conductivity (2000 m/d) aqueous concentration distributions at year 12032 for (a) Tc-99, (b) U_0.20 and (c) U_0.60.

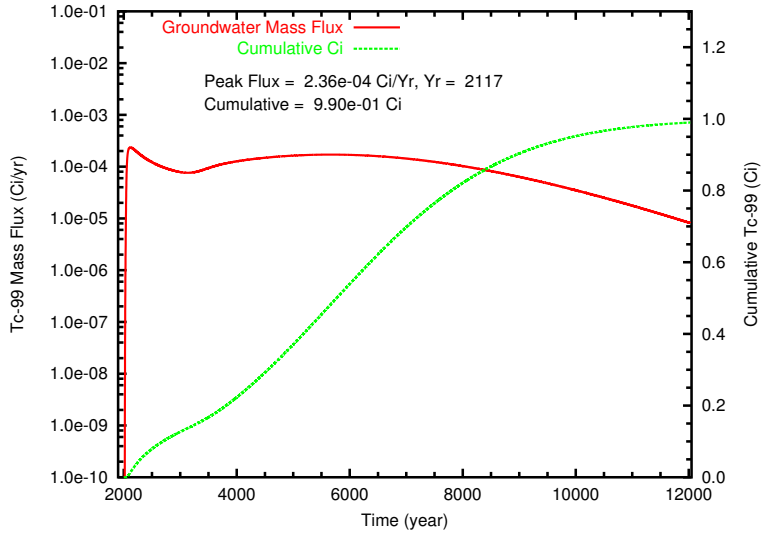

(a)

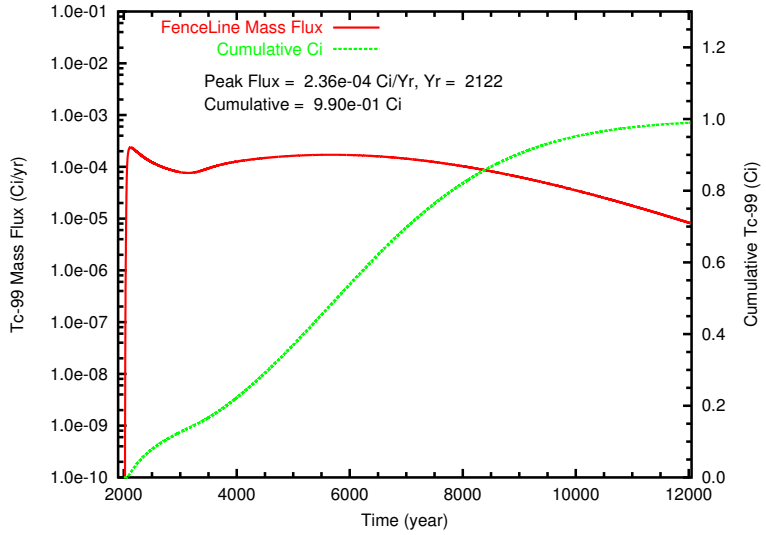

(b)

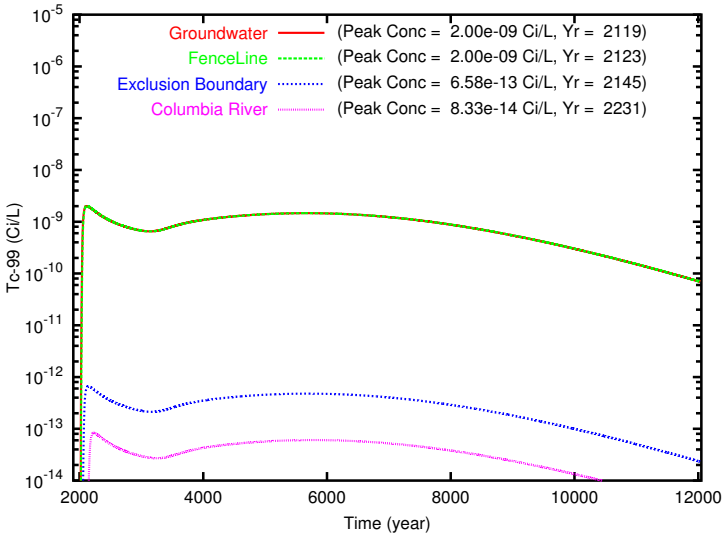

(c)

Figure D.36. Retrieval Leak: Low Aquifer Hydraulic Conductivity (2000 m/d) Tc-99 mass flux at (a) the groundwater table and (b) the fenceline; and (c) the Tc-99 concentration at groundwater, fenceline, and easterly downstream compliance points.

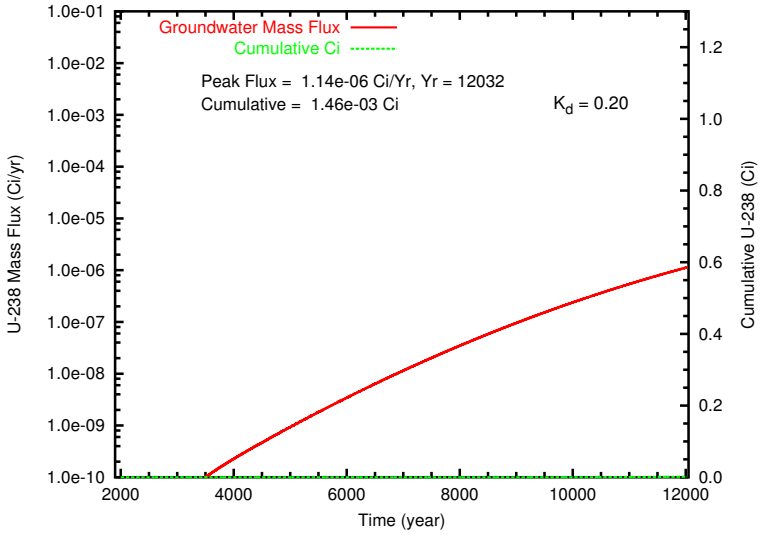

(a)

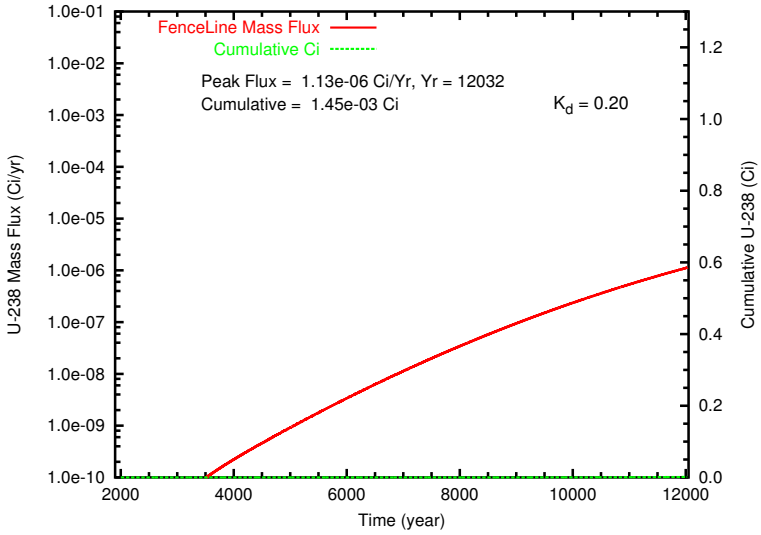

(b)

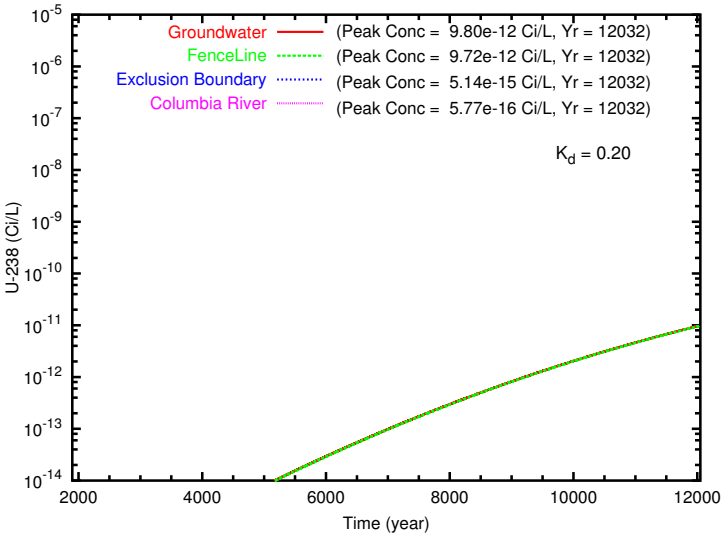

(c)

Figure D.37. Retrieval Leak: Low Aquifer Hydraulic Conductivity (2000 m/d) U_0.20 mass flux at (a) the groundwater table and (b) the fenceline; and (c) the Tc-99 concentration at groundwater, fenceline, and easterly downstream compliance points.

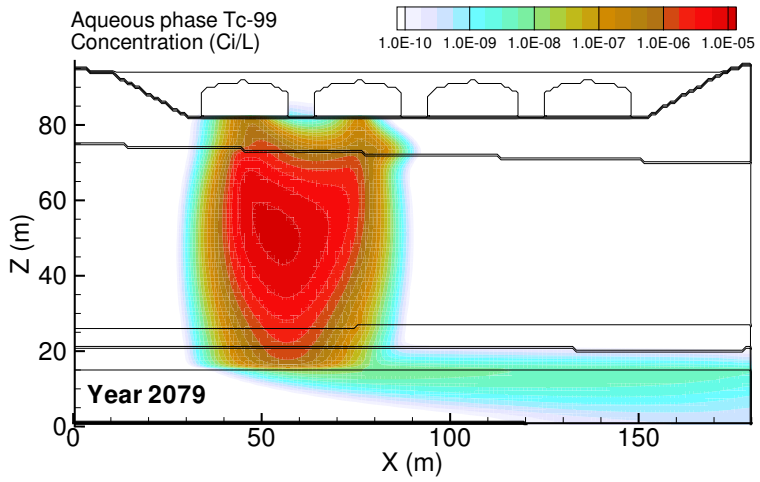

(a)

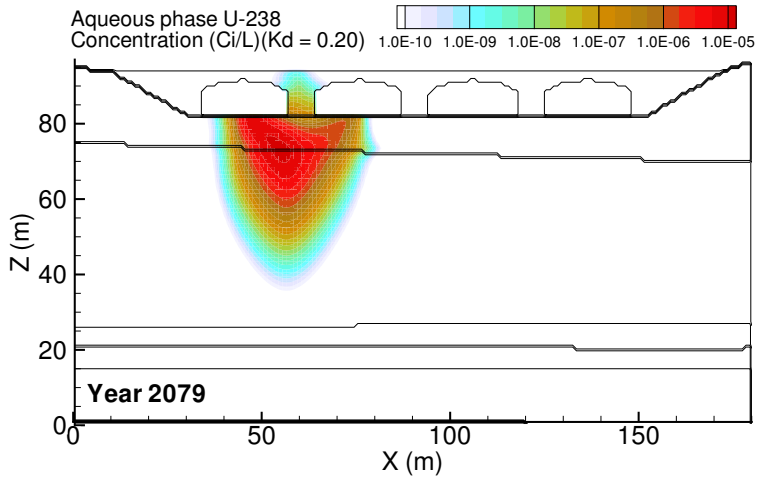

(b)

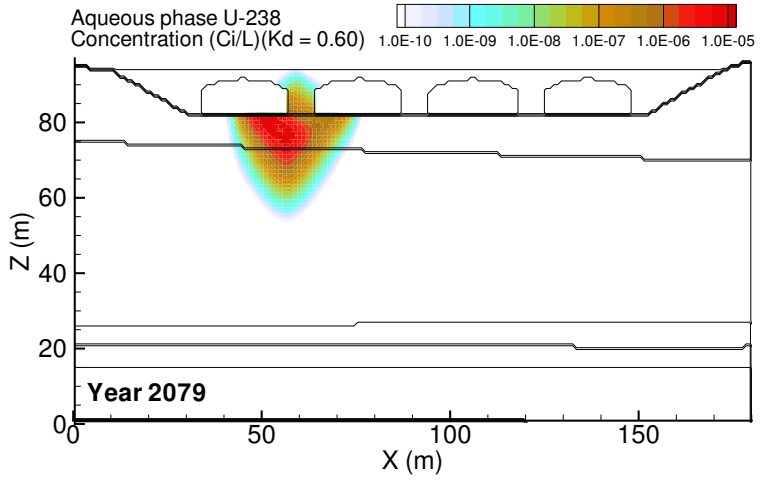

(c)

Figure D.38. Retrieval Leak: High Vadose Zone Hydraulic Conductivity ($K_{sat} \times 10$) aqueous concentration distributions at year 2079 for (a) Tc-99, (b) U_0.20 and (c) U_0.60. Year of Tc-99 peak concentration at fenceline was 2079.

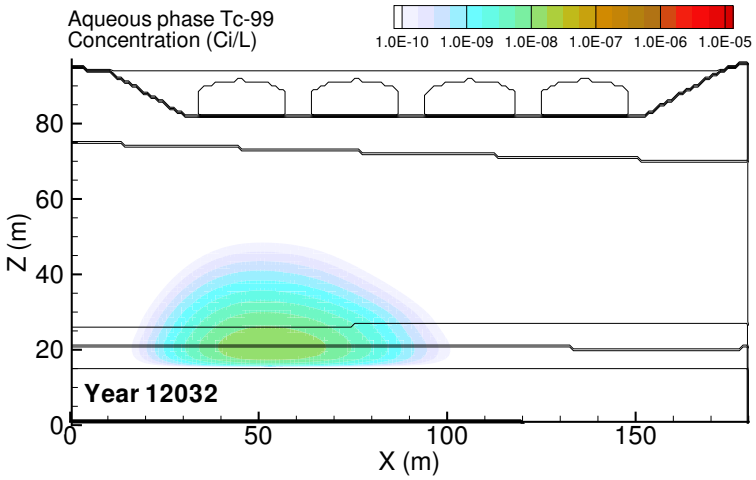

(a)

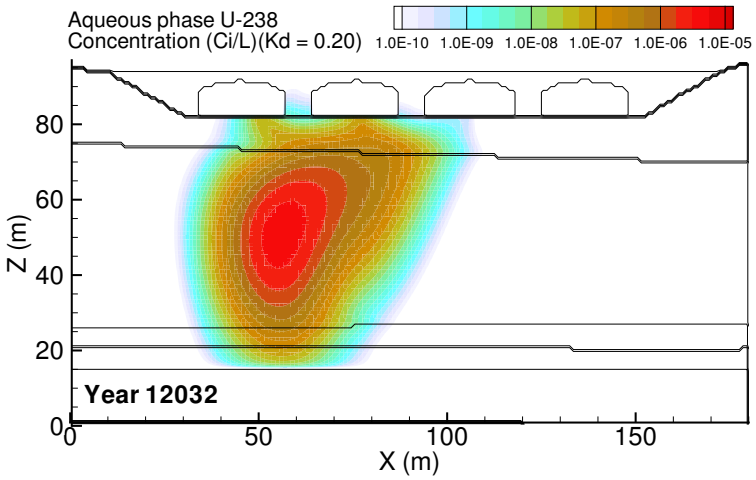

(b)

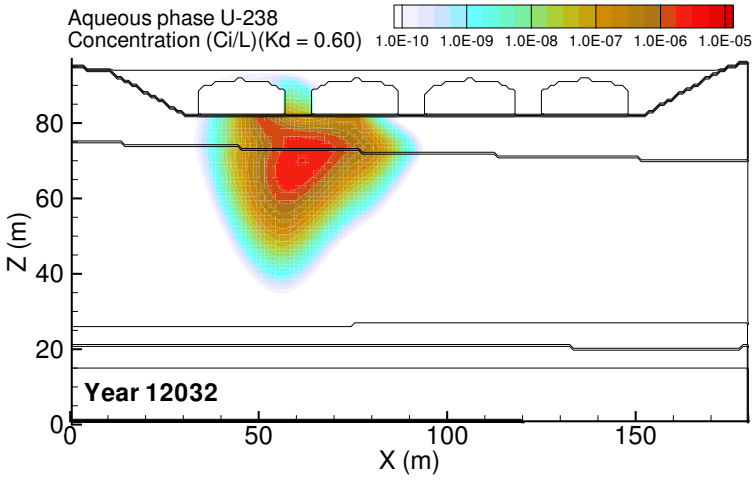

(c)

Figure D.39. Retrieval Leak: High Vadose Zone Hydraulic Conductivity ($K_{sat} \times 10$) aqueous concentration distributions at year 12032 for (a) Tc-99, (b) U_0.20 and (c) U_0.60.

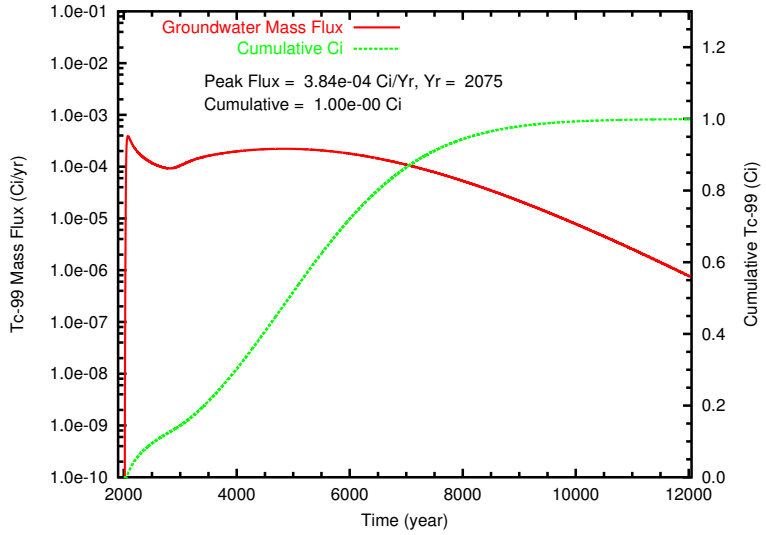

(a)

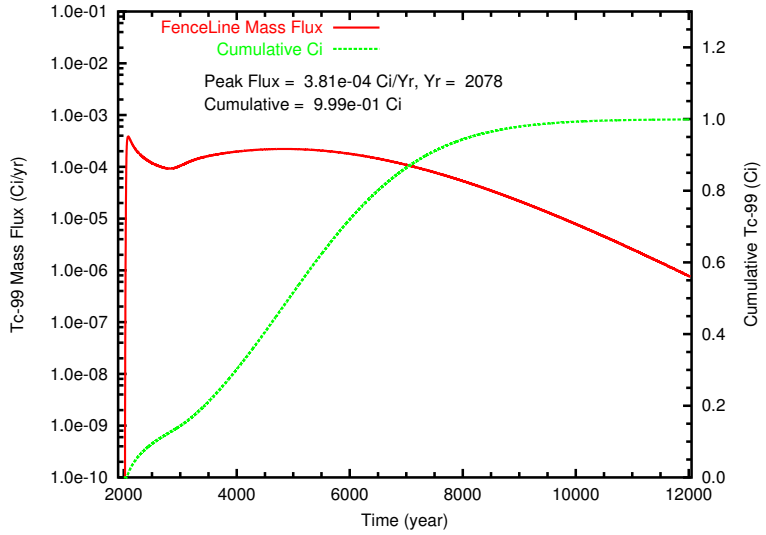

(b)

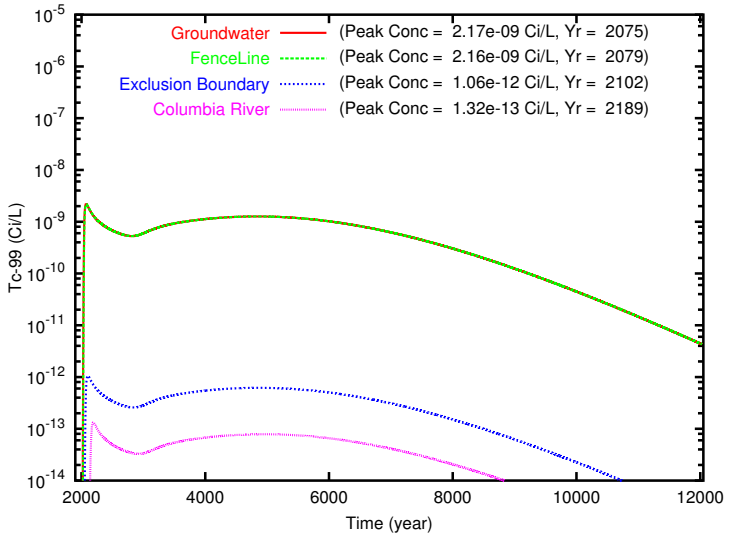

(c)

Figure D.40. Retrieval Leak: High Vadose Zone Hydraulic Conductivity ($K_{sat} \times 10$) Tc-99 mass flux at (a) the groundwater table and (b) the fenceline; and (c) the Tc-99 concentration at groundwater, fenceline, and easterly downstream compliance points.

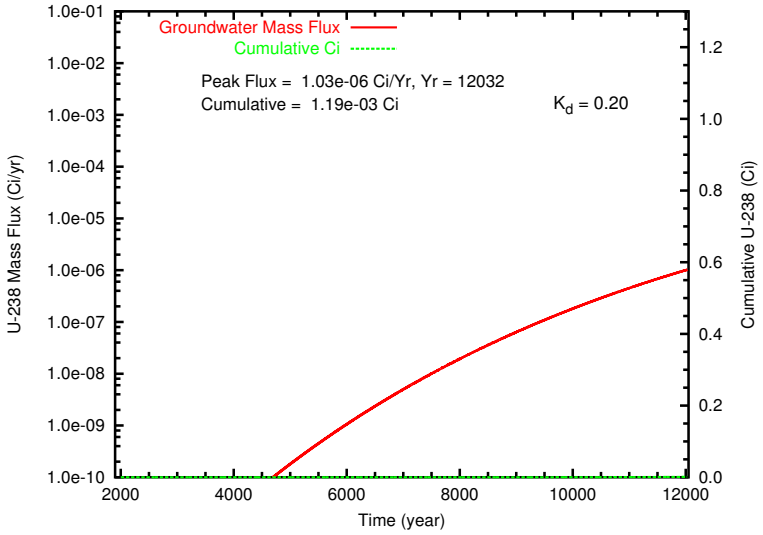

(a)

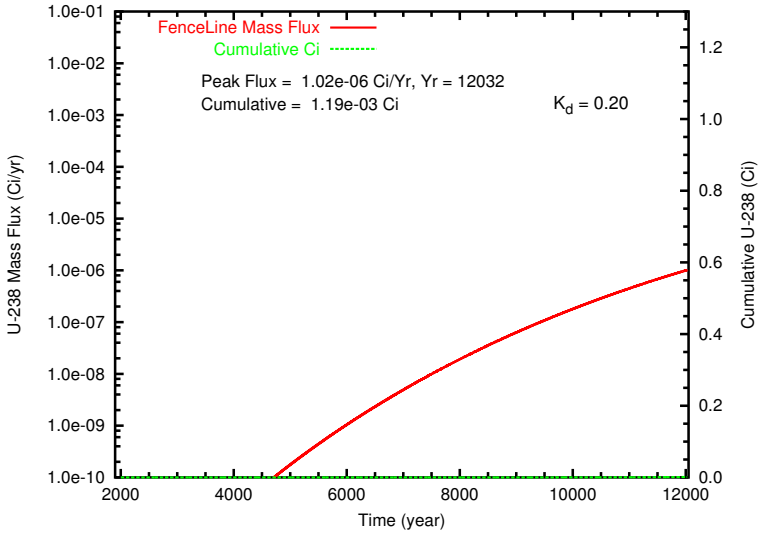

(b)

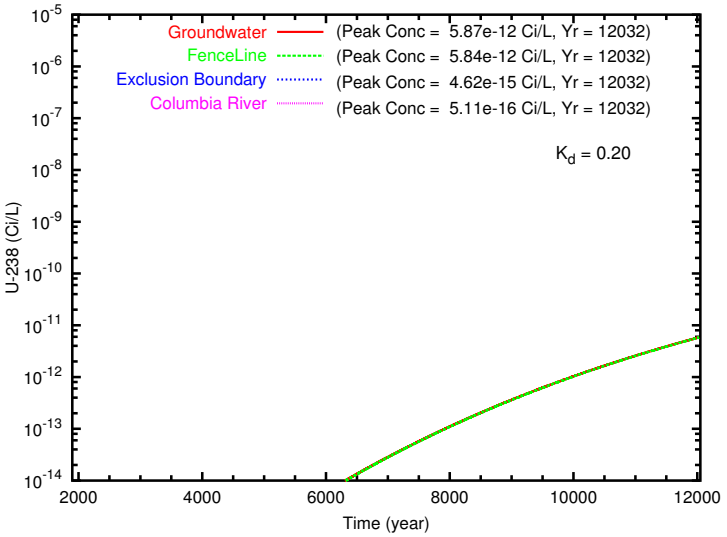

(c)

Figure D.41. Retrieval Leak: High Vadose Zone Hydraulic Conductivity ($K_{sat} \times 10$) U_0.20 mass flux at (a) the groundwater table and (b) the fenceline; and (c) the Tc-99 concentration at groundwater, fenceline, and easterly downstream compliance points.

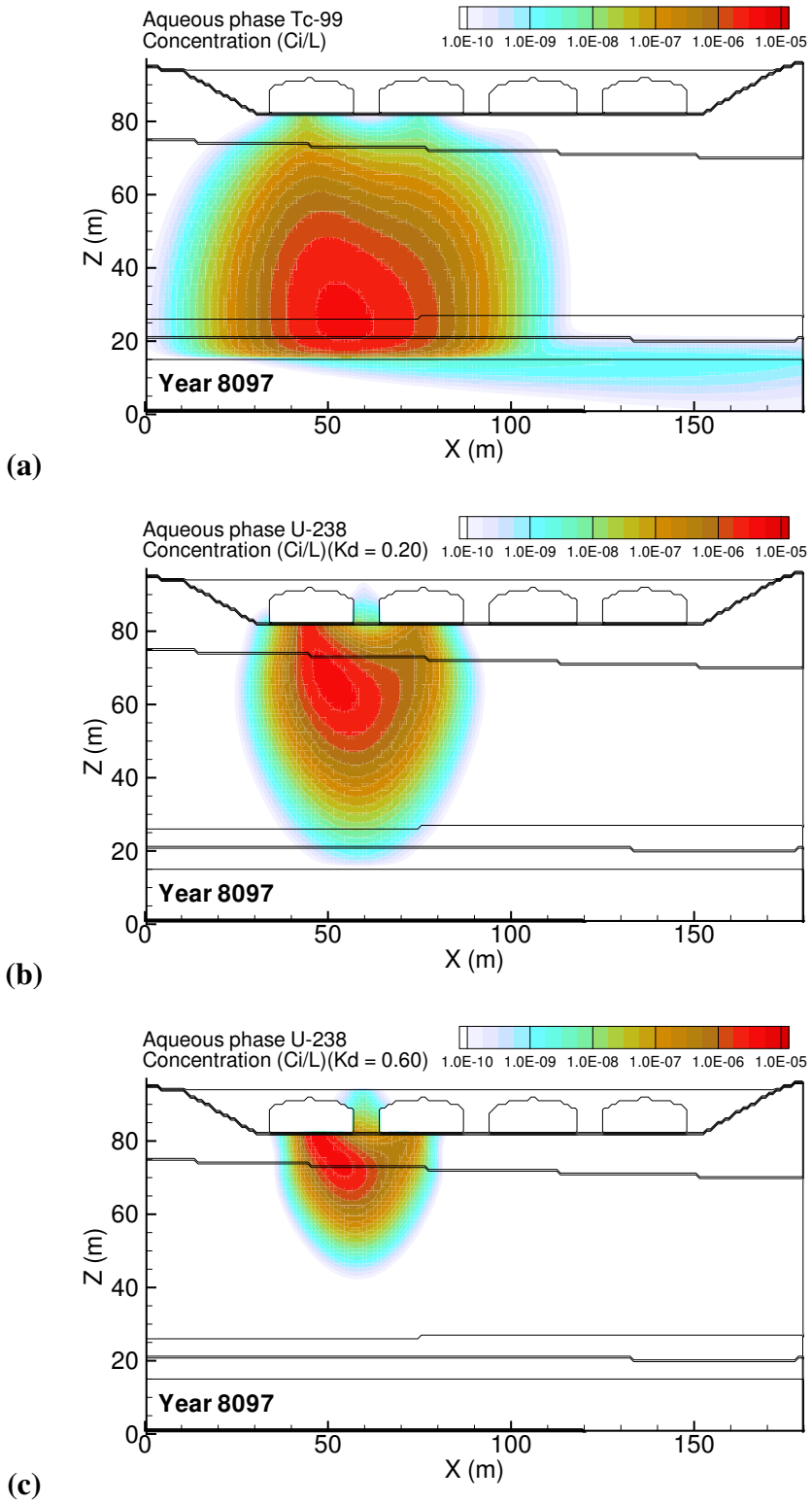

Figure D.42. Retrieval Leak: Low Vadose Zone Hydraulic Conductivity ($K_{sat} \times 0.1$) aqueous concentration distributions at year 8097 for (a) Tc-99, (b) U_0.20 and (c) U_0.60. Year of Tc-99 peak concentration at fenceline was 8097.

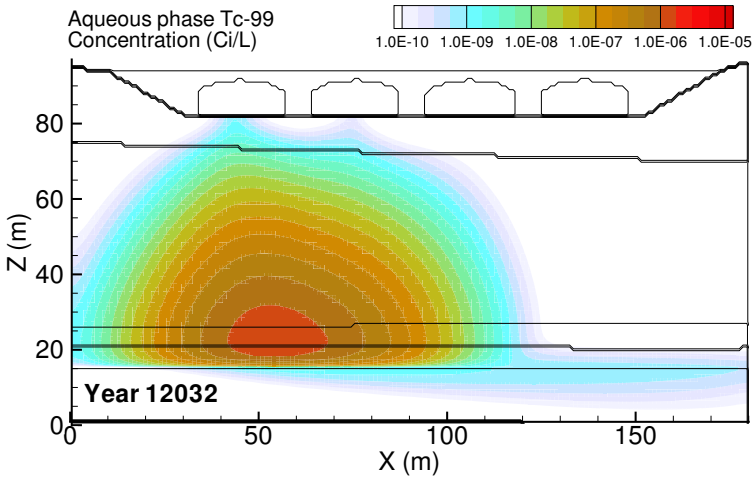

(a)

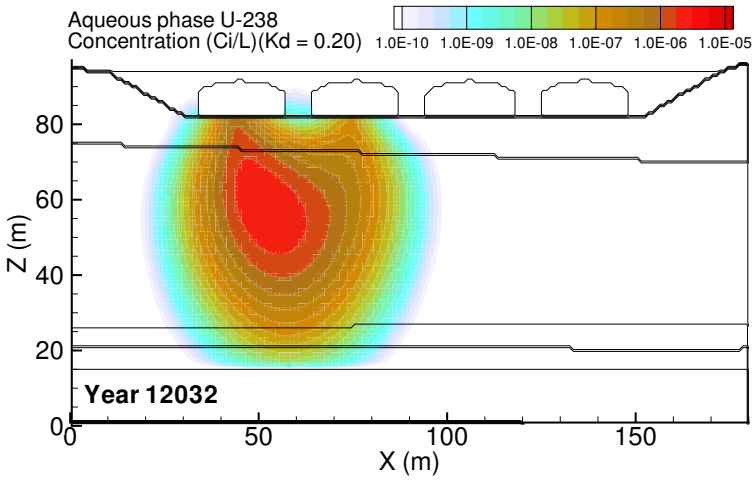

(b)

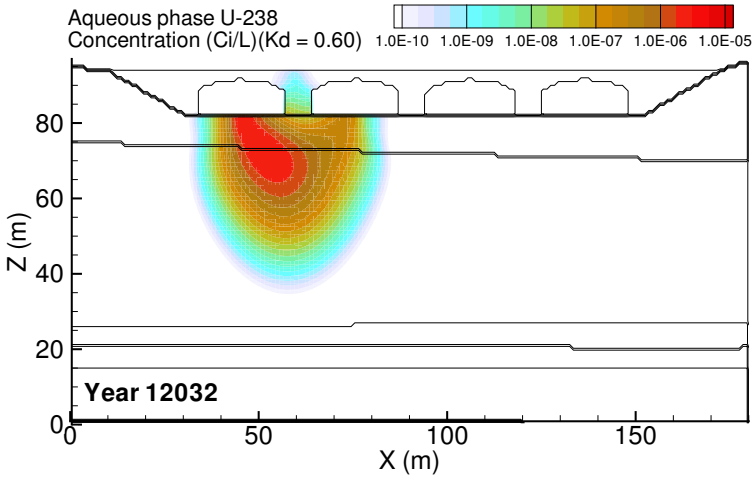

(c)

Figure D.43. Retrieval Leak: Low Vadose Zone Hydraulic Conductivity ($K_{\text{sat}} \times 0.1$) aqueous concentration distributions at year 12032 for (a) Tc-99, (b) U_0.20 and (c) U_0.60.

Appendix F

Peak Concentration, Mass Flux and Mass Balance Tables

Table F.1. Predicted Peak Tc-99 Flux (Ci/yr), Arrival Time, and Cumulative Mass (Ci) at Year 12032 for Case 1 (Past Leak)

Sub-Case		Groundwater			Fenceline		
		Flux	Time	Cm Mass	Flux	Time	Cm Mass
base		1.49E-02	2048	1.0069	1.46E-02	2051	1.0034
recharge	high	2.62E-02	2039	1.0098	2.59E-02	2042	1.0042
	low	2.10E-03	2116	1.0003	2.10E-03	2118	1.0002
barrier	high	1.49E-02	2048	1.0069	1.47E-02	2051	1.0034
	low	1.49E-02	2048	1.0069	1.46E-02	2051	1.0034
barrier_deg	high	1.49E-02	2048	1.0069	1.46E-02	2051	1.0034
	low	1.49E-02	2048	1.0061	1.46E-02	2051	1.0026
plume	high	8.44E-03	2055	1.0048	8.33E-03	2057	1.0024
	low	2.34E-02	2041	1.0071	2.32E-02	2044	1.0033
ksat_aq	high	1.49E-02	2048	1.0069	1.47E-02	2050	1.0033
	low	1.48E-02	2048	1.0069	1.45E-02	2052	1.0035
ksat_vz	high	2.52E-02	2039	1.0101	2.48E-02	2041	1.0032
	low	8.33E-03	2059	1.0038	8.25E-03	2062	1.0018

Table F.2. Predicted Peak Tc-99 Flux (Ci/yr), Arrival Time, and Cumulative Mass (Ci) at Year 12032 for Case 2 (Diffusion)

Sub-Case		Groundwater			Fenceline		
		Flux	Time	Cm Mass	Flux	Time	Cm Mass
base		2.87E-05	10480	0.1125	2.87E-05	10482	0.1124
recharge	high	2.87E-05	10479	0.1125	2.87E-05	10482	0.1125
	low	2.88E-05	10480	0.1125	2.88E-05	10482	0.1124
barrier	high	2.81E-05	10455	0.1133	2.81E-05	10457	0.1132
	low	2.93E-05	10514	0.1118	2.93E-05	10517	0.1117
barrier_deg	high	5.92E-05	5001	0.2104	5.92E-05	5004	0.2103
	low	7.33E-06	12032	0.0099	7.32E-06	12032	0.0099
diffusion	high	9.09E-05	10480	0.3558	9.09E-05	10483	0.3556
	low	9.09E-08	10479	0.0004	9.09E-08	10482	0.0004
ksat_aq	high	2.87E-05	10480	0.1125	2.87E-05	10482	0.1125
	low	2.87E-05	10479	0.1125	2.87E-05	10484	0.1124
ksat_vz	high	3.31E-05	9002	0.1459	3.31E-05	9005	0.1458
	low	2.21E-05	12032	0.0579	2.21E-05	12032	0.0578

Table F.3. Predicted Peak Tc-99 Flux (Ci/yr), Arrival Time, and Cumulative Mass (Ci) at Year 12032 for Case 3 (Retrieval Leak)

Sub-Case		Groundwater			Fenceline		
		Flux	Time	Cm Mass	Flux	Time	Cm Mass
base		2.36E-04	2117	0.9904	2.36E-04	2120	0.9903
recharge	high	6.54E-04	2080	0.9946	6.52E-04	2086	0.9943
	low	1.93E-04	6962	0.9767	1.93E-04	6963	0.9766
barrier	high	2.37E-04	2118	0.9922	2.37E-04	2121	0.9921
	low	2.35E-04	2117	0.9887	2.35E-04	2120	0.9886
barrier_deg	high	5.78E-04	3735	1.0001	5.78E-04	3738	1.0001
	low	2.36E-04	2117	0.8050	2.36E-04	2120	0.8048
ksat_aq	high	2.36E-04	2117	0.9904	2.36E-04	2119	0.9903
	low	2.36E-04	2117	0.9904	2.36E-04	2122	0.9903
ksat_vz	high	3.84E-04	2075	0.9997	3.81E-04	2078	0.9994
	low	1.27E-04	8096	0.8465	1.27E-04	8098	0.8463

Table F.4. Predicted Peak Tc-99 Flux (Ci/yr), Arrival Time, and Cumulative Mass (Ci) at Year 12032 for Case 4 (Ancillary Equipment)

Sub-Case		Groundwater			Fenceline		
		Flux	Time	Cm Mass	Flux	Time	Cm Mass
base		1.80E-04	5713	0.9899	1.80E-04	5715	0.9898
recharge	high	6.78E-04	2091	0.9955	6.77E-04	2094	0.9954
	low	2.14E-04	7536	0.9642	2.14E-04	7539	0.9641
barrier	high	1.80E-04	5471	0.9917	1.80E-04	5474	0.9917
	low	1.80E-04	5909	0.9881	1.80E-04	5913	0.9880
barrier_deg	high	6.05E-04	3757	1.0000	6.05E-04	3760	1.0000
	low	1.35E-04	2193	0.7950	1.35E-04	2196	0.7948
ksat_aq	high	1.80E-04	5713	0.9899	1.80E-04	5714	0.9898
	low	1.80E-04	5713	0.9899	1.80E-04	5716	0.9898
ksat_vz	high	2.63E-04	2093	0.9997	2.61E-04	2097	0.9995
	low	1.25E-04	7157	0.8916	1.25E-04	7160	0.8915

Table F.5. Predicted Peak U-238 (Kd = 0.02) Flux (Ci/yr), Arrival Time, and Cumulative Mass (Ci) at Year 12032 for Case 1 (Past Leak)

Sub-Case		Groundwater			Fenceline		
		Flux	Time	Cm Mass	Flux	Time	Cm Mass
base		8.30E-03	2053	1.0043	8.17E-03	2056	1.0020
recharge	high	1.78E-02	2042	1.0086	1.74E-02	2045	1.0036
	low	8.43E-04	2152	0.9983	8.43E-04	2156	0.9983
barrier	high	8.30E-03	2053	1.0044	8.18E-03	2056	1.0021
	low	8.29E-03	2053	1.0043	8.17E-03	2056	1.0020
barrier_deg	high	8.30E-03	2053	1.0047	8.17E-03	2056	1.0024
	low	8.30E-03	2053	0.9961	8.17E-03	2056	0.9938
plume	high	3.91E-03	2063	1.0012	3.88E-03	2066	1.0001
	low	1.66E-02	2045	1.0068	1.64E-02	2048	1.0033
ksat_aq	high	8.32E-03	2053	1.0043	8.20E-03	2055	1.0020
	low	8.24E-03	2053	1.0043	8.10E-03	2058	1.0021
ksat_vz	high	1.35E-02	2043	1.0073	1.32E-02	2046	1.0018
	low	5.10E-03	2066	0.9995	5.06E-03	2070	0.9982

Table F.6. Predicted Peak U-238 (Kd = 0.02) Flux (Ci/yr), Arrival Time, and Cumulative Mass (Ci) at Year 12032 for Case 2 (Diffusion)

Sub-Case		Groundwater			Fenceline		
		Flux	Time	Cm Mass	Flux	Time	Cm Mass
base		2.29E-05	12032	0.0507	2.29E-05	12032	0.0506
recharge	high	2.29E-05	12032	0.0507	2.29E-05	12032	0.0506
	low	2.29E-05	12032	0.0506	2.29E-05	12032	0.0505
barrier	high	2.27E-05	12032	0.0522	2.27E-05	12032	0.0521
	low	2.30E-05	12032	0.0493	2.30E-05	12032	0.0492
barrier_deg	high	4.94E-05	5788	0.1996	4.94E-05	5791	0.1996
	low	7.79E-07	12032	0.0007	7.76E-07	12032	0.0007
diffusion	high	7.24E-05	12032	0.1602	7.24E-05	12032	0.1599
	low	7.24E-08	12032	0.0002	7.24E-08	12032	0.0002
ksat_aq	high	2.29E-05	12032	0.0507	2.29E-05	12032	0.0506
	low	2.29E-05	12032	0.0506	2.29E-05	12032	0.0505
ksat_vz	high	2.74E-05	11821	0.0799	2.74E-05	11824	0.0798
	low	1.26E-05	12032	0.0219	1.26E-05	12032	0.0218

Table F.7. Predicted Peak U-238 (Kd = 0.02) Flux (Ci/yr), Arrival Time, and Cumulative Mass (Ci) at Year 12032 for Case 3 (Retrieval Leak)

Sub-Case		Groundwater			Fenceline		
		Flux	Time	Cm Mass	Flux	Time	Cm Mass
base		1.41E-04	7683	0.9010	1.41E-04	7687	0.9009
recharge	high	1.61E-04	2101	0.9315	1.61E-04	2104	0.9313
	low	1.53E-04	9009	0.8191	1.53E-04	9012	0.8188
barrier	high	1.41E-04	7441	0.9126	1.41E-04	7445	0.9125
	low	1.41E-04	7881	0.8907	1.41E-04	7884	0.8905
barrier_deg	high	4.77E-04	4338	1.0000	4.77E-04	4342	1.0000
	low	7.11E-05	11623	0.4821	7.11E-05	11623	0.4818
ksat_aq	high	1.41E-04	7684	0.9011	1.41E-04	7687	0.9009
	low	1.41E-04	7685	0.9010	1.41E-04	7688	0.9008
ksat_vz	high	1.75E-04	6897	0.9677	1.75E-04	6901	0.9676
	low	1.07E-04	10175	0.6192	1.07E-04	10182	0.6188

Table F.8. Predicted Peak U-238 (Kd = 0.02) Flux (Ci/yr), Arrival Time, and Cumulative Mass (Ci) at Year 12032 for Case 4 (Ancillary Equipment)

Sub-Case		Groundwater			Fenceline		
		Flux	Time	Cm Mass	Flux	Time	Cm Mass
base		1.47E-04	7839	0.8917	1.47E-04	7843	0.8915
recharge	high	1.40E-04	2129	0.9370	1.39E-04	2132	0.9369
	low	1.64E-04	9743	0.7448	1.64E-04	9746	0.7445
barrier	high	1.47E-04	7597	0.9042	1.47E-04	7601	0.9041
	low	1.47E-04	8036	0.8805	1.47E-04	8040	0.8803
barrier_deg	high	4.92E-04	4397	1.0000	4.92E-04	4400	1.0000
	low	7.41E-05	11921	0.4452	7.41E-05	11925	0.4450
ksat_aq	high	1.47E-04	7839	0.8917	1.47E-04	7842	0.8916
	low	1.47E-04	7840	0.8917	1.47E-04	7845	0.8914
ksat_vz	high	1.83E-04	6956	0.9673	1.83E-04	6960	0.9672
	low	1.06E-04	9233	0.6989	1.06E-04	9235	0.6987

Table F.9. Predicted Peak U-238 (Kd = 0.10) Flux (Ci/yr), Arrival Time, and Cumulative Mass (Ci) at Year 12032 for Case 1 (Past Leak)

Sub-Case		Groundwater			Fenceline		
		Flux	Time	Cm Mass	Flux	Time	Cm Mass
base		6.02E-04	2089	0.9343	6.01E-04	2095	0.9340
recharge	high	2.18E-03	2058	0.9622	2.14E-03	2064	0.9612
	low	1.27E-04	7171	0.8406	1.27E-04	7175	0.8403
barrier	high	6.03E-04	2089	0.9400	6.02E-04	2095	0.9397
	low	6.01E-04	2089	0.9293	6.00E-04	2094	0.9290
barrier_deg	high	6.02E-04	2089	1.0003	6.01E-04	2095	1.0002
	low	6.02E-04	2089	0.7398	6.01E-04	2095	0.7395
plume	high	1.51E-04	2130	0.8554	1.51E-04	2135	0.8552
	low	2.63E-03	2063	0.9811	2.60E-03	2068	0.9803
ksat_aq	high	6.03E-04	2089	0.9343	6.03E-04	2093	0.9340
	low	6.00E-04	2090	0.9342	5.98E-04	2098	0.9339
ksat_vz	high	5.00E-04	2063	0.9440	4.94E-04	2069	0.9435
	low	6.68E-04	2116	0.9013	6.68E-04	2121	0.9011

Table F.10. Predicted Peak U-238 (Kd = 0.10) Flux (Ci/yr), Arrival Time, and Cumulative Mass (Ci) at Year 12032 for Case 2 (Diffusion)

Sub-Case		Groundwater			Fenceline		
		Flux	Time	Cm Mass	Flux	Time	Cm Mass
base		1.94E-07	12032	0.0001	1.93E-07	12032	0.0001
recharge	high	1.94E-07	12032	0.0001	1.93E-07	12032	0.0001
	low	1.93E-07	12032	0.0001	1.92E-07	12032	0.0001
barrier	high	2.25E-07	12032	0.0002	2.23E-07	12032	0.0002
	low	1.71E-07	12032	0.0001	1.70E-07	12032	0.0001
barrier_deg	high	3.36E-05	9038	0.1459	3.36E-05	9044	0.1458
	low	7.73E-12	12032	0.0000	4.79E-12	12032	0.0000
diffusion	high	6.14E-07	12032	0.0004	6.09E-07	12032	0.0004
	low	6.13E-10	12032	0.0000	6.08E-10	12032	0.0000
ksat_aq	high	1.94E-07	12032	0.0001	1.93E-07	12032	0.0001
	low	1.94E-07	12032	0.0001	1.92E-07	12032	0.0001
ksat_vz	high	2.67E-07	12032	0.0002	2.65E-07	12032	0.0002
	low	1.37E-07	12032	0.0001	1.36E-07	12032	0.0001

Table F.11. Predicted Peak U-238 (Kd = 0.10) Flux (Ci/yr), Arrival Time, and Cumulative Mass (Ci) at Year 12032 for Case 3 (Retrieval Leak)

Sub-Case		Groundwater			Fenceline		
		Flux	Time	Cm Mass	Flux	Time	Cm Mass
base		5.07E-05	12032	0.1198	5.06E-05	12032	0.1195
recharge	high	6.13E-05	12032	0.1759	6.13E-05	12032	0.1756
	low	3.07E-05	12032	0.0531	3.06E-05	12032	0.0529
barrier	high	5.38E-05	12032	0.1325	5.37E-05	12032	0.1322
	low	4.81E-05	12032	0.1100	4.80E-05	12032	0.1098
barrier_deg	high	2.81E-04	6885	0.9948	2.81E-04	6890	0.9947
	low	4.39E-06	12032	0.0111	4.38E-06	12032	0.0111
ksat_aq	high	5.07E-05	12032	0.1198	5.06E-05	12032	0.1196
	low	5.06E-05	12032	0.1197	5.05E-05	12032	0.1193
ksat_vz	high	6.16E-05	12032	0.1373	6.16E-05	12032	0.1369
	low	2.51E-05	12032	0.0526	2.51E-05	12032	0.0525

Table F.12. Predicted Peak U-238 (Kd = 0.10) Flux (Ci/yr), Arrival Time, and Cumulative Mass (Ci) at Year 12032 for Case 4 (Ancillary Equipment)

Sub-Case		Groundwater			Fenceline		
		Flux	Time	Cm Mass	Flux	Time	Cm Mass
base		4.43E-05	12032	0.0902	4.42E-05	12032	0.0900
recharge	high	6.13E-05	12032	0.1704	6.13E-05	12032	0.1700
	low	1.48E-05	12032	0.0174	1.47E-05	12032	0.0173
barrier	high	4.76E-05	12032	0.1014	4.75E-05	12032	0.1011
	low	4.16E-05	12032	0.0818	4.15E-05	12032	0.0816
barrier_deg	high	2.83E-04	7044	0.9935	2.83E-04	7050	0.9935
	low	2.55E-06	12032	0.0050	2.54E-06	12032	0.0050
ksat_aq	high	4.43E-05	12032	0.0903	4.42E-05	12032	0.0901
	low	4.42E-05	12032	0.0902	4.41E-05	12032	0.0899
ksat_vz	high	5.21E-05	12032	0.0960	5.20E-05	12032	0.0958
	low	3.34E-05	12032	0.0792	3.33E-05	12032	0.0790

Table F.13. Predicted Peak U-238 (Kd = 0.20) Flux (Ci/yr), Arrival Time, and Cumulative Mass (Ci) at Year 12032 for Case 1 (Past Leak)

Sub-Case		Groundwater			Fenceline		
		Flux	Time	Cm Mass	Flux	Time	Cm Mass
base		7.95E-05	9613	0.5620	7.95E-05	9621	0.5615
recharge	high	1.33E-04	2092	0.6622	1.33E-04	2100	0.6617
	low	8.11E-05	12032	0.3540	8.11E-05	12032	0.3534
barrier	high	7.96E-05	9369	0.5793	7.96E-05	9376	0.5788
	low	7.95E-05	9811	0.5478	7.95E-05	9819	0.5473
barrier_deg	high	2.74E-04	5000	0.9975	2.74E-04	5007	0.9975
	low	3.82E-05	12032	0.2582	3.82E-05	12032	0.2579
plume	high	7.28E-05	12032	0.3559	7.28E-05	12032	0.3553
	low	2.35E-04	2100	0.7851	2.35E-04	2108	0.7847
ksat_aq	high	7.95E-05	9613	0.5621	7.95E-05	9616	0.5617
	low	7.95E-05	9616	0.5619	7.95E-05	9624	0.5611
ksat_vz	high	8.61E-05	10139	0.5379	8.61E-05	10145	0.5373
	low	6.80E-05	8786	0.5658	6.80E-05	8795	0.5654

Table F.14. Predicted Peak U-238 (Kd = 0.20) Flux (Ci/yr), Arrival Time, and Cumulative Mass (Ci) at Year 12032 for Case 2 (Diffusion)

Sub-Case		Groundwater			Fenceline		
		Flux	Time	Cm Mass	Flux	Time	Cm Mass
base		4.17E-11	12032	0.0000	3.97E-11	12032	0.0000
recharge	high	4.19E-11	12032	0.0000	3.99E-11	12032	0.0000
	low	4.11E-11	12032	0.0000	3.90E-11	12032	0.0000
barrier	high	5.83E-11	12032	0.0000	5.63E-11	12032	0.0000
	low	3.17E-11	12032	0.0000	2.91E-11	12032	0.0000
barrier_deg	high	2.43E-05	12032	0.0499	2.42E-05	12032	0.0497
	low	0.00E+00	12032	0.0000	0.00E+00	12032	0.0000
diffusion	high	1.32E-10	12032	0.0000	1.29E-10	12032	0.0000
	low	0.00E+00	12032	0.0000	0.00E+00	12032	0.0000
ksat_aq	high	4.17E-11	12032	0.0000	3.93E-11	12032	0.0000
	low	4.16E-11	12032	0.0000	3.95E-11	12032	0.0000
ksat_vz	high	2.46E-11	12032	0.0000	2.09E-11	12032	0.0000
	low	1.28E-10	12032	0.0000	1.25E-10	12032	0.0000

Table F.15. Predicted Peak U-238 (Kd = 0.20) Flux (Ci/yr), Arrival Time, and Cumulative Mass (Ci) at Year 12032 for Case 3 (Retrieval Leak)

Sub-Case		Groundwater			Fenceline		
		Flux	Time	Cm Mass	Flux	Time	Cm Mass
base		1.14E-06	12032	0.0015	1.14E-06	12032	0.0015
recharge	high	2.26E-06	12032	0.0033	2.25E-06	12032	0.0033
	low	2.97E-07	12032	0.0003	2.95E-07	12032	0.0003
barrier	high	1.34E-06	12032	0.0018	1.34E-06	12032	0.0017
	low	1.00E-06	12032	0.0013	9.96E-07	12032	0.0012
barrier_deg	high	1.82E-04	10148	0.7217	1.82E-04	10156	0.7207
	low	2.04E-08	12032	0.0000	2.03E-08	12032	0.0000
ksat_aq	high	1.14E-06	12032	0.0015	1.14E-06	12032	0.0015
	low	1.14E-06	12032	0.0015	1.13E-06	12032	0.0014
ksat_vz	high	1.03E-06	12032	0.0012	1.02E-06	12032	0.0012
	low	6.27E-07	12032	0.0008	6.23E-07	12032	0.0008

Table F.16. Predicted Peak U-238 (Kd = 0.20) Flux (Ci/yr), Arrival Time, and Cumulative Mass (Ci) at Year 12032 for Case 4 (Ancillary Equipment)

Sub-Case		Groundwater			Fenceline		
		Flux	Time	Cm Mass	Flux	Time	Cm Mass
base		5.48E-07	12032	0.0006	5.44E-07	12032	0.0006
recharge	high	1.87E-06	12032	0.0025	1.86E-06	12032	0.0025
	low	2.57E-08	12032	0.0000	2.55E-08	12032	0.0000
barrier	high	6.67E-07	12032	0.0007	6.63E-07	12032	0.0007
	low	4.65E-07	12032	0.0005	4.62E-07	12032	0.0005
barrier_deg	high	1.82E-04	10399	0.6853	1.82E-04	10406	0.6843
	low	3.46E-09	12032	0.0000	3.44E-09	12032	0.0000
ksat_aq	high	5.48E-07	12032	0.0006	5.46E-07	12032	0.0006
	low	5.47E-07	12032	0.0006	5.42E-07	12032	0.0006
ksat_vz	high	2.90E-07	12032	0.0003	2.88E-07	12032	0.0003
	low	1.04E-06	12032	0.0014	1.04E-06	12032	0.0014

Table F.17. Predicted Peak U-238 (Kd = 0.60) Flux (Ci/yr), Arrival Time, and Cumulative Mass (Ci) at Year 12032 for Case 1 (Past Leak)

Sub-Case		Groundwater			Fenceline		
		Flux	Time	Cm Mass	Flux	Time	Cm Mass
base		2.76E-06	12032	0.0052	2.74E-06	12032	0.0051
recharge	high	4.97E-06	12032	0.0113	4.94E-06	12032	0.0113
	low	6.50E-07	12032	0.0008	6.42E-07	12032	0.0008
barrier	high	3.04E-06	12032	0.0058	3.02E-06	12032	0.0058
	low	2.55E-06	12032	0.0047	2.53E-06	12032	0.0046
barrier_deg	high	1.14E-04	11109	0.4784	1.14E-04	11128	0.4765
	low	2.00E-07	12032	0.0004	1.99E-07	12032	0.0004
plume	high	3.67E-07	12032	0.0005	3.63E-07	12032	0.0005
	low	1.58E-05	12032	0.0454	1.57E-05	12032	0.0451
ksat_aq	high	2.76E-06	12032	0.0052	2.75E-06	12032	0.0051
	low	2.76E-06	12032	0.0052	2.73E-06	12032	0.0051
ksat_vz	high	1.69E-06	12032	0.0027	1.67E-06	12032	0.0027
	low	5.05E-06	12032	0.0120	5.03E-06	12032	0.0119

Table F.18. Predicted Peak U-238 (Kd = 0.60) Flux (Ci/yr), Arrival Time, and Cumulative Mass (Ci) at Year 12032 for Case 2 (Diffusion)

Sub-Case		Groundwater			Fenceline		
		Flux	Time	Cm Mass	Flux	Time	Cm Mass
base		0.00E+00	12032	0.0000	0.00E+00	12032	0.0000
recharge	high	0.00E+00	12032	0.0000	0.00E+00	12032	0.0000
	low	0.00E+00	12032	0.0000	0.00E+00	12032	0.0000
barrier	high	0.00E+00	12032	0.0000	0.00E+00	12032	0.0000
	low	0.00E+00	12032	0.0000	0.00E+00	12032	0.0000
barrier_deg	high	3.47E-09	12032	0.0000	3.34E-09	12032	0.0000
	low	0.00E+00	12032	0.0000	0.00E+00	12032	0.0000
diffusion	high	0.00E+00	12032	0.0000	0.00E+00	12032	0.0000
	low	0.00E+00	12032	0.0000	0.00E+00	12032	0.0000
ksat_aq	high	0.00E+00	12032	0.0000	0.00E+00	12032	0.0000
	low	0.00E+00	12032	0.0000	0.00E+00	12032	0.0000
ksat_vz	high	0.00E+00	12032	0.0000	0.00E+00	12032	0.0000
	low	0.00E+00	12032	0.0000	0.00E+00	12032	0.0000

Table F.19. Predicted Peak U-238 (Kd = 0.60) Flux (Ci/yr), Arrival Time, and Cumulative Mass (Ci) at Year 12032 for Case 3 (Retrieval Leak)

Sub-Case		Groundwater			Fenceline		
		Flux	Time	Cm Mass	Flux	Time	Cm Mass
base		0.00E+00	12032	0.0000	0.00E+00	12032	0.0000
recharge	high	0.00E+00	12032	0.0000	0.00E+00	12032	0.0000
	low	0.00E+00	12032	0.0000	0.00E+00	12032	0.0000
barrier	high	0.00E+00	12032	0.0000	0.00E+00	12032	0.0000
	low	0.00E+00	12032	0.0000	0.00E+00	12032	0.0000
barrier_deg	high	7.07E-07	12032	0.0005	6.92E-07	12032	0.0005
	low	0.00E+00	12032	0.0000	0.00E+00	12032	0.0000
ksat_aq	high	0.00E+00	12032	0.0000	0.00E+00	12032	0.0000
	low	0.00E+00	12032	0.0000	0.00E+00	12032	0.0000
ksat_vz	high	0.00E+00	12032	0.0000	0.00E+00	12032	0.0000
	low	0.00E+00	12032	0.0000	0.00E+00	12032	0.0000

Table F.20. Predicted Peak U-238 (Kd = 0.60) Flux (Ci/yr), Arrival Time, and Cumulative Mass (Ci) at Year 12032 for Case 4 (Ancillary Equipment)

Sub-Case		Groundwater			Fenceline		
		Flux	Time	Cm Mass	Flux	Time	Cm Mass
base		0.00E+00	12032	0.0000	0.00E+00	12032	0.0000
recharge	high	0.00E+00	12032	0.0000	0.00E+00	12032	0.0000
	low	0.00E+00	12032	0.0000	0.00E+00	12032	0.0000
barrier	high	0.00E+00	12032	0.0000	0.00E+00	12032	0.0000
	low	0.00E+00	12032	0.0000	0.00E+00	12032	0.0000
barrier_deg	high	3.97E-07	12032	0.0003	3.88E-07	12032	0.0003
	low	0.00E+00	12032	0.0000	0.00E+00	12032	0.0000
ksat_aq	high	0.00E+00	12032	0.0000	0.00E+00	12032	0.0000
	low	0.00E+00	12032	0.0000	0.00E+00	12032	0.0000
ksat_vz	high	0.00E+00	12032	0.0000	0.00E+00	12032	0.0000
	low	0.00E+00	12032	0.0000	0.00E+00	12032	0.0000

Table F.21. Predicted Peak U-238 (Kd = 1.00) Flux (Ci/yr), Arrival Time, and Cumulative Mass (Ci) at Year 12032 for Case 1 (Past Leak)

Sub-Case		Groundwater			Fenceline		
		Flux	Time	Cm Mass	Flux	Time	Cm Mass
base		2.20E-08	12032	0.0000	2.16E-08	12032	0.0000
recharge	high	6.34E-08	12032	0.0001	6.24E-08	12032	0.0001
	low	1.93E-09	12032	0.0000	1.88E-09	12032	0.0000
barrier	high	2.58E-08	12032	0.0000	2.54E-08	12032	0.0000
	low	1.92E-08	12032	0.0000	1.89E-08	12032	0.0000
barrier_deg	high	3.55E-05	12032	0.0649	3.52E-05	12032	0.0640
	low	5.60E-10	12032	0.0000	5.51E-10	12032	0.0000
plume	high	5.91E-10	12032	0.0000	5.75E-10	12032	0.0000
	low	7.07E-07	12032	0.0013	6.98E-07	12032	0.0012
ksat_aq	high	2.20E-08	12032	0.0000	2.17E-08	12032	0.0000
	low	2.20E-08	12032	0.0000	2.13E-08	12032	0.0000
ksat_vz	high	7.93E-09	12032	0.0000	7.75E-09	12032	0.0000
	low	9.44E-08	12032	0.0001	9.30E-08	12032	0.0001

Table F.22. Predicted Peak U-238 (Kd = 1.00) Flux (Ci/yr), Arrival Time, and Cumulative Mass (Ci) at Year 12032 for Case 2 (Diffusion)

Sub-Case		Groundwater			Fenceline		
		Flux	Time	Cm Mass	Flux	Time	Cm Mass
base		0.00E+00	12032	0.0000	0.00E+00	12032	0.0000
recharge	high	0.00E+00	12032	0.0000	0.00E+00	12032	0.0000
	low	0.00E+00	12032	0.0000	0.00E+00	12032	0.0000
barrier	high	0.00E+00	12032	0.0000	0.00E+00	12032	0.0000
	low	0.00E+00	12032	0.0000	0.00E+00	12032	0.0000
barrier_deg	high	0.00E+00	12032	0.0000	0.00E+00	12032	0.0000
	low	0.00E+00	12032	0.0000	0.00E+00	12032	0.0000
diffusion	high	0.00E+00	12032	0.0000	0.00E+00	12032	0.0000
	low	0.00E+00	12032	0.0000	0.00E+00	12032	0.0000
ksat_aq	high	0.00E+00	12032	0.0000	0.00E+00	12032	0.0000
	low	0.00E+00	12032	0.0000	0.00E+00	12032	0.0000
ksat_vz	high	0.00E+00	12032	0.0000	0.00E+00	12032	0.0000
	low	0.00E+00	12032	0.0000	0.00E+00	12032	0.0000

Table F.23. Predicted Peak U-238 (Kd = 1.00) Flux (Ci/yr), Arrival Time, and Cumulative Mass (Ci) at Year 12032 for Case 3 (Retrieval Leak)

Sub-Case		Groundwater			Fenceline		
		Flux	Time	Cm Mass	Flux	Time	Cm Mass
base		0.00E+00	12032	0.0000	0.00E+00	12032	0.0000
recharge	high	0.00E+00	12032	0.0000	0.00E+00	12032	0.0000
	low	0.00E+00	12032	0.0000	0.00E+00	12032	0.0000
barrier	high	0.00E+00	12032	0.0000	0.00E+00	12032	0.0000
	low	0.00E+00	12032	0.0000	0.00E+00	12032	0.0000
barrier_deg	high	8.88E-11	12032	0.0000	8.33E-11	12032	0.0000
	low	0.00E+00	12032	0.0000	0.00E+00	12032	0.0000
ksat_aq	high	0.00E+00	12032	0.0000	0.00E+00	12032	0.0000
	low	0.00E+00	12032	0.0000	0.00E+00	12032	0.0000
ksat_vz	high	0.00E+00	12032	0.0000	0.00E+00	12032	0.0000
	low	0.00E+00	12032	0.0000	0.00E+00	12032	0.0000

Table F.24. Predicted Peak U-238 (Kd = 1.00) Flux (Ci/yr), Arrival Time, and Cumulative Mass (Ci) at Year 12032 for Case 4 (Ancillary Equipment)

Sub-Case		Groundwater			Fenceline		
		Flux	Time	Cm Mass	Flux	Time	Cm Mass
base		0.00E+00	12032	0.0000	0.00E+00	12032	0.0000
recharge	high	0.00E+00	12032	0.0000	0.00E+00	12032	0.0000
	low	0.00E+00	12032	0.0000	0.00E+00	12032	0.0000
barrier	high	0.00E+00	12032	0.0000	0.00E+00	12032	0.0000
	low	0.00E+00	12032	0.0000	0.00E+00	12032	0.0000
barrier_deg	high	2.64E-11	12032	0.0000	2.35E-11	12032	0.0000
	low	0.00E+00	12032	0.0000	0.00E+00	12032	0.0000
ksat_aq	high	0.00E+00	12032	0.0000	0.00E+00	12032	0.0000
	low	0.00E+00	12032	0.0000	0.00E+00	12032	0.0000
ksat_vz	high	0.00E+00	12032	0.0000	0.00E+00	12032	0.0000
	low	0.00E+00	12032	0.0000	0.00E+00	12032	0.0000

Table F.25. Predicted Peak U-238 (Kd = 2.00) Flux (Ci/yr), Arrival Time, and Cumulative Mass (Ci) at Year 12032 for Case 1 (Past Leak)

Sub-Case		Groundwater			Fenceline		
		Flux	Time	Cm Mass	Flux	Time	Cm Mass
base		4.02E-13	12032	0.0000	0.00E+00	12032	0.0000
recharge	high	2.56E-12	12032	0.0000	1.42E-12	12032	0.0000
	low	0.00E+00	12032	0.0000	0.00E+00	12032	0.0000
barrier	high	5.24E-13	12032	0.0000	0.00E+00	12032	0.0000
	low	3.21E-13	12032	0.0000	0.00E+00	12032	0.0000
barrier_deg	high	1.56E-07	12032	0.0001	1.49E-07	12032	0.0001
	low	0.00E+00	12032	0.0000	0.00E+00	12032	0.0000
plume	high	0.00E+00	12032	0.0000	0.00E+00	12032	0.0000
	low	3.28E-10	12032	0.0000	3.15E-10	12032	0.0000
ksat_aq	high	4.02E-13	12032	0.0000	0.00E+00	12032	0.0000
	low	4.01E-13	12032	0.0000	0.00E+00	12032	0.0000
ksat_vz	high	3.64E-14	12032	0.0000	0.00E+00	12032	0.0000
	low	7.40E-12	12032	0.0000	5.95E-12	12032	0.0000

Table F.26. Predicted Peak U-238 (Kd = 2.00) Flux (Ci/yr), Arrival Time, and Cumulative Mass (Ci) at Year 12032 for Case 2 (Diffusion)

Sub-Case		Groundwater			Fenceline		
		Flux	Time	Cm Mass	Flux	Time	Cm Mass
base		0.00E+00	12032	0.0000	0.00E+00	12032	0.0000
recharge	high	0.00E+00	12032	0.0000	0.00E+00	12032	0.0000
	low	0.00E+00	12032	0.0000	0.00E+00	12032	0.0000
barrier	high	0.00E+00	12032	0.0000	0.00E+00	12032	0.0000
	low	0.00E+00	12032	0.0000	0.00E+00	12032	0.0000
barrier_deg	high	0.00E+00	12032	0.0000	0.00E+00	12032	0.0000
	low	0.00E+00	12032	0.0000	0.00E+00	12032	0.0000
diffusion	high	0.00E+00	12032	0.0000	0.00E+00	12032	0.0000
	low	0.00E+00	12032	0.0000	0.00E+00	12032	0.0000
ksat_aq	high	0.00E+00	12032	0.0000	0.00E+00	12032	0.0000
	low	0.00E+00	12032	0.0000	0.00E+00	12032	0.0000
ksat_vz	high	0.00E+00	12032	0.0000	0.00E+00	12032	0.0000
	low	0.00E+00	12032	0.0000	0.00E+00	12032	0.0000

Table F.27. Predicted Peak U-238 (Kd = 2.00) Flux (Ci/yr), Arrival Time, and Cumulative Mass (Ci) at Year 12032 for Case 3 (Retrieval Leak)

Sub-Case		Groundwater			Fenceline		
		Flux	Time	Cm Mass	Flux	Time	Cm Mass
base		0.00E+00	12032	0.0000	0.00E+00	12032	0.0000
recharge	high	0.00E+00	12032	0.0000	0.00E+00	12032	0.0000
	low	0.00E+00	12032	0.0000	0.00E+00	12032	0.0000
barrier	high	0.00E+00	12032	0.0000	0.00E+00	12032	0.0000
	low	0.00E+00	12032	0.0000	0.00E+00	12032	0.0000
barrier_deg	high	0.00E+00	12032	0.0000	0.00E+00	12032	0.0000
	low	0.00E+00	12032	0.0000	0.00E+00	12032	0.0000
ksat_aq	high	0.00E+00	12032	0.0000	0.00E+00	12032	0.0000
	low	0.00E+00	12032	0.0000	0.00E+00	12032	0.0000
ksat_vz	high	0.00E+00	12032	0.0000	0.00E+00	12032	0.0000
	low	0.00E+00	12032	0.0000	0.00E+00	12032	0.0000

Table F.28. Predicted Peak U-238 (Kd = 2.00) Flux (Ci/yr), Arrival Time, and Cumulative Mass (Ci) at Year 12032 for Case 4 (Ancillary Equipment)

Sub-Case		Groundwater			Fenceline		
		Flux	Time	Cm Mass	Flux	Time	Cm Mass
base		0.00E+00	12032	0.0000	0.00E+00	12032	0.0000
recharge	high	0.00E+00	12032	0.0000	0.00E+00	12032	0.0000
	low	0.00E+00	12032	0.0000	0.00E+00	12032	0.0000
barrier	high	0.00E+00	12032	0.0000	0.00E+00	12032	0.0000
	low	0.00E+00	12032	0.0000	0.00E+00	12032	0.0000
barrier_deg	high	0.00E+00	12032	0.0000	0.00E+00	12032	0.0000
	low	0.00E+00	12032	0.0000	0.00E+00	12032	0.0000
ksat_aq	high	0.00E+00	12032	0.0000	0.00E+00	12032	0.0000
	low	0.00E+00	12032	0.0000	0.00E+00	12032	0.0000
ksat_vz	high	0.00E+00	12032	0.0000	0.00E+00	12032	0.0000
	low	0.00E+00	12032	0.0000	0.00E+00	12032	0.0000

Table F.29. Predicted Peak U-238 (Kd = 5.00) Flux (Ci/yr), Arrival Time, and Cumulative Mass (Ci) at Year 12032 for Case 1 (Past Leak)

Sub-Case		Groundwater			Fenceline		
		Flux	Time	Cm Mass	Flux	Time	Cm Mass
base		0.00E+00	12032	0.0000	0.00E+00	12032	0.0000
recharge	high	0.00E+00	12032	0.0000	0.00E+00	12032	0.0000
	low	0.00E+00	12032	0.0000	0.00E+00	12032	0.0000
barrier	high	0.00E+00	12032	0.0000	0.00E+00	12032	0.0000
	low	0.00E+00	12032	0.0000	0.00E+00	12032	0.0000
barrier_deg	high	1.87E-14	12032	0.0000	0.00E+00	12032	0.0000
	low	0.00E+00	12032	0.0000	0.00E+00	12032	0.0000
plume	high	0.00E+00	12032	0.0000	0.00E+00	12032	0.0000
	low	0.00E+00	12032	0.0000	0.00E+00	12032	0.0000
ksat_aq	high	0.00E+00	12032	0.0000	0.00E+00	12032	0.0000
	low	0.00E+00	12032	0.0000	0.00E+00	12032	0.0000
ksat_vz	high	0.00E+00	12032	0.0000	0.00E+00	12032	0.0000
	low	0.00E+00	12032	0.0000	0.00E+00	12032	0.0000

Table F.30. Predicted Peak U-238 (Kd = 5.00) Flux (Ci/yr), Arrival Time, and Cumulative Mass (Ci) at Year 12032 for Case 2 (Diffusion)

Sub-Case		Groundwater			Fenceline		
		Flux	Time	Cm Mass	Flux	Time	Cm Mass
base		0.00E+00	12032	0.0000	0.00E+00	12032	0.0000
recharge	high	0.00E+00	12032	0.0000	0.00E+00	12032	0.0000
	low	0.00E+00	12032	0.0000	0.00E+00	12032	0.0000
barrier	high	0.00E+00	12032	0.0000	0.00E+00	12032	0.0000
	low	0.00E+00	12032	0.0000	0.00E+00	12032	0.0000
barrier_deg	high	0.00E+00	12032	0.0000	0.00E+00	12032	0.0000
	low	0.00E+00	12032	0.0000	0.00E+00	12032	0.0000
diffusion	high	0.00E+00	12032	0.0000	0.00E+00	12032	0.0000
	low	0.00E+00	12032	0.0000	0.00E+00	12032	0.0000
ksat_aq	high	0.00E+00	12032	0.0000	0.00E+00	12032	0.0000
	low	0.00E+00	12032	0.0000	0.00E+00	12032	0.0000
ksat_vz	high	0.00E+00	12032	0.0000	0.00E+00	12032	0.0000
	low	0.00E+00	12032	0.0000	0.00E+00	12032	0.0000

Table F.31. Predicted Peak U-238 (Kd = 5.00) Flux (Ci/yr), Arrival Time, and Cumulative Mass (Ci) at Year 12032 for Case 3 (Retrieval Leak)

Sub-Case		Groundwater			Fenceline		
		Flux	Time	Cm Mass	Flux	Time	Cm Mass
base		0.00E+00	12032	0.0000	0.00E+00	12032	0.0000
recharge	high	0.00E+00	12032	0.0000	0.00E+00	12032	0.0000
	low	0.00E+00	12032	0.0000	0.00E+00	12032	0.0000
barrier	high	0.00E+00	12032	0.0000	0.00E+00	12032	0.0000
	low	0.00E+00	12032	0.0000	0.00E+00	12032	0.0000
barrier_deg	high	0.00E+00	12032	0.0000	0.00E+00	12032	0.0000
	low	0.00E+00	12032	0.0000	0.00E+00	12032	0.0000
ksat_aq	high	0.00E+00	12032	0.0000	0.00E+00	12032	0.0000
	low	0.00E+00	12032	0.0000	0.00E+00	12032	0.0000
ksat_vz	high	0.00E+00	12032	0.0000	0.00E+00	12032	0.0000
	low	0.00E+00	12032	0.0000	0.00E+00	12032	0.0000

Table F.32. Predicted Peak U-238 (Kd = 5.00) Flux (Ci/yr), Arrival Time, and Cumulative Mass (Ci) at Year 12032 for Case 4 (Ancillary Equipment)

Sub-Case		Groundwater			Fenceline		
		Flux	Time	Cm Mass	Flux	Time	Cm Mass
base		0.00E+00	12032	0.0000	0.00E+00	12032	0.0000
recharge	high	0.00E+00	12032	0.0000	0.00E+00	12032	0.0000
	low	0.00E+00	12032	0.0000	0.00E+00	12032	0.0000
barrier	high	0.00E+00	12032	0.0000	0.00E+00	12032	0.0000
	low	0.00E+00	12032	0.0000	0.00E+00	12032	0.0000
barrier_deg	high	0.00E+00	12032	0.0000	0.00E+00	12032	0.0000
	low	0.00E+00	12032	0.0000	0.00E+00	12032	0.0000
ksat_aq	high	0.00E+00	12032	0.0000	0.00E+00	12032	0.0000
	low	0.00E+00	12032	0.0000	0.00E+00	12032	0.0000
ksat_vz	high	0.00E+00	12032	0.0000	0.00E+00	12032	0.0000
	low	0.00E+00	12032	0.0000	0.00E+00	12032	0.0000

Table F.33. Predicted Peak Tc-99 Aqueous Concentration (Ci/L) and Arrival Time (yr) Summary for Case 1 (Past Leak)

Sub-Case		Groundwater		Fenceline		Excl (East)		Col River (East)		Excl (North)		Col River (North)	
		Conc.	Time	Conc.	Time	Conc.	Time	Conc.	Time	Conc.	Time	Conc.	Time
base		8.16E-08	2048	8.07E-08	2051	3.79E-11	2075	4.27E-12	2161	1.89E-11	2055	4.09E-12	2131
recharge	high	1.40E-07	2039	1.39E-07	2042	6.38E-11	2065	6.75E-12	2150	3.34E-11	2046	6.68E-12	2121
	low	1.19E-08	2116	1.19E-08	2119	5.85E-12	2142	7.36E-13	2228	2.73E-12	2122	6.62E-13	2198
barrier	high	8.16E-08	2048	8.07E-08	2051	3.79E-11	2075	4.27E-12	2161	1.90E-11	2055	4.09E-12	2131
	low	8.15E-08	2048	8.07E-08	2051	3.79E-11	2075	4.27E-12	2161	1.89E-11	2055	4.09E-12	2131
barrier_deg	high	8.16E-08	2048	8.07E-08	2051	3.79E-11	2075	4.27E-12	2161	1.89E-11	2055	4.09E-12	2131
	low	8.16E-08	2048	8.07E-08	2051	3.79E-11	2075	4.27E-12	2161	1.89E-11	2055	4.09E-12	2131
plume	high	4.68E-08	2055	4.63E-08	2058	2.22E-11	2082	2.61E-12	2169	1.08E-11	2061	2.45E-12	2138
	low	1.27E-07	2041	1.27E-07	2044	5.92E-11	2067	6.46E-12	2152	3.00E-11	2048	6.30E-12	2122
ksat_aq	high	6.19E-08	2048	6.12E-08	2050	3.80E-11	2074	4.28E-12	2160	1.90E-11	2054	4.10E-12	2130
	low	1.19E-07	2048	1.18E-07	2052	3.77E-11	2076	4.25E-12	2162	1.88E-11	2056	4.07E-12	2132
ksat_vz	high	1.38E-07	2039	1.36E-07	2042	6.05E-11	2065	6.36E-12	2150	3.19E-11	2045	6.32E-12	2120
	low	4.60E-08	2060	4.57E-08	2062	2.23E-11	2087	2.65E-12	2173	1.07E-11	2066	2.47E-12	2143

Table F.34. Predicted Peak Tc-99 Aqueous Concentration (Ci/L) and Arrival Time (yr) Summary for Case 2 (Diffusion)

Sub-Case		Groundwater		Fenceline		Excl (East)		Col River (East)		Excl (North)		Col River (North)	
		Conc.	Time	Conc.	Time	Conc.	Time	Conc.	Time	Conc.	Time	Conc.	Time
base		1.64E-10	10480	1.64E-10	10483	8.03E-14	10504	1.02E-14	10590	3.73E-14	10485	9.12E-15	10560
recharge	high	1.64E-10	10480	1.64E-10	10483	8.03E-14	10504	1.02E-14	10592	3.73E-14	10486	9.12E-15	10558
	low	1.64E-10	10481	1.64E-10	10484	8.04E-14	10506	1.02E-14	10590	3.73E-14	10486	9.13E-15	10561
barrier	high	1.61E-10	10456	1.61E-10	10458	7.86E-14	10480	9.97E-15	10562	3.65E-14	10461	8.92E-15	10534
	low	1.67E-10	10513	1.67E-10	10517	8.18E-14	10540	1.04E-14	10626	3.80E-14	10521	9.29E-15	10594
barrier_deg	high	3.38E-10	5001	3.38E-10	5004	1.66E-13	5027	2.10E-14	5111	7.69E-14	5008	1.88E-14	5082
	low	4.19E-11	12032	4.19E-11	12032	2.02E-14	12032	2.46E-15	12032	9.49E-15	12032	2.24E-15	12032
diffusion	high	5.19E-10	10480	5.19E-10	10483	2.54E-13	10505	3.22E-14	10587	1.18E-13	10487	2.89E-14	10561
	low	5.19E-13	10479	5.19E-13	10482	2.54E-16	10504	3.22E-17	10589	1.18E-16	10486	2.88E-17	10559
ksat_aq	high	1.23E-10	10481	1.23E-10	10483	8.03E-14	10504	1.02E-14	10591	3.73E-14	10486	9.12E-15	10558
	low	2.46E-10	10480	2.46E-10	10485	8.03E-14	10507	1.02E-14	10591	3.73E-14	10488	9.12E-15	10561
ksat_vz	high	1.89E-10	9003	1.89E-10	9005	9.25E-14	9028	1.17E-14	9113	4.30E-14	9009	1.05E-14	9085
	low	1.26E-10	12032	1.26E-10	12032	6.16E-14	12032	7.76E-15	12032	2.87E-14	12032	6.96E-15	12032

Table F.35. Predicted Peak Tc-99 Aqueous Concentration (Ci/L) and Arrival Time (yr) Summary for Case 3 (Retrieval Leak)

Sub-Case		Groundwater		Fenceline		Excl (East)		Col River (East)		Excl (North)		Col River (North)	
		Conc.	Time	Conc.	Time	Conc.	Time	Conc.	Time	Conc.	Time	Conc.	Time
base		1.34E-09	2118	1.34E-09	2121	6.59E-13	2144	8.34E-14	2229	3.06E-13	2124	7.47E-14	2199
recharge	high	3.68E-09	2081	3.68E-09	2087	1.81E-12	2109	2.28E-13	2195	8.46E-13	2090	2.05E-13	2164
	low	1.10E-09	6961	1.10E-09	6964	5.40E-13	6986	6.85E-14	7070	2.51E-13	6967	6.13E-14	7042
barrier	high	1.34E-09	2119	1.34E-09	2122	6.61E-13	2144	8.36E-14	2230	3.07E-13	2125	7.50E-14	2200
	low	1.34E-09	2118	1.34E-09	2121	6.57E-13	2143	8.31E-14	2229	3.06E-13	2124	7.45E-14	2199
barrier_deg	high	3.30E-09	3735	3.30E-09	3738	1.62E-12	3761	2.05E-13	3845	7.51E-13	3742	1.84E-13	3816
	low	1.34E-09	2118	1.34E-09	2121	6.59E-13	2144	8.34E-14	2229	3.06E-13	2124	7.47E-14	2199
ksat_aq	high	1.01E-09	2118	1.01E-09	2120	6.59E-13	2143	8.34E-14	2228	3.07E-13	2123	7.48E-14	2198
	low	2.00E-09	2119	2.00E-09	2123	6.58E-13	2145	8.33E-14	2231	3.06E-13	2126	7.47E-14	2201
ksat_vz	high	2.17E-09	2075	2.16E-09	2079	1.06E-12	2102	1.32E-13	2189	4.95E-13	2082	1.19E-13	2158
	low	7.27E-10	8095	7.27E-10	8097	3.56E-13	8120	4.52E-14	8204	1.65E-13	8102	4.04E-14	8176

Table F.36. Predicted Peak Tc-99 Aqueous Concentration (Ci/L) and Arrival Time (yr) Summary for Case 4 (Ancillary Equipment)

Sub-Case		Groundwater		Fenceline		Excl (East)		Col River (East)		Excl (North)		Col River (North)	
		Conc.	Time	Conc.	Time	Conc.	Time	Conc.	Time	Conc.	Time	Conc.	Time
base		1.03E-09	5713	1.03E-09	5717	5.04E-13	5737	6.39E-14	5821	2.34E-13	5718	5.72E-14	5792
recharge	high	3.83E-09	2092	3.83E-09	2095	1.89E-12	2118	2.37E-13	2205	8.79E-13	2098	2.13E-13	2174
	low	1.22E-09	7537	1.22E-09	7540	5.98E-13	7562	7.58E-14	7645	2.78E-13	7543	6.79E-14	7617
barrier	high	1.03E-09	5471	1.03E-09	5474	5.03E-13	5496	6.39E-14	5580	2.34E-13	5477	5.71E-14	5551
	low	1.03E-09	5909	1.03E-09	5912	5.04E-13	5935	6.40E-14	6019	2.34E-13	5916	5.73E-14	5989
barrier_deg	high	3.45E-09	3757	3.45E-09	3760	1.69E-12	3783	2.15E-13	3867	7.85E-13	3764	1.92E-13	3838
	low	7.71E-10	2194	7.71E-10	2197	3.78E-13	2219	4.79E-14	2304	1.76E-13	2200	4.29E-14	2274
ksat_aq	high	7.73E-10	5712	7.73E-10	5714	5.04E-13	5736	6.39E-14	5822	2.34E-13	5719	5.72E-14	5792
	low	1.54E-09	5714	1.54E-09	5717	5.04E-13	5740	6.39E-14	5824	2.34E-13	5721	5.72E-14	5794
ksat_vz	high	1.49E-09	2094	1.48E-09	2097	7.28E-13	2121	9.17E-14	2207	3.39E-13	2101	8.24E-14	2176
	low	7.17E-10	7155	7.17E-10	7158	3.51E-13	7181	4.45E-14	7265	1.63E-13	7164	3.98E-14	7235

Table F.37. Predicted Peak U-238 (Kd = 0.02) Aqueous Concentration (Ci/L) and Arrival Time (yr) Summary for Case 1 (Past Leak)

Sub-Case		Groundwater		Fenceline		Excl (East)		Col River (East)		Excl (North)		Col River (North)	
		Conc.	Time	Conc.	Time	Conc.	Time	Conc.	Time	Conc.	Time	Conc.	Time
base		4.58E-08	2053	4.53E-08	2057	2.33E-11	2085	2.69E-12	2184	1.18E-11	2061	2.56E-12	2149
recharge	high	9.58E-08	2043	9.47E-08	2046	4.63E-11	2073	4.93E-12	2172	2.50E-11	2050	4.89E-12	2137
	low	4.79E-09	2153	4.79E-09	2156	2.56E-12	2183	3.24E-13	2281	1.22E-12	2160	2.92E-13	2246
barrier	high	4.58E-08	2053	4.53E-08	2057	2.33E-11	2085	2.69E-12	2184	1.18E-11	2061	2.56E-12	2149
	low	4.58E-08	2053	4.53E-08	2057	2.33E-11	2085	2.68E-12	2184	1.17E-11	2061	2.56E-12	2149
barrier_deg	high	4.58E-08	2053	4.53E-08	2057	2.33E-11	2085	2.69E-12	2184	1.18E-11	2061	2.56E-12	2149
	low	4.58E-08	2053	4.53E-08	2057	2.33E-11	2085	2.69E-12	2184	1.18E-11	2061	2.56E-12	2149
plume	high	2.18E-08	2063	2.17E-08	2067	1.14E-11	2095	1.38E-12	2195	5.58E-12	2071	1.28E-12	2160
	low	9.08E-08	2045	8.99E-08	2048	4.48E-11	2076	4.90E-12	2174	2.35E-11	2053	4.80E-12	2140
ksat_aq	high	3.48E-08	2053	3.43E-08	2056	2.34E-11	2084	2.69E-12	2184	1.18E-11	2060	2.56E-12	2149
	low	6.72E-08	2054	6.66E-08	2058	2.31E-11	2087	2.67E-12	2186	1.17E-11	2063	2.54E-12	2151
ksat_vz	high	7.42E-08	2043	7.29E-08	2046	3.51E-11	2074	3.77E-12	2173	1.89E-11	2051	3.72E-12	2138
	low	2.83E-08	2067	2.82E-08	2070	1.50E-11	2098	1.81E-12	2198	7.29E-12	2074	1.68E-12	2162

Table F.38. Predicted Peak U-238 (Kd = 0.02) Aqueous Concentration (Ci/L) and Arrival Time (yr) Summary for Case 2 (Diffusion)

Sub-Case		Groundwater		Fenceline		Excl (East)		Col River (East)		Excl (North)		Col River (North)	
		Conc.	Time	Conc.	Time	Conc.	Time	Conc.	Time	Conc.	Time	Conc.	Time
base		1.31E-10	12032	1.31E-10	12032	6.93E-14	12032	8.71E-15	12032	3.30E-14	12032	7.86E-15	12032
recharge	high	1.31E-10	12032	1.31E-10	12032	6.93E-14	12032	8.71E-15	12032	3.30E-14	12032	7.86E-15	12032
	low	1.31E-10	12032	1.31E-10	12032	6.93E-14	12032	8.71E-15	12032	3.30E-14	12032	7.86E-15	12032
barrier	high	1.30E-10	12032	1.30E-10	12032	6.87E-14	12032	8.65E-15	12032	3.27E-14	12032	7.80E-15	12032
	low	1.32E-10	12032	1.31E-10	12032	6.96E-14	12032	8.75E-15	12032	3.32E-14	12032	7.90E-15	12032
barrier_deg	high	2.82E-10	5788	2.82E-10	5791	1.50E-13	5818	1.91E-14	5914	7.13E-14	5796	1.72E-14	5881
	low	4.45E-12	12032	4.44E-12	12032	2.30E-15	12032	2.68E-16	12032	1.11E-15	12032	2.49E-16	12032
diffusion	high	4.14E-10	12032	4.13E-10	12032	2.19E-13	12032	2.75E-14	12032	1.04E-13	12032	2.49E-14	12032
	low	4.14E-13	12032	4.13E-13	12032	2.19E-16	12032	2.75E-17	12032	1.04E-16	12032	2.49E-17	12032
ksat_aq	high	9.81E-11	12032	9.81E-11	12032	6.93E-14	12032	8.71E-15	12032	3.30E-14	12032	7.86E-15	12032
	low	1.96E-10	12032	1.96E-10	12032	6.93E-14	12032	8.71E-15	12032	3.30E-14	12032	7.86E-15	12032
ksat_vz	high	1.57E-10	11820	1.57E-10	11824	8.34E-14	11850	1.06E-14	11947	3.96E-14	11828	9.54E-15	11913
	low	7.20E-11	12032	7.19E-11	12032	3.79E-14	12032	4.69E-15	12032	1.81E-14	12032	4.25E-15	12032

Table F.39. Predicted Peak U-238 (Kd = 0.02) Aqueous Concentration (Ci/L) and Arrival Time (yr) Summary for Case 3 (Retrieval Leak)

Sub-Case		Groundwater		Fenceline		Excl (East)		Col River (East)		Excl (North)		Col River (North)	
		Conc.	Time	Conc.	Time	Conc.	Time	Conc.	Time	Conc.	Time	Conc.	Time
base		8.07E-10	7683	8.07E-10	7687	4.29E-13	7713	5.47E-14	7809	2.04E-13	7690	4.91E-14	7775
recharge	high	9.13E-10	2102	9.13E-10	2105	4.88E-13	2132	6.18E-14	2231	2.32E-13	2109	5.58E-14	2196
	low	8.74E-10	9009	8.74E-10	9012	4.64E-13	9039	5.92E-14	9136	2.20E-13	9018	5.31E-14	9101
barrier	high	8.07E-10	7440	8.07E-10	7444	4.29E-13	7469	5.46E-14	7566	2.04E-13	7449	4.91E-14	7531
	low	8.07E-10	7880	8.07E-10	7883	4.29E-13	7910	5.47E-14	8005	2.04E-13	7888	4.91E-14	7973
barrier_deg	high	2.72E-09	4338	2.72E-09	4342	1.45E-12	4369	1.84E-13	4465	6.88E-13	4346	1.66E-13	4432
	low	4.06E-10	11623	4.06E-10	11623	2.16E-13	11650	2.75E-14	11745	1.03E-13	11629	2.47E-14	11716
ksat_aq	high	6.06E-10	7682	6.06E-10	7686	4.29E-13	7712	5.47E-14	7808	2.04E-13	7691	4.91E-14	7774
	low	1.21E-09	7683	1.21E-09	7688	4.29E-13	7714	5.47E-14	7810	2.04E-13	7693	4.91E-14	7776
ksat_vz	high	9.99E-10	6897	9.99E-10	6900	5.31E-13	6926	6.77E-14	7022	2.52E-13	6905	6.08E-14	6989
	low	6.12E-10	10175	6.12E-10	10179	3.25E-13	10204	4.14E-14	10301	1.54E-13	10186	3.72E-14	10269

Table F.40. Predicted Peak U-238 (Kd = 0.02) Aqueous Concentration (Ci/L) and Arrival Time (yr) Summary for Case 4 (Ancillary Equipment)

Sub-Case		Groundwater		Fenceline		Excl (East)		Col River (East)		Excl (North)		Col River (North)	
		Conc.	Time	Conc.	Time	Conc.	Time	Conc.	Time	Conc.	Time	Conc.	Time
base		8.40E-10	7839	8.40E-10	7842	4.47E-13	7869	5.69E-14	7964	2.12E-13	7847	5.11E-14	7930
recharge	high	7.92E-10	2130	7.92E-10	2133	4.23E-13	2159	5.37E-14	2257	2.01E-13	2137	4.84E-14	2223
	low	9.38E-10	9743	9.38E-10	9745	4.99E-13	9773	6.36E-14	9869	2.37E-13	9751	5.71E-14	9835
barrier	high	8.40E-10	7596	8.40E-10	7599	4.46E-13	7626	5.69E-14	7723	2.12E-13	7605	5.11E-14	7689
	low	8.40E-10	8035	8.40E-10	8039	4.47E-13	8065	5.69E-14	8161	2.12E-13	8044	5.11E-14	8127
barrier_deg	high	2.81E-09	4397	2.81E-09	4400	1.49E-12	4427	1.90E-13	4523	7.09E-13	4405	1.71E-13	4490
	low	4.23E-10	11921	4.23E-10	11925	2.25E-13	11954	2.87E-14	12032	1.07E-13	11929	2.57E-14	12016
ksat_aq	high	6.30E-10	7838	6.30E-10	7840	4.47E-13	7867	5.69E-14	7963	2.12E-13	7846	5.11E-14	7930
	low	1.26E-09	7841	1.26E-09	7845	4.47E-13	7870	5.69E-14	7967	2.12E-13	7849	5.11E-14	7933
ksat_vz	high	1.05E-09	6958	1.05E-09	6959	5.57E-13	6986	7.09E-14	7081	2.64E-13	6964	6.37E-14	7049
	low	6.08E-10	9233	6.08E-10	9235	3.23E-13	9261	4.12E-14	9358	1.53E-13	9240	3.70E-14	9326

Table F.41. Predicted Peak U-238 (Kd = 0.10) Aqueous Concentration (Ci/L) and Arrival Time (yr) Summary for Case 1 (Past Leak)

Sub-Case		Groundwater		Fenceline		Excl (East)		Col River (East)		Excl (North)		Col River (North)	
		Conc.	Time	Conc.	Time	Conc.	Time	Conc.	Time	Conc.	Time	Conc.	Time
base		3.40E-09	2090	3.40E-09	2095	2.29E-12	2138	2.87E-13	2290	1.18E-12	2102	2.65E-13	2236
recharge	high	1.21E-08	2058	1.20E-08	2064	7.73E-12	2108	9.00E-13	2261	4.18E-12	2071	8.66E-13	2207
	low	7.24E-10	7169	7.24E-10	7173	4.90E-13	7214	6.32E-14	7360	2.48E-13	7181	5.72E-14	7310
barrier	high	3.41E-09	2090	3.41E-09	2095	2.30E-12	2138	2.87E-13	2291	1.18E-12	2102	2.65E-13	2236
	low	3.40E-09	2090	3.40E-09	2095	2.29E-12	2138	2.86E-13	2290	1.17E-12	2102	2.64E-13	2236
barrier_deg	high	3.40E-09	2090	3.40E-09	2095	2.29E-12	2138	2.87E-13	2290	1.18E-12	2102	2.65E-13	2236
	low	3.40E-09	2090	3.40E-09	2095	2.29E-12	2138	2.87E-13	2290	1.18E-12	2102	2.65E-13	2236
plume	high	8.57E-10	2131	8.57E-10	2136	5.81E-13	2177	7.43E-14	2328	2.95E-13	2142	6.77E-14	2274
	low	1.47E-08	2063	1.46E-08	2069	9.47E-12	2113	1.12E-12	2265	5.07E-12	2075	1.07E-12	2211
ksat_aq	high	2.56E-09	2089	2.56E-09	2093	2.30E-12	2136	2.87E-13	2289	1.18E-12	2100	2.65E-13	2234
	low	5.05E-09	2091	5.05E-09	2099	2.28E-12	2141	2.85E-13	2294	1.17E-12	2105	2.64E-13	2239
ksat_vz	high	2.81E-09	2064	2.79E-09	2069	1.82E-12	2114	2.18E-13	2267	9.65E-13	2076	2.07E-13	2212
	low	3.78E-09	2117	3.78E-09	2122	2.57E-12	2163	3.26E-13	2314	1.31E-12	2128	2.98E-13	2261

Table F.42. Predicted Peak U-238 (Kd = 0.10) Aqueous Concentration (Ci/L) and Arrival Time (yr) Summary for Case 2 (Diffusion)

Sub-Case		Groundwater		Fenceline		Excl (East)		Col River (East)		Excl (North)		Col River (North)	
		Conc.	Time	Conc.	Time	Conc.	Time	Conc.	Time	Conc.	Time	Conc.	Time
base		1.11E-12	12032	1.10E-12	12032	7.10E-16	12032	7.60E-17	12032	3.74E-16	12032	7.35E-17	12032
recharge	high	1.11E-12	12032	1.10E-12	12032	7.11E-16	12032	7.61E-17	12032	3.74E-16	12032	7.36E-17	12032
	low	1.10E-12	12032	1.10E-12	12032	7.06E-16	12032	7.56E-17	12032	3.72E-16	12032	7.31E-17	12032
barrier	high	1.28E-12	12032	1.28E-12	12032	8.24E-16	12032	8.89E-17	12032	4.33E-16	12032	8.57E-17	12032
	low	9.80E-13	12032	9.73E-13	12032	6.26E-16	12032	6.65E-17	12032	3.30E-16	12032	6.45E-17	12032
barrier_deg	high	1.92E-10	9038	1.92E-10	9043	1.30E-13	9084	1.67E-14	9230	6.57E-14	9049	1.52E-14	9178
	low	4.42E-17	12032	2.74E-17	12032	1.48E-20	12032	4.05E-22	12032	9.18E-21	12032	1.01E-21	12032
diffusion	high	3.51E-12	12032	3.48E-12	12032	2.24E-15	12032	2.40E-16	12032	1.18E-15	12032	2.32E-16	12032
	low	3.50E-15	12032	3.47E-15	12032	2.24E-18	12032	2.40E-19	12032	1.18E-18	12032	2.32E-19	12032
ksat_aq	high	8.32E-13	12032	8.28E-13	12032	7.11E-16	12032	7.61E-17	12032	3.74E-16	12032	7.36E-17	12032
	low	1.66E-12	12032	1.64E-12	12032	7.07E-16	12032	7.56E-17	12032	3.72E-16	12032	7.31E-17	12032
ksat_vz	high	1.52E-12	12032	1.51E-12	12032	9.75E-16	12032	1.04E-16	12032	5.14E-16	12032	1.01E-16	12032
	low	7.84E-13	12032	7.79E-13	12032	5.04E-16	12032	5.48E-17	12032	2.64E-16	12032	5.27E-17	12032

Table F.43. Predicted Peak U-238 (Kd = 0.10) Aqueous Concentration (Ci/L) and Arrival Time (yr) Summary for Case 3 (Retrieval Leak)

Sub-Case		Groundwater		Fenceline		Excl (East)		Col River (East)		Excl (North)		Col River (North)	
		Conc.	Time	Conc.	Time	Conc.	Time	Conc.	Time	Conc.	Time	Conc.	Time
base		2.89E-10	12032	2.89E-10	12032	1.94E-13	12032	2.40E-14	12032	9.87E-14	12032	2.20E-14	12032
recharge	high	3.50E-10	12032	3.50E-10	12032	2.35E-13	12032	2.95E-14	12032	1.20E-13	12032	2.70E-14	12032
	low	1.75E-10	12032	1.75E-10	12032	1.17E-13	12032	1.41E-14	12032	5.97E-14	12032	1.31E-14	12032
barrier	high	3.07E-10	12032	3.07E-10	12032	2.06E-13	12032	2.56E-14	12032	1.05E-13	12032	2.35E-14	12032
	low	2.75E-10	12032	2.74E-10	12032	1.84E-13	12032	2.27E-14	12032	9.37E-14	12032	2.09E-14	12032
barrier_deg	high	1.60E-09	6885	1.60E-09	6890	1.09E-12	6931	1.40E-13	7077	5.49E-13	6897	1.27E-13	7026
	low	2.51E-11	12032	2.50E-11	12032	1.67E-14	12032	2.05E-15	12032	8.54E-15	12032	1.89E-15	12032
ksat_aq	high	2.17E-10	12032	2.17E-10	12032	1.94E-13	12032	2.40E-14	12032	9.88E-14	12032	2.21E-14	12032
	low	4.34E-10	12032	4.33E-10	12032	1.94E-13	12032	2.40E-14	12032	9.86E-14	12032	2.20E-14	12032
ksat_vz	high	3.52E-10	12032	3.52E-10	12032	2.36E-13	12032	2.92E-14	12032	1.20E-13	12032	2.68E-14	12032
	low	1.43E-10	12032	1.43E-10	12032	9.57E-14	12032	1.17E-14	12032	4.89E-14	12032	1.08E-14	12032

Table F.44. Predicted Peak U-238 (Kd = 0.10) Aqueous Concentration (Ci/L) and Arrival Time (yr) Summary for Case 4 (Ancillary Equipment)

Sub-Case		Groundwater		Fenceline		Excl (East)		Col River (East)		Excl (North)		Col River (North)	
		Conc.	Time	Conc.	Time	Conc.	Time	Conc.	Time	Conc.	Time	Conc.	Time
base		2.53E-10	12032	2.53E-10	12032	1.69E-13	12032	2.08E-14	12032	8.62E-14	12032	1.91E-14	12032
recharge	high	3.50E-10	12032	3.50E-10	12032	2.35E-13	12032	2.95E-14	12032	1.20E-13	12032	2.70E-14	12032
	low	8.44E-11	12032	8.42E-11	12032	5.55E-14	12032	6.48E-15	12032	2.87E-14	12032	6.08E-15	12032
barrier	high	2.72E-10	12032	2.71E-10	12032	1.82E-13	12032	2.24E-14	12032	9.27E-14	12032	2.06E-14	12032
	low	2.38E-10	12032	2.37E-10	12032	1.59E-13	12032	1.94E-14	12032	8.10E-14	12032	1.79E-14	12032
barrier_deg	high	1.61E-09	7045	1.61E-09	7050	1.09E-12	7089	1.41E-13	7236	5.53E-13	7056	1.28E-13	7186
	low	1.45E-11	12032	1.45E-11	12032	9.66E-15	12032	1.17E-15	12032	4.95E-15	12032	1.08E-15	12032
ksat_aq	high	1.90E-10	12032	1.90E-10	12032	1.69E-13	12032	2.08E-14	12032	8.63E-14	12032	1.91E-14	12032
	low	3.79E-10	12032	3.78E-10	12032	1.69E-13	12032	2.07E-14	12032	8.61E-14	12032	1.91E-14	12032
ksat_vz	high	2.98E-10	12032	2.97E-10	12032	1.99E-13	12032	2.43E-14	12032	1.01E-13	12032	2.24E-14	12032
	low	1.91E-10	12032	1.90E-10	12032	1.28E-13	12032	1.58E-14	12032	6.51E-14	12032	1.45E-14	12032

Table F.45. Predicted Peak U-238 (Kd = 0.20) Aqueous Concentration (Ci/L) and Arrival Time (yr) Summary for Case 1 (Past Leak)

Sub-Case		Groundwater		Fenceline		Excl (East)		Col River (East)		Excl (North)		Col River (North)	
		Conc.	Time	Conc.	Time	Conc.	Time	Conc.	Time	Conc.	Time	Conc.	Time
base		4.54E-10	9613	4.54E-10	9621	3.75E-13	9676	4.86E-14	9887	1.98E-13	9630	4.43E-14	9810
recharge	high	7.51E-10	2094	7.51E-10	2101	6.13E-13	2164	7.64E-14	2383	3.30E-13	2111	7.15E-14	2304
	low	4.63E-10	12032	4.63E-10	12032	3.82E-13	12032	4.93E-14	12032	2.02E-13	12032	4.51E-14	12032
barrier	high	4.55E-10	9369	4.55E-10	9376	3.75E-13	9431	4.86E-14	9637	1.98E-13	9385	4.44E-14	9567
	low	4.54E-10	9811	4.54E-10	9819	3.75E-13	9876	4.85E-14	10085	1.98E-13	9828	4.43E-14	10010
barrier_deg	high	1.56E-09	5001	1.56E-09	5007	1.29E-12	5064	1.67E-13	5274	6.82E-13	5017	1.53E-13	5201
	low	2.19E-10	12032	2.19E-10	12032	1.80E-13	12032	2.31E-14	12032	9.52E-14	12032	2.12E-14	12032
plume	high	4.16E-10	12032	4.16E-10	12032	3.43E-13	12032	4.42E-14	12032	1.81E-13	12032	4.04E-14	12032
	low	1.33E-09	2101	1.33E-09	2109	1.09E-12	2171	1.36E-13	2389	5.84E-13	2118	1.27E-13	2311
ksat_aq	high	3.41E-10	9613	3.41E-10	9616	3.75E-13	9673	4.86E-14	9884	1.98E-13	9628	4.43E-14	9809
	low	6.81E-10	9616	6.81E-10	9624	3.75E-13	9680	4.86E-14	9894	1.98E-13	9635	4.43E-14	9820
ksat_vz	high	4.92E-10	10139	4.92E-10	10145	4.06E-13	10204	5.26E-14	10410	2.15E-13	10156	4.80E-14	10340
	low	3.89E-10	8786	3.89E-10	8795	3.21E-13	8852	4.16E-14	9061	1.70E-13	8805	3.79E-14	8985

Table F.46. Predicted Peak U-238 (Kd = 0.20) Aqueous Concentration (Ci/L) and Arrival Time (yr) Summary for Case 2 (Diffusion)

Sub-Case		Groundwater		Fenceline		Excl (East)		Col River (East)		Excl (North)		Col River (North)	
		Conc.	Time	Conc.	Time	Conc.	Time	Conc.	Time	Conc.	Time	Conc.	Time
base		2.38E-16	12032	2.27E-16	12032	1.63E-19	12032	1.24E-20	12032	9.65E-20	12032	1.36E-20	12032
recharge	high	2.39E-16	12032	2.28E-16	12032	1.64E-19	12032	1.25E-20	12032	9.71E-20	12032	1.37E-20	12032
	low	2.35E-16	12032	2.23E-16	12032	1.60E-19	12032	1.22E-20	12032	9.51E-20	12032	1.33E-20	12032
barrier	high	3.33E-16	12032	3.22E-16	12032	2.34E-19	12032	1.85E-20	12032	1.37E-19	12032	2.03E-20	12032
	low	1.81E-16	12032	1.66E-16	12032	1.19E-19	12032	8.85E-21	12032	7.09E-20	12032	9.81E-21	12032
barrier_deg	high	1.39E-10	12032	1.38E-10	12032	1.13E-13	12032	1.42E-14	12032	6.03E-14	12032	1.31E-14	12032
	low	0.00E+00	12032	0.00E+00	12032	0.00E+00	12032	0.00E+00	12032	0.00E+00	12032	0.00E+00	12032
diffusion	high	7.56E-16	12032	7.38E-16	12032	5.36E-19	12032	4.30E-20	12032	3.15E-19	12032	4.64E-20	12032
	low	0.00E+00	12032	0.00E+00	12032	0.00E+00	12032	0.00E+00	12032	0.00E+00	12032	0.00E+00	12032
ksat_aq	high	1.79E-16	12032	1.69E-16	12032	1.61E-19	12032	1.23E-20	12032	9.57E-20	12032	1.36E-20	12032
	low	3.56E-16	12032	3.38E-16	12032	1.63E-19	12032	1.24E-20	12032	9.61E-20	12032	1.36E-20	12032
ksat_vz	high	1.41E-16	12032	1.20E-16	12032	8.30E-20	12032	5.58E-21	12032	5.08E-20	12032	6.48E-21	12032
	low	7.31E-16	12032	7.14E-16	12032	5.28E-19	12032	4.51E-20	12032	3.06E-19	12032	4.76E-20	12032

Table F.47. Predicted Peak U-238 (Kd = 0.20) Aqueous Concentration (Ci/L) and Arrival Time (yr) Summary for Case 3 (Retrieval Leak)

Sub-Case		Groundwater		Fenceline		Excl (East)		Col River (East)		Excl (North)		Col River (North)	
		Conc.	Time	Conc.	Time	Conc.	Time	Conc.	Time	Conc.	Time	Conc.	Time
base		6.54E-12	12032	6.50E-12	12032	5.16E-15	12032	5.79E-16	12032	2.82E-15	12032	5.55E-16	12032
recharge	high	1.29E-11	12032	1.29E-11	12032	1.03E-14	12032	1.18E-15	12032	5.58E-15	12032	1.12E-15	12032
	low	1.70E-12	12032	1.69E-12	12032	1.32E-15	12032	1.43E-16	12032	7.30E-16	12032	1.39E-16	12032
barrier	high	7.68E-12	12032	7.64E-12	12032	6.07E-15	12032	6.84E-16	12032	3.31E-15	12032	6.55E-16	12032
	low	5.72E-12	12032	5.69E-12	12032	4.51E-15	12032	5.04E-16	12032	2.46E-15	12032	4.84E-16	12032
barrier_deg	high	1.04E-09	10150	1.04E-09	10157	8.59E-13	10214	1.11E-13	10423	4.54E-13	10166	1.02E-13	10351
	low	1.16E-13	12032	1.16E-13	12032	9.27E-17	12032	1.07E-17	12032	5.03E-17	12032	1.02E-17	12032
ksat_aq	high	4.91E-12	12032	4.89E-12	12032	5.17E-15	12032	5.80E-16	12032	2.82E-15	12032	5.56E-16	12032
	low	9.80E-12	12032	9.72E-12	12032	5.14E-15	12032	5.77E-16	12032	2.81E-15	12032	5.53E-16	12032
ksat_vz	high	5.87E-12	12032	5.84E-12	12032	4.62E-15	12032	5.11E-16	12032	2.53E-15	12032	4.93E-16	12032
	low	3.58E-12	12032	3.56E-12	12032	2.82E-15	12032	3.15E-16	12032	1.54E-15	12032	3.03E-16	12032

Table F.48. Predicted Peak U-238 (Kd = 0.20) Aqueous Concentration (Ci/L) and Arrival Time (yr) Summary for Case 4 (Ancillary Equipment)

Sub-Case		Groundwater		Fenceline		Excl (East)		Col River (East)		Excl (North)		Col River (North)	
		Conc.	Time	Conc.	Time	Conc.	Time	Conc.	Time	Conc.	Time	Conc.	Time
base		3.13E-12	12032	3.11E-12	12032	2.45E-15	12032	2.65E-16	12032	1.35E-15	12032	2.58E-16	12032
recharge	high	1.07E-11	12032	1.06E-11	12032	8.47E-15	12032	9.59E-16	12032	4.61E-15	12032	9.17E-16	12032
	low	1.47E-13	12032	1.46E-13	12032	1.11E-16	12032	1.07E-17	12032	6.26E-17	12032	1.08E-17	12032
barrier	high	3.81E-12	12032	3.79E-12	12032	2.98E-15	12032	3.25E-16	12032	1.64E-15	12032	3.15E-16	12032
	low	2.66E-12	12032	2.64E-12	12032	2.07E-15	12032	2.24E-16	12032	1.14E-15	12032	2.18E-16	12032
barrier_deg	high	1.04E-09	10399	1.04E-09	10405	8.57E-13	10463	1.11E-13	10673	4.53E-13	10416	1.01E-13	10600
	low	1.98E-14	12032	1.96E-14	12032	1.55E-17	12032	1.71E-18	12032	8.50E-18	12032	1.65E-18	12032
ksat_aq	high	2.35E-12	12032	2.34E-12	12032	2.45E-15	12032	2.66E-16	12032	1.35E-15	12032	2.58E-16	12032
	low	4.69E-12	12032	4.65E-12	12032	2.44E-15	12032	2.64E-16	12032	1.34E-15	12032	2.57E-16	12032
ksat_vz	high	1.66E-12	12032	1.64E-12	12032	1.28E-15	12032	1.34E-16	12032	7.10E-16	12032	1.32E-16	12032
	low	5.95E-12	12032	5.92E-12	12032	4.71E-15	12032	5.31E-16	12032	2.56E-15	12032	5.09E-16	12032

Table F.49. Predicted Peak U-238 (Kd = 0.60) Aqueous Concentration (Ci/L) and Arrival Time (yr) Summary for Case 1 (Past Leak)

Sub-Case		Groundwater		Fenceline		Excl (East)		Col River (East)		Excl (North)		Col River (North)	
		Conc.	Time	Conc.	Time	Conc.	Time	Conc.	Time	Conc.	Time	Conc.	Time
base		1.58E-11	12032	1.57E-11	12032	1.87E-14	12032	1.99E-15	12032	1.11E-14	12032	1.97E-15	12032
recharge	high	2.84E-11	12032	2.82E-11	12032	3.40E-14	12032	3.80E-15	12032	2.00E-14	12032	3.70E-15	12032
	low	3.71E-12	12032	3.67E-12	12032	4.24E-15	12032	4.04E-16	12032	2.58E-15	12032	4.17E-16	12032
barrier	high	1.74E-11	12032	1.72E-11	12032	2.06E-14	12032	2.22E-15	12032	1.22E-14	12032	2.19E-15	12032
	low	1.46E-11	12032	1.44E-11	12032	1.72E-14	12032	1.83E-15	12032	1.02E-14	12032	1.81E-15	12032
barrier_deg	high	6.52E-10	11107	6.52E-10	11126	8.20E-13	11250	1.07E-13	11709	4.65E-13	11146	9.88E-14	11550
	low	1.14E-12	12032	1.14E-12	12032	1.36E-15	12032	1.49E-16	12032	8.02E-16	12032	1.46E-16	12032
plume	high	2.10E-12	12032	2.07E-12	12032	2.41E-15	12032	2.36E-16	12032	1.46E-15	12032	2.41E-16	12032
	low	9.01E-11	12032	8.97E-11	12032	1.10E-13	12032	1.29E-14	12032	6.36E-14	12032	1.23E-14	12032
ksat_aq	high	1.18E-11	12032	1.18E-11	12032	1.87E-14	12032	2.00E-15	12032	1.11E-14	12032	1.98E-15	12032
	low	2.36E-11	12032	2.34E-11	12032	1.86E-14	12032	1.98E-15	12032	1.10E-14	12032	1.96E-15	12032
ksat_vz	high	9.65E-12	12032	9.57E-12	12032	1.13E-14	12032	1.16E-15	12032	6.74E-15	12032	1.16E-15	12032
	low	2.89E-11	12032	2.87E-11	12032	3.47E-14	12032	3.91E-15	12032	2.03E-14	12032	3.80E-15	12032

Table F.50. Predicted Peak U-238 (Kd = 0.60) Aqueous Concentration (Ci/L) and Arrival Time (yr) Summary for Case 2 (Diffusion)

Sub-Case		Groundwater		Fenceline		Excl (East)		Col River (East)		Excl (North)		Col River (North)	
		Conc.	Time	Conc.	Time	Conc.	Time	Conc.	Time	Conc.	Time	Conc.	Time
base		0.00E+00	12032	0.00E+00	12032	0.00E+00	12032	0.00E+00	12032	0.00E+00	12032	0.00E+00	12032
recharge	high	0.00E+00	12032	0.00E+00	12032	0.00E+00	12032	0.00E+00	12032	0.00E+00	12032	0.00E+00	12032
	low	0.00E+00	12032	0.00E+00	12032	0.00E+00	12032	0.00E+00	12032	0.00E+00	12032	0.00E+00	12032
barrier	high	0.00E+00	12032	0.00E+00	12032	0.00E+00	12032	0.00E+00	12032	0.00E+00	12032	0.00E+00	12032
	low	0.00E+00	12032	0.00E+00	12032	0.00E+00	12032	0.00E+00	12032	0.00E+00	12032	0.00E+00	12032
barrier_deg	high	1.98E-14	12032	1.91E-14	12032	1.90E-17	12032	9.88E-19	12032	1.31E-17	12032	1.26E-18	12032
	low	0.00E+00	12032	0.00E+00	12032	0.00E+00	12032	0.00E+00	12032	0.00E+00	12032	0.00E+00	12032
diffusion	high	0.00E+00	12032	0.00E+00	12032	0.00E+00	12032	0.00E+00	12032	0.00E+00	12032	0.00E+00	12032
	low	0.00E+00	12032	0.00E+00	12032	0.00E+00	12032	0.00E+00	12032	0.00E+00	12032	0.00E+00	12032
ksat_aq	high	0.00E+00	12032	0.00E+00	12032	0.00E+00	12032	0.00E+00	12032	0.00E+00	12032	0.00E+00	12032
	low	0.00E+00	12032	0.00E+00	12032	0.00E+00	12032	0.00E+00	12032	0.00E+00	12032	0.00E+00	12032
ksat_vz	high	0.00E+00	12032	0.00E+00	12032	0.00E+00	12032	0.00E+00	12032	0.00E+00	12032	0.00E+00	12032
	low	0.00E+00	12032	0.00E+00	12032	0.00E+00	12032	0.00E+00	12032	0.00E+00	12032	0.00E+00	12032

Table F.51. Predicted Peak U-238 (Kd = 0.60) Aqueous Concentration (Ci/L) and Arrival Time (yr) Summary for Case 3 (Retrieval Leak)

Sub-Case		Groundwater		Fenceline		Excl (East)		Col River (East)		Excl (North)		Col River (North)	
		Conc.	Time	Conc.	Time	Conc.	Time	Conc.	Time	Conc.	Time	Conc.	Time
base		0.00E+00	12032	0.00E+00	12032	0.00E+00	12032	0.00E+00	12032	0.00E+00	12032	0.00E+00	12032
recharge	high	0.00E+00	12032	0.00E+00	12032	0.00E+00	12032	0.00E+00	12032	0.00E+00	12032	0.00E+00	12032
	low	0.00E+00	12032	0.00E+00	12032	0.00E+00	12032	0.00E+00	12032	0.00E+00	12032	0.00E+00	12032
barrier	high	0.00E+00	12032	0.00E+00	12032	0.00E+00	12032	0.00E+00	12032	0.00E+00	12032	0.00E+00	12032
	low	0.00E+00	12032	0.00E+00	12032	0.00E+00	12032	0.00E+00	12032	0.00E+00	12032	0.00E+00	12032
barrier_deg	high	4.03E-12	12032	3.95E-12	12032	4.26E-15	12032	3.08E-16	12032	2.74E-15	12032	3.51E-16	12032
	low	0.00E+00	12032	0.00E+00	12032	0.00E+00	12032	0.00E+00	12032	0.00E+00	12032	0.00E+00	12032
ksat_aq	high	0.00E+00	12032	0.00E+00	12032	0.00E+00	12032	0.00E+00	12032	0.00E+00	12032	0.00E+00	12032
	low	0.00E+00	12032	0.00E+00	12032	0.00E+00	12032	0.00E+00	12032	0.00E+00	12032	0.00E+00	12032
ksat_vz	high	0.00E+00	12032	0.00E+00	12032	0.00E+00	12032	0.00E+00	12032	0.00E+00	12032	0.00E+00	12032
	low	0.00E+00	12032	0.00E+00	12032	0.00E+00	12032	0.00E+00	12032	0.00E+00	12032	0.00E+00	12032

Table F.52. Predicted Peak U-238 (Kd = 0.60) Aqueous Concentration (Ci/L) and Arrival Time (yr) Summary for Case 4 (Ancillary Equipment)

Sub-Case		Groundwater		Fenceline		Excl (East)		Col River (East)		Excl (North)		Col River (North)	
		Conc.	Time	Conc.	Time	Conc.	Time	Conc.	Time	Conc.	Time	Conc.	Time
base		0.00E+00	12032	0.00E+00	12032	0.00E+00	12032	0.00E+00	12032	0.00E+00	12032	0.00E+00	12032
recharge	high	0.00E+00	12032	0.00E+00	12032	0.00E+00	12032	0.00E+00	12032	0.00E+00	12032	0.00E+00	12032
	low	0.00E+00	12032	0.00E+00	12032	0.00E+00	12032	0.00E+00	12032	0.00E+00	12032	0.00E+00	12032
barrier	high	0.00E+00	12032	0.00E+00	12032	0.00E+00	12032	0.00E+00	12032	0.00E+00	12032	0.00E+00	12032
	low	0.00E+00	12032	0.00E+00	12032	0.00E+00	12032	0.00E+00	12032	0.00E+00	12032	0.00E+00	12032
barrier_deg	high	2.27E-12	12032	2.22E-12	12032	2.36E-15	12032	1.61E-16	12032	1.54E-15	12032	1.87E-16	12032
	low	0.00E+00	12032	0.00E+00	12032	0.00E+00	12032	0.00E+00	12032	0.00E+00	12032	0.00E+00	12032
ksat_aq	high	0.00E+00	12032	0.00E+00	12032	0.00E+00	12032	0.00E+00	12032	0.00E+00	12032	0.00E+00	12032
	low	0.00E+00	12032	0.00E+00	12032	0.00E+00	12032	0.00E+00	12032	0.00E+00	12032	0.00E+00	12032
ksat_vz	high	0.00E+00	12032	0.00E+00	12032	0.00E+00	12032	0.00E+00	12032	0.00E+00	12032	0.00E+00	12032
	low	0.00E+00	12032	0.00E+00	12032	0.00E+00	12032	0.00E+00	12032	0.00E+00	12032	0.00E+00	12032

Table F.53. Predicted Peak U-238 (Kd = 1.00) Aqueous Concentration (Ci/L) and Arrival Time (yr) Summary for Case 1 (Past Leak)

Sub-Case		Groundwater		Fenceline		Excl (East)		Col River (East)		Excl (North)		Col River (North)	
		Conc.	Time	Conc.	Time	Conc.	Time	Conc.	Time	Conc.	Time	Conc.	Time
base		1.26E-13	12032	1.23E-13	12032	1.69E-16	12032	1.30E-17	12032	1.10E-16	12032	1.45E-17	12032
recharge	high	3.62E-13	12032	3.57E-13	12032	5.00E-16	12032	4.23E-17	12032	3.20E-16	12032	4.57E-17	12032
	low	1.10E-14	12032	1.07E-14	12032	1.38E-17	12032	8.27E-19	12032	9.48E-18	12032	1.01E-18	12032
barrier	high	1.48E-13	12032	1.45E-13	12032	1.99E-16	12032	1.55E-17	12032	1.30E-16	12032	1.73E-17	12032
	low	1.10E-13	12032	1.08E-13	12032	1.47E-16	12032	1.12E-17	12032	9.63E-17	12032	1.26E-17	12032
barrier_deg	high	2.02E-10	12032	2.01E-10	12032	2.96E-13	12032	2.93E-14	12032	1.82E-13	12032	3.00E-14	12032
	low	3.20E-15	12032	3.15E-15	12032	4.43E-18	12032	3.81E-19	12032	2.82E-18	12032	4.09E-19	12032
plume	high	3.38E-15	12032	3.29E-15	12032	4.31E-18	12032	2.79E-19	12032	2.91E-18	12032	3.31E-19	12032
	low	4.04E-12	12032	3.99E-12	12032	5.74E-15	12032	5.33E-16	12032	3.60E-15	12032	5.57E-16	12032
ksat_aq	high	9.43E-14	12032	9.30E-14	12032	1.70E-16	12032	1.31E-17	12032	1.11E-16	12032	1.46E-17	12032
	low	1.88E-13	12032	1.83E-13	12032	1.67E-16	12032	1.28E-17	12032	1.09E-16	12032	1.43E-17	12032
ksat_vz	high	4.53E-14	12032	4.43E-14	12032	5.94E-17	12032	4.19E-18	12032	3.94E-17	12032	4.83E-18	12032
	low	5.40E-13	12032	5.31E-13	12032	7.49E-16	12032	6.42E-17	12032	4.77E-16	12032	6.90E-17	12032

Table F.54. Predicted Peak U-238 (Kd = 1.00) Aqueous Concentration (Ci/L) and Arrival Time (yr) Summary for Case 2 (Diffusion)

Sub-Case		Groundwater		Fenceline		Excl (East)		Col River (East)		Excl (North)		Col River (North)	
		Conc.	Time	Conc.	Time	Conc.	Time	Conc.	Time	Conc.	Time	Conc.	Time
base		0.00E+00	12032	0.00E+00	12032	0.00E+00	12032	0.00E+00	12032	0.00E+00	12032	0.00E+00	12032
recharge	high	0.00E+00	12032	0.00E+00	12032	0.00E+00	12032	0.00E+00	12032	0.00E+00	12032	0.00E+00	12032
	low	0.00E+00	12032	0.00E+00	12032	0.00E+00	12032	0.00E+00	12032	0.00E+00	12032	0.00E+00	12032
barrier	high	0.00E+00	12032	0.00E+00	12032	0.00E+00	12032	0.00E+00	12032	0.00E+00	12032	0.00E+00	12032
	low	0.00E+00	12032	0.00E+00	12032	0.00E+00	12032	0.00E+00	12032	0.00E+00	12032	0.00E+00	12032
barrier_deg	high	0.00E+00	12032	0.00E+00	12032	0.00E+00	12032	0.00E+00	12032	0.00E+00	12032	0.00E+00	12032
	low	0.00E+00	12032	0.00E+00	12032	0.00E+00	12032	0.00E+00	12032	0.00E+00	12032	0.00E+00	12032
diffusion	high	0.00E+00	12032	0.00E+00	12032	0.00E+00	12032	0.00E+00	12032	0.00E+00	12032	0.00E+00	12032
	low	0.00E+00	12032	0.00E+00	12032	0.00E+00	12032	0.00E+00	12032	0.00E+00	12032	0.00E+00	12032
ksat_aq	high	0.00E+00	12032	0.00E+00	12032	0.00E+00	12032	0.00E+00	12032	0.00E+00	12032	0.00E+00	12032
	low	0.00E+00	12032	0.00E+00	12032	0.00E+00	12032	0.00E+00	12032	0.00E+00	12032	0.00E+00	12032
ksat_vz	high	0.00E+00	12032	0.00E+00	12032	0.00E+00	12032	0.00E+00	12032	0.00E+00	12032	0.00E+00	12032
	low	0.00E+00	12032	0.00E+00	12032	0.00E+00	12032	0.00E+00	12032	0.00E+00	12032	0.00E+00	12032

Table F.55. Predicted Peak U-238 (Kd = 1.00) Aqueous Concentration (Ci/L) and Arrival Time (yr) Summary for Case 3 (Retrieval Leak)

Sub-Case		Groundwater		Fenceline		Excl (East)		Col River (East)		Excl (North)		Col River (North)	
		Conc.	Time	Conc.	Time	Conc.	Time	Conc.	Time	Conc.	Time	Conc.	Time
base		0.00E+00	12032	0.00E+00	12032	0.00E+00	12032	0.00E+00	12032	0.00E+00	12032	0.00E+00	12032
recharge	high	0.00E+00	12032	0.00E+00	12032	0.00E+00	12032	0.00E+00	12032	0.00E+00	12032	0.00E+00	12032
	low	0.00E+00	12032	0.00E+00	12032	0.00E+00	12032	0.00E+00	12032	0.00E+00	12032	0.00E+00	12032
barrier	high	0.00E+00	12032	0.00E+00	12032	0.00E+00	12032	0.00E+00	12032	0.00E+00	12032	0.00E+00	12032
	low	0.00E+00	12032	0.00E+00	12032	0.00E+00	12032	0.00E+00	12032	0.00E+00	12032	0.00E+00	12032
barrier_deg	high	5.07E-16	12032	4.75E-16	12032	4.99E-19	12032	1.19E-20	12032	4.06E-19	12032	2.06E-20	12032
	low	0.00E+00	12032	0.00E+00	12032	0.00E+00	12032	0.00E+00	12032	0.00E+00	12032	0.00E+00	12032
ksat_aq	high	0.00E+00	12032	0.00E+00	12032	0.00E+00	12032	0.00E+00	12032	0.00E+00	12032	0.00E+00	12032
	low	0.00E+00	12032	0.00E+00	12032	0.00E+00	12032	0.00E+00	12032	0.00E+00	12032	0.00E+00	12032
ksat_vz	high	0.00E+00	12032	0.00E+00	12032	0.00E+00	12032	0.00E+00	12032	0.00E+00	12032	0.00E+00	12032
	low	0.00E+00	12032	0.00E+00	12032	0.00E+00	12032	0.00E+00	12032	0.00E+00	12032	0.00E+00	12032

Table F.56. Predicted Peak U-238 (Kd = 1.00) Aqueous Concentration (Ci/L) and Arrival Time (yr) Summary for Case 4 (Ancillary Equipment)

Sub-Case		Groundwater		Fenceline		Excl (East)		Col River (East)		Excl (North)		Col River (North)	
		Conc.	Time	Conc.	Time	Conc.	Time	Conc.	Time	Conc.	Time	Conc.	Time
base		0.00E+00	12032	0.00E+00	12032	0.00E+00	12032	0.00E+00	12032	0.00E+00	12032	0.00E+00	12032
recharge	high	0.00E+00	12032	0.00E+00	12032	0.00E+00	12032	0.00E+00	12032	0.00E+00	12032	0.00E+00	12032
	low	0.00E+00	12032	0.00E+00	12032	0.00E+00	12032	0.00E+00	12032	0.00E+00	12032	0.00E+00	12032
barrier	high	0.00E+00	12032	0.00E+00	12032	0.00E+00	12032	0.00E+00	12032	0.00E+00	12032	0.00E+00	12032
	low	0.00E+00	12032	0.00E+00	12032	0.00E+00	12032	0.00E+00	12032	0.00E+00	12032	0.00E+00	12032
barrier_deg	high	1.51E-16	12032	1.34E-16	12032	1.32E-19	12032	1.53E-21	12032	1.14E-19	12032	4.20E-21	12032
	low	0.00E+00	12032	0.00E+00	12032	0.00E+00	12032	0.00E+00	12032	0.00E+00	12032	0.00E+00	12032
ksat_aq	high	0.00E+00	12032	0.00E+00	12032	0.00E+00	12032	0.00E+00	12032	0.00E+00	12032	0.00E+00	12032
	low	0.00E+00	12032	0.00E+00	12032	0.00E+00	12032	0.00E+00	12032	0.00E+00	12032	0.00E+00	12032
ksat_vz	high	0.00E+00	12032	0.00E+00	12032	0.00E+00	12032	0.00E+00	12032	0.00E+00	12032	0.00E+00	12032
	low	0.00E+00	12032	0.00E+00	12032	0.00E+00	12032	0.00E+00	12032	0.00E+00	12032	0.00E+00	12032

Table F.57. Predicted Peak U-238 (Kd = 2.00) Aqueous Concentration (Ci/L) and Arrival Time (yr) Summary for Case 1 (Past Leak)

Sub-Case		Groundwater		Fenceline		Excl (East)		Col River (East)		Excl (North)		Col River (North)	
		Conc.	Time	Conc.	Time	Conc.	Time	Conc.	Time	Conc.	Time	Conc.	Time
base		2.30E-18	12032	0.00E+00	12032	0.00E+00	12032	0.00E+00	12032	0.00E+00	12032	0.00E+00	12032
recharge	high	1.46E-17	12032	8.11E-18	12032	6.03E-21	12032	0.00E+00	12032	8.14E-21	12032	0.00E+00	12032
	low	0.00E+00	12032	0.00E+00	12032	0.00E+00	12032	0.00E+00	12032	0.00E+00	12032	0.00E+00	12032
barrier	high	3.00E-18	12032	0.00E+00	12032	0.00E+00	12032	0.00E+00	12032	0.00E+00	12032	0.00E+00	12032
	low	1.83E-18	12032	0.00E+00	12032	0.00E+00	12032	0.00E+00	12032	0.00E+00	12032	0.00E+00	12032
barrier_deg	high	8.93E-13	12032	8.50E-13	12032	1.29E-15	12032	3.58E-17	12032	1.03E-15	12032	5.91E-17	12032
	low	0.00E+00	12032	0.00E+00	12032	0.00E+00	12032	0.00E+00	12032	0.00E+00	12032	0.00E+00	12032
plume	high	0.00E+00	12032	0.00E+00	12032	0.00E+00	12032	0.00E+00	12032	0.00E+00	12032	0.00E+00	12032
	low	1.87E-15	12032	1.80E-15	12032	2.91E-18	12032	1.19E-19	12032	2.21E-18	12032	1.67E-19	12032
ksat_aq	high	1.72E-18	12032	0.00E+00	12032	0.00E+00	12032	0.00E+00	12032	0.00E+00	12032	0.00E+00	12032
	low	3.44E-18	12032	0.00E+00	12032	0.00E+00	12032	0.00E+00	12032	0.00E+00	12032	0.00E+00	12032
ksat_vz	high	2.08E-19	12032	0.00E+00	12032	0.00E+00	12032	0.00E+00	12032	0.00E+00	12032	0.00E+00	12032
	low	4.23E-17	12032	3.40E-17	12032	4.81E-20	12032	4.08E-23	12032	4.12E-20	12032	1.32E-21	12032

Table F.58. Predicted Peak U-238 (Kd = 2.00) Aqueous Concentration (Ci/L) and Arrival Time (yr) Summary for Case 2 (Diffusion)

Sub-Case		Groundwater		Fenceline		Excl (East)		Col River (East)		Excl (North)		Col River (North)	
		Conc.	Time	Conc.	Time	Conc.	Time	Conc.	Time	Conc.	Time	Conc.	Time
base		0.00E+00	12032	0.00E+00	12032	0.00E+00	12032	0.00E+00	12032	0.00E+00	12032	0.00E+00	12032
recharge	high	0.00E+00	12032	0.00E+00	12032	0.00E+00	12032	0.00E+00	12032	0.00E+00	12032	0.00E+00	12032
	low	0.00E+00	12032	0.00E+00	12032	0.00E+00	12032	0.00E+00	12032	0.00E+00	12032	0.00E+00	12032
barrier	high	0.00E+00	12032	0.00E+00	12032	0.00E+00	12032	0.00E+00	12032	0.00E+00	12032	0.00E+00	12032
	low	0.00E+00	12032	0.00E+00	12032	0.00E+00	12032	0.00E+00	12032	0.00E+00	12032	0.00E+00	12032
barrier_deg	high	0.00E+00	12032	0.00E+00	12032	0.00E+00	12032	0.00E+00	12032	0.00E+00	12032	0.00E+00	12032
	low	0.00E+00	12032	0.00E+00	12032	0.00E+00	12032	0.00E+00	12032	0.00E+00	12032	0.00E+00	12032
diffusion	high	0.00E+00	12032	0.00E+00	12032	0.00E+00	12032	0.00E+00	12032	0.00E+00	12032	0.00E+00	12032
	low	0.00E+00	12032	0.00E+00	12032	0.00E+00	12032	0.00E+00	12032	0.00E+00	12032	0.00E+00	12032
ksat_aq	high	0.00E+00	12032	0.00E+00	12032	0.00E+00	12032	0.00E+00	12032	0.00E+00	12032	0.00E+00	12032
	low	0.00E+00	12032	0.00E+00	12032	0.00E+00	12032	0.00E+00	12032	0.00E+00	12032	0.00E+00	12032
ksat_vz	high	0.00E+00	12032	0.00E+00	12032	0.00E+00	12032	0.00E+00	12032	0.00E+00	12032	0.00E+00	12032
	low	0.00E+00	12032	0.00E+00	12032	0.00E+00	12032	0.00E+00	12032	0.00E+00	12032	0.00E+00	12032

Table F.59. Predicted Peak U-238 (Kd = 2.00) Aqueous Concentration (Ci/L) and Arrival Time (yr) Summary for Case 3 (Retrieval Leak)

Sub-Case		Groundwater		Fenceline		Excl (East)		Col River (East)		Excl (North)		Col River (North)	
		Conc.	Time	Conc.	Time	Conc.	Time	Conc.	Time	Conc.	Time	Conc.	Time
base		0.00E+00	12032	0.00E+00	12032	0.00E+00	12032	0.00E+00	12032	0.00E+00	12032	0.00E+00	12032
recharge	high	0.00E+00	12032	0.00E+00	12032	0.00E+00	12032	0.00E+00	12032	0.00E+00	12032	0.00E+00	12032
	low	0.00E+00	12032	0.00E+00	12032	0.00E+00	12032	0.00E+00	12032	0.00E+00	12032	0.00E+00	12032
barrier	high	0.00E+00	12032	0.00E+00	12032	0.00E+00	12032	0.00E+00	12032	0.00E+00	12032	0.00E+00	12032
	low	0.00E+00	12032	0.00E+00	12032	0.00E+00	12032	0.00E+00	12032	0.00E+00	12032	0.00E+00	12032
barrier_deg	high	0.00E+00	12032	0.00E+00	12032	0.00E+00	12032	0.00E+00	12032	0.00E+00	12032	0.00E+00	12032
	low	0.00E+00	12032	0.00E+00	12032	0.00E+00	12032	0.00E+00	12032	0.00E+00	12032	0.00E+00	12032
ksat_aq	high	0.00E+00	12032	0.00E+00	12032	0.00E+00	12032	0.00E+00	12032	0.00E+00	12032	0.00E+00	12032
	low	0.00E+00	12032	0.00E+00	12032	0.00E+00	12032	0.00E+00	12032	0.00E+00	12032	0.00E+00	12032
ksat_vz	high	0.00E+00	12032	0.00E+00	12032	0.00E+00	12032	0.00E+00	12032	0.00E+00	12032	0.00E+00	12032
	low	0.00E+00	12032	0.00E+00	12032	0.00E+00	12032	0.00E+00	12032	0.00E+00	12032	0.00E+00	12032

Table F.60. Predicted Peak U-238 (Kd = 2.00) Aqueous Concentration (Ci/L) and Arrival Time (yr) Summary for Case 4 (Ancillary Equipment)

Sub-Case		Groundwater		Fenceline		Excl (East)		Col River (East)		Excl (North)		Col River (North)	
		Conc.	Time	Conc.	Time	Conc.	Time	Conc.	Time	Conc.	Time	Conc.	Time
base		0.00E+00	12032	0.00E+00	12032	0.00E+00	12032	0.00E+00	12032	0.00E+00	12032	0.00E+00	12032
recharge	high	0.00E+00	12032	0.00E+00	12032	0.00E+00	12032	0.00E+00	12032	0.00E+00	12032	0.00E+00	12032
	low	0.00E+00	12032	0.00E+00	12032	0.00E+00	12032	0.00E+00	12032	0.00E+00	12032	0.00E+00	12032
barrier	high	0.00E+00	12032	0.00E+00	12032	0.00E+00	12032	0.00E+00	12032	0.00E+00	12032	0.00E+00	12032
	low	0.00E+00	12032	0.00E+00	12032	0.00E+00	12032	0.00E+00	12032	0.00E+00	12032	0.00E+00	12032
barrier_deg	high	0.00E+00	12032	0.00E+00	12032	0.00E+00	12032	0.00E+00	12032	0.00E+00	12032	0.00E+00	12032
	low	0.00E+00	12032	0.00E+00	12032	0.00E+00	12032	0.00E+00	12032	0.00E+00	12032	0.00E+00	12032
ksat_aq	high	0.00E+00	12032	0.00E+00	12032	0.00E+00	12032	0.00E+00	12032	0.00E+00	12032	0.00E+00	12032
	low	0.00E+00	12032	0.00E+00	12032	0.00E+00	12032	0.00E+00	12032	0.00E+00	12032	0.00E+00	12032
ksat_vz	high	0.00E+00	12032	0.00E+00	12032	0.00E+00	12032	0.00E+00	12032	0.00E+00	12032	0.00E+00	12032
	low	0.00E+00	12032	0.00E+00	12032	0.00E+00	12032	0.00E+00	12032	0.00E+00	12032	0.00E+00	12032

Table F.61. Predicted Peak U-238 (Kd = 5.00) Aqueous Concentration (Ci/L) and Arrival Time (yr) Summary for Case 1 (Past Leak)

Sub-Case		Groundwater		Fenceline		Excl (East)		Col River (East)		Excl (North)		Col River (North)	
		Conc.	Time	Conc.	Time	Conc.	Time	Conc.	Time	Conc.	Time	Conc.	Time
base		0.00E+00	12032	0.00E+00	12032	0.00E+00	12032	0.00E+00	12032	0.00E+00	12032	0.00E+00	12032
recharge	high	0.00E+00	12032	0.00E+00	12032	0.00E+00	12032	0.00E+00	12032	0.00E+00	12032	0.00E+00	12032
	low	0.00E+00	12032	0.00E+00	12032	0.00E+00	12032	0.00E+00	12032	0.00E+00	12032	0.00E+00	12032
barrier	high	0.00E+00	12032	0.00E+00	12032	0.00E+00	12032	0.00E+00	12032	0.00E+00	12032	0.00E+00	12032
	low	0.00E+00	12032	0.00E+00	12032	0.00E+00	12032	0.00E+00	12032	0.00E+00	12032	0.00E+00	12032
barrier_deg	high	1.07E-19	12032	0.00E+00	12032	0.00E+00	12032	0.00E+00	12032	0.00E+00	12032	0.00E+00	12032
	low	0.00E+00	12032	0.00E+00	12032	0.00E+00	12032	0.00E+00	12032	0.00E+00	12032	0.00E+00	12032
plume	high	0.00E+00	12032	0.00E+00	12032	0.00E+00	12032	0.00E+00	12032	0.00E+00	12032	0.00E+00	12032
	low	0.00E+00	12032	0.00E+00	12032	0.00E+00	12032	0.00E+00	12032	0.00E+00	12032	0.00E+00	12032
ksat_aq	high	0.00E+00	12032	0.00E+00	12032	0.00E+00	12032	0.00E+00	12032	0.00E+00	12032	0.00E+00	12032
	low	0.00E+00	12032	0.00E+00	12032	0.00E+00	12032	0.00E+00	12032	0.00E+00	12032	0.00E+00	12032
ksat_vz	high	0.00E+00	12032	0.00E+00	12032	0.00E+00	12032	0.00E+00	12032	0.00E+00	12032	0.00E+00	12032
	low	0.00E+00	12032	0.00E+00	12032	0.00E+00	12032	0.00E+00	12032	0.00E+00	12032	0.00E+00	12032

Table F.62. Predicted Peak U-238 (Kd = 5.00) Aqueous Concentration (Ci/L) and Arrival Time (yr) Summary for Case 2 (Diffusion)

Sub-Case		Groundwater		Fenceline		Excl (East)		Col River (East)		Excl (North)		Col River (North)	
		Conc.	Time	Conc.	Time	Conc.	Time	Conc.	Time	Conc.	Time	Conc.	Time
base		0.00E+00	12032	0.00E+00	12032	0.00E+00	12032	0.00E+00	12032	0.00E+00	12032	0.00E+00	12032
recharge	high	0.00E+00	12032	0.00E+00	12032	0.00E+00	12032	0.00E+00	12032	0.00E+00	12032	0.00E+00	12032
	low	0.00E+00	12032	0.00E+00	12032	0.00E+00	12032	0.00E+00	12032	0.00E+00	12032	0.00E+00	12032
barrier	high	0.00E+00	12032	0.00E+00	12032	0.00E+00	12032	0.00E+00	12032	0.00E+00	12032	0.00E+00	12032
	low	0.00E+00	12032	0.00E+00	12032	0.00E+00	12032	0.00E+00	12032	0.00E+00	12032	0.00E+00	12032
barrier_deg	high	0.00E+00	12032	0.00E+00	12032	0.00E+00	12032	0.00E+00	12032	0.00E+00	12032	0.00E+00	12032
	low	0.00E+00	12032	0.00E+00	12032	0.00E+00	12032	0.00E+00	12032	0.00E+00	12032	0.00E+00	12032
diffusion	high	0.00E+00	12032	0.00E+00	12032	0.00E+00	12032	0.00E+00	12032	0.00E+00	12032	0.00E+00	12032
	low	0.00E+00	12032	0.00E+00	12032	0.00E+00	12032	0.00E+00	12032	0.00E+00	12032	0.00E+00	12032
ksat_aq	high	0.00E+00	12032	0.00E+00	12032	0.00E+00	12032	0.00E+00	12032	0.00E+00	12032	0.00E+00	12032
	low	0.00E+00	12032	0.00E+00	12032	0.00E+00	12032	0.00E+00	12032	0.00E+00	12032	0.00E+00	12032
ksat_vz	high	0.00E+00	12032	0.00E+00	12032	0.00E+00	12032	0.00E+00	12032	0.00E+00	12032	0.00E+00	12032
	low	0.00E+00	12032	0.00E+00	12032	0.00E+00	12032	0.00E+00	12032	0.00E+00	12032	0.00E+00	12032

Table F.63. Predicted Peak U-238 (Kd = 5.00) Aqueous Concentration (Ci/L) and Arrival Time (yr) Summary for Case 3 (Retrieval Leak)

Sub-Case		Groundwater		Fenceline		Excl (East)		Col River (East)		Excl (North)		Col River (North)	
		Conc.	Time	Conc.	Time	Conc.	Time	Conc.	Time	Conc.	Time	Conc.	Time
base		0.00E+00	12032	0.00E+00	12032	0.00E+00	12032	0.00E+00	12032	0.00E+00	12032	0.00E+00	12032
recharge	high	0.00E+00	12032	0.00E+00	12032	0.00E+00	12032	0.00E+00	12032	0.00E+00	12032	0.00E+00	12032
	low	0.00E+00	12032	0.00E+00	12032	0.00E+00	12032	0.00E+00	12032	0.00E+00	12032	0.00E+00	12032
barrier	high	0.00E+00	12032	0.00E+00	12032	0.00E+00	12032	0.00E+00	12032	0.00E+00	12032	0.00E+00	12032
	low	0.00E+00	12032	0.00E+00	12032	0.00E+00	12032	0.00E+00	12032	0.00E+00	12032	0.00E+00	12032
barrier_deg	high	0.00E+00	12032	0.00E+00	12032	0.00E+00	12032	0.00E+00	12032	0.00E+00	12032	0.00E+00	12032
	low	0.00E+00	12032	0.00E+00	12032	0.00E+00	12032	0.00E+00	12032	0.00E+00	12032	0.00E+00	12032
ksat_aq	high	0.00E+00	12032	0.00E+00	12032	0.00E+00	12032	0.00E+00	12032	0.00E+00	12032	0.00E+00	12032
	low	0.00E+00	12032	0.00E+00	12032	0.00E+00	12032	0.00E+00	12032	0.00E+00	12032	0.00E+00	12032
ksat_vz	high	0.00E+00	12032	0.00E+00	12032	0.00E+00	12032	0.00E+00	12032	0.00E+00	12032	0.00E+00	12032
	low	0.00E+00	12032	0.00E+00	12032	0.00E+00	12032	0.00E+00	12032	0.00E+00	12032	0.00E+00	12032

Table F.64. Predicted Peak U-238 (Kd = 5.00) Aqueous Concentration (Ci/L) and Arrival Time (yr) Summary for Case 4 (Ancillary Equipment)

Sub-Case		Groundwater		Fenceline		Excl (East)		Col River (East)		Excl (North)		Col River (North)	
		Conc.	Time	Conc.	Time	Conc.	Time	Conc.	Time	Conc.	Time	Conc.	Time
base		0.00E+00	12032	0.00E+00	12032	0.00E+00	12032	0.00E+00	12032	0.00E+00	12032	0.00E+00	12032
recharge	high	0.00E+00	12032	0.00E+00	12032	0.00E+00	12032	0.00E+00	12032	0.00E+00	12032	0.00E+00	12032
	low	0.00E+00	12032	0.00E+00	12032	0.00E+00	12032	0.00E+00	12032	0.00E+00	12032	0.00E+00	12032
barrier	high	0.00E+00	12032	0.00E+00	12032	0.00E+00	12032	0.00E+00	12032	0.00E+00	12032	0.00E+00	12032
	low	0.00E+00	12032	0.00E+00	12032	0.00E+00	12032	0.00E+00	12032	0.00E+00	12032	0.00E+00	12032
barrier_deg	high	0.00E+00	12032	0.00E+00	12032	0.00E+00	12032	0.00E+00	12032	0.00E+00	12032	0.00E+00	12032
	low	0.00E+00	12032	0.00E+00	12032	0.00E+00	12032	0.00E+00	12032	0.00E+00	12032	0.00E+00	12032
ksat_aq	high	0.00E+00	12032	0.00E+00	12032	0.00E+00	12032	0.00E+00	12032	0.00E+00	12032	0.00E+00	12032
	low	0.00E+00	12032	0.00E+00	12032	0.00E+00	12032	0.00E+00	12032	0.00E+00	12032	0.00E+00	12032
ksat_vz	high	0.00E+00	12032	0.00E+00	12032	0.00E+00	12032	0.00E+00	12032	0.00E+00	12032	0.00E+00	12032
	low	0.00E+00	12032	0.00E+00	12032	0.00E+00	12032	0.00E+00	12032	0.00E+00	12032	0.00E+00	12032

Table F.65. STOMP Mass Balance for Tc-99 for Case 1 (Past Leak)

Sub-Case		Vadose Zone				Aquifer				Vadose Zone + Aquifer			
		Released	In Domain	Exit	%error	Released	In Domain	Exit	%error	Released	In Domain	Exit	%error
base		1.000E+00	1.001E-05	1.007E+00	-6.935E-01	1.007E+00	2.862E-08	1.003E+00	3.513E-01	1.000E+00	1.004E-05	1.003E+00	-3.398E-01
recharge	high	1.000E+00	3.500E-06	1.010E+00	-9.766E-01	1.010E+00	9.999E-09	1.004E+00	5.541E-01	1.000E+00	3.510E-06	1.004E+00	-4.170E-01
	low	1.000E+00	7.276E-05	1.000E+00	-4.057E-02	1.000E+00	2.079E-07	1.000E+00	1.007E-02	1.000E+00	7.297E-05	1.000E+00	-3.050E-02
barrier	high	1.000E+00	7.738E-06	1.007E+00	-6.936E-01	1.007E+00	2.212E-08	1.003E+00	3.512E-01	1.000E+00	7.760E-06	1.003E+00	-3.400E-01
	low	1.000E+00	1.236E-05	1.007E+00	-6.935E-01	1.007E+00	3.532E-08	1.003E+00	3.514E-01	1.000E+00	1.240E-05	1.003E+00	-3.397E-01
barrier_deg	high	1.000E+00	0.000E+00	1.007E+00	-6.935E-01	1.007E+00	0.000E+00	1.003E+00	3.513E-01	1.000E+00	0.000E+00	1.003E+00	-3.398E-01
	low	1.000E+00	8.160E-04	1.006E+00	-6.935E-01	1.006E+00	1.117E-06	1.003E+00	3.515E-01	1.000E+00	8.171E-04	1.003E+00	-3.398E-01
plume	high	1.000E+00	4.298E-05	1.005E+00	-4.822E-01	1.005E+00	1.194E-07	1.002E+00	2.340E-01	1.000E+00	4.310E-05	1.002E+00	-2.471E-01
	low	1.000E+00	1.507E-06	1.007E+00	-7.122E-01	1.007E+00	4.417E-09	1.003E+00	3.753E-01	1.000E+00	1.512E-06	1.003E+00	-3.342E-01
ksat_aq	high	1.000E+00	1.001E-05	1.007E+00	-6.946E-01	1.007E+00	2.146E-08	1.003E+00	3.586E-01	1.000E+00	1.003E-05	1.003E+00	-3.335E-01
	low	1.000E+00	1.002E-05	1.007E+00	-6.921E-01	1.007E+00	4.299E-08	1.004E+00	3.385E-01	1.000E+00	1.007E-05	1.004E+00	-3.513E-01
ksat_vz	high	1.000E+00	3.088E-07	1.010E+00	-1.015E+00	1.010E+00	1.214E-09	1.003E+00	6.875E-01	1.000E+00	3.100E-07	1.003E+00	-3.201E-01
	low	1.000E+00	5.001E-04	1.004E+00	-4.334E-01	1.004E+00	8.207E-07	1.002E+00	2.069E-01	1.000E+00	5.009E-04	1.002E+00	-2.257E-01

Table F.66. STOMP Mass Balance for Tc-99 for Case 2 (Diffusion)

Sub-Case		Vadose Zone				Aquifer				Vadose Zone + Aquifer			
		Released	In Domain	Exit	%error	Released	In Domain	Exit	%error	Released	In Domain	Exit	%error
base		2.430E-01	1.304E-01	1.125E-01	3.894E-04	1.125E-01	7.374E-05	1.124E-01	2.280E-04	2.430E-01	1.305E-01	1.124E-01	4.937E-04
recharge	high	2.430E-01	1.304E-01	1.125E-01	4.109E-04	1.125E-01	7.373E-05	1.125E-01	2.374E-04	2.430E-01	1.305E-01	1.125E-01	5.213E-04
	low	2.430E-01	1.305E-01	1.125E-01	3.649E-04	1.125E-01	7.377E-05	1.124E-01	1.994E-04	2.430E-01	1.305E-01	1.124E-01	4.569E-04
barrier	high	2.430E-01	1.297E-01	1.133E-01	4.630E-04	1.133E-01	7.244E-05	1.132E-01	2.224E-04	2.430E-01	1.298E-01	1.132E-01	5.642E-04
	low	2.430E-01	1.312E-01	1.118E-01	4.078E-04	1.118E-01	7.496E-05	1.117E-01	2.220E-04	2.430E-01	1.312E-01	1.117E-01	5.121E-04
barrier_deg	high	2.430E-01	3.261E-02	2.104E-01	3.066E-05	2.104E-01	4.203E-05	2.103E-01	-1.672E-05	2.430E-01	3.265E-02	2.103E-01	1.687E-05
	low	2.430E-01	2.331E-01	9.915E-03	6.225E-04	9.915E-03	2.133E-05	9.894E-03	5.958E-04	2.430E-01	2.331E-01	9.894E-03	6.482E-04
diffusion	high	7.683E-01	4.125E-01	3.558E-01	2.560E-04	3.558E-01	2.332E-04	3.556E-01	2.285E-04	7.683E-01	4.127E-01	3.556E-01	3.607E-04
	low	7.683E-04	4.125E-04	3.558E-04	1.076E-03	3.558E-04	2.332E-07	3.556E-04	1.796E-03	7.683E-04	4.127E-04	3.556E-04	1.909E-03
ksat_aq	high	2.430E-01	1.304E-01	1.125E-01	3.710E-04	1.125E-01	5.531E-05	1.125E-01	2.606E-04	2.430E-01	1.305E-01	1.125E-01	4.906E-04
	low	2.430E-01	1.305E-01	1.125E-01	3.772E-04	1.125E-01	1.106E-04	1.124E-01	2.678E-04	2.430E-01	1.306E-01	1.124E-01	5.029E-04
ksat_vz	high	2.430E-01	9.710E-02	1.459E-01	-2.048E-03	1.459E-01	5.920E-05	1.458E-01	7.370E-05	2.430E-01	9.716E-02	1.458E-01	-2.005E-03
	low	2.430E-01	1.850E-01	5.792E-02	4.554E-04	5.792E-02	6.822E-05	5.784E-02	2.564E-02	2.430E-01	1.851E-01	5.784E-02	6.568E-03

Table F.67. STOMP Mass Balance for Tc-99 for Case 3 (Retrieval Leak)

Sub-Case		Vadose Zone				Aquifer				Vadose Zone + Aquifer			
		Released	In Domain	Exit	%error	Released	In Domain	Exit	%error	Released	In Domain	Exit	%error
base		1.000E+00	9.719E-03	9.904E-01	-1.049E-02	9.904E-01	2.291E-05	9.903E-01	4.403E-03	1.000E+00	9.742E-03	9.903E-01	-6.124E-03
recharge	high	1.000E+00	5.876E-03	9.946E-01	-4.392E-02	9.946E-01	1.416E-05	9.943E-01	2.121E-02	1.000E+00	5.891E-03	9.943E-01	-2.283E-02
	low	1.000E+00	2.333E-02	9.767E-01	-7.525E-05	9.767E-01	5.204E-05	9.766E-01	4.876E-05	1.000E+00	2.338E-02	9.766E-01	-2.757E-05
barrier	high	1.000E+00	7.931E-03	9.922E-01	-1.049E-02	9.922E-01	1.891E-05	9.921E-01	4.396E-03	1.000E+00	7.950E-03	9.921E-01	-6.131E-03
	low	1.000E+00	1.145E-02	9.887E-01	-1.047E-02	9.887E-01	2.675E-05	9.886E-01	4.414E-03	1.000E+00	1.148E-02	9.886E-01	-6.102E-03
barrier_deg	high	1.000E+00	0.000E+00	1.000E+00	-1.050E-02	1.000E+00	0.000E+00	1.000E+00	4.398E-03	1.000E+00	0.000E+00	1.000E+00	-6.104E-03
	low	1.000E+00	1.951E-01	8.050E-01	-1.029E-02	8.050E-01	1.581E-04	8.048E-01	5.431E-03	1.000E+00	1.952E-01	8.048E-01	-5.917E-03
ksat_aq	high	1.000E+00	9.717E-03	9.904E-01	-1.052E-02	9.904E-01	1.718E-05	9.903E-01	4.344E-03	1.000E+00	9.735E-03	9.903E-01	-6.214E-03
	low	1.000E+00	9.721E-03	9.904E-01	-1.043E-02	9.904E-01	3.438E-05	9.903E-01	4.545E-03	1.000E+00	9.756E-03	9.903E-01	-5.927E-03
ksat_vz	high	1.000E+00	5.950E-04	9.997E-01	-3.154E-02	9.997E-01	2.158E-06	9.994E-01	2.864E-02	1.000E+00	5.971E-04	9.994E-01	-2.905E-03
	low	1.000E+00	1.535E-01	8.465E-01	-1.535E-04	8.465E-01	1.765E-04	8.463E-01	3.683E-03	1.000E+00	1.537E-01	8.463E-01	2.964E-03

Table F.68. STOMP Mass Balance for Tc-99 for Case 4 (Ancillary Equipment)

Sub-Case		Vadose Zone				Aquifer				Vadose Zone + Aquifer			
		Released	In Domain	Exit	%error	Released	In Domain	Exit	%error	Released	In Domain	Exit	%error
base		1.000E+00	1.016E-02	9.899E-01	-2.623E-03	9.899E-01	2.307E-05	9.898E-01	9.813E-04	1.000E+00	1.019E-02	9.898E-01	-1.652E-03
recharge	high	1.000E+00	4.839E-03	9.955E-01	-3.890E-02	9.955E-01	1.131E-05	9.954E-01	1.771E-02	1.000E+00	4.851E-03	9.954E-01	-2.127E-02
	low	1.000E+00	3.584E-02	9.642E-01	7.190E-05	9.642E-01	7.538E-05	9.641E-01	2.213E-06	1.000E+00	3.592E-02	9.641E-01	7.413E-05
barrier	high	1.000E+00	8.299E-03	9.917E-01	-2.640E-03	9.917E-01	1.905E-05	9.917E-01	9.821E-04	1.000E+00	8.318E-03	9.917E-01	-1.666E-03
	low	1.000E+00	1.197E-02	9.881E-01	-2.623E-03	9.881E-01	2.693E-05	9.880E-01	9.840E-04	1.000E+00	1.200E-02	9.880E-01	-1.651E-03
barrier_deg	high	1.000E+00	0.000E+00	1.000E+00	-2.599E-03	1.000E+00	0.000E+00	1.000E+00	8.940E-04	1.000E+00	0.000E+00	1.000E+00	-1.705E-03
	low	1.000E+00	2.050E-01	7.950E-01	-2.429E-03	7.950E-01	1.605E-04	7.948E-01	1.245E-03	1.000E+00	2.052E-01	7.948E-01	-1.439E-03
ksat_aq	high	1.000E+00	1.016E-02	9.899E-01	-2.639E-03	9.899E-01	1.730E-05	9.898E-01	9.502E-04	1.000E+00	1.018E-02	9.898E-01	-1.698E-03
	low	1.000E+00	1.016E-02	9.899E-01	-2.609E-03	9.899E-01	3.462E-05	9.898E-01	1.061E-03	1.000E+00	1.020E-02	9.898E-01	-1.559E-03
ksat_vz	high	1.000E+00	5.043E-04	9.997E-01	-2.005E-02	9.997E-01	1.799E-06	9.995E-01	1.889E-02	1.000E+00	5.061E-04	9.995E-01	-1.168E-03
	low	1.000E+00	1.084E-01	8.916E-01	-7.108E-04	8.916E-01	1.256E-04	8.915E-01	1.213E-03	1.000E+00	1.085E-01	8.915E-01	3.703E-04

Table F.69. STOMP Mass Balance for U-238 (Kd = 0.02) for Case 1 (Past Leak)

Sub-Case		Vadose Zone				Aquifer				Vadose Zone + Aquifer			
		Released	In Domain	Exit	%error	Released	In Domain	Exit	%error	Released	In Domain	Exit	%error
base		1.000E+00	3.468E-04	1.004E+00	-4.682E-01	1.004E+00	8.604E-07	1.002E+00	2.300E-01	1.000E+00	3.477E-04	1.002E+00	-2.372E-01
recharge	high	1.000E+00	1.450E-04	1.009E+00	-8.793E-01	1.009E+00	3.604E-07	1.004E+00	4.996E-01	1.000E+00	1.454E-04	1.004E+00	-3.753E-01
	low	1.000E+00	1.747E-03	9.983E-01	-9.347E-03	9.983E-01	4.302E-06	9.983E-01	2.727E-03	1.000E+00	1.751E-03	9.983E-01	-6.624E-03
barrier	high	1.000E+00	2.861E-04	1.004E+00	-4.682E-01	1.004E+00	7.106E-07	1.002E+00	2.299E-01	1.000E+00	2.869E-04	1.002E+00	-2.373E-01
	low	1.000E+00	4.056E-04	1.004E+00	-4.681E-01	1.004E+00	1.005E-06	1.002E+00	2.300E-01	1.000E+00	4.066E-04	1.002E+00	-2.371E-01
barrier_deg	high	1.000E+00	0.000E+00	1.005E+00	-4.682E-01	1.005E+00	0.000E+00	1.002E+00	2.299E-01	1.000E+00	0.000E+00	1.002E+00	-2.372E-01
	low	1.000E+00	8.550E-03	9.961E-01	-4.681E-01	9.961E-01	9.891E-06	9.938E-01	2.319E-01	1.000E+00	8.559E-03	9.938E-01	-2.371E-01
plume	high	1.000E+00	1.206E-03	1.001E+00	-2.402E-01	1.001E+00	2.867E-06	1.000E+00	1.122E-01	1.000E+00	1.209E-03	1.000E+00	-1.279E-01
	low	1.000E+00	6.621E-05	1.007E+00	-6.869E-01	1.007E+00	1.706E-07	1.003E+00	3.524E-01	1.000E+00	6.638E-05	1.003E+00	-3.321E-01
ksat_aq	high	1.000E+00	3.468E-04	1.004E+00	-4.693E-01	1.004E+00	6.451E-07	1.002E+00	2.331E-01	1.000E+00	3.474E-04	1.002E+00	-2.351E-01
	low	1.000E+00	3.471E-04	1.004E+00	-4.664E-01	1.004E+00	1.292E-06	1.002E+00	2.252E-01	1.000E+00	3.484E-04	1.002E+00	-2.402E-01
ksat_vz	high	1.000E+00	6.176E-05	1.007E+00	-7.404E-01	1.007E+00	1.973E-07	1.002E+00	5.484E-01	1.000E+00	6.196E-05	1.002E+00	-1.880E-01
	low	1.000E+00	3.399E-03	9.995E-01	-2.931E-01	9.995E-01	5.226E-06	9.982E-01	1.365E-01	1.000E+00	3.404E-03	9.982E-01	-1.566E-01

Table F.70. STOMP Mass Balance for U-238 (Kd = 0.02) for Case 2 (Diffusion)

Sub-Case		Vadose Zone				Aquifer				Vadose Zone + Aquifer			
		Released	In Domain	Exit	%error	Released	In Domain	Exit	%error	Released	In Domain	Exit	%error
base		2.430E-01	1.923E-01	5.066E-02	6.240E-04	5.066E-02	7.795E-05	5.058E-02	2.069E-04	2.430E-01	1.924E-01	5.058E-02	6.700E-04
recharge	high	2.430E-01	1.923E-01	5.067E-02	6.685E-04	5.067E-02	7.795E-05	5.059E-02	1.995E-04	2.430E-01	1.924E-01	5.059E-02	7.099E-04
	low	2.430E-01	1.924E-01	5.061E-02	6.762E-04	5.061E-02	7.798E-05	5.054E-02	2.025E-04	2.430E-01	1.924E-01	5.054E-02	7.176E-04
barrier	high	2.430E-01	1.907E-01	5.222E-02	7.605E-04	5.222E-02	7.733E-05	5.215E-02	2.169E-04	2.430E-01	1.908E-01	5.215E-02	8.095E-04
	low	2.430E-01	1.937E-01	4.930E-02	6.930E-04	4.930E-02	7.840E-05	4.922E-02	1.949E-04	2.430E-01	1.937E-01	4.922E-02	7.298E-04
barrier_deg	high	2.430E-01	4.336E-02	1.996E-01	2.300E-05	1.996E-01	5.205E-05	1.996E-01	7.406E-05	2.430E-01	4.341E-02	1.996E-01	8.433E-05
	low	2.430E-01	2.423E-01	6.981E-04	5.871E-04	6.981E-04	2.695E-06	6.954E-04	1.541E-03	2.430E-01	2.423E-01	6.954E-04	5.905E-04
diffusion	high	7.683E-01	6.081E-01	1.602E-01	8.417E-04	1.602E-01	2.465E-04	1.599E-01	1.828E-04	7.683E-01	6.084E-01	1.599E-01	8.785E-04
	low	7.683E-04	6.081E-04	1.602E-04	1.453E-03	1.602E-04	2.465E-07	1.599E-04	3.678E-03	7.683E-04	6.084E-04	1.599E-04	2.220E-03
ksat_aq	high	2.430E-01	1.923E-01	5.066E-02	6.179E-04	5.066E-02	5.848E-05	5.060E-02	2.230E-04	2.430E-01	1.924E-01	5.060E-02	6.670E-04
	low	2.430E-01	1.923E-01	5.065E-02	6.317E-04	5.065E-02	1.169E-04	5.053E-02	2.155E-04	2.430E-01	1.924E-01	5.053E-02	6.762E-04
ksat_vz	high	2.430E-01	1.631E-01	7.985E-02	-2.327E-03	7.985E-02	8.939E-05	7.976E-02	6.350E-05	2.430E-01	1.632E-01	7.976E-02	-2.306E-03
	low	2.430E-01	2.211E-01	2.186E-02	5.926E-04	2.186E-02	4.576E-05	2.181E-02	1.664E-02	2.430E-01	2.212E-01	2.181E-02	2.091E-03

Table F.71. STOMP Mass Balance for U-238 (Kd = 0.02) for Case 3 (Retrieval Leak)

Sub-Case		Vadose Zone				Aquifer				Vadose Zone + Aquifer			
		Released	In Domain	Exit	%error	Released	In Domain	Exit	%error	Released	In Domain	Exit	%error
base		1.000E+00	9.898E-02	9.010E-01	-1.631E-03	9.010E-01	1.663E-04	9.009E-01	8.095E-04	1.000E+00	9.914E-02	9.009E-01	-9.015E-04
recharge	high	1.000E+00	6.859E-02	9.315E-01	-9.280E-03	9.315E-01	1.200E-04	9.313E-01	4.747E-03	1.000E+00	6.871E-02	9.313E-01	-4.859E-03
	low	1.000E+00	1.809E-01	8.191E-01	1.922E-04	8.191E-01	2.744E-04	8.188E-01	1.286E-05	1.000E+00	1.812E-01	8.188E-01	2.027E-04
barrier	high	1.000E+00	8.738E-02	9.126E-01	-1.649E-03	9.126E-01	1.497E-04	9.125E-01	8.009E-04	1.000E+00	8.753E-02	9.125E-01	-9.179E-04
	low	1.000E+00	1.093E-01	8.907E-01	-1.637E-03	8.907E-01	1.807E-04	8.905E-01	8.214E-04	1.000E+00	1.095E-01	8.905E-01	-9.052E-04
barrier_deg	high	1.000E+00	3.437E-08	1.000E+00	-1.708E-03	1.000E+00	2.700E-10	1.000E+00	7.033E-04	1.000E+00	3.464E-08	1.000E+00	-1.005E-03
	low	1.000E+00	5.179E-01	4.821E-01	-1.311E-03	4.821E-01	2.384E-04	4.818E-01	1.527E-03	1.000E+00	5.182E-01	4.818E-01	-5.752E-04
ksat_aq	high	1.000E+00	9.896E-02	9.011E-01	-1.632E-03	9.011E-01	1.247E-04	9.009E-01	7.874E-04	1.000E+00	9.909E-02	9.009E-01	-9.224E-04
	low	1.000E+00	9.900E-02	9.010E-01	-1.621E-03	9.010E-01	2.495E-04	9.008E-01	8.570E-04	1.000E+00	9.925E-02	9.008E-01	-8.486E-04
ksat_vz	high	1.000E+00	3.230E-02	9.677E-01	-4.034E-03	9.677E-01	7.908E-05	9.676E-01	3.433E-03	1.000E+00	3.238E-02	9.676E-01	-7.119E-04
	low	1.000E+00	3.808E-01	6.192E-01	2.265E-04	6.192E-01	3.159E-04	6.188E-01	1.364E-03	1.000E+00	3.812E-01	6.188E-01	1.070E-03

Table F.72. STOMP Mass Balance for U-238 (Kd = 0.02) for Case 4 (Ancillary Equipment)

Sub-Case		Vadose Zone				Aquifer				Vadose Zone + Aquifer			
		Released	In Domain	Exit	%error	Released	In Domain	Exit	%error	Released	In Domain	Exit	%error
base		1.000E+00	1.083E-01	8.917E-01	-7.525E-05	8.917E-01	1.734E-04	8.915E-01	9.621E-05	1.000E+00	1.085E-01	8.915E-01	1.043E-05
recharge	high	1.000E+00	6.305E-02	9.370E-01	-5.703E-03	9.370E-01	1.067E-04	9.369E-01	2.676E-03	1.000E+00	6.316E-02	9.369E-01	-3.196E-03
	low	1.000E+00	2.552E-01	7.448E-01	3.606E-04	7.448E-01	3.485E-04	7.445E-01	6.963E-06	1.000E+00	2.555E-01	7.445E-01	3.666E-04
barrier	high	1.000E+00	9.576E-02	9.042E-01	-8.047E-05	9.042E-01	1.563E-04	9.041E-01	8.310E-05	1.000E+00	9.591E-02	9.041E-01	-5.215E-06
	low	1.000E+00	1.195E-01	8.805E-01	-1.036E-04	8.805E-01	1.882E-04	8.803E-01	8.096E-05	1.000E+00	1.197E-01	8.803E-01	-3.204E-05
barrier_deg	high	1.000E+00	4.277E-08	1.000E+00	-2.069E-04	1.000E+00	3.216E-10	1.000E+00	1.073E-04	1.000E+00	4.310E-08	1.000E+00	-9.968E-05
	low	1.000E+00	5.548E-01	4.452E-01	4.470E-04	4.452E-01	2.393E-04	4.450E-01	1.739E-04	1.000E+00	5.550E-01	4.450E-01	5.245E-04
ksat_aq	high	1.000E+00	1.083E-01	8.917E-01	-6.706E-05	8.917E-01	1.300E-04	8.916E-01	7.954E-05	1.000E+00	1.084E-01	8.916E-01	3.725E-06
	low	1.000E+00	1.083E-01	8.917E-01	-8.568E-05	8.917E-01	2.601E-04	8.914E-01	1.001E-04	1.000E+00	1.086E-01	8.914E-01	3.725E-06
ksat_vz	high	1.000E+00	3.270E-02	9.673E-01	-1.678E-03	9.673E-01	7.841E-05	9.672E-01	1.137E-03	1.000E+00	3.278E-02	9.672E-01	-5.785E-04
	low	1.000E+00	3.011E-01	6.989E-01	2.742E-04	6.989E-01	2.628E-04	6.987E-01	3.772E-04	1.000E+00	3.013E-01	6.987E-01	5.364E-04

Table F.73. STOMP Mass Balance for U-238 (Kd = 0.10) for Case 1 (Past Leak)

Sub-Case		Vadose Zone				Aquifer				Vadose Zone + Aquifer			
		Released	In Domain	Exit	%error	Released	In Domain	Exit	%error	Released	In Domain	Exit	%error
base		1.000E+00	6.606E-02	9.343E-01	-3.206E-02	9.343E-01	1.234E-04	9.340E-01	1.562E-02	1.000E+00	6.618E-02	9.340E-01	-1.746E-02
recharge	high	1.000E+00	3.942E-02	9.622E-01	-1.627E-01	9.622E-01	7.571E-05	9.612E-01	9.115E-02	1.000E+00	3.950E-02	9.612E-01	-7.501E-02
	low	1.000E+00	1.594E-01	8.406E-01	1.565E-04	8.406E-01	2.750E-04	8.403E-01	-2.981E-06	1.000E+00	1.597E-01	8.403E-01	1.535E-04
barrier	high	1.000E+00	6.032E-02	9.400E-01	-3.210E-02	9.400E-01	1.134E-04	9.397E-01	1.553E-02	1.000E+00	6.043E-02	9.397E-01	-1.750E-02
	low	1.000E+00	7.106E-02	9.293E-01	-3.202E-02	9.293E-01	1.319E-04	9.290E-01	1.569E-02	1.000E+00	7.119E-02	9.290E-01	-1.744E-02
barrier_deg	high	1.000E+00	7.010E-06	1.000E+00	-3.210E-02	1.000E+00	5.171E-08	1.000E+00	1.459E-02	1.000E+00	7.062E-06	1.000E+00	-1.750E-02
	low	1.000E+00	2.605E-01	7.398E-01	-3.187E-02	7.398E-01	1.990E-04	7.395E-01	1.972E-02	1.000E+00	2.607E-01	7.395E-01	-1.728E-02
plume	high	1.000E+00	1.446E-01	8.554E-01	-5.345E-03	8.554E-01	2.346E-04	8.552E-01	2.836E-03	1.000E+00	1.448E-01	8.552E-01	-2.919E-03
	low	1.000E+00	2.055E-02	9.811E-01	-1.648E-01	9.811E-01	4.342E-05	9.803E-01	8.046E-02	1.000E+00	2.059E-02	9.803E-01	-8.586E-02
ksat_aq	high	1.000E+00	6.604E-02	9.343E-01	-3.220E-02	9.343E-01	9.249E-05	9.340E-01	1.529E-02	1.000E+00	6.613E-02	9.340E-01	-1.792E-02
	low	1.000E+00	6.610E-02	9.342E-01	-3.173E-02	9.342E-01	1.851E-04	9.339E-01	1.637E-02	1.000E+00	6.628E-02	9.339E-01	-1.644E-02
ksat_vz	high	1.000E+00	5.640E-02	9.440E-01	-4.177E-02	9.440E-01	1.210E-04	9.435E-01	3.903E-02	1.000E+00	5.653E-02	9.435E-01	-4.921E-03
	low	1.000E+00	9.898E-02	9.013E-01	-3.209E-02	9.013E-01	1.334E-04	9.011E-01	1.515E-02	1.000E+00	9.912E-02	9.011E-01	-1.844E-02

Table F.74. STOMP Mass Balance for U-238 (Kd = 0.10) for Case 2 (Diffusion)

Sub-Case		Vadose Zone				Aquifer				Vadose Zone + Aquifer			
		Released	In Domain	Exit	%error	Released	In Domain	Exit	%error	Released	In Domain	Exit	%error
base		2.430E-01	2.428E-01	1.340E-04	4.538E-04	1.340E-04	1.081E-06	1.329E-04	3.288E-03	2.430E-01	2.428E-01	1.329E-04	4.529E-04
recharge	high	2.430E-01	2.428E-01	1.343E-04	5.096E-04	1.343E-04	1.083E-06	1.332E-04	3.240E-03	2.430E-01	2.428E-01	1.332E-04	5.094E-04
	low	2.430E-01	2.428E-01	1.331E-04	4.774E-04	1.331E-04	1.076E-06	1.320E-04	3.291E-03	2.430E-01	2.428E-01	1.320E-04	4.805E-04
barrier	high	2.430E-01	2.428E-01	1.619E-04	5.085E-04	1.619E-04	1.252E-06	1.607E-04	2.822E-03	2.430E-01	2.428E-01	1.607E-04	5.106E-04
	low	2.430E-01	2.429E-01	1.145E-04	4.508E-04	1.145E-04	9.556E-07	1.136E-04	3.754E-03	2.430E-01	2.429E-01	1.136E-04	4.534E-04
barrier_deg	high	2.430E-01	9.706E-02	1.459E-01	1.963E-04	1.459E-01	1.201E-04	1.458E-01	-1.043E-05	2.430E-01	9.718E-02	1.458E-01	1.901E-04
	low	2.430E-01	2.430E-01	3.099E-09	3.054E-04	3.099E-09	3.459E-11	5.637E-10	8.069E+01	2.430E-01	2.430E-01	5.637E-10	3.064E-04
diffusion	high	7.683E-01	7.679E-01	4.236E-04	6.725E-04	4.236E-04	3.419E-06	4.202E-04	1.011E-03	7.683E-01	7.679E-01	4.202E-04	6.758E-04
	low	7.683E-04	7.679E-04	4.219E-07	1.277E-03	4.219E-07	3.412E-09	4.129E-07	1.314E+00	7.683E-04	7.679E-04	4.129E-07	1.996E-03
ksat_aq	high	2.430E-01	2.428E-01	1.340E-04	4.540E-04	1.340E-04	8.119E-07	1.332E-04	3.618E-03	2.430E-01	2.428E-01	1.332E-04	4.590E-04
	low	2.430E-01	2.428E-01	1.338E-04	4.531E-04	1.338E-04	1.617E-06	1.322E-04	2.874E-03	2.430E-01	2.428E-01	1.322E-04	4.518E-04
ksat_vz	high	2.430E-01	2.428E-01	1.808E-04	3.594E-04	1.808E-04	1.450E-06	1.794E-04	4.123E-03	2.430E-01	2.428E-01	1.794E-04	3.642E-04
	low	2.430E-01	2.429E-01	1.026E-04	4.155E-04	1.026E-04	7.959E-07	1.018E-04	7.017E-03	2.430E-01	2.429E-01	1.018E-04	4.210E-04

Table F.75. STOMP Mass Balance for U-238 (Kd = 0.10) for Case 3 (Retrieval Leak)

Sub-Case		Vadose Zone				Aquifer				Vadose Zone + Aquifer			
		Released	In Domain	Exit	%error	Released	In Domain	Exit	%error	Released	In Domain	Exit	%error
base		1.000E+00	8.802E-01	1.198E-01	3.457E-04	1.198E-01	2.698E-04	1.195E-01	-2.637E-05	1.000E+00	8.805E-01	1.195E-01	3.427E-04
recharge	high	1.000E+00	8.241E-01	1.759E-01	5.469E-04	1.759E-01	3.278E-04	1.756E-01	8.933E-06	1.000E+00	8.244E-01	1.756E-01	5.499E-04
	low	1.000E+00	9.469E-01	5.307E-02	5.070E-04	5.307E-02	1.624E-04	5.291E-02	-6.307E-07	1.000E+00	9.471E-01	5.291E-02	5.048E-04
barrier	high	1.000E+00	8.675E-01	1.325E-01	5.618E-04	1.325E-01	2.864E-04	1.322E-01	9.094E-06	1.000E+00	8.678E-01	1.322E-01	5.618E-04
	low	1.000E+00	8.900E-01	1.100E-01	3.457E-04	1.100E-01	2.563E-04	1.098E-01	4.258E-06	1.000E+00	8.902E-01	1.098E-01	3.457E-04
barrier_deg	high	1.000E+00	5.227E-03	9.948E-01	3.316E-05	9.948E-01	3.224E-05	9.947E-01	8.898E-07	1.000E+00	5.260E-03	9.947E-01	3.404E-05
	low	1.000E+00	9.889E-01	1.108E-02	3.611E-04	1.108E-02	2.337E-05	1.106E-02	-2.117E-06	1.000E+00	9.889E-01	1.106E-02	3.615E-04
ksat_aq	high	1.000E+00	8.802E-01	1.198E-01	3.114E-04	1.198E-01	2.025E-04	1.196E-01	2.385E-05	1.000E+00	8.804E-01	1.196E-01	3.137E-04
	low	1.000E+00	8.803E-01	1.197E-01	4.143E-04	1.197E-01	4.044E-04	1.193E-01	2.878E-05	1.000E+00	8.807E-01	1.193E-01	4.187E-04
ksat_vz	high	1.000E+00	8.628E-01	1.373E-01	-1.010E-03	1.373E-01	3.292E-04	1.369E-01	2.212E-05	1.000E+00	8.631E-01	1.369E-01	-1.004E-03
	low	1.000E+00	9.474E-01	5.263E-02	7.764E-04	5.263E-02	1.330E-04	5.249E-02	9.346E-06	1.000E+00	9.475E-01	5.249E-02	7.764E-04

Table F.76. STOMP Mass Balance for U-238 (Kd = 0.10) for Case 4 (Ancillary Equipment)

Sub-Case		Vadose Zone				Aquifer				Vadose Zone + Aquifer			
		Released	In Domain	Exit	%error	Released	In Domain	Exit	%error	Released	In Domain	Exit	%error
base		1.000E+00	9.098E-01	9.024E-02	4.835E-04	9.024E-02	2.271E-04	9.001E-02	-1.742E-06	1.000E+00	9.100E-01	9.001E-02	4.850E-04
recharge	high	1.000E+00	8.296E-01	1.704E-01	4.753E-04	1.704E-01	3.154E-04	1.700E-01	-2.255E-06	1.000E+00	8.299E-01	1.700E-01	4.724E-04
	low	1.000E+00	9.826E-01	1.736E-02	7.559E-04	1.736E-02	7.507E-05	1.729E-02	1.211E-05	1.000E+00	9.827E-01	1.729E-02	7.587E-04
barrier	high	1.000E+00	8.986E-01	1.014E-01	5.685E-04	1.014E-01	2.440E-04	1.011E-01	3.637E-05	1.000E+00	8.989E-01	1.011E-01	5.729E-04
	low	1.000E+00	9.182E-01	8.181E-02	4.068E-04	8.181E-02	2.135E-04	8.160E-02	-1.210E-06	1.000E+00	9.184E-01	8.160E-02	4.053E-04
barrier_deg	high	1.000E+00	6.495E-03	9.935E-01	1.066E-05	9.935E-01	3.749E-05	9.935E-01	4.617E-07	1.000E+00	6.533E-03	9.935E-01	1.113E-05
	low	1.000E+00	9.950E-01	5.022E-03	4.464E-04	5.022E-03	1.311E-05	5.009E-03	6.317E-05	1.000E+00	9.950E-01	5.009E-03	4.461E-04
ksat_aq	high	1.000E+00	9.097E-01	9.025E-02	4.895E-04	9.025E-02	1.704E-04	9.008E-02	4.756E-06	1.000E+00	9.099E-01	9.008E-02	4.910E-04
	low	1.000E+00	9.098E-01	9.020E-02	4.686E-04	9.020E-02	3.403E-04	8.986E-02	5.614E-06	1.000E+00	9.101E-01	8.986E-02	4.664E-04
ksat_vz	high	1.000E+00	9.040E-01	9.602E-02	-8.352E-04	9.602E-02	2.689E-04	9.576E-02	3.267E-05	1.000E+00	9.043E-01	9.576E-02	-8.345E-04
	low	1.000E+00	9.208E-01	7.915E-02	6.005E-04	7.915E-02	1.721E-04	7.898E-02	1.206E-05	1.000E+00	9.210E-01	7.898E-02	6.042E-04

Table F.77. STOMP Mass Balance for U-238 (Kd = 0.20) for Case 1 (Past Leak)

Sub-Case		Vadose Zone				Aquifer				Vadose Zone + Aquifer			
		Released	In Domain	Exit	%error	Released	In Domain	Exit	%error	Released	In Domain	Exit	%error
base		1.000E+00	4.380E-01	5.620E-01	-3.636E-04	5.620E-01	5.384E-04	5.615E-01	5.642E-04	1.000E+00	4.385E-01	5.615E-01	-4.768E-05
recharge	high	1.000E+00	3.378E-01	6.622E-01	-7.930E-03	6.622E-01	4.563E-04	6.617E-01	6.504E-03	1.000E+00	3.383E-01	6.617E-01	-3.624E-03
	low	1.000E+00	6.460E-01	3.540E-01	3.159E-04	3.540E-01	6.140E-04	3.534E-01	-6.627E-06	1.000E+00	6.466E-01	3.534E-01	3.159E-04
barrier	high	1.000E+00	4.207E-01	5.793E-01	-4.351E-04	5.793E-01	5.270E-04	5.788E-01	5.462E-04	1.000E+00	4.212E-01	5.788E-01	-1.192E-04
	low	1.000E+00	4.522E-01	5.478E-01	-3.845E-04	5.478E-01	5.470E-04	5.473E-01	5.893E-04	1.000E+00	4.527E-01	5.473E-01	-6.258E-05
barrier_deg	high	1.000E+00	2.529E-03	9.975E-01	-6.513E-04	9.975E-01	1.728E-05	9.975E-01	3.229E-04	1.000E+00	2.546E-03	9.975E-01	-3.292E-04
	low	1.000E+00	7.418E-01	2.582E-01	-2.325E-04	2.582E-01	2.897E-04	2.579E-01	1.239E-03	1.000E+00	7.421E-01	2.579E-01	8.941E-05
plume	high	1.000E+00	6.441E-01	3.559E-01	3.845E-04	3.559E-01	5.513E-04	3.553E-01	4.038E-05	1.000E+00	6.447E-01	3.553E-01	3.994E-04
	low	1.000E+00	2.150E-01	7.851E-01	-1.146E-02	7.851E-01	3.591E-04	7.847E-01	7.167E-03	1.000E+00	2.154E-01	7.847E-01	-5.837E-03
ksat_aq	high	1.000E+00	4.379E-01	5.621E-01	-4.083E-04	5.621E-01	4.039E-04	5.617E-01	5.246E-04	1.000E+00	4.383E-01	5.617E-01	-1.132E-04
	low	1.000E+00	4.381E-01	5.619E-01	-3.666E-04	5.619E-01	8.074E-04	5.611E-01	6.523E-04	1.000E+00	4.389E-01	5.611E-01	0.000E+00
ksat_vz	high	1.000E+00	4.622E-01	5.379E-01	-2.527E-03	5.379E-01	5.968E-04	5.373E-01	1.162E-03	1.000E+00	4.627E-01	5.373E-01	-1.901E-03
	low	1.000E+00	4.342E-01	5.658E-01	-1.091E-03	5.658E-01	4.434E-04	5.654E-01	1.088E-03	1.000E+00	4.346E-01	5.654E-01	-4.768E-04

Table F.78. STOMP Mass Balance for U-238 (Kd = 0.20) for Case 2 (Diffusion)

Sub-Case		Vadose Zone				Aquifer				Vadose Zone + Aquifer			
		Released	In Domain	Exit	%error	Released	In Domain	Exit	%error	Released	In Domain	Exit	%error
base		2.430E-01	2.430E-01	1.715E-08	2.137E-04	1.715E-08	3.346E-10	1.349E-08	1.941E+01	2.430E-01	2.430E-01	1.349E-08	2.152E-04
recharge	high	2.430E-01	2.430E-01	1.727E-08	1.217E-04	1.727E-08	3.365E-10	1.360E-08	1.931E+01	2.430E-01	2.430E-01	1.360E-08	1.232E-04
	low	2.430E-01	2.430E-01	1.687E-08	1.280E-04	1.687E-08	3.297E-10	1.322E-08	1.966E+01	2.430E-01	2.430E-01	1.322E-08	1.295E-04
barrier	high	2.430E-01	2.430E-01	2.514E-08	2.166E-04	2.514E-08	4.729E-10	2.113E-08	1.409E+01	2.430E-01	2.430E-01	2.113E-08	2.182E-04
	low	2.430E-01	2.430E-01	1.257E-08	1.175E-04	1.257E-08	2.505E-10	9.215E-09	2.471E+01	2.430E-01	2.430E-01	9.215E-09	1.189E-04
barrier_deg	high	2.430E-01	1.930E-01	4.993E-02	3.956E-04	4.993E-02	1.999E-04	4.973E-02	2.396E-05	2.430E-01	1.932E-01	4.973E-02	3.986E-04
	low	2.430E-01	2.430E-01	0.000E+00	9.813E-05	0.000E+00	0.000E+00	0.000E+00	0.000E+00	2.430E-01	2.430E-01	0.000E+00	9.813E-05
diffusion	high	7.683E-01	7.683E-01	5.515E-08	3.962E-04	5.515E-08	1.082E-09	5.056E-08	6.361E+00	7.683E-01	7.683E-01	5.056E-08	3.968E-04
	low	7.683E-04	7.683E-04	0.000E+00	6.591E-04	0.000E+00	0.000E+00	0.000E+00	0.000E+00	7.683E-04	7.683E-04	0.000E+00	6.591E-04
ksat_aq	high	2.430E-01	2.430E-01	1.718E-08	2.137E-04	1.718E-08	2.500E-10	1.316E-08	2.193E+01	2.430E-01	2.430E-01	1.316E-08	2.154E-04
	low	2.430E-01	2.430E-01	1.710E-08	2.137E-04	1.710E-08	5.012E-10	1.377E-08	1.655E+01	2.430E-01	2.430E-01	1.377E-08	2.151E-04
ksat_vz	high	2.430E-01	2.430E-01	9.501E-09	3.518E-04	9.501E-09	1.847E-10	5.528E-09	3.987E+01	2.430E-01	2.430E-01	5.528E-09	3.534E-04
	low	2.430E-01	2.430E-01	6.066E-08	9.156E-05	6.066E-08	1.079E-09	5.562E-08	6.531E+00	2.430E-01	2.430E-01	5.562E-08	9.363E-05

Table F.79. STOMP Mass Balance for U-238 (Kd = 0.20) for Case 3 (Retrieval Leak)

Sub-Case		Vadose Zone				Aquifer				Vadose Zone + Aquifer			
		Released	In Domain	Exit	%error	Released	In Domain	Exit	%error	Released	In Domain	Exit	%error
base		1.000E+00	9.985E-01	1.460E-03	3.004E-04	1.460E-03	8.919E-06	1.451E-03	3.502E-04	1.000E+00	9.985E-01	1.451E-03	2.988E-04
recharge	high	1.000E+00	9.967E-01	3.300E-03	3.594E-04	3.300E-03	1.766E-05	3.282E-03	1.079E-04	1.000E+00	9.967E-01	3.282E-03	3.611E-04
	low	1.000E+00	9.997E-01	3.029E-04	6.718E-04	3.029E-04	2.313E-06	3.006E-04	2.281E-03	1.000E+00	9.997E-01	3.006E-04	6.713E-04
barrier	high	1.000E+00	9.982E-01	1.759E-03	4.408E-04	1.759E-03	1.047E-05	1.749E-03	2.435E-04	1.000E+00	9.982E-01	1.749E-03	4.397E-04
	low	1.000E+00	9.987E-01	1.252E-03	4.157E-04	1.252E-03	7.804E-06	1.244E-03	4.545E-04	1.000E+00	9.988E-01	1.244E-03	4.159E-04
barrier_deg	high	1.000E+00	2.783E-01	7.217E-01	3.010E-04	7.217E-01	1.020E-03	7.207E-01	2.016E-06	1.000E+00	2.793E-01	7.207E-01	3.010E-04
	low	1.000E+00	1.000E+00	3.479E-05	6.274E-04	3.479E-05	1.588E-07	3.463E-05	1.715E-02	1.000E+00	1.000E+00	3.463E-05	6.260E-04
ksat_aq	high	1.000E+00	9.985E-01	1.461E-03	3.004E-04	1.461E-03	6.697E-06	1.454E-03	3.917E-04	1.000E+00	9.985E-01	1.454E-03	3.032E-04
	low	1.000E+00	9.985E-01	1.459E-03	2.995E-04	1.459E-03	1.335E-05	1.446E-03	3.468E-04	1.000E+00	9.986E-01	1.446E-03	2.995E-04
ksat_vz	high	1.000E+00	9.988E-01	1.195E-03	5.977E-04	1.195E-03	8.024E-06	1.187E-03	1.078E-03	1.000E+00	9.988E-01	1.187E-03	5.968E-04
	low	1.000E+00	9.992E-01	7.681E-04	4.873E-04	7.681E-04	4.842E-06	7.632E-04	9.044E-04	1.000E+00	9.992E-01	7.632E-04	4.894E-04

Table F.80. STOMP Mass Balance for U-238 (Kd = 0.20) for Case 4 (Ancillary Equipment)

Sub-Case		Vadose Zone				Aquifer				Vadose Zone + Aquifer			
		Released	In Domain	Exit	%error	Released	In Domain	Exit	%error	Released	In Domain	Exit	%error
base		1.000E+00	9.994E-01	5.690E-04	8.338E-04	5.690E-04	4.131E-06	5.649E-04	1.197E-03	1.000E+00	9.994E-01	5.649E-04	8.363E-04
recharge	high	1.000E+00	9.975E-01	2.497E-03	5.452E-04	2.497E-03	1.412E-05	2.483E-03	1.963E-04	1.000E+00	9.975E-01	2.483E-03	5.450E-04
	low	1.000E+00	1.000E+00	1.669E-05	5.421E-04	1.669E-05	1.928E-07	1.649E-05	2.792E-02	1.000E+00	1.000E+00	1.649E-05	5.440E-04
barrier	high	1.000E+00	9.993E-01	7.141E-04	8.144E-04	7.141E-04	5.026E-06	7.091E-04	9.713E-04	1.000E+00	9.993E-01	7.091E-04	8.170E-04
	low	1.000E+00	9.995E-01	4.710E-04	9.074E-04	4.710E-04	3.508E-06	4.675E-04	1.445E-03	1.000E+00	9.995E-01	4.675E-04	9.072E-04
barrier_deg	high	1.000E+00	3.147E-01	6.853E-01	3.487E-04	6.853E-01	1.049E-03	6.843E-01	1.177E-05	1.000E+00	3.157E-01	6.843E-01	3.576E-04
	low	1.000E+00	1.000E+00	4.242E-06	3.924E-04	4.242E-06	2.610E-08	4.206E-06	2.432E-01	1.000E+00	1.000E+00	4.206E-06	3.960E-04
ksat_aq	high	1.000E+00	9.994E-01	5.693E-04	8.314E-04	5.693E-04	3.103E-06	5.661E-04	1.311E-03	1.000E+00	9.994E-01	5.661E-04	8.325E-04
	low	1.000E+00	9.994E-01	5.685E-04	8.322E-04	5.685E-04	6.180E-06	5.623E-04	1.056E-03	1.000E+00	9.994E-01	5.623E-04	8.309E-04
ksat_vz	high	1.000E+00	9.997E-01	2.543E-04	7.090E-04	2.543E-04	2.191E-06	2.521E-04	3.943E-03	1.000E+00	9.997E-01	2.521E-04	7.086E-04
	low	1.000E+00	9.986E-01	1.367E-03	3.223E-04	1.367E-03	7.878E-06	1.359E-03	4.230E-04	1.000E+00	9.986E-01	1.359E-03	3.239E-04

Table F.81. STOMP Mass Balance for U-238 (Kd = 0.60) for Case 1 (Past Leak)

Sub-Case		Vadose Zone				Aquifer				Vadose Zone + Aquifer			
		Released	In Domain	Exit	%error	Released	In Domain	Exit	%error	Released	In Domain	Exit	%error
base		1.000E+00	9.948E-01	5.158E-03	1.412E-04	5.158E-03	4.745E-05	5.111E-03	5.593E-05	1.000E+00	9.949E-01	5.111E-03	1.423E-04
recharge	high	1.000E+00	9.887E-01	1.134E-02	2.678E-04	1.134E-02	8.549E-05	1.125E-02	-3.279E-05	1.000E+00	9.887E-01	1.125E-02	2.695E-04
	low	1.000E+00	9.992E-01	8.205E-04	3.486E-04	8.205E-04	1.115E-05	8.093E-04	5.925E-04	1.000E+00	9.992E-01	8.093E-04	3.494E-04
barrier	high	1.000E+00	9.942E-01	5.836E-03	3.152E-04	5.836E-03	5.227E-05	5.784E-03	4.183E-05	1.000E+00	9.942E-01	5.784E-03	3.155E-04
	low	1.000E+00	9.953E-01	4.658E-03	1.191E-04	4.658E-03	4.378E-05	4.614E-03	7.373E-05	1.000E+00	9.954E-01	4.614E-03	1.165E-04
barrier_deg	high	1.000E+00	5.216E-01	4.784E-01	4.858E-04	4.784E-01	1.888E-03	4.765E-01	-3.212E-06	1.000E+00	5.235E-01	4.765E-01	4.858E-04
	low	1.000E+00	9.996E-01	4.424E-04	1.074E-04	4.424E-04	3.439E-06	4.389E-04	7.371E-04	1.000E+00	9.996E-01	4.389E-04	1.059E-04
plume	high	1.000E+00	9.995E-01	5.139E-04	1.637E-04	5.139E-04	6.295E-06	5.076E-04	9.912E-04	1.000E+00	9.995E-01	5.076E-04	1.619E-04
	low	1.000E+00	9.546E-01	4.538E-02	2.120E-04	4.538E-02	2.714E-04	4.511E-02	3.136E-05	1.000E+00	9.549E-01	4.511E-02	2.131E-04
ksat_aq	high	1.000E+00	9.948E-01	5.160E-03	1.393E-04	5.160E-03	3.565E-05	5.125E-03	5.689E-05	1.000E+00	9.949E-01	5.125E-03	1.399E-04
	low	1.000E+00	9.948E-01	5.153E-03	1.234E-04	5.153E-03	7.095E-05	5.082E-03	5.450E-05	1.000E+00	9.949E-01	5.082E-03	1.261E-04
ksat_vz	high	1.000E+00	9.973E-01	2.698E-03	1.744E-04	2.698E-03	2.890E-05	2.669E-03	4.147E-04	1.000E+00	9.973E-01	2.669E-03	1.744E-04
	low	1.000E+00	9.880E-01	1.200E-02	3.744E-04	1.200E-02	8.699E-05	1.191E-02	-2.395E-05	1.000E+00	9.881E-01	1.191E-02	3.711E-04

Table F.82. STOMP Mass Balance for U-238 (Kd = 0.60) for Case 2 (Diffusion)

Sub-Case		Vadose Zone				Aquifer				Vadose Zone + Aquifer			
		Released	In Domain	Exit	%error	Released	In Domain	Exit	%error	Released	In Domain	Exit	%error
base		2.430E-01	2.430E-01	0.000E+00	6.746E-05	0.000E+00	0.000E+00	0.000E+00	0.000E+00	2.430E-01	2.430E-01	0.000E+00	6.746E-05
recharge	high	2.430E-01	2.430E-01	0.000E+00	7.973E-05	0.000E+00	0.000E+00	0.000E+00	0.000E+00	2.430E-01	2.430E-01	0.000E+00	7.973E-05
	low	2.430E-01	2.430E-01	0.000E+00	6.746E-05	0.000E+00	0.000E+00	0.000E+00	0.000E+00	2.430E-01	2.430E-01	0.000E+00	6.746E-05
barrier	high	2.430E-01	2.430E-01	0.000E+00	6.746E-05	0.000E+00	0.000E+00	0.000E+00	0.000E+00	2.430E-01	2.430E-01	0.000E+00	6.746E-05
	low	2.430E-01	2.430E-01	0.000E+00	9.813E-05	0.000E+00	0.000E+00	0.000E+00	0.000E+00	2.430E-01	2.430E-01	0.000E+00	9.813E-05
barrier_deg	high	2.430E-01	2.430E-01	1.680E-06	3.082E-04	1.680E-06	6.493E-08	1.612E-06	1.676E-01	2.430E-01	2.430E-01	1.612E-06	3.116E-04
	low	2.430E-01	2.430E-01	0.000E+00	-1.227E-05	0.000E+00	0.000E+00	0.000E+00	0.000E+00	2.430E-01	2.430E-01	0.000E+00	-1.227E-05
diffusion	high	7.683E-01	7.683E-01	0.000E+00	1.086E-04	0.000E+00	0.000E+00	0.000E+00	0.000E+00	7.683E-01	7.683E-01	0.000E+00	1.086E-04
	low	7.683E-04	7.683E-04	0.000E+00	3.409E-04	0.000E+00	0.000E+00	0.000E+00	0.000E+00	7.683E-04	7.683E-04	0.000E+00	3.409E-04
ksat_aq	high	2.430E-01	2.430E-01	0.000E+00	6.746E-05	0.000E+00	0.000E+00	0.000E+00	0.000E+00	2.430E-01	2.430E-01	0.000E+00	6.746E-05
	low	2.430E-01	2.430E-01	0.000E+00	6.746E-05	0.000E+00	0.000E+00	0.000E+00	0.000E+00	2.430E-01	2.430E-01	0.000E+00	6.746E-05
ksat_vz	high	2.430E-01	2.430E-01	0.000E+00	3.066E-05	0.000E+00	0.000E+00	0.000E+00	0.000E+00	2.430E-01	2.430E-01	0.000E+00	3.066E-05
	low	2.430E-01	2.430E-01	0.000E+00	3.066E-05	0.000E+00	0.000E+00	0.000E+00	0.000E+00	2.430E-01	2.430E-01	0.000E+00	3.066E-05

Table F.83. STOMP Mass Balance for U-238 (Kd = 0.60) for Case 3 (Retrieval Leak)

Sub-Case		Vadose Zone				Aquifer				Vadose Zone + Aquifer			
		Released	In Domain	Exit	%error	Released	In Domain	Exit	%error	Released	In Domain	Exit	%error
base		1.000E+00	1.000E+00	0.000E+00	2.861E-04	0.000E+00	0.000E+00	0.000E+00	0.000E+00	1.000E+00	1.000E+00	0.000E+00	2.861E-04
recharge	high	1.000E+00	1.000E+00	0.000E+00	1.848E-04	0.000E+00	0.000E+00	0.000E+00	0.000E+00	1.000E+00	1.000E+00	0.000E+00	1.848E-04
	low	1.000E+00	1.000E+00	0.000E+00	1.907E-04	0.000E+00	0.000E+00	0.000E+00	0.000E+00	1.000E+00	1.000E+00	0.000E+00	1.907E-04
barrier	high	1.000E+00	1.000E+00	0.000E+00	1.609E-04	0.000E+00	0.000E+00	0.000E+00	0.000E+00	1.000E+00	1.000E+00	0.000E+00	1.609E-04
	low	1.000E+00	1.000E+00	0.000E+00	2.801E-04	0.000E+00	0.000E+00	0.000E+00	0.000E+00	1.000E+00	1.000E+00	0.000E+00	2.801E-04
barrier_deg	high	1.000E+00	9.995E-01	5.080E-04	2.668E-04	5.080E-04	1.238E-05	4.956E-04	6.251E-04	1.000E+00	9.995E-01	4.956E-04	2.657E-04
	low	1.000E+00	1.000E+00	0.000E+00	1.729E-04	0.000E+00	0.000E+00	0.000E+00	0.000E+00	1.000E+00	1.000E+00	0.000E+00	1.729E-04
ksat_aq	high	1.000E+00	1.000E+00	0.000E+00	2.861E-04	0.000E+00	0.000E+00	0.000E+00	0.000E+00	1.000E+00	1.000E+00	0.000E+00	2.861E-04
	low	1.000E+00	1.000E+00	0.000E+00	2.861E-04	0.000E+00	0.000E+00	0.000E+00	0.000E+00	1.000E+00	1.000E+00	0.000E+00	2.861E-04
ksat_vz	high	1.000E+00	1.000E+00	0.000E+00	2.086E-04	0.000E+00	0.000E+00	0.000E+00	0.000E+00	1.000E+00	1.000E+00	0.000E+00	2.086E-04
	low	1.000E+00	1.000E+00	0.000E+00	1.490E-04	0.000E+00	0.000E+00	0.000E+00	0.000E+00	1.000E+00	1.000E+00	0.000E+00	1.490E-04

Table F.84. STOMP Mass Balance for U-238 (Kd = 0.60) for Case 4 (Ancillary Equipment)

Sub-Case		Vadose Zone				Aquifer				Vadose Zone + Aquifer			
		Released	In Domain	Exit	%error	Released	In Domain	Exit	%error	Released	In Domain	Exit	%error
base		1.000E+00	1.000E+00	0.000E+00	2.146E-04	0.000E+00	0.000E+00	0.000E+00	0.000E+00	1.000E+00	1.000E+00	0.000E+00	2.146E-04
recharge	high	1.000E+00	1.000E+00	0.000E+00	1.431E-04	0.000E+00	0.000E+00	0.000E+00	0.000E+00	1.000E+00	1.000E+00	0.000E+00	1.431E-04
	low	1.000E+00	1.000E+00	0.000E+00	1.788E-04	0.000E+00	0.000E+00	0.000E+00	0.000E+00	1.000E+00	1.000E+00	0.000E+00	1.788E-04
barrier	high	1.000E+00	1.000E+00	0.000E+00	2.563E-04	0.000E+00	0.000E+00	0.000E+00	0.000E+00	1.000E+00	1.000E+00	0.000E+00	2.563E-04
	low	1.000E+00	1.000E+00	0.000E+00	1.431E-04	0.000E+00	0.000E+00	0.000E+00	0.000E+00	1.000E+00	1.000E+00	0.000E+00	1.431E-04
barrier_deg	high	1.000E+00	9.997E-01	2.627E-04	5.295E-04	2.627E-04	6.737E-06	2.560E-04	1.125E-03	1.000E+00	9.997E-01	2.560E-04	5.299E-04
	low	1.000E+00	1.000E+00	0.000E+00	1.073E-04	0.000E+00	0.000E+00	0.000E+00	0.000E+00	1.000E+00	1.000E+00	0.000E+00	1.073E-04
ksat_aq	high	1.000E+00	1.000E+00	0.000E+00	2.146E-04	0.000E+00	0.000E+00	0.000E+00	0.000E+00	1.000E+00	1.000E+00	0.000E+00	2.146E-04
	low	1.000E+00	1.000E+00	0.000E+00	2.146E-04	0.000E+00	0.000E+00	0.000E+00	0.000E+00	1.000E+00	1.000E+00	0.000E+00	2.146E-04
ksat_vz	high	1.000E+00	1.000E+00	0.000E+00	1.967E-04	0.000E+00	0.000E+00	0.000E+00	0.000E+00	1.000E+00	1.000E+00	0.000E+00	1.967E-04
	low	1.000E+00	1.000E+00	0.000E+00	1.729E-04	0.000E+00	0.000E+00	0.000E+00	0.000E+00	1.000E+00	1.000E+00	0.000E+00	1.729E-04

Table F.85. STOMP Mass Balance for U-238 (Kd = 1.00) for Case 1 (Past Leak)

Sub-Case		Vadose Zone				Aquifer				Vadose Zone + Aquifer			
		Released	In Domain	Exit	%error	Released	In Domain	Exit	%error	Released	In Domain	Exit	%error
base		1.000E+00	1.000E+00	2.725E-05	6.431E-05	2.725E-05	5.866E-07	2.666E-05	2.027E-02	1.000E+00	1.000E+00	2.666E-05	6.392E-05
recharge	high	1.000E+00	9.999E-01	9.376E-05	1.428E-04	9.376E-05	1.694E-06	9.206E-05	5.414E-03	1.000E+00	9.999E-01	9.206E-05	1.458E-04
	low	1.000E+00	1.000E+00	1.679E-06	1.898E-04	1.679E-06	5.129E-08	1.623E-06	2.516E-01	1.000E+00	1.000E+00	1.623E-06	1.894E-04
barrier	high	1.000E+00	1.000E+00	3.273E-05	1.657E-04	3.273E-05	6.897E-07	3.204E-05	1.693E-02	1.000E+00	1.000E+00	3.204E-05	1.637E-04
	low	1.000E+00	1.000E+00	2.344E-05	1.178E-04	2.344E-05	5.132E-07	2.292E-05	2.352E-02	1.000E+00	1.000E+00	2.292E-05	1.160E-04
barrier_deg	high	1.000E+00	9.351E-01	6.493E-02	2.444E-04	6.493E-02	9.469E-04	6.398E-02	2.331E-06	1.000E+00	9.360E-01	6.398E-02	2.421E-04
	low	1.000E+00	1.000E+00	8.799E-07	3.121E-05	8.799E-07	1.496E-08	8.573E-07	8.784E-01	1.000E+00	1.000E+00	8.573E-07	3.348E-05
plume	high	1.000E+00	1.000E+00	5.720E-07	6.797E-05	5.720E-07	1.570E-08	5.513E-07	8.777E-01	1.000E+00	1.000E+00	5.513E-07	7.004E-05
	low	1.000E+00	9.987E-01	1.257E-03	1.970E-04	1.257E-03	1.893E-05	1.239E-03	2.563E-04	1.000E+00	9.988E-01	1.239E-03	1.946E-04
ksat_aq	high	1.000E+00	1.000E+00	2.728E-05	6.773E-05	2.728E-05	4.415E-07	2.683E-05	2.211E-02	1.000E+00	1.000E+00	2.683E-05	7.077E-05
	low	1.000E+00	1.000E+00	2.720E-05	6.931E-05	2.720E-05	8.737E-07	2.632E-05	1.837E-02	1.000E+00	1.000E+00	2.632E-05	6.778E-05
ksat_vz	high	1.000E+00	1.000E+00	8.571E-06	1.085E-04	8.571E-06	2.106E-07	8.352E-06	9.965E-02	1.000E+00	1.000E+00	8.352E-06	1.065E-04
	low	1.000E+00	9.999E-01	1.428E-04	1.720E-04	1.428E-04	2.525E-06	1.402E-04	3.230E-03	1.000E+00	9.999E-01	1.402E-04	1.747E-04

Table F.86. STOMP Mass Balance for U-238 (Kd = 1.00) for Case 2 (Diffusion)

Sub-Case		Vadose Zone				Aquifer				Vadose Zone + Aquifer			
		Released	In Domain	Exit	%error	Released	In Domain	Exit	%error	Released	In Domain	Exit	%error
base		2.430E-01	2.430E-01	0.000E+00	6.133E-05	0.000E+00	0.000E+00	0.000E+00	0.000E+00	2.430E-01	2.430E-01	0.000E+00	6.133E-05
recharge	high	2.430E-01	2.430E-01	0.000E+00	3.680E-05	0.000E+00	0.000E+00	0.000E+00	0.000E+00	2.430E-01	2.430E-01	0.000E+00	3.680E-05
	low	2.430E-01	2.430E-01	0.000E+00	1.840E-05	0.000E+00	0.000E+00	0.000E+00	0.000E+00	2.430E-01	2.430E-01	0.000E+00	1.840E-05
barrier	high	2.430E-01	2.430E-01	0.000E+00	4.906E-05	0.000E+00	0.000E+00	0.000E+00	0.000E+00	2.430E-01	2.430E-01	0.000E+00	4.906E-05
	low	2.430E-01	2.430E-01	0.000E+00	3.066E-05	0.000E+00	0.000E+00	0.000E+00	0.000E+00	2.430E-01	2.430E-01	0.000E+00	3.066E-05
barrier_deg	high	2.430E-01	2.430E-01	0.000E+00	1.411E-04	0.000E+00	0.000E+00	0.000E+00	0.000E+00	2.430E-01	2.430E-01	0.000E+00	1.411E-04
	low	2.430E-01	2.430E-01	0.000E+00	-1.227E-05	0.000E+00	0.000E+00	0.000E+00	0.000E+00	2.430E-01	2.430E-01	0.000E+00	-1.227E-05
diffusion	high	7.683E-01	7.683E-01	0.000E+00	9.309E-05	0.000E+00	0.000E+00	0.000E+00	0.000E+00	7.683E-01	7.683E-01	0.000E+00	9.309E-05
	low	7.683E-04	7.683E-04	0.000E+00	2.803E-04	0.000E+00	0.000E+00	0.000E+00	0.000E+00	7.683E-04	7.683E-04	0.000E+00	2.803E-04
ksat_aq	high	2.430E-01	2.430E-01	0.000E+00	6.133E-05	0.000E+00	0.000E+00	0.000E+00	0.000E+00	2.430E-01	2.430E-01	0.000E+00	6.133E-05
	low	2.430E-01	2.430E-01	0.000E+00	6.133E-05	0.000E+00	0.000E+00	0.000E+00	0.000E+00	2.430E-01	2.430E-01	0.000E+00	6.133E-05
ksat_vz	high	2.430E-01	2.430E-01	0.000E+00	4.906E-05	0.000E+00	0.000E+00	0.000E+00	0.000E+00	2.430E-01	2.430E-01	0.000E+00	4.906E-05
	low	2.430E-01	2.430E-01	0.000E+00	-7.360E-05	0.000E+00	0.000E+00	0.000E+00	0.000E+00	2.430E-01	2.430E-01	0.000E+00	-7.360E-05

Table F.87. STOMP Mass Balance for U-238 (Kd = 1.00) for Case 3 (Retrieval Leak)

Sub-Case		Vadose Zone				Aquifer				Vadose Zone + Aquifer			
		Released	In Domain	Exit	%error	Released	In Domain	Exit	%error	Released	In Domain	Exit	%error
base		1.000E+00	1.000E+00	0.000E+00	1.609E-04	0.000E+00	0.000E+00	0.000E+00	0.000E+00	1.000E+00	1.000E+00	0.000E+00	1.609E-04
recharge	high	1.000E+00	1.000E+00	0.000E+00	1.609E-04	0.000E+00	0.000E+00	0.000E+00	0.000E+00	1.000E+00	1.000E+00	0.000E+00	1.609E-04
	low	1.000E+00	1.000E+00	0.000E+00	1.609E-04	0.000E+00	0.000E+00	0.000E+00	0.000E+00	1.000E+00	1.000E+00	0.000E+00	1.609E-04
barrier	high	1.000E+00	1.000E+00	0.000E+00	1.073E-04	0.000E+00	0.000E+00	0.000E+00	0.000E+00	1.000E+00	1.000E+00	0.000E+00	1.073E-04
	low	1.000E+00	1.000E+00	0.000E+00	7.749E-05	0.000E+00	0.000E+00	0.000E+00	0.000E+00	1.000E+00	1.000E+00	0.000E+00	7.749E-05
barrier_deg	high	1.000E+00	1.000E+00	3.995E-08	1.748E-04	3.995E-08	2.379E-09	3.524E-08	5.841E+00	1.000E+00	1.000E+00	3.524E-08	1.753E-04
	low	1.000E+00	1.000E+00	0.000E+00	1.073E-04	0.000E+00	0.000E+00	0.000E+00	0.000E+00	1.000E+00	1.000E+00	0.000E+00	1.073E-04
ksat_aq	high	1.000E+00	1.000E+00	0.000E+00	1.609E-04	0.000E+00	0.000E+00	0.000E+00	0.000E+00	1.000E+00	1.000E+00	0.000E+00	1.609E-04
	low	1.000E+00	1.000E+00	0.000E+00	1.609E-04	0.000E+00	0.000E+00	0.000E+00	0.000E+00	1.000E+00	1.000E+00	0.000E+00	1.609E-04
ksat_vz	high	1.000E+00	1.000E+00	0.000E+00	1.609E-04	0.000E+00	0.000E+00	0.000E+00	0.000E+00	1.000E+00	1.000E+00	0.000E+00	1.609E-04
	low	1.000E+00	1.000E+00	0.000E+00	4.172E-05	0.000E+00	0.000E+00	0.000E+00	0.000E+00	1.000E+00	1.000E+00	0.000E+00	4.172E-05

Table F.88. STOMP Mass Balance for U-238 (Kd = 1.00) for Case 4 (Ancillary Equipment)

Sub-Case		Vadose Zone				Aquifer				Vadose Zone + Aquifer			
		Released	In Domain	Exit	%error	Released	In Domain	Exit	%error	Released	In Domain	Exit	%error
base		1.000E+00	1.000E+00	0.000E+00	1.431E-04	0.000E+00	0.000E+00	0.000E+00	0.000E+00	1.000E+00	1.000E+00	0.000E+00	1.431E-04
recharge	high	1.000E+00	1.000E+00	0.000E+00	7.153E-05	0.000E+00	0.000E+00	0.000E+00	0.000E+00	1.000E+00	1.000E+00	0.000E+00	7.153E-05
	low	1.000E+00	1.000E+00	0.000E+00	7.153E-05	0.000E+00	0.000E+00	0.000E+00	0.000E+00	1.000E+00	1.000E+00	0.000E+00	7.153E-05
barrier	high	1.000E+00	1.000E+00	0.000E+00	1.073E-04	0.000E+00	0.000E+00	0.000E+00	0.000E+00	1.000E+00	1.000E+00	0.000E+00	1.073E-04
	low	1.000E+00	1.000E+00	0.000E+00	9.537E-05	0.000E+00	0.000E+00	0.000E+00	0.000E+00	1.000E+00	1.000E+00	0.000E+00	9.537E-05
barrier_deg	high	1.000E+00	1.000E+00	1.079E-08	2.910E-04	1.079E-08	6.702E-10	8.193E-09	1.788E+01	1.000E+00	1.000E+00	8.193E-09	2.912E-04
	low	1.000E+00	1.000E+00	0.000E+00	5.960E-05	0.000E+00	0.000E+00	0.000E+00	0.000E+00	1.000E+00	1.000E+00	0.000E+00	5.960E-05
ksat_aq	high	1.000E+00	1.000E+00	0.000E+00	1.431E-04	0.000E+00	0.000E+00	0.000E+00	0.000E+00	1.000E+00	1.000E+00	0.000E+00	1.431E-04
	low	1.000E+00	1.000E+00	0.000E+00	1.431E-04	0.000E+00	0.000E+00	0.000E+00	0.000E+00	1.000E+00	1.000E+00	0.000E+00	1.431E-04
ksat_vz	high	1.000E+00	1.000E+00	0.000E+00	1.252E-04	0.000E+00	0.000E+00	0.000E+00	0.000E+00	1.000E+00	1.000E+00	0.000E+00	1.252E-04
	low	1.000E+00	1.000E+00	0.000E+00	7.749E-05	0.000E+00	0.000E+00	0.000E+00	0.000E+00	1.000E+00	1.000E+00	0.000E+00	7.749E-05

Table F.89. STOMP Mass Balance for U-238 (Kd = 2.00) for Case 1 (Past Leak)

Sub-Case		Vadose Zone				Aquifer				Vadose Zone + Aquifer			
		Released	In Domain	Exit	%error	Released	In Domain	Exit	%error	Released	In Domain	Exit	%error
base		1.000E+00	1.000E+00	2.698E-10	6.554E-05	2.698E-10	3.728E-12	0.000E+00	9.862E+01	1.000E+00	1.000E+00	0.000E+00	6.557E-05
recharge	high	1.000E+00	1.000E+00	2.412E-09	1.249E-04	2.412E-09	1.038E-10	3.688E-10	8.041E+01	1.000E+00	1.000E+00	3.688E-10	1.251E-04
	low	1.000E+00	1.000E+00	0.000E+00	1.192E-05	0.000E+00	0.000E+00	0.000E+00	0.000E+00	1.000E+00	1.000E+00	0.000E+00	1.192E-05
barrier	high	1.000E+00	1.000E+00	3.743E-10	7.745E-05	3.743E-10	5.722E-12	0.000E+00	9.847E+01	1.000E+00	1.000E+00	0.000E+00	7.749E-05
	low	1.000E+00	1.000E+00	2.038E-10	1.192E-04	2.038E-10	2.732E-12	0.000E+00	9.866E+01	1.000E+00	1.000E+00	0.000E+00	1.192E-04
barrier_deg	high	1.000E+00	9.999E-01	1.390E-04	2.038E-04	1.390E-04	7.784E-06	1.313E-04	2.060E-03	1.000E+00	9.999E-01	1.313E-04	2.017E-04
	low	1.000E+00	1.000E+00	0.000E+00	1.311E-04	0.000E+00	0.000E+00	0.000E+00	0.000E+00	1.000E+00	1.000E+00	0.000E+00	1.311E-04
plume	high	1.000E+00	1.000E+00	0.000E+00	1.013E-04	0.000E+00	0.000E+00	0.000E+00	0.000E+00	1.000E+00	1.000E+00	0.000E+00	1.013E-04
	low	1.000E+00	1.000E+00	3.718E-07	4.626E-05	3.718E-07	1.642E-08	3.507E-07	1.280E+00	1.000E+00	1.000E+00	3.507E-07	4.838E-05
ksat_aq	high	1.000E+00	1.000E+00	2.699E-10	6.554E-05	2.699E-10	2.630E-12	0.000E+00	9.903E+01	1.000E+00	1.000E+00	0.000E+00	6.557E-05
	low	1.000E+00	1.000E+00	2.695E-10	6.554E-05	2.695E-10	5.832E-12	0.000E+00	9.784E+01	1.000E+00	1.000E+00	0.000E+00	6.557E-05
ksat_vz	high	1.000E+00	1.000E+00	9.357E-12	3.576E-05	9.357E-12	0.000E+00	0.000E+00	1.000E+02	1.000E+00	1.000E+00	0.000E+00	3.576E-05
	low	1.000E+00	1.000E+00	7.016E-09	5.294E-05	7.016E-09	3.418E-10	3.809E-09	4.084E+01	1.000E+00	1.000E+00	3.809E-09	5.326E-05

Table F.90. STOMP Mass Balance for U-238 (Kd = 2.00) for Case 2 (Diffusion)

Sub-Case		Vadose Zone				Aquifer				Vadose Zone + Aquifer			
		Released	In Domain	Exit	%error	Released	In Domain	Exit	%error	Released	In Domain	Exit	%error
base		2.430E-01	2.430E-01	0.000E+00	-1.227E-05	0.000E+00	0.000E+00	0.000E+00	0.000E+00	2.430E-01	2.430E-01	0.000E+00	-1.227E-05
recharge	high	2.430E-01	2.430E-01	0.000E+00	-1.840E-05	0.000E+00	0.000E+00	0.000E+00	0.000E+00	2.430E-01	2.430E-01	0.000E+00	-1.840E-05
	low	2.430E-01	2.430E-01	0.000E+00	1.227E-05	0.000E+00	0.000E+00	0.000E+00	0.000E+00	2.430E-01	2.430E-01	0.000E+00	1.227E-05
barrier	high	2.430E-01	2.430E-01	0.000E+00	-1.227E-05	0.000E+00	0.000E+00	0.000E+00	0.000E+00	2.430E-01	2.430E-01	0.000E+00	-1.227E-05
	low	2.430E-01	2.430E-01	0.000E+00	-3.680E-05	0.000E+00	0.000E+00	0.000E+00	0.000E+00	2.430E-01	2.430E-01	0.000E+00	-3.680E-05
barrier_deg	high	2.430E-01	2.430E-01	0.000E+00	7.360E-05	0.000E+00	0.000E+00	0.000E+00	0.000E+00	2.430E-01	2.430E-01	0.000E+00	7.360E-05
	low	2.430E-01	2.430E-01	0.000E+00	-7.973E-05	0.000E+00	0.000E+00	0.000E+00	0.000E+00	2.430E-01	2.430E-01	0.000E+00	-7.973E-05
diffusion	high	7.683E-01	7.683E-01	0.000E+00	1.552E-05	0.000E+00	0.000E+00	0.000E+00	0.000E+00	7.683E-01	7.683E-01	0.000E+00	1.552E-05
	low	7.683E-04	7.683E-04	0.000E+00	1.212E-04	0.000E+00	0.000E+00	0.000E+00	0.000E+00	7.683E-04	7.683E-04	0.000E+00	1.212E-04
ksat_aq	high	2.430E-01	2.430E-01	0.000E+00	-1.227E-05	0.000E+00	0.000E+00	0.000E+00	0.000E+00	2.430E-01	2.430E-01	0.000E+00	-1.227E-05
	low	2.430E-01	2.430E-01	0.000E+00	-1.227E-05	0.000E+00	0.000E+00	0.000E+00	0.000E+00	2.430E-01	2.430E-01	0.000E+00	-1.227E-05
ksat_vz	high	2.430E-01	2.430E-01	0.000E+00	-1.227E-05	0.000E+00	0.000E+00	0.000E+00	0.000E+00	2.430E-01	2.430E-01	0.000E+00	-1.227E-05
	low	2.430E-01	2.430E-01	0.000E+00	-6.746E-05	0.000E+00	0.000E+00	0.000E+00	0.000E+00	2.430E-01	2.430E-01	0.000E+00	-6.746E-05

Table F.91. STOMP Mass Balance for U-238 (Kd = 2.00) for Case 3 (Retrieval Leak)

Sub-Case		Vadose Zone				Aquifer				Vadose Zone + Aquifer			
		Released	In Domain	Exit	%error	Released	In Domain	Exit	%error	Released	In Domain	Exit	%error
base		1.000E+00	1.000E+00	0.000E+00	2.980E-05	0.000E+00	0.000E+00	0.000E+00	0.000E+00	1.000E+00	1.000E+00	0.000E+00	2.980E-05
recharge	high	1.000E+00	1.000E+00	0.000E+00	8.345E-05	0.000E+00	0.000E+00	0.000E+00	0.000E+00	1.000E+00	1.000E+00	0.000E+00	8.345E-05
	low	1.000E+00	1.000E+00	0.000E+00	8.941E-05	0.000E+00	0.000E+00	0.000E+00	0.000E+00	1.000E+00	1.000E+00	0.000E+00	8.941E-05
barrier	high	1.000E+00	1.000E+00	0.000E+00	5.960E-05	0.000E+00	0.000E+00	0.000E+00	0.000E+00	1.000E+00	1.000E+00	0.000E+00	5.960E-05
	low	1.000E+00	1.000E+00	0.000E+00	8.345E-05	0.000E+00	0.000E+00	0.000E+00	0.000E+00	1.000E+00	1.000E+00	0.000E+00	8.345E-05
barrier_deg	high	1.000E+00	1.000E+00	0.000E+00	2.146E-04	0.000E+00	0.000E+00	0.000E+00	0.000E+00	1.000E+00	1.000E+00	0.000E+00	2.146E-04
	low	1.000E+00	1.000E+00	0.000E+00	7.153E-05	0.000E+00	0.000E+00	0.000E+00	0.000E+00	1.000E+00	1.000E+00	0.000E+00	7.153E-05
ksat_aq	high	1.000E+00	1.000E+00	0.000E+00	2.980E-05	0.000E+00	0.000E+00	0.000E+00	0.000E+00	1.000E+00	1.000E+00	0.000E+00	2.980E-05
	low	1.000E+00	1.000E+00	0.000E+00	2.980E-05	0.000E+00	0.000E+00	0.000E+00	0.000E+00	1.000E+00	1.000E+00	0.000E+00	2.980E-05
ksat_vz	high	1.000E+00	1.000E+00	0.000E+00	9.537E-05	0.000E+00	0.000E+00	0.000E+00	0.000E+00	1.000E+00	1.000E+00	0.000E+00	9.537E-05
	low	1.000E+00	1.000E+00	0.000E+00	2.980E-05	0.000E+00	0.000E+00	0.000E+00	0.000E+00	1.000E+00	1.000E+00	0.000E+00	2.980E-05

Table F.92. STOMP Mass Balance for U-238 (Kd = 2.00) for Case 4 (Ancillary Equipment)

Sub-Case		Vadose Zone				Aquifer				Vadose Zone + Aquifer			
		Released	In Domain	Exit	%error	Released	In Domain	Exit	%error	Released	In Domain	Exit	%error
base		1.000E+00	1.000E+00	0.000E+00	1.192E-05	0.000E+00	0.000E+00	0.000E+00	0.000E+00	1.000E+00	1.000E+00	0.000E+00	1.192E-05
recharge	high	1.000E+00	1.000E+00	0.000E+00	5.364E-05	0.000E+00	0.000E+00	0.000E+00	0.000E+00	1.000E+00	1.000E+00	0.000E+00	5.364E-05
	low	1.000E+00	1.000E+00	0.000E+00	5.960E-05	0.000E+00	0.000E+00	0.000E+00	0.000E+00	1.000E+00	1.000E+00	0.000E+00	5.960E-05
barrier	high	1.000E+00	1.000E+00	0.000E+00	3.576E-05	0.000E+00	0.000E+00	0.000E+00	0.000E+00	1.000E+00	1.000E+00	0.000E+00	3.576E-05
	low	1.000E+00	1.000E+00	0.000E+00	2.980E-05	0.000E+00	0.000E+00	0.000E+00	0.000E+00	1.000E+00	1.000E+00	0.000E+00	2.980E-05
barrier_deg	high	1.000E+00	1.000E+00	0.000E+00	1.669E-04	0.000E+00	0.000E+00	0.000E+00	0.000E+00	1.000E+00	1.000E+00	0.000E+00	1.669E-04
	low	1.000E+00	1.000E+00	0.000E+00	5.364E-05	0.000E+00	0.000E+00	0.000E+00	0.000E+00	1.000E+00	1.000E+00	0.000E+00	5.364E-05
ksat_aq	high	1.000E+00	1.000E+00	0.000E+00	1.192E-05	0.000E+00	0.000E+00	0.000E+00	0.000E+00	1.000E+00	1.000E+00	0.000E+00	1.192E-05
	low	1.000E+00	1.000E+00	0.000E+00	1.192E-05	0.000E+00	0.000E+00	0.000E+00	0.000E+00	1.000E+00	1.000E+00	0.000E+00	1.192E-05
ksat_vz	high	1.000E+00	1.000E+00	0.000E+00	2.980E-05	0.000E+00	0.000E+00	0.000E+00	0.000E+00	1.000E+00	1.000E+00	0.000E+00	2.980E-05
	low	1.000E+00	1.000E+00	0.000E+00	-3.576E-05	0.000E+00	0.000E+00	0.000E+00	0.000E+00	1.000E+00	1.000E+00	0.000E+00	-3.576E-05

Table F.93. STOMP Mass Balance for U-238 (Kd = 5.00) for Case 1 (Past Leak)

Sub-Case		Vadose Zone				Aquifer				Vadose Zone + Aquifer			
		Released	In Domain	Exit	%error	Released	In Domain	Exit	%error	Released	In Domain	Exit	%error
base		1.000E+00	1.000E+00	0.000E+00	2.384E-05	0.000E+00	0.000E+00	0.000E+00	0.000E+00	1.000E+00	1.000E+00	0.000E+00	2.384E-05
recharge	high	1.000E+00	1.000E+00	0.000E+00	0.000E+00	0.000E+00	0.000E+00	0.000E+00	0.000E+00	1.000E+00	1.000E+00	0.000E+00	0.000E+00
	low	1.000E+00	1.000E+00	0.000E+00	4.172E-05	0.000E+00	0.000E+00	0.000E+00	0.000E+00	1.000E+00	1.000E+00	0.000E+00	4.172E-05
barrier	high	1.000E+00	1.000E+00	0.000E+00	2.980E-05	0.000E+00	0.000E+00	0.000E+00	0.000E+00	1.000E+00	1.000E+00	0.000E+00	2.980E-05
	low	1.000E+00	1.000E+00	0.000E+00	0.000E+00	0.000E+00	0.000E+00	0.000E+00	0.000E+00	1.000E+00	1.000E+00	0.000E+00	0.000E+00
barrier_deg	high	1.000E+00	1.000E+00	2.689E-12	1.252E-04	2.689E-12	0.000E+00	0.000E+00	1.000E+02	1.000E+00	1.000E+00	0.000E+00	1.252E-04
	low	1.000E+00	1.000E+00	0.000E+00	1.788E-05	0.000E+00	0.000E+00	0.000E+00	0.000E+00	1.000E+00	1.000E+00	0.000E+00	1.788E-05
plume	high	1.000E+00	1.000E+00	0.000E+00	1.192E-05	0.000E+00	0.000E+00	0.000E+00	0.000E+00	1.000E+00	1.000E+00	0.000E+00	1.192E-05
	low	1.000E+00	1.000E+00	0.000E+00	2.980E-05	0.000E+00	0.000E+00	0.000E+00	0.000E+00	1.000E+00	1.000E+00	0.000E+00	2.980E-05
ksat_aq	high	1.000E+00	1.000E+00	0.000E+00	2.384E-05	0.000E+00	0.000E+00	0.000E+00	0.000E+00	1.000E+00	1.000E+00	0.000E+00	2.384E-05
	low	1.000E+00	1.000E+00	0.000E+00	2.384E-05	0.000E+00	0.000E+00	0.000E+00	0.000E+00	1.000E+00	1.000E+00	0.000E+00	2.384E-05
ksat_vz	high	1.000E+00	1.000E+00	0.000E+00	7.153E-05	0.000E+00	0.000E+00	0.000E+00	0.000E+00	1.000E+00	1.000E+00	0.000E+00	7.153E-05
	low	1.000E+00	1.000E+00	0.000E+00	2.384E-05	0.000E+00	0.000E+00	0.000E+00	0.000E+00	1.000E+00	1.000E+00	0.000E+00	2.384E-05

Table F.94. STOMP Mass Balance for U-238 (Kd = 5.00) for Case 2 (Diffusion)

Sub-Case		Vadose Zone				Aquifer				Vadose Zone + Aquifer			
		Released	In Domain	Exit	%error	Released	In Domain	Exit	%error	Released	In Domain	Exit	%error
base		2.430E-01	2.430E-01	0.000E+00	-7.360E-05	0.000E+00	0.000E+00	0.000E+00	0.000E+00	2.430E-01	2.430E-01	0.000E+00	-7.360E-05
recharge	high	2.430E-01	2.430E-01	0.000E+00	-6.133E-05	0.000E+00	0.000E+00	0.000E+00	0.000E+00	2.430E-01	2.430E-01	0.000E+00	-6.133E-05
	low	2.430E-01	2.430E-01	0.000E+00	-7.973E-05	0.000E+00	0.000E+00	0.000E+00	0.000E+00	2.430E-01	2.430E-01	0.000E+00	-7.973E-05
barrier	high	2.430E-01	2.430E-01	0.000E+00	-6.133E-05	0.000E+00	0.000E+00	0.000E+00	0.000E+00	2.430E-01	2.430E-01	0.000E+00	-6.133E-05
	low	2.430E-01	2.430E-01	0.000E+00	-1.165E-04	0.000E+00	0.000E+00	0.000E+00	0.000E+00	2.430E-01	2.430E-01	0.000E+00	-1.165E-04
barrier_deg	high	2.430E-01	2.430E-01	0.000E+00	-1.227E-05	0.000E+00	0.000E+00	0.000E+00	0.000E+00	2.430E-01	2.430E-01	0.000E+00	-1.227E-05
	low	2.430E-01	2.430E-01	0.000E+00	-6.133E-05	0.000E+00	0.000E+00	0.000E+00	0.000E+00	2.430E-01	2.430E-01	0.000E+00	-6.133E-05
diffusion	high	7.683E-01	7.683E-01	0.000E+00	0.000E+00	0.000E+00	0.000E+00	0.000E+00	0.000E+00	7.683E-01	7.683E-01	0.000E+00	0.000E+00
	low	7.683E-04	7.683E-04	0.000E+00	7.576E-06	0.000E+00	0.000E+00	0.000E+00	0.000E+00	7.683E-04	7.683E-04	0.000E+00	7.576E-06
ksat_aq	high	2.430E-01	2.430E-01	0.000E+00	-7.360E-05	0.000E+00	0.000E+00	0.000E+00	0.000E+00	2.430E-01	2.430E-01	0.000E+00	-7.360E-05
	low	2.430E-01	2.430E-01	0.000E+00	-7.360E-05	0.000E+00	0.000E+00	0.000E+00	0.000E+00	2.430E-01	2.430E-01	0.000E+00	-7.360E-05
ksat_vz	high	2.430E-01	2.430E-01	0.000E+00	-7.973E-05	0.000E+00	0.000E+00	0.000E+00	0.000E+00	2.430E-01	2.430E-01	0.000E+00	-7.973E-05
	low	2.430E-01	2.430E-01	0.000E+00	-4.293E-05	0.000E+00	0.000E+00	0.000E+00	0.000E+00	2.430E-01	2.430E-01	0.000E+00	-4.293E-05

Table F.95. STOMP Mass Balance for U-238 (Kd = 5.00) for Case 3 (Retrieval Leak)

Sub-Case		Vadose Zone				Aquifer				Vadose Zone + Aquifer			
		Released	In Domain	Exit	%error	Released	In Domain	Exit	%error	Released	In Domain	Exit	%error
base		1.000E+00	1.000E+00	0.000E+00	6.557E-05	0.000E+00	0.000E+00	0.000E+00	0.000E+00	1.000E+00	1.000E+00	0.000E+00	6.557E-05
recharge	high	1.000E+00	1.000E+00	0.000E+00	5.364E-05	0.000E+00	0.000E+00	0.000E+00	0.000E+00	1.000E+00	1.000E+00	0.000E+00	5.364E-05
	low	1.000E+00	1.000E+00	0.000E+00	4.768E-05	0.000E+00	0.000E+00	0.000E+00	0.000E+00	1.000E+00	1.000E+00	0.000E+00	4.768E-05
barrier	high	1.000E+00	1.000E+00	0.000E+00	1.192E-05	0.000E+00	0.000E+00	0.000E+00	0.000E+00	1.000E+00	1.000E+00	0.000E+00	1.192E-05
	low	1.000E+00	1.000E+00	0.000E+00	5.960E-05	0.000E+00	0.000E+00	0.000E+00	0.000E+00	1.000E+00	1.000E+00	0.000E+00	5.960E-05
barrier_deg	high	1.000E+00	1.000E+00	0.000E+00	5.960E-05	0.000E+00	0.000E+00	0.000E+00	0.000E+00	1.000E+00	1.000E+00	0.000E+00	5.960E-05
	low	1.000E+00	1.000E+00	0.000E+00	5.960E-05	0.000E+00	0.000E+00	0.000E+00	0.000E+00	1.000E+00	1.000E+00	0.000E+00	5.960E-05
ksat_aq	high	1.000E+00	1.000E+00	0.000E+00	6.557E-05	0.000E+00	0.000E+00	0.000E+00	0.000E+00	1.000E+00	1.000E+00	0.000E+00	6.557E-05
	low	1.000E+00	1.000E+00	0.000E+00	6.557E-05	0.000E+00	0.000E+00	0.000E+00	0.000E+00	1.000E+00	1.000E+00	0.000E+00	6.557E-05
ksat_vz	high	1.000E+00	1.000E+00	0.000E+00	3.576E-05	0.000E+00	0.000E+00	0.000E+00	0.000E+00	1.000E+00	1.000E+00	0.000E+00	3.576E-05
	low	1.000E+00	1.000E+00	0.000E+00	8.941E-05	0.000E+00	0.000E+00	0.000E+00	0.000E+00	1.000E+00	1.000E+00	0.000E+00	8.941E-05

Table F.96. STOMP Mass Balance for U-238 (Kd = 5.00) for Case 4 (Ancillary Equipment)

Sub-Case		Vadose Zone				Aquifer				Vadose Zone + Aquifer			
		Released	In Domain	Exit	%error	Released	In Domain	Exit	%error	Released	In Domain	Exit	%error
base		1.000E+00	1.000E+00	0.000E+00	0.000E+00	0.000E+00	0.000E+00	0.000E+00	0.000E+00	1.000E+00	1.000E+00	0.000E+00	0.000E+00
recharge	high	1.000E+00	1.000E+00	0.000E+00	4.768E-05	0.000E+00	0.000E+00	0.000E+00	0.000E+00	1.000E+00	1.000E+00	0.000E+00	4.768E-05
	low	1.000E+00	1.000E+00	0.000E+00	1.192E-05	0.000E+00	0.000E+00	0.000E+00	0.000E+00	1.000E+00	1.000E+00	0.000E+00	1.192E-05
barrier	high	1.000E+00	1.000E+00	0.000E+00	-1.192E-05	0.000E+00	0.000E+00	0.000E+00	0.000E+00	1.000E+00	1.000E+00	0.000E+00	-1.192E-05
	low	1.000E+00	1.000E+00	0.000E+00	1.192E-05	0.000E+00	0.000E+00	0.000E+00	0.000E+00	1.000E+00	1.000E+00	0.000E+00	1.192E-05
barrier_deg	high	1.000E+00	1.000E+00	0.000E+00	0.000E+00	0.000E+00	0.000E+00	0.000E+00	0.000E+00	1.000E+00	1.000E+00	0.000E+00	0.000E+00
	low	1.000E+00	1.000E+00	0.000E+00	1.192E-05	0.000E+00	0.000E+00	0.000E+00	0.000E+00	1.000E+00	1.000E+00	0.000E+00	1.192E-05
ksat_aq	high	1.000E+00	1.000E+00	0.000E+00	0.000E+00	0.000E+00	0.000E+00	0.000E+00	0.000E+00	1.000E+00	1.000E+00	0.000E+00	0.000E+00
	low	1.000E+00	1.000E+00	0.000E+00	0.000E+00	0.000E+00	0.000E+00	0.000E+00	0.000E+00	1.000E+00	1.000E+00	0.000E+00	0.000E+00
ksat_vz	high	1.000E+00	1.000E+00	0.000E+00	0.000E+00	0.000E+00	0.000E+00	0.000E+00	0.000E+00	1.000E+00	1.000E+00	0.000E+00	0.000E+00
	low	1.000E+00	1.000E+00	0.000E+00	1.192E-05	0.000E+00	0.000E+00	0.000E+00	0.000E+00	1.000E+00	1.000E+00	0.000E+00	1.192E-05

Distribution

No. of
Copies

Fluor Federal Services

R. Khaleel E6-17

10 CH2M-HILL Hanford Group, Inc.

M. Connelly E6-35

8 Pacific Northwest National Laboratory

V.L. Freedman (2) K9-36
Z.F. Zhang K9-36
S.R. Waichler K9-36
S.K. Wurstner K9-36
D.H. Bacon K9-36
Information Release (2) P8-55

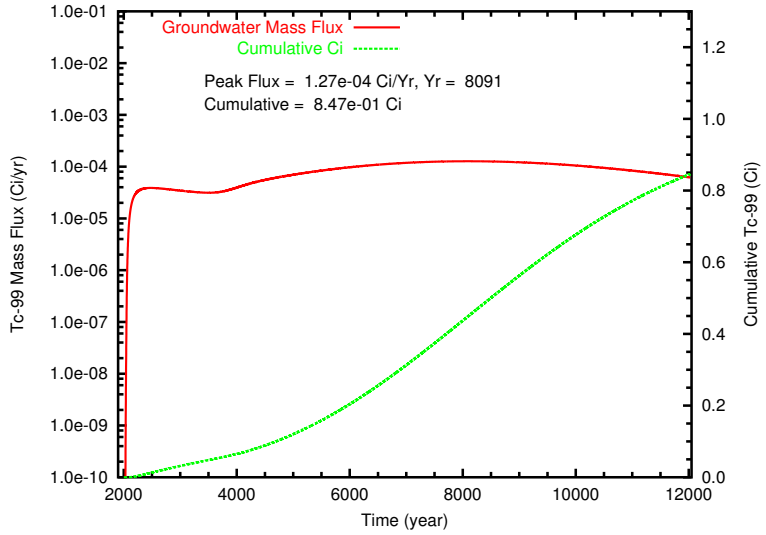

(a)

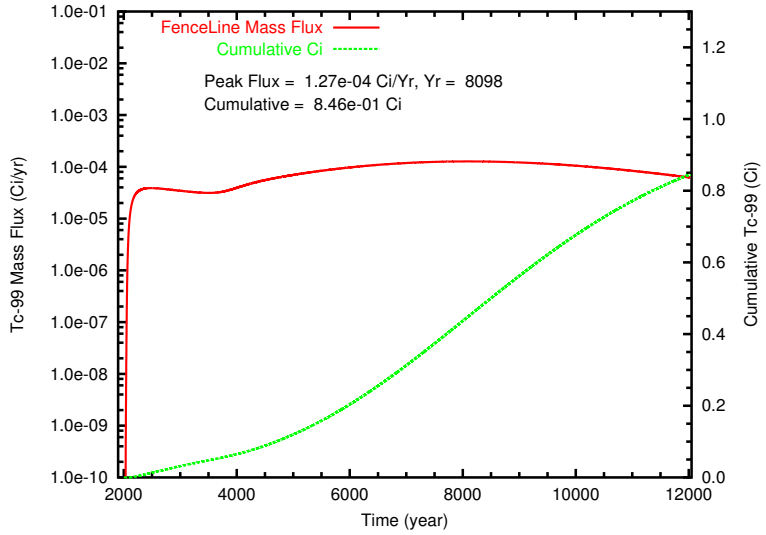

(b)

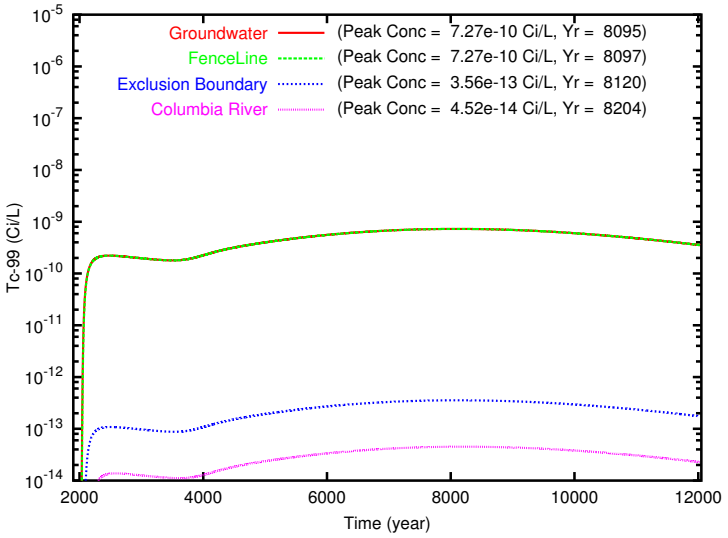

(c)

Figure D.44. Retrieval Leak: Low Vadose Zone Hydraulic Conductivity ($K_{sat} \times 0.1$) Tc-99 mass flux at (a) the groundwater table and (b) the fenceline; and (c) the Tc-99 concentration at groundwater, fenceline, and easterly downstream compliance points.

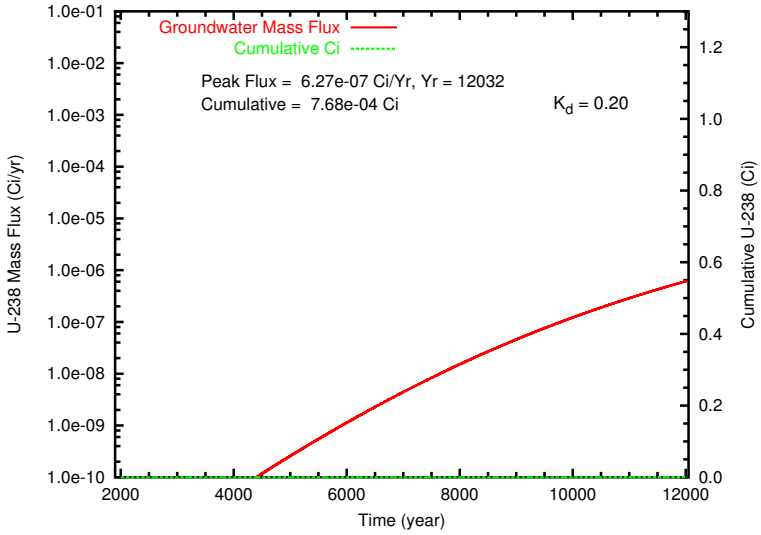

(a)

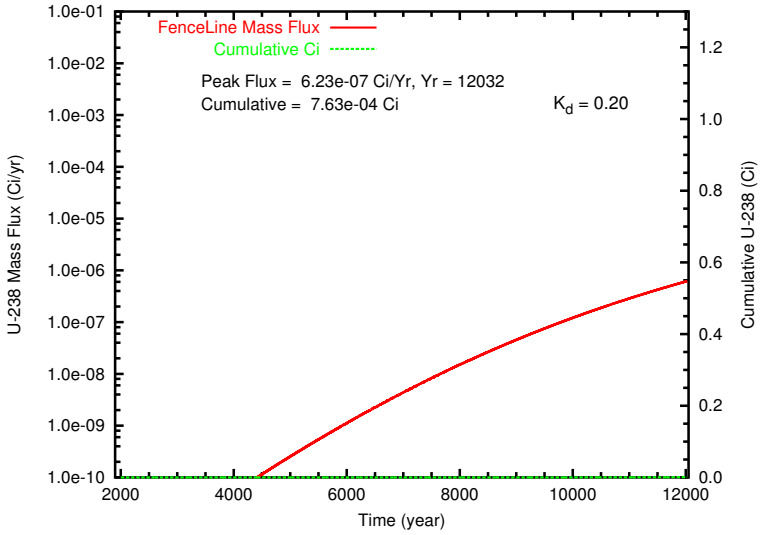

(b)

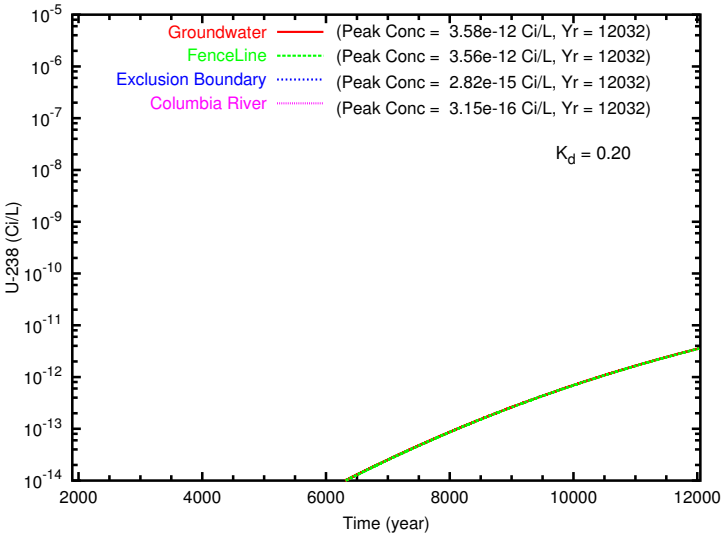

(c)

Figure D.45. Retrieval Leak: Low Vadose Zone Hydraulic Conductivity ($K_{sat} \times 0.1$) U_0.20 mass flux at (a) the groundwater table and (b) the fenceline; and (c) the Tc-99 concentration at groundwater, fenceline, and easterly downstream compliance points.

Appendix F

Peak Concentration, Mass Flux and Mass Balance Tables

Table F.1. Predicted Peak Tc-99 Flux (Ci/yr), Arrival Time, and Cumulative Mass (Ci) at Year 12032 for Case 1 (Past Leak)

Sub-Case		Groundwater			Fenceline		
		Flux	Time	Cm Mass	Flux	Time	Cm Mass
base		1.49E-02	2048	1.0069	1.46E-02	2051	1.0034
recharge	high	2.62E-02	2039	1.0098	2.59E-02	2042	1.0042
	low	2.10E-03	2116	1.0003	2.10E-03	2118	1.0002
barrier	high	1.49E-02	2048	1.0069	1.47E-02	2051	1.0034
	low	1.49E-02	2048	1.0069	1.46E-02	2051	1.0034
barrier_deg	high	1.49E-02	2048	1.0069	1.46E-02	2051	1.0034
	low	1.49E-02	2048	1.0061	1.46E-02	2051	1.0026
plume	high	8.44E-03	2055	1.0048	8.33E-03	2057	1.0024
	low	2.34E-02	2041	1.0071	2.32E-02	2044	1.0033
ksat_aq	high	1.49E-02	2048	1.0069	1.47E-02	2050	1.0033
	low	1.48E-02	2048	1.0069	1.45E-02	2052	1.0035
ksat_vz	high	2.52E-02	2039	1.0101	2.48E-02	2041	1.0032
	low	8.33E-03	2059	1.0038	8.25E-03	2062	1.0018

Table F.2. Predicted Peak Tc-99 Flux (Ci/yr), Arrival Time, and Cumulative Mass (Ci) at Year 12032 for Case 2 (Diffusion)

Sub-Case		Groundwater			Fenceline		
		Flux	Time	Cm Mass	Flux	Time	Cm Mass
base		2.87E-05	10480	0.1125	2.87E-05	10482	0.1124
recharge	high	2.87E-05	10479	0.1125	2.87E-05	10482	0.1125
	low	2.88E-05	10480	0.1125	2.88E-05	10482	0.1124
barrier	high	2.81E-05	10455	0.1133	2.81E-05	10457	0.1132
	low	2.93E-05	10514	0.1118	2.93E-05	10517	0.1117
barrier_deg	high	5.92E-05	5001	0.2104	5.92E-05	5004	0.2103
	low	7.33E-06	12032	0.0099	7.32E-06	12032	0.0099
diffusion	high	9.09E-05	10480	0.3558	9.09E-05	10483	0.3556
	low	9.09E-08	10479	0.0004	9.09E-08	10482	0.0004
ksat_aq	high	2.87E-05	10480	0.1125	2.87E-05	10482	0.1125
	low	2.87E-05	10479	0.1125	2.87E-05	10484	0.1124
ksat_vz	high	3.31E-05	9002	0.1459	3.31E-05	9005	0.1458
	low	2.21E-05	12032	0.0579	2.21E-05	12032	0.0578

Table F.3. Predicted Peak Tc-99 Flux (Ci/yr), Arrival Time, and Cumulative Mass (Ci) at Year 12032 for Case 3 (Retrieval Leak)

Sub-Case		Groundwater			Fenceline		
		Flux	Time	Cm Mass	Flux	Time	Cm Mass
base		2.36E-04	2117	0.9904	2.36E-04	2120	0.9903
recharge	high	6.54E-04	2080	0.9946	6.52E-04	2086	0.9943
	low	1.93E-04	6962	0.9767	1.93E-04	6963	0.9766
barrier	high	2.37E-04	2118	0.9922	2.37E-04	2121	0.9921
	low	2.35E-04	2117	0.9887	2.35E-04	2120	0.9886
barrier_deg	high	5.78E-04	3735	1.0001	5.78E-04	3738	1.0001
	low	2.36E-04	2117	0.8050	2.36E-04	2120	0.8048
ksat_aq	high	2.36E-04	2117	0.9904	2.36E-04	2119	0.9903
	low	2.36E-04	2117	0.9904	2.36E-04	2122	0.9903
ksat_vz	high	3.84E-04	2075	0.9997	3.81E-04	2078	0.9994
	low	1.27E-04	8096	0.8465	1.27E-04	8098	0.8463

Table F.4. Predicted Peak Tc-99 Flux (Ci/yr), Arrival Time, and Cumulative Mass (Ci) at Year 12032 for Case 4 (Ancillary Equipment)

Sub-Case		Groundwater			Fenceline		
		Flux	Time	Cm Mass	Flux	Time	Cm Mass
base		1.80E-04	5713	0.9899	1.80E-04	5715	0.9898
recharge	high	6.78E-04	2091	0.9955	6.77E-04	2094	0.9954
	low	2.14E-04	7536	0.9642	2.14E-04	7539	0.9641
barrier	high	1.80E-04	5471	0.9917	1.80E-04	5474	0.9917
	low	1.80E-04	5909	0.9881	1.80E-04	5913	0.9880
barrier_deg	high	6.05E-04	3757	1.0000	6.05E-04	3760	1.0000
	low	1.35E-04	2193	0.7950	1.35E-04	2196	0.7948
ksat_aq	high	1.80E-04	5713	0.9899	1.80E-04	5714	0.9898
	low	1.80E-04	5713	0.9899	1.80E-04	5716	0.9898
ksat_vz	high	2.63E-04	2093	0.9997	2.61E-04	2097	0.9995
	low	1.25E-04	7157	0.8916	1.25E-04	7160	0.8915

Table F.5. Predicted Peak U-238 (Kd = 0.02) Flux (Ci/yr), Arrival Time, and Cumulative Mass (Ci) at Year 12032 for Case 1 (Past Leak)

Sub-Case		Groundwater			Fenceline		
		Flux	Time	Cm Mass	Flux	Time	Cm Mass
base		8.30E-03	2053	1.0043	8.17E-03	2056	1.0020
recharge	high	1.78E-02	2042	1.0086	1.74E-02	2045	1.0036
	low	8.43E-04	2152	0.9983	8.43E-04	2156	0.9983
barrier	high	8.30E-03	2053	1.0044	8.18E-03	2056	1.0021
	low	8.29E-03	2053	1.0043	8.17E-03	2056	1.0020
barrier_deg	high	8.30E-03	2053	1.0047	8.17E-03	2056	1.0024
	low	8.30E-03	2053	0.9961	8.17E-03	2056	0.9938
plume	high	3.91E-03	2063	1.0012	3.88E-03	2066	1.0001
	low	1.66E-02	2045	1.0068	1.64E-02	2048	1.0033
ksat_aq	high	8.32E-03	2053	1.0043	8.20E-03	2055	1.0020
	low	8.24E-03	2053	1.0043	8.10E-03	2058	1.0021
ksat_vz	high	1.35E-02	2043	1.0073	1.32E-02	2046	1.0018
	low	5.10E-03	2066	0.9995	5.06E-03	2070	0.9982

Table F.6. Predicted Peak U-238 (Kd = 0.02) Flux (Ci/yr), Arrival Time, and Cumulative Mass (Ci) at Year 12032 for Case 2 (Diffusion)

Sub-Case		Groundwater			Fenceline		
		Flux	Time	Cm Mass	Flux	Time	Cm Mass
base		2.29E-05	12032	0.0507	2.29E-05	12032	0.0506
recharge	high	2.29E-05	12032	0.0507	2.29E-05	12032	0.0506
	low	2.29E-05	12032	0.0506	2.29E-05	12032	0.0505
barrier	high	2.27E-05	12032	0.0522	2.27E-05	12032	0.0521
	low	2.30E-05	12032	0.0493	2.30E-05	12032	0.0492
barrier_deg	high	4.94E-05	5788	0.1996	4.94E-05	5791	0.1996
	low	7.79E-07	12032	0.0007	7.76E-07	12032	0.0007
diffusion	high	7.24E-05	12032	0.1602	7.24E-05	12032	0.1599
	low	7.24E-08	12032	0.0002	7.24E-08	12032	0.0002
ksat_aq	high	2.29E-05	12032	0.0507	2.29E-05	12032	0.0506
	low	2.29E-05	12032	0.0506	2.29E-05	12032	0.0505
ksat_vz	high	2.74E-05	11821	0.0799	2.74E-05	11824	0.0798
	low	1.26E-05	12032	0.0219	1.26E-05	12032	0.0218

Table F.7. Predicted Peak U-238 (Kd = 0.02) Flux (Ci/yr), Arrival Time, and Cumulative Mass (Ci) at Year 12032 for Case 3 (Retrieval Leak)

Sub-Case		Groundwater			Fenceline		
		Flux	Time	Cm Mass	Flux	Time	Cm Mass
base		1.41E-04	7683	0.9010	1.41E-04	7687	0.9009
recharge	high	1.61E-04	2101	0.9315	1.61E-04	2104	0.9313
	low	1.53E-04	9009	0.8191	1.53E-04	9012	0.8188
barrier	high	1.41E-04	7441	0.9126	1.41E-04	7445	0.9125
	low	1.41E-04	7881	0.8907	1.41E-04	7884	0.8905
barrier_deg	high	4.77E-04	4338	1.0000	4.77E-04	4342	1.0000
	low	7.11E-05	11623	0.4821	7.11E-05	11623	0.4818
ksat_aq	high	1.41E-04	7684	0.9011	1.41E-04	7687	0.9009
	low	1.41E-04	7685	0.9010	1.41E-04	7688	0.9008
ksat_vz	high	1.75E-04	6897	0.9677	1.75E-04	6901	0.9676
	low	1.07E-04	10175	0.6192	1.07E-04	10182	0.6188

Table F.8. Predicted Peak U-238 (Kd = 0.02) Flux (Ci/yr), Arrival Time, and Cumulative Mass (Ci) at Year 12032 for Case 4 (Ancillary Equipment)

Sub-Case		Groundwater			Fenceline		
		Flux	Time	Cm Mass	Flux	Time	Cm Mass
base		1.47E-04	7839	0.8917	1.47E-04	7843	0.8915
recharge	high	1.40E-04	2129	0.9370	1.39E-04	2132	0.9369
	low	1.64E-04	9743	0.7448	1.64E-04	9746	0.7445
barrier	high	1.47E-04	7597	0.9042	1.47E-04	7601	0.9041
	low	1.47E-04	8036	0.8805	1.47E-04	8040	0.8803
barrier_deg	high	4.92E-04	4397	1.0000	4.92E-04	4400	1.0000
	low	7.41E-05	11921	0.4452	7.41E-05	11925	0.4450
ksat_aq	high	1.47E-04	7839	0.8917	1.47E-04	7842	0.8916
	low	1.47E-04	7840	0.8917	1.47E-04	7845	0.8914
ksat_vz	high	1.83E-04	6956	0.9673	1.83E-04	6960	0.9672
	low	1.06E-04	9233	0.6989	1.06E-04	9235	0.6987

Table F.9. Predicted Peak U-238 (Kd = 0.10) Flux (Ci/yr), Arrival Time, and Cumulative Mass (Ci) at Year 12032 for Case 1 (Past Leak)

Sub-Case		Groundwater			Fenceline		
		Flux	Time	Cm Mass	Flux	Time	Cm Mass
base		6.02E-04	2089	0.9343	6.01E-04	2095	0.9340
recharge	high	2.18E-03	2058	0.9622	2.14E-03	2064	0.9612
	low	1.27E-04	7171	0.8406	1.27E-04	7175	0.8403
barrier	high	6.03E-04	2089	0.9400	6.02E-04	2095	0.9397
	low	6.01E-04	2089	0.9293	6.00E-04	2094	0.9290
barrier_deg	high	6.02E-04	2089	1.0003	6.01E-04	2095	1.0002
	low	6.02E-04	2089	0.7398	6.01E-04	2095	0.7395
plume	high	1.51E-04	2130	0.8554	1.51E-04	2135	0.8552
	low	2.63E-03	2063	0.9811	2.60E-03	2068	0.9803
ksat_aq	high	6.03E-04	2089	0.9343	6.03E-04	2093	0.9340
	low	6.00E-04	2090	0.9342	5.98E-04	2098	0.9339
ksat_vz	high	5.00E-04	2063	0.9440	4.94E-04	2069	0.9435
	low	6.68E-04	2116	0.9013	6.68E-04	2121	0.9011

Table F.10. Predicted Peak U-238 (Kd = 0.10) Flux (Ci/yr), Arrival Time, and Cumulative Mass (Ci) at Year 12032 for Case 2 (Diffusion)

Sub-Case		Groundwater			Fenceline		
		Flux	Time	Cm Mass	Flux	Time	Cm Mass
base		1.94E-07	12032	0.0001	1.93E-07	12032	0.0001
recharge	high	1.94E-07	12032	0.0001	1.93E-07	12032	0.0001
	low	1.93E-07	12032	0.0001	1.92E-07	12032	0.0001
barrier	high	2.25E-07	12032	0.0002	2.23E-07	12032	0.0002
	low	1.71E-07	12032	0.0001	1.70E-07	12032	0.0001
barrier_deg	high	3.36E-05	9038	0.1459	3.36E-05	9044	0.1458
	low	7.73E-12	12032	0.0000	4.79E-12	12032	0.0000
diffusion	high	6.14E-07	12032	0.0004	6.09E-07	12032	0.0004
	low	6.13E-10	12032	0.0000	6.08E-10	12032	0.0000
ksat_aq	high	1.94E-07	12032	0.0001	1.93E-07	12032	0.0001
	low	1.94E-07	12032	0.0001	1.92E-07	12032	0.0001
ksat_vz	high	2.67E-07	12032	0.0002	2.65E-07	12032	0.0002
	low	1.37E-07	12032	0.0001	1.36E-07	12032	0.0001

Table F.11. Predicted Peak U-238 (Kd = 0.10) Flux (Ci/yr), Arrival Time, and Cumulative Mass (Ci) at Year 12032 for Case 3 (Retrieval Leak)

Sub-Case		Groundwater			Fenceline		
		Flux	Time	Cm Mass	Flux	Time	Cm Mass
base		5.07E-05	12032	0.1198	5.06E-05	12032	0.1195
recharge	high	6.13E-05	12032	0.1759	6.13E-05	12032	0.1756
	low	3.07E-05	12032	0.0531	3.06E-05	12032	0.0529
barrier	high	5.38E-05	12032	0.1325	5.37E-05	12032	0.1322
	low	4.81E-05	12032	0.1100	4.80E-05	12032	0.1098
barrier_deg	high	2.81E-04	6885	0.9948	2.81E-04	6890	0.9947
	low	4.39E-06	12032	0.0111	4.38E-06	12032	0.0111
ksat_aq	high	5.07E-05	12032	0.1198	5.06E-05	12032	0.1196
	low	5.06E-05	12032	0.1197	5.05E-05	12032	0.1193
ksat_vz	high	6.16E-05	12032	0.1373	6.16E-05	12032	0.1369
	low	2.51E-05	12032	0.0526	2.51E-05	12032	0.0525

Table F.12. Predicted Peak U-238 (Kd = 0.10) Flux (Ci/yr), Arrival Time, and Cumulative Mass (Ci) at Year 12032 for Case 4 (Ancillary Equipment)

Sub-Case		Groundwater			Fenceline		
		Flux	Time	Cm Mass	Flux	Time	Cm Mass
base		4.43E-05	12032	0.0902	4.42E-05	12032	0.0900
recharge	high	6.13E-05	12032	0.1704	6.13E-05	12032	0.1700
	low	1.48E-05	12032	0.0174	1.47E-05	12032	0.0173
barrier	high	4.76E-05	12032	0.1014	4.75E-05	12032	0.1011
	low	4.16E-05	12032	0.0818	4.15E-05	12032	0.0816
barrier_deg	high	2.83E-04	7044	0.9935	2.83E-04	7050	0.9935
	low	2.55E-06	12032	0.0050	2.54E-06	12032	0.0050
ksat_aq	high	4.43E-05	12032	0.0903	4.42E-05	12032	0.0901
	low	4.42E-05	12032	0.0902	4.41E-05	12032	0.0899
ksat_vz	high	5.21E-05	12032	0.0960	5.20E-05	12032	0.0958
	low	3.34E-05	12032	0.0792	3.33E-05	12032	0.0790

Table F.13. Predicted Peak U-238 (Kd = 0.20) Flux (Ci/yr), Arrival Time, and Cumulative Mass (Ci) at Year 12032 for Case 1 (Past Leak)

Sub-Case		Groundwater			Fenceline		
		Flux	Time	Cm Mass	Flux	Time	Cm Mass
base		7.95E-05	9613	0.5620	7.95E-05	9621	0.5615
recharge	high	1.33E-04	2092	0.6622	1.33E-04	2100	0.6617
	low	8.11E-05	12032	0.3540	8.11E-05	12032	0.3534
barrier	high	7.96E-05	9369	0.5793	7.96E-05	9376	0.5788
	low	7.95E-05	9811	0.5478	7.95E-05	9819	0.5473
barrier_deg	high	2.74E-04	5000	0.9975	2.74E-04	5007	0.9975
	low	3.82E-05	12032	0.2582	3.82E-05	12032	0.2579
plume	high	7.28E-05	12032	0.3559	7.28E-05	12032	0.3553
	low	2.35E-04	2100	0.7851	2.35E-04	2108	0.7847
ksat_aq	high	7.95E-05	9613	0.5621	7.95E-05	9616	0.5617
	low	7.95E-05	9616	0.5619	7.95E-05	9624	0.5611
ksat_vz	high	8.61E-05	10139	0.5379	8.61E-05	10145	0.5373
	low	6.80E-05	8786	0.5658	6.80E-05	8795	0.5654

Table F.14. Predicted Peak U-238 (Kd = 0.20) Flux (Ci/yr), Arrival Time, and Cumulative Mass (Ci) at Year 12032 for Case 2 (Diffusion)

Sub-Case		Groundwater			Fenceline		
		Flux	Time	Cm Mass	Flux	Time	Cm Mass
base		4.17E-11	12032	0.0000	3.97E-11	12032	0.0000
recharge	high	4.19E-11	12032	0.0000	3.99E-11	12032	0.0000
	low	4.11E-11	12032	0.0000	3.90E-11	12032	0.0000
barrier	high	5.83E-11	12032	0.0000	5.63E-11	12032	0.0000
	low	3.17E-11	12032	0.0000	2.91E-11	12032	0.0000
barrier_deg	high	2.43E-05	12032	0.0499	2.42E-05	12032	0.0497
	low	0.00E+00	12032	0.0000	0.00E+00	12032	0.0000
diffusion	high	1.32E-10	12032	0.0000	1.29E-10	12032	0.0000
	low	0.00E+00	12032	0.0000	0.00E+00	12032	0.0000
ksat_aq	high	4.17E-11	12032	0.0000	3.93E-11	12032	0.0000
	low	4.16E-11	12032	0.0000	3.95E-11	12032	0.0000
ksat_vz	high	2.46E-11	12032	0.0000	2.09E-11	12032	0.0000
	low	1.28E-10	12032	0.0000	1.25E-10	12032	0.0000

Table F.15. Predicted Peak U-238 (Kd = 0.20) Flux (Ci/yr), Arrival Time, and Cumulative Mass (Ci) at Year 12032 for Case 3 (Retrieval Leak)

Sub-Case		Groundwater			Fenceline		
		Flux	Time	Cm Mass	Flux	Time	Cm Mass
base		1.14E-06	12032	0.0015	1.14E-06	12032	0.0015
recharge	high	2.26E-06	12032	0.0033	2.25E-06	12032	0.0033
	low	2.97E-07	12032	0.0003	2.95E-07	12032	0.0003
barrier	high	1.34E-06	12032	0.0018	1.34E-06	12032	0.0017
	low	1.00E-06	12032	0.0013	9.96E-07	12032	0.0012
barrier_deg	high	1.82E-04	10148	0.7217	1.82E-04	10156	0.7207
	low	2.04E-08	12032	0.0000	2.03E-08	12032	0.0000
ksat_aq	high	1.14E-06	12032	0.0015	1.14E-06	12032	0.0015
	low	1.14E-06	12032	0.0015	1.13E-06	12032	0.0014
ksat_vz	high	1.03E-06	12032	0.0012	1.02E-06	12032	0.0012
	low	6.27E-07	12032	0.0008	6.23E-07	12032	0.0008

Table F.16. Predicted Peak U-238 (Kd = 0.20) Flux (Ci/yr), Arrival Time, and Cumulative Mass (Ci) at Year 12032 for Case 4 (Ancillary Equipment)

Sub-Case		Groundwater			Fenceline		
		Flux	Time	Cm Mass	Flux	Time	Cm Mass
base		5.48E-07	12032	0.0006	5.44E-07	12032	0.0006
recharge	high	1.87E-06	12032	0.0025	1.86E-06	12032	0.0025
	low	2.57E-08	12032	0.0000	2.55E-08	12032	0.0000
barrier	high	6.67E-07	12032	0.0007	6.63E-07	12032	0.0007
	low	4.65E-07	12032	0.0005	4.62E-07	12032	0.0005
barrier_deg	high	1.82E-04	10399	0.6853	1.82E-04	10406	0.6843
	low	3.46E-09	12032	0.0000	3.44E-09	12032	0.0000
ksat_aq	high	5.48E-07	12032	0.0006	5.46E-07	12032	0.0006
	low	5.47E-07	12032	0.0006	5.42E-07	12032	0.0006
ksat_vz	high	2.90E-07	12032	0.0003	2.88E-07	12032	0.0003
	low	1.04E-06	12032	0.0014	1.04E-06	12032	0.0014

Table F.17. Predicted Peak U-238 (Kd = 0.60) Flux (Ci/yr), Arrival Time, and Cumulative Mass (Ci) at Year 12032 for Case 1 (Past Leak)

Sub-Case		Groundwater			Fenceline		
		Flux	Time	Cm Mass	Flux	Time	Cm Mass
base		2.76E-06	12032	0.0052	2.74E-06	12032	0.0051
recharge	high	4.97E-06	12032	0.0113	4.94E-06	12032	0.0113
	low	6.50E-07	12032	0.0008	6.42E-07	12032	0.0008
barrier	high	3.04E-06	12032	0.0058	3.02E-06	12032	0.0058
	low	2.55E-06	12032	0.0047	2.53E-06	12032	0.0046
barrier_deg	high	1.14E-04	11109	0.4784	1.14E-04	11128	0.4765
	low	2.00E-07	12032	0.0004	1.99E-07	12032	0.0004
plume	high	3.67E-07	12032	0.0005	3.63E-07	12032	0.0005
	low	1.58E-05	12032	0.0454	1.57E-05	12032	0.0451
ksat_aq	high	2.76E-06	12032	0.0052	2.75E-06	12032	0.0051
	low	2.76E-06	12032	0.0052	2.73E-06	12032	0.0051
ksat_vz	high	1.69E-06	12032	0.0027	1.67E-06	12032	0.0027
	low	5.05E-06	12032	0.0120	5.03E-06	12032	0.0119

Table F.18. Predicted Peak U-238 (Kd = 0.60) Flux (Ci/yr), Arrival Time, and Cumulative Mass (Ci) at Year 12032 for Case 2 (Diffusion)

Sub-Case		Groundwater			Fenceline		
		Flux	Time	Cm Mass	Flux	Time	Cm Mass
base		0.00E+00	12032	0.0000	0.00E+00	12032	0.0000
recharge	high	0.00E+00	12032	0.0000	0.00E+00	12032	0.0000
	low	0.00E+00	12032	0.0000	0.00E+00	12032	0.0000
barrier	high	0.00E+00	12032	0.0000	0.00E+00	12032	0.0000
	low	0.00E+00	12032	0.0000	0.00E+00	12032	0.0000
barrier_deg	high	3.47E-09	12032	0.0000	3.34E-09	12032	0.0000
	low	0.00E+00	12032	0.0000	0.00E+00	12032	0.0000
diffusion	high	0.00E+00	12032	0.0000	0.00E+00	12032	0.0000
	low	0.00E+00	12032	0.0000	0.00E+00	12032	0.0000
ksat_aq	high	0.00E+00	12032	0.0000	0.00E+00	12032	0.0000
	low	0.00E+00	12032	0.0000	0.00E+00	12032	0.0000
ksat_vz	high	0.00E+00	12032	0.0000	0.00E+00	12032	0.0000
	low	0.00E+00	12032	0.0000	0.00E+00	12032	0.0000

Table F.19. Predicted Peak U-238 (Kd = 0.60) Flux (Ci/yr), Arrival Time, and Cumulative Mass (Ci) at Year 12032 for Case 3 (Retrieval Leak)

Sub-Case		Groundwater			Fenceline		
		Flux	Time	Cm Mass	Flux	Time	Cm Mass
base		0.00E+00	12032	0.0000	0.00E+00	12032	0.0000
recharge	high	0.00E+00	12032	0.0000	0.00E+00	12032	0.0000
	low	0.00E+00	12032	0.0000	0.00E+00	12032	0.0000
barrier	high	0.00E+00	12032	0.0000	0.00E+00	12032	0.0000
	low	0.00E+00	12032	0.0000	0.00E+00	12032	0.0000
barrier_deg	high	7.07E-07	12032	0.0005	6.92E-07	12032	0.0005
	low	0.00E+00	12032	0.0000	0.00E+00	12032	0.0000
ksat_aq	high	0.00E+00	12032	0.0000	0.00E+00	12032	0.0000
	low	0.00E+00	12032	0.0000	0.00E+00	12032	0.0000
ksat_vz	high	0.00E+00	12032	0.0000	0.00E+00	12032	0.0000
	low	0.00E+00	12032	0.0000	0.00E+00	12032	0.0000

Table F.20. Predicted Peak U-238 (Kd = 0.60) Flux (Ci/yr), Arrival Time, and Cumulative Mass (Ci) at Year 12032 for Case 4 (Ancillary Equipment)

Sub-Case		Groundwater			Fenceline		
		Flux	Time	Cm Mass	Flux	Time	Cm Mass
base		0.00E+00	12032	0.0000	0.00E+00	12032	0.0000
recharge	high	0.00E+00	12032	0.0000	0.00E+00	12032	0.0000
	low	0.00E+00	12032	0.0000	0.00E+00	12032	0.0000
barrier	high	0.00E+00	12032	0.0000	0.00E+00	12032	0.0000
	low	0.00E+00	12032	0.0000	0.00E+00	12032	0.0000
barrier_deg	high	3.97E-07	12032	0.0003	3.88E-07	12032	0.0003
	low	0.00E+00	12032	0.0000	0.00E+00	12032	0.0000
ksat_aq	high	0.00E+00	12032	0.0000	0.00E+00	12032	0.0000
	low	0.00E+00	12032	0.0000	0.00E+00	12032	0.0000
ksat_vz	high	0.00E+00	12032	0.0000	0.00E+00	12032	0.0000
	low	0.00E+00	12032	0.0000	0.00E+00	12032	0.0000

Table F.21. Predicted Peak U-238 (Kd = 1.00) Flux (Ci/yr), Arrival Time, and Cumulative Mass (Ci) at Year 12032 for Case 1 (Past Leak)

Sub-Case		Groundwater			Fenceline		
		Flux	Time	Cm Mass	Flux	Time	Cm Mass
base		2.20E-08	12032	0.0000	2.16E-08	12032	0.0000
recharge	high	6.34E-08	12032	0.0001	6.24E-08	12032	0.0001
	low	1.93E-09	12032	0.0000	1.88E-09	12032	0.0000
barrier	high	2.58E-08	12032	0.0000	2.54E-08	12032	0.0000
	low	1.92E-08	12032	0.0000	1.89E-08	12032	0.0000
barrier_deg	high	3.55E-05	12032	0.0649	3.52E-05	12032	0.0640
	low	5.60E-10	12032	0.0000	5.51E-10	12032	0.0000
plume	high	5.91E-10	12032	0.0000	5.75E-10	12032	0.0000
	low	7.07E-07	12032	0.0013	6.98E-07	12032	0.0012
ksat_aq	high	2.20E-08	12032	0.0000	2.17E-08	12032	0.0000
	low	2.20E-08	12032	0.0000	2.13E-08	12032	0.0000
ksat_vz	high	7.93E-09	12032	0.0000	7.75E-09	12032	0.0000
	low	9.44E-08	12032	0.0001	9.30E-08	12032	0.0001

Table F.22. Predicted Peak U-238 (Kd = 1.00) Flux (Ci/yr), Arrival Time, and Cumulative Mass (Ci) at Year 12032 for Case 2 (Diffusion)

Sub-Case		Groundwater			Fenceline		
		Flux	Time	Cm Mass	Flux	Time	Cm Mass
base		0.00E+00	12032	0.0000	0.00E+00	12032	0.0000
recharge	high	0.00E+00	12032	0.0000	0.00E+00	12032	0.0000
	low	0.00E+00	12032	0.0000	0.00E+00	12032	0.0000
barrier	high	0.00E+00	12032	0.0000	0.00E+00	12032	0.0000
	low	0.00E+00	12032	0.0000	0.00E+00	12032	0.0000
barrier_deg	high	0.00E+00	12032	0.0000	0.00E+00	12032	0.0000
	low	0.00E+00	12032	0.0000	0.00E+00	12032	0.0000
diffusion	high	0.00E+00	12032	0.0000	0.00E+00	12032	0.0000
	low	0.00E+00	12032	0.0000	0.00E+00	12032	0.0000
ksat_aq	high	0.00E+00	12032	0.0000	0.00E+00	12032	0.0000
	low	0.00E+00	12032	0.0000	0.00E+00	12032	0.0000
ksat_vz	high	0.00E+00	12032	0.0000	0.00E+00	12032	0.0000
	low	0.00E+00	12032	0.0000	0.00E+00	12032	0.0000

Table F.23. Predicted Peak U-238 (Kd = 1.00) Flux (Ci/yr), Arrival Time, and Cumulative Mass (Ci) at Year 12032 for Case 3 (Retrieval Leak)

Sub-Case		Groundwater			Fenceline		
		Flux	Time	Cm Mass	Flux	Time	Cm Mass
base		0.00E+00	12032	0.0000	0.00E+00	12032	0.0000
recharge	high	0.00E+00	12032	0.0000	0.00E+00	12032	0.0000
	low	0.00E+00	12032	0.0000	0.00E+00	12032	0.0000
barrier	high	0.00E+00	12032	0.0000	0.00E+00	12032	0.0000
	low	0.00E+00	12032	0.0000	0.00E+00	12032	0.0000
barrier_deg	high	8.88E-11	12032	0.0000	8.33E-11	12032	0.0000
	low	0.00E+00	12032	0.0000	0.00E+00	12032	0.0000
ksat_aq	high	0.00E+00	12032	0.0000	0.00E+00	12032	0.0000
	low	0.00E+00	12032	0.0000	0.00E+00	12032	0.0000
ksat_vz	high	0.00E+00	12032	0.0000	0.00E+00	12032	0.0000
	low	0.00E+00	12032	0.0000	0.00E+00	12032	0.0000

Table F.24. Predicted Peak U-238 (Kd = 1.00) Flux (Ci/yr), Arrival Time, and Cumulative Mass (Ci) at Year 12032 for Case 4 (Ancillary Equipment)

Sub-Case		Groundwater			Fenceline		
		Flux	Time	Cm Mass	Flux	Time	Cm Mass
base		0.00E+00	12032	0.0000	0.00E+00	12032	0.0000
recharge	high	0.00E+00	12032	0.0000	0.00E+00	12032	0.0000
	low	0.00E+00	12032	0.0000	0.00E+00	12032	0.0000
barrier	high	0.00E+00	12032	0.0000	0.00E+00	12032	0.0000
	low	0.00E+00	12032	0.0000	0.00E+00	12032	0.0000
barrier_deg	high	2.64E-11	12032	0.0000	2.35E-11	12032	0.0000
	low	0.00E+00	12032	0.0000	0.00E+00	12032	0.0000
ksat_aq	high	0.00E+00	12032	0.0000	0.00E+00	12032	0.0000
	low	0.00E+00	12032	0.0000	0.00E+00	12032	0.0000
ksat_vz	high	0.00E+00	12032	0.0000	0.00E+00	12032	0.0000
	low	0.00E+00	12032	0.0000	0.00E+00	12032	0.0000

Table F.25. Predicted Peak U-238 (Kd = 2.00) Flux (Ci/yr), Arrival Time, and Cumulative Mass (Ci) at Year 12032 for Case 1 (Past Leak)

Sub-Case		Groundwater			Fenceline		
		Flux	Time	Cm Mass	Flux	Time	Cm Mass
base		4.02E-13	12032	0.0000	0.00E+00	12032	0.0000
recharge	high	2.56E-12	12032	0.0000	1.42E-12	12032	0.0000
	low	0.00E+00	12032	0.0000	0.00E+00	12032	0.0000
barrier	high	5.24E-13	12032	0.0000	0.00E+00	12032	0.0000
	low	3.21E-13	12032	0.0000	0.00E+00	12032	0.0000
barrier_deg	high	1.56E-07	12032	0.0001	1.49E-07	12032	0.0001
	low	0.00E+00	12032	0.0000	0.00E+00	12032	0.0000
plume	high	0.00E+00	12032	0.0000	0.00E+00	12032	0.0000
	low	3.28E-10	12032	0.0000	3.15E-10	12032	0.0000
ksat_aq	high	4.02E-13	12032	0.0000	0.00E+00	12032	0.0000
	low	4.01E-13	12032	0.0000	0.00E+00	12032	0.0000
ksat_vz	high	3.64E-14	12032	0.0000	0.00E+00	12032	0.0000
	low	7.40E-12	12032	0.0000	5.95E-12	12032	0.0000

Table F.26. Predicted Peak U-238 (Kd = 2.00) Flux (Ci/yr), Arrival Time, and Cumulative Mass (Ci) at Year 12032 for Case 2 (Diffusion)

Sub-Case		Groundwater			Fenceline		
		Flux	Time	Cm Mass	Flux	Time	Cm Mass
base		0.00E+00	12032	0.0000	0.00E+00	12032	0.0000
recharge	high	0.00E+00	12032	0.0000	0.00E+00	12032	0.0000
	low	0.00E+00	12032	0.0000	0.00E+00	12032	0.0000
barrier	high	0.00E+00	12032	0.0000	0.00E+00	12032	0.0000
	low	0.00E+00	12032	0.0000	0.00E+00	12032	0.0000
barrier_deg	high	0.00E+00	12032	0.0000	0.00E+00	12032	0.0000
	low	0.00E+00	12032	0.0000	0.00E+00	12032	0.0000
diffusion	high	0.00E+00	12032	0.0000	0.00E+00	12032	0.0000
	low	0.00E+00	12032	0.0000	0.00E+00	12032	0.0000
ksat_aq	high	0.00E+00	12032	0.0000	0.00E+00	12032	0.0000
	low	0.00E+00	12032	0.0000	0.00E+00	12032	0.0000
ksat_vz	high	0.00E+00	12032	0.0000	0.00E+00	12032	0.0000
	low	0.00E+00	12032	0.0000	0.00E+00	12032	0.0000

Table F.27. Predicted Peak U-238 (Kd = 2.00) Flux (Ci/yr), Arrival Time, and Cumulative Mass (Ci) at Year 12032 for Case 3 (Retrieval Leak)

Sub-Case		Groundwater			Fenceline		
		Flux	Time	Cm Mass	Flux	Time	Cm Mass
base		0.00E+00	12032	0.0000	0.00E+00	12032	0.0000
recharge	high	0.00E+00	12032	0.0000	0.00E+00	12032	0.0000
	low	0.00E+00	12032	0.0000	0.00E+00	12032	0.0000
barrier	high	0.00E+00	12032	0.0000	0.00E+00	12032	0.0000
	low	0.00E+00	12032	0.0000	0.00E+00	12032	0.0000
barrier_deg	high	0.00E+00	12032	0.0000	0.00E+00	12032	0.0000
	low	0.00E+00	12032	0.0000	0.00E+00	12032	0.0000
ksat_aq	high	0.00E+00	12032	0.0000	0.00E+00	12032	0.0000
	low	0.00E+00	12032	0.0000	0.00E+00	12032	0.0000
ksat_vz	high	0.00E+00	12032	0.0000	0.00E+00	12032	0.0000
	low	0.00E+00	12032	0.0000	0.00E+00	12032	0.0000

Table F.28. Predicted Peak U-238 (Kd = 2.00) Flux (Ci/yr), Arrival Time, and Cumulative Mass (Ci) at Year 12032 for Case 4 (Ancillary Equipment)

Sub-Case		Groundwater			Fenceline		
		Flux	Time	Cm Mass	Flux	Time	Cm Mass
base		0.00E+00	12032	0.0000	0.00E+00	12032	0.0000
recharge	high	0.00E+00	12032	0.0000	0.00E+00	12032	0.0000
	low	0.00E+00	12032	0.0000	0.00E+00	12032	0.0000
barrier	high	0.00E+00	12032	0.0000	0.00E+00	12032	0.0000
	low	0.00E+00	12032	0.0000	0.00E+00	12032	0.0000
barrier_deg	high	0.00E+00	12032	0.0000	0.00E+00	12032	0.0000
	low	0.00E+00	12032	0.0000	0.00E+00	12032	0.0000
ksat_aq	high	0.00E+00	12032	0.0000	0.00E+00	12032	0.0000
	low	0.00E+00	12032	0.0000	0.00E+00	12032	0.0000
ksat_vz	high	0.00E+00	12032	0.0000	0.00E+00	12032	0.0000
	low	0.00E+00	12032	0.0000	0.00E+00	12032	0.0000

Table F.29. Predicted Peak U-238 (Kd = 5.00) Flux (Ci/yr), Arrival Time, and Cumulative Mass (Ci) at Year 12032 for Case 1 (Past Leak)

Sub-Case		Groundwater			Fenceline		
		Flux	Time	Cm Mass	Flux	Time	Cm Mass
base		0.00E+00	12032	0.0000	0.00E+00	12032	0.0000
recharge	high	0.00E+00	12032	0.0000	0.00E+00	12032	0.0000
	low	0.00E+00	12032	0.0000	0.00E+00	12032	0.0000
barrier	high	0.00E+00	12032	0.0000	0.00E+00	12032	0.0000
	low	0.00E+00	12032	0.0000	0.00E+00	12032	0.0000
barrier_deg	high	1.87E-14	12032	0.0000	0.00E+00	12032	0.0000
	low	0.00E+00	12032	0.0000	0.00E+00	12032	0.0000
plume	high	0.00E+00	12032	0.0000	0.00E+00	12032	0.0000
	low	0.00E+00	12032	0.0000	0.00E+00	12032	0.0000
ksat_aq	high	0.00E+00	12032	0.0000	0.00E+00	12032	0.0000
	low	0.00E+00	12032	0.0000	0.00E+00	12032	0.0000
ksat_vz	high	0.00E+00	12032	0.0000	0.00E+00	12032	0.0000
	low	0.00E+00	12032	0.0000	0.00E+00	12032	0.0000

Table F.30. Predicted Peak U-238 (Kd = 5.00) Flux (Ci/yr), Arrival Time, and Cumulative Mass (Ci) at Year 12032 for Case 2 (Diffusion)

Sub-Case		Groundwater			Fenceline		
		Flux	Time	Cm Mass	Flux	Time	Cm Mass
base		0.00E+00	12032	0.0000	0.00E+00	12032	0.0000
recharge	high	0.00E+00	12032	0.0000	0.00E+00	12032	0.0000
	low	0.00E+00	12032	0.0000	0.00E+00	12032	0.0000
barrier	high	0.00E+00	12032	0.0000	0.00E+00	12032	0.0000
	low	0.00E+00	12032	0.0000	0.00E+00	12032	0.0000
barrier_deg	high	0.00E+00	12032	0.0000	0.00E+00	12032	0.0000
	low	0.00E+00	12032	0.0000	0.00E+00	12032	0.0000
diffusion	high	0.00E+00	12032	0.0000	0.00E+00	12032	0.0000
	low	0.00E+00	12032	0.0000	0.00E+00	12032	0.0000
ksat_aq	high	0.00E+00	12032	0.0000	0.00E+00	12032	0.0000
	low	0.00E+00	12032	0.0000	0.00E+00	12032	0.0000
ksat_vz	high	0.00E+00	12032	0.0000	0.00E+00	12032	0.0000
	low	0.00E+00	12032	0.0000	0.00E+00	12032	0.0000

Table F.31. Predicted Peak U-238 (Kd = 5.00) Flux (Ci/yr), Arrival Time, and Cumulative Mass (Ci) at Year 12032 for Case 3 (Retrieval Leak)

Sub-Case		Groundwater			Fenceline		
		Flux	Time	Cm Mass	Flux	Time	Cm Mass
base		0.00E+00	12032	0.0000	0.00E+00	12032	0.0000
recharge	high	0.00E+00	12032	0.0000	0.00E+00	12032	0.0000
	low	0.00E+00	12032	0.0000	0.00E+00	12032	0.0000
barrier	high	0.00E+00	12032	0.0000	0.00E+00	12032	0.0000
	low	0.00E+00	12032	0.0000	0.00E+00	12032	0.0000
barrier_deg	high	0.00E+00	12032	0.0000	0.00E+00	12032	0.0000
	low	0.00E+00	12032	0.0000	0.00E+00	12032	0.0000
ksat_aq	high	0.00E+00	12032	0.0000	0.00E+00	12032	0.0000
	low	0.00E+00	12032	0.0000	0.00E+00	12032	0.0000
ksat_vz	high	0.00E+00	12032	0.0000	0.00E+00	12032	0.0000
	low	0.00E+00	12032	0.0000	0.00E+00	12032	0.0000

Table F.32. Predicted Peak U-238 (Kd = 5.00) Flux (Ci/yr), Arrival Time, and Cumulative Mass (Ci) at Year 12032 for Case 4 (Ancillary Equipment)

Sub-Case		Groundwater			Fenceline		
		Flux	Time	Cm Mass	Flux	Time	Cm Mass
base		0.00E+00	12032	0.0000	0.00E+00	12032	0.0000
recharge	high	0.00E+00	12032	0.0000	0.00E+00	12032	0.0000
	low	0.00E+00	12032	0.0000	0.00E+00	12032	0.0000
barrier	high	0.00E+00	12032	0.0000	0.00E+00	12032	0.0000
	low	0.00E+00	12032	0.0000	0.00E+00	12032	0.0000
barrier_deg	high	0.00E+00	12032	0.0000	0.00E+00	12032	0.0000
	low	0.00E+00	12032	0.0000	0.00E+00	12032	0.0000
ksat_aq	high	0.00E+00	12032	0.0000	0.00E+00	12032	0.0000
	low	0.00E+00	12032	0.0000	0.00E+00	12032	0.0000
ksat_vz	high	0.00E+00	12032	0.0000	0.00E+00	12032	0.0000
	low	0.00E+00	12032	0.0000	0.00E+00	12032	0.0000

Table F.33. Predicted Peak Tc-99 Aqueous Concentration (Ci/L) and Arrival Time (yr) Summary for Case 1 (Past Leak)

Sub-Case		Groundwater		Fenceline		Excl (East)		Col River (East)		Excl (North)		Col River (North)	
		Conc.	Time	Conc.	Time	Conc.	Time	Conc.	Time	Conc.	Time	Conc.	Time
base		8.16E-08	2048	8.07E-08	2051	3.79E-11	2075	4.27E-12	2161	1.89E-11	2055	4.09E-12	2131
recharge	high	1.40E-07	2039	1.39E-07	2042	6.38E-11	2065	6.75E-12	2150	3.34E-11	2046	6.68E-12	2121
	low	1.19E-08	2116	1.19E-08	2119	5.85E-12	2142	7.36E-13	2228	2.73E-12	2122	6.62E-13	2198
barrier	high	8.16E-08	2048	8.07E-08	2051	3.79E-11	2075	4.27E-12	2161	1.90E-11	2055	4.09E-12	2131
	low	8.15E-08	2048	8.07E-08	2051	3.79E-11	2075	4.27E-12	2161	1.89E-11	2055	4.09E-12	2131
barrier_deg	high	8.16E-08	2048	8.07E-08	2051	3.79E-11	2075	4.27E-12	2161	1.89E-11	2055	4.09E-12	2131
	low	8.16E-08	2048	8.07E-08	2051	3.79E-11	2075	4.27E-12	2161	1.89E-11	2055	4.09E-12	2131
plume	high	4.68E-08	2055	4.63E-08	2058	2.22E-11	2082	2.61E-12	2169	1.08E-11	2061	2.45E-12	2138
	low	1.27E-07	2041	1.27E-07	2044	5.92E-11	2067	6.46E-12	2152	3.00E-11	2048	6.30E-12	2122
ksat_aq	high	6.19E-08	2048	6.12E-08	2050	3.80E-11	2074	4.28E-12	2160	1.90E-11	2054	4.10E-12	2130
	low	1.19E-07	2048	1.18E-07	2052	3.77E-11	2076	4.25E-12	2162	1.88E-11	2056	4.07E-12	2132
ksat_vz	high	1.38E-07	2039	1.36E-07	2042	6.05E-11	2065	6.36E-12	2150	3.19E-11	2045	6.32E-12	2120
	low	4.60E-08	2060	4.57E-08	2062	2.23E-11	2087	2.65E-12	2173	1.07E-11	2066	2.47E-12	2143

Table F.34. Predicted Peak Tc-99 Aqueous Concentration (Ci/L) and Arrival Time (yr) Summary for Case 2 (Diffusion)

Sub-Case		Groundwater		Fenceline		Excl (East)		Col River (East)		Excl (North)		Col River (North)	
		Conc.	Time	Conc.	Time	Conc.	Time	Conc.	Time	Conc.	Time	Conc.	Time
base		1.64E-10	10480	1.64E-10	10483	8.03E-14	10504	1.02E-14	10590	3.73E-14	10485	9.12E-15	10560
recharge	high	1.64E-10	10480	1.64E-10	10483	8.03E-14	10504	1.02E-14	10592	3.73E-14	10486	9.12E-15	10558
	low	1.64E-10	10481	1.64E-10	10484	8.04E-14	10506	1.02E-14	10590	3.73E-14	10486	9.13E-15	10561
barrier	high	1.61E-10	10456	1.61E-10	10458	7.86E-14	10480	9.97E-15	10562	3.65E-14	10461	8.92E-15	10534
	low	1.67E-10	10513	1.67E-10	10517	8.18E-14	10540	1.04E-14	10626	3.80E-14	10521	9.29E-15	10594
barrier_deg	high	3.38E-10	5001	3.38E-10	5004	1.66E-13	5027	2.10E-14	5111	7.69E-14	5008	1.88E-14	5082
	low	4.19E-11	12032	4.19E-11	12032	2.02E-14	12032	2.46E-15	12032	9.49E-15	12032	2.24E-15	12032
diffusion	high	5.19E-10	10480	5.19E-10	10483	2.54E-13	10505	3.22E-14	10587	1.18E-13	10487	2.89E-14	10561
	low	5.19E-13	10479	5.19E-13	10482	2.54E-16	10504	3.22E-17	10589	1.18E-16	10486	2.88E-17	10559
ksat_aq	high	1.23E-10	10481	1.23E-10	10483	8.03E-14	10504	1.02E-14	10591	3.73E-14	10486	9.12E-15	10558
	low	2.46E-10	10480	2.46E-10	10485	8.03E-14	10507	1.02E-14	10591	3.73E-14	10488	9.12E-15	10561
ksat_vz	high	1.89E-10	9003	1.89E-10	9005	9.25E-14	9028	1.17E-14	9113	4.30E-14	9009	1.05E-14	9085
	low	1.26E-10	12032	1.26E-10	12032	6.16E-14	12032	7.76E-15	12032	2.87E-14	12032	6.96E-15	12032

Table F.35. Predicted Peak Tc-99 Aqueous Concentration (Ci/L) and Arrival Time (yr) Summary for Case 3 (Retrieval Leak)

Sub-Case		Groundwater		Fenceline		Excl (East)		Col River (East)		Excl (North)		Col River (North)	
		Conc.	Time	Conc.	Time	Conc.	Time	Conc.	Time	Conc.	Time	Conc.	Time
base		1.34E-09	2118	1.34E-09	2121	6.59E-13	2144	8.34E-14	2229	3.06E-13	2124	7.47E-14	2199
recharge	high	3.68E-09	2081	3.68E-09	2087	1.81E-12	2109	2.28E-13	2195	8.46E-13	2090	2.05E-13	2164
	low	1.10E-09	6961	1.10E-09	6964	5.40E-13	6986	6.85E-14	7070	2.51E-13	6967	6.13E-14	7042
barrier	high	1.34E-09	2119	1.34E-09	2122	6.61E-13	2144	8.36E-14	2230	3.07E-13	2125	7.50E-14	2200
	low	1.34E-09	2118	1.34E-09	2121	6.57E-13	2143	8.31E-14	2229	3.06E-13	2124	7.45E-14	2199
barrier_deg	high	3.30E-09	3735	3.30E-09	3738	1.62E-12	3761	2.05E-13	3845	7.51E-13	3742	1.84E-13	3816
	low	1.34E-09	2118	1.34E-09	2121	6.59E-13	2144	8.34E-14	2229	3.06E-13	2124	7.47E-14	2199
ksat_aq	high	1.01E-09	2118	1.01E-09	2120	6.59E-13	2143	8.34E-14	2228	3.07E-13	2123	7.48E-14	2198
	low	2.00E-09	2119	2.00E-09	2123	6.58E-13	2145	8.33E-14	2231	3.06E-13	2126	7.47E-14	2201
ksat_vz	high	2.17E-09	2075	2.16E-09	2079	1.06E-12	2102	1.32E-13	2189	4.95E-13	2082	1.19E-13	2158
	low	7.27E-10	8095	7.27E-10	8097	3.56E-13	8120	4.52E-14	8204	1.65E-13	8102	4.04E-14	8176

Table F.36. Predicted Peak Tc-99 Aqueous Concentration (Ci/L) and Arrival Time (yr) Summary for Case 4 (Ancillary Equipment)

Sub-Case		Groundwater		Fenceline		Excl (East)		Col River (East)		Excl (North)		Col River (North)	
		Conc.	Time	Conc.	Time	Conc.	Time	Conc.	Time	Conc.	Time	Conc.	Time
base		1.03E-09	5713	1.03E-09	5717	5.04E-13	5737	6.39E-14	5821	2.34E-13	5718	5.72E-14	5792
recharge	high	3.83E-09	2092	3.83E-09	2095	1.89E-12	2118	2.37E-13	2205	8.79E-13	2098	2.13E-13	2174
	low	1.22E-09	7537	1.22E-09	7540	5.98E-13	7562	7.58E-14	7645	2.78E-13	7543	6.79E-14	7617
barrier	high	1.03E-09	5471	1.03E-09	5474	5.03E-13	5496	6.39E-14	5580	2.34E-13	5477	5.71E-14	5551
	low	1.03E-09	5909	1.03E-09	5912	5.04E-13	5935	6.40E-14	6019	2.34E-13	5916	5.73E-14	5989
barrier_deg	high	3.45E-09	3757	3.45E-09	3760	1.69E-12	3783	2.15E-13	3867	7.85E-13	3764	1.92E-13	3838
	low	7.71E-10	2194	7.71E-10	2197	3.78E-13	2219	4.79E-14	2304	1.76E-13	2200	4.29E-14	2274
ksat_aq	high	7.73E-10	5712	7.73E-10	5714	5.04E-13	5736	6.39E-14	5822	2.34E-13	5719	5.72E-14	5792
	low	1.54E-09	5714	1.54E-09	5717	5.04E-13	5740	6.39E-14	5824	2.34E-13	5721	5.72E-14	5794
ksat_vz	high	1.49E-09	2094	1.48E-09	2097	7.28E-13	2121	9.17E-14	2207	3.39E-13	2101	8.24E-14	2176
	low	7.17E-10	7155	7.17E-10	7158	3.51E-13	7181	4.45E-14	7265	1.63E-13	7164	3.98E-14	7235

Table F.37. Predicted Peak U-238 (Kd = 0.02) Aqueous Concentration (Ci/L) and Arrival Time (yr) Summary for Case 1 (Past Leak)

Sub-Case		Groundwater		Fenceline		Excl (East)		Col River (East)		Excl (North)		Col River (North)	
		Conc.	Time	Conc.	Time	Conc.	Time	Conc.	Time	Conc.	Time	Conc.	Time
base		4.58E-08	2053	4.53E-08	2057	2.33E-11	2085	2.69E-12	2184	1.18E-11	2061	2.56E-12	2149
recharge	high	9.58E-08	2043	9.47E-08	2046	4.63E-11	2073	4.93E-12	2172	2.50E-11	2050	4.89E-12	2137
	low	4.79E-09	2153	4.79E-09	2156	2.56E-12	2183	3.24E-13	2281	1.22E-12	2160	2.92E-13	2246
barrier	high	4.58E-08	2053	4.53E-08	2057	2.33E-11	2085	2.69E-12	2184	1.18E-11	2061	2.56E-12	2149
	low	4.58E-08	2053	4.53E-08	2057	2.33E-11	2085	2.68E-12	2184	1.17E-11	2061	2.56E-12	2149
barrier_deg	high	4.58E-08	2053	4.53E-08	2057	2.33E-11	2085	2.69E-12	2184	1.18E-11	2061	2.56E-12	2149
	low	4.58E-08	2053	4.53E-08	2057	2.33E-11	2085	2.69E-12	2184	1.18E-11	2061	2.56E-12	2149
plume	high	2.18E-08	2063	2.17E-08	2067	1.14E-11	2095	1.38E-12	2195	5.58E-12	2071	1.28E-12	2160
	low	9.08E-08	2045	8.99E-08	2048	4.48E-11	2076	4.90E-12	2174	2.35E-11	2053	4.80E-12	2140
ksat_aq	high	3.48E-08	2053	3.43E-08	2056	2.34E-11	2084	2.69E-12	2184	1.18E-11	2060	2.56E-12	2149
	low	6.72E-08	2054	6.66E-08	2058	2.31E-11	2087	2.67E-12	2186	1.17E-11	2063	2.54E-12	2151
ksat_vz	high	7.42E-08	2043	7.29E-08	2046	3.51E-11	2074	3.77E-12	2173	1.89E-11	2051	3.72E-12	2138
	low	2.83E-08	2067	2.82E-08	2070	1.50E-11	2098	1.81E-12	2198	7.29E-12	2074	1.68E-12	2162

Table F.38. Predicted Peak U-238 (Kd = 0.02) Aqueous Concentration (Ci/L) and Arrival Time (yr) Summary for Case 2 (Diffusion)

Sub-Case		Groundwater		Fenceline		Excl (East)		Col River (East)		Excl (North)		Col River (North)	
		Conc.	Time	Conc.	Time	Conc.	Time	Conc.	Time	Conc.	Time	Conc.	Time
base		1.31E-10	12032	1.31E-10	12032	6.93E-14	12032	8.71E-15	12032	3.30E-14	12032	7.86E-15	12032
recharge	high	1.31E-10	12032	1.31E-10	12032	6.93E-14	12032	8.71E-15	12032	3.30E-14	12032	7.86E-15	12032
	low	1.31E-10	12032	1.31E-10	12032	6.93E-14	12032	8.71E-15	12032	3.30E-14	12032	7.86E-15	12032
barrier	high	1.30E-10	12032	1.30E-10	12032	6.87E-14	12032	8.65E-15	12032	3.27E-14	12032	7.80E-15	12032
	low	1.32E-10	12032	1.31E-10	12032	6.96E-14	12032	8.75E-15	12032	3.32E-14	12032	7.90E-15	12032
barrier_deg	high	2.82E-10	5788	2.82E-10	5791	1.50E-13	5818	1.91E-14	5914	7.13E-14	5796	1.72E-14	5881
	low	4.45E-12	12032	4.44E-12	12032	2.30E-15	12032	2.68E-16	12032	1.11E-15	12032	2.49E-16	12032
diffusion	high	4.14E-10	12032	4.13E-10	12032	2.19E-13	12032	2.75E-14	12032	1.04E-13	12032	2.49E-14	12032
	low	4.14E-13	12032	4.13E-13	12032	2.19E-16	12032	2.75E-17	12032	1.04E-16	12032	2.49E-17	12032
ksat_aq	high	9.81E-11	12032	9.81E-11	12032	6.93E-14	12032	8.71E-15	12032	3.30E-14	12032	7.86E-15	12032
	low	1.96E-10	12032	1.96E-10	12032	6.93E-14	12032	8.71E-15	12032	3.30E-14	12032	7.86E-15	12032
ksat_vz	high	1.57E-10	11820	1.57E-10	11824	8.34E-14	11850	1.06E-14	11947	3.96E-14	11828	9.54E-15	11913
	low	7.20E-11	12032	7.19E-11	12032	3.79E-14	12032	4.69E-15	12032	1.81E-14	12032	4.25E-15	12032

Table F.39. Predicted Peak U-238 (Kd = 0.02) Aqueous Concentration (Ci/L) and Arrival Time (yr) Summary for Case 3 (Retrieval Leak)

Sub-Case		Groundwater		Fenceline		Excl (East)		Col River (East)		Excl (North)		Col River (North)	
		Conc.	Time	Conc.	Time	Conc.	Time	Conc.	Time	Conc.	Time	Conc.	Time
base		8.07E-10	7683	8.07E-10	7687	4.29E-13	7713	5.47E-14	7809	2.04E-13	7690	4.91E-14	7775
recharge	high	9.13E-10	2102	9.13E-10	2105	4.88E-13	2132	6.18E-14	2231	2.32E-13	2109	5.58E-14	2196
	low	8.74E-10	9009	8.74E-10	9012	4.64E-13	9039	5.92E-14	9136	2.20E-13	9018	5.31E-14	9101
barrier	high	8.07E-10	7440	8.07E-10	7444	4.29E-13	7469	5.46E-14	7566	2.04E-13	7449	4.91E-14	7531
	low	8.07E-10	7880	8.07E-10	7883	4.29E-13	7910	5.47E-14	8005	2.04E-13	7888	4.91E-14	7973
barrier_deg	high	2.72E-09	4338	2.72E-09	4342	1.45E-12	4369	1.84E-13	4465	6.88E-13	4346	1.66E-13	4432
	low	4.06E-10	11623	4.06E-10	11623	2.16E-13	11650	2.75E-14	11745	1.03E-13	11629	2.47E-14	11716
ksat_aq	high	6.06E-10	7682	6.06E-10	7686	4.29E-13	7712	5.47E-14	7808	2.04E-13	7691	4.91E-14	7774
	low	1.21E-09	7683	1.21E-09	7688	4.29E-13	7714	5.47E-14	7810	2.04E-13	7693	4.91E-14	7776
ksat_vz	high	9.99E-10	6897	9.99E-10	6900	5.31E-13	6926	6.77E-14	7022	2.52E-13	6905	6.08E-14	6989
	low	6.12E-10	10175	6.12E-10	10179	3.25E-13	10204	4.14E-14	10301	1.54E-13	10186	3.72E-14	10269

Table F.40. Predicted Peak U-238 (Kd = 0.02) Aqueous Concentration (Ci/L) and Arrival Time (yr) Summary for Case 4 (Ancillary Equipment)

Sub-Case		Groundwater		Fenceline		Excl (East)		Col River (East)		Excl (North)		Col River (North)	
		Conc.	Time	Conc.	Time	Conc.	Time	Conc.	Time	Conc.	Time	Conc.	Time
base		8.40E-10	7839	8.40E-10	7842	4.47E-13	7869	5.69E-14	7964	2.12E-13	7847	5.11E-14	7930
recharge	high	7.92E-10	2130	7.92E-10	2133	4.23E-13	2159	5.37E-14	2257	2.01E-13	2137	4.84E-14	2223
	low	9.38E-10	9743	9.38E-10	9745	4.99E-13	9773	6.36E-14	9869	2.37E-13	9751	5.71E-14	9835
barrier	high	8.40E-10	7596	8.40E-10	7599	4.46E-13	7626	5.69E-14	7723	2.12E-13	7605	5.11E-14	7689
	low	8.40E-10	8035	8.40E-10	8039	4.47E-13	8065	5.69E-14	8161	2.12E-13	8044	5.11E-14	8127
barrier_deg	high	2.81E-09	4397	2.81E-09	4400	1.49E-12	4427	1.90E-13	4523	7.09E-13	4405	1.71E-13	4490
	low	4.23E-10	11921	4.23E-10	11925	2.25E-13	11954	2.87E-14	12032	1.07E-13	11929	2.57E-14	12016
ksat_aq	high	6.30E-10	7838	6.30E-10	7840	4.47E-13	7867	5.69E-14	7963	2.12E-13	7846	5.11E-14	7930
	low	1.26E-09	7841	1.26E-09	7845	4.47E-13	7870	5.69E-14	7967	2.12E-13	7849	5.11E-14	7933
ksat_vz	high	1.05E-09	6958	1.05E-09	6959	5.57E-13	6986	7.09E-14	7081	2.64E-13	6964	6.37E-14	7049
	low	6.08E-10	9233	6.08E-10	9235	3.23E-13	9261	4.12E-14	9358	1.53E-13	9240	3.70E-14	9326

Table F.41. Predicted Peak U-238 (Kd = 0.10) Aqueous Concentration (Ci/L) and Arrival Time (yr) Summary for Case 1 (Past Leak)

Sub-Case		Groundwater		Fenceline		Excl (East)		Col River (East)		Excl (North)		Col River (North)	
		Conc.	Time	Conc.	Time	Conc.	Time	Conc.	Time	Conc.	Time	Conc.	Time
base		3.40E-09	2090	3.40E-09	2095	2.29E-12	2138	2.87E-13	2290	1.18E-12	2102	2.65E-13	2236
recharge	high	1.21E-08	2058	1.20E-08	2064	7.73E-12	2108	9.00E-13	2261	4.18E-12	2071	8.66E-13	2207
	low	7.24E-10	7169	7.24E-10	7173	4.90E-13	7214	6.32E-14	7360	2.48E-13	7181	5.72E-14	7310
barrier	high	3.41E-09	2090	3.41E-09	2095	2.30E-12	2138	2.87E-13	2291	1.18E-12	2102	2.65E-13	2236
	low	3.40E-09	2090	3.40E-09	2095	2.29E-12	2138	2.86E-13	2290	1.17E-12	2102	2.64E-13	2236
barrier_deg	high	3.40E-09	2090	3.40E-09	2095	2.29E-12	2138	2.87E-13	2290	1.18E-12	2102	2.65E-13	2236
	low	3.40E-09	2090	3.40E-09	2095	2.29E-12	2138	2.87E-13	2290	1.18E-12	2102	2.65E-13	2236
plume	high	8.57E-10	2131	8.57E-10	2136	5.81E-13	2177	7.43E-14	2328	2.95E-13	2142	6.77E-14	2274
	low	1.47E-08	2063	1.46E-08	2069	9.47E-12	2113	1.12E-12	2265	5.07E-12	2075	1.07E-12	2211
ksat_aq	high	2.56E-09	2089	2.56E-09	2093	2.30E-12	2136	2.87E-13	2289	1.18E-12	2100	2.65E-13	2234
	low	5.05E-09	2091	5.05E-09	2099	2.28E-12	2141	2.85E-13	2294	1.17E-12	2105	2.64E-13	2239
ksat_vz	high	2.81E-09	2064	2.79E-09	2069	1.82E-12	2114	2.18E-13	2267	9.65E-13	2076	2.07E-13	2212
	low	3.78E-09	2117	3.78E-09	2122	2.57E-12	2163	3.26E-13	2314	1.31E-12	2128	2.98E-13	2261

Table F.42. Predicted Peak U-238 (Kd = 0.10) Aqueous Concentration (Ci/L) and Arrival Time (yr) Summary for Case 2 (Diffusion)

Sub-Case		Groundwater		Fenceline		Excl (East)		Col River (East)		Excl (North)		Col River (North)	
		Conc.	Time	Conc.	Time	Conc.	Time	Conc.	Time	Conc.	Time	Conc.	Time
base		1.11E-12	12032	1.10E-12	12032	7.10E-16	12032	7.60E-17	12032	3.74E-16	12032	7.35E-17	12032
recharge	high	1.11E-12	12032	1.10E-12	12032	7.11E-16	12032	7.61E-17	12032	3.74E-16	12032	7.36E-17	12032
	low	1.10E-12	12032	1.10E-12	12032	7.06E-16	12032	7.56E-17	12032	3.72E-16	12032	7.31E-17	12032
barrier	high	1.28E-12	12032	1.28E-12	12032	8.24E-16	12032	8.89E-17	12032	4.33E-16	12032	8.57E-17	12032
	low	9.80E-13	12032	9.73E-13	12032	6.26E-16	12032	6.65E-17	12032	3.30E-16	12032	6.45E-17	12032
barrier_deg	high	1.92E-10	9038	1.92E-10	9043	1.30E-13	9084	1.67E-14	9230	6.57E-14	9049	1.52E-14	9178
	low	4.42E-17	12032	2.74E-17	12032	1.48E-20	12032	4.05E-22	12032	9.18E-21	12032	1.01E-21	12032
diffusion	high	3.51E-12	12032	3.48E-12	12032	2.24E-15	12032	2.40E-16	12032	1.18E-15	12032	2.32E-16	12032
	low	3.50E-15	12032	3.47E-15	12032	2.24E-18	12032	2.40E-19	12032	1.18E-18	12032	2.32E-19	12032
ksat_aq	high	8.32E-13	12032	8.28E-13	12032	7.11E-16	12032	7.61E-17	12032	3.74E-16	12032	7.36E-17	12032
	low	1.66E-12	12032	1.64E-12	12032	7.07E-16	12032	7.56E-17	12032	3.72E-16	12032	7.31E-17	12032
ksat_vz	high	1.52E-12	12032	1.51E-12	12032	9.75E-16	12032	1.04E-16	12032	5.14E-16	12032	1.01E-16	12032
	low	7.84E-13	12032	7.79E-13	12032	5.04E-16	12032	5.48E-17	12032	2.64E-16	12032	5.27E-17	12032

Table F.43. Predicted Peak U-238 (Kd = 0.10) Aqueous Concentration (Ci/L) and Arrival Time (yr) Summary for Case 3 (Retrieval Leak)

Sub-Case		Groundwater		Fenceline		Excl (East)		Col River (East)		Excl (North)		Col River (North)	
		Conc.	Time	Conc.	Time	Conc.	Time	Conc.	Time	Conc.	Time	Conc.	Time
base		2.89E-10	12032	2.89E-10	12032	1.94E-13	12032	2.40E-14	12032	9.87E-14	12032	2.20E-14	12032
recharge	high	3.50E-10	12032	3.50E-10	12032	2.35E-13	12032	2.95E-14	12032	1.20E-13	12032	2.70E-14	12032
	low	1.75E-10	12032	1.75E-10	12032	1.17E-13	12032	1.41E-14	12032	5.97E-14	12032	1.31E-14	12032
barrier	high	3.07E-10	12032	3.07E-10	12032	2.06E-13	12032	2.56E-14	12032	1.05E-13	12032	2.35E-14	12032
	low	2.75E-10	12032	2.74E-10	12032	1.84E-13	12032	2.27E-14	12032	9.37E-14	12032	2.09E-14	12032
barrier_deg	high	1.60E-09	6885	1.60E-09	6890	1.09E-12	6931	1.40E-13	7077	5.49E-13	6897	1.27E-13	7026
	low	2.51E-11	12032	2.50E-11	12032	1.67E-14	12032	2.05E-15	12032	8.54E-15	12032	1.89E-15	12032
ksat_aq	high	2.17E-10	12032	2.17E-10	12032	1.94E-13	12032	2.40E-14	12032	9.88E-14	12032	2.21E-14	12032
	low	4.34E-10	12032	4.33E-10	12032	1.94E-13	12032	2.40E-14	12032	9.86E-14	12032	2.20E-14	12032
ksat_vz	high	3.52E-10	12032	3.52E-10	12032	2.36E-13	12032	2.92E-14	12032	1.20E-13	12032	2.68E-14	12032
	low	1.43E-10	12032	1.43E-10	12032	9.57E-14	12032	1.17E-14	12032	4.89E-14	12032	1.08E-14	12032

Table F.44. Predicted Peak U-238 (Kd = 0.10) Aqueous Concentration (Ci/L) and Arrival Time (yr) Summary for Case 4 (Ancillary Equipment)

Sub-Case		Groundwater		Fenceline		Excl (East)		Col River (East)		Excl (North)		Col River (North)	
		Conc.	Time	Conc.	Time	Conc.	Time	Conc.	Time	Conc.	Time	Conc.	Time
base		2.53E-10	12032	2.53E-10	12032	1.69E-13	12032	2.08E-14	12032	8.62E-14	12032	1.91E-14	12032
recharge	high	3.50E-10	12032	3.50E-10	12032	2.35E-13	12032	2.95E-14	12032	1.20E-13	12032	2.70E-14	12032
	low	8.44E-11	12032	8.42E-11	12032	5.55E-14	12032	6.48E-15	12032	2.87E-14	12032	6.08E-15	12032
barrier	high	2.72E-10	12032	2.71E-10	12032	1.82E-13	12032	2.24E-14	12032	9.27E-14	12032	2.06E-14	12032
	low	2.38E-10	12032	2.37E-10	12032	1.59E-13	12032	1.94E-14	12032	8.10E-14	12032	1.79E-14	12032
barrier_deg	high	1.61E-09	7045	1.61E-09	7050	1.09E-12	7089	1.41E-13	7236	5.53E-13	7056	1.28E-13	7186
	low	1.45E-11	12032	1.45E-11	12032	9.66E-15	12032	1.17E-15	12032	4.95E-15	12032	1.08E-15	12032
ksat_aq	high	1.90E-10	12032	1.90E-10	12032	1.69E-13	12032	2.08E-14	12032	8.63E-14	12032	1.91E-14	12032
	low	3.79E-10	12032	3.78E-10	12032	1.69E-13	12032	2.07E-14	12032	8.61E-14	12032	1.91E-14	12032
ksat_vz	high	2.98E-10	12032	2.97E-10	12032	1.99E-13	12032	2.43E-14	12032	1.01E-13	12032	2.24E-14	12032
	low	1.91E-10	12032	1.90E-10	12032	1.28E-13	12032	1.58E-14	12032	6.51E-14	12032	1.45E-14	12032

Table F.45. Predicted Peak U-238 (Kd = 0.20) Aqueous Concentration (Ci/L) and Arrival Time (yr) Summary for Case 1 (Past Leak)

Sub-Case		Groundwater		Fenceline		Excl (East)		Col River (East)		Excl (North)		Col River (North)	
		Conc.	Time	Conc.	Time	Conc.	Time	Conc.	Time	Conc.	Time	Conc.	Time
base		4.54E-10	9613	4.54E-10	9621	3.75E-13	9676	4.86E-14	9887	1.98E-13	9630	4.43E-14	9810
recharge	high	7.51E-10	2094	7.51E-10	2101	6.13E-13	2164	7.64E-14	2383	3.30E-13	2111	7.15E-14	2304
	low	4.63E-10	12032	4.63E-10	12032	3.82E-13	12032	4.93E-14	12032	2.02E-13	12032	4.51E-14	12032
barrier	high	4.55E-10	9369	4.55E-10	9376	3.75E-13	9431	4.86E-14	9637	1.98E-13	9385	4.44E-14	9567
	low	4.54E-10	9811	4.54E-10	9819	3.75E-13	9876	4.85E-14	10085	1.98E-13	9828	4.43E-14	10010
barrier_deg	high	1.56E-09	5001	1.56E-09	5007	1.29E-12	5064	1.67E-13	5274	6.82E-13	5017	1.53E-13	5201
	low	2.19E-10	12032	2.19E-10	12032	1.80E-13	12032	2.31E-14	12032	9.52E-14	12032	2.12E-14	12032
plume	high	4.16E-10	12032	4.16E-10	12032	3.43E-13	12032	4.42E-14	12032	1.81E-13	12032	4.04E-14	12032
	low	1.33E-09	2101	1.33E-09	2109	1.09E-12	2171	1.36E-13	2389	5.84E-13	2118	1.27E-13	2311
ksat_aq	high	3.41E-10	9613	3.41E-10	9616	3.75E-13	9673	4.86E-14	9884	1.98E-13	9628	4.43E-14	9809
	low	6.81E-10	9616	6.81E-10	9624	3.75E-13	9680	4.86E-14	9894	1.98E-13	9635	4.43E-14	9820
ksat_vz	high	4.92E-10	10139	4.92E-10	10145	4.06E-13	10204	5.26E-14	10410	2.15E-13	10156	4.80E-14	10340
	low	3.89E-10	8786	3.89E-10	8795	3.21E-13	8852	4.16E-14	9061	1.70E-13	8805	3.79E-14	8985

Table F.46. Predicted Peak U-238 (Kd = 0.20) Aqueous Concentration (Ci/L) and Arrival Time (yr) Summary for Case 2 (Diffusion)

Sub-Case		Groundwater		Fenceline		Excl (East)		Col River (East)		Excl (North)		Col River (North)	
		Conc.	Time	Conc.	Time	Conc.	Time	Conc.	Time	Conc.	Time	Conc.	Time
base		2.38E-16	12032	2.27E-16	12032	1.63E-19	12032	1.24E-20	12032	9.65E-20	12032	1.36E-20	12032
recharge	high	2.39E-16	12032	2.28E-16	12032	1.64E-19	12032	1.25E-20	12032	9.71E-20	12032	1.37E-20	12032
	low	2.35E-16	12032	2.23E-16	12032	1.60E-19	12032	1.22E-20	12032	9.51E-20	12032	1.33E-20	12032
barrier	high	3.33E-16	12032	3.22E-16	12032	2.34E-19	12032	1.85E-20	12032	1.37E-19	12032	2.03E-20	12032
	low	1.81E-16	12032	1.66E-16	12032	1.19E-19	12032	8.85E-21	12032	7.09E-20	12032	9.81E-21	12032
barrier_deg	high	1.39E-10	12032	1.38E-10	12032	1.13E-13	12032	1.42E-14	12032	6.03E-14	12032	1.31E-14	12032
	low	0.00E+00	12032	0.00E+00	12032	0.00E+00	12032	0.00E+00	12032	0.00E+00	12032	0.00E+00	12032
diffusion	high	7.56E-16	12032	7.38E-16	12032	5.36E-19	12032	4.30E-20	12032	3.15E-19	12032	4.64E-20	12032
	low	0.00E+00	12032	0.00E+00	12032	0.00E+00	12032	0.00E+00	12032	0.00E+00	12032	0.00E+00	12032
ksat_aq	high	1.79E-16	12032	1.69E-16	12032	1.61E-19	12032	1.23E-20	12032	9.57E-20	12032	1.36E-20	12032
	low	3.56E-16	12032	3.38E-16	12032	1.63E-19	12032	1.24E-20	12032	9.61E-20	12032	1.36E-20	12032
ksat_vz	high	1.41E-16	12032	1.20E-16	12032	8.30E-20	12032	5.58E-21	12032	5.08E-20	12032	6.48E-21	12032
	low	7.31E-16	12032	7.14E-16	12032	5.28E-19	12032	4.51E-20	12032	3.06E-19	12032	4.76E-20	12032

Table F.47. Predicted Peak U-238 (Kd = 0.20) Aqueous Concentration (Ci/L) and Arrival Time (yr) Summary for Case 3 (Retrieval Leak)

Sub-Case		Groundwater		Fenceline		Excl (East)		Col River (East)		Excl (North)		Col River (North)	
		Conc.	Time	Conc.	Time	Conc.	Time	Conc.	Time	Conc.	Time	Conc.	Time
base		6.54E-12	12032	6.50E-12	12032	5.16E-15	12032	5.79E-16	12032	2.82E-15	12032	5.55E-16	12032
recharge	high	1.29E-11	12032	1.29E-11	12032	1.03E-14	12032	1.18E-15	12032	5.58E-15	12032	1.12E-15	12032
	low	1.70E-12	12032	1.69E-12	12032	1.32E-15	12032	1.43E-16	12032	7.30E-16	12032	1.39E-16	12032
barrier	high	7.68E-12	12032	7.64E-12	12032	6.07E-15	12032	6.84E-16	12032	3.31E-15	12032	6.55E-16	12032
	low	5.72E-12	12032	5.69E-12	12032	4.51E-15	12032	5.04E-16	12032	2.46E-15	12032	4.84E-16	12032
barrier_deg	high	1.04E-09	10150	1.04E-09	10157	8.59E-13	10214	1.11E-13	10423	4.54E-13	10166	1.02E-13	10351
	low	1.16E-13	12032	1.16E-13	12032	9.27E-17	12032	1.07E-17	12032	5.03E-17	12032	1.02E-17	12032
ksat_aq	high	4.91E-12	12032	4.89E-12	12032	5.17E-15	12032	5.80E-16	12032	2.82E-15	12032	5.56E-16	12032
	low	9.80E-12	12032	9.72E-12	12032	5.14E-15	12032	5.77E-16	12032	2.81E-15	12032	5.53E-16	12032
ksat_vz	high	5.87E-12	12032	5.84E-12	12032	4.62E-15	12032	5.11E-16	12032	2.53E-15	12032	4.93E-16	12032
	low	3.58E-12	12032	3.56E-12	12032	2.82E-15	12032	3.15E-16	12032	1.54E-15	12032	3.03E-16	12032

Table F.48. Predicted Peak U-238 (Kd = 0.20) Aqueous Concentration (Ci/L) and Arrival Time (yr) Summary for Case 4 (Ancillary Equipment)

Sub-Case		Groundwater		Fenceline		Excl (East)		Col River (East)		Excl (North)		Col River (North)	
		Conc.	Time	Conc.	Time	Conc.	Time	Conc.	Time	Conc.	Time	Conc.	Time
base		3.13E-12	12032	3.11E-12	12032	2.45E-15	12032	2.65E-16	12032	1.35E-15	12032	2.58E-16	12032
recharge	high	1.07E-11	12032	1.06E-11	12032	8.47E-15	12032	9.59E-16	12032	4.61E-15	12032	9.17E-16	12032
	low	1.47E-13	12032	1.46E-13	12032	1.11E-16	12032	1.07E-17	12032	6.26E-17	12032	1.08E-17	12032
barrier	high	3.81E-12	12032	3.79E-12	12032	2.98E-15	12032	3.25E-16	12032	1.64E-15	12032	3.15E-16	12032
	low	2.66E-12	12032	2.64E-12	12032	2.07E-15	12032	2.24E-16	12032	1.14E-15	12032	2.18E-16	12032
barrier_deg	high	1.04E-09	10399	1.04E-09	10405	8.57E-13	10463	1.11E-13	10673	4.53E-13	10416	1.01E-13	10600
	low	1.98E-14	12032	1.96E-14	12032	1.55E-17	12032	1.71E-18	12032	8.50E-18	12032	1.65E-18	12032
ksat_aq	high	2.35E-12	12032	2.34E-12	12032	2.45E-15	12032	2.66E-16	12032	1.35E-15	12032	2.58E-16	12032
	low	4.69E-12	12032	4.65E-12	12032	2.44E-15	12032	2.64E-16	12032	1.34E-15	12032	2.57E-16	12032
ksat_vz	high	1.66E-12	12032	1.64E-12	12032	1.28E-15	12032	1.34E-16	12032	7.10E-16	12032	1.32E-16	12032
	low	5.95E-12	12032	5.92E-12	12032	4.71E-15	12032	5.31E-16	12032	2.56E-15	12032	5.09E-16	12032

Table F.49. Predicted Peak U-238 (Kd = 0.60) Aqueous Concentration (Ci/L) and Arrival Time (yr) Summary for Case 1 (Past Leak)

Sub-Case		Groundwater		Fenceline		Excl (East)		Col River (East)		Excl (North)		Col River (North)	
		Conc.	Time	Conc.	Time	Conc.	Time	Conc.	Time	Conc.	Time	Conc.	Time
base		1.58E-11	12032	1.57E-11	12032	1.87E-14	12032	1.99E-15	12032	1.11E-14	12032	1.97E-15	12032
recharge	high	2.84E-11	12032	2.82E-11	12032	3.40E-14	12032	3.80E-15	12032	2.00E-14	12032	3.70E-15	12032
	low	3.71E-12	12032	3.67E-12	12032	4.24E-15	12032	4.04E-16	12032	2.58E-15	12032	4.17E-16	12032
barrier	high	1.74E-11	12032	1.72E-11	12032	2.06E-14	12032	2.22E-15	12032	1.22E-14	12032	2.19E-15	12032
	low	1.46E-11	12032	1.44E-11	12032	1.72E-14	12032	1.83E-15	12032	1.02E-14	12032	1.81E-15	12032
barrier_deg	high	6.52E-10	11107	6.52E-10	11126	8.20E-13	11250	1.07E-13	11709	4.65E-13	11146	9.88E-14	11550
	low	1.14E-12	12032	1.14E-12	12032	1.36E-15	12032	1.49E-16	12032	8.02E-16	12032	1.46E-16	12032
plume	high	2.10E-12	12032	2.07E-12	12032	2.41E-15	12032	2.36E-16	12032	1.46E-15	12032	2.41E-16	12032
	low	9.01E-11	12032	8.97E-11	12032	1.10E-13	12032	1.29E-14	12032	6.36E-14	12032	1.23E-14	12032
ksat_aq	high	1.18E-11	12032	1.18E-11	12032	1.87E-14	12032	2.00E-15	12032	1.11E-14	12032	1.98E-15	12032
	low	2.36E-11	12032	2.34E-11	12032	1.86E-14	12032	1.98E-15	12032	1.10E-14	12032	1.96E-15	12032
ksat_vz	high	9.65E-12	12032	9.57E-12	12032	1.13E-14	12032	1.16E-15	12032	6.74E-15	12032	1.16E-15	12032
	low	2.89E-11	12032	2.87E-11	12032	3.47E-14	12032	3.91E-15	12032	2.03E-14	12032	3.80E-15	12032

Table F.50. Predicted Peak U-238 (Kd = 0.60) Aqueous Concentration (Ci/L) and Arrival Time (yr) Summary for Case 2 (Diffusion)

Sub-Case		Groundwater		Fenceline		Excl (East)		Col River (East)		Excl (North)		Col River (North)	
		Conc.	Time	Conc.	Time	Conc.	Time	Conc.	Time	Conc.	Time	Conc.	Time
base		0.00E+00	12032	0.00E+00	12032	0.00E+00	12032	0.00E+00	12032	0.00E+00	12032	0.00E+00	12032
recharge	high	0.00E+00	12032	0.00E+00	12032	0.00E+00	12032	0.00E+00	12032	0.00E+00	12032	0.00E+00	12032
	low	0.00E+00	12032	0.00E+00	12032	0.00E+00	12032	0.00E+00	12032	0.00E+00	12032	0.00E+00	12032
barrier	high	0.00E+00	12032	0.00E+00	12032	0.00E+00	12032	0.00E+00	12032	0.00E+00	12032	0.00E+00	12032
	low	0.00E+00	12032	0.00E+00	12032	0.00E+00	12032	0.00E+00	12032	0.00E+00	12032	0.00E+00	12032
barrier_deg	high	1.98E-14	12032	1.91E-14	12032	1.90E-17	12032	9.88E-19	12032	1.31E-17	12032	1.26E-18	12032
	low	0.00E+00	12032	0.00E+00	12032	0.00E+00	12032	0.00E+00	12032	0.00E+00	12032	0.00E+00	12032
diffusion	high	0.00E+00	12032	0.00E+00	12032	0.00E+00	12032	0.00E+00	12032	0.00E+00	12032	0.00E+00	12032
	low	0.00E+00	12032	0.00E+00	12032	0.00E+00	12032	0.00E+00	12032	0.00E+00	12032	0.00E+00	12032
ksat_aq	high	0.00E+00	12032	0.00E+00	12032	0.00E+00	12032	0.00E+00	12032	0.00E+00	12032	0.00E+00	12032
	low	0.00E+00	12032	0.00E+00	12032	0.00E+00	12032	0.00E+00	12032	0.00E+00	12032	0.00E+00	12032
ksat_vz	high	0.00E+00	12032	0.00E+00	12032	0.00E+00	12032	0.00E+00	12032	0.00E+00	12032	0.00E+00	12032
	low	0.00E+00	12032	0.00E+00	12032	0.00E+00	12032	0.00E+00	12032	0.00E+00	12032	0.00E+00	12032

Table F.51. Predicted Peak U-238 (Kd = 0.60) Aqueous Concentration (Ci/L) and Arrival Time (yr) Summary for Case 3 (Retrieval Leak)

Sub-Case		Groundwater		Fenceline		Excl (East)		Col River (East)		Excl (North)		Col River (North)	
		Conc.	Time	Conc.	Time	Conc.	Time	Conc.	Time	Conc.	Time	Conc.	Time
base		0.00E+00	12032	0.00E+00	12032	0.00E+00	12032	0.00E+00	12032	0.00E+00	12032	0.00E+00	12032
recharge	high	0.00E+00	12032	0.00E+00	12032	0.00E+00	12032	0.00E+00	12032	0.00E+00	12032	0.00E+00	12032
	low	0.00E+00	12032	0.00E+00	12032	0.00E+00	12032	0.00E+00	12032	0.00E+00	12032	0.00E+00	12032
barrier	high	0.00E+00	12032	0.00E+00	12032	0.00E+00	12032	0.00E+00	12032	0.00E+00	12032	0.00E+00	12032
	low	0.00E+00	12032	0.00E+00	12032	0.00E+00	12032	0.00E+00	12032	0.00E+00	12032	0.00E+00	12032
barrier_deg	high	4.03E-12	12032	3.95E-12	12032	4.26E-15	12032	3.08E-16	12032	2.74E-15	12032	3.51E-16	12032
	low	0.00E+00	12032	0.00E+00	12032	0.00E+00	12032	0.00E+00	12032	0.00E+00	12032	0.00E+00	12032
ksat_aq	high	0.00E+00	12032	0.00E+00	12032	0.00E+00	12032	0.00E+00	12032	0.00E+00	12032	0.00E+00	12032
	low	0.00E+00	12032	0.00E+00	12032	0.00E+00	12032	0.00E+00	12032	0.00E+00	12032	0.00E+00	12032
ksat_vz	high	0.00E+00	12032	0.00E+00	12032	0.00E+00	12032	0.00E+00	12032	0.00E+00	12032	0.00E+00	12032
	low	0.00E+00	12032	0.00E+00	12032	0.00E+00	12032	0.00E+00	12032	0.00E+00	12032	0.00E+00	12032

Table F.52. Predicted Peak U-238 (Kd = 0.60) Aqueous Concentration (Ci/L) and Arrival Time (yr) Summary for Case 4 (Ancillary Equipment)

Sub-Case		Groundwater		Fenceline		Excl (East)		Col River (East)		Excl (North)		Col River (North)	
		Conc.	Time	Conc.	Time	Conc.	Time	Conc.	Time	Conc.	Time	Conc.	Time
base		0.00E+00	12032	0.00E+00	12032	0.00E+00	12032	0.00E+00	12032	0.00E+00	12032	0.00E+00	12032
recharge	high	0.00E+00	12032	0.00E+00	12032	0.00E+00	12032	0.00E+00	12032	0.00E+00	12032	0.00E+00	12032
	low	0.00E+00	12032	0.00E+00	12032	0.00E+00	12032	0.00E+00	12032	0.00E+00	12032	0.00E+00	12032
barrier	high	0.00E+00	12032	0.00E+00	12032	0.00E+00	12032	0.00E+00	12032	0.00E+00	12032	0.00E+00	12032
	low	0.00E+00	12032	0.00E+00	12032	0.00E+00	12032	0.00E+00	12032	0.00E+00	12032	0.00E+00	12032
barrier_deg	high	2.27E-12	12032	2.22E-12	12032	2.36E-15	12032	1.61E-16	12032	1.54E-15	12032	1.87E-16	12032
	low	0.00E+00	12032	0.00E+00	12032	0.00E+00	12032	0.00E+00	12032	0.00E+00	12032	0.00E+00	12032
ksat_aq	high	0.00E+00	12032	0.00E+00	12032	0.00E+00	12032	0.00E+00	12032	0.00E+00	12032	0.00E+00	12032
	low	0.00E+00	12032	0.00E+00	12032	0.00E+00	12032	0.00E+00	12032	0.00E+00	12032	0.00E+00	12032
ksat_vz	high	0.00E+00	12032	0.00E+00	12032	0.00E+00	12032	0.00E+00	12032	0.00E+00	12032	0.00E+00	12032
	low	0.00E+00	12032	0.00E+00	12032	0.00E+00	12032	0.00E+00	12032	0.00E+00	12032	0.00E+00	12032

Table F.53. Predicted Peak U-238 (Kd = 1.00) Aqueous Concentration (Ci/L) and Arrival Time (yr) Summary for Case 1 (Past Leak)

Sub-Case		Groundwater		Fenceline		Excl (East)		Col River (East)		Excl (North)		Col River (North)	
		Conc.	Time	Conc.	Time	Conc.	Time	Conc.	Time	Conc.	Time	Conc.	Time
base		1.26E-13	12032	1.23E-13	12032	1.69E-16	12032	1.30E-17	12032	1.10E-16	12032	1.45E-17	12032
recharge	high	3.62E-13	12032	3.57E-13	12032	5.00E-16	12032	4.23E-17	12032	3.20E-16	12032	4.57E-17	12032
	low	1.10E-14	12032	1.07E-14	12032	1.38E-17	12032	8.27E-19	12032	9.48E-18	12032	1.01E-18	12032
barrier	high	1.48E-13	12032	1.45E-13	12032	1.99E-16	12032	1.55E-17	12032	1.30E-16	12032	1.73E-17	12032
	low	1.10E-13	12032	1.08E-13	12032	1.47E-16	12032	1.12E-17	12032	9.63E-17	12032	1.26E-17	12032
barrier_deg	high	2.02E-10	12032	2.01E-10	12032	2.96E-13	12032	2.93E-14	12032	1.82E-13	12032	3.00E-14	12032
	low	3.20E-15	12032	3.15E-15	12032	4.43E-18	12032	3.81E-19	12032	2.82E-18	12032	4.09E-19	12032
plume	high	3.38E-15	12032	3.29E-15	12032	4.31E-18	12032	2.79E-19	12032	2.91E-18	12032	3.31E-19	12032
	low	4.04E-12	12032	3.99E-12	12032	5.74E-15	12032	5.33E-16	12032	3.60E-15	12032	5.57E-16	12032
ksat_aq	high	9.43E-14	12032	9.30E-14	12032	1.70E-16	12032	1.31E-17	12032	1.11E-16	12032	1.46E-17	12032
	low	1.88E-13	12032	1.83E-13	12032	1.67E-16	12032	1.28E-17	12032	1.09E-16	12032	1.43E-17	12032
ksat_vz	high	4.53E-14	12032	4.43E-14	12032	5.94E-17	12032	4.19E-18	12032	3.94E-17	12032	4.83E-18	12032
	low	5.40E-13	12032	5.31E-13	12032	7.49E-16	12032	6.42E-17	12032	4.77E-16	12032	6.90E-17	12032

Table F.54. Predicted Peak U-238 (Kd = 1.00) Aqueous Concentration (Ci/L) and Arrival Time (yr) Summary for Case 2 (Diffusion)

Sub-Case		Groundwater		Fenceline		Excl (East)		Col River (East)		Excl (North)		Col River (North)	
		Conc.	Time	Conc.	Time	Conc.	Time	Conc.	Time	Conc.	Time	Conc.	Time
base		0.00E+00	12032	0.00E+00	12032	0.00E+00	12032	0.00E+00	12032	0.00E+00	12032	0.00E+00	12032
recharge	high	0.00E+00	12032	0.00E+00	12032	0.00E+00	12032	0.00E+00	12032	0.00E+00	12032	0.00E+00	12032
	low	0.00E+00	12032	0.00E+00	12032	0.00E+00	12032	0.00E+00	12032	0.00E+00	12032	0.00E+00	12032
barrier	high	0.00E+00	12032	0.00E+00	12032	0.00E+00	12032	0.00E+00	12032	0.00E+00	12032	0.00E+00	12032
	low	0.00E+00	12032	0.00E+00	12032	0.00E+00	12032	0.00E+00	12032	0.00E+00	12032	0.00E+00	12032
barrier_deg	high	0.00E+00	12032	0.00E+00	12032	0.00E+00	12032	0.00E+00	12032	0.00E+00	12032	0.00E+00	12032
	low	0.00E+00	12032	0.00E+00	12032	0.00E+00	12032	0.00E+00	12032	0.00E+00	12032	0.00E+00	12032
diffusion	high	0.00E+00	12032	0.00E+00	12032	0.00E+00	12032	0.00E+00	12032	0.00E+00	12032	0.00E+00	12032
	low	0.00E+00	12032	0.00E+00	12032	0.00E+00	12032	0.00E+00	12032	0.00E+00	12032	0.00E+00	12032
ksat_aq	high	0.00E+00	12032	0.00E+00	12032	0.00E+00	12032	0.00E+00	12032	0.00E+00	12032	0.00E+00	12032
	low	0.00E+00	12032	0.00E+00	12032	0.00E+00	12032	0.00E+00	12032	0.00E+00	12032	0.00E+00	12032
ksat_vz	high	0.00E+00	12032	0.00E+00	12032	0.00E+00	12032	0.00E+00	12032	0.00E+00	12032	0.00E+00	12032
	low	0.00E+00	12032	0.00E+00	12032	0.00E+00	12032	0.00E+00	12032	0.00E+00	12032	0.00E+00	12032

Table F.55. Predicted Peak U-238 (Kd = 1.00) Aqueous Concentration (Ci/L) and Arrival Time (yr) Summary for Case 3 (Retrieval Leak)

Sub-Case		Groundwater		Fenceline		Excl (East)		Col River (East)		Excl (North)		Col River (North)	
		Conc.	Time	Conc.	Time	Conc.	Time	Conc.	Time	Conc.	Time	Conc.	Time
base		0.00E+00	12032	0.00E+00	12032	0.00E+00	12032	0.00E+00	12032	0.00E+00	12032	0.00E+00	12032
recharge	high	0.00E+00	12032	0.00E+00	12032	0.00E+00	12032	0.00E+00	12032	0.00E+00	12032	0.00E+00	12032
	low	0.00E+00	12032	0.00E+00	12032	0.00E+00	12032	0.00E+00	12032	0.00E+00	12032	0.00E+00	12032
barrier	high	0.00E+00	12032	0.00E+00	12032	0.00E+00	12032	0.00E+00	12032	0.00E+00	12032	0.00E+00	12032
	low	0.00E+00	12032	0.00E+00	12032	0.00E+00	12032	0.00E+00	12032	0.00E+00	12032	0.00E+00	12032
barrier_deg	high	5.07E-16	12032	4.75E-16	12032	4.99E-19	12032	1.19E-20	12032	4.06E-19	12032	2.06E-20	12032
	low	0.00E+00	12032	0.00E+00	12032	0.00E+00	12032	0.00E+00	12032	0.00E+00	12032	0.00E+00	12032
ksat_aq	high	0.00E+00	12032	0.00E+00	12032	0.00E+00	12032	0.00E+00	12032	0.00E+00	12032	0.00E+00	12032
	low	0.00E+00	12032	0.00E+00	12032	0.00E+00	12032	0.00E+00	12032	0.00E+00	12032	0.00E+00	12032
ksat_vz	high	0.00E+00	12032	0.00E+00	12032	0.00E+00	12032	0.00E+00	12032	0.00E+00	12032	0.00E+00	12032
	low	0.00E+00	12032	0.00E+00	12032	0.00E+00	12032	0.00E+00	12032	0.00E+00	12032	0.00E+00	12032

Table F.56. Predicted Peak U-238 (Kd = 1.00) Aqueous Concentration (Ci/L) and Arrival Time (yr) Summary for Case 4 (Ancillary Equipment)

Sub-Case		Groundwater		Fenceline		Excl (East)		Col River (East)		Excl (North)		Col River (North)	
		Conc.	Time	Conc.	Time	Conc.	Time	Conc.	Time	Conc.	Time	Conc.	Time
base		0.00E+00	12032	0.00E+00	12032	0.00E+00	12032	0.00E+00	12032	0.00E+00	12032	0.00E+00	12032
recharge	high	0.00E+00	12032	0.00E+00	12032	0.00E+00	12032	0.00E+00	12032	0.00E+00	12032	0.00E+00	12032
	low	0.00E+00	12032	0.00E+00	12032	0.00E+00	12032	0.00E+00	12032	0.00E+00	12032	0.00E+00	12032
barrier	high	0.00E+00	12032	0.00E+00	12032	0.00E+00	12032	0.00E+00	12032	0.00E+00	12032	0.00E+00	12032
	low	0.00E+00	12032	0.00E+00	12032	0.00E+00	12032	0.00E+00	12032	0.00E+00	12032	0.00E+00	12032
barrier_deg	high	1.51E-16	12032	1.34E-16	12032	1.32E-19	12032	1.53E-21	12032	1.14E-19	12032	4.20E-21	12032
	low	0.00E+00	12032	0.00E+00	12032	0.00E+00	12032	0.00E+00	12032	0.00E+00	12032	0.00E+00	12032
ksat_aq	high	0.00E+00	12032	0.00E+00	12032	0.00E+00	12032	0.00E+00	12032	0.00E+00	12032	0.00E+00	12032
	low	0.00E+00	12032	0.00E+00	12032	0.00E+00	12032	0.00E+00	12032	0.00E+00	12032	0.00E+00	12032
ksat_vz	high	0.00E+00	12032	0.00E+00	12032	0.00E+00	12032	0.00E+00	12032	0.00E+00	12032	0.00E+00	12032
	low	0.00E+00	12032	0.00E+00	12032	0.00E+00	12032	0.00E+00	12032	0.00E+00	12032	0.00E+00	12032

Table F.57. Predicted Peak U-238 (Kd = 2.00) Aqueous Concentration (Ci/L) and Arrival Time (yr) Summary for Case 1 (Past Leak)

Sub-Case		Groundwater		Fenceline		Excl (East)		Col River (East)		Excl (North)		Col River (North)	
		Conc.	Time	Conc.	Time	Conc.	Time	Conc.	Time	Conc.	Time	Conc.	Time
base		2.30E-18	12032	0.00E+00	12032	0.00E+00	12032	0.00E+00	12032	0.00E+00	12032	0.00E+00	12032
recharge	high	1.46E-17	12032	8.11E-18	12032	6.03E-21	12032	0.00E+00	12032	8.14E-21	12032	0.00E+00	12032
	low	0.00E+00	12032	0.00E+00	12032	0.00E+00	12032	0.00E+00	12032	0.00E+00	12032	0.00E+00	12032
barrier	high	3.00E-18	12032	0.00E+00	12032	0.00E+00	12032	0.00E+00	12032	0.00E+00	12032	0.00E+00	12032
	low	1.83E-18	12032	0.00E+00	12032	0.00E+00	12032	0.00E+00	12032	0.00E+00	12032	0.00E+00	12032
barrier_deg	high	8.93E-13	12032	8.50E-13	12032	1.29E-15	12032	3.58E-17	12032	1.03E-15	12032	5.91E-17	12032
	low	0.00E+00	12032	0.00E+00	12032	0.00E+00	12032	0.00E+00	12032	0.00E+00	12032	0.00E+00	12032
plume	high	0.00E+00	12032	0.00E+00	12032	0.00E+00	12032	0.00E+00	12032	0.00E+00	12032	0.00E+00	12032
	low	1.87E-15	12032	1.80E-15	12032	2.91E-18	12032	1.19E-19	12032	2.21E-18	12032	1.67E-19	12032
ksat_aq	high	1.72E-18	12032	0.00E+00	12032	0.00E+00	12032	0.00E+00	12032	0.00E+00	12032	0.00E+00	12032
	low	3.44E-18	12032	0.00E+00	12032	0.00E+00	12032	0.00E+00	12032	0.00E+00	12032	0.00E+00	12032
ksat_vz	high	2.08E-19	12032	0.00E+00	12032	0.00E+00	12032	0.00E+00	12032	0.00E+00	12032	0.00E+00	12032
	low	4.23E-17	12032	3.40E-17	12032	4.81E-20	12032	4.08E-23	12032	4.12E-20	12032	1.32E-21	12032

Table F.58. Predicted Peak U-238 (Kd = 2.00) Aqueous Concentration (Ci/L) and Arrival Time (yr) Summary for Case 2 (Diffusion)

Sub-Case		Groundwater		Fenceline		Excl (East)		Col River (East)		Excl (North)		Col River (North)	
		Conc.	Time	Conc.	Time	Conc.	Time	Conc.	Time	Conc.	Time	Conc.	Time
base		0.00E+00	12032	0.00E+00	12032	0.00E+00	12032	0.00E+00	12032	0.00E+00	12032	0.00E+00	12032
recharge	high	0.00E+00	12032	0.00E+00	12032	0.00E+00	12032	0.00E+00	12032	0.00E+00	12032	0.00E+00	12032
	low	0.00E+00	12032	0.00E+00	12032	0.00E+00	12032	0.00E+00	12032	0.00E+00	12032	0.00E+00	12032
barrier	high	0.00E+00	12032	0.00E+00	12032	0.00E+00	12032	0.00E+00	12032	0.00E+00	12032	0.00E+00	12032
	low	0.00E+00	12032	0.00E+00	12032	0.00E+00	12032	0.00E+00	12032	0.00E+00	12032	0.00E+00	12032
barrier_deg	high	0.00E+00	12032	0.00E+00	12032	0.00E+00	12032	0.00E+00	12032	0.00E+00	12032	0.00E+00	12032
	low	0.00E+00	12032	0.00E+00	12032	0.00E+00	12032	0.00E+00	12032	0.00E+00	12032	0.00E+00	12032
diffusion	high	0.00E+00	12032	0.00E+00	12032	0.00E+00	12032	0.00E+00	12032	0.00E+00	12032	0.00E+00	12032
	low	0.00E+00	12032	0.00E+00	12032	0.00E+00	12032	0.00E+00	12032	0.00E+00	12032	0.00E+00	12032
ksat_aq	high	0.00E+00	12032	0.00E+00	12032	0.00E+00	12032	0.00E+00	12032	0.00E+00	12032	0.00E+00	12032
	low	0.00E+00	12032	0.00E+00	12032	0.00E+00	12032	0.00E+00	12032	0.00E+00	12032	0.00E+00	12032
ksat_vz	high	0.00E+00	12032	0.00E+00	12032	0.00E+00	12032	0.00E+00	12032	0.00E+00	12032	0.00E+00	12032
	low	0.00E+00	12032	0.00E+00	12032	0.00E+00	12032	0.00E+00	12032	0.00E+00	12032	0.00E+00	12032

Table F.59. Predicted Peak U-238 (Kd = 2.00) Aqueous Concentration (Ci/L) and Arrival Time (yr) Summary for Case 3 (Retrieval Leak)

Sub-Case		Groundwater		Fenceline		Excl (East)		Col River (East)		Excl (North)		Col River (North)	
		Conc.	Time	Conc.	Time	Conc.	Time	Conc.	Time	Conc.	Time	Conc.	Time
base		0.00E+00	12032	0.00E+00	12032	0.00E+00	12032	0.00E+00	12032	0.00E+00	12032	0.00E+00	12032
recharge	high	0.00E+00	12032	0.00E+00	12032	0.00E+00	12032	0.00E+00	12032	0.00E+00	12032	0.00E+00	12032
	low	0.00E+00	12032	0.00E+00	12032	0.00E+00	12032	0.00E+00	12032	0.00E+00	12032	0.00E+00	12032
barrier	high	0.00E+00	12032	0.00E+00	12032	0.00E+00	12032	0.00E+00	12032	0.00E+00	12032	0.00E+00	12032
	low	0.00E+00	12032	0.00E+00	12032	0.00E+00	12032	0.00E+00	12032	0.00E+00	12032	0.00E+00	12032
barrier_deg	high	0.00E+00	12032	0.00E+00	12032	0.00E+00	12032	0.00E+00	12032	0.00E+00	12032	0.00E+00	12032
	low	0.00E+00	12032	0.00E+00	12032	0.00E+00	12032	0.00E+00	12032	0.00E+00	12032	0.00E+00	12032
ksat_aq	high	0.00E+00	12032	0.00E+00	12032	0.00E+00	12032	0.00E+00	12032	0.00E+00	12032	0.00E+00	12032
	low	0.00E+00	12032	0.00E+00	12032	0.00E+00	12032	0.00E+00	12032	0.00E+00	12032	0.00E+00	12032
ksat_vz	high	0.00E+00	12032	0.00E+00	12032	0.00E+00	12032	0.00E+00	12032	0.00E+00	12032	0.00E+00	12032
	low	0.00E+00	12032	0.00E+00	12032	0.00E+00	12032	0.00E+00	12032	0.00E+00	12032	0.00E+00	12032

Table F.60. Predicted Peak U-238 (Kd = 2.00) Aqueous Concentration (Ci/L) and Arrival Time (yr) Summary for Case 4 (Ancillary Equipment)

Sub-Case		Groundwater		Fenceline		Excl (East)		Col River (East)		Excl (North)		Col River (North)	
		Conc.	Time	Conc.	Time	Conc.	Time	Conc.	Time	Conc.	Time	Conc.	Time
base		0.00E+00	12032	0.00E+00	12032	0.00E+00	12032	0.00E+00	12032	0.00E+00	12032	0.00E+00	12032
recharge	high	0.00E+00	12032	0.00E+00	12032	0.00E+00	12032	0.00E+00	12032	0.00E+00	12032	0.00E+00	12032
	low	0.00E+00	12032	0.00E+00	12032	0.00E+00	12032	0.00E+00	12032	0.00E+00	12032	0.00E+00	12032
barrier	high	0.00E+00	12032	0.00E+00	12032	0.00E+00	12032	0.00E+00	12032	0.00E+00	12032	0.00E+00	12032
	low	0.00E+00	12032	0.00E+00	12032	0.00E+00	12032	0.00E+00	12032	0.00E+00	12032	0.00E+00	12032
barrier_deg	high	0.00E+00	12032	0.00E+00	12032	0.00E+00	12032	0.00E+00	12032	0.00E+00	12032	0.00E+00	12032
	low	0.00E+00	12032	0.00E+00	12032	0.00E+00	12032	0.00E+00	12032	0.00E+00	12032	0.00E+00	12032
ksat_aq	high	0.00E+00	12032	0.00E+00	12032	0.00E+00	12032	0.00E+00	12032	0.00E+00	12032	0.00E+00	12032
	low	0.00E+00	12032	0.00E+00	12032	0.00E+00	12032	0.00E+00	12032	0.00E+00	12032	0.00E+00	12032
ksat_vz	high	0.00E+00	12032	0.00E+00	12032	0.00E+00	12032	0.00E+00	12032	0.00E+00	12032	0.00E+00	12032
	low	0.00E+00	12032	0.00E+00	12032	0.00E+00	12032	0.00E+00	12032	0.00E+00	12032	0.00E+00	12032

Table F.61. Predicted Peak U-238 (Kd = 5.00) Aqueous Concentration (Ci/L) and Arrival Time (yr) Summary for Case 1 (Past Leak)

Sub-Case		Groundwater		Fenceline		Excl (East)		Col River (East)		Excl (North)		Col River (North)	
		Conc.	Time	Conc.	Time	Conc.	Time	Conc.	Time	Conc.	Time	Conc.	Time
base		0.00E+00	12032	0.00E+00	12032	0.00E+00	12032	0.00E+00	12032	0.00E+00	12032	0.00E+00	12032
recharge	high	0.00E+00	12032	0.00E+00	12032	0.00E+00	12032	0.00E+00	12032	0.00E+00	12032	0.00E+00	12032
	low	0.00E+00	12032	0.00E+00	12032	0.00E+00	12032	0.00E+00	12032	0.00E+00	12032	0.00E+00	12032
barrier	high	0.00E+00	12032	0.00E+00	12032	0.00E+00	12032	0.00E+00	12032	0.00E+00	12032	0.00E+00	12032
	low	0.00E+00	12032	0.00E+00	12032	0.00E+00	12032	0.00E+00	12032	0.00E+00	12032	0.00E+00	12032
barrier_deg	high	1.07E-19	12032	0.00E+00	12032	0.00E+00	12032	0.00E+00	12032	0.00E+00	12032	0.00E+00	12032
	low	0.00E+00	12032	0.00E+00	12032	0.00E+00	12032	0.00E+00	12032	0.00E+00	12032	0.00E+00	12032
plume	high	0.00E+00	12032	0.00E+00	12032	0.00E+00	12032	0.00E+00	12032	0.00E+00	12032	0.00E+00	12032
	low	0.00E+00	12032	0.00E+00	12032	0.00E+00	12032	0.00E+00	12032	0.00E+00	12032	0.00E+00	12032
ksat_aq	high	0.00E+00	12032	0.00E+00	12032	0.00E+00	12032	0.00E+00	12032	0.00E+00	12032	0.00E+00	12032
	low	0.00E+00	12032	0.00E+00	12032	0.00E+00	12032	0.00E+00	12032	0.00E+00	12032	0.00E+00	12032
ksat_vz	high	0.00E+00	12032	0.00E+00	12032	0.00E+00	12032	0.00E+00	12032	0.00E+00	12032	0.00E+00	12032
	low	0.00E+00	12032	0.00E+00	12032	0.00E+00	12032	0.00E+00	12032	0.00E+00	12032	0.00E+00	12032

Table F.62. Predicted Peak U-238 (Kd = 5.00) Aqueous Concentration (Ci/L) and Arrival Time (yr) Summary for Case 2 (Diffusion)

Sub-Case		Groundwater		Fenceline		Excl (East)		Col River (East)		Excl (North)		Col River (North)	
		Conc.	Time	Conc.	Time	Conc.	Time	Conc.	Time	Conc.	Time	Conc.	Time
base		0.00E+00	12032	0.00E+00	12032	0.00E+00	12032	0.00E+00	12032	0.00E+00	12032	0.00E+00	12032
recharge	high	0.00E+00	12032	0.00E+00	12032	0.00E+00	12032	0.00E+00	12032	0.00E+00	12032	0.00E+00	12032
	low	0.00E+00	12032	0.00E+00	12032	0.00E+00	12032	0.00E+00	12032	0.00E+00	12032	0.00E+00	12032
barrier	high	0.00E+00	12032	0.00E+00	12032	0.00E+00	12032	0.00E+00	12032	0.00E+00	12032	0.00E+00	12032
	low	0.00E+00	12032	0.00E+00	12032	0.00E+00	12032	0.00E+00	12032	0.00E+00	12032	0.00E+00	12032
barrier_deg	high	0.00E+00	12032	0.00E+00	12032	0.00E+00	12032	0.00E+00	12032	0.00E+00	12032	0.00E+00	12032
	low	0.00E+00	12032	0.00E+00	12032	0.00E+00	12032	0.00E+00	12032	0.00E+00	12032	0.00E+00	12032
diffusion	high	0.00E+00	12032	0.00E+00	12032	0.00E+00	12032	0.00E+00	12032	0.00E+00	12032	0.00E+00	12032
	low	0.00E+00	12032	0.00E+00	12032	0.00E+00	12032	0.00E+00	12032	0.00E+00	12032	0.00E+00	12032
ksat_aq	high	0.00E+00	12032	0.00E+00	12032	0.00E+00	12032	0.00E+00	12032	0.00E+00	12032	0.00E+00	12032
	low	0.00E+00	12032	0.00E+00	12032	0.00E+00	12032	0.00E+00	12032	0.00E+00	12032	0.00E+00	12032
ksat_vz	high	0.00E+00	12032	0.00E+00	12032	0.00E+00	12032	0.00E+00	12032	0.00E+00	12032	0.00E+00	12032
	low	0.00E+00	12032	0.00E+00	12032	0.00E+00	12032	0.00E+00	12032	0.00E+00	12032	0.00E+00	12032

Table F.63. Predicted Peak U-238 (Kd = 5.00) Aqueous Concentration (Ci/L) and Arrival Time (yr) Summary for Case 3 (Retrieval Leak)

Sub-Case		Groundwater		Fenceline		Excl (East)		Col River (East)		Excl (North)		Col River (North)	
		Conc.	Time	Conc.	Time	Conc.	Time	Conc.	Time	Conc.	Time	Conc.	Time
base		0.00E+00	12032	0.00E+00	12032	0.00E+00	12032	0.00E+00	12032	0.00E+00	12032	0.00E+00	12032
recharge	high	0.00E+00	12032	0.00E+00	12032	0.00E+00	12032	0.00E+00	12032	0.00E+00	12032	0.00E+00	12032
	low	0.00E+00	12032	0.00E+00	12032	0.00E+00	12032	0.00E+00	12032	0.00E+00	12032	0.00E+00	12032
barrier	high	0.00E+00	12032	0.00E+00	12032	0.00E+00	12032	0.00E+00	12032	0.00E+00	12032	0.00E+00	12032
	low	0.00E+00	12032	0.00E+00	12032	0.00E+00	12032	0.00E+00	12032	0.00E+00	12032	0.00E+00	12032
barrier_deg	high	0.00E+00	12032	0.00E+00	12032	0.00E+00	12032	0.00E+00	12032	0.00E+00	12032	0.00E+00	12032
	low	0.00E+00	12032	0.00E+00	12032	0.00E+00	12032	0.00E+00	12032	0.00E+00	12032	0.00E+00	12032
ksat_aq	high	0.00E+00	12032	0.00E+00	12032	0.00E+00	12032	0.00E+00	12032	0.00E+00	12032	0.00E+00	12032
	low	0.00E+00	12032	0.00E+00	12032	0.00E+00	12032	0.00E+00	12032	0.00E+00	12032	0.00E+00	12032
ksat_vz	high	0.00E+00	12032	0.00E+00	12032	0.00E+00	12032	0.00E+00	12032	0.00E+00	12032	0.00E+00	12032
	low	0.00E+00	12032	0.00E+00	12032	0.00E+00	12032	0.00E+00	12032	0.00E+00	12032	0.00E+00	12032

Table F.64. Predicted Peak U-238 (Kd = 5.00) Aqueous Concentration (Ci/L) and Arrival Time (yr) Summary for Case 4 (Ancillary Equipment)

Sub-Case		Groundwater		Fenceline		Excl (East)		Col River (East)		Excl (North)		Col River (North)	
		Conc.	Time	Conc.	Time	Conc.	Time	Conc.	Time	Conc.	Time	Conc.	Time
base		0.00E+00	12032	0.00E+00	12032	0.00E+00	12032	0.00E+00	12032	0.00E+00	12032	0.00E+00	12032
recharge	high	0.00E+00	12032	0.00E+00	12032	0.00E+00	12032	0.00E+00	12032	0.00E+00	12032	0.00E+00	12032
	low	0.00E+00	12032	0.00E+00	12032	0.00E+00	12032	0.00E+00	12032	0.00E+00	12032	0.00E+00	12032
barrier	high	0.00E+00	12032	0.00E+00	12032	0.00E+00	12032	0.00E+00	12032	0.00E+00	12032	0.00E+00	12032
	low	0.00E+00	12032	0.00E+00	12032	0.00E+00	12032	0.00E+00	12032	0.00E+00	12032	0.00E+00	12032
barrier_deg	high	0.00E+00	12032	0.00E+00	12032	0.00E+00	12032	0.00E+00	12032	0.00E+00	12032	0.00E+00	12032
	low	0.00E+00	12032	0.00E+00	12032	0.00E+00	12032	0.00E+00	12032	0.00E+00	12032	0.00E+00	12032
ksat_aq	high	0.00E+00	12032	0.00E+00	12032	0.00E+00	12032	0.00E+00	12032	0.00E+00	12032	0.00E+00	12032
	low	0.00E+00	12032	0.00E+00	12032	0.00E+00	12032	0.00E+00	12032	0.00E+00	12032	0.00E+00	12032
ksat_vz	high	0.00E+00	12032	0.00E+00	12032	0.00E+00	12032	0.00E+00	12032	0.00E+00	12032	0.00E+00	12032
	low	0.00E+00	12032	0.00E+00	12032	0.00E+00	12032	0.00E+00	12032	0.00E+00	12032	0.00E+00	12032

Table F.65. STOMP Mass Balance for Tc-99 for Case 1 (Past Leak)

Sub-Case		Vadose Zone				Aquifer				Vadose Zone + Aquifer			
		Released	In Domain	Exit	%error	Released	In Domain	Exit	%error	Released	In Domain	Exit	%error
base		1.000E+00	1.001E-05	1.007E+00	-6.935E-01	1.007E+00	2.862E-08	1.003E+00	3.513E-01	1.000E+00	1.004E-05	1.003E+00	-3.398E-01
recharge	high	1.000E+00	3.500E-06	1.010E+00	-9.766E-01	1.010E+00	9.999E-09	1.004E+00	5.541E-01	1.000E+00	3.510E-06	1.004E+00	-4.170E-01
	low	1.000E+00	7.276E-05	1.000E+00	-4.057E-02	1.000E+00	2.079E-07	1.000E+00	1.007E-02	1.000E+00	7.297E-05	1.000E+00	-3.050E-02
barrier	high	1.000E+00	7.738E-06	1.007E+00	-6.936E-01	1.007E+00	2.212E-08	1.003E+00	3.512E-01	1.000E+00	7.760E-06	1.003E+00	-3.400E-01
	low	1.000E+00	1.236E-05	1.007E+00	-6.935E-01	1.007E+00	3.532E-08	1.003E+00	3.514E-01	1.000E+00	1.240E-05	1.003E+00	-3.397E-01
barrier_deg	high	1.000E+00	0.000E+00	1.007E+00	-6.935E-01	1.007E+00	0.000E+00	1.003E+00	3.513E-01	1.000E+00	0.000E+00	1.003E+00	-3.398E-01
	low	1.000E+00	8.160E-04	1.006E+00	-6.935E-01	1.006E+00	1.117E-06	1.003E+00	3.515E-01	1.000E+00	8.171E-04	1.003E+00	-3.398E-01
plume	high	1.000E+00	4.298E-05	1.005E+00	-4.822E-01	1.005E+00	1.194E-07	1.002E+00	2.340E-01	1.000E+00	4.310E-05	1.002E+00	-2.471E-01
	low	1.000E+00	1.507E-06	1.007E+00	-7.122E-01	1.007E+00	4.417E-09	1.003E+00	3.753E-01	1.000E+00	1.512E-06	1.003E+00	-3.342E-01
ksat_aq	high	1.000E+00	1.001E-05	1.007E+00	-6.946E-01	1.007E+00	2.146E-08	1.003E+00	3.586E-01	1.000E+00	1.003E-05	1.003E+00	-3.335E-01
	low	1.000E+00	1.002E-05	1.007E+00	-6.921E-01	1.007E+00	4.299E-08	1.004E+00	3.385E-01	1.000E+00	1.007E-05	1.004E+00	-3.513E-01
ksat_vz	high	1.000E+00	3.088E-07	1.010E+00	-1.015E+00	1.010E+00	1.214E-09	1.003E+00	6.875E-01	1.000E+00	3.100E-07	1.003E+00	-3.201E-01
	low	1.000E+00	5.001E-04	1.004E+00	-4.334E-01	1.004E+00	8.207E-07	1.002E+00	2.069E-01	1.000E+00	5.009E-04	1.002E+00	-2.257E-01

Table F.66. STOMP Mass Balance for Tc-99 for Case 2 (Diffusion)

Sub-Case		Vadose Zone				Aquifer				Vadose Zone + Aquifer			
		Released	In Domain	Exit	%error	Released	In Domain	Exit	%error	Released	In Domain	Exit	%error
base		2.430E-01	1.304E-01	1.125E-01	3.894E-04	1.125E-01	7.374E-05	1.124E-01	2.280E-04	2.430E-01	1.305E-01	1.124E-01	4.937E-04
recharge	high	2.430E-01	1.304E-01	1.125E-01	4.109E-04	1.125E-01	7.373E-05	1.125E-01	2.374E-04	2.430E-01	1.305E-01	1.125E-01	5.213E-04
	low	2.430E-01	1.305E-01	1.125E-01	3.649E-04	1.125E-01	7.377E-05	1.124E-01	1.994E-04	2.430E-01	1.305E-01	1.124E-01	4.569E-04
barrier	high	2.430E-01	1.297E-01	1.133E-01	4.630E-04	1.133E-01	7.244E-05	1.132E-01	2.224E-04	2.430E-01	1.298E-01	1.132E-01	5.642E-04
	low	2.430E-01	1.312E-01	1.118E-01	4.078E-04	1.118E-01	7.496E-05	1.117E-01	2.220E-04	2.430E-01	1.312E-01	1.117E-01	5.121E-04
barrier_deg	high	2.430E-01	3.261E-02	2.104E-01	3.066E-05	2.104E-01	4.203E-05	2.103E-01	-1.672E-05	2.430E-01	3.265E-02	2.103E-01	1.687E-05
	low	2.430E-01	2.331E-01	9.915E-03	6.225E-04	9.915E-03	2.133E-05	9.894E-03	5.958E-04	2.430E-01	2.331E-01	9.894E-03	6.482E-04
diffusion	high	7.683E-01	4.125E-01	3.558E-01	2.560E-04	3.558E-01	2.332E-04	3.556E-01	2.285E-04	7.683E-01	4.127E-01	3.556E-01	3.607E-04
	low	7.683E-04	4.125E-04	3.558E-04	1.076E-03	3.558E-04	2.332E-07	3.556E-04	1.796E-03	7.683E-04	4.127E-04	3.556E-04	1.909E-03
ksat_aq	high	2.430E-01	1.304E-01	1.125E-01	3.710E-04	1.125E-01	5.531E-05	1.125E-01	2.606E-04	2.430E-01	1.305E-01	1.125E-01	4.906E-04
	low	2.430E-01	1.305E-01	1.125E-01	3.772E-04	1.125E-01	1.106E-04	1.124E-01	2.678E-04	2.430E-01	1.306E-01	1.124E-01	5.029E-04
ksat_vz	high	2.430E-01	9.710E-02	1.459E-01	-2.048E-03	1.459E-01	5.920E-05	1.458E-01	7.370E-05	2.430E-01	9.716E-02	1.458E-01	-2.005E-03
	low	2.430E-01	1.850E-01	5.792E-02	4.554E-04	5.792E-02	6.822E-05	5.784E-02	2.564E-02	2.430E-01	1.851E-01	5.784E-02	6.568E-03

Table F.67. STOMP Mass Balance for Tc-99 for Case 3 (Retrieval Leak)

Sub-Case		Vadose Zone				Aquifer				Vadose Zone + Aquifer			
		Released	In Domain	Exit	%error	Released	In Domain	Exit	%error	Released	In Domain	Exit	%error
base		1.000E+00	9.719E-03	9.904E-01	-1.049E-02	9.904E-01	2.291E-05	9.903E-01	4.403E-03	1.000E+00	9.742E-03	9.903E-01	-6.124E-03
recharge	high	1.000E+00	5.876E-03	9.946E-01	-4.392E-02	9.946E-01	1.416E-05	9.943E-01	2.121E-02	1.000E+00	5.891E-03	9.943E-01	-2.283E-02
	low	1.000E+00	2.333E-02	9.767E-01	-7.525E-05	9.767E-01	5.204E-05	9.766E-01	4.876E-05	1.000E+00	2.338E-02	9.766E-01	-2.757E-05
barrier	high	1.000E+00	7.931E-03	9.922E-01	-1.049E-02	9.922E-01	1.891E-05	9.921E-01	4.396E-03	1.000E+00	7.950E-03	9.921E-01	-6.131E-03
	low	1.000E+00	1.145E-02	9.887E-01	-1.047E-02	9.887E-01	2.675E-05	9.886E-01	4.414E-03	1.000E+00	1.148E-02	9.886E-01	-6.102E-03
barrier_deg	high	1.000E+00	0.000E+00	1.000E+00	-1.050E-02	1.000E+00	0.000E+00	1.000E+00	4.398E-03	1.000E+00	0.000E+00	1.000E+00	-6.104E-03
	low	1.000E+00	1.951E-01	8.050E-01	-1.029E-02	8.050E-01	1.581E-04	8.048E-01	5.431E-03	1.000E+00	1.952E-01	8.048E-01	-5.917E-03
ksat_aq	high	1.000E+00	9.717E-03	9.904E-01	-1.052E-02	9.904E-01	1.718E-05	9.903E-01	4.344E-03	1.000E+00	9.735E-03	9.903E-01	-6.214E-03
	low	1.000E+00	9.721E-03	9.904E-01	-1.043E-02	9.904E-01	3.438E-05	9.903E-01	4.545E-03	1.000E+00	9.756E-03	9.903E-01	-5.927E-03
ksat_vz	high	1.000E+00	5.950E-04	9.997E-01	-3.154E-02	9.997E-01	2.158E-06	9.994E-01	2.864E-02	1.000E+00	5.971E-04	9.994E-01	-2.905E-03
	low	1.000E+00	1.535E-01	8.465E-01	-1.535E-04	8.465E-01	1.765E-04	8.463E-01	3.683E-03	1.000E+00	1.537E-01	8.463E-01	2.964E-03

Table F.68. STOMP Mass Balance for Tc-99 for Case 4 (Ancillary Equipment)

Sub-Case		Vadose Zone				Aquifer				Vadose Zone + Aquifer			
		Released	In Domain	Exit	%error	Released	In Domain	Exit	%error	Released	In Domain	Exit	%error
base		1.000E+00	1.016E-02	9.899E-01	-2.623E-03	9.899E-01	2.307E-05	9.898E-01	9.813E-04	1.000E+00	1.019E-02	9.898E-01	-1.652E-03
recharge	high	1.000E+00	4.839E-03	9.955E-01	-3.890E-02	9.955E-01	1.131E-05	9.954E-01	1.771E-02	1.000E+00	4.851E-03	9.954E-01	-2.127E-02
	low	1.000E+00	3.584E-02	9.642E-01	7.190E-05	9.642E-01	7.538E-05	9.641E-01	2.213E-06	1.000E+00	3.592E-02	9.641E-01	7.413E-05
barrier	high	1.000E+00	8.299E-03	9.917E-01	-2.640E-03	9.917E-01	1.905E-05	9.917E-01	9.821E-04	1.000E+00	8.318E-03	9.917E-01	-1.666E-03
	low	1.000E+00	1.197E-02	9.881E-01	-2.623E-03	9.881E-01	2.693E-05	9.880E-01	9.840E-04	1.000E+00	1.200E-02	9.880E-01	-1.651E-03
barrier_deg	high	1.000E+00	0.000E+00	1.000E+00	-2.599E-03	1.000E+00	0.000E+00	1.000E+00	8.940E-04	1.000E+00	0.000E+00	1.000E+00	-1.705E-03
	low	1.000E+00	2.050E-01	7.950E-01	-2.429E-03	7.950E-01	1.605E-04	7.948E-01	1.245E-03	1.000E+00	2.052E-01	7.948E-01	-1.439E-03
ksat_aq	high	1.000E+00	1.016E-02	9.899E-01	-2.639E-03	9.899E-01	1.730E-05	9.898E-01	9.502E-04	1.000E+00	1.018E-02	9.898E-01	-1.698E-03
	low	1.000E+00	1.016E-02	9.899E-01	-2.609E-03	9.899E-01	3.462E-05	9.898E-01	1.061E-03	1.000E+00	1.020E-02	9.898E-01	-1.559E-03
ksat_vz	high	1.000E+00	5.043E-04	9.997E-01	-2.005E-02	9.997E-01	1.799E-06	9.995E-01	1.889E-02	1.000E+00	5.061E-04	9.995E-01	-1.168E-03
	low	1.000E+00	1.084E-01	8.916E-01	-7.108E-04	8.916E-01	1.256E-04	8.915E-01	1.213E-03	1.000E+00	1.085E-01	8.915E-01	3.703E-04

Table F.69. STOMP Mass Balance for U-238 (Kd = 0.02) for Case 1 (Past Leak)

Sub-Case		Vadose Zone				Aquifer				Vadose Zone + Aquifer			
		Released	In Domain	Exit	%error	Released	In Domain	Exit	%error	Released	In Domain	Exit	%error
base		1.000E+00	3.468E-04	1.004E+00	-4.682E-01	1.004E+00	8.604E-07	1.002E+00	2.300E-01	1.000E+00	3.477E-04	1.002E+00	-2.372E-01
recharge	high	1.000E+00	1.450E-04	1.009E+00	-8.793E-01	1.009E+00	3.604E-07	1.004E+00	4.996E-01	1.000E+00	1.454E-04	1.004E+00	-3.753E-01
	low	1.000E+00	1.747E-03	9.983E-01	-9.347E-03	9.983E-01	4.302E-06	9.983E-01	2.727E-03	1.000E+00	1.751E-03	9.983E-01	-6.624E-03
barrier	high	1.000E+00	2.861E-04	1.004E+00	-4.682E-01	1.004E+00	7.106E-07	1.002E+00	2.299E-01	1.000E+00	2.869E-04	1.002E+00	-2.373E-01
	low	1.000E+00	4.056E-04	1.004E+00	-4.681E-01	1.004E+00	1.005E-06	1.002E+00	2.300E-01	1.000E+00	4.066E-04	1.002E+00	-2.371E-01
barrier_deg	high	1.000E+00	0.000E+00	1.005E+00	-4.682E-01	1.005E+00	0.000E+00	1.002E+00	2.299E-01	1.000E+00	0.000E+00	1.002E+00	-2.372E-01
	low	1.000E+00	8.550E-03	9.961E-01	-4.681E-01	9.961E-01	9.891E-06	9.938E-01	2.319E-01	1.000E+00	8.559E-03	9.938E-01	-2.371E-01
plume	high	1.000E+00	1.206E-03	1.001E+00	-2.402E-01	1.001E+00	2.867E-06	1.000E+00	1.122E-01	1.000E+00	1.209E-03	1.000E+00	-1.279E-01
	low	1.000E+00	6.621E-05	1.007E+00	-6.869E-01	1.007E+00	1.706E-07	1.003E+00	3.524E-01	1.000E+00	6.638E-05	1.003E+00	-3.321E-01
ksat_aq	high	1.000E+00	3.468E-04	1.004E+00	-4.693E-01	1.004E+00	6.451E-07	1.002E+00	2.331E-01	1.000E+00	3.474E-04	1.002E+00	-2.351E-01
	low	1.000E+00	3.471E-04	1.004E+00	-4.664E-01	1.004E+00	1.292E-06	1.002E+00	2.252E-01	1.000E+00	3.484E-04	1.002E+00	-2.402E-01
ksat_vz	high	1.000E+00	6.176E-05	1.007E+00	-7.404E-01	1.007E+00	1.973E-07	1.002E+00	5.484E-01	1.000E+00	6.196E-05	1.002E+00	-1.880E-01
	low	1.000E+00	3.399E-03	9.995E-01	-2.931E-01	9.995E-01	5.226E-06	9.982E-01	1.365E-01	1.000E+00	3.404E-03	9.982E-01	-1.566E-01

Table F.70. STOMP Mass Balance for U-238 (Kd = 0.02) for Case 2 (Diffusion)

Sub-Case		Vadose Zone				Aquifer				Vadose Zone + Aquifer			
		Released	In Domain	Exit	%error	Released	In Domain	Exit	%error	Released	In Domain	Exit	%error
base		2.430E-01	1.923E-01	5.066E-02	6.240E-04	5.066E-02	7.795E-05	5.058E-02	2.069E-04	2.430E-01	1.924E-01	5.058E-02	6.700E-04
recharge	high	2.430E-01	1.923E-01	5.067E-02	6.685E-04	5.067E-02	7.795E-05	5.059E-02	1.995E-04	2.430E-01	1.924E-01	5.059E-02	7.099E-04
	low	2.430E-01	1.924E-01	5.061E-02	6.762E-04	5.061E-02	7.798E-05	5.054E-02	2.025E-04	2.430E-01	1.924E-01	5.054E-02	7.176E-04
barrier	high	2.430E-01	1.907E-01	5.222E-02	7.605E-04	5.222E-02	7.733E-05	5.215E-02	2.169E-04	2.430E-01	1.908E-01	5.215E-02	8.095E-04
	low	2.430E-01	1.937E-01	4.930E-02	6.930E-04	4.930E-02	7.840E-05	4.922E-02	1.949E-04	2.430E-01	1.937E-01	4.922E-02	7.298E-04
barrier_deg	high	2.430E-01	4.336E-02	1.996E-01	2.300E-05	1.996E-01	5.205E-05	1.996E-01	7.406E-05	2.430E-01	4.341E-02	1.996E-01	8.433E-05
	low	2.430E-01	2.423E-01	6.981E-04	5.871E-04	6.981E-04	2.695E-06	6.954E-04	1.541E-03	2.430E-01	2.423E-01	6.954E-04	5.905E-04
diffusion	high	7.683E-01	6.081E-01	1.602E-01	8.417E-04	1.602E-01	2.465E-04	1.599E-01	1.828E-04	7.683E-01	6.084E-01	1.599E-01	8.785E-04
	low	7.683E-04	6.081E-04	1.602E-04	1.453E-03	1.602E-04	2.465E-07	1.599E-04	3.678E-03	7.683E-04	6.084E-04	1.599E-04	2.220E-03
ksat_aq	high	2.430E-01	1.923E-01	5.066E-02	6.179E-04	5.066E-02	5.848E-05	5.060E-02	2.230E-04	2.430E-01	1.924E-01	5.060E-02	6.670E-04
	low	2.430E-01	1.923E-01	5.065E-02	6.317E-04	5.065E-02	1.169E-04	5.053E-02	2.155E-04	2.430E-01	1.924E-01	5.053E-02	6.762E-04
ksat_vz	high	2.430E-01	1.631E-01	7.985E-02	-2.327E-03	7.985E-02	8.939E-05	7.976E-02	6.350E-05	2.430E-01	1.632E-01	7.976E-02	-2.306E-03
	low	2.430E-01	2.211E-01	2.186E-02	5.926E-04	2.186E-02	4.576E-05	2.181E-02	1.664E-02	2.430E-01	2.212E-01	2.181E-02	2.091E-03

Table F.71. STOMP Mass Balance for U-238 (Kd = 0.02) for Case 3 (Retrieval Leak)

Sub-Case		Vadose Zone				Aquifer				Vadose Zone + Aquifer			
		Released	In Domain	Exit	%error	Released	In Domain	Exit	%error	Released	In Domain	Exit	%error
base		1.000E+00	9.898E-02	9.010E-01	-1.631E-03	9.010E-01	1.663E-04	9.009E-01	8.095E-04	1.000E+00	9.914E-02	9.009E-01	-9.015E-04
recharge	high	1.000E+00	6.859E-02	9.315E-01	-9.280E-03	9.315E-01	1.200E-04	9.313E-01	4.747E-03	1.000E+00	6.871E-02	9.313E-01	-4.859E-03
	low	1.000E+00	1.809E-01	8.191E-01	1.922E-04	8.191E-01	2.744E-04	8.188E-01	1.286E-05	1.000E+00	1.812E-01	8.188E-01	2.027E-04
barrier	high	1.000E+00	8.738E-02	9.126E-01	-1.649E-03	9.126E-01	1.497E-04	9.125E-01	8.009E-04	1.000E+00	8.753E-02	9.125E-01	-9.179E-04
	low	1.000E+00	1.093E-01	8.907E-01	-1.637E-03	8.907E-01	1.807E-04	8.905E-01	8.214E-04	1.000E+00	1.095E-01	8.905E-01	-9.052E-04
barrier_deg	high	1.000E+00	3.437E-08	1.000E+00	-1.708E-03	1.000E+00	2.700E-10	1.000E+00	7.033E-04	1.000E+00	3.464E-08	1.000E+00	-1.005E-03
	low	1.000E+00	5.179E-01	4.821E-01	-1.311E-03	4.821E-01	2.384E-04	4.818E-01	1.527E-03	1.000E+00	5.182E-01	4.818E-01	-5.752E-04
ksat_aq	high	1.000E+00	9.896E-02	9.011E-01	-1.632E-03	9.011E-01	1.247E-04	9.009E-01	7.874E-04	1.000E+00	9.909E-02	9.009E-01	-9.224E-04
	low	1.000E+00	9.900E-02	9.010E-01	-1.621E-03	9.010E-01	2.495E-04	9.008E-01	8.570E-04	1.000E+00	9.925E-02	9.008E-01	-8.486E-04
ksat_vz	high	1.000E+00	3.230E-02	9.677E-01	-4.034E-03	9.677E-01	7.908E-05	9.676E-01	3.433E-03	1.000E+00	3.238E-02	9.676E-01	-7.119E-04
	low	1.000E+00	3.808E-01	6.192E-01	2.265E-04	6.192E-01	3.159E-04	6.188E-01	1.364E-03	1.000E+00	3.812E-01	6.188E-01	1.070E-03

Table F.72. STOMP Mass Balance for U-238 (Kd = 0.02) for Case 4 (Ancillary Equipment)

Sub-Case		Vadose Zone				Aquifer				Vadose Zone + Aquifer			
		Released	In Domain	Exit	%error	Released	In Domain	Exit	%error	Released	In Domain	Exit	%error
base		1.000E+00	1.083E-01	8.917E-01	-7.525E-05	8.917E-01	1.734E-04	8.915E-01	9.621E-05	1.000E+00	1.085E-01	8.915E-01	1.043E-05
recharge	high	1.000E+00	6.305E-02	9.370E-01	-5.703E-03	9.370E-01	1.067E-04	9.369E-01	2.676E-03	1.000E+00	6.316E-02	9.369E-01	-3.196E-03
	low	1.000E+00	2.552E-01	7.448E-01	3.606E-04	7.448E-01	3.485E-04	7.445E-01	6.963E-06	1.000E+00	2.555E-01	7.445E-01	3.666E-04
barrier	high	1.000E+00	9.576E-02	9.042E-01	-8.047E-05	9.042E-01	1.563E-04	9.041E-01	8.310E-05	1.000E+00	9.591E-02	9.041E-01	-5.215E-06
	low	1.000E+00	1.195E-01	8.805E-01	-1.036E-04	8.805E-01	1.882E-04	8.803E-01	8.096E-05	1.000E+00	1.197E-01	8.803E-01	-3.204E-05
barrier_deg	high	1.000E+00	4.277E-08	1.000E+00	-2.069E-04	1.000E+00	3.216E-10	1.000E+00	1.073E-04	1.000E+00	4.310E-08	1.000E+00	-9.968E-05
	low	1.000E+00	5.548E-01	4.452E-01	4.470E-04	4.452E-01	2.393E-04	4.450E-01	1.739E-04	1.000E+00	5.550E-01	4.450E-01	5.245E-04
ksat_aq	high	1.000E+00	1.083E-01	8.917E-01	-6.706E-05	8.917E-01	1.300E-04	8.916E-01	7.954E-05	1.000E+00	1.084E-01	8.916E-01	3.725E-06
	low	1.000E+00	1.083E-01	8.917E-01	-8.568E-05	8.917E-01	2.601E-04	8.914E-01	1.001E-04	1.000E+00	1.086E-01	8.914E-01	3.725E-06
ksat_vz	high	1.000E+00	3.270E-02	9.673E-01	-1.678E-03	9.673E-01	7.841E-05	9.672E-01	1.137E-03	1.000E+00	3.278E-02	9.672E-01	-5.785E-04
	low	1.000E+00	3.011E-01	6.989E-01	2.742E-04	6.989E-01	2.628E-04	6.987E-01	3.772E-04	1.000E+00	3.013E-01	6.987E-01	5.364E-04

Table F.73. STOMP Mass Balance for U-238 (Kd = 0.10) for Case 1 (Past Leak)

Sub-Case		Vadose Zone				Aquifer				Vadose Zone + Aquifer			
		Released	In Domain	Exit	%error	Released	In Domain	Exit	%error	Released	In Domain	Exit	%error
base		1.000E+00	6.606E-02	9.343E-01	-3.206E-02	9.343E-01	1.234E-04	9.340E-01	1.562E-02	1.000E+00	6.618E-02	9.340E-01	-1.746E-02
recharge	high	1.000E+00	3.942E-02	9.622E-01	-1.627E-01	9.622E-01	7.571E-05	9.612E-01	9.115E-02	1.000E+00	3.950E-02	9.612E-01	-7.501E-02
	low	1.000E+00	1.594E-01	8.406E-01	1.565E-04	8.406E-01	2.750E-04	8.403E-01	-2.981E-06	1.000E+00	1.597E-01	8.403E-01	1.535E-04
barrier	high	1.000E+00	6.032E-02	9.400E-01	-3.210E-02	9.400E-01	1.134E-04	9.397E-01	1.553E-02	1.000E+00	6.043E-02	9.397E-01	-1.750E-02
	low	1.000E+00	7.106E-02	9.293E-01	-3.202E-02	9.293E-01	1.319E-04	9.290E-01	1.569E-02	1.000E+00	7.119E-02	9.290E-01	-1.744E-02
barrier_deg	high	1.000E+00	7.010E-06	1.000E+00	-3.210E-02	1.000E+00	5.171E-08	1.000E+00	1.459E-02	1.000E+00	7.062E-06	1.000E+00	-1.750E-02
	low	1.000E+00	2.605E-01	7.398E-01	-3.187E-02	7.398E-01	1.990E-04	7.395E-01	1.972E-02	1.000E+00	2.607E-01	7.395E-01	-1.728E-02
plume	high	1.000E+00	1.446E-01	8.554E-01	-5.345E-03	8.554E-01	2.346E-04	8.552E-01	2.836E-03	1.000E+00	1.448E-01	8.552E-01	-2.919E-03
	low	1.000E+00	2.055E-02	9.811E-01	-1.648E-01	9.811E-01	4.342E-05	9.803E-01	8.046E-02	1.000E+00	2.059E-02	9.803E-01	-8.586E-02
ksat_aq	high	1.000E+00	6.604E-02	9.343E-01	-3.220E-02	9.343E-01	9.249E-05	9.340E-01	1.529E-02	1.000E+00	6.613E-02	9.340E-01	-1.792E-02
	low	1.000E+00	6.610E-02	9.342E-01	-3.173E-02	9.342E-01	1.851E-04	9.339E-01	1.637E-02	1.000E+00	6.628E-02	9.339E-01	-1.644E-02
ksat_vz	high	1.000E+00	5.640E-02	9.440E-01	-4.177E-02	9.440E-01	1.210E-04	9.435E-01	3.903E-02	1.000E+00	5.653E-02	9.435E-01	-4.921E-03
	low	1.000E+00	9.898E-02	9.013E-01	-3.209E-02	9.013E-01	1.334E-04	9.011E-01	1.515E-02	1.000E+00	9.912E-02	9.011E-01	-1.844E-02

Table F.74. STOMP Mass Balance for U-238 (Kd = 0.10) for Case 2 (Diffusion)

Sub-Case		Vadose Zone				Aquifer				Vadose Zone + Aquifer			
		Released	In Domain	Exit	%error	Released	In Domain	Exit	%error	Released	In Domain	Exit	%error
base		2.430E-01	2.428E-01	1.340E-04	4.538E-04	1.340E-04	1.081E-06	1.329E-04	3.288E-03	2.430E-01	2.428E-01	1.329E-04	4.529E-04
recharge	high	2.430E-01	2.428E-01	1.343E-04	5.096E-04	1.343E-04	1.083E-06	1.332E-04	3.240E-03	2.430E-01	2.428E-01	1.332E-04	5.094E-04
	low	2.430E-01	2.428E-01	1.331E-04	4.774E-04	1.331E-04	1.076E-06	1.320E-04	3.291E-03	2.430E-01	2.428E-01	1.320E-04	4.805E-04
barrier	high	2.430E-01	2.428E-01	1.619E-04	5.085E-04	1.619E-04	1.252E-06	1.607E-04	2.822E-03	2.430E-01	2.428E-01	1.607E-04	5.106E-04
	low	2.430E-01	2.429E-01	1.145E-04	4.508E-04	1.145E-04	9.556E-07	1.136E-04	3.754E-03	2.430E-01	2.429E-01	1.136E-04	4.534E-04
barrier_deg	high	2.430E-01	9.706E-02	1.459E-01	1.963E-04	1.459E-01	1.201E-04	1.458E-01	-1.043E-05	2.430E-01	9.718E-02	1.458E-01	1.901E-04
	low	2.430E-01	2.430E-01	3.099E-09	3.054E-04	3.099E-09	3.459E-11	5.637E-10	8.069E+01	2.430E-01	2.430E-01	5.637E-10	3.064E-04
diffusion	high	7.683E-01	7.679E-01	4.236E-04	6.725E-04	4.236E-04	3.419E-06	4.202E-04	1.011E-03	7.683E-01	7.679E-01	4.202E-04	6.758E-04
	low	7.683E-04	7.679E-04	4.219E-07	1.277E-03	4.219E-07	3.412E-09	4.129E-07	1.314E+00	7.683E-04	7.679E-04	4.129E-07	1.996E-03
ksat_aq	high	2.430E-01	2.428E-01	1.340E-04	4.540E-04	1.340E-04	8.119E-07	1.332E-04	3.618E-03	2.430E-01	2.428E-01	1.332E-04	4.590E-04
	low	2.430E-01	2.428E-01	1.338E-04	4.531E-04	1.338E-04	1.617E-06	1.322E-04	2.874E-03	2.430E-01	2.428E-01	1.322E-04	4.518E-04
ksat_vz	high	2.430E-01	2.428E-01	1.808E-04	3.594E-04	1.808E-04	1.450E-06	1.794E-04	4.123E-03	2.430E-01	2.428E-01	1.794E-04	3.642E-04
	low	2.430E-01	2.429E-01	1.026E-04	4.155E-04	1.026E-04	7.959E-07	1.018E-04	7.017E-03	2.430E-01	2.429E-01	1.018E-04	4.210E-04

Table F.75. STOMP Mass Balance for U-238 (Kd = 0.10) for Case 3 (Retrieval Leak)

Sub-Case		Vadose Zone				Aquifer				Vadose Zone + Aquifer			
		Released	In Domain	Exit	%error	Released	In Domain	Exit	%error	Released	In Domain	Exit	%error
base		1.000E+00	8.802E-01	1.198E-01	3.457E-04	1.198E-01	2.698E-04	1.195E-01	-2.637E-05	1.000E+00	8.805E-01	1.195E-01	3.427E-04
recharge	high	1.000E+00	8.241E-01	1.759E-01	5.469E-04	1.759E-01	3.278E-04	1.756E-01	8.933E-06	1.000E+00	8.244E-01	1.756E-01	5.499E-04
	low	1.000E+00	9.469E-01	5.307E-02	5.070E-04	5.307E-02	1.624E-04	5.291E-02	-6.307E-07	1.000E+00	9.471E-01	5.291E-02	5.048E-04
barrier	high	1.000E+00	8.675E-01	1.325E-01	5.618E-04	1.325E-01	2.864E-04	1.322E-01	9.094E-06	1.000E+00	8.678E-01	1.322E-01	5.618E-04
	low	1.000E+00	8.900E-01	1.100E-01	3.457E-04	1.100E-01	2.563E-04	1.098E-01	4.258E-06	1.000E+00	8.902E-01	1.098E-01	3.457E-04
barrier_deg	high	1.000E+00	5.227E-03	9.948E-01	3.316E-05	9.948E-01	3.224E-05	9.947E-01	8.898E-07	1.000E+00	5.260E-03	9.947E-01	3.404E-05
	low	1.000E+00	9.889E-01	1.108E-02	3.611E-04	1.108E-02	2.337E-05	1.106E-02	-2.117E-06	1.000E+00	9.889E-01	1.106E-02	3.615E-04
ksat_aq	high	1.000E+00	8.802E-01	1.198E-01	3.114E-04	1.198E-01	2.025E-04	1.196E-01	2.385E-05	1.000E+00	8.804E-01	1.196E-01	3.137E-04
	low	1.000E+00	8.803E-01	1.197E-01	4.143E-04	1.197E-01	4.044E-04	1.193E-01	2.878E-05	1.000E+00	8.807E-01	1.193E-01	4.187E-04
ksat_vz	high	1.000E+00	8.628E-01	1.373E-01	-1.010E-03	1.373E-01	3.292E-04	1.369E-01	2.212E-05	1.000E+00	8.631E-01	1.369E-01	-1.004E-03
	low	1.000E+00	9.474E-01	5.263E-02	7.764E-04	5.263E-02	1.330E-04	5.249E-02	9.346E-06	1.000E+00	9.475E-01	5.249E-02	7.764E-04

Table F.76. STOMP Mass Balance for U-238 (Kd = 0.10) for Case 4 (Ancillary Equipment)

Sub-Case		Vadose Zone				Aquifer				Vadose Zone + Aquifer			
		Released	In Domain	Exit	%error	Released	In Domain	Exit	%error	Released	In Domain	Exit	%error
base		1.000E+00	9.098E-01	9.024E-02	4.835E-04	9.024E-02	2.271E-04	9.001E-02	-1.742E-06	1.000E+00	9.100E-01	9.001E-02	4.850E-04
recharge	high	1.000E+00	8.296E-01	1.704E-01	4.753E-04	1.704E-01	3.154E-04	1.700E-01	-2.255E-06	1.000E+00	8.299E-01	1.700E-01	4.724E-04
	low	1.000E+00	9.826E-01	1.736E-02	7.559E-04	1.736E-02	7.507E-05	1.729E-02	1.211E-05	1.000E+00	9.827E-01	1.729E-02	7.587E-04
barrier	high	1.000E+00	8.986E-01	1.014E-01	5.685E-04	1.014E-01	2.440E-04	1.011E-01	3.637E-05	1.000E+00	8.989E-01	1.011E-01	5.729E-04
	low	1.000E+00	9.182E-01	8.181E-02	4.068E-04	8.181E-02	2.135E-04	8.160E-02	-1.210E-06	1.000E+00	9.184E-01	8.160E-02	4.053E-04
barrier_deg	high	1.000E+00	6.495E-03	9.935E-01	1.066E-05	9.935E-01	3.749E-05	9.935E-01	4.617E-07	1.000E+00	6.533E-03	9.935E-01	1.113E-05
	low	1.000E+00	9.950E-01	5.022E-03	4.464E-04	5.022E-03	1.311E-05	5.009E-03	6.317E-05	1.000E+00	9.950E-01	5.009E-03	4.461E-04
ksat_aq	high	1.000E+00	9.097E-01	9.025E-02	4.895E-04	9.025E-02	1.704E-04	9.008E-02	4.756E-06	1.000E+00	9.099E-01	9.008E-02	4.910E-04
	low	1.000E+00	9.098E-01	9.020E-02	4.686E-04	9.020E-02	3.403E-04	8.986E-02	5.614E-06	1.000E+00	9.101E-01	8.986E-02	4.664E-04
ksat_vz	high	1.000E+00	9.040E-01	9.602E-02	-8.352E-04	9.602E-02	2.689E-04	9.576E-02	3.267E-05	1.000E+00	9.043E-01	9.576E-02	-8.345E-04
	low	1.000E+00	9.208E-01	7.915E-02	6.005E-04	7.915E-02	1.721E-04	7.898E-02	1.206E-05	1.000E+00	9.210E-01	7.898E-02	6.042E-04

Table F.77. STOMP Mass Balance for U-238 (Kd = 0.20) for Case 1 (Past Leak)

Sub-Case		Vadose Zone				Aquifer				Vadose Zone + Aquifer			
		Released	In Domain	Exit	%error	Released	In Domain	Exit	%error	Released	In Domain	Exit	%error
base		1.000E+00	4.380E-01	5.620E-01	-3.636E-04	5.620E-01	5.384E-04	5.615E-01	5.642E-04	1.000E+00	4.385E-01	5.615E-01	-4.768E-05
recharge	high	1.000E+00	3.378E-01	6.622E-01	-7.930E-03	6.622E-01	4.563E-04	6.617E-01	6.504E-03	1.000E+00	3.383E-01	6.617E-01	-3.624E-03
	low	1.000E+00	6.460E-01	3.540E-01	3.159E-04	3.540E-01	6.140E-04	3.534E-01	-6.627E-06	1.000E+00	6.466E-01	3.534E-01	3.159E-04
barrier	high	1.000E+00	4.207E-01	5.793E-01	-4.351E-04	5.793E-01	5.270E-04	5.788E-01	5.462E-04	1.000E+00	4.212E-01	5.788E-01	-1.192E-04
	low	1.000E+00	4.522E-01	5.478E-01	-3.845E-04	5.478E-01	5.470E-04	5.473E-01	5.893E-04	1.000E+00	4.527E-01	5.473E-01	-6.258E-05
barrier_deg	high	1.000E+00	2.529E-03	9.975E-01	-6.513E-04	9.975E-01	1.728E-05	9.975E-01	3.229E-04	1.000E+00	2.546E-03	9.975E-01	-3.292E-04
	low	1.000E+00	7.418E-01	2.582E-01	-2.325E-04	2.582E-01	2.897E-04	2.579E-01	1.239E-03	1.000E+00	7.421E-01	2.579E-01	8.941E-05
plume	high	1.000E+00	6.441E-01	3.559E-01	3.845E-04	3.559E-01	5.513E-04	3.553E-01	4.038E-05	1.000E+00	6.447E-01	3.553E-01	3.994E-04
	low	1.000E+00	2.150E-01	7.851E-01	-1.146E-02	7.851E-01	3.591E-04	7.847E-01	7.167E-03	1.000E+00	2.154E-01	7.847E-01	-5.837E-03
ksat_aq	high	1.000E+00	4.379E-01	5.621E-01	-4.083E-04	5.621E-01	4.039E-04	5.617E-01	5.246E-04	1.000E+00	4.383E-01	5.617E-01	-1.132E-04
	low	1.000E+00	4.381E-01	5.619E-01	-3.666E-04	5.619E-01	8.074E-04	5.611E-01	6.523E-04	1.000E+00	4.389E-01	5.611E-01	0.000E+00
ksat_vz	high	1.000E+00	4.622E-01	5.379E-01	-2.527E-03	5.379E-01	5.968E-04	5.373E-01	1.162E-03	1.000E+00	4.627E-01	5.373E-01	-1.901E-03
	low	1.000E+00	4.342E-01	5.658E-01	-1.091E-03	5.658E-01	4.434E-04	5.654E-01	1.088E-03	1.000E+00	4.346E-01	5.654E-01	-4.768E-04

Table F.78. STOMP Mass Balance for U-238 (Kd = 0.20) for Case 2 (Diffusion)

Sub-Case		Vadose Zone				Aquifer				Vadose Zone + Aquifer			
		Released	In Domain	Exit	%error	Released	In Domain	Exit	%error	Released	In Domain	Exit	%error
base		2.430E-01	2.430E-01	1.715E-08	2.137E-04	1.715E-08	3.346E-10	1.349E-08	1.941E+01	2.430E-01	2.430E-01	1.349E-08	2.152E-04
recharge	high	2.430E-01	2.430E-01	1.727E-08	1.217E-04	1.727E-08	3.365E-10	1.360E-08	1.931E+01	2.430E-01	2.430E-01	1.360E-08	1.232E-04
	low	2.430E-01	2.430E-01	1.687E-08	1.280E-04	1.687E-08	3.297E-10	1.322E-08	1.966E+01	2.430E-01	2.430E-01	1.322E-08	1.295E-04
barrier	high	2.430E-01	2.430E-01	2.514E-08	2.166E-04	2.514E-08	4.729E-10	2.113E-08	1.409E+01	2.430E-01	2.430E-01	2.113E-08	2.182E-04
	low	2.430E-01	2.430E-01	1.257E-08	1.175E-04	1.257E-08	2.505E-10	9.215E-09	2.471E+01	2.430E-01	2.430E-01	9.215E-09	1.189E-04
barrier_deg	high	2.430E-01	1.930E-01	4.993E-02	3.956E-04	4.993E-02	1.999E-04	4.973E-02	2.396E-05	2.430E-01	1.932E-01	4.973E-02	3.986E-04
	low	2.430E-01	2.430E-01	0.000E+00	9.813E-05	0.000E+00	0.000E+00	0.000E+00	0.000E+00	2.430E-01	2.430E-01	0.000E+00	9.813E-05
diffusion	high	7.683E-01	7.683E-01	5.515E-08	3.962E-04	5.515E-08	1.082E-09	5.056E-08	6.361E+00	7.683E-01	7.683E-01	5.056E-08	3.968E-04
	low	7.683E-04	7.683E-04	0.000E+00	6.591E-04	0.000E+00	0.000E+00	0.000E+00	0.000E+00	7.683E-04	7.683E-04	0.000E+00	6.591E-04
ksat_aq	high	2.430E-01	2.430E-01	1.718E-08	2.137E-04	1.718E-08	2.500E-10	1.316E-08	2.193E+01	2.430E-01	2.430E-01	1.316E-08	2.154E-04
	low	2.430E-01	2.430E-01	1.710E-08	2.137E-04	1.710E-08	5.012E-10	1.377E-08	1.655E+01	2.430E-01	2.430E-01	1.377E-08	2.151E-04
ksat_vz	high	2.430E-01	2.430E-01	9.501E-09	3.518E-04	9.501E-09	1.847E-10	5.528E-09	3.987E+01	2.430E-01	2.430E-01	5.528E-09	3.534E-04
	low	2.430E-01	2.430E-01	6.066E-08	9.156E-05	6.066E-08	1.079E-09	5.562E-08	6.531E+00	2.430E-01	2.430E-01	5.562E-08	9.363E-05

Table F.79. STOMP Mass Balance for U-238 (Kd = 0.20) for Case 3 (Retrieval Leak)

Sub-Case		Vadose Zone				Aquifer				Vadose Zone + Aquifer			
		Released	In Domain	Exit	%error	Released	In Domain	Exit	%error	Released	In Domain	Exit	%error
base		1.000E+00	9.985E-01	1.460E-03	3.004E-04	1.460E-03	8.919E-06	1.451E-03	3.502E-04	1.000E+00	9.985E-01	1.451E-03	2.988E-04
recharge	high	1.000E+00	9.967E-01	3.300E-03	3.594E-04	3.300E-03	1.766E-05	3.282E-03	1.079E-04	1.000E+00	9.967E-01	3.282E-03	3.611E-04
	low	1.000E+00	9.997E-01	3.029E-04	6.718E-04	3.029E-04	2.313E-06	3.006E-04	2.281E-03	1.000E+00	9.997E-01	3.006E-04	6.713E-04
barrier	high	1.000E+00	9.982E-01	1.759E-03	4.408E-04	1.759E-03	1.047E-05	1.749E-03	2.435E-04	1.000E+00	9.982E-01	1.749E-03	4.397E-04
	low	1.000E+00	9.987E-01	1.252E-03	4.157E-04	1.252E-03	7.804E-06	1.244E-03	4.545E-04	1.000E+00	9.988E-01	1.244E-03	4.159E-04
barrier_deg	high	1.000E+00	2.783E-01	7.217E-01	3.010E-04	7.217E-01	1.020E-03	7.207E-01	2.016E-06	1.000E+00	2.793E-01	7.207E-01	3.010E-04
	low	1.000E+00	1.000E+00	3.479E-05	6.274E-04	3.479E-05	1.588E-07	3.463E-05	1.715E-02	1.000E+00	1.000E+00	3.463E-05	6.260E-04
ksat_aq	high	1.000E+00	9.985E-01	1.461E-03	3.004E-04	1.461E-03	6.697E-06	1.454E-03	3.917E-04	1.000E+00	9.985E-01	1.454E-03	3.032E-04
	low	1.000E+00	9.985E-01	1.459E-03	2.995E-04	1.459E-03	1.335E-05	1.446E-03	3.468E-04	1.000E+00	9.986E-01	1.446E-03	2.995E-04
ksat_vz	high	1.000E+00	9.988E-01	1.195E-03	5.977E-04	1.195E-03	8.024E-06	1.187E-03	1.078E-03	1.000E+00	9.988E-01	1.187E-03	5.968E-04
	low	1.000E+00	9.992E-01	7.681E-04	4.873E-04	7.681E-04	4.842E-06	7.632E-04	9.044E-04	1.000E+00	9.992E-01	7.632E-04	4.894E-04

Table F.80. STOMP Mass Balance for U-238 (Kd = 0.20) for Case 4 (Ancillary Equipment)

Sub-Case		Vadose Zone				Aquifer				Vadose Zone + Aquifer			
		Released	In Domain	Exit	%error	Released	In Domain	Exit	%error	Released	In Domain	Exit	%error
base		1.000E+00	9.994E-01	5.690E-04	8.338E-04	5.690E-04	4.131E-06	5.649E-04	1.197E-03	1.000E+00	9.994E-01	5.649E-04	8.363E-04
recharge	high	1.000E+00	9.975E-01	2.497E-03	5.452E-04	2.497E-03	1.412E-05	2.483E-03	1.963E-04	1.000E+00	9.975E-01	2.483E-03	5.450E-04
	low	1.000E+00	1.000E+00	1.669E-05	5.421E-04	1.669E-05	1.928E-07	1.649E-05	2.792E-02	1.000E+00	1.000E+00	1.649E-05	5.440E-04
barrier	high	1.000E+00	9.993E-01	7.141E-04	8.144E-04	7.141E-04	5.026E-06	7.091E-04	9.713E-04	1.000E+00	9.993E-01	7.091E-04	8.170E-04
	low	1.000E+00	9.995E-01	4.710E-04	9.074E-04	4.710E-04	3.508E-06	4.675E-04	1.445E-03	1.000E+00	9.995E-01	4.675E-04	9.072E-04
barrier_deg	high	1.000E+00	3.147E-01	6.853E-01	3.487E-04	6.853E-01	1.049E-03	6.843E-01	1.177E-05	1.000E+00	3.157E-01	6.843E-01	3.576E-04
	low	1.000E+00	1.000E+00	4.242E-06	3.924E-04	4.242E-06	2.610E-08	4.206E-06	2.432E-01	1.000E+00	1.000E+00	4.206E-06	3.960E-04
ksat_aq	high	1.000E+00	9.994E-01	5.693E-04	8.314E-04	5.693E-04	3.103E-06	5.661E-04	1.311E-03	1.000E+00	9.994E-01	5.661E-04	8.325E-04
	low	1.000E+00	9.994E-01	5.685E-04	8.322E-04	5.685E-04	6.180E-06	5.623E-04	1.056E-03	1.000E+00	9.994E-01	5.623E-04	8.309E-04
ksat_vz	high	1.000E+00	9.997E-01	2.543E-04	7.090E-04	2.543E-04	2.191E-06	2.521E-04	3.943E-03	1.000E+00	9.997E-01	2.521E-04	7.086E-04
	low	1.000E+00	9.986E-01	1.367E-03	3.223E-04	1.367E-03	7.878E-06	1.359E-03	4.230E-04	1.000E+00	9.986E-01	1.359E-03	3.239E-04

Table F.81. STOMP Mass Balance for U-238 (Kd = 0.60) for Case 1 (Past Leak)

Sub-Case		Vadose Zone				Aquifer				Vadose Zone + Aquifer			
		Released	In Domain	Exit	%error	Released	In Domain	Exit	%error	Released	In Domain	Exit	%error
base		1.000E+00	9.948E-01	5.158E-03	1.412E-04	5.158E-03	4.745E-05	5.111E-03	5.593E-05	1.000E+00	9.949E-01	5.111E-03	1.423E-04
recharge	high	1.000E+00	9.887E-01	1.134E-02	2.678E-04	1.134E-02	8.549E-05	1.125E-02	-3.279E-05	1.000E+00	9.887E-01	1.125E-02	2.695E-04
	low	1.000E+00	9.992E-01	8.205E-04	3.486E-04	8.205E-04	1.115E-05	8.093E-04	5.925E-04	1.000E+00	9.992E-01	8.093E-04	3.494E-04
barrier	high	1.000E+00	9.942E-01	5.836E-03	3.152E-04	5.836E-03	5.227E-05	5.784E-03	4.183E-05	1.000E+00	9.942E-01	5.784E-03	3.155E-04
	low	1.000E+00	9.953E-01	4.658E-03	1.191E-04	4.658E-03	4.378E-05	4.614E-03	7.373E-05	1.000E+00	9.954E-01	4.614E-03	1.165E-04
barrier_deg	high	1.000E+00	5.216E-01	4.784E-01	4.858E-04	4.784E-01	1.888E-03	4.765E-01	-3.212E-06	1.000E+00	5.235E-01	4.765E-01	4.858E-04
	low	1.000E+00	9.996E-01	4.424E-04	1.074E-04	4.424E-04	3.439E-06	4.389E-04	7.371E-04	1.000E+00	9.996E-01	4.389E-04	1.059E-04
plume	high	1.000E+00	9.995E-01	5.139E-04	1.637E-04	5.139E-04	6.295E-06	5.076E-04	9.912E-04	1.000E+00	9.995E-01	5.076E-04	1.619E-04
	low	1.000E+00	9.546E-01	4.538E-02	2.120E-04	4.538E-02	2.714E-04	4.511E-02	3.136E-05	1.000E+00	9.549E-01	4.511E-02	2.131E-04
ksat_aq	high	1.000E+00	9.948E-01	5.160E-03	1.393E-04	5.160E-03	3.565E-05	5.125E-03	5.689E-05	1.000E+00	9.949E-01	5.125E-03	1.399E-04
	low	1.000E+00	9.948E-01	5.153E-03	1.234E-04	5.153E-03	7.095E-05	5.082E-03	5.450E-05	1.000E+00	9.949E-01	5.082E-03	1.261E-04
ksat_vz	high	1.000E+00	9.973E-01	2.698E-03	1.744E-04	2.698E-03	2.890E-05	2.669E-03	4.147E-04	1.000E+00	9.973E-01	2.669E-03	1.744E-04
	low	1.000E+00	9.880E-01	1.200E-02	3.744E-04	1.200E-02	8.699E-05	1.191E-02	-2.395E-05	1.000E+00	9.881E-01	1.191E-02	3.711E-04

Table F.82. STOMP Mass Balance for U-238 (Kd = 0.60) for Case 2 (Diffusion)

Sub-Case		Vadose Zone				Aquifer				Vadose Zone + Aquifer			
		Released	In Domain	Exit	%error	Released	In Domain	Exit	%error	Released	In Domain	Exit	%error
base		2.430E-01	2.430E-01	0.000E+00	6.746E-05	0.000E+00	0.000E+00	0.000E+00	0.000E+00	2.430E-01	2.430E-01	0.000E+00	6.746E-05
recharge	high	2.430E-01	2.430E-01	0.000E+00	7.973E-05	0.000E+00	0.000E+00	0.000E+00	0.000E+00	2.430E-01	2.430E-01	0.000E+00	7.973E-05
	low	2.430E-01	2.430E-01	0.000E+00	6.746E-05	0.000E+00	0.000E+00	0.000E+00	0.000E+00	2.430E-01	2.430E-01	0.000E+00	6.746E-05
barrier	high	2.430E-01	2.430E-01	0.000E+00	6.746E-05	0.000E+00	0.000E+00	0.000E+00	0.000E+00	2.430E-01	2.430E-01	0.000E+00	6.746E-05
	low	2.430E-01	2.430E-01	0.000E+00	9.813E-05	0.000E+00	0.000E+00	0.000E+00	0.000E+00	2.430E-01	2.430E-01	0.000E+00	9.813E-05
barrier_deg	high	2.430E-01	2.430E-01	1.680E-06	3.082E-04	1.680E-06	6.493E-08	1.612E-06	1.676E-01	2.430E-01	2.430E-01	1.612E-06	3.116E-04
	low	2.430E-01	2.430E-01	0.000E+00	-1.227E-05	0.000E+00	0.000E+00	0.000E+00	0.000E+00	2.430E-01	2.430E-01	0.000E+00	-1.227E-05
diffusion	high	7.683E-01	7.683E-01	0.000E+00	1.086E-04	0.000E+00	0.000E+00	0.000E+00	0.000E+00	7.683E-01	7.683E-01	0.000E+00	1.086E-04
	low	7.683E-04	7.683E-04	0.000E+00	3.409E-04	0.000E+00	0.000E+00	0.000E+00	0.000E+00	7.683E-04	7.683E-04	0.000E+00	3.409E-04
ksat_aq	high	2.430E-01	2.430E-01	0.000E+00	6.746E-05	0.000E+00	0.000E+00	0.000E+00	0.000E+00	2.430E-01	2.430E-01	0.000E+00	6.746E-05
	low	2.430E-01	2.430E-01	0.000E+00	6.746E-05	0.000E+00	0.000E+00	0.000E+00	0.000E+00	2.430E-01	2.430E-01	0.000E+00	6.746E-05
ksat_vz	high	2.430E-01	2.430E-01	0.000E+00	3.066E-05	0.000E+00	0.000E+00	0.000E+00	0.000E+00	2.430E-01	2.430E-01	0.000E+00	3.066E-05
	low	2.430E-01	2.430E-01	0.000E+00	3.066E-05	0.000E+00	0.000E+00	0.000E+00	0.000E+00	2.430E-01	2.430E-01	0.000E+00	3.066E-05

Table F.83. STOMP Mass Balance for U-238 (Kd = 0.60) for Case 3 (Retrieval Leak)

Sub-Case		Vadose Zone				Aquifer				Vadose Zone + Aquifer			
		Released	In Domain	Exit	%error	Released	In Domain	Exit	%error	Released	In Domain	Exit	%error
base		1.000E+00	1.000E+00	0.000E+00	2.861E-04	0.000E+00	0.000E+00	0.000E+00	0.000E+00	1.000E+00	1.000E+00	0.000E+00	2.861E-04
recharge	high	1.000E+00	1.000E+00	0.000E+00	1.848E-04	0.000E+00	0.000E+00	0.000E+00	0.000E+00	1.000E+00	1.000E+00	0.000E+00	1.848E-04
	low	1.000E+00	1.000E+00	0.000E+00	1.907E-04	0.000E+00	0.000E+00	0.000E+00	0.000E+00	1.000E+00	1.000E+00	0.000E+00	1.907E-04
barrier	high	1.000E+00	1.000E+00	0.000E+00	1.609E-04	0.000E+00	0.000E+00	0.000E+00	0.000E+00	1.000E+00	1.000E+00	0.000E+00	1.609E-04
	low	1.000E+00	1.000E+00	0.000E+00	2.801E-04	0.000E+00	0.000E+00	0.000E+00	0.000E+00	1.000E+00	1.000E+00	0.000E+00	2.801E-04
barrier_deg	high	1.000E+00	9.995E-01	5.080E-04	2.668E-04	5.080E-04	1.238E-05	4.956E-04	6.251E-04	1.000E+00	9.995E-01	4.956E-04	2.657E-04
	low	1.000E+00	1.000E+00	0.000E+00	1.729E-04	0.000E+00	0.000E+00	0.000E+00	0.000E+00	1.000E+00	1.000E+00	0.000E+00	1.729E-04
ksat_aq	high	1.000E+00	1.000E+00	0.000E+00	2.861E-04	0.000E+00	0.000E+00	0.000E+00	0.000E+00	1.000E+00	1.000E+00	0.000E+00	2.861E-04
	low	1.000E+00	1.000E+00	0.000E+00	2.861E-04	0.000E+00	0.000E+00	0.000E+00	0.000E+00	1.000E+00	1.000E+00	0.000E+00	2.861E-04
ksat_vz	high	1.000E+00	1.000E+00	0.000E+00	2.086E-04	0.000E+00	0.000E+00	0.000E+00	0.000E+00	1.000E+00	1.000E+00	0.000E+00	2.086E-04
	low	1.000E+00	1.000E+00	0.000E+00	1.490E-04	0.000E+00	0.000E+00	0.000E+00	0.000E+00	1.000E+00	1.000E+00	0.000E+00	1.490E-04

Table F.84. STOMP Mass Balance for U-238 (Kd = 0.60) for Case 4 (Ancillary Equipment)

Sub-Case		Vadose Zone				Aquifer				Vadose Zone + Aquifer			
		Released	In Domain	Exit	%error	Released	In Domain	Exit	%error	Released	In Domain	Exit	%error
base		1.000E+00	1.000E+00	0.000E+00	2.146E-04	0.000E+00	0.000E+00	0.000E+00	0.000E+00	1.000E+00	1.000E+00	0.000E+00	2.146E-04
recharge	high	1.000E+00	1.000E+00	0.000E+00	1.431E-04	0.000E+00	0.000E+00	0.000E+00	0.000E+00	1.000E+00	1.000E+00	0.000E+00	1.431E-04
	low	1.000E+00	1.000E+00	0.000E+00	1.788E-04	0.000E+00	0.000E+00	0.000E+00	0.000E+00	1.000E+00	1.000E+00	0.000E+00	1.788E-04
barrier	high	1.000E+00	1.000E+00	0.000E+00	2.563E-04	0.000E+00	0.000E+00	0.000E+00	0.000E+00	1.000E+00	1.000E+00	0.000E+00	2.563E-04
	low	1.000E+00	1.000E+00	0.000E+00	1.431E-04	0.000E+00	0.000E+00	0.000E+00	0.000E+00	1.000E+00	1.000E+00	0.000E+00	1.431E-04
barrier_deg	high	1.000E+00	9.997E-01	2.627E-04	5.295E-04	2.627E-04	6.737E-06	2.560E-04	1.125E-03	1.000E+00	9.997E-01	2.560E-04	5.299E-04
	low	1.000E+00	1.000E+00	0.000E+00	1.073E-04	0.000E+00	0.000E+00	0.000E+00	0.000E+00	1.000E+00	1.000E+00	0.000E+00	1.073E-04
ksat_aq	high	1.000E+00	1.000E+00	0.000E+00	2.146E-04	0.000E+00	0.000E+00	0.000E+00	0.000E+00	1.000E+00	1.000E+00	0.000E+00	2.146E-04
	low	1.000E+00	1.000E+00	0.000E+00	2.146E-04	0.000E+00	0.000E+00	0.000E+00	0.000E+00	1.000E+00	1.000E+00	0.000E+00	2.146E-04
ksat_vz	high	1.000E+00	1.000E+00	0.000E+00	1.967E-04	0.000E+00	0.000E+00	0.000E+00	0.000E+00	1.000E+00	1.000E+00	0.000E+00	1.967E-04
	low	1.000E+00	1.000E+00	0.000E+00	1.729E-04	0.000E+00	0.000E+00	0.000E+00	0.000E+00	1.000E+00	1.000E+00	0.000E+00	1.729E-04

Table F.85. STOMP Mass Balance for U-238 (Kd = 1.00) for Case 1 (Past Leak)

Sub-Case		Vadose Zone				Aquifer				Vadose Zone + Aquifer			
		Released	In Domain	Exit	%error	Released	In Domain	Exit	%error	Released	In Domain	Exit	%error
base		1.000E+00	1.000E+00	2.725E-05	6.431E-05	2.725E-05	5.866E-07	2.666E-05	2.027E-02	1.000E+00	1.000E+00	2.666E-05	6.392E-05
recharge	high	1.000E+00	9.999E-01	9.376E-05	1.428E-04	9.376E-05	1.694E-06	9.206E-05	5.414E-03	1.000E+00	9.999E-01	9.206E-05	1.458E-04
	low	1.000E+00	1.000E+00	1.679E-06	1.898E-04	1.679E-06	5.129E-08	1.623E-06	2.516E-01	1.000E+00	1.000E+00	1.623E-06	1.894E-04
barrier	high	1.000E+00	1.000E+00	3.273E-05	1.657E-04	3.273E-05	6.897E-07	3.204E-05	1.693E-02	1.000E+00	1.000E+00	3.204E-05	1.637E-04
	low	1.000E+00	1.000E+00	2.344E-05	1.178E-04	2.344E-05	5.132E-07	2.292E-05	2.352E-02	1.000E+00	1.000E+00	2.292E-05	1.160E-04
barrier_deg	high	1.000E+00	9.351E-01	6.493E-02	2.444E-04	6.493E-02	9.469E-04	6.398E-02	2.331E-06	1.000E+00	9.360E-01	6.398E-02	2.421E-04
	low	1.000E+00	1.000E+00	8.799E-07	3.121E-05	8.799E-07	1.496E-08	8.573E-07	8.784E-01	1.000E+00	1.000E+00	8.573E-07	3.348E-05
plume	high	1.000E+00	1.000E+00	5.720E-07	6.797E-05	5.720E-07	1.570E-08	5.513E-07	8.777E-01	1.000E+00	1.000E+00	5.513E-07	7.004E-05
	low	1.000E+00	9.987E-01	1.257E-03	1.970E-04	1.257E-03	1.893E-05	1.239E-03	2.563E-04	1.000E+00	9.988E-01	1.239E-03	1.946E-04
ksat_aq	high	1.000E+00	1.000E+00	2.728E-05	6.773E-05	2.728E-05	4.415E-07	2.683E-05	2.211E-02	1.000E+00	1.000E+00	2.683E-05	7.077E-05
	low	1.000E+00	1.000E+00	2.720E-05	6.931E-05	2.720E-05	8.737E-07	2.632E-05	1.837E-02	1.000E+00	1.000E+00	2.632E-05	6.778E-05
ksat_vz	high	1.000E+00	1.000E+00	8.571E-06	1.085E-04	8.571E-06	2.106E-07	8.352E-06	9.965E-02	1.000E+00	1.000E+00	8.352E-06	1.065E-04
	low	1.000E+00	9.999E-01	1.428E-04	1.720E-04	1.428E-04	2.525E-06	1.402E-04	3.230E-03	1.000E+00	9.999E-01	1.402E-04	1.747E-04

Table F.86. STOMP Mass Balance for U-238 (Kd = 1.00) for Case 2 (Diffusion)

Sub-Case		Vadose Zone				Aquifer				Vadose Zone + Aquifer			
		Released	In Domain	Exit	%error	Released	In Domain	Exit	%error	Released	In Domain	Exit	%error
base		2.430E-01	2.430E-01	0.000E+00	6.133E-05	0.000E+00	0.000E+00	0.000E+00	0.000E+00	2.430E-01	2.430E-01	0.000E+00	6.133E-05
recharge	high	2.430E-01	2.430E-01	0.000E+00	3.680E-05	0.000E+00	0.000E+00	0.000E+00	0.000E+00	2.430E-01	2.430E-01	0.000E+00	3.680E-05
	low	2.430E-01	2.430E-01	0.000E+00	1.840E-05	0.000E+00	0.000E+00	0.000E+00	0.000E+00	2.430E-01	2.430E-01	0.000E+00	1.840E-05
barrier	high	2.430E-01	2.430E-01	0.000E+00	4.906E-05	0.000E+00	0.000E+00	0.000E+00	0.000E+00	2.430E-01	2.430E-01	0.000E+00	4.906E-05
	low	2.430E-01	2.430E-01	0.000E+00	3.066E-05	0.000E+00	0.000E+00	0.000E+00	0.000E+00	2.430E-01	2.430E-01	0.000E+00	3.066E-05
barrier_deg	high	2.430E-01	2.430E-01	0.000E+00	1.411E-04	0.000E+00	0.000E+00	0.000E+00	0.000E+00	2.430E-01	2.430E-01	0.000E+00	1.411E-04
	low	2.430E-01	2.430E-01	0.000E+00	-1.227E-05	0.000E+00	0.000E+00	0.000E+00	0.000E+00	2.430E-01	2.430E-01	0.000E+00	-1.227E-05
diffusion	high	7.683E-01	7.683E-01	0.000E+00	9.309E-05	0.000E+00	0.000E+00	0.000E+00	0.000E+00	7.683E-01	7.683E-01	0.000E+00	9.309E-05
	low	7.683E-04	7.683E-04	0.000E+00	2.803E-04	0.000E+00	0.000E+00	0.000E+00	0.000E+00	7.683E-04	7.683E-04	0.000E+00	2.803E-04
ksat_aq	high	2.430E-01	2.430E-01	0.000E+00	6.133E-05	0.000E+00	0.000E+00	0.000E+00	0.000E+00	2.430E-01	2.430E-01	0.000E+00	6.133E-05
	low	2.430E-01	2.430E-01	0.000E+00	6.133E-05	0.000E+00	0.000E+00	0.000E+00	0.000E+00	2.430E-01	2.430E-01	0.000E+00	6.133E-05
ksat_vz	high	2.430E-01	2.430E-01	0.000E+00	4.906E-05	0.000E+00	0.000E+00	0.000E+00	0.000E+00	2.430E-01	2.430E-01	0.000E+00	4.906E-05
	low	2.430E-01	2.430E-01	0.000E+00	-7.360E-05	0.000E+00	0.000E+00	0.000E+00	0.000E+00	2.430E-01	2.430E-01	0.000E+00	-7.360E-05

Table F.87. STOMP Mass Balance for U-238 (Kd = 1.00) for Case 3 (Retrieval Leak)

Sub-Case		Vadose Zone				Aquifer				Vadose Zone + Aquifer			
		Released	In Domain	Exit	%error	Released	In Domain	Exit	%error	Released	In Domain	Exit	%error
base		1.000E+00	1.000E+00	0.000E+00	1.609E-04	0.000E+00	0.000E+00	0.000E+00	0.000E+00	1.000E+00	1.000E+00	0.000E+00	1.609E-04
recharge	high	1.000E+00	1.000E+00	0.000E+00	1.609E-04	0.000E+00	0.000E+00	0.000E+00	0.000E+00	1.000E+00	1.000E+00	0.000E+00	1.609E-04
	low	1.000E+00	1.000E+00	0.000E+00	1.609E-04	0.000E+00	0.000E+00	0.000E+00	0.000E+00	1.000E+00	1.000E+00	0.000E+00	1.609E-04
barrier	high	1.000E+00	1.000E+00	0.000E+00	1.073E-04	0.000E+00	0.000E+00	0.000E+00	0.000E+00	1.000E+00	1.000E+00	0.000E+00	1.073E-04
	low	1.000E+00	1.000E+00	0.000E+00	7.749E-05	0.000E+00	0.000E+00	0.000E+00	0.000E+00	1.000E+00	1.000E+00	0.000E+00	7.749E-05
barrier_deg	high	1.000E+00	1.000E+00	3.995E-08	1.748E-04	3.995E-08	2.379E-09	3.524E-08	5.841E+00	1.000E+00	1.000E+00	3.524E-08	1.753E-04
	low	1.000E+00	1.000E+00	0.000E+00	1.073E-04	0.000E+00	0.000E+00	0.000E+00	0.000E+00	1.000E+00	1.000E+00	0.000E+00	1.073E-04
ksat_aq	high	1.000E+00	1.000E+00	0.000E+00	1.609E-04	0.000E+00	0.000E+00	0.000E+00	0.000E+00	1.000E+00	1.000E+00	0.000E+00	1.609E-04
	low	1.000E+00	1.000E+00	0.000E+00	1.609E-04	0.000E+00	0.000E+00	0.000E+00	0.000E+00	1.000E+00	1.000E+00	0.000E+00	1.609E-04
ksat_vz	high	1.000E+00	1.000E+00	0.000E+00	1.609E-04	0.000E+00	0.000E+00	0.000E+00	0.000E+00	1.000E+00	1.000E+00	0.000E+00	1.609E-04
	low	1.000E+00	1.000E+00	0.000E+00	4.172E-05	0.000E+00	0.000E+00	0.000E+00	0.000E+00	1.000E+00	1.000E+00	0.000E+00	4.172E-05

Table F.88. STOMP Mass Balance for U-238 (Kd = 1.00) for Case 4 (Ancillary Equipment)

Sub-Case		Vadose Zone				Aquifer				Vadose Zone + Aquifer			
		Released	In Domain	Exit	%error	Released	In Domain	Exit	%error	Released	In Domain	Exit	%error
base		1.000E+00	1.000E+00	0.000E+00	1.431E-04	0.000E+00	0.000E+00	0.000E+00	0.000E+00	1.000E+00	1.000E+00	0.000E+00	1.431E-04
recharge	high	1.000E+00	1.000E+00	0.000E+00	7.153E-05	0.000E+00	0.000E+00	0.000E+00	0.000E+00	1.000E+00	1.000E+00	0.000E+00	7.153E-05
	low	1.000E+00	1.000E+00	0.000E+00	7.153E-05	0.000E+00	0.000E+00	0.000E+00	0.000E+00	1.000E+00	1.000E+00	0.000E+00	7.153E-05
barrier	high	1.000E+00	1.000E+00	0.000E+00	1.073E-04	0.000E+00	0.000E+00	0.000E+00	0.000E+00	1.000E+00	1.000E+00	0.000E+00	1.073E-04
	low	1.000E+00	1.000E+00	0.000E+00	9.537E-05	0.000E+00	0.000E+00	0.000E+00	0.000E+00	1.000E+00	1.000E+00	0.000E+00	9.537E-05
barrier_deg	high	1.000E+00	1.000E+00	1.079E-08	2.910E-04	1.079E-08	6.702E-10	8.193E-09	1.788E+01	1.000E+00	1.000E+00	8.193E-09	2.912E-04
	low	1.000E+00	1.000E+00	0.000E+00	5.960E-05	0.000E+00	0.000E+00	0.000E+00	0.000E+00	1.000E+00	1.000E+00	0.000E+00	5.960E-05
ksat_aq	high	1.000E+00	1.000E+00	0.000E+00	1.431E-04	0.000E+00	0.000E+00	0.000E+00	0.000E+00	1.000E+00	1.000E+00	0.000E+00	1.431E-04
	low	1.000E+00	1.000E+00	0.000E+00	1.431E-04	0.000E+00	0.000E+00	0.000E+00	0.000E+00	1.000E+00	1.000E+00	0.000E+00	1.431E-04
ksat_vz	high	1.000E+00	1.000E+00	0.000E+00	1.252E-04	0.000E+00	0.000E+00	0.000E+00	0.000E+00	1.000E+00	1.000E+00	0.000E+00	1.252E-04
	low	1.000E+00	1.000E+00	0.000E+00	7.749E-05	0.000E+00	0.000E+00	0.000E+00	0.000E+00	1.000E+00	1.000E+00	0.000E+00	7.749E-05

Table F.89. STOMP Mass Balance for U-238 (Kd = 2.00) for Case 1 (Past Leak)

Sub-Case		Vadose Zone				Aquifer				Vadose Zone + Aquifer			
		Released	In Domain	Exit	%error	Released	In Domain	Exit	%error	Released	In Domain	Exit	%error
base		1.000E+00	1.000E+00	2.698E-10	6.554E-05	2.698E-10	3.728E-12	0.000E+00	9.862E+01	1.000E+00	1.000E+00	0.000E+00	6.557E-05
recharge	high	1.000E+00	1.000E+00	2.412E-09	1.249E-04	2.412E-09	1.038E-10	3.688E-10	8.041E+01	1.000E+00	1.000E+00	3.688E-10	1.251E-04
	low	1.000E+00	1.000E+00	0.000E+00	1.192E-05	0.000E+00	0.000E+00	0.000E+00	0.000E+00	1.000E+00	1.000E+00	0.000E+00	1.192E-05
barrier	high	1.000E+00	1.000E+00	3.743E-10	7.745E-05	3.743E-10	5.722E-12	0.000E+00	9.847E+01	1.000E+00	1.000E+00	0.000E+00	7.749E-05
	low	1.000E+00	1.000E+00	2.038E-10	1.192E-04	2.038E-10	2.732E-12	0.000E+00	9.866E+01	1.000E+00	1.000E+00	0.000E+00	1.192E-04
barrier_deg	high	1.000E+00	9.999E-01	1.390E-04	2.038E-04	1.390E-04	7.784E-06	1.313E-04	2.060E-03	1.000E+00	9.999E-01	1.313E-04	2.017E-04
	low	1.000E+00	1.000E+00	0.000E+00	1.311E-04	0.000E+00	0.000E+00	0.000E+00	0.000E+00	1.000E+00	1.000E+00	0.000E+00	1.311E-04
plume	high	1.000E+00	1.000E+00	0.000E+00	1.013E-04	0.000E+00	0.000E+00	0.000E+00	0.000E+00	1.000E+00	1.000E+00	0.000E+00	1.013E-04
	low	1.000E+00	1.000E+00	3.718E-07	4.626E-05	3.718E-07	1.642E-08	3.507E-07	1.280E+00	1.000E+00	1.000E+00	3.507E-07	4.838E-05
ksat_aq	high	1.000E+00	1.000E+00	2.699E-10	6.554E-05	2.699E-10	2.630E-12	0.000E+00	9.903E+01	1.000E+00	1.000E+00	0.000E+00	6.557E-05
	low	1.000E+00	1.000E+00	2.695E-10	6.554E-05	2.695E-10	5.832E-12	0.000E+00	9.784E+01	1.000E+00	1.000E+00	0.000E+00	6.557E-05
ksat_vz	high	1.000E+00	1.000E+00	9.357E-12	3.576E-05	9.357E-12	0.000E+00	0.000E+00	1.000E+02	1.000E+00	1.000E+00	0.000E+00	3.576E-05
	low	1.000E+00	1.000E+00	7.016E-09	5.294E-05	7.016E-09	3.418E-10	3.809E-09	4.084E+01	1.000E+00	1.000E+00	3.809E-09	5.326E-05

Table F.90. STOMP Mass Balance for U-238 (Kd = 2.00) for Case 2 (Diffusion)

Sub-Case		Vadose Zone				Aquifer				Vadose Zone + Aquifer			
		Released	In Domain	Exit	%error	Released	In Domain	Exit	%error	Released	In Domain	Exit	%error
base		2.430E-01	2.430E-01	0.000E+00	-1.227E-05	0.000E+00	0.000E+00	0.000E+00	0.000E+00	2.430E-01	2.430E-01	0.000E+00	-1.227E-05
recharge	high	2.430E-01	2.430E-01	0.000E+00	-1.840E-05	0.000E+00	0.000E+00	0.000E+00	0.000E+00	2.430E-01	2.430E-01	0.000E+00	-1.840E-05
	low	2.430E-01	2.430E-01	0.000E+00	1.227E-05	0.000E+00	0.000E+00	0.000E+00	0.000E+00	2.430E-01	2.430E-01	0.000E+00	1.227E-05
barrier	high	2.430E-01	2.430E-01	0.000E+00	-1.227E-05	0.000E+00	0.000E+00	0.000E+00	0.000E+00	2.430E-01	2.430E-01	0.000E+00	-1.227E-05
	low	2.430E-01	2.430E-01	0.000E+00	-3.680E-05	0.000E+00	0.000E+00	0.000E+00	0.000E+00	2.430E-01	2.430E-01	0.000E+00	-3.680E-05
barrier_deg	high	2.430E-01	2.430E-01	0.000E+00	7.360E-05	0.000E+00	0.000E+00	0.000E+00	0.000E+00	2.430E-01	2.430E-01	0.000E+00	7.360E-05
	low	2.430E-01	2.430E-01	0.000E+00	-7.973E-05	0.000E+00	0.000E+00	0.000E+00	0.000E+00	2.430E-01	2.430E-01	0.000E+00	-7.973E-05
diffusion	high	7.683E-01	7.683E-01	0.000E+00	1.552E-05	0.000E+00	0.000E+00	0.000E+00	0.000E+00	7.683E-01	7.683E-01	0.000E+00	1.552E-05
	low	7.683E-04	7.683E-04	0.000E+00	1.212E-04	0.000E+00	0.000E+00	0.000E+00	0.000E+00	7.683E-04	7.683E-04	0.000E+00	1.212E-04
ksat_aq	high	2.430E-01	2.430E-01	0.000E+00	-1.227E-05	0.000E+00	0.000E+00	0.000E+00	0.000E+00	2.430E-01	2.430E-01	0.000E+00	-1.227E-05
	low	2.430E-01	2.430E-01	0.000E+00	-1.227E-05	0.000E+00	0.000E+00	0.000E+00	0.000E+00	2.430E-01	2.430E-01	0.000E+00	-1.227E-05
ksat_vz	high	2.430E-01	2.430E-01	0.000E+00	-1.227E-05	0.000E+00	0.000E+00	0.000E+00	0.000E+00	2.430E-01	2.430E-01	0.000E+00	-1.227E-05
	low	2.430E-01	2.430E-01	0.000E+00	-6.746E-05	0.000E+00	0.000E+00	0.000E+00	0.000E+00	2.430E-01	2.430E-01	0.000E+00	-6.746E-05

Table F.91. STOMP Mass Balance for U-238 (Kd = 2.00) for Case 3 (Retrieval Leak)

Sub-Case		Vadose Zone				Aquifer				Vadose Zone + Aquifer			
		Released	In Domain	Exit	%error	Released	In Domain	Exit	%error	Released	In Domain	Exit	%error
base		1.000E+00	1.000E+00	0.000E+00	2.980E-05	0.000E+00	0.000E+00	0.000E+00	0.000E+00	1.000E+00	1.000E+00	0.000E+00	2.980E-05
recharge	high	1.000E+00	1.000E+00	0.000E+00	8.345E-05	0.000E+00	0.000E+00	0.000E+00	0.000E+00	1.000E+00	1.000E+00	0.000E+00	8.345E-05
	low	1.000E+00	1.000E+00	0.000E+00	8.941E-05	0.000E+00	0.000E+00	0.000E+00	0.000E+00	1.000E+00	1.000E+00	0.000E+00	8.941E-05
barrier	high	1.000E+00	1.000E+00	0.000E+00	5.960E-05	0.000E+00	0.000E+00	0.000E+00	0.000E+00	1.000E+00	1.000E+00	0.000E+00	5.960E-05
	low	1.000E+00	1.000E+00	0.000E+00	8.345E-05	0.000E+00	0.000E+00	0.000E+00	0.000E+00	1.000E+00	1.000E+00	0.000E+00	8.345E-05
barrier_deg	high	1.000E+00	1.000E+00	0.000E+00	2.146E-04	0.000E+00	0.000E+00	0.000E+00	0.000E+00	1.000E+00	1.000E+00	0.000E+00	2.146E-04
	low	1.000E+00	1.000E+00	0.000E+00	7.153E-05	0.000E+00	0.000E+00	0.000E+00	0.000E+00	1.000E+00	1.000E+00	0.000E+00	7.153E-05
ksat_aq	high	1.000E+00	1.000E+00	0.000E+00	2.980E-05	0.000E+00	0.000E+00	0.000E+00	0.000E+00	1.000E+00	1.000E+00	0.000E+00	2.980E-05
	low	1.000E+00	1.000E+00	0.000E+00	2.980E-05	0.000E+00	0.000E+00	0.000E+00	0.000E+00	1.000E+00	1.000E+00	0.000E+00	2.980E-05
ksat_vz	high	1.000E+00	1.000E+00	0.000E+00	9.537E-05	0.000E+00	0.000E+00	0.000E+00	0.000E+00	1.000E+00	1.000E+00	0.000E+00	9.537E-05
	low	1.000E+00	1.000E+00	0.000E+00	2.980E-05	0.000E+00	0.000E+00	0.000E+00	0.000E+00	1.000E+00	1.000E+00	0.000E+00	2.980E-05

Table F.92. STOMP Mass Balance for U-238 (Kd = 2.00) for Case 4 (Ancillary Equipment)

Sub-Case		Vadose Zone				Aquifer				Vadose Zone + Aquifer			
		Released	In Domain	Exit	%error	Released	In Domain	Exit	%error	Released	In Domain	Exit	%error
base		1.000E+00	1.000E+00	0.000E+00	1.192E-05	0.000E+00	0.000E+00	0.000E+00	0.000E+00	1.000E+00	1.000E+00	0.000E+00	1.192E-05
recharge	high	1.000E+00	1.000E+00	0.000E+00	5.364E-05	0.000E+00	0.000E+00	0.000E+00	0.000E+00	1.000E+00	1.000E+00	0.000E+00	5.364E-05
	low	1.000E+00	1.000E+00	0.000E+00	5.960E-05	0.000E+00	0.000E+00	0.000E+00	0.000E+00	1.000E+00	1.000E+00	0.000E+00	5.960E-05
barrier	high	1.000E+00	1.000E+00	0.000E+00	3.576E-05	0.000E+00	0.000E+00	0.000E+00	0.000E+00	1.000E+00	1.000E+00	0.000E+00	3.576E-05
	low	1.000E+00	1.000E+00	0.000E+00	2.980E-05	0.000E+00	0.000E+00	0.000E+00	0.000E+00	1.000E+00	1.000E+00	0.000E+00	2.980E-05
barrier_deg	high	1.000E+00	1.000E+00	0.000E+00	1.669E-04	0.000E+00	0.000E+00	0.000E+00	0.000E+00	1.000E+00	1.000E+00	0.000E+00	1.669E-04
	low	1.000E+00	1.000E+00	0.000E+00	5.364E-05	0.000E+00	0.000E+00	0.000E+00	0.000E+00	1.000E+00	1.000E+00	0.000E+00	5.364E-05
ksat_aq	high	1.000E+00	1.000E+00	0.000E+00	1.192E-05	0.000E+00	0.000E+00	0.000E+00	0.000E+00	1.000E+00	1.000E+00	0.000E+00	1.192E-05
	low	1.000E+00	1.000E+00	0.000E+00	1.192E-05	0.000E+00	0.000E+00	0.000E+00	0.000E+00	1.000E+00	1.000E+00	0.000E+00	1.192E-05
ksat_vz	high	1.000E+00	1.000E+00	0.000E+00	2.980E-05	0.000E+00	0.000E+00	0.000E+00	0.000E+00	1.000E+00	1.000E+00	0.000E+00	2.980E-05
	low	1.000E+00	1.000E+00	0.000E+00	-3.576E-05	0.000E+00	0.000E+00	0.000E+00	0.000E+00	1.000E+00	1.000E+00	0.000E+00	-3.576E-05

Table F.93. STOMP Mass Balance for U-238 (Kd = 5.00) for Case 1 (Past Leak)

Sub-Case		Vadose Zone				Aquifer				Vadose Zone + Aquifer			
		Released	In Domain	Exit	%error	Released	In Domain	Exit	%error	Released	In Domain	Exit	%error
base		1.000E+00	1.000E+00	0.000E+00	2.384E-05	0.000E+00	0.000E+00	0.000E+00	0.000E+00	1.000E+00	1.000E+00	0.000E+00	2.384E-05
recharge	high	1.000E+00	1.000E+00	0.000E+00	0.000E+00	0.000E+00	0.000E+00	0.000E+00	0.000E+00	1.000E+00	1.000E+00	0.000E+00	0.000E+00
	low	1.000E+00	1.000E+00	0.000E+00	4.172E-05	0.000E+00	0.000E+00	0.000E+00	0.000E+00	1.000E+00	1.000E+00	0.000E+00	4.172E-05
barrier	high	1.000E+00	1.000E+00	0.000E+00	2.980E-05	0.000E+00	0.000E+00	0.000E+00	0.000E+00	1.000E+00	1.000E+00	0.000E+00	2.980E-05
	low	1.000E+00	1.000E+00	0.000E+00	0.000E+00	0.000E+00	0.000E+00	0.000E+00	0.000E+00	1.000E+00	1.000E+00	0.000E+00	0.000E+00
barrier_deg	high	1.000E+00	1.000E+00	2.689E-12	1.252E-04	2.689E-12	0.000E+00	0.000E+00	1.000E+02	1.000E+00	1.000E+00	0.000E+00	1.252E-04
	low	1.000E+00	1.000E+00	0.000E+00	1.788E-05	0.000E+00	0.000E+00	0.000E+00	0.000E+00	1.000E+00	1.000E+00	0.000E+00	1.788E-05
plume	high	1.000E+00	1.000E+00	0.000E+00	1.192E-05	0.000E+00	0.000E+00	0.000E+00	0.000E+00	1.000E+00	1.000E+00	0.000E+00	1.192E-05
	low	1.000E+00	1.000E+00	0.000E+00	2.980E-05	0.000E+00	0.000E+00	0.000E+00	0.000E+00	1.000E+00	1.000E+00	0.000E+00	2.980E-05
ksat_aq	high	1.000E+00	1.000E+00	0.000E+00	2.384E-05	0.000E+00	0.000E+00	0.000E+00	0.000E+00	1.000E+00	1.000E+00	0.000E+00	2.384E-05
	low	1.000E+00	1.000E+00	0.000E+00	2.384E-05	0.000E+00	0.000E+00	0.000E+00	0.000E+00	1.000E+00	1.000E+00	0.000E+00	2.384E-05
ksat_vz	high	1.000E+00	1.000E+00	0.000E+00	7.153E-05	0.000E+00	0.000E+00	0.000E+00	0.000E+00	1.000E+00	1.000E+00	0.000E+00	7.153E-05
	low	1.000E+00	1.000E+00	0.000E+00	2.384E-05	0.000E+00	0.000E+00	0.000E+00	0.000E+00	1.000E+00	1.000E+00	0.000E+00	2.384E-05

Table F.94. STOMP Mass Balance for U-238 (Kd = 5.00) for Case 2 (Diffusion)

Sub-Case		Vadose Zone				Aquifer				Vadose Zone + Aquifer			
		Released	In Domain	Exit	%error	Released	In Domain	Exit	%error	Released	In Domain	Exit	%error
base		2.430E-01	2.430E-01	0.000E+00	-7.360E-05	0.000E+00	0.000E+00	0.000E+00	0.000E+00	2.430E-01	2.430E-01	0.000E+00	-7.360E-05
recharge	high	2.430E-01	2.430E-01	0.000E+00	-6.133E-05	0.000E+00	0.000E+00	0.000E+00	0.000E+00	2.430E-01	2.430E-01	0.000E+00	-6.133E-05
	low	2.430E-01	2.430E-01	0.000E+00	-7.973E-05	0.000E+00	0.000E+00	0.000E+00	0.000E+00	2.430E-01	2.430E-01	0.000E+00	-7.973E-05
barrier	high	2.430E-01	2.430E-01	0.000E+00	-6.133E-05	0.000E+00	0.000E+00	0.000E+00	0.000E+00	2.430E-01	2.430E-01	0.000E+00	-6.133E-05
	low	2.430E-01	2.430E-01	0.000E+00	-1.165E-04	0.000E+00	0.000E+00	0.000E+00	0.000E+00	2.430E-01	2.430E-01	0.000E+00	-1.165E-04
barrier_deg	high	2.430E-01	2.430E-01	0.000E+00	-1.227E-05	0.000E+00	0.000E+00	0.000E+00	0.000E+00	2.430E-01	2.430E-01	0.000E+00	-1.227E-05
	low	2.430E-01	2.430E-01	0.000E+00	-6.133E-05	0.000E+00	0.000E+00	0.000E+00	0.000E+00	2.430E-01	2.430E-01	0.000E+00	-6.133E-05
diffusion	high	7.683E-01	7.683E-01	0.000E+00	0.000E+00	0.000E+00	0.000E+00	0.000E+00	0.000E+00	7.683E-01	7.683E-01	0.000E+00	0.000E+00
	low	7.683E-04	7.683E-04	0.000E+00	7.576E-06	0.000E+00	0.000E+00	0.000E+00	0.000E+00	7.683E-04	7.683E-04	0.000E+00	7.576E-06
ksat_aq	high	2.430E-01	2.430E-01	0.000E+00	-7.360E-05	0.000E+00	0.000E+00	0.000E+00	0.000E+00	2.430E-01	2.430E-01	0.000E+00	-7.360E-05
	low	2.430E-01	2.430E-01	0.000E+00	-7.360E-05	0.000E+00	0.000E+00	0.000E+00	0.000E+00	2.430E-01	2.430E-01	0.000E+00	-7.360E-05
ksat_vz	high	2.430E-01	2.430E-01	0.000E+00	-7.973E-05	0.000E+00	0.000E+00	0.000E+00	0.000E+00	2.430E-01	2.430E-01	0.000E+00	-7.973E-05
	low	2.430E-01	2.430E-01	0.000E+00	-4.293E-05	0.000E+00	0.000E+00	0.000E+00	0.000E+00	2.430E-01	2.430E-01	0.000E+00	-4.293E-05

Table F.95. STOMP Mass Balance for U-238 (Kd = 5.00) for Case 3 (Retrieval Leak)

Sub-Case		Vadose Zone				Aquifer				Vadose Zone + Aquifer			
		Released	In Domain	Exit	%error	Released	In Domain	Exit	%error	Released	In Domain	Exit	%error
base		1.000E+00	1.000E+00	0.000E+00	6.557E-05	0.000E+00	0.000E+00	0.000E+00	0.000E+00	1.000E+00	1.000E+00	0.000E+00	6.557E-05
recharge	high	1.000E+00	1.000E+00	0.000E+00	5.364E-05	0.000E+00	0.000E+00	0.000E+00	0.000E+00	1.000E+00	1.000E+00	0.000E+00	5.364E-05
	low	1.000E+00	1.000E+00	0.000E+00	4.768E-05	0.000E+00	0.000E+00	0.000E+00	0.000E+00	1.000E+00	1.000E+00	0.000E+00	4.768E-05
barrier	high	1.000E+00	1.000E+00	0.000E+00	1.192E-05	0.000E+00	0.000E+00	0.000E+00	0.000E+00	1.000E+00	1.000E+00	0.000E+00	1.192E-05
	low	1.000E+00	1.000E+00	0.000E+00	5.960E-05	0.000E+00	0.000E+00	0.000E+00	0.000E+00	1.000E+00	1.000E+00	0.000E+00	5.960E-05
barrier_deg	high	1.000E+00	1.000E+00	0.000E+00	5.960E-05	0.000E+00	0.000E+00	0.000E+00	0.000E+00	1.000E+00	1.000E+00	0.000E+00	5.960E-05
	low	1.000E+00	1.000E+00	0.000E+00	5.960E-05	0.000E+00	0.000E+00	0.000E+00	0.000E+00	1.000E+00	1.000E+00	0.000E+00	5.960E-05
ksat_aq	high	1.000E+00	1.000E+00	0.000E+00	6.557E-05	0.000E+00	0.000E+00	0.000E+00	0.000E+00	1.000E+00	1.000E+00	0.000E+00	6.557E-05
	low	1.000E+00	1.000E+00	0.000E+00	6.557E-05	0.000E+00	0.000E+00	0.000E+00	0.000E+00	1.000E+00	1.000E+00	0.000E+00	6.557E-05
ksat_vz	high	1.000E+00	1.000E+00	0.000E+00	3.576E-05	0.000E+00	0.000E+00	0.000E+00	0.000E+00	1.000E+00	1.000E+00	0.000E+00	3.576E-05
	low	1.000E+00	1.000E+00	0.000E+00	8.941E-05	0.000E+00	0.000E+00	0.000E+00	0.000E+00	1.000E+00	1.000E+00	0.000E+00	8.941E-05

Table F.96. STOMP Mass Balance for U-238 (Kd = 5.00) for Case 4 (Ancillary Equipment)

Sub-Case		Vadose Zone				Aquifer				Vadose Zone + Aquifer			
		Released	In Domain	Exit	%error	Released	In Domain	Exit	%error	Released	In Domain	Exit	%error
base		1.000E+00	1.000E+00	0.000E+00	0.000E+00	0.000E+00	0.000E+00	0.000E+00	0.000E+00	1.000E+00	1.000E+00	0.000E+00	0.000E+00
recharge	high	1.000E+00	1.000E+00	0.000E+00	4.768E-05	0.000E+00	0.000E+00	0.000E+00	0.000E+00	1.000E+00	1.000E+00	0.000E+00	4.768E-05
	low	1.000E+00	1.000E+00	0.000E+00	1.192E-05	0.000E+00	0.000E+00	0.000E+00	0.000E+00	1.000E+00	1.000E+00	0.000E+00	1.192E-05
barrier	high	1.000E+00	1.000E+00	0.000E+00	-1.192E-05	0.000E+00	0.000E+00	0.000E+00	0.000E+00	1.000E+00	1.000E+00	0.000E+00	-1.192E-05
	low	1.000E+00	1.000E+00	0.000E+00	1.192E-05	0.000E+00	0.000E+00	0.000E+00	0.000E+00	1.000E+00	1.000E+00	0.000E+00	1.192E-05
barrier_deg	high	1.000E+00	1.000E+00	0.000E+00	0.000E+00	0.000E+00	0.000E+00	0.000E+00	0.000E+00	1.000E+00	1.000E+00	0.000E+00	0.000E+00
	low	1.000E+00	1.000E+00	0.000E+00	1.192E-05	0.000E+00	0.000E+00	0.000E+00	0.000E+00	1.000E+00	1.000E+00	0.000E+00	1.192E-05
ksat_aq	high	1.000E+00	1.000E+00	0.000E+00	0.000E+00	0.000E+00	0.000E+00	0.000E+00	0.000E+00	1.000E+00	1.000E+00	0.000E+00	0.000E+00
	low	1.000E+00	1.000E+00	0.000E+00	0.000E+00	0.000E+00	0.000E+00	0.000E+00	0.000E+00	1.000E+00	1.000E+00	0.000E+00	0.000E+00
ksat_vz	high	1.000E+00	1.000E+00	0.000E+00	0.000E+00	0.000E+00	0.000E+00	0.000E+00	0.000E+00	1.000E+00	1.000E+00	0.000E+00	0.000E+00
	low	1.000E+00	1.000E+00	0.000E+00	1.192E-05	0.000E+00	0.000E+00	0.000E+00	0.000E+00	1.000E+00	1.000E+00	0.000E+00	1.192E-05

Distribution

No. of
Copies

Fluor Federal Services

R. Khaleel E6-17

10 CH2M-HILL Hanford Group, Inc.

M. Connelly E6-35

8 Pacific Northwest National Laboratory

V.L. Freedman (2) K9-36
Z.F. Zhang K9-36
S.R. Waichler K9-36
S.K. Wurstner K9-36
D.H. Bacon K9-36
Information Release (2) P8-55